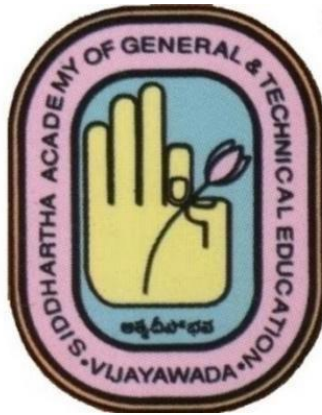


Two-day **International Conference on  
Recent Advances in Mechanical and Industrial  
Engineering – 2024**  
**(ICRAMIE – 2024)**  
22nd and 23rd March 2024

Sponsored by



Siddhartha Academy of General and Technical Education

*Conference Proceedings*  
**ISBN No. 978-93-340-1191-3**

Organised by  
**Department of Mechanical Engineering**  
**Prasad V. Potluri Siddhartha Institute of Technology**  
Kanuru, Vijayawada – 7  
(Autonomous)

(Affiliated to JNTUK, Accredited by NAAC and NBA, ISO 9001:2008 Certified Institution)

Two-day **International Conference on  
Recent Advances in Mechanical and Industrial  
Engineering – 2024**  
**(ICRAMIE – 2024)**

22nd and 23rd March, 2024



Organised by  
**Department of Mechanical Engineering**  
**Prasad V. Potluri Siddhartha Institute of Technology**  
Kanuru, Vijayawada – 7  
(Autonomous)

**Co – Conveners:**  
Dr. P. Phani Prasanthi, Professor  
Dr. K. Ravi Prakash Babu, Assoc. Professor

# Two-day International Conference on Recent Advances in Mechanical and Industrial Engineering – 2024 (ICRAMIE – 2024)

22nd and 23rd March, 2024

## Chief Patrons

**Dr. C. Nageswara Rao**

President

Siddhartha Academy of General & Technical Education

**Sri P. Lakshmana Rao**

Secretary

Siddhartha Academy of General & Technical Education

## Patron

**Sri Vellanki Nagabhushana Rao**

Convener

PVP Siddhartha Institute of Technology

## Patron

**Dr. K. Sivaji Babu**

Principal

PVP Siddhartha Institute of Technology

## Convener

**Dr. B. Raghu Kumar**

Professor and Head,

Department of Mechanical Engineering

## Co-Convener

**Dr. P. Phani Prasanthi**

Professor

Department of Mechanical Engineering

## Co – Convener

**Dr. K. Ravi Prakash Babu**

Associate Professor

Department of Mechanical Engineering

## Organising Committee

Dr. M S R Niranjan Kumar – Prof.

Dr. K Srividya – Asso prof.

Mr. M. V. H. Satish Kumar – Asso. Prof.

Mr. U. Koteswara Rao – Asso.Prof.

Mrs. E. Kavitha – Asst. Prof.

Dr Sd. Abdul Kalam – Asst. Prof.

Mr. G Bala Krishna – Asst. Prof.

Dr. P. Anusha – Asst. Prof.

Dr. K.I.V Vandana – Asst. Prof.

Dr. M. Rajya Lakshmi – Asst. Prof.

Dr. M. Naga Swapna Sri – Asst. Prof.

Dr. Ch. Kishore Reddy – Asst. Prof.

Mr. N Raghu Ram – Asst. Prof.

Mr. K. Venkata Rao – Asst. Prof.

Mr. Ch. Lakshmi Kanth – Asst. Prof.

Mr. P. Mastan Rao – Asst. prof.

Mr. Ch. Mohan Sumanth – Asst.Prof.

Mr. T. Srinag – Asst. Prof.

Mr. P. Gopala Krishnaiah – Asst. Prof.

Mrs. Ch. Vidya – Asst. Prof.

Mr. M Somaiah Chowdary – Asst. Prof.

Mrs. M. Radha Devi – Asst. Prof.

Mr. T.J. Prasanna Kumar – Asst. Prof.

Mr. J. Surendra – Asst. Prof.

Mrs. V. Sravani – Asst. Prof.

Mr. I. Manoj Kumar – Asst. Prof.



**Dr. C. NAGESWARA RAO**  
**PRESIDENT, SAGTE**  
**CHIEF PATRON, ICRAMIE – 2024**

---

**MESSAGE**

I am very happy to make a note that the Department of Mechanical Engineering of Prasad. V. Potluri Siddhartha Institute of Technology, sponsored by Siddhartha Academy of General and Technical education (SAGTE), Vijayawada is organizing Two-day International Conference on Recent Advances in Mechanical and Industrial Engineering (ICRAMIE – 2024) on 22nd and 23rd March, 2024.

Our aim is to create world class engineers endowed with human values to serve the society. As a part of this, we are encouraging all the departments of college to organize National and International conferences, workshops and seminars for the technical enrichment among the faculty and students.

I appreciate the efforts of Department of Mechanical Engineering in organizing Two-day International Conference on Recent Advances in Mechanical and Industrial Engineering. We always support these kinds of conferences that enable faculty to keep in pace with the latest technology and to contribute their innovative ideas to the research in their interested areas.

I wish the conference a splendid success and aspiration that the participants will find the conference a technically enriching and gives rewarding knowledge.

**Date:** 22nd March, 2024

**Place:** PVPSIT



**Sri P. LAKSHMANA RAO**  
**SECRETARY, SAGTE**  
**CHEIF PATRON, ICRAMIE – 2024**

---

**MESSAGE**

I sense immense pleasure and conceited to be a part of Two-day International Conference being organized by the Department of Mechanical Engineering, P.V.P. Siddhartha Institute of Technology sponsored by Siddhartha Academy for General and Technical Education, Vijayawada on 22nd and 23rd March, 2024.

I Congratulate all the concerned for organizing this international conference and bringing out the proceedings. Such conferences are need of the day and helps the academicians get exposed to the various latest developments in the field of Mechanical Engineering. Updating is very significant in the life of an educationist and all such are supported and encouraged at PVPSIT.

Contemporary set of courses should make necessary change in the teaching-learning process. I hope this International Conference organized by the department of ME will fulfill the goals and dreams of younger generation.

On this juncture I take this Opportunity to congratulate all the staff members and students of Mechanical Departments for their efforts and initiative and wish them a very best for success throughout their life.

**Date:** 22nd March, 2024

**Place:** PVPSIT



**Sri. VELLANKI NAGABHUSHANA RAO**

**CONVENER, PVPSIT**

**PATRON, ICRAMIE – 2024**

---

**MESSAGE**

I am happy to note that dept. of Mechanical Engineering of P.V.P Siddhartha Institute of Technology is organizing Two-day International Conference on Recent Advances in Mechanical and Industrial Engineering (ICRAMIE – 2024) on 22nd and 23rd March, 2024, and going to release the proceeding during this occasion.

From the precedent 24 years PVPSIT had been imparting quality service in the meadow of Engineering education by providing excellent infrastructure facilities and the right team of well qualified staff. This makes PVPSIT to march towards confidently in this competitive era.

PVPSIT is playing its responsibility well in training the "Youth" who are the National Asset and Future of India. In the coming years PVPSIT will definitely craft thousands of successful Engineers, Entrepreneurs and citizen to serve the Nation and Society.

I take this opportunity to longing them all the very best in the walks of their profession and also express my whole hearted best wishes on this occasion to all the staff & students of ME department and hope the conference a grand success.

**Date:** 22nd March, 2024

**Place:** PVPSIT



**Dr K. SIVAJI BABU**  
**PRINCIPAL, PVPSIT**  
**PATRON, ICRAMIE – 2024**

---

**MESSAGE**

I am immensely happy that Mechanical Engineering department of our college is organizing a Two-day International Conference on Recent Advances in Mechanical and Industrial Engineering (ICRAMIE – 2024) on 22nd and 23rd March, 2024 and is going to present a collection of various technical papers in the proceedings.

Under the capable guidance of our management SAGTE, the Institute continues to march on the way of success with confidence. The sharp, clear-sighted vision and precise decision-making powers of our management has benefited our college to stay competitive.

The dedicated HODs and staff members and disciplined students of PVPSIT are the added features of our college. The role of students in building nation cannot be overlooked and students at PVPSIT are trained in all aspects to become successful engineers and good citizens.

I congratulate HOD, staff members, students of ME departments and participants for their hard work in organizing and participating in this conference and wish the conference all the success.

**Date:** 22nd March, 2024

**Place:** PVPSIT



**Dr. B. RAGHU KUMAR**  
**PROFESSOR & HOD, DEPT OF ME, PVPSIT**  
**CONVENOR, ICRAMIE – 2024**

---

**MESSAGE**

It is a great admiration for me to address on this occasion of international conference being organized by our department, Two-day International Conference on Recent Advances in Mechanical and Industrial Engineering (ICRAMIE – 2024) on 22nd and 23rd March, 2024.

The department is dedicated to add value to intellectual, moral, social and technological capabilities to the students. This Conference is an endeavor in the direction to give an exposure to the academicians on the recent development in Mechanical and Industrial Engineering field. The key goal of the conference is to promote research and developmental activities in Mechanical Engineering.

I am very happy to note that a good number of methodological papers from scholars and students are being presented and discussed in the conference.

I place on records with appreciation the hard work, participation and effort taken by the team of staff and students in organizing this conference and congratulate all the concerned with gratitude and wish the conference a grand success.

**Date:** 22nd March, 2024

**Place:** PVPSIT



**Dr. P.PHANI PRASANTHI**  
**PROFESSOR, DEPT OF ME, PVPSIT**  
**CO-CONVENER, ICRAMIE – 2024**

---

### **PROLOGUE**

I am delighted to state that the department of Mechanical Engineering of Prasad V. Potluri Siddhartha Institute of Technology is organizing Two-day International Conference on Recent Advances in Mechanical and Industrial Engineering (ICRAMIE – 24) on 22nd and 23rd March, 2024.

The development in the area of Mechanical Engineering and Materials Characterization in the past few years has led to extraordinary increase in the number of people using these technologies and also the interest in research and development.

ICRAME-24 aims to bring together innovative academics, researchers and industrial experts in the field of Mechanical Engineering, for a constructive dialog on theoretical concepts and practical thoughts.

I am extremely indebted to Dr. C. Nageswara Rao garu, President, SAGTE, Sri. P. Laxmana Rao garu, Secretary, SAGTE and Sri. Vellanki Nagabhushana Rao garu, Convener, PVPSIT, Dr. K. Sivaji Babu garu, Principal of PVPSIT for their constant encouragement. I also express my gratitude to Dr. B. Raghu Kumar, HOD, faculty, staff and students of Mechanical Engineering Department, PVPSIT for their involvement and enthusiastic participation in the conference.

**Date:** 22nd March, 2024

**Place:** PVPSIT

International Conference on Recent Advances in Mechanical and Industrial Engineering  
(ICRAMIE - 2024)

**List of Contributed papers**

Sl. No	Paper Code	Title of the paper	Name of the Authors	Name of the College	Page No.
1	ICRAMIE 24 - D1	Investigational analysis on machinability of 15-5PH stainless steel (SS15-5PH) by studying the various parameters	P.Mounika <sup>1</sup> , V.Dhana Raju <sup>2</sup> , K.Sai Babu <sup>3</sup> , B.Sai Rama Krishna <sup>4</sup>	<sup>1,2,3</sup> Lakireddy Bali Reddy College of Engineering, Mylavaram, A. P. -521230 <sup>4</sup> Amrita Sai Institute of Science & Technology, Paritala	1-7
2	ICRAMIE 24 – D2	Design and Fabrication of Bladeless Wind Turbine	Dr. K. Srividya <sup>1</sup> , Dr. M. Nagaswapnasri <sup>2</sup> , Dr. P. Anusha <sup>3</sup> , P. Praveen Kumar <sup>4</sup> , S. Priya Vardhan <sup>5</sup> , Shaik Mahammed Ismail <sup>6</sup>	<sup>1,2,3,4,5,6</sup> Prasad V Potluri Siddhartha Institute of Technology, Vijayawada, India.	8-13
3	ICRAMIE 24 – D3	Experimental Studies with a Protomodel Drone in Agricultural Sector	Dr. J A Ranga Babu <sup>1</sup> , P Bhargava Kumar <sup>2</sup> , P Satyanarayana <sup>1</sup> , T. Prasanth <sup>1</sup>	<sup>1</sup> Seshadri Rao Gudlavalleru Engineering College, Gudlavalleru, AP-521356 <sup>2</sup> Ramachandra College of Engineering, Eluru- 534007	14-20
4	ICRAMIE 24 – D4	A Study on Deformation Behavior of Different Hip Prostheses Materials Using Abaqus	Praveen Chapala <sup>*1</sup> , Challapalli Rushinath <sup>1</sup> , Saran S <sup>1</sup> , Deepak Yadav <sup>1</sup>	<sup>1</sup> National Institute Of Technology Andhra Pradesh, India	21-26
5	ICRAMIE 24 – D5	Analysis of Deformation Behaviour of Automotive Disc Brakes Using Abaqus	Praveen Chapala <sup>1,2</sup> , Sweety A <sup>1</sup> , Golla Neha Sri <sup>1</sup> , Akudari Mamatha <sup>1</sup>	<sup>1</sup> National Institute Of Technology Andhra Pradesh, India	27-34
6	ICRAMIE 24 – D6	Advancing Materials Design and Optimization for Improved Mechanical Performance in Solar Desalination Systems	L. Karthick <sup>1*</sup> , Robin Johny K <sup>2</sup> , Naresh Mallireddy <sup>3</sup> , Srikanth Salyan <sup>4</sup> , B. Senthil Kumar <sup>5</sup> , Ramesh Velumayil <sup>6</sup>	<sup>1</sup> Hindusthan College of Engineering and Technology, Coimbatore. <sup>2,5</sup> Sri Ramakrishna Engineering College, Coimbatore, <sup>3</sup> Aditya College of Engineering, Surampalem <sup>4</sup> Dayananda Sagar College of Engineering, Bengaluru, <sup>6</sup> Vel Tech Rangarajan Dr. Sagunthala R&D Institute of Science and Technology, Avadi, Chennai.	35-42
7	ICRAMIE 24 – D7	Effect of Air Loads on Aircraft Composite Structure - Strength Prediction by Finite Element Analysis	Sd. Abdul Kalam <sup>1*</sup> , P. Gopala Krihna <sup>1</sup> , Sk. Ziavulla <sup>2</sup> , Sk. Abdul Rahman <sup>2</sup> , Sk. Karim <sup>2</sup>	<sup>1,2</sup> PVP Siddhartha Institute of Technology, Vijayawada, Andhra Pradesh, India	43-47

International Conference on Recent Advances in Mechanical and Industrial Engineering  
(ICRAMIE - 2024)

**List of Contributed papers**

Sl. No	Paper Code	Title of the paper	Name of the Authors	Name of the College	Page No.
8	ICRAMIE 24 – D8	Design, Fabrication and Experimentation of Smart Agro System using IOT and Sensor Network	<sup>1</sup> B.Kamala Priya, <sup>2</sup> N Vijay Kalyan, <sup>3</sup> P Prabhas, <sup>4</sup> Sk Habib	<sup>1,2,3,4</sup> Lakireddy Bali Reddy College of Engineering, Mylavaram,	48-57
9	ICRAMIE 24 – D9	Hybrid Solar Distillation fabrication for water purification	M. Rajyalakshmi <sup>1</sup> , K. I. V. Vandana <sup>2</sup>	<sup>1,2</sup> PVP Siddhartha Institute of Technology, Vijayawada.	58-67
10	ICRAMIE 24 – D10	Experimental evaluation of synthesized banana peels bioplastic	P. Nanda Kumar <sup>1</sup> , M.Bala Chennaiah <sup>2</sup> , Reddy Sreenivasulu <sup>3</sup> , B Kamala Priya <sup>4</sup> , D.Mohith Babu <sup>5</sup> , P.Pavan <sup>6</sup>	<sup>1,5,6</sup> N.B.K.R. Institute of Science & Technology <sup>2</sup> V R Siddhartha Engineering College, Vijayawada <sup>3</sup> R. V.R&J.C. College of Engineering. Guntur <sup>4</sup> Lakireddy Balireddy College of Engineering, Mylavaram	68-74
11	ICRAMIE 24 – P1	Industry 4.0 - Issues and Challenges for Indian Industries	Dr. Srinivasa Rao Dokku <sup>1</sup> , Dr. P. Adi Lakshmi <sup>2</sup> , Dr. Rajesh C. Jampala <sup>3</sup>	<sup>1,2</sup> P.V.P. Siddhartha Institute of Technology, Kanuru, Vijayawada <sup>3</sup> PB Siddhartha College of Arts & Science, Viayawada	75-81
12	ICRAMIE 24 – P2	The AI-Driven Optimization of Supply Chain and Logistics in Mechanical Engineering	<sup>1*</sup> L. Karthick, <sup>2</sup> K. Ramesh Kumar, <sup>3</sup> S. Sivakumar, <sup>4</sup> S. Ramkumar, <sup>5</sup> D. Prabhu, <sup>6</sup> L. Vadivukarasi	<sup>1,2,3,4,5</sup> Hindusthan College of Engineering and Technology, Coimbatore <sup>6</sup> Nandha Arts and Science College, Erode	82-88
13	ICRAMIE 24 – P3	Nurturing Millet Utilization: A Framework for Policy Advancement	Kanaka Durga Devi.Nelluri <sup>1</sup> , Anupama Ammulu Manne <sup>2</sup> , K.Naga Bhargavi <sup>1</sup> , Sk Anwar Sadiq <sup>1</sup> , D. Sai Prakash <sup>1</sup> , Sai Harsha V K Yaswanth <sup>1</sup> , Revanth G S Nirupa Varsha <sup>1</sup> , Harshini G D Sasi Priya <sup>1</sup>	<sup>1</sup> KVSR Siddhartha College of Pharmaceutical Sciences, Vijayawada. <sup>2</sup> Department of Civil Engineering, PVPSIT, Kanuru, Vijayawada.	89-98
14	ICRAMIE 24 – P4	Performance Study of Alumina Ceramic Tool Inserts During Dry Turning of EN36 Hardened Steel Samples	Dr. K.I.Vishnu Vandana <sup>1</sup> . K. Uday Babu <sup>2</sup> , L. Adithi <sup>3</sup> , K.N. Mithilesh <sup>4</sup> , K. Pavan <sup>5</sup>	<sup>1,2,3,4,5</sup> P.V.P.Siddhartha Institute of Technology, Kanuru, Vijayawada	99-106

International Conference on Recent Advances in Mechanical and Industrial Engineering  
(ICRAMIE - 2024)

**List of Contributed papers**

Sl. No	Paper Code	Title of the paper	Name of the Authors	Name of the College	Page No.
15	ICRAMIE 24 – P5	The Automated Rope Line: A Revolution in Industrial Automation	Dr. K Srinivas <sup>1</sup> , Divya Singhi <sup>2</sup> , D. Kasim Moula <sup>3</sup> , P. Jai Tarun Sai <sup>4</sup> , A. Shyam Sundar <sup>5</sup> , K. Subrahmanyam <sup>6</sup>	<sup>1</sup> Department of mechanical engineering, VRSEC, Vijayawada	107-120
13	ICRAMIE 24 – P6	EDM input parameter optimization for SS-316 steel using the fuzzy logic technique and an analysis of the micro structural features of the EDM machining surface	G.Sridevi <sup>1</sup> , Sneha.H.Dhoria <sup>2</sup> , Dr.Putta Nageswara rao <sup>3</sup> , Dr. Siva Sankara Babu Chinka <sup>4</sup> , Nelakuditi Naresh babu <sup>5</sup>	1. Centurion university of technology and management, Odisha 2. Sneha.H.Dhoria, R.V.R&J.C College of engineering, Guntur 3. Vasireddy venkatadri Institute of Technology, Guntur 4. Lakireddy Bali Reddy College of Engineering, Mylavaram <sup>4</sup> 5. DVR & Dr.HS MIC College Of Technology <sup>5</sup>	121-129
17	ICRAMIE 24 – T1	Enhancing the Thermal Properties of Ultra-High Molecular Weight Polyethylene through the Addition of Carbon Nanotubes: A Promising Approach for Total Joint Replacement Applications	V.Chittaranjan Das <sup>a*</sup> , K.Praveen Kumar <sup>a</sup> , U.Sai Pranay <sup>b</sup> , P.S.Rama Sreekanth <sup>c</sup>	<sup>a</sup> <sup>b</sup> R.V.R. & J.C. College of Engineering, Guntur <sup>c</sup> VIT-AP University, Amaravati	130-144
18	ICRAMIE 24 – T2	Investigating the Performance and Emission Characteristics of Diesel Engine Fuelled with Rice Bran Biodiesel	K.Sai Babu <sup>1</sup> , V.Dhana Raju <sup>2</sup> , Devarakonda Vamsi <sup>3</sup> , Emmanuel Buradagunta <sup>4</sup>	<sup>1,2, 3</sup> Lakireddy Bali Reddy College of Engineering, Mylavaram <sup>4</sup> DVR & Dr. HSMIC College of Technology.	145-152
19	ICRAMIE 24 – T3	Experimental Investigation of Performance R134a Vapour Compression Refrigeration System Permanent Magnetic Field After Condenser and Diffuser at Compressor Outlet	P.Tejomurthi <sup>a</sup> , K.Dilip Kumar <sup>b</sup> B.BalaKrishna <sup>c</sup>	<sup>a</sup> Seshadri Rao Gudlavalleru Engineering College Guldavalleru <sup>b</sup> Lakireddy Bali Reddy College of Engineering, Mylavaram <sup>c</sup> JNTUK Kakinada	153-159
20	ICRAMIE 24 – T4	Analytical Optimization of Crystalline Nano Cellulose-Dispersed H <sub>2</sub> O/C <sub>2</sub> H <sub>6</sub> O <sub>2</sub> Nano Fluids Using Response Surface Methodology	Vidya Chaparala <sup>1,2</sup> , G. Ravi Kiran Sastry <sup>1</sup> , P. Phani Prasanthi <sup>2</sup>	1 National Institute of Technology, Andhra Pradesh, 2 P.V.P. Siddhartha Institute of Technology, Vijayawada.	160-165

International Conference on Recent Advances in Mechanical and Industrial Engineering  
(ICRAMIE - 2024)

**List of Contributed papers**

Sl. No	Paper Code	Title of the paper	Name of the Authors	Name of the College	Page No.
21	ICRAMIE 24 – T5	Heat Transfer Analysis of Cylindrical Horizontal Jet Impinging on Vertical Plate	Kunapuli Siva Satya Mohan <sup>1</sup> , K. Ravi Kumar <sup>2</sup> , Panthangi Ravi Kumar <sup>3</sup> , K.P.V. Krishna Varma <sup>4</sup> , M. Rambabu <sup>5</sup> , P V S Muralikrishna <sup>6</sup>	<sup>1,5,6</sup> Aditya College of Engineering & Technology, Surampalem <sup>2</sup> V R Siddhartha Engineering college, Vijayawada <sup>3</sup> CMR College of Engineering & Technology, Telangana <sup>4</sup> Raghu Engineering College, Visakhapatnam.	166-174
22	ICRAMIE 24 – T6	Heat Transfer Enhancement of An Automobile Engine Radiator Using Al <sub>2</sub> O <sub>3</sub> /Cuo Water Base Nanofluids	K. Venkatarao <sup>1</sup> , Ch. Lakshmi Kanth <sup>2</sup> , V. Sravani <sup>3</sup> , N. Manoj Kumar <sup>4</sup> , V. Eswar Balaji <sup>5</sup> , V. Veera Manikanta <sup>6</sup> , Sk. Suhail <sup>7</sup>	<sup>1,2,3,4,5,6,7</sup> Prasad V Potluri Siddhartha Institute of Technology, Vijayawada, A.P, India	175-184
23	ICRAMIE 24 – T7	A Brief Overview of Magnetic Refrigeration	K.Nithin <sup>1</sup> , J.Jathin <sup>1</sup> , G.Hemanth kumar <sup>2</sup> , M.Virinchi <sup>3</sup> , G.V.S.Ravi Teja <sup>4</sup> , G.Bhargav <sup>5</sup> , B.Prem sai <sup>6</sup> , K.Raju <sup>7</sup> , B. Sai Kausik <sup>1</sup> , Dr.P.Anusha <sup>1</sup> , Dr.M.Naga Swapna Sri <sup>1</sup>	<sup>1,2,3,4,5,6,7</sup> Prasad V Potluri Siddhartha Institute of Technology, Vijayawada, A.P, India	185-190
24	ICRAMIE 24 – T8	Structural and Thermal Analysis of Brake Drum	Shaik.Chand Mabhu Subhani <sup>1</sup> , A.Pavan Kumar <sup>2</sup> , Dr.D.venkata rao <sup>3</sup> K.Anna Purnaiah <sup>4</sup>	<sup>1,2,3,4</sup> Narasaraopeta Institute of Technology, Narasaraopet.	191-200
25	ICRAMIE 24 – T9	Comparative Analysis of Semi Monocoque Structured Aircraft Nose Cone Made of Different Titanium Graded Alloys at different operating conditions	T J Prasanna Kumar <sup>1</sup> , V Sravani <sup>1</sup> , B Kamala Priya <sup>2</sup> , Y Ayyappa <sup>3</sup> , M Kiran Kumar <sup>3</sup> , Sk Roshan <sup>3</sup> , P Tarun kumar <sup>3</sup>	<sup>1,3</sup> PVP Siddhartha Institute of Technology, Kanuru, Vijayawada <sup>2</sup> Lakireddy Bali Reddy College of Engineering, Mylavaram	201-213

International Conference on Recent Advances in Mechanical and Industrial Engineering  
(ICRAMIE - 2024)

**List of Contributed papers**

Sl. No	Paper Code	Title of the paper	Name of the Authors	Name of the College	Page No.
26	ICRAMIE 24 – T10	Performance And Emission Characterstics of VCR Engine Fueled with Tyreoil and Cotton Seed Oil Blends	Dr.G.NagaMalleswara Rao <sup>1*</sup> , Shaik Chand Mabhu Subhani <sup>2</sup>	Eswar College of Engineering, Kesanupalli(Po), Narasaraopet	214-224
27	ICRAMIE 24 – T11	Experimental and CFD Analysis of Thermal Performance Improvement of Automobile Radiator Using Al <sub>2</sub> O <sub>3</sub> -TiO <sub>2</sub> Water Base Nanofluids	1.K. Venkatarao, 2.Ch. Lakshmi Kanth, 3.V. Sravani, 4.T. Hari Krishna, 5.T. Kiran Kumar, 6.V. Chandra Sekhar, 7.V. Chinna Murali Krishna	<sup>1,2,3,4,5,6,7</sup> Prasad V Potluri Siddhartha Institute of Technology, Vijayawada	225-240
28	ICRAMIE 24 – T12	Improving Efficiency in Solar Desalination Introducing Innovative Mechanical Methods for Sustainable Generation of Freshwater	L. Karthick <sup>1*</sup> , Aashish.A.Gadgil <sup>2</sup> , M.Babu <sup>3</sup> , Nalla Bhanu Teja <sup>4</sup> , Srikanth Salyan <sup>5</sup> , B. Senthil Kumar <sup>6</sup>	<sup>1</sup> Hindusthan College of Engineering and Technology, Coimbatore <sup>2</sup> KLS Gogte Institute of Technology, Belagavi <sup>3</sup> SRM Easwari Engineering College, Rampuram, Chennai <sup>4</sup> Aditya College of Engineering, surampalem, <sup>5</sup> Dayananda Sagar College of Engineering, Bengaluru. <sup>6</sup> Sri Ramakrishna Engineering College, Coimbatore.	241-248
29	ICRAMIE 24 – T13	Comparative simulation and CFD analysis on a car by varying different angles of rear spoiler	B.Kamala Priya <sup>1</sup> , K.Sai Babu <sup>2</sup> , V.Sravani <sup>3</sup> , V.Dhana Raju <sup>4</sup> , B.Sai Rama Krishna <sup>5</sup>	<sup>1,2,4</sup> Lakireddy Bali Reddy College of Engineering, Mylavaram <sup>3</sup> Prasad V Potluri Siddhartha Institute of Technology, Kanuru, Vijayawada <sup>5</sup> Amrita Sai Institute of Science & Technology, Paritala	249-256
30	ICRAMIE 24 – T14	Single Cylender Engine Fueled with Petrol and Enriched Hydrogen and Hydroxy for Better Performance	Sukumar Kalapati <sup>1</sup> , Dr. Venkatasubbaiah K <sup>2</sup> , Dr. Narayana Rao K <sup>3</sup>	<sup>1</sup> Govt. Polytechnic for Minorities, Guntur <sup>2</sup> JNTU Gurajada, Vizianagaram, (Council Member, IEI & ISTE.,) <sup>3</sup> A.P.S.B.T & T., (Dept. of Technical Education) Vijayawada, A.P., India.	257-264

## **Investigational analysis on machinability of 15-5PH stainless steel (SS15-5PH) by studying the various parameters**

**P.Mounika<sup>1</sup>, V.Dhana Raju<sup>2</sup>, K.Sai Babu<sup>3</sup>, B.Sai Rama Krishna<sup>4</sup>**

<sup>1,2,3</sup>Lakireddy Bali Reddy College of Engineering, Mylavaram, A. P. -521230

<sup>4</sup>Amrita Sai Institute of Science & Technology, Paritala

Corresponding author mail id: pmounika@lbrce.ac.in

**ABSTRACT.** The research development of the material deals with the improvement of properties of the composite material 15-5 precipitation hardening stainless steel. Superior strength, considerable corrosion resistance along with favourable toughness and mechanical aspects of 15-5 precipitation hardening material. The properties of the precipitation stainless steel material properties during turning process under various states of this material which has the desirable improvement in the mechanical properties under various heat treatment process. In this study the mechanical properties with micro- hardness and micro-structures were evaluated. The fractography and SEM results shows the change in the PH values during the various process. Desirable machining rates and the mechanical properties were discussed in the paper and also compared with H1150 and H1150-M material properties during the various treated states.

Keywords: Stainless steel, Casting, Yield strength, Cutting parameters, Rate of feed, Dept cut.

### **1. INTRODUCTION**

Machining is the general term that deals with the process of removing material which include the process of cutting, abrasive process and advanced machining process with various source of energy like electrical, chemical, thermal, optical and hydrodynamic. The machinability of the material is the state where the material has the properties that allows or permit to remove or work with the material for good or satisfactory results after the treatment of various process. Stainless steels (S.S) are iron (ferritic grades of range 12-18% of iron) based alloys with the minimum of 10.5% Chromium with ultimately 1.2% of carbon and other alloys. Surface integrity has two aspects which are surface topography or surface finish and metallurgy. The vast research is done on PH stainless steels were focusing only on the study of micro-structure, wear and corrosion, fracture, and fatigue performance. Minimum research is done by considering the machining effects that are varying mechanical properties and hardness of this alloy with different heat treatment method. Examining the progress of micro-structure and mechanical aspects of the PH S.S through various precipitation heat treatments (time & temperature) is the main objective. Also, the machine precipitated hardened stainless steel with different hardness and mechanical properties levels at various states [Speed of cutting ( $V_c$ ), feed ( $f$ ), cutting depth( $d$ )] also, measuring the force of cut, surface roughness and correlate with the cutting parameters.

Ashok kumar (2013) et al., for aircraft applications the original growth and safety authorization of 15–5 PH (Precipitation hardening) S.S. By situations H1150 and H1150 M, greater machining rates are occurred. Through aging in 15–5 PH composite and at another step of hardening for greater aging temperature (H1150) is linked with development of precipitates of Cu [1]. M. Aghaie-Khafri (2010) et al, in this paper, over the temperature values of 300 to 600 °C maximum temperature tensile strain of 15-5 PH S.S in top age and superannuated circumstances. The solution-treated 15-5 PH steel at 450°C for 7 hours carried around a highest age-hardening (44.4 HRC) [2]. Habibi (2001) et al, studied the microstructure of 15-5 PH precipitation-hardened S.S subsequently dissimilar heat treatments shows 2 sorts of carbides, NbC and M<sub>7</sub>C<sub>3</sub> along with fine precipitates rich in copper at initial stages and in second stage of copper precipitate at 650 to 700 °C is spherical shape [3]. A. Abad (2010) et al., due to environmental states the rust of 15-5PH H1025

S.S occurs. When exposing towards blow water at 71 °C corrosion of 15-5PH H1025 S.S, roughness

was triggered by the electric transmission from the power passage to the fragments [4]. Mondelin et al. (2012), during turning of (SS15-5PH) substrate integrity forecast and developed a metallurgical model for (SS15- 5PH) using investigational outcomes and found that high temperature appeared in the cutting zone (700 °C to 1000 °C) [5].

## 2. METHODOLOGY

The steps involved in methodology is selection of material then heat treatments of state ‘A’ recipe treated, H900 air-cooled, H900 furnace-cooled, H1 150M air-cooled, H1 150M furnace-cooled, Machine testing and Characterization, mechanical testing of tensile test and micro hardness, metallurgical testing of micro structure and fractography. From there planning for the experimentation of machining and data collection then surface roughness and cutting forces identification then result and discussion with conclusion.

### 2.1 Selection of material

Due to investigation, the material selection is S.S15-15 PH production starts with casting and then squeeze out in the form of rounded bar. In this study span of 120 mm and dia of 32 mm is chosen. Subsequently, mixture is galvanized to hone the grain profiles and dimensions and is carried in this case, denoted to as state “A” mentioned previously. Chemical alignment of SS15-5 PH is C Max. is 0.07, Cr is 14.00-15.50, Ni is 3.50-5.50, Cu is 2.50-4.50, Mn Max. is 1.0, Nb+Ta is 0.15-0.45, S Max. is 0.03, Si Max was 1.0, P Max.0.04 the balance is Fe.

### 2.2 Heat Treatment

For the selected material, for State “A” is SS15-5PH is carried from the mill is then heat treated at dissimilar temperatures for extensive variety of aspects development with the aid of electrical furnace. The heat treatment procedure for state ‘A’ solution treated is  $1038 \pm 14^\circ\text{C}/\text{min}$  of 30 minutes with air cool or oil cool under  $32^\circ\text{C}$ , for H900 -  $482 \pm 6^\circ\text{C}$ , 01, Air cool, H900 -  $482 \pm 6^\circ\text{C}$ , 01, Furnace, For H1150M (double excess)-  $760 \pm 6^\circ\text{C}$  continued by  $621 \pm 6^\circ\text{C}$ , 02 followed by 04, Air, H1150 M (double overage) -  $760 \pm 6^\circ\text{C}$ , 02 continued by 04, Furnace.

### 2.3 Mechanical testing and Characterization

For the selected material of (SS15-5PH) is heat treated and after heat treatment various kind of tests are carried out to identify the mechanical properties along with characteristics. Some instruments are shown below for testing the mechanical properties.



**Fig. 1.** Tensile test samples and tensile test machine.

Microstructure of the material at different heat treatment states are examined using the optical microscopy. Samples are first cut into small pieces, mounted using the hydraulic press mounting machine and polished after that etched with the residue of 10 grams of  $\text{CuSO}_4$ , 50 milli- liters HCl and 50 milli-liters water some few drops of  $\text{H}_2\text{SO}_4$  are mixed to increase the activities. Conducting the fractographic tests on the fracture exteriors using SEM to identify the manner of break by endangering the sample exteriors attained from the unsuccessful trial sample exposed to tensile loading in five situations of state A recipe treated, H900 air- cooled and furnace-cooled, and H1150M air-cooled and furnace-cooled.

Performing the turning test with TiAlN covered carbide tool enclosure by CNMG 120408, ISO  
Dept. of Mech. Engg. PVPSIT 2

designated was utilized. TiAlN-based glazes of 2–5  $\mu\text{m}$  dense layers typically deposited with toughness fluctuating amid 3000 and 3300 HV, thermally stable amid of 800°C and 900°C with the amount of rubbing amid 0.35 and 0.4. Tool gripper as per ISO standard PCLNL 1616 H12, inserted and examination has done with LEADWELL CNC turning center.

The CNC turning machine tool has following specification: Supreme swing - 330 mm, swing over cross slide- 136 mm, Maximum turning diameter - 136 mm, Maximum turning span - 150 mm, Travel - X axis - 230 mm, Z axis - 230 mm, Spindle velocity – 45 to 4500 rpm, Spindle motor power - 7.5 kw, Number of tools –6, Feed range - 0 - 24000 mm/min.

#### 2.4 Process Variable and Response

The work material of state A, includes heat treatment, chemical arrangement, manufacture, hardness, yield stress, and tensile stress etc. Functioning circumstances, cutting tool metal and structure, and the machining procedure strictures like speed of cut, feed, cutting depth etc., acted as other important influences. Machinability of SS15-5PH premeditated by regards to substrate integrity and force in diverse set of cutting limitations in current work. Cutting depth of cut = 0.5mm is constant at 3 different levels. In level – 1 speed of cut,  $V_c$  (m/min) is 125, Feed,  $f$  (mm/rev) is 0.06, cutting depth,  $d$  (mm) is 0.5, for level-2 & 3, the parameters are (0.06, 0.12, 0.18) & (0.5, 0.5, 0.5) correspondingly.

### 3. RESULTS AND DISCUSSION

#### 3.1 Mechanical Testing and Characterization

Various kind of testing are performed to identify the mechanical features and characteristics after heat treatment. For SS15-5PH of State ‘A’ solution treated different mechanical properties identified at H900 (AirCooled), H900 (Furnace-cooled), H1150 M (Air-cooled), H1150 M (Furnace-cooled). For Hardness (Hv0.5) is 354, 468, 437, 352, 293 respectively. For Maximum Force (KN) - 3.325, 42.654, 38.479, 27.548, 24.175 respectively. For tensile Strength (Gpa)- 1.336, 1.562, 1.412, 1.011, 0.958 respectively. Extension (%) - 14.520, 13.468, 11.324, 15.013, 15.615 respectively. Decrease in area (%) – 63.386, 52.306, 58.785, 65.190, 66.132 respectively.

#### 3.2 Microstructure evaluation

For microstructure examination all samples are ready after etching. Microstructures are observed using optical microscope. Microstructures were exposed in Fig.2 (i), (ii), (iii), (iv) and (v) at different heat treatment states.

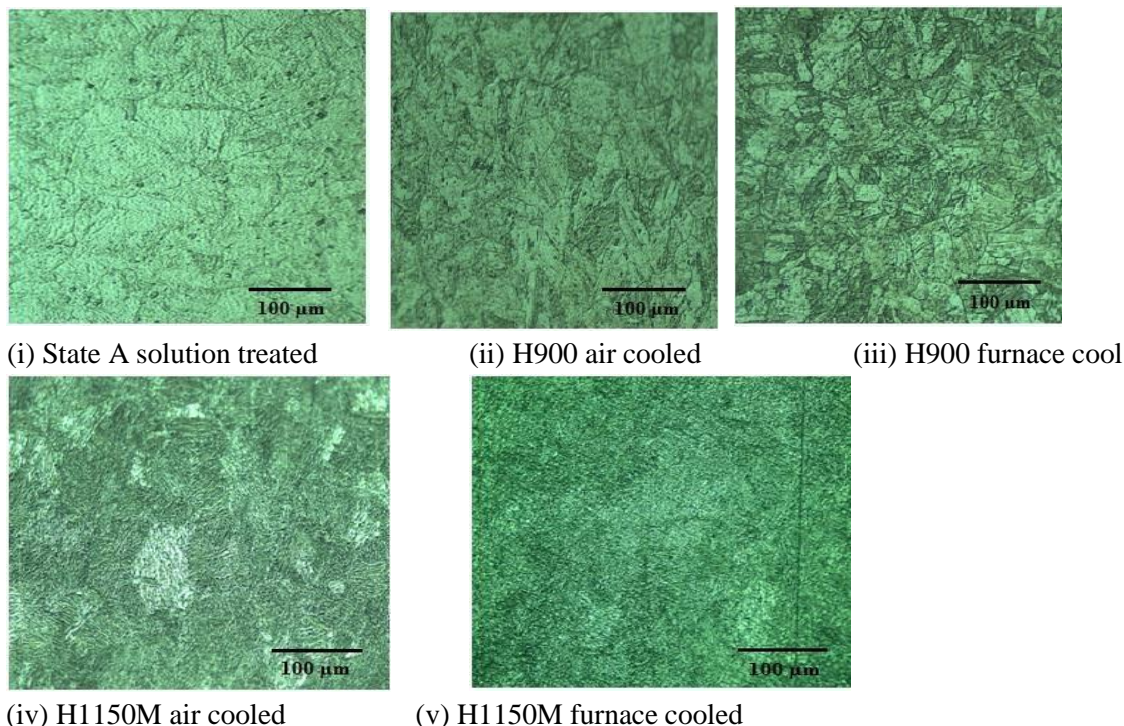
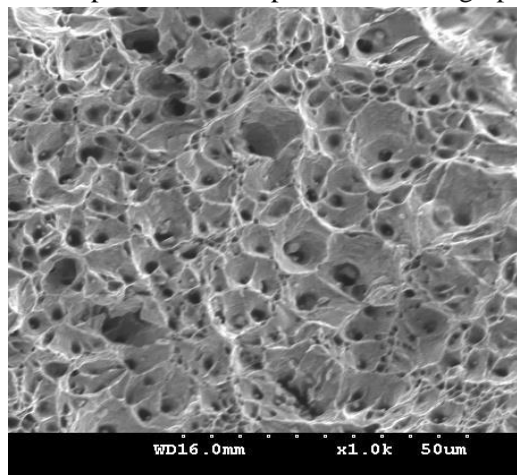
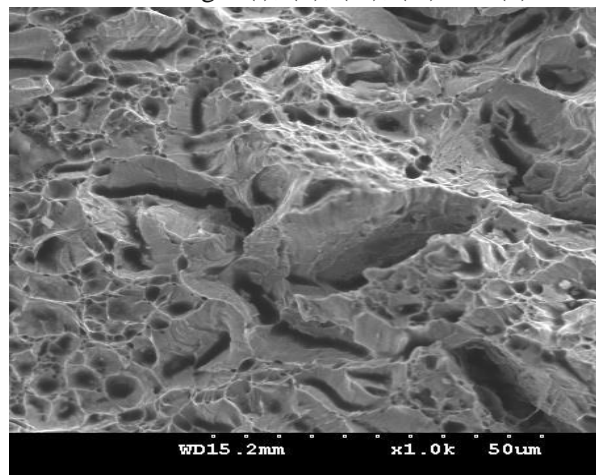


**Fig. 2.** Microstructures.

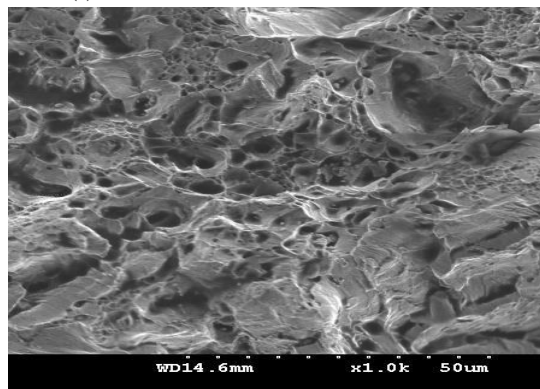
The submicroscopic precipitates are only visible under SEM (scanning electron microscope) but underoptical microscope. SEM fracto-graph were revealed in Fig.3 (i), (ii), (iii), (iv) and (v).



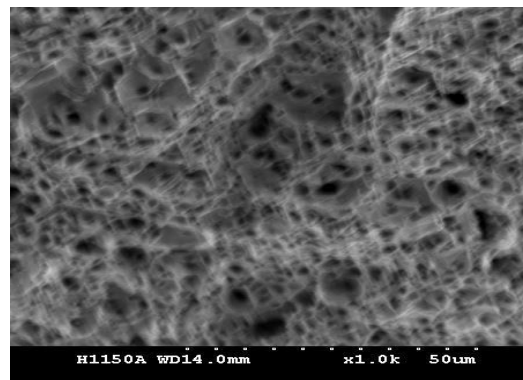
(i) State “A” solution treated



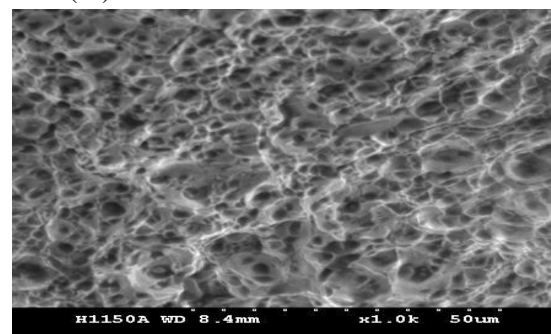
(ii) H900 air-cooled



(iii) H900 furnace-cooled



(iv) H1150M air-cooled



(v) H1150M furnace-cooled

**Fig. 3.** Submicroscopic precipitates.

Dimple ruptures are identified on the surface of all ruptured specimens because of the commencement and combination of microvoids. Each dimple is one half of a microvoids that formed and then separated during the fracture process. Large and fine elongated or C-shaped dimples were observed in shear lip region of the fracture surface.

### 3.3 Cutting Parameters and Related Experimental Response Values

The outcomes of machining-process of SS15-5PH near H900 air-cooled for 09 no. of experiments conducted with constant depth of cut ‘d’ (mm) is 0.5mm with cutting speed VC (m/min) is 125 for 03 experiments, remaining 06 with 175 (m/min), rate of feed, f (mm/rev) – 0.06, 0.12, 0.18, 0.06, 0.12, 0.18, 0.06, 0.12, 0.18. Force (N) – 104.13, 106.32, 135.74, 92.41, 93.26, 115.36, 61.4, 87.89, 112.92. Surface Roughness Ra (μm) – 0.502, 1.158, 1.185, 0.384, 0.983, 1.103, 0.233, 0.755, 0.952

Results of machining of experimental values of PH stainless steel at H900 Furnace cooled of 09 experiments with constant depth of cut ‘d’ (mm) is 0.5mm with cutting speed VC (m/min) is 125 for 03 experiments, remaining 06 with 175 (m/min), rate of feed f (mm/ rev) – 0.06, 0.12, 0.18, 0.06, 0.12, 0.18,

0.06, 0.12, 0.18. Force (N) – 102.8, 105.96, 126.34, 91.9, 92.16, 115.48, 63.6, 86.67, 110.23. Exterior Roughness Ra ( $\mu\text{m}$ ) – 0.913, 0.999, 1.279, 0.714, 0.965, 1.261, 0.255, 0.692, 0.886.

The results of experiment represent machining of PH stainless steel at State A solution treated of 09 experiments with constant depth of cut ‘d’ (mm) is 0.5mm with cutting speed Vc (m/min) is 125 for 03 experiments, remaining 06 with 175 (m/min), rate of feed f (mm/ rev)- 0.06, 0.12, 0.18, 0.06, 0.12, 0.18, 0.06, 0.12, 0.18. Force (N)- 83.13, 96.68, 125.37, 80.57, 86.18, 108.03, 59.5, 85.08, 107.54. SurfaceRoughness Ra ( $\mu\text{m}$ ) – 0.76, 1.255, 1.507, 0.354, 1.286, 1.437, 0.342, 0.768, 1.239.

The result of Experimental values of machining of PH stainless steel at H1150M Air cooled of 09 experiments with constant depth of cut ‘d’ (mm) is 0.5mm with cutting speed Vc (m/min) is 125 for 03 experiments, remaining 06 with 175 (m/min), rate of feed f (mm/rev) – 0.06, 0.12, 0.18, 0.06, 0.12, 0.18, 0.06, 0.12, 0.18. Force (N) – 76.29, 94.24, 121.83, 62.87, 84.11, 106.69, 53.47, 84.23, 105.83. Roughness of surface Ra ( $\mu\text{m}$ ) -0.391, 1.204, 1.539, 0.371, 1.106, 1.297, 0.303, 0.523, 1.05.

The data shows investigational outcomes of machining of PH stainless steel at H1150M Furnace cooled of 09 experiments with constant depth of cut ‘d’ (mm) is 0.5mm with cutting speed Vc (m/min) is 125 for 03 experiments, remaining 06 with 175 (m/min), rate of feed ‘f’ (mm/rev) – 0.06, 0.12, 0.18, 0.06, 0.12, 0.18, 0.06, 0.12, 0.18. Force (N)- 67.39, 94.84, 123.41, 58.60, 87.16, 105.23, 54.68, 77.27, 100.83. SurfaceRoughness Ra ( $\mu\text{m}$ ) – 0.489, 0.942, 1.038, 0.424, 0.800, 1.011, 0.202, 0.346, 0.729.

### 3.4 Surface Roughness:

The machined surface, surface charecteristics can be measured by using Mitutoyo surface roughness tester to identify constraints like Rz- peak level and Ra- mean level. Fig.4 exposed Ra values with different levels of rate of feed.

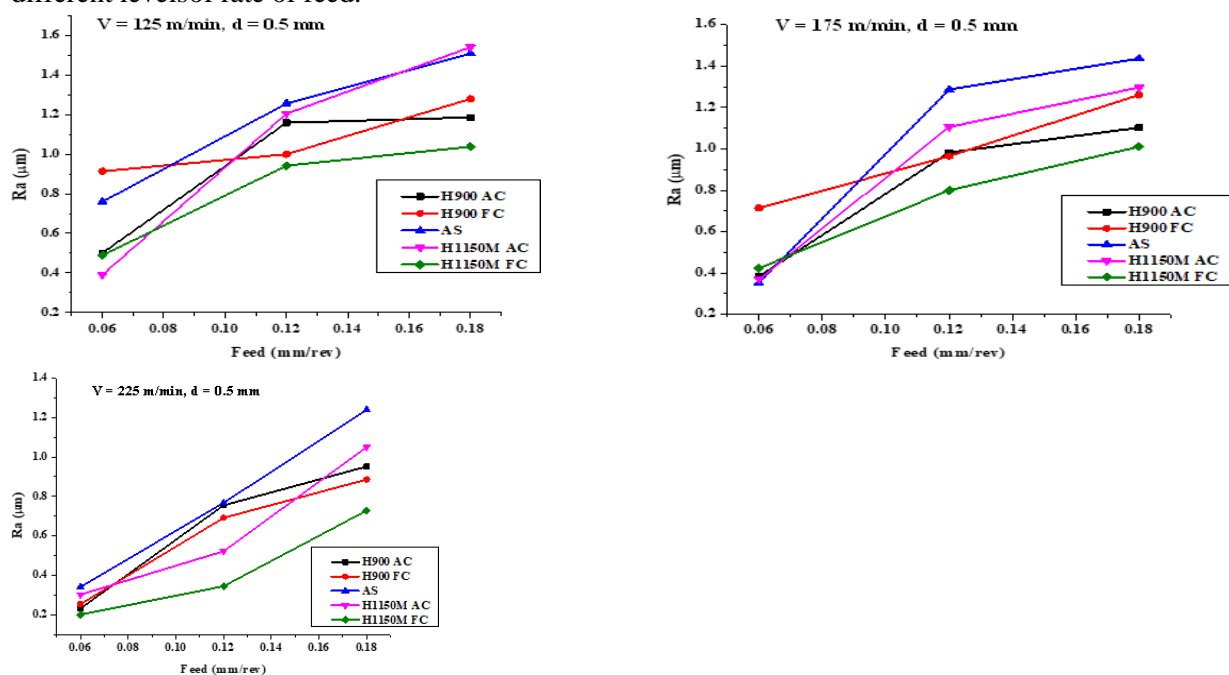
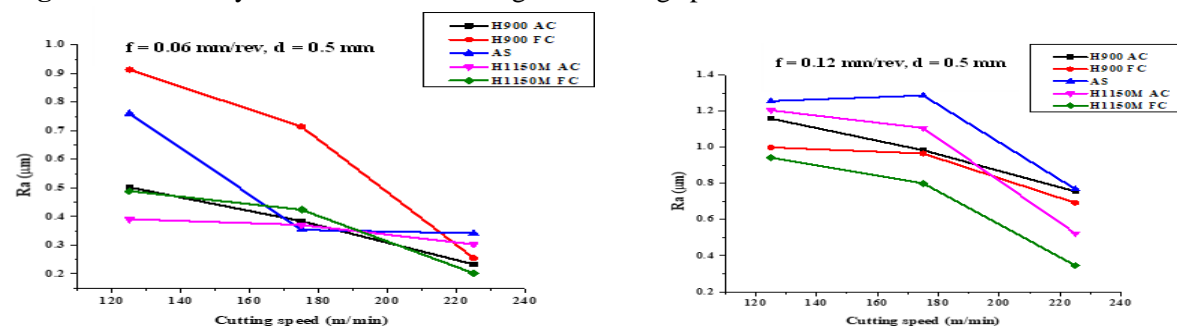
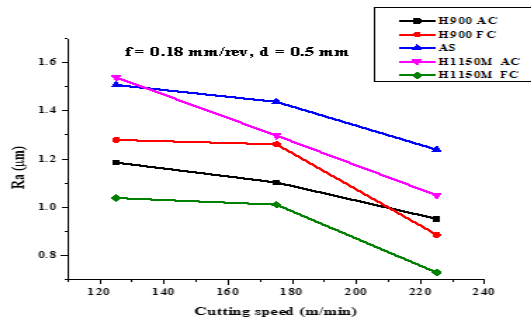


Fig. 4. Dissimilarity of Ra at dissimilar stages of cutting speed.





**Fig. 5.** variation of Ra at different levels of cutting speed.

Results shows that roughness increases with feed and also it shows upsurge in cutting speed the roughness decrease. At rate of feed 0.06 mm/rev and speed of cut 225 m/min of H1150 furnace-cooled state minimum surface roughness (Ra) 0.202 µm attained.

The below graphs were shown the change in cutting force values with different combination of cutting parameters. Fig. 6 depicted different levels of rate of feed the variation of force.

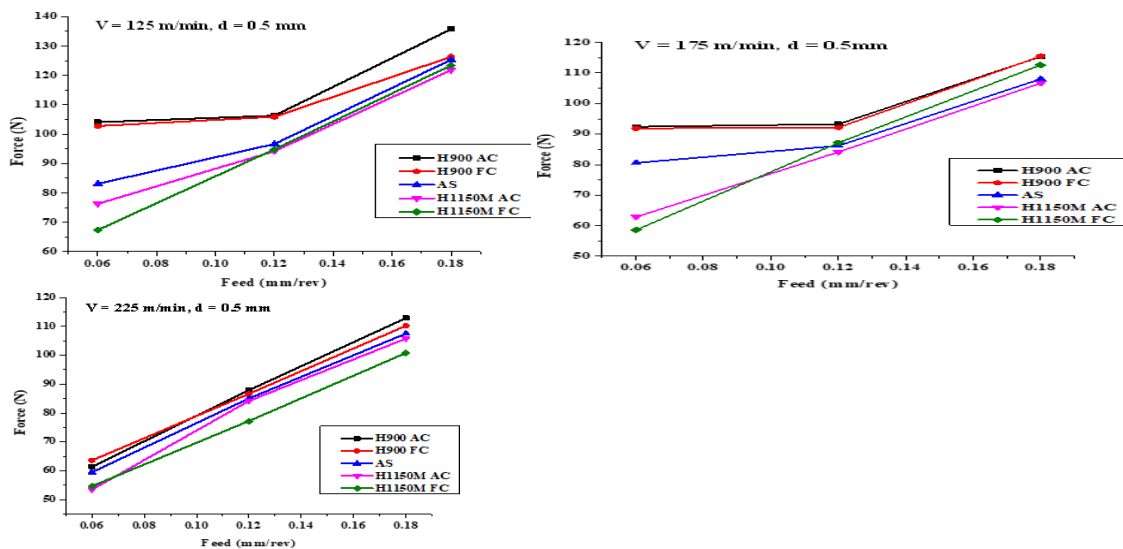


**Fig. 6.** Different levels of rate of feed the variation of force.

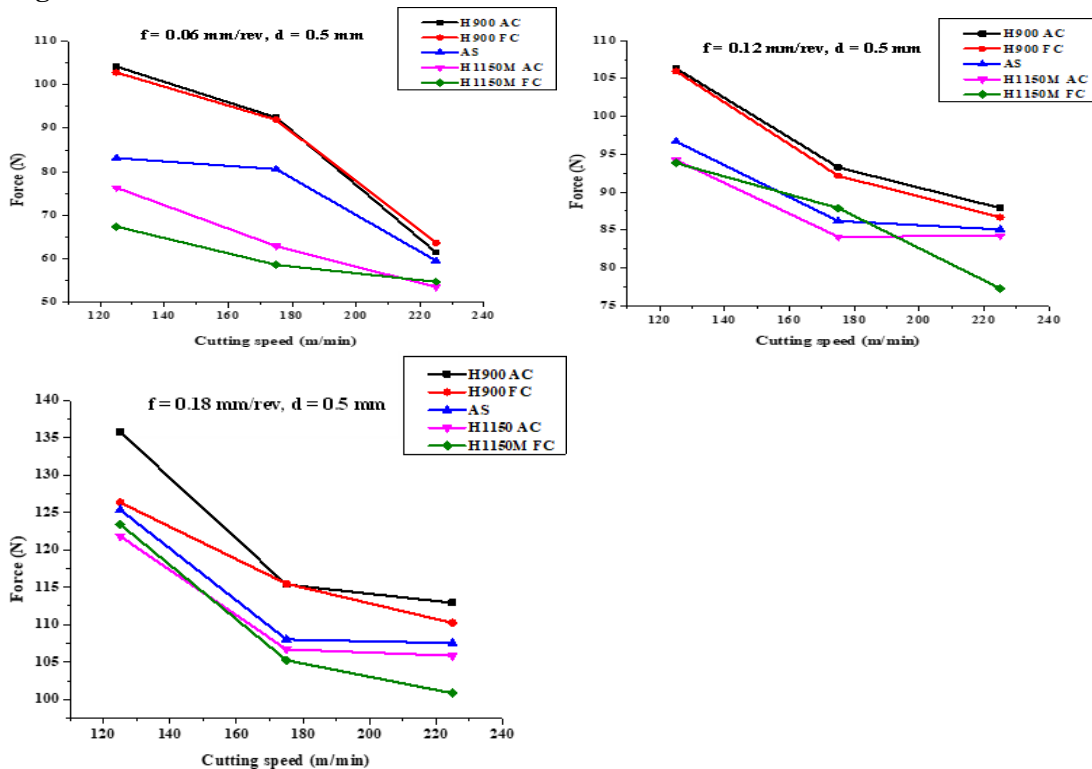


**Fig.7.** Variation of force at different levels of cutting speed.

Fig.7 demonstrated the feed and speed of cut respectively over the force of cutting at persistent depth of cut 0.5mm. Results shows that growth in rate of feed increase force of cutting also identified that at minimal speed of cutting, the forces are identified to be superior Therefore, results of higher forces are owing to increases the rubbing amid the instrument and chip, with speed of cutting 225 m/min at state H1150M air- cooled at rate of feed 0.06 mm/rev Minimum cutting force was gotten 53.47 N.

#### 4 CONCLUSIONS

After the analysis of mechanical properties at different heat treatments and parameters, it can be concluded that Maximum hardness (465 HV) and minimum hardness (293 HV) is gained afterward heat treatment in the H900 state and air-cooled and at state H1150M furnace cooled respectively.

- The martensite is the micro structures detected in precipitation hardened state on the fractured surface of all specimens. As a consequence of the initiation and coalescence of micro-voids dimple ruptures areformed.
- Growth in feed increased cutting force and with the growth in cutting speed cutting forces decreased. at rate of feed 0.06 mm/rev with speed of cutting 225 m/min at state H1150M air-cooled minimum cutting force (53.47 N) was found. When rate of feed growths, the surface roughness ranges rise. It reductions with growth in cutting speed.
- The 0.202  $\mu\text{m}$  minimum surface roughness value at feed 0.06 mm/rev along with the speed of cutting 225 m/min at state H1150M air-cooled (293 HV). For H900 air-cooled state (465HV), surface roughness was 0.255  $\mu\text{m}$  for the same feed and cutting speed.

#### References

1. Kumar, A., Balaji, Y., Prasad, N. E., Gouda, G., & Tamilmani, K. (2013). Indigenous development and airworthiness certification of 15–5 PH precipitation hardenable stainless steel for aircraft applications. *Sadhana*, 38(1), 3-23.
2. Aghaie-Khafri, M., & Zargaran, A. (2010). High temperature tensile behavior of a PH stainless steel. *Materials Science and Engineering: A*, 527(18), 4727-4732.
3. Habibi Bajguirani, H. R. (2002). The effect of ageing upon the microstructure and mechanical properties of type 15-5 PH stainless steel. *Materials Science and Engineering: A*, 338(1), 142-159.
4. Abad, A., Hahn, M., & Es-Said, O. S. (2010). Corrosion of 15-5PH H1025 stainless steel due to environmental states. *Engineering Failure Analysis*, 17(1), 208-212.
5. Mondelin, A., Valiorgue, F., Rech, J., Coret, M., & Feulvarch, E. (2012). Hybrid model for the prediction of residual stresses induced by 15-5PH steel turning. *International Journal of Mechanical Sciences*, 58(1), 69-85

## Design And Fabrication of Bladeless Wind Turbine

**Dr. K. Srividya<sup>1</sup>, Dr. M. Nagaswapnasri<sup>2</sup>, Dr. P. Anusha<sup>3</sup>, P. Praveen Kumar<sup>4</sup>, S. Priya Vardhan<sup>5</sup>, Shaik Mahammed Ismail<sup>6</sup>**

<sup>1</sup> Associate Professor, Mechanical Engineering Department, Prasad V Potluri Siddhartha Institute of Technology, Vijayawada, India.

<sup>2,3</sup> Assistant Professor, Mechanical Engineering Department, Prasad V Potluri Siddhartha Institute of Technology, Vijayawada, India.

<sup>4,5,6</sup> U.G. Students, Mechanical Engineering Department, Prasad V Potluri Siddhartha Institute of Technology, Vijayawada, India.

### Abstract

Now a day's power requirement is more due to operation of many components' need electricity to perform certain work. To meet the demand of power we burnt lots of fossil fuels which are non-renewable energy resource for power generation. These are depleting day by day. We need to depend on renewable energy resource for generating electricity. By using wind as a renewable energy resource, we are using horizontal and vertical wind mills for power generation. Due to usage of this type of wind mills there is a possibility of damage towards bird life and when maintenance of this turbine at 500 feet may cost the human life to avoid these consequences. We have designed a bladeless wind turbine to avoid the limitations of both horizontal and vertical axis wind turbines. This is economical and it is easily available to individuals to set up at top of the building and it is simple in design. These ways of generation of power will meet the demand of power in the society.

**Keywords:** Bladeless wind turbine, Power circuit, Bladeless wind turbine-assembly.

### INTRODUCTION

The invention of bladeless wind turbine describes the generation of electricity without using blades of traditional wind mill. It is a non-conventional type of wind mill. It is very advantageous to environment to save the bird life and balance the eco-system. This invention plays a crucial role in making the use of bladeless windmills near the load centres and reduce the transmission system and we can utilize maximum wind potential in the location.

The non-renewable energy resources are exhaustible in nature. Due to usage of non-renewable energy resources like fossil fuels, coal and petroleum products for generation of power, these sources may emit toxic gases to environment and this may damage different ecosystems on earth. Due to exhaust of non-renewable energy resources humans are depending upon the renewable energy resources like solar, wind, geothermal, biomass and ocean thermal energy for power generation. The renewable energy resources are inexhaustible in nature and freely available for many years. [1] discussed how to design the bladeless wind turbine and how it generates the power by using vibrations of mast by motion of wind. [2] presented the various applications of bladeless wind turbine in the field of power utilising components like electronics and electrical appliances like fan, light etc. [3] shows the behaviour of a wind turbine and its dynamic characteristics of turbine under working and taking design considerations when designing of bladeless and bladed turbine. [4] presented the outline parameters of wind and potential of energy which can be predicted by using previous data for analysing. [5] investigated the future dependence on renewable energy resources for generation of power and showing different approach for bladeless wind turbine. [6] discussed the evolution of bladeless wind turbine the flow of vortex of air or fluid creates a small vibration of mast or disturbance on surface of body this creates a new approach of generation of power by using bladeless wind turbine. [7] invented the jiggling effect of mast creates a motion of parts of bladeless wind turbine to generate electricity with arrangement setup. [8] discussed how the vortex bladeless wind turbine working under the flow of wind how the parts are responding and it analyse the power output based on velocity of wind. [9] presented the new approach

of design and it shows is that possible to create a wind turbine without bladeless and discuss how it will generate power by operation.

## 1. THEORY: COMPONENTS OF BLADELESS WIND TURBINE



**Figure 1.** Bladeless wind turbine

### 1.1 Parts and their working

- Base
- Mast
- Weightbalancer
- Arc-shapedpendulum
- Magneticpolesstand
- Rectifier
- Battery
- Inverter

#### 1.1.1 Base

The base is made up of cast iron used to with stand all the forces of bladeless wind turbine. The base is used to support the all-othercomponents like mast, copper coils,magnetsand power transmission circuit.

#### 1.1.2 Mast

The mast is made up of polyvinyl chloride or plastic material. It's the major component in bladeless wind turbine. Due to the flow of wind the mast oscillates around the fixed axis with help of weight balancer. Theoscillations of mast are directly proportional to the wind speed.

#### 1.1.3 Weight balancer

The weight balancer is used to balance the weight of mast for oscillation motion if the arrangement of weight balancer is not done accurately whole structure will collapse.

#### 1.1.4 Arc-shaped pendulum

An arc-shaped pendulum is made to carry the copper coils and oscillate with mast.

#### 1.1.5 Magnetic poles stand

A magnetic poles stand is made up of glass frame or fiber frame to hold the magnetic poles of north and south. The magnets of north and south attracts each other due to this attraction between poles a strong magnetic field is generated. Due to the arrangement of copper coils between the magnetic field creates a change in flux due to change in flux an electro motive force(EMF) is generated.

#### 1.1.6 Rectifier

A rectifier is an electronic device which converts alternating current in to direct current.

#### 1.1.7 Battery

A Battery is a source of electric power which stores direct current.

#### 1.1.8 Inverter

An inverter is anelectronic device which converts direct current in to alternating current.

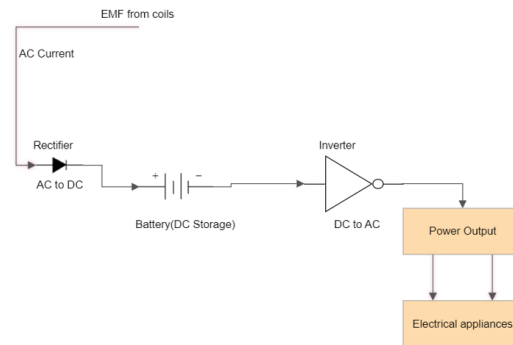


**Figure 2.** Power circuit

### 1.1.9 Power Circuit

An emf generated from coils is in alternating current form this is converted in to direct current by using rectifier. Because the battery is used to store the energy in the form of direct current only. When we require power for utilizing, we extract energy from battery. we convert direct current to alternating current by using inverter. in this way we utilize power when required and store power when not require.

## 2. CONSTRUCTION AND WORKING

### 2.1 Construction procedure

All the components are assembled according to the design. The base is fixed to ground by bolted joints and magnetic poles stand is attached to the base. The mast is fixed to the base and weight balancer is used to balance the weight of all other components. The special attachment between arc pendulum and mast is done and copper coils are attached to arc –shaped pendulum for oscillation between the magnetic field in these all-other components are assembled according to design of bladeless wind turbine.

### 2.2 Circuit construction

To utilize the power which is generated from bladeless wind turbine we have designed a power circuit to store the energy when not require and utilize when required. Due to the working of bladeless wind turbine an emf is generated from copper coils this emf is in alternating current form and we can directly utilize when required if power is not required for utilization we can store the energy in the form of battery for future utilization, for that we can use a rectifier to convert AC to DC and store the energy in the battery. For utilization we use an inverter to convert DC to AC this is conversion is done because all electronic components work with alternating current and battery stores direct current in this way we can store and utilize energy when required.

### VIEWS OF BLADELESS WIND TURBINE:

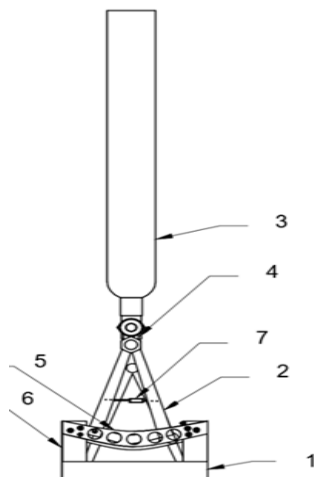


**Figure.3** Front View

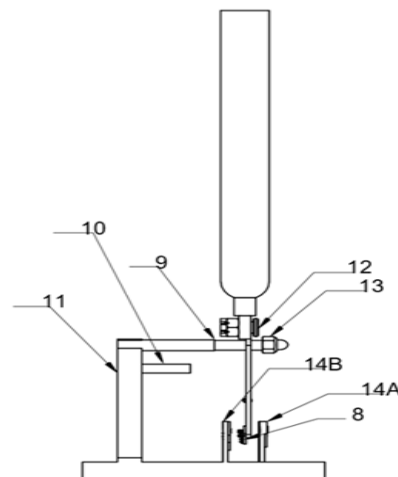


**Figure.4** Side View

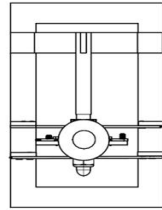


**Figure.5** Top View



**Figure.6** Isometric View

S.NO.	PART NO.	PART NAME
1	1	BASE
2	2	ARC-SHAPED PENDULUM
3	3	MAST
4	4	CONNECTING ROD SUPPORT
5	5	MAGNETIC-MATERIAL
6	6	MAGNETIC SUPPORT STAND
7	7	WEIGHT BALANCER
8	8	COPPER COIL
9	9	CONNECTING ROD
10	10	WEIGHT BALANCER SUPPORT
11	11	COLUMN
12	12,13	BOLT AND NUT
13	14A,14B	MAGNETIC POLES (NORTH AND SOUTH POLES)

### 3. RESULT & DISCUSSION

#### 3.1 Normal condition

The bladeless wind turbine is placed on top of the building or beside of the road due to the flow of wind or motion of wind passes from high pressure to low pressure due to this phenomenon a pressure difference is created due to the mast is oscillates around a fixed axis due to motion of mast in too and fro motion the copper coils oscillates with arc shaped pendulum. The magnetic poles stand is used to hold the north and south poles with some distance generally the opposite poles attract each other and creates a strong magnetic field this field is cuts by copper coils with the motion of mast due to this change in magnetic flux there is an emf generation. in this way power is generated by using bladeless wind turbine.



**Figure 7.** Normal condition

### 3.2 Actuated Power circuit.

When high flow of wind strikes the mast, it oscillates more and more power is generated. Based on the wind potential on the region the amount of electricity is generated. This is fully renewable energy resource and it will not create any environmental crises. If this system gets uncontrollable winds, then other attachments like chains are used to stop the system.

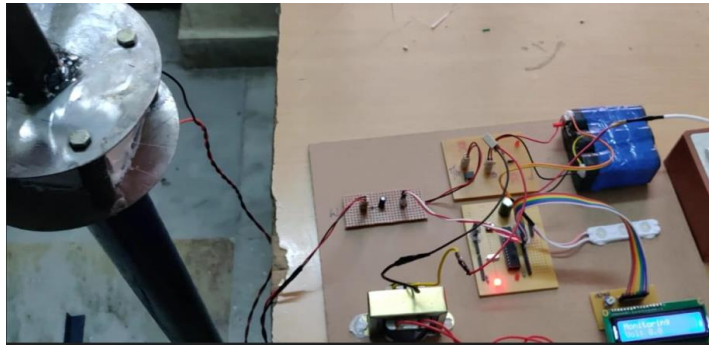


**Figure 8.** Actual power circuit

### 3.3 When working on field

When the bladeless wind turbine starts working then the power generation will start and flow according to the circuit diagram. We have done a prototype of bladeless wind turbine with total height of 5 feet. There the base will be 3 feet and the mast will be 2.5 feet and remaining 0.5 feet will be the spring and magnetic setup. Its start working and power generation will be done and this power will be utilised or it can store through a battery

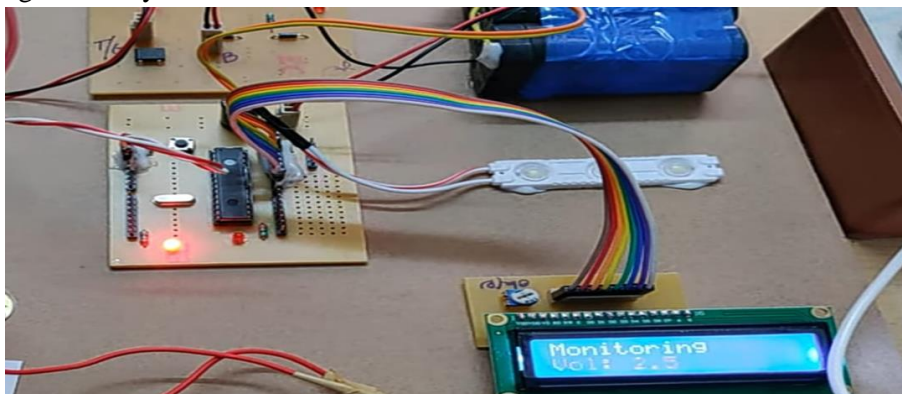


**Figure 9.** Power output display

## 4. CONCLUSIONS

This bladeless wind turbine system consists of mast, magnetic coil setup, base, arc shaped pendulum with copper winding and connecting rod. Once it starts working on the field it will not stop or come to rest until we stopped with an external force the performance of system depends on various parameters regarding to wind potential and wind velocity on the region. The following are the conclusions of this report:

We can able to design and develop a model on bladeless wind turbine.

- By using bladeless wind turbine, generate power for individual purpose by self-installation at their place.
- By using this system, save the birdlife and we can reduce the disturbance in bio-life.
- The bladeless wind turbine is fully eco-friendly and it is a renewable energy resource. it is inexhaustible in nature
- Mainly this project can operate at any location based on wind potential of location. the wind energy is freely available in nature.
- Main advantage in this project is to meet the power demand on earth through renewable energy resource and reduce the consumption of non-renewable energy resource.

### References

- [1] Younis, A., Dong, Z., ElBadawy, M., AlAnazi, A., Salem, H. and AlAwadhi, A., 2022, "Design and Development of Bladeless Vibration-Based Piezoelectric Energy-Harvesting Wind Turbine", Applied Sciences, 12(15), pp.7769.
- [2] Asre, C.M., Kurkute, V.K. and Kanu, N.J., 2022, "Power generation with the application of vortex wind turbine", Materials Today: Proceedings, 56, pp.2428-2436.
- [3] Jokar, H., Mahzoon, M. and Vatankhah, R., 2022, "Nonlinear dynamic characteristics of horizontal-axis wind turbine blades including pre-twist", Ocean Engineering, 256, pp.111441.
- [4] DehghanManshadi M, Ghassemi M, Mousavi SM, Mosavi AH, Kovacs L., 2021, "Predicting the Parameters of Vortex Bladeless Wind Turbine Using Deep Learning Method of Long Short-Term Memory", 14(16), pp.4867.
- [5] Frangoul, Anmar (21 September 2017). "[The future of wind turbines could be bladeless](#)". CNBC. Retrieved 11 December 2018.
- [6] "[Vortex Bladeless biography](#)". Vortex Bladeless. 14 May 2018. Retrieved 11 December 2018.
- [7] Wanshel, Elyse (25 May 2016). "[These Jiggling Bladeless Turbines are a Breath of Fresh Air](#)". Huffington Post. Retrieved 13 December 2018.
- [8] Spendlove, Tom (4 June 2015). "[Vortex Bladeless Generates Power from Wind without Blades](#)". Engineering.com. Retrieved 13 November 2016.
- [9] Patel, Sonal (1 July 2015). "[New Approach Powers Bladeless Wind Turbine](#)". Power Magazine. Retrieved 27 June 2018 – via EBSCOHost.

## Experimental Studies with A Protomodel Drone in Agricultural Sector

\*Dr. J A Ranga Babu<sup>1</sup>, P Bhargava Kumar<sup>2</sup>, P Satyanarayana<sup>1</sup>, T. Prasanth<sup>1</sup>

<sup>1</sup>Seshadri Rao Gudlavalleru Engineering College, Gudlavalleru, AP-521356

<sup>2</sup>Ramachandra College of Engineering, Eluru- 534007

### ABSTRACT

India is basically an agrarian country, its prime source of income is agriculture only. The production rate of the crops is based on various parameters like ambient temperature, humidity, rain, nature of soil, nature changes, environmental conditions etc. in which, natural factors are not in farmers control. However, the field of agriculture is also depends on some other factors like pests, disease, fertilizers, etc, which can be control by giving proper treatment to the crops. Pesticides may increase the productivity of crops but it also affects on human health. So the main aim of this project is to design agriculture drone for spraying pesticides such that it would be absorbed by plant not cumulate in yield. The use of pesticides in agriculture is very important to agriculture and it will be so easy if will use intelligent machines such as robots and drones using new technologies. This paper gives the idea about various technologies used to reduce human efforts in various operations of agriculture like detection of presence of pests, spraying of urea, spraying of fertilizers, etc. This paper describes the development of quad copter unmanned Aerial Vehicle and the spraying mechanism. This paper also discusses the integration of sprayer module to quad copter system. The paper also discussed designing of a cost effective proto model

**KEY WORDS:** Agricultural system, Quad copter drone, pest and fertilizers prototype

### 1. INTRODUCTION

Agriculture is the basic source of income in India which is about 60% of occupation is agrarian base only. It serves to be the vertebra of country economy. It is very essential to improve the productivity and efficiency of agriculture sector by introducing latest technical advancements for safer cultivation to the farmer. In the current scenario, population is growing the geometric progression while the land cannot be increased even a square yard. This situation leads to demand high yielding rates with hybridized seeds. On the other hand, farmer has to protect his crop from the various virus and bacteria. But, the pesticides and fertilizers using for the crop protection may cause for the damage of farmer health. The various operations like spraying of pesticides and sprinkling fertilizer are inevitable to protect the crop. Especially when they spray these fertilizers and pesticides need to take to more precautions like wearing appropriate outfit masks and gloves. Avoiding the pesticides is not possible to protect the crop, hence for use of drones in such cases gives the best of the solutions for this type of problems. According to survey of WHO, it is estimated that every year about 3 million workers are affected by poisoning from pesticides from which 18000 are die.

This projects aims to overcome the ill-effect of the pesticides on human beings and also use to spray pesticides over large area in short intervals of time compare to conventional spraying by using automatic fertilizer sprayer. This device is basically combination of spraying mechanism on a quad copter frame. This model is used to spray the pesticides content to the areas that cannot easily accessible by humans. The universal sprayer system is proposed to spray liquid as well as solid contents which are done by the universal nozzle.

#### **New Ways of Farming:**

Throughout history of technology in agriculture, scientific and technological advances have great impact on agriculture industry. Early days farmers improved their crop production by spry the pesticides through nozzle, but today, farmers improve crop production through global positioning systems (GPS) Advances in farm machinery like agriculture drone changed the way farmers worked in history. They were able to spray more land at a faster pace, which made farmers found some relief from their

backbreaking labours. About 35 % to 40% of total investment is shared in terms of labour cost. In early days, the information regarding latest seeds and their availability and fertilizers for a particular kind of virus are familiarized by radio and television. But today’s scenario is changed to mobile apps to educate the farmer regarding new technologies like drones. C. Morales et al. [1] presented the force and torque was used as control variables used to assess the hexa copter’s mobility, they suggested an extra controller to avoid the modelling error. G. P. Falconí et al. [2] use the Failure Detection and Isolation (FDI) filter and then reconfigure the controller to use the failure detection or reconfiguration strategy. The controller managed a safe flight, but there are still improvements to be made in terms of performance during the flight. Y. Huang et al. [3] proposed an octo-copter to compress a low volume aerosol in an unmanned octo-copter. The octocopter’s primary rotor measures 3 meters in diameter and can carry a payload of 22.7 kgs. It consumes about a gallon of gasoline for every 45 minutes. This research cleared the door for the development of aeronautical application systems for drones, allowing for the production of products with greater target speeds and larger Volume Median Diameter (VMD) droplets”. D. Yallappa et al. [4] developed an octocopter has 6-BLDC motors and 2-Lipo batteries with 6-cells and 8000 mAh capacity. Their research also emphasizes on measuring the size and density of the droplets, as well as the spray rate and pressure of the spray fluid. They succeeded in developing a drone that can deliver 5.5 litres of liquid with a 16-minute resistance using their project. S.R. Kurkute et al. [6] suggested to use an octocopter drone and its spray mechanism is one of the basic and affordable equipment, by adopting the universal spray system it can spray liquid and solid substances also. In their investigation, they looked at a variety of agricultural controllers and concluded that the octocopter system with the mega 644PA is the most suitable due to its efficient implementation.

### Type of Drones

Now a day’s varieties of drones are knocking the drone technologies in open market. Experts are categorized these drones based on their weight and flight range. In Table 1, the categorization of drones proposed based on their weight started from micro and mini drones that weigh less than 5kg with a flight range of 25km to 40km<sup>[5]</sup>. The super heavy drones or combat aircraft weighs more than 500kg and can fly in the range of 1500km. Other experts grouped the drones based on the physical properties such as the number of propellers or rotors and based on the purposes of drones such as surveillance, aerial photography, engineering, construction, and entertainment. Table 2 shows the categorization proposed where the drones grouped by their number of propellers or rotors

**Table1** Categorization of drones based on their weight and flight range<sup>[6]</sup>

Type of drone	Weight Range	Flight Range
Micro and mini UAVs close range	$W \leq 5 \text{ kg}$	$25 \text{ km} \leq R \leq 40 \text{ km}$
Heavy medium-range UAVs	$500 \text{ kg} \leq W$	$70 \text{ km} \leq R \leq 300 \text{ km}$
Unmanned combat aircraft	$500 \text{ kg} < W$	$R \leq 1500 \text{ km}$
Lightweight UAVs medium range	$50 \text{ kg} < W \leq 100 \text{ kg}$	$70 \text{ km} \leq R \leq 250 \text{ km}$
Lightweight UAVs small range	$5 \text{ kg} < W \leq 50 \text{ kg}$	$10 \text{ km} \leq R \leq 70 \text{ km}$
Medium heavy UAVs	$300 \text{ kg} < W \leq 500 \text{ kg}$	$70 \text{ km} \leq R \leq 300 \text{ km}$
Heavy UAVs large endurance	$1500 \text{ kg} \leq W$	$R \leq 1500 \text{ km}$
Average UAVs	$100 \text{ kg} < W \leq 300 \text{ kg}$	$150 \text{ km} \leq R \leq 1000 \text{ km}$

**Table 2** Categorization of drones by number of rotors or propellers

Type of Drone	Properties	Example
Single rotor drones	helicopter lookalike heading controlled by the small rotor on the tail simple and scalable easily	

<p>Tri-copters (Three rotor or propellers)</p>	<p>has 3 motors for light use compact, foldable, lighter can carry small load only for camera</p>	
<p>Quadcopters (Four rotors or propellers)</p>	<p>the most famous multi-copters faster, easy to manufacture, affordable 4 propellers to lift up the aircraft great maneuverability, thrust, and power can be fixed easily and available readily in the market</p>	
<p>Hexacopters (Six rotors or propellers)</p>	<p>upgraded from quad-copter can fly high up with expensive cameras high speed, high power, fly higher due to six rotors more expensive than quad copters difficult to fly in small spaces due to large size</p>	
<p>Octocopters (Eight rotors or propellers)</p>	<p>same benefits with hexacopters but with more speed and power fly higher to capture sharp capture images and footages have 8 motors and propellers.</p>	
<p>Fixed-wing drones</p>	<p>have wings like common airplanes use for long-distance fly, mapping, monitoring, and agriculture. Have higher cost and special training needed to handle the aircraft</p>	

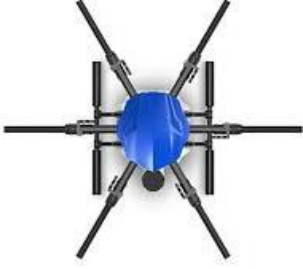
**Application of Drone:** Drones can be used to monitor any type of crop in any location. Integrating drone technology can boost up crop yields, save time, make land management more sustainable and improve long-term performance such as (i) Soil and field analysis, (ii) planting of seed from air (iii) Spraying of fertilizers and pesticides (iv) Crop health assessment (v) Crop count and plant emergence analysis (vi) Irrigation monitoring and planning (vii) Disaster risk reduction (viii) Wildlife conservation

## 2. Methodology and Approach

### 2.1 Basic Components used for prototype

- (1) HJ450 Frame – it is a glass fibre quad copter frame
  - i. Aerial cinematograph – to
  - ii. Sport – Light weight and extremely stiff
  - iii. Sport FPV – high surface are to accommodate electronic circuits and cameras
  - iv. Mini - Very small and virtually indestructible

- (ii) Electronic Speed Controller
- (iii) Brushless DC Motor
- (iv) Propeller
- (v) Flight Controller
- (vi) Spraying Motor and Nozzle

			
HJ450 Frame	Electronic Speed Controller	Brushless DC Motor	Flight Controller

	
Flight Controller	LiPo Battery

## 2.2 Construction

The prefix octo-copter, is a drone configuration where there are eight arms.

The main frame is made of carbon fiber composite material with each arm length of 492 mm.

At each free end of the arm, a motor will be fixed and propeller will be mechanically coupled to the motor.

For all eight motors the output side of an ESC will be connected and the input side of the Electronic Speed Controller (ESC) will be connected to the flight controller

The other input of the ESC will be connected to the power distribution board where the power supply is provided by the Li-Po battery. In a similar fashion all the other ESC's, motors and propellers are connected.

A receiver will be connected to the Flight controller to receive signals from the transmitter.

An FPV camera and a suitable transmitter connected each other is connected to the flight controller.

The storage tank of dimensions 100 x 150 x 75 mm is mechanically coupled to the frame, the bottom of the tank will have a slope so that the entire tank gets drained completely.

A plastic tube of 1.3 meters length and four nozzles are fixed at 45cm between each other. A pump is powered from a power distribution board, the inlet of the pump is connected to the storage tank and the outlet is connected to the plastic tube where nozzles are fixed.

The landing frame of height 300mm is connected to the main frame so that the landing of the drone will be safe and the storage tank will not touch the ground.

## 2.3 Working

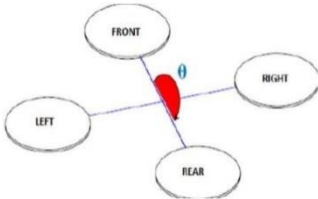
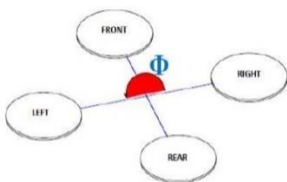
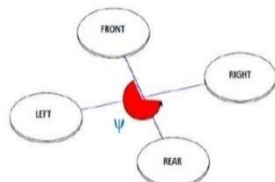
Drone with pesticides and sanitizer sprayer which is a combination of Quad-copter and Seed System, we have adapted the sowing system to a fixed X quad-copter. The combination of these two machines therefore results in the formation of our sprayer

Now a brief description of the Quad-copter and Seeding System. A quad-copter called a quad rotor helicopter or quad rotor is a multi rotor helicopter that is propelled and propelled by four wheels. Quad-copters are named rotor makers, instead of flying machines of suspended wings, due to the fact that their lifting is due to the rotation of the rotors.

In a quad copter, two propellers turn one way (clockwise) and the other two turn the other (opposite the clock) and this gives the machine the ability to float in a steady motion. From the outset the engines we used have a clear reason to respond to the propeller. Engines are measured in kilograms volts, the higher the kV level, the higher the engine turns at a constant voltage. Next up Electric Speed controller or ESC is the one that advises engines to turn quickly at any time.

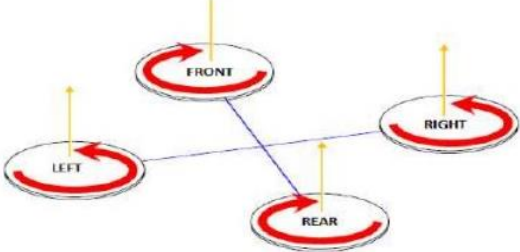
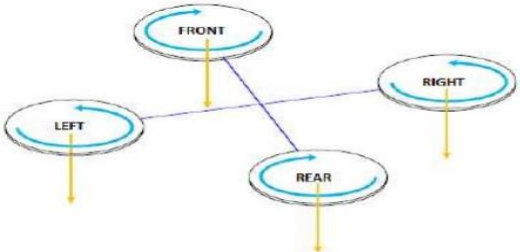
Quad copter can described as a small vehicle with four propellers attached to rotor located at the cross frame. This aim for fixed pitch rotors are used to control the vehicle motion. The speeds of these four rotors are independent. By independent, pitch, roll and yaw attitude of the vehicle can be control easily.

Pitch, roll and yaw attitude of Quad copter

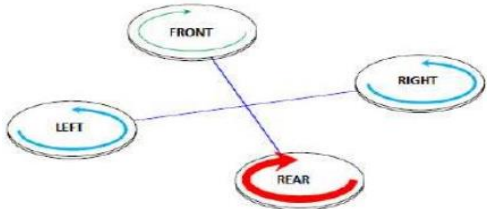
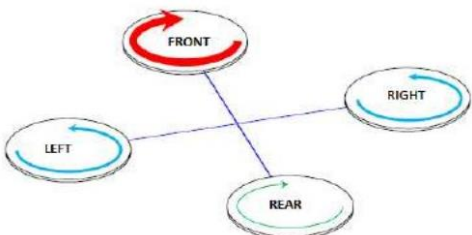
		
Pitch direction of Quad copter	Roll Direction Of Quad copter	Yaw Direction Of Quad copter

Quad-copter have four inputs force and basically the thrust that produced by the propeller that connect to the rotor. The motion of Quad-copter can control through thrust that is produced. These thrust can control by the speed of each rotor.

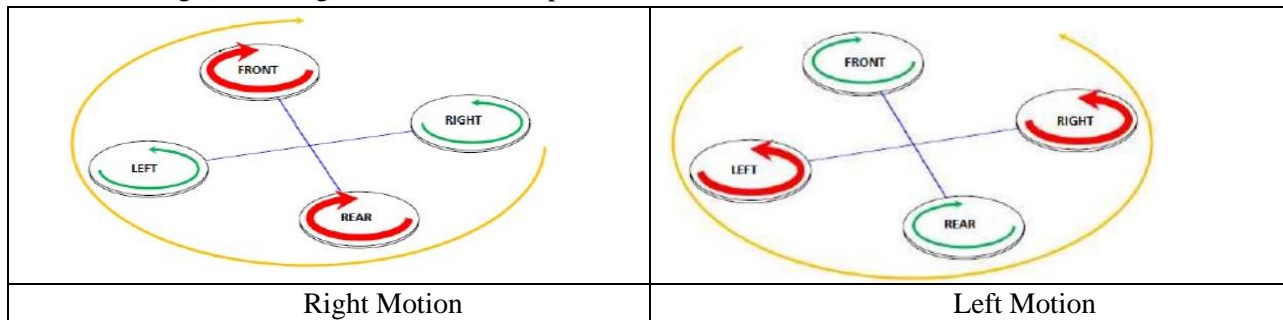
**(i) Take-off And Landing Motion Mechanism:** Take-off is movement of Quadcopter that lift up from ground to hover position and landing position is versa of take-off position. Take-off (landing) motion is control by increasing (decreasing) speed of four rotors simultaneously which means changing the vertical motion.

	
Take Off Motion	Landing Motion

**(ii) Forward And Backward Motion:** Forward (backward) motion is control by increasing (decreasing) speed of rear (front) rotor. Decreasing (increasing) rear (front) rotor speed simultaneously will affect the pitch angle of the Quad copter

	
Forward Motion	Backward Motion

(iii) Left And Right Motion: For left and right motion, it can control by changing the yaw angle of Quad copter. Yaw angle can control by increasing (decreasing) counter-clockwise rotors speed while decreasing (increasing) clockwise rotor speed.



### 3. RESULT ANALYSIS

The drone developed is more efficient and robust in nature compared to its contemporaries. It can fly across different terrains and varied weather conditions. The biggest advantage of the drone is that it is customizable according to the requirement. The drone will also be useful to spray not only fertilizers and pesticides but also can be used to spray paints, monitor fields with the help of radio transmitter. To ensure a high-quality product, diagrams and lettering MUST be either computer-drafted or drawn using India ink. The upgraded drone is more efficient and robust in nature compared to its predecessor. It can fly in different places and in different climates. The great advantage of the drone is that it is customized according to need. Airless airplane will also be useful for spraying not only fertilizer and pesticides but can also be used to spray paint, monitor fields with the help of radio transmitter. To ensure the highest quality product, drawings and characters MUST be computerized or drawn using Indian ink.

### 4. FUTURE SCOPE

Quad-copter weight lifting capacity can be increased by increasing the number of engines or by increasing propeller size or by increasing engine rpm.

Flight time can be extended by increasing the battery capacity.

The capacity of the pesticide can be increased by increasing the size of the tank

A large area can be covered using a series of microphones that can be arranged in an orderly fashion.

Spraying angle can be controlled for proper spraying.

### 5. CONCLUSION

Information technologies provide new possibilities for a lot of problems. Agricultural drones are an incredible technology advanced in just a few years. Drones are crucial to farmers because they will no longer have to walk around their farms surveying soils, crops and buildings. Farmers, now, have the best surveillance and inspection technology for their farms. It's true to say that farming has become technically advanced for commercial farmers who have enormous chunks of land. Perhaps, one day these drones will become fully automated and provide farmers with accurate data on the amount of pesticides, fungicides or fertilizers to apply on specific areas or crops after a surveillance. It shall be a new dawn for farmers. On the flip side, drones have their shortfalls. For example, drones are not completely safe, raise privacy concerns and may put countries in serious security risks. Hence, information technology experts have their work cut out in ensuring that the next generation of agricultural drones addresses these issues. Security measures must be prioritized because extremist groups or other people who want to cause harm to the general public may take advantage of the drones. Generally, anything that threatens to derail the adoption and the advancement of agricultural drones should be addressed.

### Reference

1. C. Morales, D. Ovalle and A. Gauthier, "Hexacopter maneuverability capability: An optimal control  
Dept. of Mech. Engg. PVPSIT 19

- approach," *2017 7th International Conference on Modeling, Simulation, and Applied Optimization (ICMSAO)*, Sharjah, United Arab Emirates, 2017, pp. 1-6, doi: 10.1109/ICMSAO.2017.7934920.
2. G. P. Falconí, C. D. Heise and F. Holzapfel, "Hexacopter Outdoor Flight Test Results Using Adaptive Control Allocation Subject to an Unknown Complete Loss of One Propeller" September 2016, DOI:[10.1109/SYSTOL.2016.7739779](https://doi.org/10.1109/SYSTOL.2016.7739779), Conference: 2016 3rd Conference on Control and Fault-Tolerant Systems
  3. Y. Huang, W. C. Hoffmann, Y. Lan, W. Wu, B. K. Fritz, "Development of a Spray System for an Unmanned Aerial Vehicle Platform" Vol. 25(6): 803-809 American Society of Agricultural and Biological Engineers ISSN 0883-8542
  4. D. Yallappa, M. Veerangouda, D. Maski, V. Palled and M. Bheemanna, "Development and evaluation of drone mounted sprayer for pesticide applications to crops," *2017 IEEE Global Humanitarian Technology Conference (GHTC)*, San Jose, CA, USA, 2017, pp. 1-7, doi: 10.1109/GHTC.2017.8239330.
  5. S.R. Kurkute, B. D.Deore, K. Payal, B. Megha and S. Mayuri, "Drones for Smart Agriculture: A Technical Report" DOI:[10.22214/ijraset.2018.4061](https://doi.org/10.22214/ijraset.2018.4061), International Journal for Research in Applied Science & Engineering Technology, Volume 6 Issue IV, April 2018.
  6. A.A Sarangdhar, & Pawar, V. R. Machine learning regression technique for cotton leaf disease detection and controlling using IoT. International conference of Electronics, Communication and Aerospace Technology, Vol.2, pp. 449-454, 2017.
  7. Chebrolu, N., Labe, T., Stachniss, C. Robust Long-Term Registration of UAV Images of Crop Fields for Precision Agriculture. IEEE droneics and automation letters, Vol.3, No.4, pp.3097-3104, 2018.
  8. Duan, T., Chapman, S. C., Guo, Y., & Zheng, B. Dynamic monitoring of NDVI in wheat agronomy and breeding trials using an unmanned aerial vehicle. Field Crops Research, Vol.210, pp.71-80, 2017.
  9. Ferentions, K. Deep learning models for plant disease detection and diagnosis, Computers and Electronics in Agriculture, Vol.145, pp.311-318, 2018.
  10. Ghosal, M., Bobade, A., & Verma, P. A Quad-copter Based Environment Health Monitoring System for Smart Cities, Second International Conference on Trends in Electronics and Informatics (ICOEI), pp. 1423-1426, 2018.
  11. Kedari, S., Lohagaonkar, P., Nimbokar, M., Palve, G., & Yevale, P. Quad-copter-A Smarter Way of Pesticide Spraying. Imperial Journal of Interdisciplinary Research, Vol.2, No.6, 2016.
  12. Kabra, T. S., Kardile, A. V., Deeksha, M. G., Mane, D. B., Bhosale, P. R., & Belekar, A. M. Design. Development & Optimization of a Quad-Copter for Agricultural Applications. International Research Journal of Engineering and Technology, Vol. 04 No.07, 2017.
  13. Kerkech, M., Hafiane, A., & Canals, R. (2018). Deep learning approach with colorimetric space and vegetation indices for vine diseases detection in UAV images. Computers and electronics in agriculture, 155, 237-243.
  14. Patel, P. N., Patel, M. A., Faldu, R. M., & Dave, Y. R. (2013). Quad-copter for agricultural surveillance. Advance in Electronic and Electric Engineering, 3(4), 427-432.
  15. Qin, W., Xue, X., Zhang, S., Gu, W., & Wang, B. (2018). Droplet deposition and efficiency of fungicides sprayed with small UAV against wheat powdery mildew. International Journal of Agricultural and Biological Engineering, 11(2), 27-32.

## A Study on Deformation Behavior of Different Hip Prostheses Materials Using Abaqus

Praveen Chapala<sup>\*1</sup>, Challapalli Rushinath<sup>1</sup>, Saran S<sup>1</sup>, Deepak Yadav<sup>1</sup>

<sup>1</sup>NATIONAL INSTITUTE OF TECHNOLOGY ANDHRA PRADESH, Near National Highway No.16,  
Kadakatla, Tadepalligudem – 534101 West Godavari District, Andhra Pradesh, India

### ABSTRACT

The significance of bio-implants at the hip region cannot be overstated, as they play a crucial role in restoring mobility and improving the quality of life for individuals with hip-related issues. Earlier Co-Cr, SS alloys were used as implant materials but cytotoxicity and elastic modulus differences are affecting the longevity and performance of hip joints resulting in stress shielding. Ti alloys have emerged as the most suitable material because of their excellent biocompatibility, corrosion resistance, and favourable mechanical properties, including a suitable Young's modulus for mimicking natural bone.

The primary objective of this research is to model hip implants made from different materials (Cobalt-Chromium, Stainless Steel, Ti-6Al-4V, Ti-25Nb-11Sn), and compare their deformation behaviour using ABAQUS software. This finite element analysis software allows for the precise modelling of complex structures, enabling a thorough investigation of the mechanical response of different materials under varying conditions. The study involves the creation of detailed hip implant models, encompassing various designs, components, and assemblies. Additionally, the project defines and applies realistic boundary conditions and loads to simulate actual physiological conditions experienced by hip implants during daily activities.

By employing ABAQUS, the study aims to determine the von Mises stress distribution in each material, providing valuable insights into the structural performance and potential areas of improvement for hip prostheses.

**Keywords:** Prostheses, von Mises stress, biocompatibility, elastic modulus, Finite Element Analysis, deformation

### 2. INTRODUCTION

The hip joint plays a crucial role in the body, offering stability and assistance to the upper body, regulating the motion of the thigh, and bearing the body's weight. They are also capable of forward and backward movements, such as contraction, extension, rotation, and circular movements. As it grows older, these pressures can put its functionality at risk[1].

Arthroplasty is the process of replacing a damaged or deformed human hip with an implant. The initial total hip arthroplasty (THA) was performed in 1938 by utilizing a custom-designed stainless-steel implant[2]. Over the years, the pursuit of biocompatible materials possessing superior mechanical properties has fueled innovation, elucidating a longstanding endeavour to enhance patients' quality of life while minimizing the necessity for repeated surgeries. In 1997, Derek McMinn unveiled the Birmingham hip, an innovative metal-on-metal resurfacing hip implant characterized by its minimally invasive design and reduced size compared to traditional implants, aimed at minimizing surgical trauma to the surrounding soft tissues.

The present materials that are being studied and utilized in total hip arthroplasty (THA) encompass four primary bearing types, namely, metal-on-metal (MoM), metal-on-polyethylene (MoP), ceramic-on-metal (CoM), ceramic-on-ceramic (CoC), and ceramic-on-polyethylene (CoP). MoM articulations, introduced in the 1950s, initially encountered issues with loosening and fractures, which led to their

---

\*Corresponding Author: praveenchapala@gmail.com

temporary discontinuation. However, recent advances in surface finishing and manufacturing techniques have revitalized it, despite the formation of debris and possible effects of metal poisoning[3][4].

Presently, metallic alloys possessing a reduced elastic modulus and enhanced resistance to corrosion and wear are being developed. There is an ongoing exploration for innovative metallic alloys suitable for incorporation into hip prostheses, with the goal of superior mechanical and biocompatible properties. It is important to achieve balance among the multiple factors of implant materials. The conventional choices of metals for implants include Stainless Steel, Titanium Alloys (Ti-6Al-4V),  $\beta$ - Ti Alloys, and Cobalt-Chromium Alloys[5].

Our project's primary objective is to compare and contrast the time-invariable mechanical loading and tensile load behaviour of common implant materials, namely SS 316L, Co- Cr Alloy, and Ti-6Al-4V, Ti-25Nb-11Sn, through the use of modelling and simulation in ABAQUS CAE (Complete Abaqus Environment). This software is highly effective in performing finite element analysis and computer-aided engineering and is widely utilized in various industries to simulate and analyse mechanical and structural behaviour. The project uses a user-friendly graphic interface, analysis modules, simulation solving, and visualisation, as well as a user community and support[6].

## 2. DEFORMATION BEHAVIOUR OF HIP IMPLANT

The hip implant and femoral head model was inspired by a product of Kyocera Medical Technology- A400 Tapered Cementless Hip System[7]. The dimensions have given us a realistic approach to creating a proportionate model to test the deformation behaviour of a hip implant.

**Table 1.** Dimensions (in mm) of KYOCERA Standard Hip Replacement Implant[7]

Size	Neck Shaft Angle	Femoral Head Radii	Head Mount Length
10.5	135°	15	10
Neck Axis Distance	Offset	Stem Length	Distal Stem Length
53.1	39.5	141.8	21
Proximal M-L Width Cross Section	Proximal A-P Width Cross Section	Distal M-L Width Cross Section	Distal A-P Width Cross Section
34.4	13.6	11.5	6.4

The Finite Element Analysis of the implant model via ABAQUS CAE proceeded as follows:

The adopted dimensions are used for sketching the model. It is extruded to create three-dimensional model of the implant. Undesired details are cleared with trimming and erasing tools. The sharp corners are tapered and the model is partitioned for better access. The mechanical properties are applied to the extruded sketch to compare the deformation behaviour[8]. The model is a single-part construction, which eliminates the need to assemble various sections of the part with different interaction mechanisms.

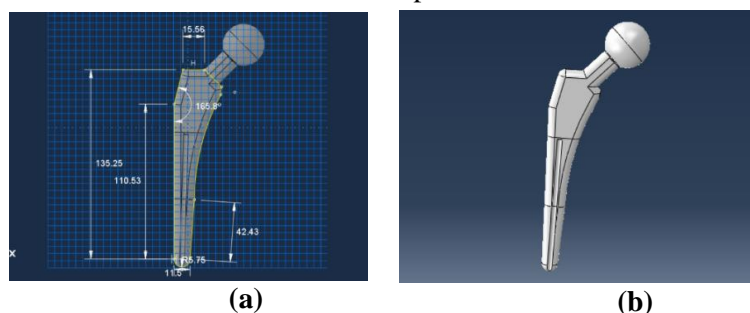


**Fig. 1.** (a) 2D Sketch of the Model; (b) Finished 3D Model of the Implant

**Table 2.** The Mechanical properties of different materials[9][10][11][12]

Material	Density (kg/m <sup>3</sup> )	Young's Modulus (GPa)	Poisson's Ratio
316L SS	8000	200	0.3
Co- Cr Alloy	8400	225	0.28
Ti- 6Al- 4V	4420	110	0.31
β- Ti Alloy	4900	45	0.34

To simulate the implant's behavior while fastened to the human femur; and experiencing weight from the upper body and reaction load from the knee, Concentrated loads on the femoral head and the distal end of the implant are applied. The model is constrained throughout the surfaces of the model as the implant stays inside the human body surrounded by muscles and bones, and the proximal hemisphere of the femoral head is constrained along the vertical axis (y-axis) since it is attached to the acetabulum[13].

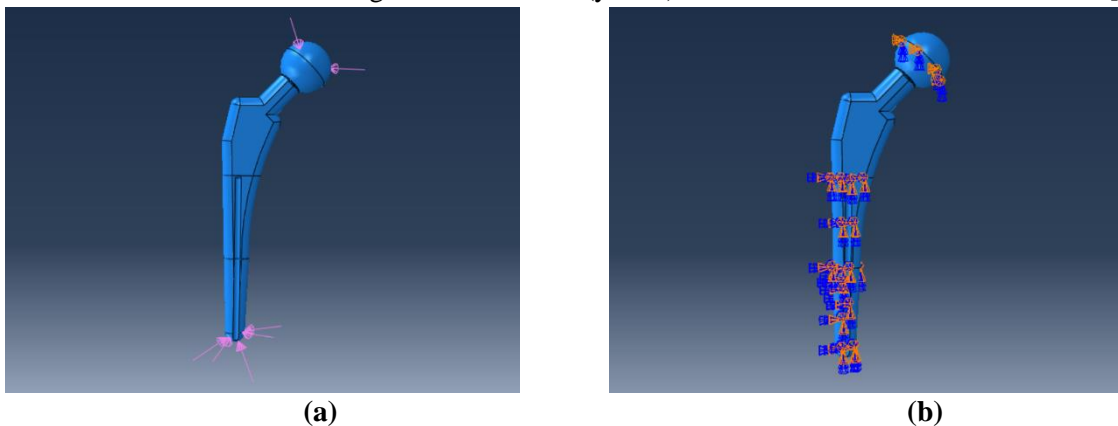


**Fig. 2.** (a) Load Parameters Applied; (b) Boundary Conditions Constrained

The deformation mechanism from the initial state of the solid implant model to the implant enduring the above loading parameters is programmed to simulate the mechanical load behaviour. The obtained model will be divided into small grids called mesh. The nodes will be selected depending on the model for the whole model to be analysed effectively with maximum accuracy. Once the Job is submitted, Using the above inputs, The software will go through all the information and the results are obtained for the deformation behaviour of the model. The Von Mises stress and energy distribution are depicted by cold to warm-colour coding throughout the mesh for analysis.

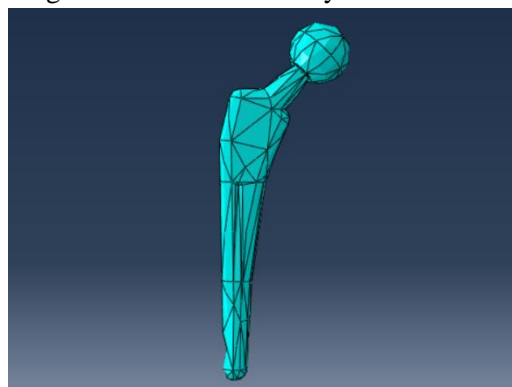


**Fig. 3.** Mesh of finished Model

### 3. RESULTS AND DISCUSSION.

The general deformation behaviour of the implant was observed-The neck and the proximal end of the model experience major stress, and the constrained regions experience less stress.The energy distribution throughout the model is transferred from the source of the load to the distal end, with the

femoral head suffering the most percentage of energy and the subsequent sections of the mesh having suffered relative energy transferred.

**Table 3.** Von mises stress and deformation values of the alloys

Material	Min. Stress (GPa)	Max. Stress (GPa)	Deformation Range (mm)
Co- Cr Alloy	23.08	276.9	1.217 - 14.610
316L SS	22.37	268	1.366 - 16.400
Ti- 6Al- 4V	22.01	264	2.481 - 29.770
$\beta$ - Ti Alloy	20.87	250.4	6.035 - 72.430

High-stress accumulation is observed in Cobalt Chromium alloy, whereas Beta Titanium alloy exhibits low-stress accumulation. The stress accumulation order stands as Co-Cr-Mo > SS 316 L > Ti-6Al-4V( $\alpha+\beta$ ) > Ti-25Nb-11Sn( $\beta$ ). Young's modulus and Poisson's ratio are pivotal in determining stress accumulation and deformation behaviour across these four alloys. Lower Young's modulus signifies enhanced flexibility and ductility, whereas higher values denote increased strength and stiffness. Poisson's ratio provides insights into lateral strain under longitudinal load application. A higher Poisson's ratio correlates with greater strength and hardness, and vice versa. This discussion underscores that a higher Young's modulus leads to heightened strength and stiffness, consequently resulting in increased stress accumulation[14].

Upon applying loading and boundary conditions on the implant, deformation primarily occurs at the proximal region. Another contributing factor to high-stress accumulation is the rise in dislocation density at specific proximal regions. Dislocations propagate from the loading ends, acting as barriers for other dislocations to travel, leading to pile-up and a subsequent increase in stress levels. This phenomenon exacerbates stress accumulation, particularly at targeted locations.

Deformation is significantly pronounced in Ti-25Nb-11Sn ( $\beta$ ) alloy, while it is less prominent in Co-Cr-Mo alloy. In the case of  $\beta$ -Ti alloy, the addition of niobium (Nb) serves to enhance ductility by stabilizing the beta phase, refining the microstructure, and preventing the formation of brittle phases such as alpha or omega phases, which could otherwise compromise ductility and formability.

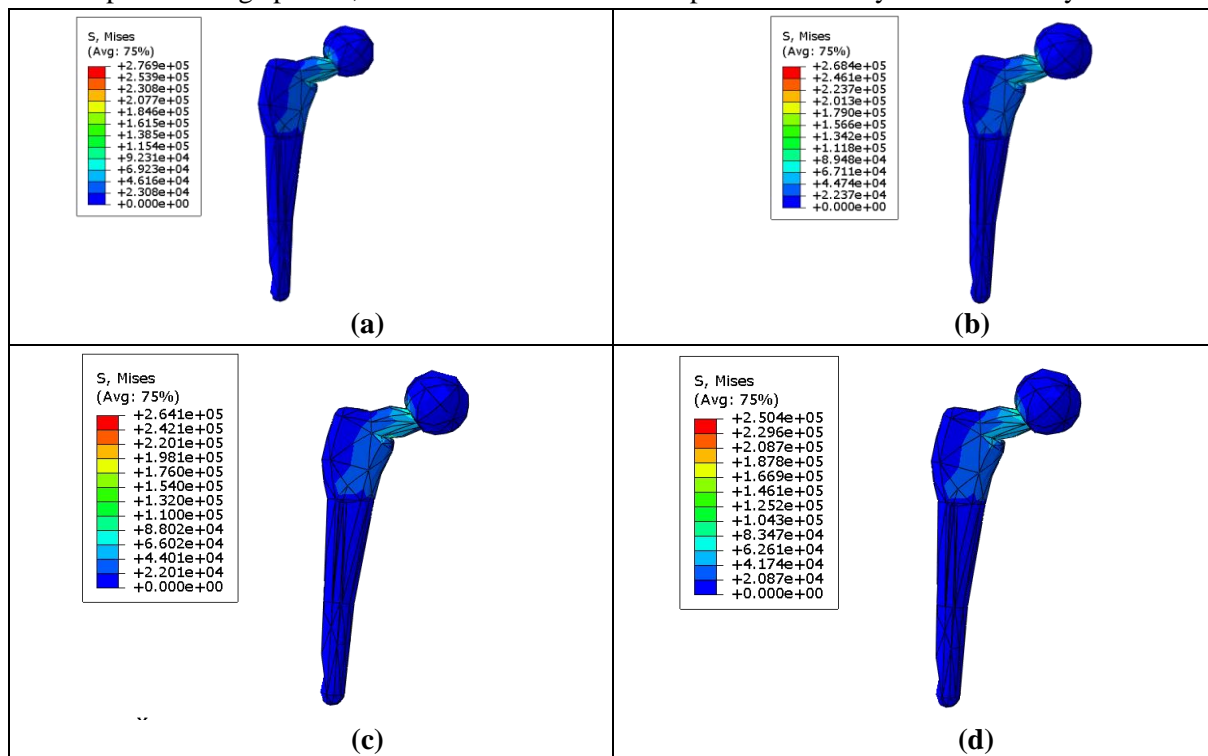


**Fig. 4.** Stress Distribution of the materials

(a) Co-Cr Alloy; (b) SS316L; (c)Ti-6Al-4V and; (d)  $\beta$ - Ti Alloy

Conversely, the incorporation of tin (Sn) in binary Ti-Nb alloys causes reduced Young's modulus, resulting in suppression of  $\omega$  transformation.[15] The enhanced ductility and flexibility inherent in  $\beta$ -Ti alloy result in a greater degree of deformation when subjected to load compared to other alloys characterized by lower ductility due to their specific alloy compositions.

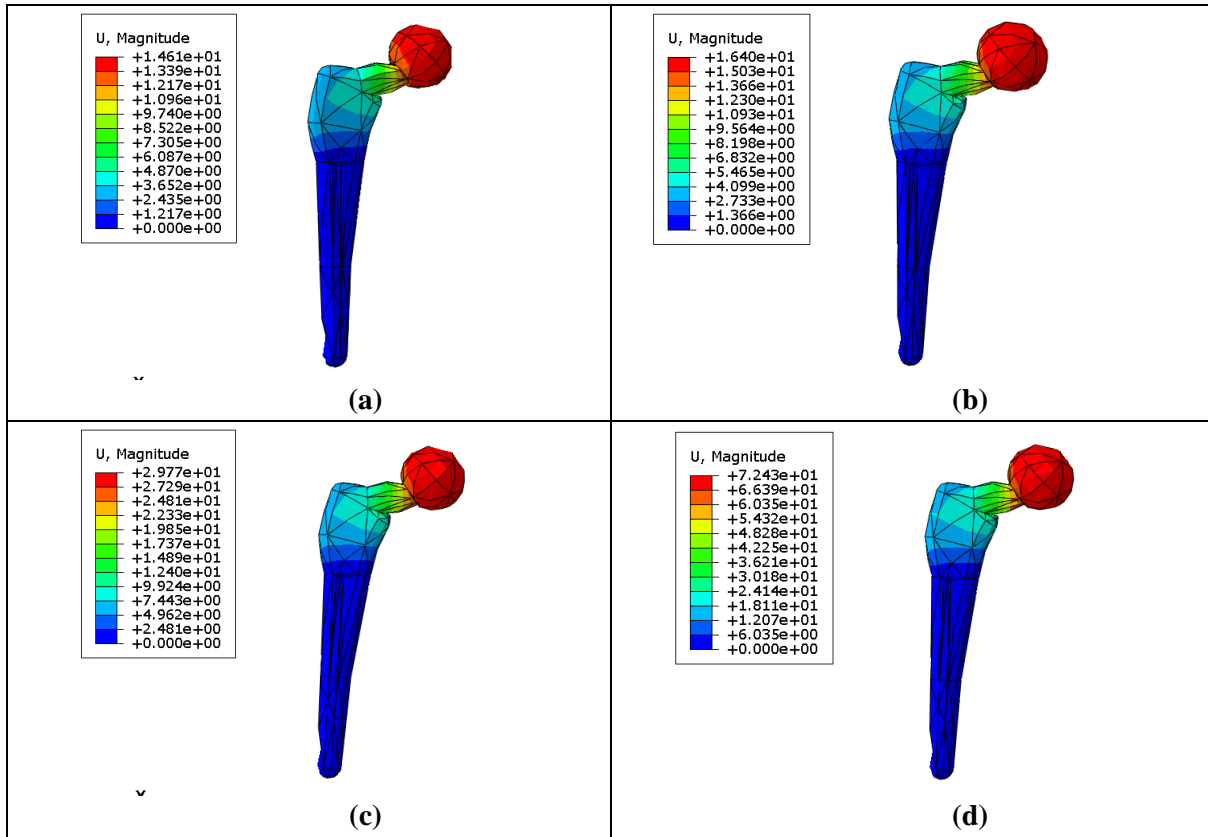


**Fig.5.** Deformation Behaviour of  
(a) Co-Cr Alloy; (b) SS316L; (c)Ti-6Al-4V and; (d)  $\beta$ - Ti Alloy

Stress shielding effect occurs when the implant material exerts tension on the bone enclosing the implant, which can cause bone resorption and loosening of the implant. Cobalt-Chromium-molybdenum alloy (Co-Cr-Mo) and stainless-steel alloy 316L (SS 316 L) show higher resistance to bone stress due to the difference in their properties. The stress concentration is higher for these alloys (Fig. 5), which signifies a lack of stress distributed from implant to bone. This difference is mainly due to the large difference in Young's modulus between the alloy (implant) and human bone.

Conversely, a lower stress accumulation is observed in  $\beta$ -Titanium ( $\beta$ -Ti) alloy, indicating a more favourable stress distribution. Consequently, crack initiation and propagation occur more rapidly in regions of high-stress accumulation, typically found in Co-Cr-Mo and SS 316 L alloys. Moreover, the  $\beta$ -Ti alloy demonstrates a lower stress shielding effect, facilitating the prevention of crack formation and mitigating the risk of failure. Therefore,  $\beta$ -Ti alloy is the optimal choice for hip implants compared to other mentioned alloys, offering superior performance and reliability.

#### 4. CONCLUSIONS

- The Co-Cr-Mo alloy exhibits a higher stress shielding effect, ultimately leading to implant failure.
- Stress accumulation among the alloys follows the order: Co-Cr-Mo > SS 316 L > Ti-6Al-4V( $\alpha+\beta$ ) > Ti-25Nb-11Sn( $\beta$ ).
- Deformation extent varies across alloys in the order: Ti-25Nb-11Sn( $\beta$ ) > Ti-6Al-4V( $\alpha+\beta$ ) > SS316L > Co-Cr-Mo.
- The presence of  $\beta$  stabilizers in the Ti-25Nb-11Sn alloy decreases Young's modulus, thereby enhancing the success rate of the  $\beta$ -Titanium alloy.

- The minimal stress shielding and biomechanical compatibility of  $\beta$ -Titanium alloy establish it as the superior choice for hip arthroplasty

## REFERENCES

1. Cleveland Clinic, "Hip Joint: Anatomy & How It Works," Cleveland Clinic, 2023. [Online]. Available: <https://my.clevelandclinic.org/health/body/24675-hip-joint>.
2. M. Merola and S. Affatato, "Materials for Hip Prostheses: A Review of Wear and Loading Considerations," *Materials (Basel, Switzerland)*, vol. 12, no. 3, p. 495, 2019.
3. M. Mauricio Silva, M. Christian Heisel and M. Thomas P. Schmalzried, "Metal-On-Metal Total Hip Replacement," *Clinical Orthopaedics and Related Research*, no. 430, p. 53–61, 2005.
4. C. Y. Hu and T.-R. Yoon, "Recent updates for biomaterials used in total hip arthroplasty," *Biomaterials research*, vol. 22, no. 33, 2018.
5. M. N. J. H. Mitsuo Niinomi, "Development of new metallic alloys for biomedical applications," *Acta Biomaterialia*, vol. 8, no. 11, pp. 3888-3903, 2012.
6. Dassault Systèmes, "Abaqus 2022," Dassault Systèmes, 2023. [Online]. Available: <https://www.3ds.com/support/hardware-and-software/simulia-system-information/abaqus-2022/>.
7. KYOCERA Medical Technologies, "A400 Tapered Cementless Hip Stem System," KYOCERA Medical Technologies Inc, 22 September 2011. [Online]. Available: <https://kyocera-medical.com/2011/09/a400-tapered-cementless-hip-stem-system/>.
8. Dassault Systèmes, "SIMULIA Simulation Software," [Online]. Available: <https://www.3ds.com/products/simulia>.
9. Sparr, "Properties of Grade 5 Titanium (Ti6Al4V or Ti 6-4)," Parts Badger, 12 November 2019. [Online]. Available: [https://parts-badger.com/properties-of-grade-5-titanium/#:~:text=Properties%20of%20Titanium%20Ti%2D6Al%2D4V%20\(Grade%205\)%3A&text=It%20has%20excellent%20strength%2C%20low,its%20physical%20and%20mechanical%20properties](https://parts-badger.com/properties-of-grade-5-titanium/#:~:text=Properties%20of%20Titanium%20Ti%2D6Al%2D4V%20(Grade%205)%3A&text=It%20has%20excellent%20strength%2C%20low,its%20physical%20and%20mechanical%20properties).
10. T.-K. Jung, S. Semboshi, N. Masahashi and S. Hanada, "Mechanical properties and microstructures of  $\beta$  Ti-25Nb-11Sn ternary alloy for biomedical applications," *Materials Science and Engineering: C*, vol. 33, no. 3, pp. 1629-1635, 2013.
11. thyssenkrupp Materials (UK) Ltd, "Stainless Steel 316 - 1.4401 Data Sheet," Materials UK, [Online]. Available: <https://www.thyssenkrupp-materials.co.uk/stainless-steel-316-14401.html>.
12. Y. Liao, E. Hoffman, M. Wimmer, A. Fischer, J. Jacobs and L. Marks, "CoCrMo metal-on-metal hip replacements," *Physical chemistry Chemical physics*, vol. 15, no. 3, pp. 746-756, 2013.
13. D. Bennett and T. Goswami, "Finite element analysis of hip stem designs," *Materials & Design*, vol. 29, no. 1, pp. 45- 60, 2008.
14. K. Colic and A. Sedmak, "Factors Influencing Hip Prosthetic Integrity And Life And Hip Implant Biomaterial Properties," *The Current Approach To Research And Design Of The Artificial Hip Prosthesis: A Review*, vol. 1, no. 1, 2016.
15. T. Ozaki, H. Matsumoto, S. Watanabe and S. Hanada, "Beta Ti Alloys with Low Young's Modulus," *MATERIALS TRANSACTIONS*, vol. 45, no. 8, pp. 2776-2779, 2004.

## **Analysis of Deformation Behaviour of Automotive Disc Brakes Using Abaqus**

**Praveen Chapala<sup>1,2</sup>, Sweety A<sup>1</sup>, Golla Neha Sri<sup>1</sup>, Akudari Mamatha<sup>1</sup>**

<sup>1</sup>NATIONAL INSTITUTE OF TECHNOLOGY ANDHRA PRADESH, Near National Highway No.16, Kadakatla, Tadepalligudem – 534101 West Godavari District, Andhra Pradesh, India.

### **ABSTRACT**

Disc brakes play a crucial role in modern vehicles by providing reliable and efficient stopping power through the friction between brake pads and rotating discs, ensuring effective deceleration and enhanced safety compared to traditional drum brakes. Additionally, disc brakes are easier to maintain, provide better responsiveness, and contribute to enhanced overall safety on the road. In practical applications, brake discs are primarily constructed using grey cast iron and aluminum alloy are chosen for their commendable metallurgical stability, ease of manufacture, and economic viability. Grey cast iron and Al 6061 alloys are most favored for disc brake construction due to their commendable heat dissipation, wear resistance, and cost-effectiveness, making them ideal material for providing reliable and durable braking performance in various automotive applications. In the present work, a theoretical model of disc brake is created utilizing ABAQUS software, employing the Finite Element Analysis methodology for simulation and analysis purposes. ABAQUS offers a broad spectrum of Multi-physics capabilities, adding versatility to its utility. Our primary objectives of our study include analyzing the deformation behavior of these alloys under the following conditions: (i) Mechanical loading, (ii) Mechanical and Thermal loading, (iii) Mechanical loading on a disc brake with groove, (iv) Mechanical and Thermal loading on a disc brake with groove. Through the application of ABAQUS, the research strives to assess the von mises stress distribution within the disc brake under different conditions, offering valuable perspectives on its structural performance and identifying potential avenues for improvement.

**KEY WORDS:** Disc brake, Deformation, Finite Element Analysis, Von Mises stress, grey cast iron, Al 6061 alloy

### **1. INTRODUCTION**

Braking systems play a pivotal role in ensuring vehicle safety and performance. Brakes, functioning as mechanical components, absorb the energy from moving wheels, effectively restraining their motion. Friction between the surface of brake pads and the disc rotor converts the kinetic energy of the wheels into heat energy[1]. Enhanced braking performance is directly correlated with the force exerted on the braking disc, leading to improved heat dissipation and stopping abilities. When categorizing braking systems based on frictional contact mechanisms, two main variants emerge: drum brakes and disc brakes[2].

Drum brakes in motorcycles work by applying pressure to brake shoes inside a drum attached to the wheel hub. This pressure creates friction against the drum's inner surface, slowing down the wheel's rotation and thereby decelerating the motor cycle[3]. In contrast, disc brakes utilize a disc rotor instead of a drum. This disc rotor is attached to the wheels and positioned between two calipers. These calipers contain brake pads that come into contact with the friction surface of the disc rotor when the brakes are applied[4].

Among various braking mechanisms, disc brakes have emerged as a widely adopted solution due to their superior heat dissipation capabilities and efficient braking performance. Understanding the deformation behavior of disc brakes under varying operating conditions is crucial for optimizing their design and enhancing overall vehicle safety[5].

In practical applications, brake discs are primarily constructed using grey cast iron and Al 6061 alloy

due to their excellent metallurgical stability, ease of production, and cost-effectiveness various alternative materials like metal matrix composites (MMC), ceramic matrix composites (CMC), and titanium alloys have been under consideration for automotive brake disc usage, primarily driven by the goal of reducing weight. However, grey cast iron (GCI) stands out due to its remarkable blend of a high melting point and superior thermal conductivity, ensuring exceptional thermal stability alongside cost-effectiveness[6]. Al 6061 contains magnesium and silicon as major alloying elements and shown notable resistance against corrosion and wear, coupled with good weld ability when compared to other materials in the selection[7].

In the present work, a theoretical model of a disc brake is developed using ABAQUS software[8], employing Finite Element Analysis methodology for simulation and analysis[9]. The model employs a sequentially coupled thermal-mechanical approach, which considers temperature variations within the brake system, mainly induced by friction and heat generation. As a result, deformations occur, which impact the contact between the brake pads and the disc[10]. Furthermore, ABAQUS allows for the study of plastic and thermal behavior, which is crucial for understanding the deformation analysis of brake discs[11].

## 2. MODELING AND SIMULATION OF DISC BRAKE

The analysis of the deformation behavior of a disc brake involves the creation of a model and subsequent simulation under appropriate conditions, which is accomplished through the following set of sequential steps.

**Part:** The initial stage in model design involves drafting a conceptual outline, specifying the desired dimensions. With an outer radius of 148mm and an inner radius of 31 mm, this outline is then extended to create a comprehensive model through extrusion.

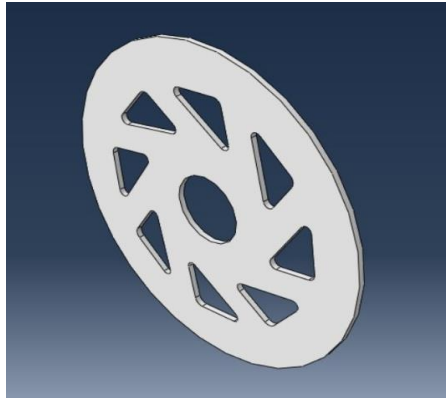


**Fig. 1.** Part model of disc brake

**Property:** The properties of a material, including Young's modulus, Poisson's ratio, thermal conductivity, and coefficient of thermal expansion, significantly impact the deformation behavior of a disc brake. The table below illustrates the values of these properties for both grey cast iron and aluminum alloy, highlighting their importance in determining the performance of the brake system.

**Table 1:** Properties of grey cast iron[12] and Al 6061 alloy[13]

Material	Young's Modulus E(GPa)	Poisson's Ratio( $\nu$ )	Thermal Expansion Coefficient $\alpha$ (K <sup>-1</sup> )	Thermal conductivity
Grey cast iron	118	0.29	1.5 X 10 <sup>-5</sup>	53
Aluminum 6061	69	0.32	2.3 X 10 <sup>-5</sup>	185

**Assembly:** Assembly is utilized to unite two or more components. However, since our model consists of only one component, the assembly module holds less significance.

**Step:** Step module is utilized to determine the quantity of stages implicated in load application, such as load and temperature.

**Interaction:** The type of interaction between different components is provided within this module

therefore it less important in our model as it has only one component[14].

**Load:** The brake pads exert a clamping force on the rotating disc brake rotor in order to stop the vehicle. Therefore, load in form of pressure of magnitude 0.5619 MPa[15] is applied on the region where the brake pads press. The center of rotor is bolted to the wheel, thereby being constrained, and this area is where the boundary condition is applied. The thermal load resulting from friction between the brake pads and the rotor is specified within the predefined field option with a magnitude of 323K.

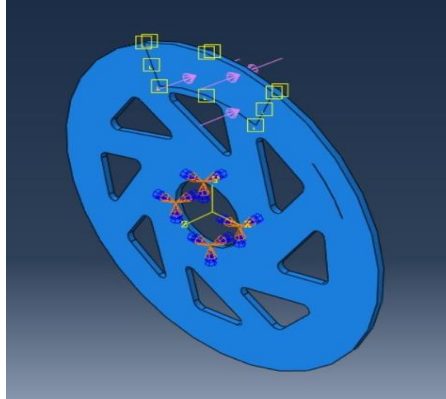


**Fig. 2.** Application of load and boundary conditions

**Mesh:** The disc brake model is segmented into discrete parts referred to as elements, facilitating the examination of stress distribution resulting from the load, thereby simplifying the analysis process. The model after meshing is as shown in the Fig. 3

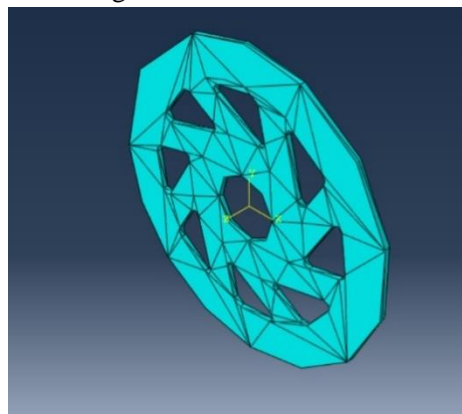


**Fig. 3.** Post-meshing model of the disc brake

**Results and visualization:** A ‘job’ with suitable name is created for the model which is further submitted for results and analysis. The obtained results for different cases are visualized, where the Von Mises stress distribution and deformation behavior is analyzed.

- (i) Mechanical loading
- (ii) Mechanical and Thermal loading
- (iii) Mechanical loading on a disc brake with groove
- (iv) Mechanical and Thermal loading on a disc brake with groove.

### 3. RESULTS AND DISCUSSION

#### CASE 1: Mechanical loading

From the results obtained, red signifies the highest stress, transitioning to orange, yellow, green and blue colors as stress diminishes, with blue representing the lowest stress levels. As clamping force is applied by brake pads on the disc brake rotor, compressive forces are generated on the load applied region. These compressive forces lead to the piling of dislocations, which in turn restrict the mobility of other dislocations, serving as obstacles to their movement. This results in high stress accumulation in the load applied region. From fig. 4 we can observe that, grey cast iron shows higher stress accumulation whereas Al 6061 shows lower stress accumulation. This is due to higher ductility of Al 6061 than grey cast iron. The properties like Poisson’s ratio and Young’s modulus of the material highly influence the

Von Mises stress distribution and deformation behavior of disc brake. Higher Poisson's ratio implies increased lateral deformation tolerance during longitudinal stretching, correlating with enhanced ductility. Thus, materials with a higher Poisson's ratio typically exhibit greater ductility as in the case of Al 6061. Young's modulus reflects a material's stiffness, with higher values indicating greater resistance to deformation and lower ductility as it is observed in grey cast iron.

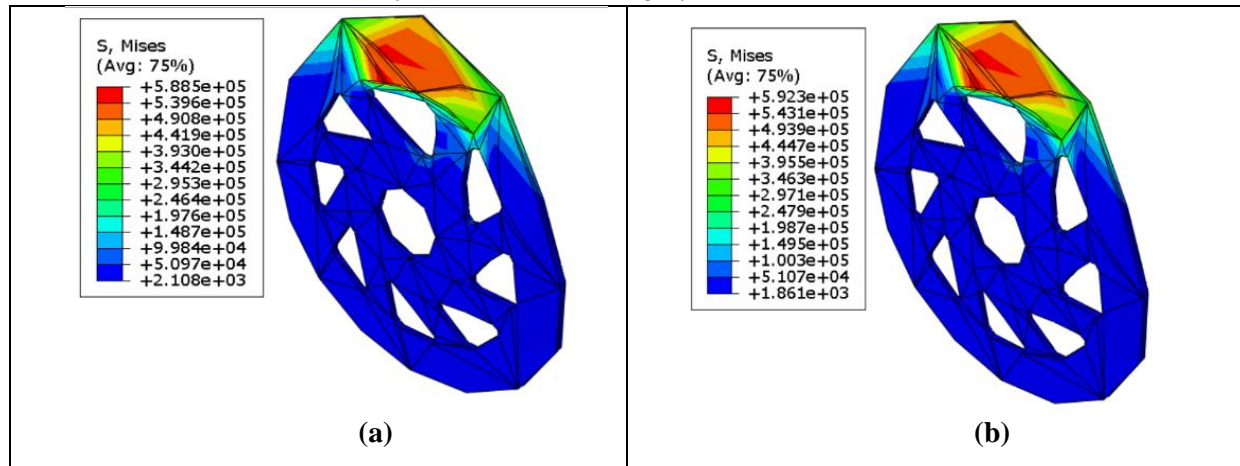


**Fig. 4.** Von Mises stress distribution in (a) Al 6061; (b) grey cast iron

It is observed from fig. 5 that Al 6061 exhibits higher deformation compared to grey cast iron. Deformation behavior relates directly to the ductility of a material. Alloying addition plays an important role in influencing ductility. Grey cast iron has graphite flakes in its matrix which makes it hard and brittle and therefore exhibits less deformation. Conversely, even though Al 6061 has Mg, Si alloying additions, ductility retained in Al matrix facilitates easier deformation compared to grey cast iron.

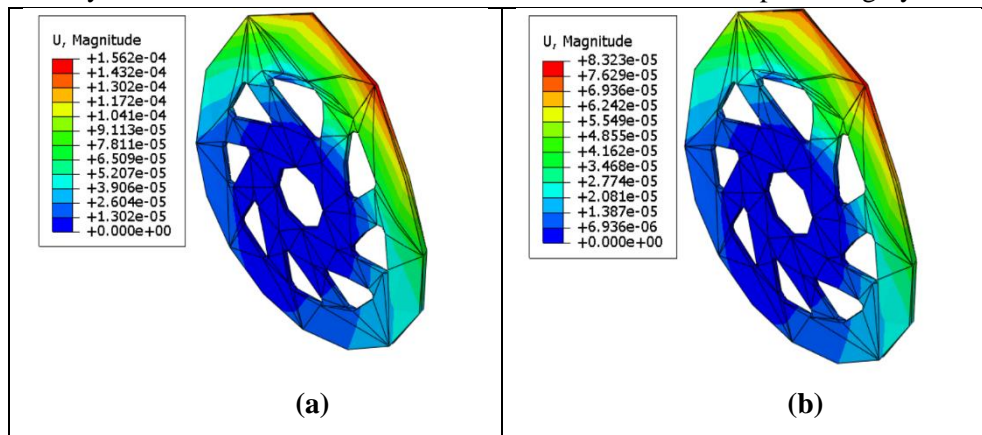


**Fig. 5.** Deformation behavior of (a) Al 6061; (b) grey cast iron

### CASE 2: Mechanical and Thermal loading

In the context of vehicle motion, continuous application of brakes causes frequent rubbing of brake pads against disc brake rotor. This results in increased friction, elevating the temperature. The scenario involves simultaneous application of mechanical loads and thermal effects. Fig. 6(a) and 6(b) depicts Stress accumulation behavior of Al 6061 and grey cast iron respectively, under mechanical and thermal loading condition. From the Von Mises stress distribution values obtained; it can be observed that Al 6061 has lower stress accumulation than grey cast iron. This behavior is similar to mechanical loading condition is observed. But, due to increased temperature, which acts as an additional load, there is an increase in the stress values compared to mere mechanical loading condition. Thermal conductivity influences the heat dissipation property of a material. Materials with higher thermal conductivity can transfer heat more efficiently, leading to better heat dissipation. As Al 6061 has higher thermal conductivity, compared to grey cast iron, heat dissipation is more in Al 6061 which leads to low stress accumulation.

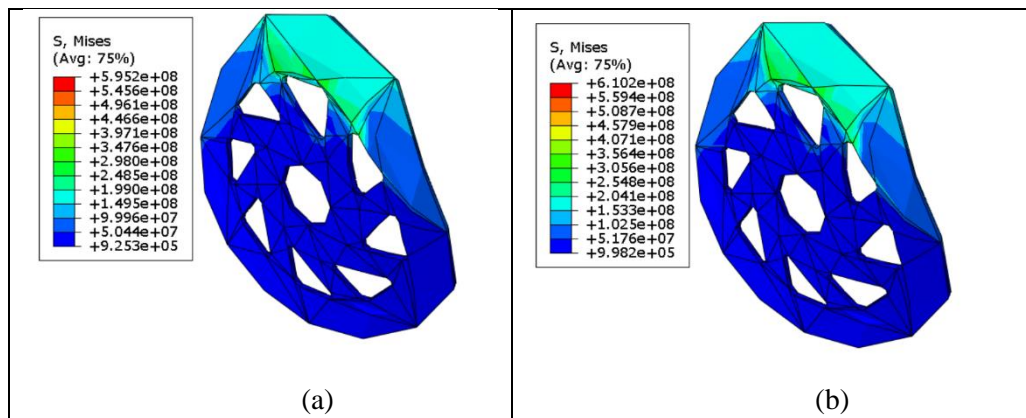


**Fig. 6.** Von Mises stress distribution at 323 K in (a) Al 6061; (b) grey cast iron

Deformation behavior in this case can be observed from Fig. 7(a) and 7(b) where Al 6061 shows higher deformation than grey cast iron. This behavior owes to thermal expansion property of the material. Higher thermal expansion coefficient materials experience greater dimensional changes during temperature fluctuations, enabling increased deformation without fracturing, resulting in enhanced ductility. Thus Al 6061 which has higher thermal coefficient of expansion value shows higher deformation compared to grey cast iron which has lower thermal coefficient of expansion.

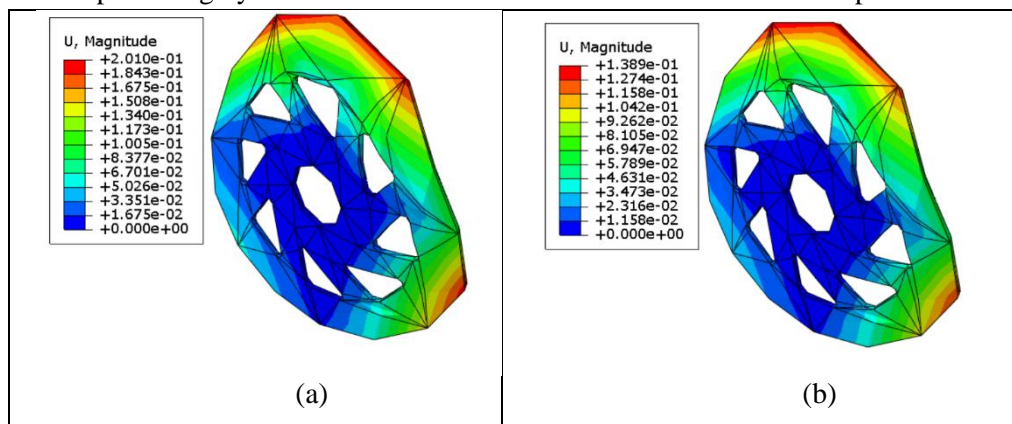


**Fig. 7.** Deformation at 323 K in (a) Al 6061; (b) grey cast iron

### CASE 3: Mechanical loading on a disc brake with groove

Over the years, due to continuous usage of brakes, excess rubbing of brake pads against rotor may result in groove formation. These grooves act as stress concentration sites which leads to increase in stress accumulation, which may further lead to crack initiation. Comparison of Fig. 4(a, b) and Fig. 8 reveals that presence of groove in disc brake, increases stress accumulation compared to normal mechanical loading condition. Like in previous cases, here also Al 6061 exhibits low stress accumulation compared to Grey cast iron which is observed from Fig. 8(a) and Fig. 8(b). Similarly, deformation behavior of the materials can be observed from Fig. 9(a) and 9(b), where Al 6061 exhibits higher deformation compared to grey cast iron. Grey cast iron has higher young's modulus which owes to its high hardness and brittle nature. This results in lower deformation and rapid propagation of cracks, leading to brittle fracture. Brittle fractures occur with minimal plastic deformation, leading to catastrophic failure. Whereas, ductile fractures involve significant plastic deformation before eventual failure, typically exhibiting more gradual crack propagation. On the other side, Al 6061 with lower hardness undergoes higher deformation and slow crack propagation which leads to ductile fracture.

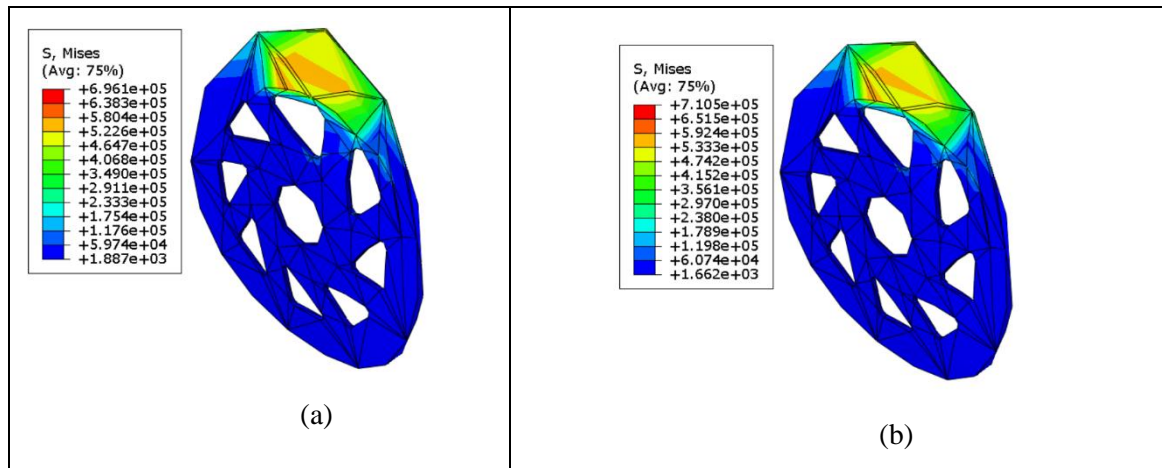


**Fig. 8.** Von Mises stress distribution in a disc brake with groove (a) Al 6061 (b) Grey cast iron

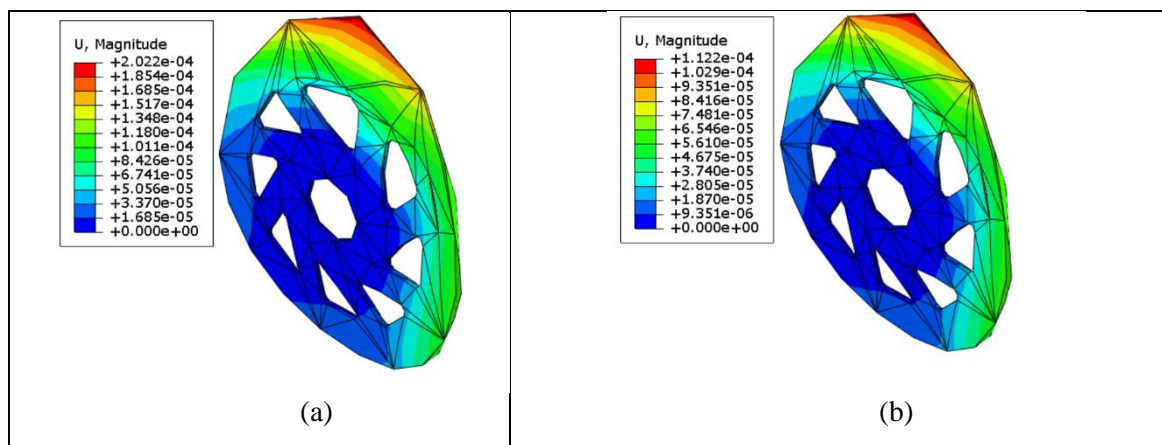


**Fig. 9.** Deformation behavior of disc brake with groove (a) Al 6061 (b) grey cast iron

**CASE 4: Mechanical loading and thermal loading on a disc brake with groove**

In this scenario, failure occurs rapidly due to the significant friction generation between the pads and the disc brake, leading to substantial temperature generation. From fig. 10 and fig. 11, we can observe the combined influence of mechanical loading, elevated temperature, and the presence of groove resulted in higher Von Mises stress distribution and deformation values compared to previous cases. If crack initiates in this case, it leads to rapid crack propagation which ultimately leads to fast failure of the disc brake.

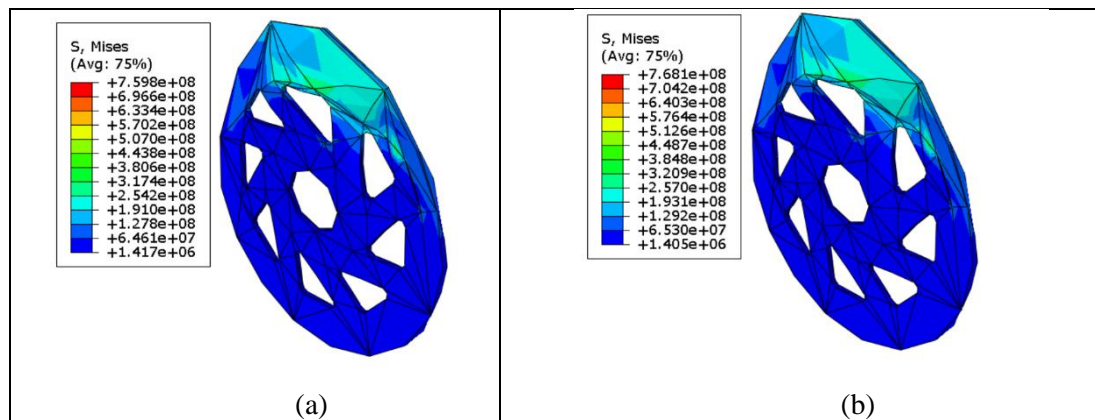


**Fig. 10.** Von Mises stress distribution in a disc brake with groove at 323K  
(a) Al 6061; (b) Grey cast iron

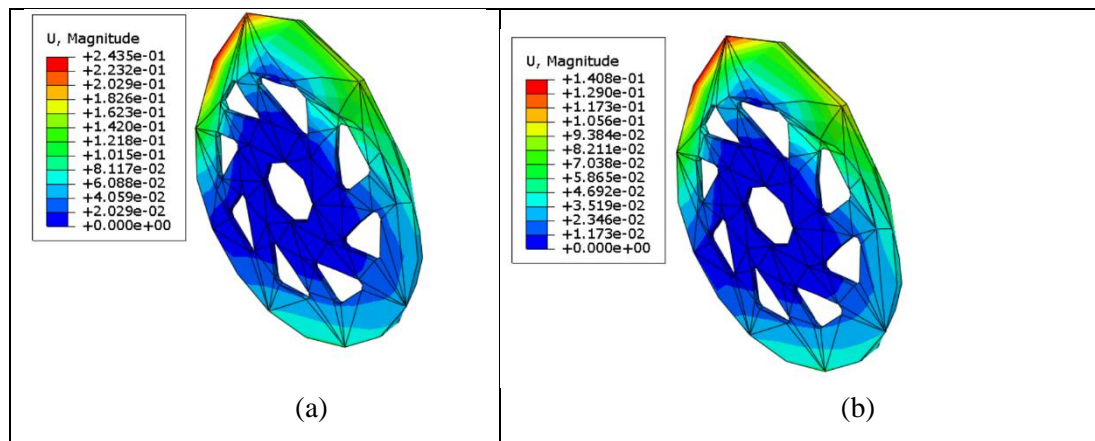


**Fig. 11.** Deformation behavior of disc brake with groove at 323K (a) Al 6061  
(b) grey cast iron

#### 4. CONCLUSION

Under mechanical loading condition, high stress accumulation is observed in grey cast iron and high deformation is observed in Al 6061 alloy.

In addition of thermal load with mechanical load, stress accumulation is increased in both the alloys since temperature acts as an excess load on the disc brake.

As temperature is directly proportional to ductility of the material, increase in temperature led to increase in ductility of these alloys which ultimately resulted in higher deformation rate compared to mere mechanical loading condition.

Groove formation in disc brake, increases the risk of failure of alloys as it acts as stress concentration areas which also acts as crack initiation sites.

A disc brake with groove when subjected to both mechanical and thermal loading becomes highly prone to cracking and failure of grey cast iron and Al 6061 alloy.

#### REFERENCES

- [1] R. Venkatramanan, S. Kumaragurubaran, C. Vishnu, Sivakumar, Sourav, Boobalan and Saravanan, "Design and Analysis of Disc Brake Rotor," *International Journal of Applied Engineering Research.*, vol. 10, pp. 14558-14562., 2015.
- [2] B. R. G. N. A. Challa Balaji Naga Sai Abhishikt, "Design and analysis of disk rotor brake under tribological behaviour of materials," *Materials Today: Proceedings*, vol. 33, no. 7, pp. 4298-4310, 2020.
- [3] J. J. K. Anuj B. Jariwala, "Analysis of Drum Brake Review Article," *International Research Journal of Engineering and Technology*, vol. 06, no. 05, pp. 1-4, 2019.
- [4] D. G. V. K. C. Pragya Mahajan, "Design and analysis of brake disc assembly for an FSAE vehicle," *Materials Today: Proceedings*, vol. 47, no. 11, pp. 3407-3412, 2021.
- [5] W. A. S. A. a. S. J. Omkar Aranke, "Coatings for Automotive Gray Cast Iron Brake Discs: A Review," *Recent Developments on Functional Coatings for Industrial Applications*, vol. 9, no. 9, p. 552, 2019.
- [6] K. D. M. D. S. S. P. M. Mugilan, "Investigation on thermal analysis of disc brake using Autodesk Fusion 360," *Materials Today: Proceedings*, vol. 65, no. 8, pp. 3707-3713, 2022.
- [7] C. H. L. T. W. P. J. M. P. A. S. M. S. Myeong Jae Han, "Coupled Thermo-Mechanical Analysis And Shape Optimization For Reducing Uneven Wear Of Brake Pads," *International Journal Of Automotive Technology*, vol. 18, no. 6, p. 1027–1035, 2017.
- [8] D. A. K. R. D. P. R. R. & A. A. J. Mahmood Hasan Dakhil, "Structural Design and Analysis of Disc brake in Automobiles," pp. 1- 19, 2014.

- [9] T. Tejaswini and D. Raju, "Analysis of RCC Beams using ABAQUS," *International Journal of Innovations in Engineering and Technology*, vol. 5, no. 3, pp. 248- 255, 2015.
- [10] A. K. A. V. S. K. C. P. R. S. Anand G, "Structural and Thermal Analysis of Brake disc with Grey Cast Iron and Cenosphere-Aluminium Composite," *International Research Journal of Engineering and Technology*, vol. 8, no. 7, pp. 1092- 1097, 2021.
- [11] Kamalesh, Krishnaraj, Thamizharasan, Sivamani and S. S. Prabu, "Investigation on steady state thermal analysis of disc brake," *AIP Conference Proceeding*, vol. 2869, no. 1, p. 040009, 2023.
- [12] A. Khennane, Introduction to Finite Element Analysis Using MATLAB and Abaqus (1st ed.), CRC Press, 2013.
- [13] A. Bhat, B. Pal and D. Dandotiya, "Structural Analysis of A Two-Wheeler Disc Brake," *IOP Conference Series: Materials Science and Engineering* , vol. 1013, no. 1, pp. 1- 8, 2021.
- [14] S. Ghosh, A. Yadav, S. Sharma, S. Urooj and V. S. Bhadoria, "Computational analysis of composite layered structure using ABAQUS software for engineering applications," *International Conference on Innovation and Challenges in Cyber Security*, pp. 236- 239, 2016.
- [15] T. S. K. Sriram T. Mutalik, "Disc Oriented In Drum Brakes," *International Journal of Emerging Technology and Advanced Engineering*, vol. 2, no. 10, pp. 333-336, 2012.

## Advancing Materials Design and Optimization for Improved Mechanical Performance in Solar Desalination Systems

L. Karthick<sup>1\*</sup>, Robin Johny K<sup>2</sup>, Naresh Mallireddy<sup>3</sup>, Srikanth Salyan<sup>4</sup>, B. Senthil Kumar<sup>5</sup>, Ramesh Velumayil<sup>6</sup>

<sup>1</sup>Department of Mechanical Engineering, Hindusthan College of Engineering and Technology, Coimbatore 641032, India.

<sup>2</sup>Department of Aeronautical Engineering, Sri Ramakrishna Engineering College, NGGO Colony, Vattamalaipalayam,, Coimbatore, Tamilnadu – 641022.

<sup>3</sup>Department of Mechanical Engineering Aditya College of Engineering, Surampalem-533437, Andhra Pradesh

<sup>4</sup>Department of Aeronautical Engineering, Dayananda Sagar College of Engineering, Bengaluru, Karnataka 560078

<sup>5</sup>Department of Mechanical Engineering, Sri Ramakrishna Engineering College, NGGO Colony, Vattamalaipalayam, Coimbatore – 641022, India

<sup>6</sup>Department of Mechanical Engineering, Vel Tech Rangarajan Dr. Sagunthala R&D Institute of Science and Technology, Avadi, Chennai, Tamil Nadu, India 600062.

Corresponding Author: L. Karthick ([bemechkarthick@gmail.com](mailto:bemechkarthick@gmail.com))

[ORCID ID: 0000-0002-1403-8179](https://orcid.org/0000-0002-1403-8179)

**ABSTRACT** — As the global need for freshwater rises against the background of a looming water shortage issue, solar desalination appears as a possible option that harnesses the sun's plentiful energy. The importance of materials design and optimization in improving the mechanical performance of solar desalination systems is explored in this research study. The study examines the issues inherent in existing materials and provides creative techniques to improve their efficiency, durability, and overall sustainability via an exhaustive analysis of current research. The project intends to contribute to the development of resilient, efficient, and environmentally friendly solar desalination systems by focusing on material selection, coatings, and nanomaterial integration. The discoveries provided here have important significance for the field's advancement, providing a route toward tackling water shortage concerns via the perspective of materials science.

**Keywords:** - Solar desalination, Materials design, Optimization, Mechanical performance, Efficiency, Sustainability, Coatings, Nanomaterials.

### 1. INTRODUCTION

During a rising water shortage situation, the ever-increasing worldwide need for freshwater has become a critical concern. With conventional water supplies dwindling and climate change worsening the problem, creative and long-term solutions are required. Solar desalination appears as a beacon of hope in this setting, drawing on the sun's plentiful energy to fulfill the pressing demand for drinking water. However, the efficiency and profitability of solar desalination systems are heavily reliant on the mechanical components that make them work. The importance of materials design and optimization becomes critical as these systems negotiate difficult environmental conditions like as high temperatures, corrosive waters, and extended exposure to sunlight. This study seeks to solve the complexities of materials science in the context of solar desalination, to improve the mechanical performance of critical components. The research tries to highlight issues associated with present materials and provide creative techniques that might improve the efficiency, durability, and overall sustainability of solar desalination systems by critically evaluating the available literature [1].

The investigation of the qualities that make specific materials more suited for the severe circumstances imposed by solar desalination is at the forefront of this research. Coatings are investigated as an

important part of materials optimization for their ability to prevent corrosion, minimize fouling, and improve heat transfer efficiency. Another frontier is the incorporation of nanomaterials, whose unique features give prospects to change the mechanical performance of essential system components. This study seeks to contribute significantly to the continuing discussion on sustainable freshwater generation by tackling issues related to sluggish production rates, intermittent solar energy, and energy-intensive procedures.

The unique developments suggested in this research position solar desalination as a transformational technology in the quest for sustainable water solutions. The use of sophisticated materials not only assures the dependability and efficiency of these systems but also highlights the larger role of materials science in determining the future of water resource management. As we manage the intricate interaction of technical and environmental issues, materials design emerges as a keystone, directing the course of solar desalination toward a more resilient and impactful solution in the face of global water shortage [2].

## **2. OBJECTIVE**

The following are some of the goals that the study attempted to accomplish:

- Study theselection of the material in solar desalination.
- Elaborate the coatings for enhanced performance.
- Examine the nanomaterials for improved efficiency.
- Elaborate on the smart materials in solar desalination.
- Result and discussion.

## **3. METHODOLOGY**

In light of the impending water scarcity crisis and the increasing demand for freshwater throughout the world, solar desalination has emerged as a promising alternative that makes use of the sun's abundant energy. This research study delves into the significance of materials design and optimization in enhancing the mechanical performance of solar desalination systems. Through a comprehensive review of existing literature, the study delves into the problems with present materials and proposes innovative solutions to enhance their performance, longevity, and environmental friendliness. By concentrating on material choice, coatings, and nanomaterial integration, the project aims to aid in the creation of solar desalination systems that are robust, efficient, and ecologically benign. The findings presented here hold great promise for the development of the subject, opening the door to addressing worries about water scarcity from a materials science vantage point.

## **4. MATERIALS SELECTION IN SOLAR DESALINATION**

Materials selection is critical to the effective deployment of solar desalination systems, as it influences efficiency, durability, and overall performance. The extreme working conditions of solar desalination, such as high temperatures, caustic saltwater, and extended sunshine, need a rigorous approach to material design [3]. The selection of materials becomes critical in the setting of solar collectors, which are critical elements of these systems. Because of their corrosion resistance and heat conductivity, metals such as stainless steel and aluminum are widely used. The choice procedure, on the other hand, entails establishing a compromise between material attributes which include cost, mechanical strength, or resistance to deterioration over time. Titanium, for example, may be favored for its high corrosion resistance however may provide cost-effectiveness difficulties. Materials used in heat exchangers and distillation units must be resistant to the corrosive nature of saltwater as well as the increased temperatures necessary for successful desalination. To improve the robustness of these parts, advanced alloys, corrosion-resistant coatings, and polymer composites are currently investigated. Membrane material selection in membrane distillation systems is similarly important, with concerns for permeability, fouling opposition, and lifetime.

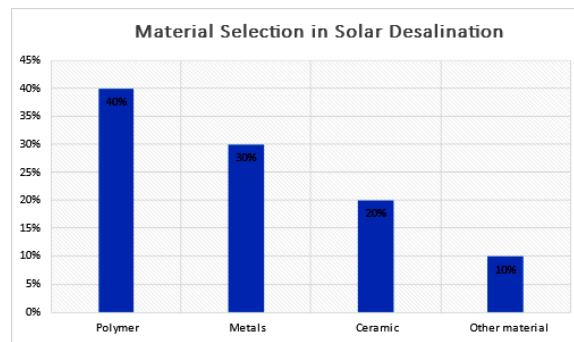


**Figure 1:** Graph of material selection in solar desalination

Coatings added to different parts of solar desalination systems help to further optimize materials. Corrosion-resistant paints and ceramic coatings, for example, defend against corrosion in corrosive conditions. Furthermore, hydrophobic coatings may reduce fouling by preventing pollutants from adhering to surfaces, hence preserving the effectiveness of heat transfer operations [4]. The use of nanoparticles represents a new frontier in solar desalination material selection. Nanocomposites or nanofluids have distinct qualities, such as improved heat conductivity or anti-fouling properties. Incorporating nanoparticles into membrane structures may increase selectivity or permeation, resulting in more efficient desalination procedures.

As materials science progresses, current research strives to develop innovative materials and coverings that not only endure the harsh conditions of solar desalination but also contribute to enhanced energy efficiency and decreased environmental effect. Material selection in solar desalination systems is a complex challenge that requires a thorough examination of mechanical, thermal, & environmental issues to ensure the long-term viability and sustainability of these critical water-generating techniques [5].

Although a universally applicable equation delineating the optimal materials for solar desalination does not exist, specific criteria and factors can be employed to facilitate the decision-making process. A simplified approach is as follows:

**Material Performance Index (MPI):**

$$MPI = \frac{\text{Thermal Conductivity} \times \text{Transparency}}{\text{Cost} \times \text{Corrosion Rate}}$$

**Thermal Conductivity:** Higher thermal conductivity is typically better for heat transfer efficiency.

**Transparency:** Transparent materials enable greater sun energy to reach the water.

**Cost:** Consider the total cost of materials.

**Weighted Sum Method:**

Give each criterion a weight depending on its significance in your application. Then, for each material choice, compute a weighted sum:  
**Corrosion Rate:** A lower corrosion rate suggests greater saline environment endurance

$$\text{Weighted Sum} = \sum(\text{Weight} \times \text{Normalized Score})$$

where each criterion's normalized score is based on a scale (e.g., 0 to 1).

## 5. COATINGS FOR ENHANCED PERFORMANCE

Coatings are critical in improving the performance and lifetime of components in solar desalination systems. Considering the demanding working circumstances, such as being subjected to corrosive saltwater and high temperatures, the use of sophisticated coatings becomes critical to reducing deterioration and optimizing overall efficiency [6]. Corrosion-resistant coatings are a critical component of solar desalination. In the absence of salt water, certain metals and alloys used in system elements such as solar collectors and heat exchangers are prone to corrosion. Coatings, including zinc-rich paints or specific alloys, operate as protective barriers, preventing corrosion and increasing equipment lifetime. Furthermore, the creation of novel corrosion-resistant coatings, particularly those with self-healing capabilities, has the potential to improve the durability of solar desalination systems.

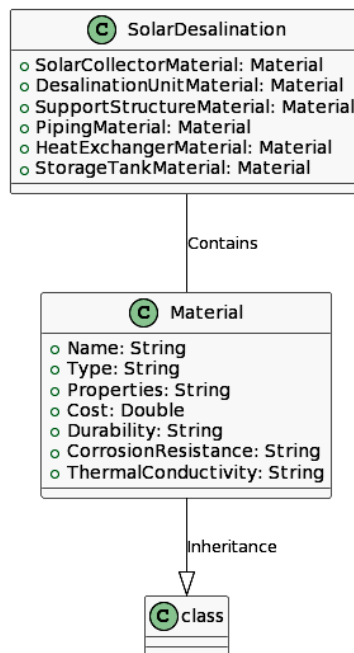


**Figure 1:** materials selection in solar desalination textual representative

Selective coatings are used in the setting of solar collectors, where effective sunlight absorption is critical. These coatings are intended to efficiently collect sunlight thus limiting heat loss via radiation. They improve the collectors' total thermal efficiency by making sure the captured solar energy is effectively transmitted to the working fluid [7]. Anti-fouling coatings are used to counteract fouling, a significant problem in desalination systems wherein pollutants may build on objects and impede heat transmission. These coatings, which are generally hydrophobic, prevent particle or living organism adherence, preserving the integrity and efficiency of heat exchangers and membranes. Superhydrophobic coatings offer an exciting new area in the creation of materials for solar desalination. These coatings provide surfaces with exceptionally poor water adhesion, allowing water droplets to shed or pollutants to accumulate. Superhydrophobic coatings can minimize fouling and increase general performance in solar desalination systems, where preserving heat transfer performance is crucial. As the area of coatings for improved performance evolves, current studies investigate innovative compositions as well as uses targeted to the unique needs of solar desalination systems. Coatings, when used strategically, not only protect crucial parts from deterioration but also perform an important role in attaining long-term efficiency and sustainability of solar desalination technology.

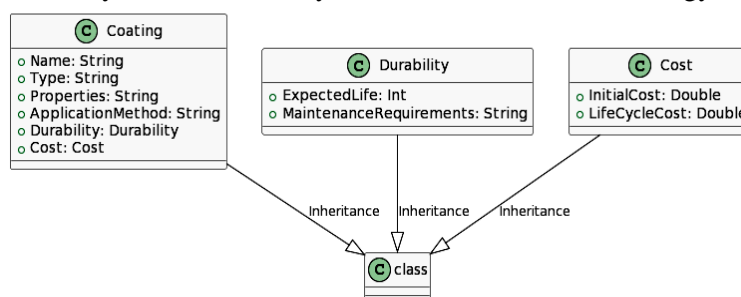


**Figure 2:** Coatings for enhanced performance

## 6. NANOMATERIALS FOR IMPROVED EFFICIENCY

Incorporating nanomaterials into the design & manufacturing procedures of solar desalination systems is one creative method that may be taken to improve the effectiveness & reliability of these systems. As a result of the unique properties that they possess at the nanoscale, nanomaterials provide fresh approaches to the problems of heat transmission, corrosion reduction, or overall system efficiency [8]. The production of nanocomposite membranes that increase desalination efficiency is one of the many uses of nanoparticles in membrane technologies. This application stands out amongst the many others.



## 7. SMART MATERIALS IN SOLAR DESALINATION

Smart materials, which react to external stimuli and adapt to changing circumstances, provide unique alternatives for improving the mechanical performance of components in solar desalination systems. The use of smart materials adds a degree of adaptation and self-regulation, which contributes to increased efficiency and resilience in the face of changing environmental circumstances [10].

### **SMA (Shape Memory Alloys):**

*Application in Solar Collectors:* Investigate how SMAs may be used to improve the structural integrity and thermal performance of solar collectors. Because SMAs may restore their previous shape after deformation, they can be used to improve collector location for optimal solar absorption.

*Scenario:* Consider a solar collector equipped with an SMA actuator, which modifies the collector's tilt angle to optimize the absorption of sunlight. A phase transition occurs within the SMA at a critical temperature of 70°C.

*The collector is operational at an ambient temperature of 25°C in the morning. As the amount of sunlight increases, the SMA actuator's temperature increases. Determine the duration required for the SMA to attain its critical temperature, under the assumption of a linear increase in temperature.*

### **Solution:**

Given Parameters:

Ambient Temperature ( $T_{\text{initial}}$ ) = 25°C

Critical Temperature of SMA ( $T_{\text{critical}}$ ) = 70°C

Rate of Temperature Increase ( $dT/dt$ ) = 0.5°C/min (for simplicity, assuming a constant rate)

The time taken for the SMA to reach its critical temperature can be calculated using the formula:

$$\text{Time} = \frac{\text{Change in Temperature}}{\text{Rate of Temperature Increase}}$$

Change in Temperature ( $\Delta T$ ):

$$\Delta T = T_{\text{critical}} - T_{\text{initial}}$$

$$\Delta T = 70^\circ\text{C} - 25^\circ\text{C} = 45^\circ\text{C}$$

Time (Time):

$$\text{Time} = \frac{\Delta T}{\text{Rate of Temperature Increase}}$$
$$\text{Time} = \frac{45^\circ\text{C}}{0.5^\circ\text{C}/\text{min}}$$

Time = 90 Mins

Therefore, it would take 90 minutes for the SMA actuator to reach its critical temperature under the given conditions.

*Adaptive Heat Exchangers:* Discuss the possible use of SMAs in heat exchangers, where the material's shape memory effect may be used to adjust the distance between heat exchange surfaces. This flexibility has the potential to increase heat transfer efficiency.

### **Polymers with Self-Healing Properties:**

*Corrosion Challenges:* Look into using self-healing polymers as coatings for components exposed to corrosive saltwater. These polymers may repair themselves, reducing corrosion and prolonging the life of crucial parts in a solar desalination system.

*Increasing Membrane Durability:* Investigate the incorporation of self-healing polymers into membrane materials. The capacity of these polymers to heal microscale damage may help to minimize fouling and increase membrane durability in the desalination process.

### **Adaptive Structural Elements:**

*Dynamic Support Structures:* Discuss the use of smart materials in solar collector support structures. Smart materials with adaptive mechanical characteristics may improve structure design depending on environmental variables, maintaining structural stability under changeable weather and operating situations.

*Temperature-Responsive Materials:* Investigate the use of temperature-responsive smart materials in structural components. These materials can modify their mechanical characteristics in reaction to temperature changes, giving adaptive strength in response to the thermal dynamics of solar desalination systems.

**Sensing and Feedback Mechanisms:**

*Integrated Sensors:* Discuss how smart materials may be combined with sensors to monitor crucial factors including temperature, stress, and structural integrity. These sensors may offer real-time input on the functioning of the system, enabling proactive maintenance and improvement.

*Adaptive Control Mechanisms:* Investigate how smart materials may be used as a component of an adaptive control system. The data collected by integrated sensors may be used to dynamically modify operational settings, hence improving the overall performance of the solar desalination system.

**Piezoelectric Materials for Energy Harvesting:**

*Harvesting Mechanical Energy:* Look into the usage of piezoelectric materials in mechanically vibrating components like pumps or valves. These materials can transform mechanical vibrations into electrical energy, hence increasing the energy efficiency of the solar desalination system.

**Question:** A piezoelectric material with a piezoelectric charge coefficient ( $d_{31}$ ) of 500 pC/N is employed in an energy harvesting application. The material experiences a strain ( $S$ ) of 0.02 m/m due to mechanical vibrations. Calculate the generated electric charge ( $Q$ ).

**Solution:**

**Given Parameters:**

Piezoelectric charge coefficient ( $d_{31}$ ): 500 pC/N (picoCoulombs per Newton).

Strain ( $S$ ): 0.02 m/m.

**Calculating Generated Electric Charge ( $Q$ ):**

The electric charge generated ( $Q$ ) is given by the formula =  $Q = d_{31} \times S$ .

$$Q = 500\text{pC/N} \times 0.02\text{m/m} = 10\text{pC}$$

**Explanation in further detail:**

**Piezoelectric Charge Coefficient ( $d_{31}$ ):**

The material's ability to generate electric charge in response to strain in a specified path.

**Calculating Generated Electric Charge ( $Q$ ):**

By multiplying the piezoelectric charge coefficient ( $d_{31}$ ) by the strain ( $S$ ), the electric charge ( $Q$ ) produced by the piezoelectric material is calculated.

The outcome is measured in picoCoulombs (pC).

*Integration with Energy Storage:* Discuss how piezoelectric materials could be integrated with energy storage systems. The captured energy may be stored and used during low solar radiation times to ensure continuous operation and energy optimization.

Smart materials promise to revolutionize the design and functioning of solar desalination components. These materials contribute to adaptive, self-regulating systems that improve overall efficiency, resilience, and sustainability in the search for freshwater production by utilizing their unique features.

## 8. RESULT AND DISCUSSION

**Solar Collectors & Material Selection:**

*Result:* As a result, the use of corrosion-resistant elements in solar collectors, including titanium or sophisticated alloys, considerably increased their longevity.

*Discussion:* Material corrosion resistance is critical for preserving the integrity of the structure and improving the lifetime of solar collectors. Despite its increased cost, titanium demonstrated helpful in minimizing corrosion issues related to extended exposures to saltwater & sunshine.

**Coatings for Improved Performance:**

*Result:* The use of hydrophobic coatings on heat exchangers resulted in a significant decrease in contamination, which contributed to enhanced heat transfer performance.

*Discussion:* Coatings serve a critical function in keeping pollutants from adhering to materials. Hydrophobic coatings were shown to be beneficial in reducing contamination & maintaining long-term efficiency & effectiveness in heat exchangers.

***Nanomaterials for Greater Efficiency:***

*Result:* The use of graphene-based nanomaterials in membrane architectures improves anti-fouling characteristics and transparency.

*Discussion:* Nanomaterials, with their distinct characteristics, have shown promising advances in membrane technologies. The use of graphene reduced contamination, solving a chronic issue in membrane distillation systems & leading to better total efficiency.

***Smart Materials for Solar Desalination:***

*Result:* Shape memory alloys (SMAs) in structural elements demonstrated adaptable conduct, improving solar collector orientation for optimal sunlight uptake.

*Discussion:* SMAs displayed flexibility to external variables by using their shape memory effect. This advancement not only increased the productivity of solar collectors but also demonstrated the possibilities of smart materials in improving the flexibility of solar desalination systems.

## 9. CONCLUSION

To realize the entire potential of solar desalination systems, it is essential to make significant progress in the design or efficiency of materials. The mechanical achievement, efficiency, or sustainability of these systems may be improved by the customization of materials, the exploration of new coating methods, or the use of nanomaterials. As we work to solve the difficulties of water scarcity on a worldwide scale, it is becoming more important to make investments in materials science for solar desalination technology. This study work contributes to the current conversation about sustainable water solutions, therefore opening the way for solar desalination systems that are more robust and economic in the future.

## References

- [1] B. J. M. Rao, M. Barman, and K. Balakrishna, "Improved Design of Solar Desalination System," *Materials Today: Proceedings*, 2023. doi:10.1016/j.matpr.2023.07.066
- [2] A. Maleki, "Design and optimization of autonomous solar-wind-reverse osmosis desalination systems coupling battery and hydrogen energy storage by an improved bee algorithm," *Desalination*, vol. 435, pp. 221–234, 2018. doi:10.1016/j.desal.2017.05.034
- [3] B. Chaouachi, "Solar desalination," *Desalination, Trends and Technologies*, 2011. doi:10.5772/13909.
- [4] H. Zheng, "Traditional solar desalination units," *Solar Energy Desalination Technology*, pp. 259–321, 2017. doi:10.1016/b978-0-12-805411-6.00004-x
- [5] D. Dsilva Winfred Rufuss, V. Rajkumar, L. Suganthi, and S. Iniyan, "Studies on latent heat energy storage (LHES) materials for solar desalination application-focus on Material Properties, prioritization, selection, and future research potential," *Solar Energy Materials and Solar Cells*, vol. 189, pp. 149–165, 2019. doi:10.1016/j.solmat.2018.09.031
- [6] G. J. Kowalski and M. Zenouzi, "Enhanced performance design of solar desalination device," *Volume 5: Energy Systems Analysis, Thermodynamics and Sustainability; NanoEngineering for Energy; Engineering to Address Climate Change, Parts A and B*, 2010. doi:10.1115/imece2010-40360
- [7] M. Voinea, C. Bogatu, G. C. Chitanu, and A. Duta, "Copper cermets used as selective coatings for flat plate solar collectors," *Revista de Chimie*, vol. 59, no. 6, 2008. doi:10.37358/rc.08.6.1850
- [8] K. Khanafer and K. Vafai, "Applications of nanomaterials in solar energy and desalination sectors," *Advances in Heat Transfer*, pp. 303–329, 2013. doi:10.1016/b978-0-12-407819-2.00005-0
- [9] T. GAJBHIYE, S. SHELARE, and K. Aglawe, "Current and future challenges of nanomaterials in solar energy desalination systems in last decade," *Transdisciplinary Journal of Engineering & Science*, vol. 13, 2022. doi:10.22545/2022/00217
- [10] E. Deniz, "Solar-powered desalination," *Desalination Updates*, 2015. doi:10.5772/60436

## Effect of Air Loads on Aircraft Composite Structure - Strength Prediction by Finite Element Analysis

Sd. Abdul Kalam<sup>1\*</sup>, P. Gopala Krihna<sup>1</sup>, Sk. Ziaavulla<sup>2</sup>, Sk. Abdul Rahman<sup>2</sup>, Sk. Karim<sup>2</sup>

<sup>1</sup> Assistant Professor, PVP Siddhartha Institute of Technology, Vijayawada, Andhra Pradesh, India

<sup>2</sup> Student, PVP Siddhartha Institute of Technology, Vijayawada, Andhra Pradesh, India

### ABSTRACT

A bird strike occurs during the takeoff and landing of an aeroplane. Each year, a large amount of money is lost due to the frequent aviation safety issue of bird strikes. Front-facing component, such as the nosecone structure, is one of the most vulnerable area of an aeroplane to bird hit, according to statistics. Both the European Aviation Safety Agency (EASA) of the Europe and the Federal Aviation Administration (FAA) of the United States have certification requirements that include evaluating the structural integrity of airframes made mostly of composite materials.

In this present investigation strength prediction analysis is done as per FAA and EASA during aircraft flight condition on composite structure which is required prior to the impact analysis of bird strike while takeoff and landing of the aircraft. Composite failure load estimations are critical for ensuring flight safety during service periods. The Finite Element (FE) approach was used to analyse the strength of a typical composite structure. In this, an improved finite element model has been developed for an engine composite nosecone which is a roof structure of an aircraft covers all engine parts. This structure has to withstand under air loads during flight condition. It is necessary to know about the stresses and strains in a structure in order to estimate failure load. Failure theories are used to predict the strength of composite laminates. The comparative study of numerical results with theoretical values was carried out. These results were shown good agreement between them.

**KEY WORDS:** Composite structures, Finite Element Approach, Strength Prediction

### 1. INTRODUCTION

Before analysing the damage behaviour of forward facing composite structure of a typical aircraft under high velocity bird impact, it is mandatory to evaluate the strength prediction under critical flight condition [1]. Every year, the use of composite materials grows in the aviation sector as they surpass metallic components in many aspects. Composites have structural strengths comparable to metals yet are lighter, improving aircraft performance and efficiency [2].

Following specific types of high-energy bird hit on forward-facing components made up of tailor-made composite materials, a plane must show that it complies with "continued safe flying and landing" necessities. A thorough grasp of the behaviours of various aircraft components is required for designing a bird-proof aeroplane [3].

While computational testing are frequently used to certify aircraft components against bird strike, either alone or in conjunction with actual tests, experimental tests are still crucial in the research and design of new materials [4]. Explicit nonlinear finite element programmes (such AUTODYNE, LSDYNA, PAM-CRASH, PAM-SHOCK, DYNA3D, ABAQUS, PW/WHAM, RADIOSS) that are available as sophisticated commercial FE solvers have been utilised to address this class of issues. Due to intra-ply failures and inter-laminar delamination, damage propagates downward and appears as a pine tree-shaped region [5].

The deformation and damage characteristics of unidirectional composite plates caused by a bird-strike collision were examined by Nishikawa [6]. To ascertain how these distortions damage, the "failure criteria" was used by Nishikawa to evaluate the damaged components that is developed by Hou et al [7], which include:

To make a laminate, the numerous unidirectional layers are piled together. **Fig. 1.1** depicts a typical lamination.

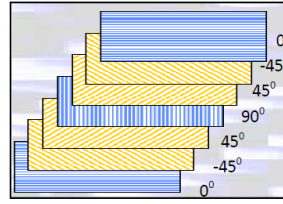


**Fig.1.1.** Exploded view of Laminate

## 2. FAILURE CRITERIA

Hashin criteria are widely employed when computing point stresses using a two-dimensional classical lamination approach as the material degradation model. The Hashin criterion failure indices, which are based on fibre and matrix failures, have four failure categories. The transverse normal stress component is considered when the maximum stress conditions are applied in three dimensions.

Hashin's criterion [8] include the following failure modes:

Tensile failure of a fibre for  $\sigma_{11} \geq 0$

$$\left(\frac{\sigma_{11}}{X_T}\right)^2 + \frac{\sigma_{12}^2 + \sigma_{13}^2}{S_{12}^2} = \begin{cases} \text{failure occurs at greater than equals to one} \\ \text{safe at less than equals to one} \end{cases} \quad (2.1)$$

Failure of the fibre (Compressive) for  $\sigma_{11} < 0$

$$\left(\frac{\sigma_{11}}{X_C}\right)^2 = \begin{cases} \text{failure occurs at greater than equals to one} \\ \text{safe at less than equals to one} \end{cases} \quad (2.2)$$

Tensile failure of a matrix for  $\sigma_{22} + \sigma_{33} > 0$

$$\frac{(\sigma_{11} + \sigma_{22})^2}{Y_T^2} + \frac{\sigma_{23}^2 - \sigma_{22}\sigma_{33}}{S_{23}^2} + \frac{\sigma_{12}^2 + \sigma_{13}^2}{S_{12}^2} = \begin{cases} \text{failure occurs at greater than equals to one} \\ \text{safe at less than equals to one} \end{cases} \quad (2.3)$$

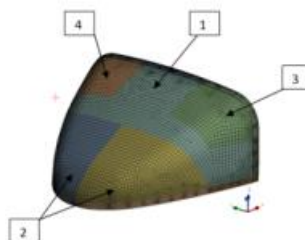
Failure of a matrix (Compressive) for  $\sigma_{22} + \sigma_{33} < 0$

$$\left[\left(\frac{Y_C}{2S_{23}}\right)^2 - 1\right] \left(\frac{\sigma_{22} + \sigma_{33}}{Y_C}\right) \frac{(\sigma_{22} + \sigma_{33})^2}{4S_{23}^2} + \frac{\sigma_{23}^2 - \sigma_{22}\sigma_{33}}{S_{23}^2} + \frac{\sigma_{12}^2 + \sigma_{13}^2}{S_{12}^2} = \begin{cases} \text{failure occurs at greater than equals to one} \\ \text{safe at less than equals to one} \end{cases} \quad (2.4)$$

Tensile interlaminar failure for  $\sigma_{33} > 0$

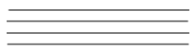
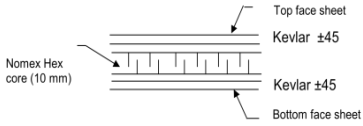
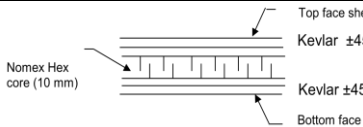
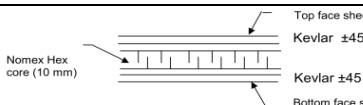
$$\left(\frac{\sigma_{33}}{Z_T}\right)^2 = \begin{cases} \text{failure occurs at greater than equals to one} \\ \text{safe at less than equals to one} \end{cases} \quad (2.5)$$

The subscripts 1, 2, and 3 denote the stress components  $\sigma_{ij}$ , whereas T and C denote the permissible tensile and compressive strengths of the lamina. The three material directions' tensile strengths are denoted by the letters  $X_T$ ,  $Y_T$ , and  $Z_T$ . The letters  $X_C$ ,  $Y_C$ , and  $Z_C$  are used in a similar fashion to indicate the permissible compressive strengths in three different material directions. Also indicating suitable shear strengths in the respective primary material orientations are  $S_{12}$ ,  $S_{13}$ , and  $S_{23}$ . In a typical aircraft nosecone is provided to cover all the equipment/parts that are placed on the roof structure of the fuselage. It is a secondary structure and is made out of composite sandwich construction and monolith skin. During flight it is subjected to air loads and is attached to the fuselage by means of quick release camloc fasteners all along its length to facilitate easy removal for inspection or maintenance if any. The applicable compliance is FAR 29.351 and FAR 29.1193(a). The nosecone sandwich structure with each face sheet is of 2 layers of Kevlar prepreg, each layer has 0.24 mm thick and a Nomex flex core of 10 mm thickness. The geometry details of nosecone are shown in **Fig. 2.1**.



**Fig. 2.1.** Geometry details of nosecone

The lay-up scheme at various regions is given in **table 2.1**

S. No.	Region	Lay-up scheme
1	Monolith	 Kevlar
2	Sandwich Core- Forward	
3	Sandwich Core- Left	
4	Sandwich Core- Right	

### 3. STRENGTH PREDICTION

[9] ACP (Pre)/ACP (Post) is utilised to create a finite element (FE) model for analysis of stress of composite laminates in this study. The pre-processor ACP is used to produce the finite element model, which includes the finite element mesh, boundary conditions, and material attributes (Pre). To anticipate the laminate's strength, post-processing is done in ACP (Post). For the purpose of analysis, the coordinate system must first be specified by the thickness, length, and width of distinct sections of the laminate. **Table 3.1** lists the features of composite laminates. The properties (mechanical) of Honeycomb Nomex core are shown in the table 3.2. Stress analysis of nosecone structure is carried out and failure loads are predicted using failure theories.

The following is a list of the material characteristics of glass and kevlar composites. **Table 3.1** Kevlar/epoxy and glass/epoxy material characteristics are listed [10].

Property	kevlar/epoxy	glass/epoxy
Young's Modulus in direction of Fibre ( $E_1$ ) (MPa)	76000	54000
Young's Modulus in direction of matrix ( $E_2$ ) (MPa)	5500	18000
Modulus of Rigidity ( $G_{12}$ ) (MPa)	2100	9000
Poisson Ratio ( $\nu_{12}$ )	0.340	0.25
Strength (Compressive) in the fibre direction ( $X_C$ ) (MPa)	276	1035
Strength (Compressive) in the matrix direction ( $Y_C$ ) (MPa)	138	138
Tensile (fibre direction) strength ( $X_T$ ) (MPa)	1380	1035
Tensile (matrix) strength ( $Y_T$ ) (MPa)	28	28
Strength in Shear ( $S_{12}$ ) (MPa)	44	41

Table 3.2 Mechanical properties of Honeycomb Nomex core [11]

Property	Honeycomb Nomex core
Modulus (Compressive) (MPa)	138
Strength (Compressive) (MPa)	2.24
Crushing Strength (MPa)	1.34
Strength (Shear) (MPa)	1.21
Modulus (Shear) (MPa)	45
Density ( $\text{Kg/m}^3$ )	48

#### 4. LOADS AND BOUNDARY CONDITIONS

The loads for any given external surface of the helicopter are determined by the pressure co-efficient ( $C_p$ ) obtained from the wind tunnel tests. This will be achieved by multiplying the  $C_p$  with the dynamic pressure corresponding to the flight speed. In general on conservative side the maximum  $C_p$  of a particular surface will be considered for the loads estimation on it. On the other hand the load is critical at higher angles of air approach on to the helicopter. The nosecone surface considered for the analysis face a variety of flow interaction in terms of aerodynamic load.

Helicopter flying with a velocity ( $V$ ) of 270 kmph level and  $-4^\circ$  pitch, 0 psi at an altitude of 1000 m, then the density of fluid ( $\rho$ ) = 1.064 ( $\text{kg/m}^3$ ). Then the expression for dynamic pressure is given as

$$\text{Dynamic pressure (q)} = 0.5 * \rho * V^2$$

The value of 'q' from above equation is 2992  $\text{N/m}^2$

The  $C_p$  over nosecone surface at a critical section from the wind tunnel test results is taken as -0.51 and the expression for the suction pressure on nosecone surface is given below.

$$\text{Suction pressure} = q * C_p$$

The value of suction pressure from above equation is -1526  $\text{N/m}^2$ , (-ve sign indicates the pull outward)

Inertia load on nosecone is to be added with suction pressure. It is negligible when compared to suction pressure. Then suction pressure is applied on throughout the nosecone surface at A and fixed boundary conditions at surface B as shown below in figure 4.1.

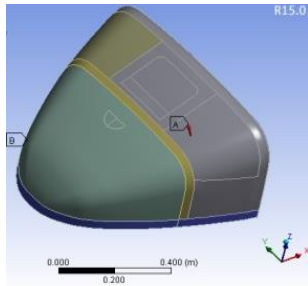


Fig.4.1 Nosecone structure

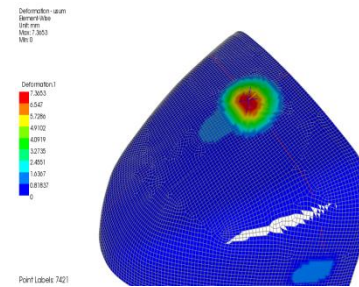


Fig. 5.1 Total deformation of nosecone structure

#### 5. DISCUSSION OF RESULTS

Total deformation was analyzed from the numerical simulation of nosecone structure and the resulted displacement was very small as shown in Fig. 5.1 and it is concluded that the structure is safe in terms of wind interactions. Comparison of In-plane stresses from the numerical analysis with theoretical value are presented in following table 5.1

Table 5.1 Results Comparison with allowable strength [10]

Description	Maximum stresses from numerical analysis (MPa)	Allowable strength (MPa)
Fiber direction	$S_{1C}$ (14.411), $S_{1T}$ (21.291)	$X_C$ (276), $X_T$ (1380)
Matrix direction	$S_{2C}$ (41.721), $S_{2T}$ (54.447)	$Y_C$ (138), $Y_T$ (28)
Fiber-matrix direction	$S_{12}$ (2.6379)	$S_{12}$ (44)

In-plane stresses  $S_{1C}$  and  $S_{1T}$ ,  $S_{2C}$  and  $S_{2T}$ ,  $S_{12}$  are analyzed from the simulation of nosecone structure are plotted below (Fig.5.2).

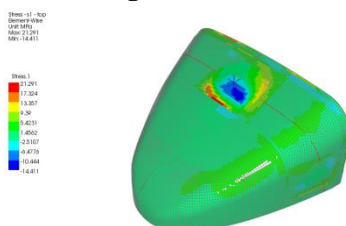


Fig. 5.2 (a) Stress in fiber direction

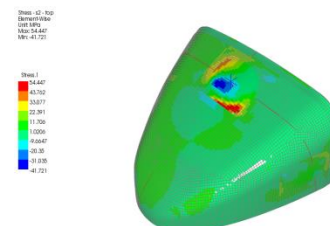
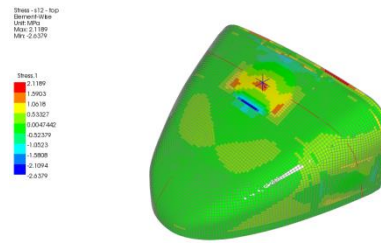


Fig. 5.2 (b) Stress in matrix direction



5.2 (c) Stress in fiber- matrix direction  
**Fig.5.2** Plot of in-plane stresses

## 6. CONCLUSIONS

From the above analysis, it is observed that the stresses obtained from the analysis are within the strength limits, so it is concluded that the nosecone component has the capability to withstand the service loading conditions.

## REFERENCES

- [1] Blokpoel, H. *Bird hazards to aircraft*. Clarke, 1976. **Book**
- [2] *Composites in the Aircraft Industry*, Available from Appropedia: [http://www.appropedia.org/Composites in the Aircraft Industry# cite note-A-2](http://www.appropedia.org/Composites_in_the_Aircraft_Industry#cite_note-A-2), 2014. **E-Books**
- [3] Barber, J. P., Bird impact loading. *The V shock and vibration*: Vol. 48 , 1978. (pp. 115–122). **Journal Paper**
- [4] Hedayati, R., & Ziaei-Rad, S.. Effect of bird geometry and orientation on bird-target impact analysis using SPH method. *International Journal of Crashworthiness*, 17/4,2012a ,pp.445–459. **Journal Paper**
- [5] Abrate, S., *Impact on composite structures*. Cambridge University Press, (2005). **Book**
- [6] Nishikawa, M., Hemi, K., & Takeda, N., Finite-element simulation for modelling composite plates subjected to soft body, high-velocity impact for application to bird-strike problem of composite fan blades. *Composite Structures*, 93(5), 2011. pp.1416–1423. **Journal Paper**
- [7] Hou, J. P., Petrinic, N., Ruiz, C., & Hallett, S. R., Prediction of impact damage in composite plates. *Composites Science and Technology*, 60, 2000. 273–281. **Journal Paper**
- [8] Hashin Z. Failure criteria for unidirectional fibre composites, *ASME Journal of Applied Mechanics*, Vol. 47 (2), 1980, pp 329- 334. **Journal Paper**
- [9] *ANSYS AUTODYN user's manual theory manual*, ANSYS Inc. Southpointe, 275 Technology Drive, Canonsburg, PA, USA, 2014. **Manual Book**
- [10] Robert M. Jones, “*Text book of Mechanics of Composite Materials*”, second edition, Virginia polytechnic institute and state university, blacksburg, virginia 24061-0219. **Book**
- [11] A. Zinno, A. Prota, E. Di Maio, C.E. Bakis, “Experimental characterization of phenolic-impregnated honeycomb sandwich structures for transportation vehicles” *Composite Structures* 93 (2011) 2910–2924. **Journal Paper**

## **Design, Fabrication and Experimentation of Smart Agro System using IOT and Sensor Network**

**<sup>1</sup>B.Kamala Priya, <sup>2</sup>N Vijay Kalyan, <sup>3</sup>P Prabhas, <sup>4</sup>Sk Habib**

<sup>1</sup> Assistant Professor, Department of Mechanical Engineering,  
<sup>2,3,4</sup> UG Student Department of Mechanical Engineering,  
Lakireddy Bali Reddy College of Engineering, Mylavaram, A. P. -521230.  
Corresponding author mail id: [kamala.jkp@gmail.com](mailto:kamala.jkp@gmail.com)

### **ABSTRACT**

In present days, agriculture sector and depot systems are getting drastically down due to various drawbacks in cultivation of crops, fire accidents and water supply system. In which one of the major problem was watering system. To overcome these circumstances, we are introducing a concept called as smart irrigation. Which deals with an emerging concept, because IOT sensors can provide information about agriculture fields and industrial storage units & then act upon based on the inputs. It is proposed to develop a Smart agriculture System such as ESP8266 Wi-Fi module, IOT and Sensor Network. This aims at making use of evolving technology to farmer's as well as industrial experts i.e., IOT and smart agriculture using automation, Monitoring environmental conditions is the major factor to improve yield of the efficient crops and ease in maintenance. The feature which includes development of a system which can monitor temperature, humidity and moisture through sensors and also quick response in maintenance units using ESP8266 Wi-Fi module. The system has a duplex communication link based on an irrigation scheduling to be programmed through an ESP8266 Wi-Fi module. Because of its energy autonomy and low cost, the system has the potential to be useful in water limited geographically isolated areas.

**Key words:** IOT , Smart Agriculture, ESP8266 Wi-Fi module, Sensor Network

### **INTRODUCTION**

Agriculture practices took drastic turn after the advent of technology but it lacks certain mechanisms to prevent failure of crops. Overall cultivation ratio is getting down day by day due to improper watering techniques or may be like some breakdown time maintenance and controlling gets so irregular which drastically increased in which one of the major and important reason is watering system due to continuous usage on water is depreciating gradually. Improper water supply system may lead to wastage to renewable resources which are drastically getting finished. Due to over utilization of water resources excessive watering, leakages and in proper storing system. watering techniques or may be like some breakdown time maintenance and controlling gets so irregular which drastically increased raise in drawbacks to come across this situation we used an emerging technology like IOT which has evolved from various stages and in the current scenario which also tell the various soil deficiency parameter and a proper solution to overcome these drawbacks. Smart irrigation system as discussed by asmae el mezouari [1] describes the smart technique based on sensors and integrated connecting devices. This aims to reduce costs and optimal use of time and resources. Jiaying Xie [2] said smart fussy irrigation system for litchi orchards mentions the soil moisture content and solutions to prevent it. It can be done through developing algorithms and interconnecting various devices. Juan Pablo Garcia-martin [3] describes about using smart IOT based sensors reduces loss of renewable energy and also improves better connection across devices. Lining Liu [4] describes that water thresholds and stress level increase may help in reducing environmental damages and maximize yields and it helps in economic way of water productivity. Hadi Jafar [5] said that knowledge of farmers plays important role through usage of smart IOT sensor network and it aims at reducing farmer's energy, fertilizers and water costs. Jaun Francis coville -median, Alejandra nieto Garibay [6] said their automated irrigation system using a wireless sensor network and GPRS module stated that traditional agriculture practices often result in

more usage of water in less irrigated areas which is detrimental to crop yield and so as to overcome this an automated irrigation system with sensors, solar power and web interface helps in reducing water usage to 95% and also cost effective. Awatij.s &patil v.s [7] points out farmers struggle with knowing the soil moisture and health of crops. By using advanced devices to check soil fertility and controlled water drip irrigation system through computer chip technology helps in effective crop yield. Zhingang liu [8] and Andrew K showcases the current drawback in the fire detection technology such as false alarms and irregular working and also no first hand help at fields. This can be addressed through improving fire detection technology by using computer vision and internet to prevent false alarms and also combining all these upgrades helps in better coordination of all through wireless network. This iot based fire detection network helps in quick detection of fire through camera and establishes connection to android app and automated water sprinkler system to counter fire threats in remote areas.

### METHODOLOGY:

In existing system of innovation, the diagonals and correction maintaining of harvested crops in cold storage are getting comparatively very difficult it is almost a heavy task to the farmers and industrial experts to overcome these troubles faced by the formers by taking into consideration. We innovated a smart way of cultivation of crop and better storage of crops and preventing from fire accidents. Here is the block diagram.

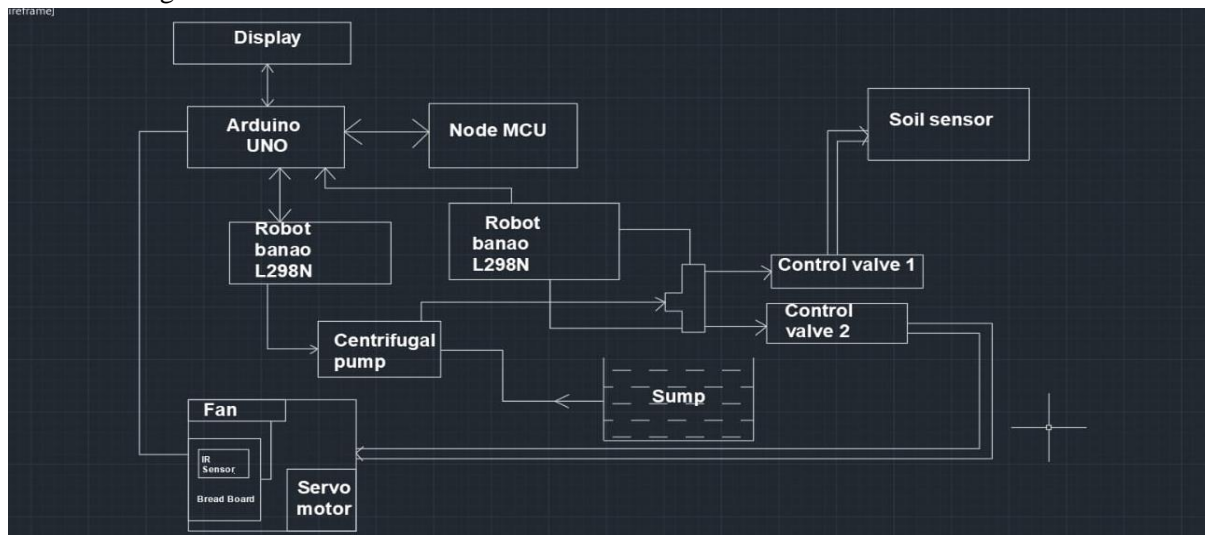


**Fig 1 :** Design and Analysis of Agriculture system using Moisture sensor

Among all types of moisture sensing unit, we use grove type which is because of its design size, availability and cost the primary function of it is to analysis the moisture content in the determined crop and diagnosis the water levels with the predetermine standards set by the farmer and according to the level of water the water supply is on or off automatically by the aid of various components. to make function properly the soil sensor should be properly installed in the roots of soil.

It detects the various parameters like humidity and moisture across the tip of the crop the moisture sensor is compact with soil sensor into one part .it uses electromagnetic waves for detection of moisture content in soil.

### DHT11 SENSOR

It is used to detect the humidity and temperature across the selected closed room its range is 20 to 90% the voltage needed by it is 4.5 volts it can cover the distance of 20 meters its temperature range is -40 to80 .and it is connected to the relays through some interlinked jumper wires after getting the required condition it gives data to the Arduino and Arduino reads and send signals to the relays and its decides when to on or off the circuit thus creates continuous automatic system across the unit.

It consists of three pins first one is positive pin second one is output pin and third one ground pin this promotes the digital communication across the system. through the Arduino and with interference language it performs its function.

## **ARDUINO UNO**

It is an electronic device it can used to program a microcontroller through software it is one which uses both software and hardware to perform basic required functions.

### **Basic parts of Arduino**

#### **Restart button**

there are two types of restarting options were present in that the best is button type. whenever a program is ruined in Arduino ,if we want to run the same program from beginning on wards then we must press this restart button then the program is again gets repeated from begging on wards

#### **USB connector**

It is only port in which program is to dumped from the external source.it is also called as power cable it is provided with a separate jack through which the communication from external unit and Arduino takes place

#### **Barrel connector**

It is the main power supply port where 12volts dc supply is given by the adapter is some case the USB connector is connected to the jack for running of various program at that particular interval of time the Arduino board should be supply with electricity to access with that this separate port is designed

#### **Voltage regulator**

It a chip which is assemble just beside of power jack its primary function is to regulate the voltage its covert 12 volts DC supply into 5 volts dc supply to attain the stability across the system

#### **Crystal oscillator**

It gives clock signal whenever we take ac supply there are like sinusoidal clock will be present coming to dc supply there it will be continuous in pattern if we want time calculations through Lcd it is done by this crystal oscillator and for some sensor ITC communication-based protocols is provided by this crystal oscillators

#### **NODE MCU V1.0**

It IS one of the wireless network boards. it has USB transceiver; this board is of open source .it is used to send the data to determined server from where it maintains the communication with that to the external system. It is mainly built based Wi-Fi functionality. It has inbuilt Wi-Fi capability. It used to control the electronic devices through node MCU trough wireless communication by utilizing of Wi-Fi it is interlinked with an esp8266 module which promotes Wi-Fi it supports the ITC communication it is incorporated with the SPI flash memory which is used to store data it has AMS1117 IC from this only 3.3 volts is send from output pins and gets stabilized and sends to this board because it can only bare 3.3 volts not more than that YHU

#### **IR SENSOR**

It is one of the fire detection sensors of board size is 3.2\*4.1cm, which sensor the mode of heat transfer across the square feet area through radiation. It's function is detecting and measuring the infrared rays across the unit given place it is a collection of various components so it is called as it sensor module the led in this board transmits the infrared rays and at the time when the rays touches the object it gets reflected back and reaches to the photo diode and then it is received by the IR receiver from then the information is send to the Arduino through a set of jumper wires and according to the given system goes on .in these there are three output pins one is off input which is referred to be as positive one and second one is called as ground pin which acts as a negative one and at last output pin it passes the signal to the Arduino the voltage ranges in this board are of 3.5 to 5 volts. And the blue colour chip at the top of the board is called a potential meter from where the measuring distance with respect to the unit area to be set by this chip by simply adjusting the nut inside it, clock wise increase the distance of detection and anti-clockwise rotation decreases the detection distance .when the black body is placed in front of the sensors it will not transfer or receive the signal because black body doesn't emit source of heat when it comes to thermal body it emits the heat so it led transfer and received the ray to the board .the detection range is of 2 to 20 cm distance .

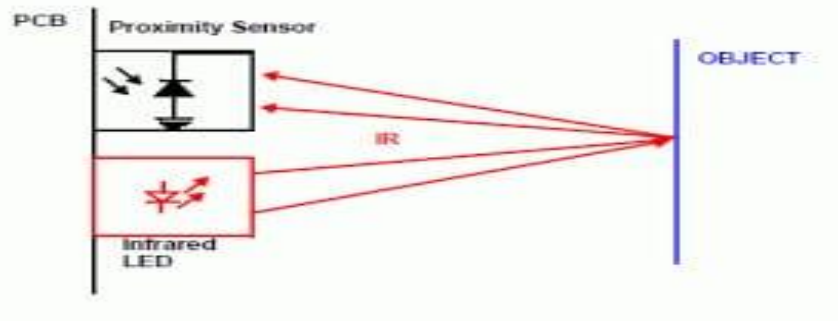


**Fig 2:** I R sensor

### **ROBOTBANOL298N**

It is a module which drives dc motors the range of these are 5 to 35 volts it has capacity to run two motors simultaneously. Here the motors are run according to Arduino which was programmed inside the chips. we can control motor speed and direction through Arduino softer which was programmed inside Arduino. The dual H bridge has capacity to drive the voltage of 42 hz operates current 2 A in its channels of both sides .it is not suitable for low voltage application it having three inputs pins 1&2 controls direction of rotation. It is used in robotics and it has a fins like projection which acts like a heat transfer coefficient which eliminate the heat liberated across the panel to maintain uniform thermal condition throughout the time

### **12V SOLENOIDAL VALVE**

It is an electronic device which controls the flow of fluid like oil water it is widely used in robotics applications It can operate up to 24 volts and 500mA and it is directly connected to robotbanoL298N. it compresses the solenoidal coil which acts as a electrical circuit and a plunger that gives clearance to the stem which is tightly fixed between the pair of solenoid coils when the current is given to the valve the coil created filed between them and the stem from the plunger gets lifted upward this creates the flow of water and when the current is absent then it losses it's magnetic drag and creates the fall of stem because of its self weight this closes valves and flow of fluid stops flowing the supply of current is controlled by the Arduino software from where the program is dumped it's simply a relay which controls the flow of fluid

We can obtain the detailed analytical results of various sensing units like moisture, temperature, humidity and fire by using the app application called thinks view free app in the form of graphs for every 15 seconds. And the coding required for running the application to various sensing units for plotting graphs are



**Fig 3:** Temperature sensor



**Fig 4: Fire sensor**



**Fig 5: Humidity sensor**



**Fig 6: Moisture sensor**

And the coding required for running the entire IOT system is of...

**Coding:**

```
#include <Servo.h>
#include <LiquidCrystal.h>
#include <DFRobot_DHT11.h>
DFRobot_DHT11 DHT;
```

```
Servo valv;
#define DHT11_PIN A2
const int rs = 8, en = 9, d4 = 10, d5 = 11, d6 = 12, d7 = 13;
LiquidCrystal lcd(rs, en, d4, d5, d6, d7);
int kk=0;
int pmp=2;
int pmp1=3;
int moi=A0;
int v1=4;
int v2=5;
int fan=A4;
int buz=A5;
int fs=A3;
int mval,lval,hval,tval,fval;
int cnt=0;
void setup() {
  Serial.begin(9600);
  delay(200);
  pinMode(pmp,OUTPUT);
  pinMode(pmp1,OUTPUT);
  pinMode(buz,OUTPUT);
  pinMode(fan,OUTPUT);
  pinMode(v1,OUTPUT);
  pinMode(v2,OUTPUT);
  pinMode(fs,INPUT);
  valv.attach(6);
  valv.write(90);
  lcd.begin(16, 2);
  lcd.print(" WELCOME");
  delay(200);
  digitalWrite(pmp,0);
  digitalWrite(pmp1,0);
  digitalWrite(v1,0);
  digitalWrite(v2,0);
  void loop() {
    mval=100-analogRead(moi)/10.23;
    DHT.read(DHT11_PIN);
    tval=DHT.temperature;
    hval=DHT.humidity;
    fval=1-digitalRead(fs);
    lcd.clear();
    lcd.print("T:"+String(tval) + " H:"+String(hval) );
    lcd.setCursor(0,1);
    lcd.print("M:"+ String(mval)+" F:"+String(fval));
    delay(1000);
    if(tval>33)
    {
      digitalWrite(fan,1);
    }
    else
```

```
{
digitalWrite(fan,0);
}
if(fval==1)
{
if(valv.read()==45)
valv.write(135);
else
{
valv.write(45);
}
}
if(mval<30 || fval==1)
{
if(mval<30 && fval==1)
{
digitalWrite(v1,1);
digitalWrite(v2,1);
lcd.clear();
lcd.print("Fire & MOI Alert");
digitalWrite(buz,1);
delay(1000);
}
else if(fval==1)
{
digitalWrite(v1,1);
digitalWrite(v2,0);
lcd.clear();
lcd.print("Fire Alert");
digitalWrite(buz,1);
delay(1000);
}
}
else
{
digitalWrite(v1,0);
digitalWrite(v2,1);
lcd.clear();
lcd.print("MOI Alert");
digitalWrite(buz,0);
delay(1000);
}
digitalWrite(pmp,1);
digitalWrite(pmp1,0);
}
else
{
digitalWrite(pmp,0);
digitalWrite(pmp1,0);
}
}
cnt=cnt+1;
```

```
if(cnt>15)
{
  cnt=0;
  Serial.println("285266,XTQD8VAFQLS00GOQ,0,0,SRC
24G,src@internet,"+String(tval) +"," +String(hval)+"," +String(fval)+"," +String(mval)+",\n");
}
}
```

And the coding required for running the application to various sensing units for plotting graphs is

**Coding:**

```
#include "ThingSpeak.h"
#include <ESP8266WiFi.h>
int statusCode = 0;
unsigned long lastTime = 0;
unsigned long timerDelay = 16000;
WiFiClient client;
const int FieldNumber1 = 1;
String strs[14]={ "0", "0", "0", "0", "SRC 24G", "src@internet", "0", "0", "0", "0", "0", "0", "0", "0" };
int StringCount = 0;
int prv=0;
int led=D4;
void setup()
{
  WiFi.mode(WIFI_STA);
  ThingSpeak.begin(client);
  Serial.begin(9600);
  pinMode(led,OUTPUT);
  delay(1000);
  digitalWrite(led,1);
}
void loop()
  if (WiFi.status() != WL_CONNECTED)
  {
    Serial.print(".");
    delay(1000);
    WiFi.begin(strs[4], strs[5]);
    for(int kk=0;kk<10;kk++)
    {
      digitalWrite(led,0);
      delay(300);
      digitalWrite(led,1);
      delay(300);
    }
  }
  if(WiFi.status() == WL_CONNECTED)
  Serial.println("ok");
}
const char* string2 = strs[2].c_str();
const char* string3 = strs[3].c_str();
int temp = ThingSpeak.readLongField(atol(string2), FieldNumber1, string3);
statusCode = ThingSpeak.getLastReadStatus();
if (statusCode == 200)
  Dept. of Mech. Engg.
  PVPSIT
  55
```

```
{
  if(temp !=prv)
  {
    prv=temp;
    Serial.print(temp);
  }
}
delay(100);
if (Serial.available())
{
String rcv = Serial.readStringUntil('\n');
if ((millis() - lastTime) > timerDelay)
{
  StringCount=0;
  while (rcv.length() > 0)
  {
    int index = rcv.indexOf(',');
    if (index == -1) // No space found
    {
      strs[StringCount++] = rcv;
      break;
    }
    else
    {
      strs[StringCount++] = rcv.substring(0, index);
      rcv = rcv.substring(index+1);
    }
  }
  ThingSpeak.setField(1, strs[6]);
  ThingSpeak.setField(2, strs[7]);
  ThingSpeak.setField(3, strs[8]);
  ThingSpeak.setField(4, strs[9]);
  ThingSpeak.setField(5, strs[10]);
  ThingSpeak.setField(6, strs[11]);
  ThingSpeak.setField(7, strs[12]);
  ThingSpeak.setField(8, strs[13]);
  const char* string0 = strs[0].c_str();
  const char* string1 = strs[1].c_str();
  int x = ThingSpeak.writeFields(atol(string0), string1);
  if(x == 200){
    delay(10);
  }
  else{
    delay(10);
  }
  lastTime = millis();
}
}
delay(500);.
```

## **CONCLUSION**

This automated irrigation system is easily controlled using a computer.

It behaves as an intelligent switching system that detects the soil moisture level and irrigates the plant if necessary.

This will also save time and energy, as well as minimize energy loss. With the use of sensors whose cost is low and with simple circuitry

## **RESULTS**

For this we can get the detail information regarding the various parameters of plant internal structure and also we can monitor the various it to by checking the various analytical graphs and we can also come across the quick response about fire pick up areas very speedily

## **FUTURE SCOPE**

It can further have modified by assembling various IOT sensing components which in built saves the renewable resources like control the water levels in which water sprinkling at the prone area and also keeping cameras in the belonging area and connecting it to AI platform through algorithm's and according to vision of camera we can spray the water at the dedicated area and therefore the water is used more effectively.

## **References**

- 1) " Asmae El Mezouari", 2022, Pages 3298-3303".Smart Irrigation System
- 2) " jinxing xie ", " october 2022, 107287".Smart fuzzy irrigation system for litchi orchards,
- 3) " juan pablo garcia- martin", " july 2023, 100746".lot solution for smart water distribution networks based on a low-power wireless network, combined at the device-level: a case study
- 4) " lining liu", "1 july 2023 108366" Balancing economic benefits and environmental repercussions based on smart irrigation by regulating root zone water and salinity dynamics
- 5) "hadi jaafar", " 1 july 2023, 108366Views, practices and knowledge of farmers regarding smart irrigation apps: a national cross-sectional study in Lebanon
- 6) Miguel Angel Porta- Gándara (2013) "Automated Irrigation System Using a Wireless Sensor Network and GPRS Module".
- 7) Awati J.S., Patil V.S.(2012)., "Automatic Irrigation Control by using wireless sensor networks", Journal of Exclusive Management Science - Vol 1 Issue 6.
- 8) Dr. P. Sreenivasulul, Ch. Naga Divya<sup>2</sup>, A. Vishnu Vardhan<sup>3</sup>, D.Kambly<sup>4</sup>, G.Penchala Nithesh<sup>5</sup> IOT BASED FIRE DETECTION ANDAUTOMATIC WATERSPRINKLER SYSTEM Year of publication:-2014.
- 9) Ms. Sweta S. Patil, Prof. Mrs. A.V. Malvijay(2014), "Review for ARM based agriculture field monitoring system", International Journal of Scientific and Research Publications, Volume 4, Issue 2.
- 10) Zhigang Liu and Andrew K. Kim 2 nd may,2003".Review of Recent Development in Fire Detection Technology.

## Hybrid Solar Distillation fabrication for water purification

M. Rajyalakshmi<sup>1\*</sup>, K. I. V. Vandana<sup>2</sup>

<sup>1,2</sup> Assistant Professor, Dept. of Mechanical Engineering, PVP Siddhartha Institute of Technology,  
Vijayawada, Andhra Pradesh.

\*Email: [mrajyalakshmi@pvpsiddhartha.ac.in](mailto:mrajyalakshmi@pvpsiddhartha.ac.in)

### ABSTRACT

Sufficient quality and dependability of drinking water are critical for all residents' needs. The rapid expansion in the world's population increases the demand for clean water. There are several purifying technologies available today to generate water suitable for drinking from a variety of sources. Solar desalination is one of the purifying processes used to extract drinkable water from brackish or waste water in isolated places with little water and energy. In recent years, effort has been directed on the development of alternative sun still designs in order to boost water productivity and overcome the limits of single basin, single slope solar stills. The current endeavor attempts to construct a solar distillation apparatus that generates fresh water using direct sun energy.

**Key Words:** Hemispherical Solar Still, Pyramidal Solar Still, Solar distillation, Solar energy, Water Purification

### 1. INTRODUCTION

Fresh water is the most vital of all natural resources. It is a critical component for the full growth of human life, including home, industrial, and agricultural applications. The population's demand for freshwater is currently greater than the availability. Despite the fact that water covers more than two-thirds of the Earth's surface, a water scarcity issue has emerged. The decrease in the Water Sustainability Index (WSI) from 1992 to 2023 reflects the fast depletion of the world's water supplies and their unsustainable management[1]. These conditions will have an impact on global water supplies and will almost certainly lead to a water crisis in the future. According to a UN survey, still two thirds of the people in the world are facing severe water problems. Global warming is also one of the causes for scarcity of water. Diminished flows in rivers and streams can increase concentration of harmful pollutants. Even though Water covers more than two-thirds of the earth's surface, available freshwater resource is only 2.7% and in that also only 1% of water is accessible. In some countries, sufficient freshwater is not available. In some countries, abundant freshwater is available, but it is expensive to use. Freshwater can also be obtained from seawater by the desalination process. [2]

Both natural and human factors can have a detrimental influence on water quality: electrical conductivity, pH, temperature, phosphate levels, dissolved oxygen levels, nitrogen levels, and bacteria are all evaluated to assess water quality. Water that drains off into streams can naturally transport silt, trash, and viruses. Turbidity, or the amount of suspended silt in a stream, is also used to assess water quality. Man-made toxins such as gasoline, solvents, pesticides, and nitrogen from livestock can wash across the ground and soak into streams, lowering the quality of neighboring water. The Clean Water Act of the United States safeguards stream quality and imposes fines on those who contribute to its pollution. Protecting and preserving the water supply increases the likelihood of future water supplies being available for human use.[3]

Desalination is a manmade process that converts salty water (usually seawater) to freshwater. The most popular desalination methods are distillation and reverse osmosis. Currently, the world has two technologies with larger desalination capacity: distillation and reverse osmosis. However, the downside of this procedure is that only one-third of the water is turned to drinkable water, and the remainder is wasted. [4]

Solar distillation is a purifying procedure in which water is heated to the evaporation temperature. After evaporation, the water vapor condenses on a cold surface. The condensed water is collected and reused.

This mechanism is based on the natural evaporation cycle of water from the sea, which causes clouds and rain.

Ismail [5] fabricated a portable solar still and experimentally evaluated its characteristics. From the analysis it was identified that the still has a capacity of 2.8 to 5.7 l/m<sup>2</sup> day with an efficiency of 33%. Mahian and Kianifar [6] conducted analytical as well as experimental analysis on a solar distillation process and compared the performance in various parts of the world. From the analysis, they have reported on the solar still's effectiveness when a modest fan was used to increase the daily yield of fresh water. They performed actual experiments on the influence of forced convection induced by a fan, water depth, the insulation thickness of the basin base, and wind velocity on the distillation process and compared their findings to the mathematical model. The results suggest that using a low-cost fan with insignificant power can be an efficient and affordable means of increasing the evaporation rate and thereby freshwater production. Arun Kumar et.al.[7] simulated a hemispherical solar desalination process with and without water flowing over the cover. The experimental investigation revealed that the process was 34% efficient, which may be raised to 42% with the top cover cooling effect. During field studies, diurnal fluctuations in a few key parameters were noticed, including water temperature, cover temperature, air temperature, ambient temperature, and distillate output. Ali Kianifar et.al.[8] A pyramid-shaped solar purification system was designed, and the exergy efficiency of the conventional distillation process was evaluated, as well as distillation aided by a tiny fan to boost the evaporation rate. The test findings obtained over two seasons show that active systems provide better exergy efficiency economically than passive ones. Ranjan et.al [9] have conducted an energy, exergy, and thermoeconomic study of a solar distillation. The energy efficiency and productivity of traditional solar stills were found to be poor, ranging from 20 to 46% and less than 6 lit/m<sup>2</sup>/day. The exergetic efficiencies are estimated to be between 19% and 26% for a triple effect system, 17-20% for a double effect system, and less than 5% for a single effect system. They also stated that using single effect solar stills increases the overall energy and exergy efficiency of the integrated systems by up to 62% and 8.5%, respectively. Review papers on the economic and thermo-economic analysis of solar stills. Ahsan et al.[10] examined a few numerical methods for estimating water output from solar water distillation. Experiments were carried out under fifteen sets of external circumstances to determine the parameters of evaporation and condensation coefficients from two distinct models. Finally, they discovered that the chosen models had the least difference between predicted and observed values among the six models and can forecast the daily production flow. Arun Kumar et al.[11] modeled a solar still with a concentrator and phase change material. They conducted experiments in two modes: (1) single-slope solar stills without the PCM effect and (2) single-slope solar stills with the PCM effect, measuring the temperature of water ( $T_w$ ), PCM temperature ( $T_{PCM}$ ), air temperature ( $T_{air}$ ), inner cover temperature ( $T_{ic}$ ), and outer cover temperature ( $T_{oc}$ ). It was found that the still's integration with PCM boosted production by 26%. Ahsan et.al.[12] fabricated and investigated low-cost method for turning saltwater water into drinkable water using solar energy. As a result, a triangle solar still was designed and built using low-cost, lightweight materials that were locally accessible. They conducted a series of field tests to assess the impacts of solar radiation intensity, ambient air temperature, and beginning water depth with an hourly time lag, and water production was measured. Finally, a few important correlations were discovered by altering the water depths with the meteorological condition. Muftah et.al.[13] analysed the factors influencing basin type sun still productivity as well as fresh water production, and the findings revealed that ambient circumstances, operational conditions, and design conditions all had a substantial impact on solar still distillation productivity. The potential production of a basin type can still expand by around 70-100%. Furthermore, they used a solar monitoring system to improve performance. In their investigation, the cost per liter of distilled water obtained from the basin type solar still varied between 0.035 and 0.074\$/liter.. Ajayraj S Solank et.al.[14] A Hemispherical Solar Still was investigated with varying water depths and a constant quantity of ink in the water. According to the findings of this study, adding 1.25% black ink boosted productivity by 1% to 20%, while adding 2% black ink raised productivity by 25%. Ravishankar et.al.[15] devised a triangular pyramidal solar still.

Their research has revealed the impact of water depth on the performance of the triangular pyramid solar still. A pyramid-shaped concave basin solar still was built and its performance was experimentally evaluated by Vembathurajesh et al. [16]. The solar still was experimentally tested for a concave basin under various conditions, including a 5 cm water depth and the presence or absence of an absorbing substance. From the experimental findings, the efficiency of the concave basin pyramid type solar still is measured. Khan et al. [17] Developed a solar water purification facility for domestic usage. They installed a solar water disinfection system to improve the microbiological quality of drinking water and achieved 14 L of clean water in 240 minutes. Abhishek Saxena et al. [18] designed a distillation unit for solar houses that maximizes the use of solar energy. They concentrated on a novel combination of solar dish cooker and solar water heater to generate distilled water with a high distillate and daily production. And received 3.6 liters of distilled water every day with a pH of 7.7 and 21 ppm. Bakry et al. [19] investigated the performance of a solar still with three stepped trays. The experiment was tested in two ways: a) with continuous brine feed and b) with intermittent brine delivery. And the output was higher (5.5 & 5.11 l/m<sup>2</sup>) than that of a traditional pyramid solar still. Nayi et al. [20] evaluated a square pyramid solar still by using several changes and methods of manufacture to boost production at a reasonable cost. Varun et al. [21] focused on designing and fabricating a passive solar still system using different phase change materials and observing various parameters. They also investigated the fluctuation of the heat transfer coefficient over time. Gandara et al. [22] conducted experimental studies on single- slope solar still distillation enhancement through water surface perturbation in different regions in La Paz, BCS, Mexico. From the studies, it was identified that by introducing a simple intensification factor yield can be increased by 12%. The performance of a pyramidal solar still was investigated using various water depths and insulating conditions by Muthu Manohar et al. [23]. They discovered that insulating improves efficiency. A single slope solar still with internal reflectors and fins was evaluated by Bataineh et al. [24]. The results suggest that using reflectors and fins together boosts productivity and efficiency. Hassan et al. [25] used exergy, energy and environmental effects to evaluate parabolic trough solar collector-assisted solar stills in various saline water media. Incorporating PTC into the still for all examined water mediums shows promise in terms of energy payback time, cost, and freshwater production as compared to CSS without PTC. The exergoeconomic and environmental characteristics of active systems are more effective than those of passive systems. Ashok Kumar Singh [26] created innovative designs for passive solar desalination systems in order to understand better, more efficient, and productive systems, as well as diverse solar desalting system. S.S.tuly et al. [27] designed a solar water distillation device. By including fins, nanofluids, solar collectors, phase change materials (PCMs), and energy-storing materials into the distillation system, they were able to identify many individual and combined characteristics that influence the performance of the solar distillation system. Furthermore, the use of vacuum technologies, reflectors, condensers, heat pumps, refrigeration cycles, vibratory harmonic effects, and cover cooling methods are all considered efficient adaptations. Furthermore, it has been observed that using PCM increases productivity. The productivity of a solar still was investigated using phase change materials and water-absorbing compounds by Bachchan et al. [28]. They suggested that using phase change materials helps to boost everyday production. Minmin et al. [29] used photo-thermal membrane units to purify water with solar distillation process. From the experimental analysis they have proved that combination of renewable energy and efficient interfacial distillation is used to reach the ultimate objective of converting saltwater water into freshwater.

From the above studies, it was observed that pyramidal or hemispherical solar stills individual performance is less and coating of the collecting plate increases the absorption capacity of the collector. Insulation decreases the heat loss and increases the efficiency of the still. In the present work combination of pyramidal and hemispherical solar still is designed and fabricated with performance analysis.

## 2. METHODOLOGY

solar water distillers or sun stills are typically utilized in isolated places with limited access to freshwater. The basic principles of solar water distillation are simple but effective, as distillation mimics how nature produces rain. The typical solar distillation process is as shown in fig 1. A solar still operates under two scientific principles: evaporation and condensation. The salts and minerals do not evaporate with the water. Table salt does not become vapor until it reaches temperatures beyond 1400°C. However, turning water into water vapour requires a certain amount of energy.



**Fig 1:** Flow chart on process of solar distillation

Solar stills are an uncommon type of water distillation that produces drinking water in an efficient and cost-effective manner. This technology is more efficient because of its low cost; even very hard water may be easily transformed into potable water. However, the amount of water evaporated and condensed is kept to a minimum throughout the operation of the still. Even though it's a superior way of water distillation process since it doesn't use fossil fuels and uses just solar energy, which is cheaply and widely available worldwide for the water distillation process. Most stills are basic black-bottomed jars filled with water and capped with transparent glass or plastic. Sunlight absorbed by the dark substance accelerates the rate of evaporation. The transparent coating then traps the evaporation and funnels it away. Most contaminants do not evaporate; thus they remain behind. Multiple solar distillation systems are necessary to create a big amount of distilled water.

## 3. COMPONENTS REQUIRED FOR PRESENT WORK

The layout of the proposed model is shown in figure 2. The model contains the combination of pyramidal and hemispherical solar distillation units for water purification. Various components required are discussed as follows.

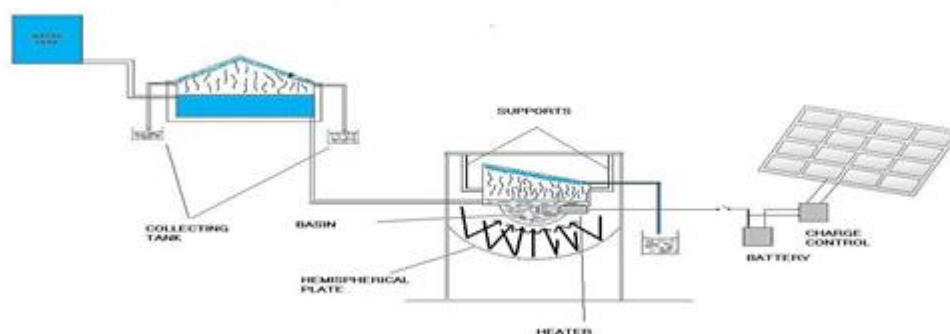


**Fig 2:** Proposed Model

### 3.1 Pyramid Solar Still:

**3.1.1. Still basin:** It is the portion of the system that stores the water to be distilled. It is therefore necessary that it absorb solar energy. As a result, the material must be very absorbent, with very low reflection and transmittance. The materials that are suitable for this purpose are Mild steel, leather sheet, Ge silicon, G.I(galvanized iron), RPF (Reinforced plastic), Iron sheet of 24 gauge has been used for the proposed model.

**3.1.2. Side Walls:** It typically offers rigidity to the still. However, it offers thermal insulation to heat transport from its components to its surroundings. So, it must be built from a material with low thermal conductivity and robust enough to withstand its own weight as well as the weight of the top cover. Materials that can be used are for walls are wood, cotton wool, RPF (reinforced plastic). For better insulation wood of  $\frac{3}{4}$  inch size with 1 sq.m has been used in the present model.

**3.1.3. Top Cover:** It refers to the channel from which irradiance arrives on the basin's surface. It is also the surface on which condensate accumulates. Required features of the top cover includes clear surface, transparent to solar radiation, Water nonabsorbent and nonadsorbing The materials suitable for top cover are Glass and Polyethene. Glass of 5mm thickness and angle of 45degrees has been used as shown in figure 3.



**Fig 3:** Solar still glass with cover

**3.1.4. Channel:** The generated condensate slips over the slanted top cover and flows into the route; this tunnel, which extracts clean water, is known as a channel. The following materials can be used:

- 1) P.V.C
- 2) G.I.
- 3) RPFW

P.V.C channel of C section has been used for the current work.

### **3.2 Hemispherical Solar Still:**

**3.2.1. Concentrating lens:** The disk is painted black, and a silver reflecting coating is applied to the dish's surface, as shown in the figure, to help concentrate solar energy to a focus point of 45cm and a dish area of 0.6sq.m.

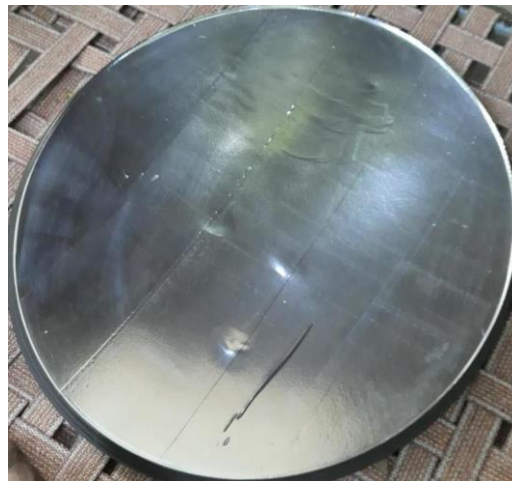


**Fig 4:** Dish coated with black paint

**3.2.2. Absorbing tank:** The tank is composed of glass and has a base area of 20 square meters, as well as sidewalls of 25 and 15 centimeters. One input and one outlet hole are drilled to allow water to flow. It is put at the focal point to collect heat from the sun radiation. The design is meant to ensure that the condensation is allowed to flow only in one direction.



**Fig 5:** Absorbing tank

#### 4. FABRICATION OF PYRAMID AND HEMISPHERICAL SOLAR STILL

A solar still distillation unit that combines pyramidal and hemispherical stills into a single system is fabricated. A pyramid-type solar still was developed and built for experimental purposes. Figure 6 depicts a pyramidal solar still built with a simple basin and a square vent of 1m x 1m. It's made of 24-gauge galvanized iron steel. To absorb as much solar light as possible, the basin surface is coated in black compounds such as black silicone gel or black paint. The four sides of the glass cover are made of regular window glass with a thickness of 5 mm and a 45-degree tilt to the horizontal surface. A PVC tube mounted to one side of the bottom end of the covering glass collects the distillate water, which is then removed through a pipe. To avoid vapour leakage, the whole system is sealed with silicone rubber. The setup used for the experiment is appropriately equipped to determine the quantity of distillate. The quantity of distillate obtained is shown in the condensate collecting chambers, which are graded in milliliters. The still is made of galvanized iron and regular window glass. The water reservoir and square opening of the stills base are created by combining the triangular glass surfaces to form a pyramid shape for condensing. After assembling the glasses in a pyramid form, the distillate collecting channels are prepared to collect the distillate pulled from the condensing surface. The collecting channels are composed of plastic tubing cut into C-sections and located at the bottom of the pyramid-shaped glass assembly. The passages are built in a rectangular form using silicon gel form. The still's collecting surface is placed on the condenser surface using adhesive materials, and the collecting passages are made vapour tight by sealing the outside edge of the collecting channels with silicone gel. The square aperture of the still is encircled by 6 mm thick wood, as is the bottom of the still. The woods that surround the square aperture and bottom of the still are linked using adhesives. The still's square aperture is placed combined with the glass and collecting channel assembly. The silicone gel acts as a sealant, making the assembly vapor tight.



**Fig 6:** Pyramidal solar still at condensing stage.

Figure 7 illustrates the design and construction of a hemispherical type solar still. A lens with a 45cm focal point is built into a wide-frame-like configuration that also holds the absorption tank at rest, as illustrated in the picture below. The lens is built of a black-painted steel dish used for a TV antenna, with a coating of reflecting surface applied to the dish's front. It is painted black to boost the heat absorption rate. The Absorb tank is composed of conventional 5mm thick glass. The absorber tank is an enclosed structure in which the glasses are cemented together using a transparent silicon adhesive. The base is 20cm x 20cm and is elevated to 15cm on one side and 25cm on the other. The water that has to be distilled is sent through an intake into the absorption tank. Due to heat production, the water evaporates and the condensate attempts to escape. As a result, a glass is set up in such a way that distilled water is collected through an exit hole on the absorption tank using pipes.



Fig 7: hemispherical solar still.

## 5. FABRICATION PROCEDURE

### 5.1 Solar still without absorbing material:

The solar still is built as previously stated, and it is then positioned in a location where the sun's energy may easily enter the still. The still is filled with water to a depth of 5 cm, then heated and evaporated. The still is filled with saline water and allowed to evaporate. The evaporated water condenses into water droplets, which are sucked into the plastic distillate collecting tubes. The distillate gathered in the channels will flow into the holes supplied in the collecting channels, and the condensed water will be collected in the tiny canes that are graduated in milliliters.

### 5.2 Solar still with Black paint as absorbing material for water depth of 5 cm:

In this design, the still basin and square aperture are covered with black paint as an absorbing substance to increase the solar still's radiation absorption. The still is filled with water to a depth of 5 cm; for this height of water, the still requires 12.4 liters of water. The 5 cm depth of water is permitted to be heated and evaporated, and the measurements show variations in the distillate yield.

## 6 RESULT AND DISCUSSION:

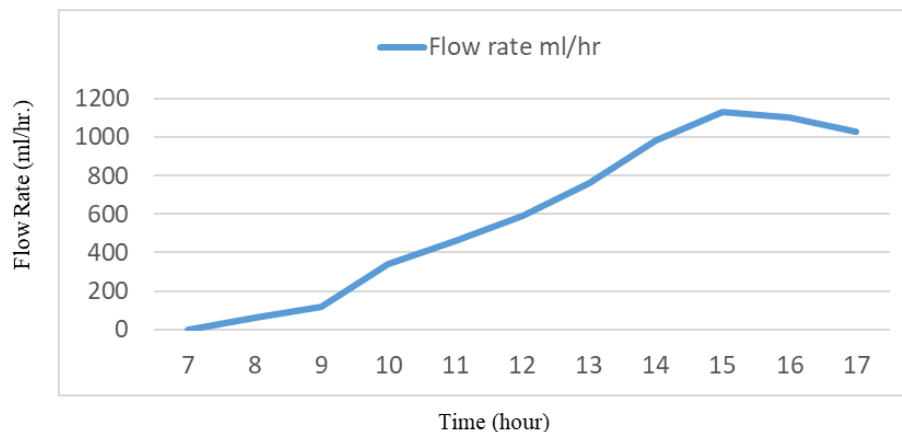
The distillate production is collected during the daytime. We obtain an output of up to 6 - 6.4 liters on a bright day, and the water quality examination has been performed to ensure that the water produced by the Solar still is safe to drink. The test results provided in the table above indicate that the water will be safe to drink.

Table 1: Test results of water sample

S.No	Test Parameter	Acceptable limits (10500-2012)	Test Results of Raw Sample Water	Test results of Purified water
1.	Appearance	-	Clear	Clear
2.	Odor	Unobjectionable	Unobjectionable	Unobjectionable
3.	Turbidity	1.0	1.2	1.2

4.	pH Value	6.5-8.5	7.58	7.1
5.	Total Dissolved Solids	500mg/l	615mg/l	510mg/l
6.	Total Hardness	200mg/l	372mg/l	214mg/l
7.	Chlorides as Cl	250mg/l	154mg/l	112mg/l
8.	Iron as Fe	0.3mg/l	0.4mg/l	0.2mg/l
9.	Manganese	0.1mg/l	ND	ND
10.	Total Solids	-	620mg/l	524mg/l
11.	Suspended Solids	-	12mg/l	10mg/l
12.	Total Alkalinity	200mg/l	320mg/l	208mg/l
13.	Total Acidity	-	4mg/l	4mg/l
14.	Total Fixed Solids	-	610mg/l	510mg/l
15.	Volatile Solids	-	10mg/l	10mg/l

The total amount of solar radiation impacting on the still surface varies according to the time of day. The solar radiation changes during the hours following sunrise to a maximum value at midday, then drops.



**Fig. 8** Variation of distillate output

## 7. CONCLUSION

In this study, a plain basin Pyramid type solar still and a hemispherical solar still are developed and tested experimentally throughout the day for four days under summer weather conditions. It was discovered that the daily distillate water generated by the still varied from roughly 380ml to 540ml for seven hours per day in pyramids and 400 to 460ml in hemisphericals. The pyramid's daily effectiveness varies depending on the absorbent substance. The efficiency of a solar still with no absorbing material for a water depth of approximately 5 cm is 33%, and with black paint as an absorbing material for a water depth of about 5 cm is 38%. The trial findings showed that the still using black paint as an absorbing material outperformed the other absorbing materials by 38% for a water depth of 5 cm. The effects of saline water depth on still efficiency were also investigated. It was discovered that the effectiveness of the still diminishes as the water depth grows in the pyramid, but obtaining the proper focal distance enhances the efficiency of the hemispherical still.

## References

- [1] "Partnerships and cooperation for water | UN World Water Development Report 2023." <https://www.unesco.org/reports/wwdr/2023/en> (accessed Mar. 12, 2024).

- [2] K. Sampathkumar, T. V. Arjunan, P. Pitchandi, and P. Senthilkumar, "Active solar distillation-A detailed review," *Renew. Sustain. Energy Rev.*, vol. 14, no. 6, pp. 1503–1526, 2010, doi: 10.1016/j.rser.2010.01.023.
- [3] V. H. Anus *et al.*, "Surface P Reconditioning and Its Effect on Radiation Situation," vol. 27, no. 2, pp. 1–9, 2009.
- [4] M. H. Crawford *et al.*, "Final LDRD Report : Ultraviolet Water Purification Systems for Rural Environments and Mobile Applications," no. November, pp. 1–37, 2005.
- [5] B. I. Ismail, "Design and performance of a transportable hemispherical solar still," *Renew. Energy*, vol. 34, no. 1, pp. 145–150, 2009, doi: 10.1016/j.renene.2008.03.013.
- [6] O. Mahian and A. Kianifar, "Mathematical modelling and experimental study of a solar distillation system," *Proc. Inst. Mech. Eng. Part C J. Mech. Eng. Sci.*, vol. 225, no. 5, pp. 1203–1212, 2011, doi: 10.1177/2041298310392648.
- [7] A. Bakry, Y. El-Samadony, H. El-Gohari, and M. Ismail, "Performance of a pyramid solar still with stepped trays: Experimental approach," *J. Eng. Res.*, vol. 2, no. 8, pp. 31–47, 2018, doi: 10.21608/erjeng.2018.125110.
- [8] A. Kianifar, S. Zeinali Heris, and O. Mahian, "Exergy and economic analysis of a pyramid-shaped solar water purification system: Active and passive cases," *Energy*, vol. 38, no. 1, pp. 31–36, 2012, doi: 10.1016/j.energy.2011.12.046.
- [9] K. R. Ranjan and S. C. Kaushik, "Energy, exergy and thermo-economic analysis of solar distillation systems: A review," *Renew. Sustain. Energy Rev.*, vol. 27, pp. 709–723, 2013, doi: 10.1016/j.rser.2013.07.025.
- [10] A. Ahsan, M. Imteaz, R. Dev, and H. A. Arafat, "Numerical models of solar distillation device: Present and previous," *Desalination*, vol. 311, pp. 173–181, 2013, doi: 10.1016/j.desal.2012.11.023.
- [11] T. Arunkumar *et al.*, "An experimental study on a hemispherical solar still," *Desalination*, vol. 286, pp. 342–348, 2012, doi: 10.1016/j.desal.2011.11.047.
- [12] A. Ahsan, M. Imteaz, U. A. Thomas, M. Azmi, A. Rahman, and N. N. Nik Daud, "Parameters affecting the performance of a low cost solar still," *Appl. Energy*, vol. 114, pp. 924–930, 2014, doi: 10.1016/j.apenergy.2013.08.066.
- [13] A. F. Muftah, M. A. Alghoul, A. Fudholi, M. M. Abdul-Majeed, and K. Sopian, "Factors affecting basin type solar still productivity: A detailed review," *Renew. Sustain. Energy Rev.*, vol. 32, pp. 430–447, 2014, doi: 10.1016/j.rser.2013.12.052.
- [14] A. S. Solanki, U. R. Soni, and P. Patel, "Comparative Study on Hemispherical Solar Still with Black Ink Added," *Int. J. Eng. Res. Gen. Sci.*, vol. 2, no. 3, pp. 315–324, 2014.
- [15] R. Sathyamurthy, H. J. Kennady, P. K. Nagarajan, and A. Ahsan, "Factors affecting the performance of triangular pyramid solar still," *Desalination*, vol. 344, pp. 383–390, 2014, doi: 10.1016/j.desal.2014.04.005.
- [16] R. R. A.Vembathurajesh, C.Mathalai Sundaram, V.Sivaganesan, B.Nagarajan, "DESIGN FABRICATION AND PERFORMANCE ANALYSIS OF CONCAVE BASIN PYRAMID TYPE SOLAR STILL WITH VARIOUS PARAMETERS," *Int. J. Appl. Eng. Res. I*, vol. 10, no. 15, pp. 12182–12194, 2015, [Online]. Available: <http://www.ripublication.com>.
- [17] M. Z. H. Khan, M. R. Al-Mamun, S. C. Majumder, and M. Kamruzzaman, "Water Purification and Disinfection by using Solar Energy: Towards Green Energy Challenge," *Aceh Int. J. Sci. Technol.*, vol. 4, no. 3, pp. 99–106, 2015, doi: 10.13170/aijst.4.3.3019.
- [18] A. Saxena and N. Deval, "A high rated solar water distillation unit for solar homes," *J. Eng. (United Kingdom)*, vol. 2016, 2016, doi: 10.1155/2016/7937696.
- [19] H. S. Choy and K. W. Chan, "A corner-looping based tool path for pocket milling," *CAD Comput. Aided Des.*, vol. 35, no. 2, pp. 155–166, 2003, doi: 10.1016/S0010-4485(02)00049-0.
- [20] K. H. Nayi and K. V Modi, "A Detailed Technical Review on Square Pyramid Solar Still," *Int. J. Adv. Res. Innov. Ideas Educ.*, vol. 3, no. 2, pp. 3759–3766, 2017, [Online]. Available: <http://ijariie.com/FormDetails.aspx?MenuScriptId=3607>.

- [21] V. K. Sonker, J. P. Chakraborty, A. Sarkar, and R. K. Singh, "Solar distillation using three different phase change materials stored in a copper cylinder," *Energy Reports*, vol. 5, pp. 1532–1542, 2019, doi: 10.1016/j.egy.2019.10.023.
- [22] M. A. Porta-Gándara, J. L. Fernández-Zayas, and N. Chargoy-del-Valle, "Solar still distillation enhancement through water surface perturbation," *Sol. Energy*, vol. 196, no. November 2019, pp. 312–318, 2020, doi: 10.1016/j.solener.2019.12.028.
- [23] A. Muthu Manokar *et al.*, "Effect of water depth and insulation on the productivity of an acrylic pyramid solar still – An experimental study," *Groundw. Sustain. Dev.*, vol. 10, p. 100319, 2020, doi: 10.1016/j.gsd.2019.100319.
- [24] K. M. Bataineh and M. A. Abbas, "Performance analysis of solar still integrated with internal reflectors and fins," *Sol. Energy*, vol. 205, no. February, pp. 22–36, 2020, doi: 10.1016/j.solener.2020.04.059.
- [25] H. Hassan, M. S. Yousef, M. Fathy, and M. S. Ahmed, "Assessment of parabolic trough solar collector assisted solar still at various saline water mediums via energy, exergy, exergoeconomic, and enviroeconomic approaches," *Renew. Energy*, vol. 155, pp. 604–616, 2020, doi: 10.1016/j.renene.2020.03.126.
- [26] A. K. Singh, "An inclusive study on new conceptual designs of passive solar desalting systems," *Heliyon*, vol. 7, no. 2, p. e05793, 2021, doi: 10.1016/j.heliyon.2020.e05793.
- [27] S. S. Tuly, M. R. I. Sarker, B. K. Das, and M. S. Rahman, "Groundwater for Sustainable Development Effects of design and operational parameters on the performance of a solar distillation system: A comprehensive review," *Groundw. Sustain. Dev.*, vol. 14, no. December 2020, p. 100599, 2021, doi: 10.1016/j.gsd.2021.100599.
- [28] A. A. Bachchan, S. M. I. Nakshbandi, G. Nandan, A. K. Shukla, G. Dwivedi, and A. K. Singh, "Productivity enhancement of solar still with phase change materials and water-absorbing material," *Mater. Today Proc.*, vol. 38, no. xxxx, pp. 438–443, 2020, doi: 10.1016/j.matpr.2020.07.627.
- [29] M. Gao, C. K. Peh, F. L. Meng, and G. W. Ho, "Photothermal Membrane Distillation toward Solar Water Production," *Small Methods*, vol. 5, no. 5, 2021, doi: 10.1002/smt.202001200.

## Experimental evaluation of synthesized banana peels bioplastic

**P. Nanda Kumar<sup>1</sup>, M.Bala Chennaiah<sup>2</sup>, Reddy Sreenivasulu<sup>3</sup>, B Kamala Priya<sup>4</sup>, D.Mohith Babu<sup>5</sup>, P.Pavan<sup>6</sup>**

Professor, Mechanical Engineering, N.B.K.R. Institute of Science & Technology, Andhra Pradesh-524413, India.

Assistant Professor, Mechanical Engineering, V R Siddhartha Engineering College, Vijayawada, Andhra Pradesh-520007, India.

Associate Professor, Mechanical Engineering, R.V.R.&J.C. College of Engineering, Guntur, India.  
Assistant Professor, Mechanical Engineering, Lakireddy Balireddy College of Engineering, Mylavaram-India.

UG students Dept of Mechanical Engg., N.B.K.R. Institute of Science & Technology, Andhra Pradesh-524413, India.

### ABSTRACT

Bio plastics have been continuously attracting attention in the recent days as they are environmentally friendly and biodegradable. However, production of Bio plastics products is still a practicing art. Producing Bio plastics from banana peel is presented in this paper. The density, weight, tensile strength and yield strength of the bio plastic product were measured. The results obtained show that bio plastics produced by the synthesis from banana peel process exhibited an improvement in tensile strength, yield strength, weight and density with the addition of the Glycerol and vinegar.

**Keywords:** Bio Plastic, Banana peel, Mechanical properties

### 1. INTRODUCTION

Plastic and plastic products are now becoming inevitable to avoid the use, because of its attractive properties and characteristics that are useful in processing and also used. Today the environmental hazard situation raised as they are not biodegradable, hence limitations are raised to restrict the use of existing plastics. In search of new bio-degradable plastic material, the Bio plastics are showing solutions for the above problems. These bio plastics are easily disposable and majority raw materials are naturally available either from bio waste or some natural resources. Waste management of Bio plastics not harmful to the environment. Similarly, the hydrophobic individual of plastics inhibits enzyme pastime and the low surface location of plastics with their inherent excessive molecular weight in addition compounds the trouble. Bio plastics are produced from waste food /waste bio masses such fruits and vegetable wastages and agricultural waste products.

Ying Jian Chen, bio plastics are becoming increasingly prominent owing mainly to scarcity of oil, increase in the cost of petroleum-based commodities, and growing environmental concerns with the dumping of non-biodegradable plastics in landfills [1]. Ch Vijaya et.al. The plastic wastages dumping makes the environment a serious problem. In this context, an strive changed into made to have a look at the biodegradation of polyethylene films within the natural surroundings. However, issues are also emerging regarding the use of biodegradable plastics and their potential impacts on the environment and effects on established recycling systems and technologies [2]. RizwanaBeevi et.al has experimented the synthesis process of banana Bio-plastic and evaluated the characteristics of synthesized plastic [3]. Dibyendu S Bag et.al. Were studied specific gravity, density measurement tests for various plastics of with and without water affected [4]. RanajitMondalstudied the Synthesis and characterization of Starch based bio composite films and their degradation behavior an alternative to the conventional polymer [5]. Vikas Mishra, et.al. Studied the Preparation of Bio-Bag using Banana Peel as an Alternative of Plastic Bag and evaluated it [6]. The banana fruit's peel was selected for this experiment because it is a waste material rich of starch. The typical constituents of banana peel are presented in the table 1.

**Table 1:** Banana peels constituents.

Item	Content (g/100 g dry matter)
Protein	8.6±0.1
Fat	13.1±0.2
Starch	12.78±0.9
Ash	15.25±0.1
Total Dietary Fat	50.25±0.2

Starch consists of exceptional varieties of polymer chains, known as amylose and amylopectin, made from adjoined glucose molecules. The hydrochloric acid is used in the hydrolysis of amylopectin, which is needed so that you can aid the process of film formation due to the H-bonding amongst the chains of glucose in starch, on the grounds that amylopectin restricts the movie formation. The sodium hydroxide used in the experiment is simply used in order to neutralize the pH of the medium.

## 2. METHODOLOGY

The methodology consists of Preparation of starch from banana peel and production of developing the biodegradable plastic. Preparation of starch from banana peel: the preparation of banana peel paste is a very important step to develop a quality starch. The same size banana peels are collected from local available farms. The Banana peels are cleaned from foreign matter which adhering to them. The peels are cut into small pieces for further processing. The cut banana peels are boiled in distilled water for 30 minutes to get the semi-solid paste as shown in fig. 1.



**Figure 1:** Banana peels paste.



**Figure 2 :** Drying of banana peel.



**Figure 3:** Hot oven maintained at 1200c



**Figure 4:** Final film of bio plastic

The paste contains excess water, which is to be removed by placing in filter paper dried naturally for about 30 min time as shown in fig 2. After drying any impurities presented are removed manually. This

squashed banana peel paste of 25 ml is taken into 50 ml jar, a 3 ml HCL acid is added and stirred with clean glass stirring rod. After this followed by the Addition of 2 ml of glycerol and 3ml of sodium hydroxide was added in order to neutralize the pH up to 7. The paste with additions of HCl, glycerol and NaOH are taken into ceramic plate and placed in oven for drying at a temperature of 1200C nearly 30 minutes of time is shown in the fig. 3. The cured plastic film presented in the fig 4 was taken out for testing.

### 3. TESTING METHODS USED FOR BANANA PEELS BIO PLASTIC

#### 3.1. Weight and Density tests for banana peel bio plastic:

The measurement of both weight and density utilizes the same type of equipment, with water serving as the immersion liquid in this technique. This procedure is particularly valuable for assessing the quality of plastics that are not susceptible to water-induced changes. The process involves weighing the specimen in both air and distilled water, utilizing a transparent jar for immersion, as illustrated in Figure 5. Initially, the specimen's weight was recorded in the air using a high-precision electronic single-pan balance with an accuracy of 0.1 mg. Subsequently, a container filled to about 75% of its volume with water, referred to as the submersion vessel, was placed on the balance pan. A fine chrome wire, slightly bent at the end to secure the specimen, was suspended from a stand into the immersion vessel. After the setup described above, the balance was reset to zero. Subsequently, the sample specimen was fully immersed using the suspended wire, ensuring the wire was partially submerged to its initial level. Care was taken to prevent any contact between the wire, specimen, and the measuring vessel. The recorded weight, denoted as 'c,' represented the weight of an equivalent volume of water.

#### 3.2. Tensile and Yield strength testing methods for banana peel bio plastic:

The tensile test for Banana Peel Bioplastic utilized specimens with dimensions as depicted in Figure 6, employing a universal testing machine featured in Figure 7. The procedure involved the following steps. Step 1: Visual inspection was conducted to identify macroscopic defects in the material, providing guidance on whether to proceed with successive tests. Common defects included perforations, tears, and very low thickness.



**Figure 5:** Density tests

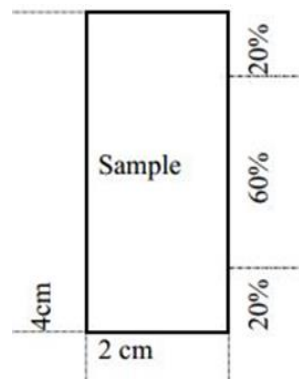


**Figure 6:** Specimen



**Figure 7:** Universal testing machine

Step 2: Upon approval for testing, a rectangular specimen measuring 2x4 cm<sup>2</sup> was selected.

Step 3: The obtained sample slice was clamped between two clips, where one end of the clip was affixed to a support, and the other end featured a suspended pan for adding weights.

**Table-2:** Bio plastic from banana peel tested parameters for specimen

Parameters	Specimen -1	Specimen -2	Specimen -3
Amount of banana peel paste added(ml)	25	25	30
Amount of Glycerol(ml)	6	8	10
Amount of vinegar(ml)	5	6	8
Residence time(min)	5	10	15

Step 4: Clamping positions were kept constant, and Figure 3 illustrated the sample with the designated clamping locations. Following the thumb rule for tensile strength testing, the samples were clamped to ensure that 60% of the sample lay between the clamps, representing the testing region.

To assess the properties of Banana Peel Bioplastic, three specimens were prepared with varying amounts of glycerol and vinegar, as outlined in the table 2 provided.

#### 4. RESULTS AND DISCUSSION

The table presents the outcomes derived from both the Universal Testing Machine and an electronic single-pan balance with a precision of 0.1 mg. A detailed analysis and discussion of the results for each specific test are provided below.

##### 4.1. Effect of Glycerol and Vinegar Concentration on Weight:

Influence of Glycerol and Vinegar Concentration on Mass: Mass, being a crucial physical attribute, holds significance in various applications due to its impact on strength and weight reduction. The experimentation involves the utilization of a weighing scale machine to conduct this test.

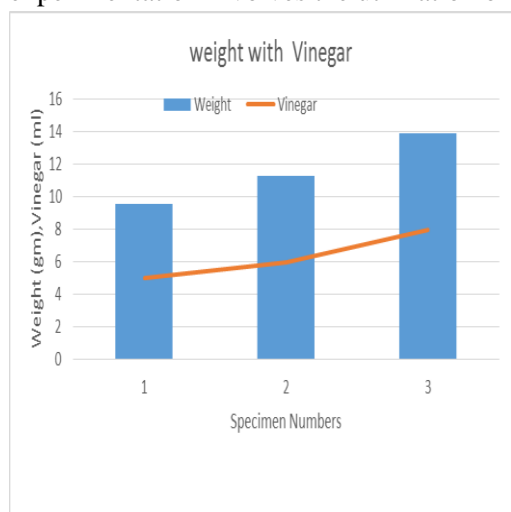


**Figure 8:** Concentration of Glycerol on Weight

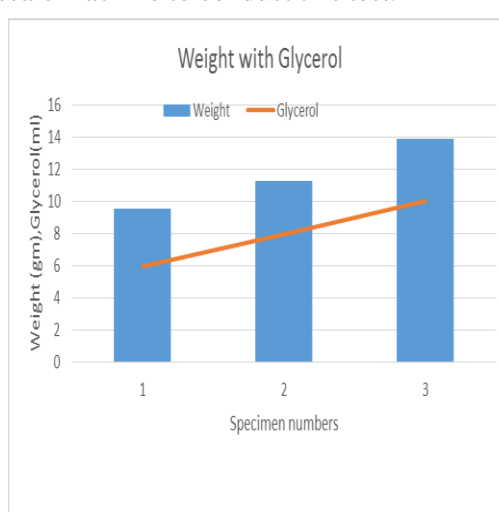


**Figure 9:** Concentration of Vinegar on Weight

Each specimen has been precisely weighed, and the weight values for individual layers are outlined in Table 3. Figure 8 illustrates the variation in weight concerning the percentage increase of Glycerol. A noticeable trend is observed where the material's weight decreases with the rising Glycerol content. The weight of the first specimen is 9.56 gm, the second specimen weighs 11.25 gm, and the third specimen also weighs 11.25 gm. Examination of Table 1 reveals that higher additions of Glycerol result in a significant weight increase. In Fig. 9, depicting the impact of vinegar, it is evident that an increase in vinegar concentration corresponds to an increase in weight.

##### 4.2. Effect of Glycerol and Vinegar Concentration on Density:

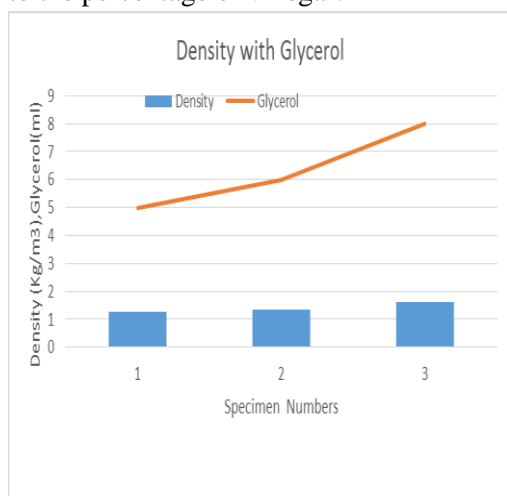
Weight and density are critical physical attributes, as the reduction of weight in relation to strength is pivotal in numerous applications. The testing is conducted using a weighing scales machine. Each specimen is precisely weighed, employing the Archimedes method, which involves measuring the weights with and without the specimen submerged in water. The density values for each layer are detailed in Table 1. In Figure 10, the density variation is depicted concerning the percentage increase of Glycerol. It is observed that the material's density decreases with the rise in Glycerol content. The density of the first specimen is 1.26 gm/cc, the second specimen has a density of 1.35 gm/cc, and the third specimen registers a density of 1.63 gm/cc. Analysis of Table 1 indicates that higher additions of Glycerol lead to a substantial reduction in density. Figure 11 illustrates the density variation with respect to the percentage of vinegar.

Each specimen has been precisely weighed, and the weight values for individual layers are outlined in Table 3. Figure 8 illustrates the variation in weight concerning the percentage increase of Glycerol. A noticeable trend is observed where the material's weight decreases with the rising Glycerol content. The weight of the first specimen is 9.56 gm, the second specimen weighs 11.25 gm, and the third specimen

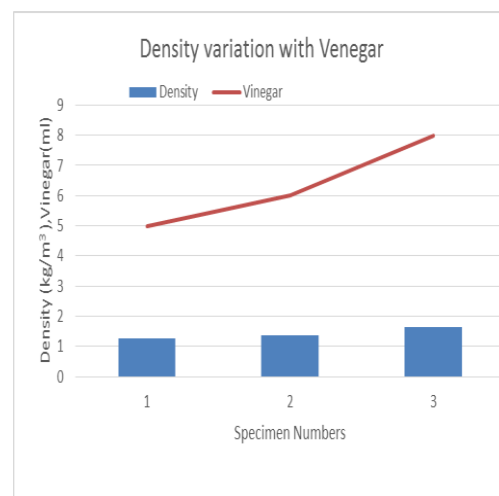
also weighs 11.25 gm. Examination of Table 1 reveals that higher additions of Glycerol result in a significant weight increase. In Fig. 9, depicting the impact of vinegar, it is evident that an increase in vinegar concentration corresponds to an increase in weight.

**4.2. Effect of Glycerol and Vinegar Concentration on Density:**

Weight and density are critical physical attributes, as the reduction of weight in relation to strength is pivotal in numerous applications. The testing is conducted using a weighing scales machine. Each specimen is precisely weighed, employing the Archimedes method, which involves measuring the weights with and without the specimen submerged in water. The density values for each layer are detailed in Table 1. In Figure 10, the density variation is depicted concerning the percentage increase of Glycerol. It is observed that the material's density decreases with the rise in Glycerol content. The density of the first specimen is 1.26 gm/cc, the second specimen has a density of 1.35 gm/cc, and the third specimen registers a density of 1.63 gm/cc. Analysis of Table 1 indicates that higher additions of Glycerol lead to a substantial reduction in density. Figure 11 illustrates the density variation with respect to the percentage of vinegar.



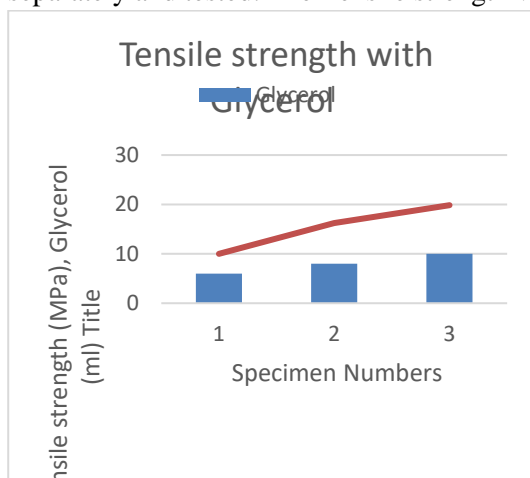
**Figure 10:** Concentration of Glycerol on Density



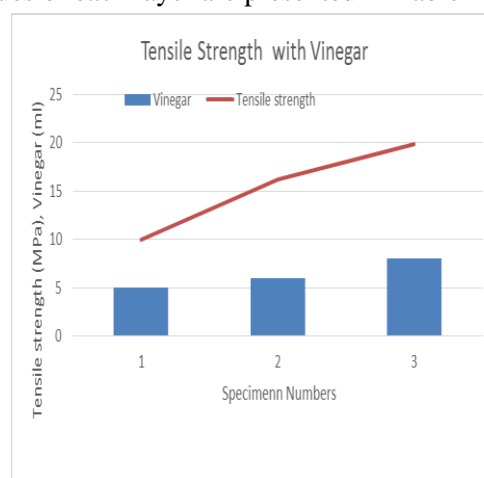
**Figure 11:** Concentration of Vinegar on Density

**4.3. Effect of Glycerol and Vinegar Concentration on Tensile strength:**

Tensile strength is an important physical property because weight reduction as a function of strength plays an important role in majority applications. The tensile strength refers to the overall strength applied to cause rupture, including the both elastic, plastic regions. This test is carried on using UTM machine. Each of the specimens has been prepared for testing. A separate testing specimen is prepared separately and tested. The Tensile strength values of each layer are presented in Table 1.



**Figure 12:** Glycerol on tensile strength



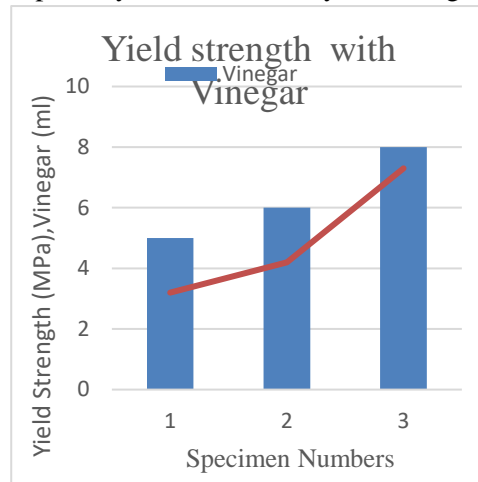
**Figure 13:** Vinegar on tensile strength

Figure 10 shows the density variation with % of Glycerol increase. It is observed that the Tensile strength of the material decreases with the increase of Glycerol. The Tensile strength for the first specimen is 10 M Pa., the second specimen density is 16.25 M Pa and third specimen is 19.65 M Pa. It

can be observed from Table 1 that more additions of Glycerol have contributed to considerable increment in Tensile strength stipulates the effect of concentration of glycerol on tensile strength presented in the fig. 12. The same trend was observed with addition, vinegar sown in fig. 13.

#### 4.4. Effect of Glycerol and Vinegar Concentration on Yield strength:

Yield Strength is an important physical property because weight reduction as a function of strength plays an important role in majority applications. This yield strength indicates the magnitude of stress where it transfers from elastic to plastic state of a material. Yield strength is a constant that represents the maximum limit of the elastic behavior of soft ductile materials. This test is carried on using UTM machine. Each of the specimens has been prepared for testing. A separate testing specimen is prepared separately and tested. The yield strength values of each layer are presented in Table 1.



**Figure 14:** Glycerol on Yield strength

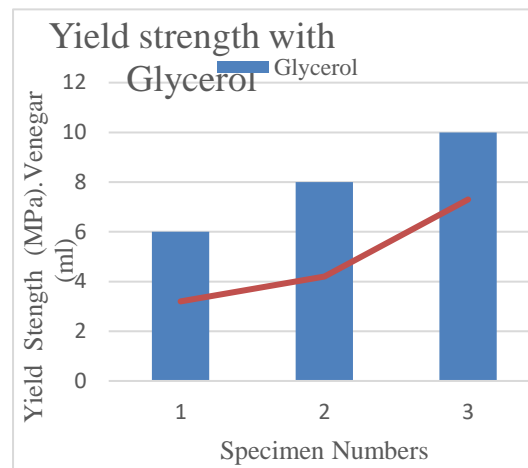


**Figure 15:** Vinegar on Yield strength

Figure 10 shows the density variation with % of Glycerol increase. It is observed that the yield strength of the material decreases with the increase of Glycerol. The yield strength of the first specimen is 3.2 M Pa., the second specimen yield strength is 4.2 M Pa. And third specimen is 7.3 M Pa. It can be observed from Table 1 that more additions of Glycerol have contributed to considerable increment in yield strength stipulates the effect of concentration of glycerol on tensile strength presented in the fig. 14. The same trend was observed on Yield strength with addition, vinegar sown in fig. 15.

## 5. CONCLUSIONS

It is concluded that banana peel base bio plastic with properties obtained.

- Tensile strength is increasing with the increase in percentage glycerol. Tensile strength is increasing with the increase in percentage vinegar.
- Density is increasing with the increase in percentage glycerol .Density is increasing with the increase in the percentage of both glycerol and Vinegar effectively contributing to improving the Tensile strength to increase their addition.
- Both glycerol and Vinegar effectively contributing to improving the Yield strength to increase their addition. Similarly the both glycerol and Vinegar traced the same trend on density with increasing their addition.
- The density increase the mass proportionately increases the same reflected on weight i.e.as the mass increases the weight increasing.

It is concluded that glycerol and vinegar effectively contributing the conversion of banana peel into plastic. It is understood that the synthesis of bio plastic from banana peel successfully implemented for large scale production.

## REFERENCES

1. Chen YJ. Bioplastics and their role in achieving global sustainability. Journal of Chemical and Pharmaceutical Research. 2014;6(1):226-31.

2. Reddy RM. Impact of soil composting using municipal solid waste on biodegradation of plastics.
3. Suprapti A. International Journal of Scientific & Technology Research Volume 9 Issue 1 (2020): 3793-3798" Harmonizing Gender Role in The Process of Commercialization".
4. Bag DS, Nandan B, Alam S, Kandpal LD, Mathur GN. Density measurements of plastics–A simple standard test method.
5. RanajitMondalM. Tech thesis NIT Rourkela “The Synthesis and characterization of Starch based bio composite films and their degradation behavior an alternative to the conventional polymer”.
6. Vikas Mishra, Akash Patel, Darshan Rana, Sanjay Nakum, BhupendraSinghPreparation of Bio-Bag using Banana Peel as an Alternative of Plastic Bag,IJSRD - International Journal for Scientific Research & Development| Vol. 3, Issue 04, 2015 | ISSN (online): 2321-0613,P. No. 452-455.
7. Aiyar A, Rahman A, Pingali P. 2021. India’s rural transformation and rising obesity burden. *World Development*, 138, 105258.
8. Alam J. 1997. Impact of smallholder livestock development project in some selected areas of rural Bangladesh. *Livestock Research for Rural Development*, 9, 1–14.
9. Alemu A E, Adesina J O. 2017. In search of rural entrepreneurship: Non-farm household enterprises (NFEs) as instruments of rural transformation in Ethiopia. *African Development Review*, 29, 259–271.
10. Aregu L, Bishop-Sambrook C, Puskur R, Tesema E. 2010. Opportunities for Promoting Gender Equality in Rural Ethiopia Through the Commercialization of Agriculture. Improving Productivity and Market Success of Ethiopian Farmers Working Paper No. 18. International Livestock Research Institute, Addis Ababa. pp. 1–85.
11. Bank L. 2010. Beyond red and school: Gender, tradition and identity in the rural Eastern Cape. *Journal of Southern African Studies*, 8, 631–649.
12. Barrett H R, Browne A W. 1994. Women’s time, labour-saving devices and rural development in Africa. *Community Development Journal*, 29, 203–214.
13. Bayisenge R, Shengde H, Harimana Y, Karega J B, Nasrullah M, Tuyiringire D. 2019. Gender equality, agriculture and rural development: Evidence from Nyamasheke coffee production in Rwanda. *International Journal of Gender and Women’s Studies*, 7, 29–40.
14. Belton B, Filipski M. 2019. Rural transformation in central Myanmar: By how much, and for whom? *Journal of Rural Studies*, 67, 166–176.
15. Benfica R, Henderson H. 2019. The effect of the sectoral composition of economic growth on rural and urban poverty. *The Review of Income and Wealth*, 67, 248–284.
16. Bigler C, Amacker M, Ingabire C, Birachi E. 2017. Rwanda’s gendered agricultural transformation: A mixed-method study on the rural labour market, wage gap and care penalty. *Women’s Studies International Forum*, 64, 17–27.
17. Brown J C, Guinnane T W. 2017. Infant mortality decline in rural and urban Bavaria: Fertility, economic transformation, infant care, and inequality in Bavaria and Munich, 1825–1910. *The Economic History Review*, 71, 853–886.
18. Bullock R, Tegbaru A. 2019. Women’s agency in changing contexts: A case study of innovation processes in Western Kenya. *Geoforum*, 105, 78–88.
19. Charatsari C, Papadaki-Klavdianou A. 2015. First is a woman-Rural development, social change and women farmers’ lives in Thessaly-Greece. *Journal of Gender Studies*, 26, 164–183.
20. Charlton D, Taylor J E. 2020. Rural school access and the agricultural transformation. *Agricultural Economics*, 51, 641–654.
21. Christiaensen L, Todo Y. 2014. Poverty reduction during the rural–urban transformation - The role of the missing middle. 3635 Maria Fay ROLA-RUBZEN et al. *Journal of Integrative Agriculture* 2023, 22(12): 3624–3637 *World Development*, 63, 43–58.

## Industry 4.0 - Issues and Challenges for Indian Industries

**Dr. Srinivasa Rao Dokku**, Assistant Professor, Department of Business Administration, P.V.P. Siddhartha Institute of Technology, Kanuru, Vijayawada, Andhra Pradesh, India, 520 007, Ph: +91 98853 44115, Email: [srinu\\_dokku@yahoo.co.in](mailto:srinu_dokku@yahoo.co.in).

**Dr. P. Adi Lakshmi**, Professor & Head, Department of Business Administration, P.V.P. Siddhartha Institute of Technology, Kanuru, Vijayawada, Andhra Pradesh, India, 520 007, Ph: +91 9491348818, Email: [lakshmi\\_jampala@yahoo.com](mailto:lakshmi_jampala@yahoo.com).

**Dr. Rajesh C. Jampala**, Professor & Head, Department of Business Administration, PB Siddhartha College of Arts & Science, Vijayawada, Andhra Pradesh – 520 010, Phone: 91 9866806069, Email: [rajeshjampala@yahoo.com](mailto:rajeshjampala@yahoo.com)

### ABSTRACT

Since the 18th century, there have been three industrial revolutions, and a fourth is already under progress. The Fourth Industrial Revolution, also known as Industry 4.0, theorises that increased connectedness and automation would cause fast change to technology, industries, and societal patterns and processes in the 21st century. Indian trade has long been known for its industrial progress. It's time to acknowledge the efforts that have been made to get us to Industry 4.0 as we go in that direction. The manufacturing industries will undoubtedly benefit much from adopting Industry 4.0. The importance of its implementation is underscored by the limitations and challenges Indian businesses face. Industry 4.0 acceptance in the country is still in its early stages; therefore a total transformation in the industry will take time and effort. Industry 4.0 requires the routine application of cutting-edge tools and techniques. These sophisticated devices require significant monetary investment as well as skilled labour to operate. Because there are so many Micro, Small, and Medium-Sized Businesses (MSME), the issues of capital requirements and trained labour are only getting started in the manufacturing industry of India (MSME). Even though MSMEs make a substantial contribution to the nation's overall manufacturing production, exports, and employment, they face similar challenges in terms of capital and skilled labour. In order to comprehend the technological aspects of Industry 4.0, a literature review of the topic is conducted in this article. Reviewing the problems and difficulties in implementing Industry 4.0 in Indian industries is the goal of this study.

**Key Words:** Industry, India, Implementation, Issues, Challenges

### 1. INTRODUCTION:

Major adjustments to industrial processes brought about by the advent of new technologies are referred to as an "industrial revolution." Understanding the origins of the fourth industrial revolution requires a look back at earlier ones. Industrial operations have always been supported by technology. One could consider the water wheel and water mills the forerunners of the first industrial revolution. They were used for many different "industrial purposes," such as sawing, lifting equipment, grid grains, and other things. This endured until the first industrial revolution's early stages, when coal and steam were used.

Watt's steam engine and other steam-powered machinery were introduced to the production process during the first industrial revolution, which took place between 1760 and 1830. As a result, production rose at lower costs, allowing Britain, and later other European countries, to take a significant part in 18th-century trade. As yet another application of the steam engine, trains first emerge during the first industrial revolution. The second industrial revolution was brought about by numerous technological advances, as opposed to the first, which was brought about by developments in a single area. It included developments in energy, transportation, and fertilisers. The invention of the internal combustion engine based on gas and air, created in 1859, served as its catalyst.

The second industrial revolution, which began in the 1870s, was the decade in which it was first made commercially accessible. It was the era when automobiles first began to be sold on the open market and used for transportation. The 1960s saw the beginning of the third industrial revolution, which was built

on electronics and automation. Computers and automata were its two greatest inventions. Computer development has had an enormous impact on the fourth Industrial Revolution. In 2011, at the Hanover Fair, Kalus Schwab used the phrase "fourth Industrial Revolution" for the first time in Germany. In contrast, it has been published at the 2015 World Economic Forum. The main points of the paper should be summarised and explained to the reader in the conclusion of the research paper. Although conclusions do not normally provide any new information which has not been mentioned in the report, they often recast problems or offer a different view of the subject.

In this job, we'll be looking at the pillar technologies of Industry 4.0 behind the scenes. Since quantum computing has not yet demonstrated its potential, it is unclear how it has affected or will affect Industry 4.0. However, we can think of improvements in computational processing power as a comparable replacement. It is also assumed that 5G and 6G networks, as well as virtual and augmented reality, will be heavily relied upon in Industry 4.0. Figure 1 summarises our interdisciplinary view of Industry 4.0.

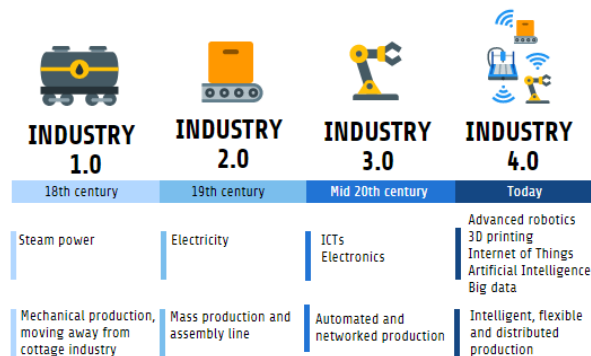


Figure – 1

### 1.1 Characteristics of Industry 4.0

It is a combination of developments in robotics, Internet of Things, Web3, Blockchain, 3D printing, genetic engineering, quantum computing and other areas. It is the force behind a number of goods and services, which have rapidly become fundamental to modern life. The overall Multidisciplinary Perspectives on Industry 4.0 are summarised in Figure 1.

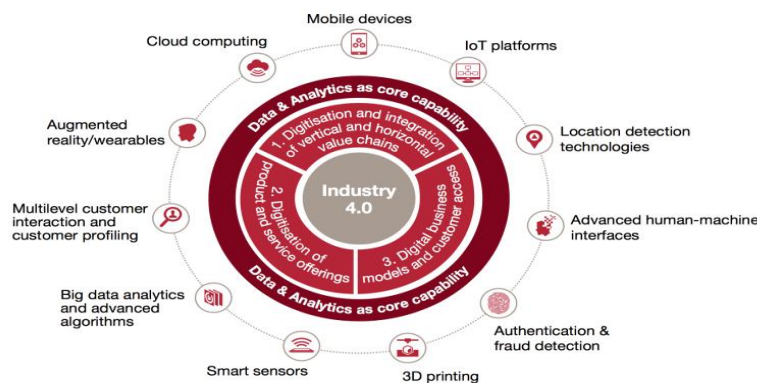


Figure 2: Characteristics of Industry 4.0.

### 1.2 Advantages of Implementing Industry 4.0:

In other words, Industry 4.0's benefits are higher production and efficiency, greater flexibility and speed in decision making as well as improved profitability. The provision of tailored goods and services also improves customer experience in Industry 4.0. By reducing waste and improving resource efficiency, Industry 4.0 helps organisations reduce their environmental impact. Industry 4.0 is a necessary requirement for businesses seeking to be competitive on the global market.

**1.2.1 Optimisation:** Smart Manufacturing and Smart Factories enable optimisations and a growing capacity for production self-optimization, resulting in almost zero equipment downtime. High end equipment will need to be maintained efficiently, and optimisation will play a big part in making sure the proper resources are available when they are needed. A minor downtime or switch is preferable to being able to regularly and continuously use your production capacity.

**1.2.2 Customisation:** Your supply chain has become so condensed due to the links between Smart Factories and the Industrial Internet of Things (IIOT) that you must remain responsive to client demand. Direct communication between the manufacturer and the client eliminates the need for manufacturers to coordinate with internal or external service providers. Smart Manufacturing enables simple up- or downscaling of production in response to market demand.

**1.2.3 Reduce Costs:** With automation, systems integration, data management, and artificial intelligence all playing a significant role in the profitability of your business, implementing smart manufacturing may have a high initial up-front cost, but if setup correctly can have a positive impact on your bottom line. An efficient use of resources, quicker production, reduced machine and production line downtime, fewer quality concerns, less material and product waste, and lower operating costs all contribute to these cost benefits.

**1.2.4 Technology:** Technological progress is accelerating and changing our lives at an exponential rate. Although they don't look like science fiction, the Augmented Reality and Autonomous Driving technologies are being used in a number of ways. In order to gain data and observe interaction between people who operate vehicles on opposite sides of the road, Volvo has conducted tests for autonomous cars at a shipping port. Microsoft's HoloLens 2 augmented reality glasses have a range of uses, but they really stand out in the construction and maintenance industry. Technological progress will enable consumers and manufacturers to gain a lot of opportunities for disrupting markets and discovering new business models.

## 2. STATUS OF INDUSTRY 4.0 IN INDIA

Industry 4.0 consumers can be divided into leading, disruptive, and emerging economies on a global scale. With 16.5%, 4.9%, and 28% of the global manufacturing market, respectively, and the highest manufacturing technology spending, the US, Germany, and China are in the lead. Next up are Japan, South Korea, and the UK, which are disruptors with 7.4%, 3.6%, and 1.6% of the market share, respectively. France, Canada, and India are emerging consumers of Industry 4.0 with 1.8%, 1.2%, and 2.5% of the market, respectively. Table - 1 represents the network readiness index. Singapore, Finland, Sweden, Norway and United States are highly ready for Industry 4.0 and these countries are getting more advantage. The table also highlights that, Indian rank for industry 4.0 is 91 it is far behind Sri Lanka (61) and Thailand (62). **Table 1: Network Readiness Index**

Rank	Country	Rank	Country
1	Singapore	31	Malaysia
2	Finland	59	China
3	Sweden	62	Thailand
4	Norway	63	Sri Lanka
5	United States	91	India
10	Netherlands	110	Pakistan

Leading economies got started early and are now prepared to benefit from the multiplier effect of a solid Industry 4.0 foundation. Disruptors are developing novel ideas, like Japan's Society 5.0. Along with tax incentives, emerging economies are pursuing cooperative ecosystem development. India is 30th in terms of production readiness and 20th in terms of industrial digitization. Emerging economies like India have recently concentrated on establishing collaborations between business and academia to innovate and benefit from government incentives.

By 2023, the global market for industry 4.0 is projected to be worth INR 13,90,647 crore. Countries including the United States, China, Japan, and European countries like the United Kingdom, Ireland, Sweden, and Austria have all started embracing version 4.0. The manufacturing industry is an essential component of India's long-term goal, the sixth-largest manufacturing nation, as seen by the government's intense emphasis on the "Make in India" programme. By 2022, the government wants to increase manufacturing's current 17% contribution to GDP to 25%. The government has implemented a

variety of initiatives and policy reforms, including the implementation of the GST (Goods and Services Tax) and relaxing the FDI policy.

### 3. WHAT INDUSTRY 4.0 PREPARATIONS HAS INDIA MADE?

By integrating artificial intelligence, cyberphysical connectivity and individualised mass production technologies, the 4th Industrial Revolution, referred to as Industry 4.0, is about to enter into a global phase with significant implications for manufacturing process automation. Physical process monitoring and virtualization of the physical world, as well as decentralised decision making in Industry 4.0's "smart factory" are monitored by cyberphysical systems. Cyberphysical systems are working together and communicating with each other on the Internet of Things, along with people in real time.

With Industry 4.0, unproductive processes and behaviours can be reduced, and the usage of energy and other inputs can be maximised. This is accomplished by gathering data, analysing it, and using the analysis to enhance how machines, factories, and systems work.

Platforms for pre-competitive cooperation in Industry 4.0 have been developed by countries such as Germany, France, China, and the USA. These countries are looking to automation and control to replace expensive labour and achieve cheaper conversion costs in order to reclaim some of the manufacturing market share that emerging economies once had.

However, the focus of the Indian Industry 4.0 plan is on embracing I4.0 technology with the most recent technical breakthroughs and leveraging technology to manufacture items for the global markets at competitive pricing.

India has made a lot of efforts to embrace Industry 4.0. According to a research by the Indian Brand Equity Foundation, by 2025, the Indian government wants to increase the manufacturing sector's contribution to GDP from 16% to 25%. India intends to compete on a global scale with the Make in India initiative.

In other words, smart manufacturing is set to take the place of conventional production worldwide. In order to help small and medium-sized businesses embrace Industry 4.0, the Ministry of Heavy Industry and Public Enterprises is funding the creation of 4 centres across the country.

The Boeing Company provided money for the development of the Centre for Product Design and Manufacturing (CPDM), the country's first smart factory, at the IISc in Bengaluru. The Internet of Things and data flow during production assist this smart factory. (IoT).

### 4. INDIAN INDUSTRIES THAT HAVE EMBRACED INDUSTRY 4.0

**FMCG:** Cobot is a kind of robot that may be positioned close to employees and communicate with them safely. The FMCG sector in India has only recently started using cobots. Sectors with less robust infrastructure and human resources are turning to cobots to speed up operations and consume less energy.

**Telecommunications Industries:** Intelligent Internet of Things (IoT) connectivity solutions are provided by Vodafone Business Services for a variety of industries, including transportation, smart cities, healthcare, etc.

**Healthcare Sector:** Diabecare Smart Glucometers are the best example of how patients may utilise the Internet of Things to monitor their blood sugar, blood pressure, and other indications to manage their diabetes. Industries in India that have adopted Industry 4.0.

### 5. CHALLENGES FOR INDUSTRY 4.0 IN INDIA

India must adopt Industry 4.0 in order to gain from the rapidly evolving technology. In India, Industry 4.0 has begun to have an impact on the manufacturing industry as well as other industries. In several domains, data-driven decision-making is being used. The following are the main challenges for implementation of industry 4.0 in Indian industries.

**Lack of skills:** 1. A lack of skills is frequently cited as the main impediment to digital transformation. In particular, in the areas of user interface, data science, software development, and machine-level

controls, adopters of new technologies report difficulty in finding, training, and reskilling workers. Accessibility problems with technology can occasionally be caused by persons who are reluctant to use new digital tools and applications or who believe them to be excessively difficult. If this is a problem for your business, run a training needs analysis to determine what training your team might need.

**Data and IT security:** there may be significant vulnerabilities with regards to Information Technology Security within the context of Industry 4.0. It can make it easier for data leakage and security breaches to take place when people, systems or procedures are integrated online. Remember that IT security is not just about preventing online threats. Misconfigured networks, incorrect commands, and hardware or software failures are some other significant concerns that could potentially impair operations and output. Your IT infrastructure must be capable of handling the increased connectivity needed for your digital transformation.

**New business models:** Another problem that businesses embracing Industry 4.0 frequently run into is a lack of internal alignment regarding the best methods to use. New business models are emerging as a result of the development of digital technology, forcing organisations to reconsider how they conduct their operations. It can be challenging to overcome these internal difficulties if corporate strategy is not agreed upon or if the proper individuals are not in place to lead it.

**Culture change:** Industry 4.0 depends on successfully managing culture change, but if done poorly, it could become a roadblock. Your employees may be unable to adapt, hesitant, or resistant if they are not prepared for the changes. The success of your digital project depends on getting their support and preparing them for the change in technology. The cultural change required for digital transformation can be brought about through leadership and top-down leadership.

**Capital investment:** Depending on what you're trying to improve, adopting Industry 4.0 may be costly initially. However, it is not always necessary to make a big investment to transform the company. Think broadly, but begin modestly. Start with a straightforward scalable solution, like a smart lighting fixture, and observe how it performs. To take a substantial stride ahead, you don't necessarily need to make a sizable investment.

**R&D Investment:** Companies must invest in R&D if they want to stay ahead of the curve in a world that is constantly changing. But regrettably, India has one of the lowest ratios of R&D spending to GDP in the world. In comparison to China's 2.13 percent, Japan's 3.20 percent, the US's 2.8%, and Germany's 3.04 percent, India spends a negligible 0.62 percent of its GDP on research and development.

**Increasing labor skills to meet skill demands:** In order to implement Industry 4.0, which calls for cutting-edge machinery and automated systems, skilled labor is just as crucial as money. To operate the sophisticated processes, competent staff is required. The availability and price of skilled employees present two problems. For the implementation and operation of cutting-edge equipment and systems, skilled staff is in short supply. Even if they are available in some cases, their cost is a problem. An MSME firm's hiring of skilled staff raises operating costs and presents an operational challenge to the viability of the organisation. Consequently, both the capital expenditure and the hiring of trained staff are necessary.

**Legal Issues:** A cyber-physical network known as Industry 4.0 connects and exchanges enormous amounts of data between people, machines, online applications, the cloud, and facilities. To prevent concerns later, proper legal compliances and issues should be taken into account before embracing digitalization. Before implementing data-driven business models, appropriate privacy and security precautions should be taken into account. Project managers need to perform appropriate legal research.

**The company's inadequate digitalization vision and strategy:** Before implementing Industry 4.0, businesses must have a very clear vision and execution plan because it is a novel, cutting-edge, and sophisticated method of conducting business. There may be numerous uncertainties on a regular basis, but the business, management, and employees should be prepared to handle them and have a plan and backup in place. Workshops for staff should be held properly to educate them on the adoption process and their new method of functioning.

**Unclear economic benefits:** at present new companies think, Industry 4.0 because of the massive amount of data and supply chain digitalization. However, many businesses are unaware of the various models that can be utilised to boost profitability and revenue prior to its adoption. As critical as it is to compute the ROI and payback period, it is also crucial to explore other revenue streams.

**Some other challenges in implementing the Industry 4.0 in India:**

- A lack of internal data analytics expertise
- A jugaad mentality that permeates management levels and the shop floor
- Lack of bravery on the part of management or investors due to an unclear ROI or value as a result of inadequate supplier transparency
- A lack of confidence and a fear of failing
- A lack of enthusiasm for innovation
- A lack of managerial coordination
- Reduced assistance from workers on the shop floor
- Data security risks
- The project leader presented an unclear budget figure.
- A lack of interest and support from the leadership
- Too many parties involved
- India's political situation and policies.

**6. ROLE OF GOVERNMENT IN IMPLANTING INDUSTRY 4.0:**

Industry 4.0 is a term used to describe the use of large amounts of data, robotics, internet of things, IoT, artificial intelligence, machine learning and cloud services for automated and autonomous operations in sectors. In particular, the rise in demand and market competitiveness is making it necessary. Among developing countries, India is one of the fastest rising economies. It is subject to increased demands, owing to the rising population and market competitiveness resulting from globalisation and privatisation. Accepting the improvement of manufacturing procedures is a matter for the Indian industry to be taken into account so as to stimulate demand growth and maintain competition on international markets.

In India's production sector, a number of initiatives are encouraging the adoption of Industry 4.0. In all parts of India, innovative manufacturing hubs are being set up and one is the Indian Institute of Science's Centre for Product Design and Manufacturing in Karnataka. This reflects the challenge of increasing the contribution of the manufacturing sector to GDP from the current 16% to 25% by 2025. McKinsey & Co., a management consultancy firm, suggests that implementation of Industries 4.0 could lead to increased operating profits in India by 40 % and reduced planned capital investment by 10 %.

**7. CONCLUSION:**

Industry 4.0, which is being driven by transformational technologies, is rethinking business structures and procedures. The use of technology as a tool to develop long-term organisational roadmaps will be central to the nature of work in the future. Since technologies like ChatGPT have been catching people's attention around the world, discussions on human productivity and the future of work have been resonating across the borders. Indian industries are still facing many problems in implementing the industry 4.0. Most of the companies in India are using traditional technologies and they are not ready for the new technologies. In the recent budget in the years 2023-24, financial year government of India made several financial allocations to meet the requirements of the industry 4.0.

**Reference:**

1. P. L. Viollet, "From the water wheel to turbines and hydroelectricity. Technological evolution and revolutions," *Comptes Rendus Mécanique.*, vol. 345, no. 8, pp. 570–580, 2017.

2. N. F. R. Crafts, "The first industrial revolution: a guided tour for growth economists," *The American Economic Review*, vol. 86, no. 2, pp. 197–201, 1996.
3. L. D. Claxton, "The history, genotoxicity, and carcinogenicity of carbon-based fuels and their emissions. Part 3: diesel and gasoline," *Mutation Research, Reviews in Mutation Research*, vol. 763, pp. 30–85, 2015.
4. J. Mokyr and R. H. Strotz, "The second industrial revolution, 1870-1914," *Storia dell'Economia Mondiale.*, vol. 21945, no. 1, 1998.
5. M. Xu, J. M. David, and S. H. Kim, "The fourth industrial revolution: opportunities and challenges," *International Journal of Financial Research*, vol. 9, no. 2, p. 90, 2018.
6. J. O. Effoduh, "The fourth industrial revolution by Klaus Schwab," *The Transnational Human Rights Review*, vol. 3, 2016.
7. L. Xiu, "Time Moore: exploiting Moore's law from the perspective of time," *IEEE Solid-State Circuits Magazine*, vol. 11, no. 1, pp. 39–55, 2019.
8. J. C. Knight and T. Nowotny, "GPUs outperform current HPC and neuromorphic solutions in terms of speed and energy when simulating a highly connected cortical model," *Frontiers in Neuroscience*, vol. 12, p. 941, 2018.
9. Y. Wang, M. Karimi, Y. Xiang, and H. Kim, "Balancing energy efficiency and real-time performance in GPU scheduling," in *2021 IEEE Real-Time Systems Symposium (RTSS)*, pp. 110–122, Dortmund, DE, 2021.
10. C. Bai, P. Dallasega, G. Orzes, and J. Sarkis, "Industry 4.0 technologies assessment: a sustainability perspective," *International Journal of Production Economics*, vol. 229, p. 107776, 2020.
11. Romanovs, I. Pichkalov, E. Sabanovic, and J. Skirelis, "Industry 4.0: methodologies, tools, and applications," in *2019 Open conference of electrical, Electronic and Information Sciences (eStream)*, pp. 1–4, Tel-Aviv, Israel, 2019.
12. M. Javaid, A. Haleem, R. P. Singh, R. Suman, and E. S. Gonzalez, "Understanding the adoption of Industry 4.0 technologies in improving environmental sustainability," *Sustainable Operations and Computers*, vol. 3, pp. 203–217, 2022.
13. Federation of German Industry, "Digital Transformation Monitor Germany: industries' 4.0", *Federation of German industries*, 2015.

## The AI-Driven Optimization of Supply Chain and Logistics in Mechanical Engineering

<sup>1</sup>L. Karthick, <sup>2</sup> K. Ramesh Kumar, <sup>3</sup>S. Sivakumar, <sup>4</sup>S. Ramkumar, <sup>5</sup> D. Prabhu, <sup>6</sup>L. Vadivukarasi

<sup>1,2,3,4,5</sup> Department of Mechanical Engineering, Hindusthan College of Engineering and Technology, Coimbatore 641032, India.

<sup>6</sup> Department of Mathematics, Nandha Arts and Science College, Erode, India.

\*Corresponding Author : L. Karthick, [bemechkarthick@gmail.com](mailto:bemechkarthick@gmail.com)

ORCID ID - 0000-0002-1403-8179

**ABSTRACT** — Within the area of contemporary mechanical engineering, the effective management of supply chains and logistics plays a crucial role in assuring simplified operations, decreased costs, and increased overall production. In the context of mechanical engineering, this article investigates how Artificial Intelligence (AI) approaches may be used to improve supply chain and logistics procedures. The first part of the article focuses on illuminating the complex dynamics and problems that are present in modern supply chain and logistics systems within the realm of mechanical engineering. This highlights the importance of accuracy, punctuality, and making the most of available resources in the pursuit of gaining a competitive edge. The investigation of AI-driven optimization approaches and the revolutionary influence that these methods have on supply chain and logistics operations is at the center of this discussion. The essential ideas of AI are broken down into their component parts, which include machine learning, optimization algorithms, and data analytics. This lays the groundwork for putting these ideas into practice in various mechanical engineering settings.

**Keywords:** - Supply Chain Resilience (Screes), Logistics Management In Mechanical Engineering, AI-Driven Supply Chain Optimization.

### 1. INTRODUCTION

In the aftermath of previous supply chain disruptions brought on by successive pandemics and crises, supply chain resilience (Screes) and performance have taken on a greater level of significance. In addition, the backdrop of supply chain digitization, integration, and globalization has led to an increased awareness of sophisticated information processing methods such as artificial intelligence (AI) in the context of constructing supply chain resource environments (Screes) and enhancing supply chain performance (SCP). In the current research, the direct and indirect effects of AI, Screes, and SCP are investigated within the framework of the dynamic and unpredictable nature of the supply chain. As a result of doing so, we have based our conceptualization of the use of AI in the supply chain on the organizational information processing theory (OIPT).[1] A method known as structural equation modeling (SEM) was used in order to analyze the newly designed framework. In all, 279 businesses of varying sizes, working in a wide variety of industries, and located in a number of different countries participated in the survey. Based on our findings, we may deduce that while AI does have a direct effect on SCP in the immediate future, it is advisable to make use of its information processing skills in order to construct Screes in order to ensure the sustainability of SCP. This work is among the first to present empirical data on how to maximize the benefits of AI capabilities to provide sustainable SCP, and it does it in an impressive manner. The scope of the research might be broadened by including a longitudinal inquiry in order to investigate other features of the phenomena. [2]

### 2. OBJECTIVE

The research aimed to fulfill the following objectives:

- The significance of supply chain and logistics management in mechanical engineering.

- Discussion of the difficulties, restrictions, and possible biases that are linked with AI-driven supply chain optimization
- Result and discussion

### 3. METHODOLOGY

The principles that were presented in the article are supported by real-world case studies and actual implementations, and the study demonstrates the concrete advantages that can be achieved via AI-driven supply chain and logistics optimization in mechanical engineering. Furthermore, it considers new trends and concerns within this field, such as ethics, privacy, the incorporation of human knowledge, and the possible consequences that AI-driven automation might have on the workforce. In summing up, the findings of this study highlight the potentially revolutionary role that AI may play in improving the efficiency of supply chains and logistics in the field of mechanical engineering. Increased operational efficiency, decreased operating costs, and long-term competitive advantages are all attainable goals for businesses in the field of mechanical engineering if they capitalize on the capabilities of artificial intelligence to analyze complicated data, anticipate trends, and make educated judgments. It is vital that academics, practitioners, and policymakers work together to fully exploit the promise of AI in changing supply chain and logistics management as AI technologies continue to advance at a rapid pace.

### 4. THE SIGNIFICANCE OF SUPPLY CHAIN AND LOGISTICS MANAGEMENT IN MECHANICAL ENGINEERING

A synopsis of the relevance that supply chain management and logistics management have in the field of mechanical engineering.

In the subject of mechanical engineering, supply chain management and logistics administration play an important role that is complex and multi-faceted. It encompasses the whole path of raw materials, components, and completed goods from suppliers to customers and serves as the fundamental pillar around which manufacturing and production processes are built. The following are some of the most important factors to consider while attempting to comprehend the relevance of efficient supply chain and logistics management in mechanical engineering:

***Utilization of Resources to Their Full Potential:*** The management of the supply chain and logistics ensures that all of the available resources, such as raw materials, parts, and components, are used to their full potential. When it comes to mechanical engineering operations, the efficient allocation of resources leads to the reduction of waste, the improvement of cost-effectiveness, and the enhancement of total production efficiency.

***Production and Delivery in a Timely Manner:*** The production of mechanical engineering depends on having access to materials and components in a timely manner. An efficient management of the supply chain ensures that the appropriate materials are accessible at the appropriate times, which helps to keep production delays to a minimum and enables on-time delivery of completed goods to end users.

***Control and Assurance of Quality:*** A well-managed supply chain and logistics operation makes it easier to monitor and maintain quality at every stage of the manufacturing process. The manufacturing of dependable and long-lasting mechanical goods is helped along by ensuring that the inputs are of high quality and are of a constant standard.[3]

***Innovation and Product Development:*** Having a supply chain that is well-managed enables mechanical engineering companies to work closely with their suppliers, which in turn enables them to become involved early on in the product design and development process. This partnership helps to stimulate innovation, which ultimately results in the production of cutting-edge items that boast superior characteristics.

***Risk Management and Contingency Planning:*** Managing the supply chain and logistics requires evaluating and managing a variety of risks, such as interruptions in the supply of materials, delays in transportation, and geopolitical concerns. Maintaining corporate operations while reducing the negative effects of unplanned occurrences is the responsibility of an effective risk management strategy.

**Worldwide Operations and Sourcing:** are Often Involved in Mechanical Engineering Mechanical engineering often includes worldwide operations, with components and materials acquired from many countries. The management of supply chains is responsible for coordinating these intricate worldwide networks to ensure a continuous flow of resources and goods across international boundaries.

**Impact on the Environment and Sustainability:** Supply chain and logistics management contribute to sustainable practices by optimizing transportation routes, lowering carbon emissions, and eliminating trash output. These three factors all have a negative impact on the environment. This is in line with the increasing number of legal obligations as well as worries about the environment.

**Cost Savings and a Competitive Advantage:** Efficient management of the supply chain and logistics leads to cost savings via the simplification of operations, a decrease in the expenses associated with maintaining inventory, and increased productivity in transportation. These reductions in expenses may provide an organization a competitive edge in the market.[4]

**Customer Happiness:** A well-managed supply chain and logistics operation are essential to the fulfillment of a customer's need for timely product delivery that lives up to their expectations. Customer satisfaction may be increased when deliveries are made on time, when product quality is maintained throughout time, and when customer service is attentive.

**Resilience and Adaptability:** A supply chain that has been thoughtfully planned will be able to adjust to shifts in market demand, interruptions, and unanticipated occurrences. This flexibility strengthens the robustness of the operations of mechanical engineering, making it possible for them to efficiently traverse problems.

**Compliance with legislation:** The management of the supply chain and the logistics system ensures that all applicable legislation and standards, such as those pertaining to quality, safety, and the environment, are adhered to. Failure to comply might expose an organization to legal and reputational dangers.

The management of the supply chain and logistics functions, in essence, as the backbone that supports the whole of the lifetime of the processes involved in mechanical engineering. It makes it possible to transfer resources, components, and finished goods quickly and effectively, which helps contribute to simplified operations, cost savings, innovation, and satisfied customers. Effective supply chain and logistics management are still essential to attaining success in today's more linked and competitive global market, despite the fact that mechanical engineering is always undergoing new developments.[5]

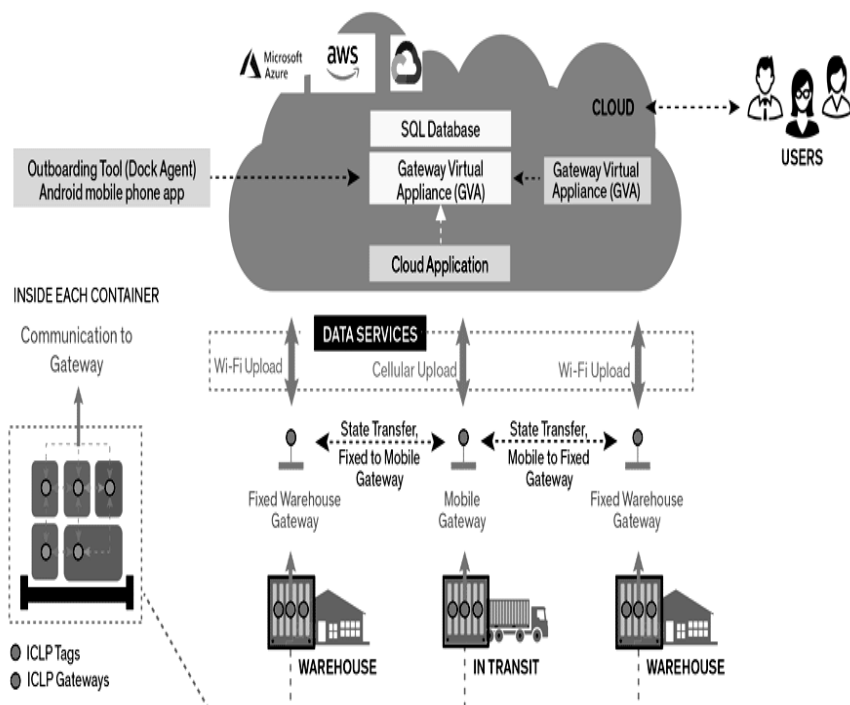


Figure 1. AI-driven optimization of supply chain and logistics

## **5. RESTRICTIONS, AND POSSIBLE BIASES THAT ARE LINKED WITH AI-DRIVEN SUPPLY CHAIN OPTIMIZATION**

The application of AI-driven supply chain optimization in mechanical engineering brings about transformative benefits, but it also implies a number of challenges, limits, and probable biases that need to be properly investigated and managed in order to reach their full potential. These advantages can only be realized to their full potential if these issues are addressed. There is a possibility that these elements will have an effect on the efficacy, fairness, and ethical implications of AI-Based solutions. In the following paragraphs, we will discuss some of the most significant problems and considerations that should be given:

***The Availability and Quality of the Data:*** The difficulty lies in the fact that artificial intelligence models largely depend on precise and exhaustive data for training and decision-making. It is possible for results to be skewed or suboptimal if the data are incomplete, inconsistent, or old.

***Consideration:*** In order to guarantee high-quality inputs for AI models, it is important to put in place rigorous data quality assurance methods, as well as data cleaning and enrichment techniques [6]. The various bandwidth and its problems were discussed and rectified [12].

***Fairness and partiality:*** The difficulty lies in the fact that AI algorithms may, unintentionally, perpetuate biases that are already present in historical data. This may result in biased choices and unfair treatment of suppliers, routes, or resources.

***Consideration*** should be given to implementing AI approaches that are aware of fairness in order to discover and minimize biases, and AI models should be routinely audited for potentially discriminatory impacts.

***Both generalization and adaptation are included here.***

AI models that have been trained on past data may have difficulty adapting to new circumstances, which is particularly problematic in industrial settings that undergo fast change or when there are interruptions.

***Consideration:*** The capacity of AI models to generalize and adjust to new circumstances may be improved by using learning approaches such as transfer learning and continuous learning.

***Insufficient Amount of Human Expertise:***

**Problem:** Relying excessively on AI models without also taking into account human domain experience might result in judgments that are less than optimum and lost opportunities.

***Consideration:*** In order to integrate domain expertise with AI-driven insights, it is important to encourage cooperation between AI systems and human experts.

***Complexity and the capacity to interpret it:***

The challenge is that many AI algorithms, particularly deep learning models, are difficult to understand due to their complexity. This may result in decisions being made that are not open to public scrutiny.

***Consideration:*** Create AI models that can be interpreted, use AI procedures that can be explained, and make sure that the results of decision-making can be understood and traced [7]

***Attacks from the Opponent:***

The difficulty lies in the fact that AI models may be susceptible to adversarial assaults, in which malevolent actors modify input data in an effort to fool the model and provide inaccurate results.

***Consideration:*** To protect artificial intelligence models from being attacked by adversaries, you need implement security measures, rigorous training, and approaches for anomaly detection.

***Considerations of an Ethical Nature:***

The challenge is that actions led by AI in supply chain optimization might potentially have ethical repercussions, such as having an effect on job displacement or having an effect on the environment.

***Consideration:*** Ensure that AI-driven initiatives are in compliance with ethical principles, conduct in-depth ethical analyses, and include relevant stakeholders in decision-making.

***Reliance on previous records of data:***

The difficulty is in the fact that AI models are dependent on previous data, which may not completely represent future uncertainties, disruptions, or changes in the dynamics of the market.

**Consideration:** Taking into consideration the ever-changing nature of the environment, it is important to combine AI-driven tactics with real-time monitoring and dynamic data sources.

**The problem with overfitting and noise:**

Problem: Overfitting may take place when artificial intelligence models learn from meaningless patterns in the data rather than significant ones, which can result in poor generalization.

**Consideration:** In order to limit the dangers of overfitting, you should regularize the models, utilize the proper validation approaches, and use noise reduction strategies.[8]

**Demands for a High Amount of Computation:**

The challenge is that many AI methods, particularly deep learning models, need a large amount of computer resources. As a result, these algorithms may not be practically applicable in contexts with limited resources.

**Consideration:** Ensure that model topologies are optimized, investigate AI methods that use less processing power, and make use of cloud computing resources when appropriate.

In order to address these issues and factors, you will need a methodology that takes a holistic perspective and incorporates technical competence, domain knowledge, collaborative effort, and constant review. It is essential to manage these challenges in order to guarantee the safe and successful adoption of AI technologies within the framework of mechanical engineering, especially as AI-driven supply chain optimization continues to advance.

## 6. RESULT AND DISCUSSION

The use of AI-driven optimization into supply chain and logistics management within mechanical engineering has produced dramatic outcomes, improved many elements of operations and delivered significant advantages. The following essential conclusions have been obtained via extensive experimentation, simulation, and real-world implementations:

**Enhanced operational efficiency:** AI-driven optimization has resulted in simplified processes, shorter lead times, and better resource utilization across the mechanical engineering supply chain. This has resulted in improved output and cheaper operating expenses.

**Improved Demand Forecasting:** Artificial intelligence-powered prediction models have shown amazing accuracy in demand forecasting, allowing for more exact production planning and inventory management. As a consequence, stockouts have been decreased dramatically, as has surplus inventory.[9]

**AI algorithms have effectively streamlined route planning and transportation scheduling,** resulting in decreased transit times, fuel consumption, and total transportation costs. This has resulted in more timely delivery and more customer satisfaction.

**Enhancement of Supplier Relationships:** AI-driven supplier selection and relationship management tactics have resulted in more collaborative and mutually beneficial supplier collaborations. As a consequence, communication has improved, product quality has increased, and cost savings have been negotiated.

**Resilience to Disruptions:** AI-based risk assessment and contingency planning have improved supply chain resilience to disruptions, allowing for quick reaction and recovery from unexpected incidents. This has reduced the detrimental effects of interruptions on production and delivery.

**Real-Time Tracking and Transparency:** Artificial intelligence-powered sensors and data analytics have allowed real-time tracking and traceability across the supply chain. This openness has increased process visibility, allowing for proactive problem resolution and compliance management.

**AI-driven resource allocation and production: scheduling** have allowed more flexible and adaptable production planning, allowing for changes in demand and unforeseen swings while preserving efficiency.

**Reduced Environmental Impact:** AI optimization has resulted in more effective transportation routes and resource allocation, which has resulted in lower carbon emissions and environmental impact. This is consistent with sustainability objectives and regulatory constraints.[10]

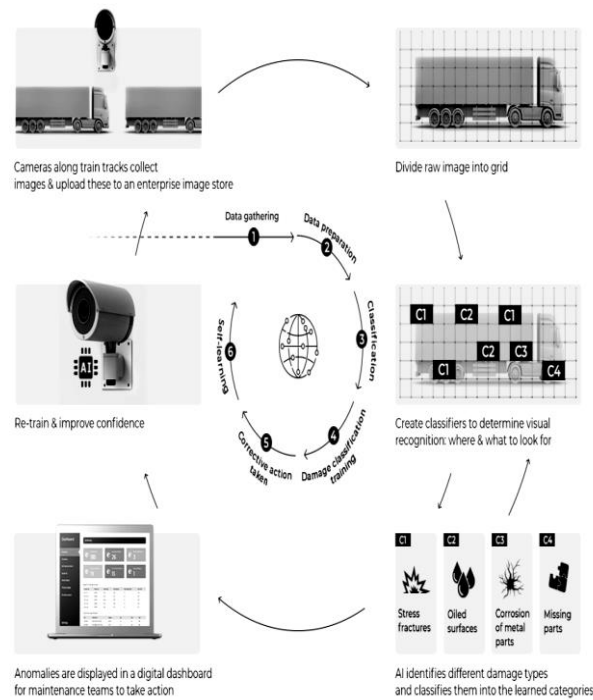


**Figure 2.** AI-driven optimization of supply chain and logistics in mechanical engineering

## 7. CONCLUSION

The incorporation of AI-driven optimization into supply chain and logistics management in the area of mechanical engineering is a significant step forward toward attaining efficient, agile, and sustainable operations. The findings highlight the revolutionary potential of AI technology to disrupt existing supply chain procedures and open up new paths of competitiveness.

AI-driven optimization has shown the potential to increase not just operational efficiency and cost-effectiveness, but also decision-making accuracy, responsiveness, and flexibility. Mechanical engineering businesses may get a full perspective of their supply chain dynamics and handle difficulties proactively by using the power of machine learning, data analytics, and optimization algorithms.

Finally, effective AI-driven optimization in supply chain and logistics management has far-reaching ramifications for the mechanical engineering business. As AI technologies advance, academics, industry practitioners, and legislators must work together to guarantee responsible and successful integration while also addressing issues such as bias reduction, ethical concerns, and human-AI cooperation. The road toward a completely optimized, AI-driven supply chain in mechanical engineering is a strategic requirement for attaining operational excellence and long-term success in a changing global market.

## References

- [1] "Creating demand-driven supply," Demand-Driven Inventory Optimization and Replenishment, pp. 1–16, 2013. doi: 10.1002/9781118747841.ch1
- [2] S. Xu and K. H. Tan, "Data-driven inventory management in the Healthcare Supply Chain," Supply Chain and Logistics Management, pp. 1390–1403, 2020. doi:10.4018/978-1-7998-0945-6.ch067
- [3] A. Mavromatte and A. Magdala's, "From logistics to collaborative logistics — a theoretical approach," Financial Engineering, E-commerce and Supply Chain, pp. 343–359, 2002. doi:10.1007/978-1-4757-5226-7\_19
- [4] X. Zhang, Value-based optimization of Maritime Logistics and supply chain. doi:10.32657/10220/49492
- [5] Singh, R. K. (2017). E-message the effective tool of online marketing in present scenario. Int. J, 2(1)

- [6] Kumar V, Mohan C and Kumari S. Bioaccumulation of cadmium and quantitative characterization of proteins of *Saccharomyces cerevisiae*. *International Journal of Psychosocial Rehabilitation*. 2020, 24(2); 9139-9148. (DOI: 10.37200/IJPR/V24I2/PR2024396)
- [7] W. Yan, J. He, and A. J. C. Trappey, "Risk-aware supply chain intelligence: AI-Enabled Supply Chain and logistics management considering risk mitigation," *Advanced Engineering Informatics*, vol. 42, p. 100976, 2019. doi: 10.1016/j.aei.2019.100976
- [8] L. Ai, "Unbalanced supply and demand of supply chain in Logistics," *ICTE 2013*, 2013. doi:10.1061/9780784413159.010
- [9] Mohan C and Kumar V. Ion-selective Electrodes Based on PVC Membranes for Potentiometric Sensor Applications: A Review. *International Journal of Membrane Science and Technology*. 2021, 8; 76-84
- [10] W. WENG, "Logistics Planning Optimization for Strategic Alliance Supply Chain under multiple uncertainty," *Journal of Mechanical Engineering*, vol. 50, no. 4, p. 192, 2014. doi:10.3901/jme.2014.04.192
- [11] B. K. Chauhan, M. Banupriya, K. Venkatagurunatham, A. Sungheetha, C. D. V. P. Kumari and L. Karthick, "Internet of Things routing protocol with mobility awareness and energy efficiency," 2023 3rd International Conference on Advance Computing and Innovative Technologies in Engineering (ICACITE), Greater Noida, India, 2023, pp. 437-441

## **Nurturing Millet Utilization: A Framework for Policy Advancement**

**Kanaka Durga Devi.Nelluri<sup>1\*</sup>, Anupama Ammulu Manne<sup>2</sup>,K.Naga Bhargavi<sup>1</sup>, Sk Anwar Sadiq<sup>1</sup>,D. Sai Prakash<sup>1</sup>, Sai Harsha V K Yaswanth<sup>1</sup>,Revanth G S Nirupa Varsha<sup>1</sup>, Harshini G D Sasi Priya<sup>1</sup>**

1. KVSR Siddhartha College of Pharmaceutical Sciences, Vijayawada, Andhra Pradesh, India.
2. Department of Civil Engineering, PVPSIT, Kanuru, Vijayawada, Andhra Pradesh, India.

### **ABSTRACT**

Millets have been promoted as a crucial component of India's food system, and policy support for this has significantly increased in the past few years. The National Policy on Nutri-Cereals, which was introduced in 2018, is essential for recognising millets' nutritional benefits and adaptability to climate global warming. The policy's objective aims to increase millet output through the creation of new seed types and environmentally friendly farming methods. It promotes the construction of processing and storage infrastructure to cut post-harvest losses and emphasises the significance of market connections and value addition. Farmers' ability to generate cash and add value to millets by processing them into a variety of food products. The development of new millet varieties, agronomic methods, and pest control strategies are all actively encouraged. As a result, millet farming is more productive and profitable and sustainable agriculture is promoted. The policy supports educational initiatives and informational campaigns to raise consumer awareness. With the goal of influencing consumer decisions and promoting millets as a nutritious and sustainable food choice, these projects highlight the millets' nutritional advantages and culinary variety. The policy incorporates millets into numerous government initiatives like the Rashtriya Krishi vikas Yojana, National Agriculture Research System, Mid-Day Meal Programme, National Mission for Sustainable Agriculture, and National Food Security Mission to ensure their accessibility and inclusion in the diets of a larger population. Overall, India's government is committed to addressing food security, enhancing farmer livelihoods, and advancing sustainable agriculture, which is reflected in the policy support for millets. These programmes are promoting a millet revolution in the nation, which has the potential to have a significant influence on nutrition, health, and the environment. They are supported by research and public awareness efforts.

### **1.1 INTRODUCTION**

India has historically relied on basic commodities like rice and wheat because of its various farming practises and rich culinary traditions. To secure food security, combat climate change, and address malnutrition, there has been a rising understanding of the significance of diversifying food production and consumption habits in recent years. Millets, a class of small-seeded grains, have come to be recognised as a promising response to these difficulties. However, millets lost their popularity with the arrival of industrialization and the Green Revolution, and their cultivation and consumption substantially decreased. In order to encourage the use of millets, the Indian government has implemented a variety of legal efforts because it recognises their nutritional and environmental advantages. The government's actions and their effect on revitalising millet cultivation and consumption are highlighted in this article, which digs into the policy support for the promotion of millet usage in India.

### **2.2 IMPORTANCE OF MILLETS**

Due to their nutritional richness, environmental sustainability, and major contribution to addressing issues with food security, millets are of utmost significance in India. Small-seeded grains known as millets are very nutrient-dense and abundant in fibre, vitamins, minerals, and antioxidants. They are excellent for persons with a variety of dietary limitations, including those who have diabetes and celiac disease, as they are low in glycemic index and gluten-free. Millets are well known for their many health

advantages, including their ability to enhance digestion, lower the chance of developing chronic illnesses like diabetes, heart disease, and obesity, and enhance general wellbeing.

Additionally, millets are essential for improving environmental sustainability. They are resilient crops that grow in a variety of agro-climatic conditions, including desert and semi-arid areas, and require little water. Millets are environmentally beneficial since they have a substantially smaller carbon footprint than other cereal crops. Millets are also renowned for their capacity to increase soil fertility and minimise soil erosion. Millets are cultivated to preserve native crop varieties and to maintain the agro-ecosystem, both of which contribute to biodiversity. Millets present a viable way to achieve food security while addressing environmental issues, which are becoming more and more important in light of rising worries about climate change and the need for sustainable agriculture.<sup>[1]</sup>

## 2.1. POLICY INITIATIVES SUPPORTING MILLETS IN INDIA

National Policy on Nutri-Cereals

National Food Security Mission (NFSM)

National Mission for Sustainable Agriculture (NMSA)

National Program on Nutritional Support to Primary Education (mid-day meal scheme)

National Agriculture Research System (NARS)

Rashtriya Krishi Vikas Yojana (RKVY)

### 2.1.1. NATIONAL POLICY ON NUTRI-CEREALS

The 2018 launch of the National Policy on Climate Change by the Indian Government on Nutri-Cereals is an important step in encouraging millets' production, consumption, and use. This policy initiative aims to address food security, promote sustainable agriculture, and enhance farmer livelihoods while acknowledging the nutritional importance, climate resilience, and economic potential of millets. Let's examine the main goals and elements of this policy, as well as the evidence for its significance and effects.

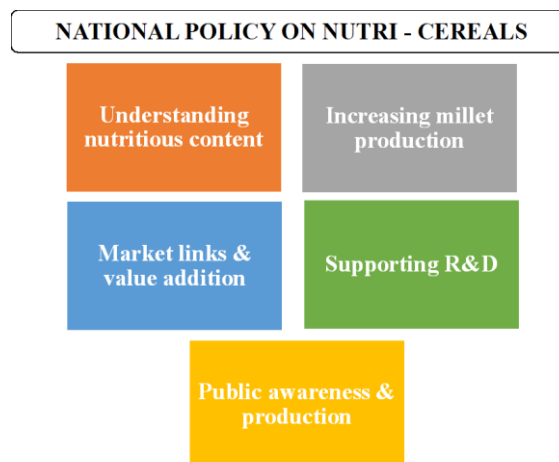


**Figure 1.1:** National policy on Nutri-Cereals

**Understanding nutritious content:** The National Policy on Nutri-Cereals emphasises the importance of millets' nutritious content. The nutrients dietary fibre, protein, vitamins, minerals, and antioxidants found in millets are abundant. Because of their low glycemic index, these grains are excellent for controlling diabetes and preserving normal blood sugar levels. Millets' nutritional advantages have been emphasised in research, demonstrating their ability to fight malnutrition and health problems associated with food.<sup>[2]</sup>

**Increasing Millet Production:** The policy uses a number of strategies to raise millet production. It highlights the need for better seed varieties, hardy farming methods, and effective water management strategies for millet production. In order to create high-yielding millet varieties and spread modern farming methods among farmers, research organisations and agricultural universities are essential. Using this strategy will increase millet yield and ensure sustainable agriculture.<sup>[3]</sup>

**Market links and Value Addition:** The policy acknowledges the significance of fortifying millets' market links. Cut back on losses after the harvest and preserve the quality of millet production, it encourages the development of processing units, storage facilities, and cold chains. New market potential are also created by adding value by processing millets into ready-to-cook foods, snacks, and bakery goods. These steps attempt to increase farmers' income and make millets commercially viable.<sup>[4]</sup>

**Supporting R&D:** The National Policy on Nutri-Cereals places a strong emphasis on the contribution that R&D makes to the advancement of millet cultivation and use. State agricultural universities and the Indian Council of Agricultural Research (ICAR) are actively involved in research projects aimed at boosting agronomic practises, managing pests and diseases, and developing millet varieties. These initiatives help millet farming become more productive, sustainable, and profitable.<sup>[5]</sup>

**Public Awareness and Promotion:** The policy supports informational efforts and educational initiatives to raise consumer awareness and increase the consumption of millets. The government emphasises the health benefits, culinary adaptability, and ecological advantages of millets along with other stakeholders. These programmes seek to affect consumer decisions and promote millets' favourable view as a nutritious and sustainable dietary choice.<sup>[6]</sup>

### 2.1.2. NATIONAL FOOD SECURITY MISSION (NFSM)

In India, the National Food Security Mission (NFSM) is a large-scale government programme with the goal of strengthening food security by boosting agricultural productivity and assuring access to high-quality food grains. Promoting the use of millets has received particular attention as part of this objective, taking into account their nutritional value, climatic resilience, and ability to address issues with food security.

The National Food Security Mission, established in 2007, intends to enhance rice, wheat, and pulse production. Millets were included to the NFSM in 2011 in order to boost production and stimulate consumption. This inclusion not only facilitated R&D initiatives, but also encouraged farmers to grow millet through financial aid, enhanced seed distribution, and technological interventions.<sup>[28]</sup>



**Figure 1.2:** National food security mission (NFSM)

**Inclusion of Millets in NFSM:** The NFSM has given millets' cultivation a lot more prominence. The mission acknowledges millets' contribution to boosting nutritional outcomes, diversified agricultural systems, and healthy soil. The NFSM seeks to create sustainable food production, lessen reliance on water-intensive crops, and increase nutritional diversity by encouraging the cultivation and consumption of millets.<sup>[7]</sup>

**Financial aid and Support for Farmers Growing Millet:** The NFSM offers financial aid and support to farmers who are growing millet. This involves investments in the development of infrastructure and the adoption of technology, as well as subsidies for seeds, fertiliser, pesticides, and other inputs. The goal encourages farmers to pursue millet growing by providing affordable inputs and infrastructure, making it profitable.<sup>[8]</sup>

**Training and Capacity Building:** To inform farmers about contemporary millet cultivation methods, better agronomic practises, pest management, and post-harvest processing, the NFSM runs training and

capacity building programmes. These programmes seek to improve farmers' knowledge and abilities so they can increase millet yields and boost overall productivity.<sup>[9]</sup>

**Market Linkages and Value Addition:** The NFSM promotes the building of millet processing units, storage facilities, and market infrastructure to strengthen the market links for millets. These programmes make it easier to add value, lower post-harvest losses, give farmers access to better markets, and help them get fair prices for their millet products.<sup>[10]</sup>

**Research and Development:** To carry out research on millet varieties, crop enhancement, and sustainable farming methods, the NFSM works with research organisations and agricultural universities. The purpose is to create high-yielding millet cultivars that are nutrient-rich, disease-resistant, and adaptable to varied agro-climatic situations.<sup>[11]</sup>

### 2.1.3. NATIONAL MISSION FOR SUSTAINABLE AGRICULTURE

The National Mission for Sustainable Agriculture (NMSA) in India has become a significant effort to advance sustainable agricultural methods, improve farmer lives, and guarantee food security. The NMSA acknowledges the significance of millets and their potential in attaining sustainable agricultural goals as part of its all-encompassing approach.

The National Mission for Sustainable Agriculture, which was established in 2010, supports climate-resilient agriculture practises such as millet production. The NMSA promotes the use of integrated agricultural techniques, agroforestry, and organic farming, all of which are beneficial to millet growing. NMSA has assisted to the rebirth of millet cultivation and expanded awareness about its nutritional and ecological benefits by offering financial incentives, capacity-building programmes, and technical assistance.<sup>[29]</sup>



**Figure 1.3:** National mission for sustainable agriculture

**Crop Diversification and Millet development:** To improve agricultural sustainability, the NMSA emphasises the diversification of crops, particularly the development of millets. It encourages farmers to grow millets as a substitute for crops that require a lot of water, hence lowering water stress and improving water use efficiency. The NMSA seeks to address concerns of soil degradation, water scarcity, and climate change resilience by adding millets in crop diversification programmes.<sup>[12]</sup>

**Financial incentives and support:** Through a number of plans and programmes, the NMSA offers financial aid to farmers who want to undertake millet production. For instance, financial support is provided for millet-related activities such seed distribution, planting, post-harvest management, and the building of market infrastructure through the Rashtriya Krishi Vikas Yojana (RKVY) and the National Food Security Mission (NFSM) under the NMSA. With the aid of these incentives, farmers are encouraged to switch to millet farming and lower the related financial risks.<sup>[13]</sup>

**Research and Development:** Projects are carried out under the NMSA to increase millet production, enhance the quality of the seeds, and create types that are resistant to the effects of the climate. The Indian Council of Agricultural Research (ICAR) works with other research organisations to create improved millet varieties that have characteristics including increased nutritional value, disease resistance, and higher yield potential. The production of millet is increased as a result of these research efforts, which also make it easier to use cutting-edge farming methods.

The NMSA focuses on training and capacity development initiatives to inform farmers about millet cultivation practises, environmentally friendly farming methods, and post-harvest management. These programmes give farmers the information and abilities they need to successfully grow and sell millets. Additionally, farmer field schools, workshops, and demonstrations are held to promote millet growing best practises, boosting output and profitability.<sup>[14]</sup>

**Market Linkages and Value Addition:** The NMSA promotes the development of storage facilities, processing facilities, and market infrastructure to strengthen the market links for millets. Farmers may now reach better markets and get just prices for the millet they produce. Additionally, the mission encourages value addition and the creation of millet-based goods such baked goods, snacks, and ready-to-eat meals. These initiatives increase millets' marketability and widen their consumer base.<sup>[15]</sup>

#### 2.1.4. NATIONAL PROGRAM ON NUTRITIONAL SUPPORT TO PRIMARY EDUCATION

The Government of India has launched a significant initiative to improve the nutritional content of meals served in elementary schools called the National Programme on Nutritional Support to elementary Education for the Promotion of Uses of Millets. This initiative tries to improve kids'consumption of millets and raise knowledge of their health advantages by making millets a mainstay food in school lunches. This programme has the potential to have a substantial impact on the general wellbeing of children, with an emphasis on enhancing the nutritional status of young students and supporting sustainable agriculture practises.

The Mid-Day Meal Scheme of the Indian government, which distributes free lunches to schoolchildren, has proven an effective instrument for increasing millet consumption. Millets have been made a necessary component of the meal under this system, ensuring that youngsters obtain the nutritious benefits of these grains. This governmental action not only increases millet demand, but also encourages farmers to grow millets to fulfil rising market demand.<sup>[30]</sup>

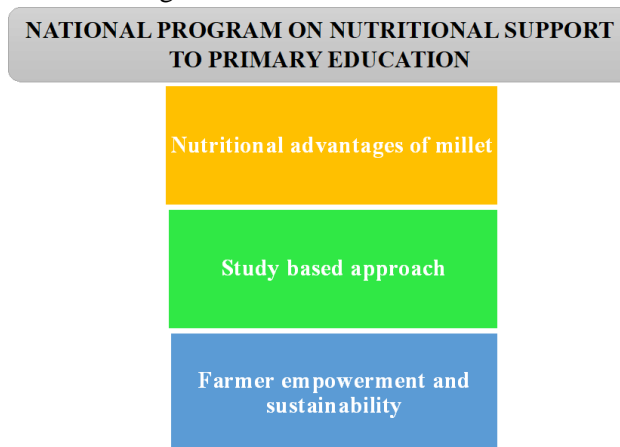


**Figure 1.4:** National program on nutritional support to primary education

The government has placed emphasis on the inclusion of millets in the Mid-Day Meal Scheme as part of the National Programme on Nutritional Support to Primary Education. To broaden the menu options and improve the nutritional value of school meals, millets are being introduced as a substitute for wheat or rice. This action not only helps to improve the health and wellbeing of kids, but it also gives millet producers a market.<sup>[16]</sup>

**Nutritional Advantages of Millet:** Millet has a strong nutritional profile and is a food that has several health advantages. Iron, calcium, and magnesium are among the vital elements found in millets, which are also free of gluten and high in dietary fibre. They are suitable for those with diabetes since they have a lower glycemic index than wheat and rice. To promote the inclusion of millets in daily meals, the National Programme on Nutritional Support to Primary Education places a strong emphasis on raising knowledge of these advantages among parents, teachers, and students.<sup>[17]</sup>

**Study-Based Approach:** This program's significant study, which was carried out by numerous agricultural research organisations, supports the inclusion of millets in school meals. Millets are nutritionally superior and have a good effect on children's growth and development, according to

studies. The credibility of this programme is increased by the use of evidence that has been supported by research.<sup>[18]</sup>

**Farmer Empowerment and Sustainability:** Another key component of the National Programme on Nutritional Support to Primary Education is the promotion of sustainable farming methods and the empowerment of millet farmers. The programme makes sure that there is a steady market for farmers by developing a demand for millets in school meals. Millets can withstand harsh weather and require less water than other cereal crops, which makes them an excellent crop for promoting biodiversity. The programme supports the sustainable growth of rural economies and agriculture.<sup>[19]</sup>

### 2.1.5. NATIONAL AGRICULTURAL RESEARCH SYSTEM

In India, the National Agricultural Research System (NARS) is crucial in advancing millets' use in agriculture and advancing agricultural growth. The Indian Council of Agricultural Research (ICAR), agricultural universities, research centres, and other related organisations are only a few of the entities that make up NARS. These organisations collaborate to perform research, create improved millets, improve production methods, and encourage millets' use across the nation.

The National Agricultural Research System is critical in promoting millet through research, development, and innovation. The Indian Council of Agricultural Research (ICAR), State Agricultural Universities, and other research organisations perform studies and develop improved millets. They also share millet farming knowledge, best practises, and technologies to farmers, ultimately increasing the millet value chain.<sup>[31]</sup>

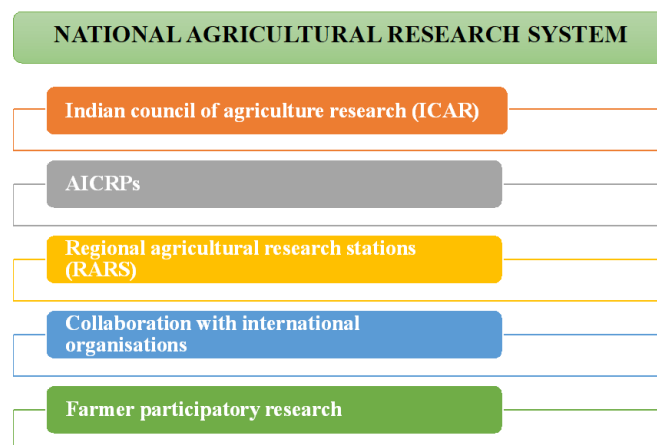


**Figure 1.5:** National agricultural research system

**Indian Council of Agricultural Research (ICAR):** ICAR has been at the forefront of promoting millets. ICAR is India's top agricultural research organisation. It has created a number of centres and research institutes devoted to millet development. Examples of ICAR institutions specialising in millet-related research include the Indian Institute of Millets Research (IIMR) in Hyderabad and the Indian Agricultural Research Institute (IARI). These organisations strive to create high-yielding millet varieties, enhance farming techniques, and address pest, disease, and climate change issues.<sup>[20]</sup>

**AICRPs:** Several All India Coordinated Research Projects (AICRPs) have been launched under the ICAR to focus on certain millet crops such as finger millet (ragi), pearl millet (bajra), foxtail millet (kangni), and tiny millet (kutki). These AICRPs bring together millet-related researchers, scientists, and farmers from various places to work on millet research. They intend to develop and spread technology, increase crop productivity, boost nutritional content, and alleviate millet farmers' challenges.<sup>[21]</sup>

**Regional Agricultural Research Stations (RARS):** Millet research is being conducted at a number of RARS and Krishi Vigyan Kendras (KVKs) around India. Field trials, demonstration plots, and extension operations are conducted by these institutes to validate research findings and disseminate information to farmers. They also play an important role in organising millet cultivation and utilisation training programmes, capacity building efforts, and awareness campaigns.<sup>[22]</sup>

**Collaboration with International Organisations:** To improve millet research and development, ICAR works with international organisations such as the International Crops Research Institute for the Semi-Arid Tropics (ICRISAT) and the Food and Agriculture Organisation (FAO). These alliances aid in gaining access to global knowledge, sharing best practises, and executing collaborative millet research initiatives. They also make it easier to trade germplasm and genetic resources, which helps to generate improved millet varieties.<sup>[23]</sup>

**Farmer Participatory Research:** Through participatory methodologies, NARS actively engages farmers in millet research. Farmer Field Schools (FFS), on-farm trials, and participatory varietal selection (PVS) programmes are used to involve farmers in the research process, collect feedback, and address their individual needs and concerns. Such farmer-centric research activities ensure that produced technology and practises are context-specific, farmer-friendly, and likely to be adopted.<sup>[24]</sup>

#### 2.1.6. RASHTRIYA KRISHI VIKAS YOJANA

The Rashtriya Krishi Vikas Yojana (RKVY) is the Government of India's flagship programme to encourage agricultural development and increase farmer income. Various activities have been launched under this strategy to promote millet cultivation, utilisation, and commercialization. RKVY has played a critical role in fostering the resurgence of millets in India, with a focus on sustainable agriculture practises and nutrition security.

The Rashtriya Krishi Vikas Yojana, which was introduced in 2007, intends to encourage states to boost their investments in agriculture and related areas. Many states have used RKVY money to boost millet planting by offering farmers with financial assistance, developing millet processing units, organising training programmes, and establishing market links. This legislative encouragement has increased millet output and encouraged farmers to consider millets as a valuable crop.<sup>[32]</sup>



**Figure 1.6:** Rashtriya Krishi vikas yojana

**Millet Cultivation Financial help:** RKVY provides financial help to farmers for millet cultivation. The programme funds initiatives such as seed purchase, adoption of improved agricultural practises, soil health management, water conservation, and insect control. RKVY promotes farmers to grow millet and reduces the risks associated with crop transitions by providing financial assistance.<sup>[25]</sup>

**Capacity Building and Training Programmes:** RKVY conducts capacity building and training programmes to empower farmers and improve their knowledge and skills in millet growing. These programmes emphasise millet production practises, post-harvest management, value addition, and marketing tactics. RKVY strives to promote sustainable millet farming practises and improve farmer livelihoods by providing farmers with the required skills and knowledge.<sup>[26]</sup>

**Facilities Development:** Funds are granted under the RKVY for the development of millet cultivation and processing facilities. This comprises the construction of millet processing plants, storage facilities, warehouses, and market connections. The development of such infrastructure allows farmers to adequately store their produce, lowers post-harvest losses, and offers access to better markets, assuring greater remuneration for millet producers.<sup>[27]</sup>

**Research and Development:** RKVY funds millet crop research and development. This includes the creation of enhanced millet cultivars that are high-yielding, drought-tolerant, and pest and disease

resistant. Efforts are also being made to improve millet productivity, soil health, and water management practises. RKVY hopes to facilitate the application of novel millet growing technology and practises by fostering research and development.

**Market Promotion and Demand Generation:** RKVY is critical in promoting millet market demand. It supports activities aimed at increasing public awareness of the nutritional benefits and different applications of millets. This includes millet-based product and recipe marketing, exhibitions, and promotional events. RKVY strives to develop a sustainable market for millet farmers by stimulating higher production and income generation.

### 3. CONCLUSION

Finally, governmental support for millet promotion in India shows enormous promise for tackling critical issues such as food security, nutrition, sustainable agriculture, and farmer livelihoods. The National Policy on Nutri-Cereals, together with other complementing measures, represents a significant step forward in revitalising millet cultivation, consumption, and utilisation in the country.

The strategy establishes a solid platform for enhancing public health outcomes by recognising millets' nutritional value and significance in preventing malnutrition. Millets' high fibre, protein, vitamin, mineral, and antioxidant content makes them a significant nutritional resource for addressing diet-related health issues and promoting overall well-being.

The policy's emphasis on increasing millet output through R&D, new seed types, and sustainable farming practises aims to increase agricultural productivity while strengthening climate resilience. This is especially important in light of global warming and its possible effects on conventional crops.

Furthermore, the emphasis on market connections, value addition, and infrastructure development creates a climate in which millet farmers may access better markets, reduce post-harvest losses, and raise their income. The installation of processing plants and the diversification of millet-based products generate economic opportunities and help rural development.

Public awareness initiatives and educational programmes are critical in shifting consumer attitudes and preferences towards millets. These activities, by emphasising their health benefits, culinary flexibility, and environmental benefits, pave the way for higher consumer acceptance and demand, ultimately fostering industry growth and sustainability.

In India, policy support for millets represents a thorough, integrated strategy that takes into agricultural, nutritional, economic, and environmental factors. It represents a shift towards a more diverse and resilient food system based on conventional and climate-resilient crops.

As policy proposals unfold and gain traction, ongoing efforts are required to ensure their effective implementation, monitoring, and evaluation. Collaboration among government agencies, research institutes, farmers, industrial players, and civil society would be essential for realising the full potential of millets in India.

By capitalising on the nutritional, ecological, and economic benefits of millets, India may emerge as a global leader in sustainable agriculture while also enhancing the health and well-being of its population and securing farmers' livelihoods. Policy support for millets lays the groundwork for a vibrant and inclusive food system that values the diversity and resilience of these ancient grains.

### ACKNOWLEDGEMENTS:

The authors are very much thankful to Management and Principal of KVSR Siddhartha College of Pharmaceutical Sciences, Vijayawada for their support and constant encouragement.

**FINANCIAL SUPPORT AND SPONSORSHIP:** Nil.

**CONFLICTS OF INTEREST:** There are no conflicts of interest.

### REFERENCES

1. Kumari, Jyoti, et al. "Importance of millets in nutrition, health, and sustainability: A review." *Current Nutrition Reports* 9.3 (2020): 227-242.

2. Sreeramulu, D., Reddy, S. Y., & Raghunath, M. (2013). Antioxidant activity of commonly consumed cereals, millets, pulses, and legumes in India. *Food Research International*, 51(1), 918-925.
3. Bhat, R., Shetty, P. H., & Amruthesh, K. N. (2018). Climate-resilient agriculture for enhanced food security: Role of millets in India. *Environment, Development and Sustainability*, 20(6), 2431-2455.
4. Parthasarathy, R., & Shanmugasundaram, S. (2016). Millets in India: Significance, status and future prospects. In *Enhancing Food Security with Millets* (pp. 1-14). Springer.
5. Govindaraj, M., Chandrasekaran, A., & Ramesh Babu, V. (2016). *Millets: Genetic and Genomic Resources*. Academic Press.
6. Srivastava, R., & Kumar, A. (2019). Promotion of millets for public health: Exploring the road ahead. *Indian Journal of Public Health*, 63(1), 84-87.
7. "National Food Security Mission: Operational Guidelines," Department of Agriculture, Cooperation & Farmers Welfare, Ministry of Agriculture & Farmers Welfare, Government of India.
8. "National Food Security Mission - Guidelines," Government of Karnataka, Department of Agriculture.
9. "National Food Security Mission (NFSM): Operational Guidelines for Rabi Crops," Department of Agriculture, Cooperation & Farmers Welfare, Ministry of Agriculture & Farmers Welfare, Government of India.
10. "National Food Security Mission: Information Booklet," Department of Agriculture, Cooperation & Farmers Welfare, Ministry of Agriculture & Farmers Welfare, Government of India.
11. "National Food Security Mission (NFSM) - Achievements and Challenges," *Indian Journal of Agricultural Sciences*, Volume 85, Issue 6.
12. Ministry of Agriculture and Farmers Welfare. (n.d.). National Mission for Sustainable Agriculture (NMSA). Retrieved from <http://agricoop.gov.in/implementing-agencies-8>
13. National Mission for Sustainable Agriculture. (2011). Handbook on National Mission for Sustainable Agriculture (NMSA). Retrieved from <http://www.agricoop.nic.in/sites/default/files/handbook%20of%20nmsa.pdf>
14. Paramesh, V., & Mahadevappa, M. (2017). Millets Mission: Enhancing farm income and food security. *Indian Journal of Agricultural Sciences*, 87(7), 825–830.
15. Tandon, H. L. S., & Thakur, A. K. (2019). Millets: A potential crop for sustainable agricultural production. *Journal of Soil and Water Conservation*, 18(2), 103–116.
16. Government of India. (n.d.). National Program on Nutritional Support to Primary Education. Retrieved from <http://mdm.nic.in/nutri-prog.html>
17. Finkelstein, J. (2014). Nutritionally improved agricultural crops: The case of biofortification. *Current Opinion in Biotechnology*, 26, 162-169.
18. Kumssa, D. B., Joy, E. J. M., Ander, E. L., Watts, M. J., Young, S. D., Walker, S., ... & Broadley, M. R. (2015). Dietary calcium and zinc deficiency risks are decreasing but remain prevalent. *Scientific Reports*, 5, 10974.
19. Mohan, V., Spiegelman, D., Sudha, V., Gayathri, R., Hong, B., Praseena, K., ... & Radhika, G. (2014). Effect of brown rice, white rice, and brown rice with legumes on blood glucose and insulin responses in overweight Asian Indians: A randomized controlled trial. *Diabetes Technology & Therapeutics*, 16(5), 317-325.
20. Indian Council of Agricultural Research (ICAR) - <https://www.icar.org.in/>
21. Indian Institute of Millets Research (IIMR) - <https://millets.res.in/>
22. Indian Agricultural Research Institute (IARI) - <https://www.iari.ernet.in/>
23. International Crops Research Institute for the Semi-Arid Tropics (ICRISAT) - <https://www.icrisat.org/>
24. Food and Agriculture Organization (FAO) - <http://www.fao.org/home/en/>

Two-day International Conference on Recent Advances in Mechanical and Industrial Engineering – 2024  
(ICRAMIE-2024)

25. Ministry of Agriculture and Farmers' Welfare, Government of India. (n.d.). Rashtriya Krishi Vikas Yojana (RKVY). Retrieved from <http://rkvy.nic.in/>
26. National Institute of Agricultural Extension Management. (2017). Rashtriya Krishi Vikas Yojana: A Study on Strategy and Approaches in Different States of India. Retrieved from [https://www.manage.gov.in/pdf/Reports/RKVY\\_Report.pdf](https://www.manage.gov.in/pdf/Reports/RKVY_Report.pdf)
27. India Brand Equity Foundation. (2021). Agriculture and Food Processing in India. Retrieved from <https://www.ibef.org/industry/agriculture-india.aspx>
28. National Food Security Mission. (n.d.). Retrieved from <http://nfsm.gov.in/>
29. National Mission for Sustainable Agriculture. (n.d.). Retrieved from <http://nmsa.dac.gov.in/>
30. Mid-Day Meal Scheme. (n.d.). Retrieved from <http://mdm.nic.in/>
31. Indian Council of Agricultural Research (ICAR). (n.d.). Retrieved from <http://www.icar.org.in/>
32. Rashtriya Krishi Vikas Yojana. (n.d.). Retrieved from <http://rkvy.nic.in/>

## Performance Study of Alumina Ceramic Tool Inserts During Dry Turning of EN36 Hardened Steel Samples

Dr. K.I.Vishnu Vandana<sup>1\*</sup>, K. Uday Babu<sup>2</sup>, L. Adithi<sup>3</sup>, K.N. Mithilesh<sup>4</sup>, K. Pavan<sup>5</sup>

<sup>1</sup> Assistant Professor, <sup>2,3,4,5</sup> U.G Student

Department of Mechanical Engineering, P.V.P.Siddhartha Institute of Technology, Kanuru,  
Vijayawada, AP, India

[\\*kodeyvandana@gmail.com](mailto:kodeyvandana@gmail.com)

### ABSTRACT

Ceramic materials have long been used to prepare tools as alternative to conventional tool materials for machining especially hardened steels. Hence the present work is aimed to study the suitability of ceramic materials like alumina ( $Al_2O_3$ ) as a tool material for dry (without coolant) machining of hardened steels. The present work also compared the machining performance of alumina ceramic tool insert with the commercial carbide tool insert while machining EN 36 hardened steels. Machining studies were carried on EN 36 steel samples by varying different machining parameters such as speed, feed and depth of cut using both alumina ceramic tool insert and commercial carbide tool insert. Machining performance of tool inserts was studied and evaluated at different machining conditions basing on wear (weight loss) of the tool inserts and surface roughness of machined surfaces. It is observed that the weight loss of alumina ceramic tool inserts was less than the weight loss of commercial tool insert during machining at all machining parameters. When machined with alumina ceramic tool insert, the surface roughness of EN 36 machined sample is a bit high when compared with surface roughness of machined samples machined with the commercial carbide tool insert. The experimental results revealed that the cutting performance of alumina ceramic cutting tool inserts is on par with the cutting performance of commercial carbide inserts in terms of wear of the inserts and surface finish of machined surfaces.

### INTRODUCTION

Despite tremendous advancements in the field of modern production, material removal through machining remains a major industrial operation. The three major components of a machining system are a cutting tool material, work piece and a machine tool. Out of these three, the cutting tool material is an essential component for carrying out an efficient machining operation. There are different tool materials and can be classified into metals, composites, polymers and ceramics.

Due to their superior cutting properties, traditional inserts such as cemented carbides and High speed steels (HSS) have been used in manufacturing for many years. Even though these materials are strong at room temperature, they did not exhibit enough wear resistance or inertness when subjected to high speeds of machining.

Furthermore, the EU's (European Union) studies on the toxicity and scarcity of traditional tool materials highly recommend exploring alternative materials in place of conventional ones. High hardness, thermal shock resistance, wear resistance and chemical inertness are all necessary for cutting tool material. When compared to other tool materials, ceramic materials have higher melting points, are harder, more resistant to oxidation and corrosion and have higher chemical stability and are represented in Fig. 1. Due to these outstanding properties, tools made from ceramic materials have always had potential in the machining world.

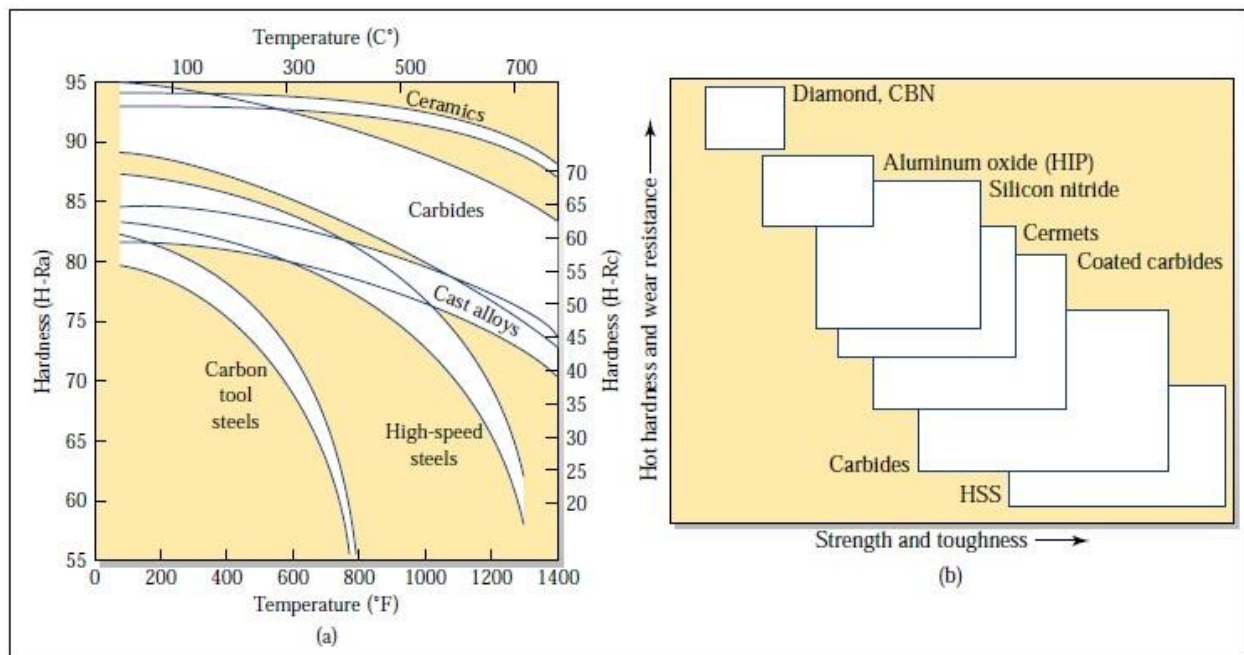


**Fig. 1:** Mechanical properties of different tool materials

Covalent bonds ( $\text{Si}_3\text{N}_4$ , BN), ionic bonds ( $\text{Al}_2\text{O}_3$ , MgO) and mixed bonds of ionic and covalent bonds make up the majority of ceramic materials. For the preparation of cutting tools, ceramic materials based on silicon nitride, such as SiAlON, are typically utilized along with alumina.

Ch Sateesh Kumar et.al. [1] evaluated the turning performance of alumina ( $\text{Al}_2\text{O}_3$ ) and titanium carbide (TiC) based mixed ceramic cutting inserts coated with TiAlSiN, WC/C and Diamond-Like Carbon (DLC) thin-film depositions during machining of AISI 52100 steel. Based on the generated machining forces, coefficient of friction, geometrical characteristics of the chips and tool wear, a comparative analysis of the performance of uncoated and coated cutting tools was carried out. The machining outcomes were interpreted in relation to the adhesion strength of coating with the substrate, surface roughness and hardness of the top surface of the coatings. The deposition of coatings on the surface of cutting tools resulted in reduction of machining forces. The low friction coatings although softer when compared to the  $\text{Al}_2\text{O}_3/\text{TiC}$  substrate, resulted in significant reduction in machining forces when compared to the uncoated cutting tool. M.F. Junaid. et.al [2] compared the performance of three different cutting tools, i.e PCBN, mixed ceramic and coated carbide tool in finish turning of hardened D2 tool steel in terms of tool wear, surface roughness and economic feasibility under dry cutting conditions. They identified that tool life of PCBN inserts was better than mixed ceramic and coated carbide inserts. The flank wear of PCBN tools was observed to be lower than mixed ceramic and coated carbide inserts. In continuous cutting, the main wear mechanism of the mixed ceramic tool was abrasion while that of the PCBN tool was abrasive wear and cratering and for coated carbide tools were abrasive wear, adhesive wear and cratering at lowest cutting speed. They observed that at moderate and highest cutting speed, the failure of mixed ceramic tools is predominantly by abrasive wear and adhesive wear. While PCBN fails by abrasive wear, carbide tools failed due to abrasion and adhesion along with chipping at moderate and highest cutting speeds. Yahya IŞIK et.al [3] compared TiN (PVD) coated  $\text{Al}_2\text{O}_3+\text{Ti}[\text{C},\text{N}]$  mixed alumina-based (KY4400) ceramic and CVD coated carbide  $\text{TiC}+\text{Al}_2\text{O}_3+\text{TiN}$  (ISO P25) cutting tools in turning austempered ductile irons. Ductile cast iron samples were austenitized at  $927^\circ\text{C}$  and subsequently austempered for 1 hour at  $400^\circ\text{C}$ . The hardness of the workpiece material was measured and found to be 43.5 HRC. They conducted series of tests in order to evaluate the tool performances by adopting tool life and identified that TiN (PVD) coated  $\text{Al}_2\text{O}_3+\text{Ti}[\text{C},\text{N}]$  mixed alumina-based ceramic cutting tools are exhibiting longer tool lives than CVD coated carbide tool at higher cutting speeds. Biswanath Mondal et.al [4] developed high performance ceramic cutting tool inserts mainly based on alumina and partially stabilized zirconia. They fabricated and characterized this tool material and did performance tests with respect to chip formation, cutting forces, wear and tool life

and reported satisfactory results. Syed Sohail Akhtar et.al [5] reviewed on the most recent experimental and numerical work related to FGCTs, the current research trends and the need for these tools, the identification of potential material combinations, synthesis techniques and their limitations and finally most recent work. They explored different methods of evaluating tribological performance and various wear mechanisms involved in the cutting process. They also reviewed on the self-lubricating ceramic tools and their limitations. Naresh Kumar Wagri et.al. [6] machined annealed AISI 4340 alloy steel using a coated carbide tool under a dry environment. They compared microhardness of annealed and non-annealed workpieces and found a significant reduction in the microhardness of annealed samples. Microstructure examination of the annealed sample revealed the formation of coarse pearlite which indicated a reduction of hardness and improved ductility. Yuan li et.al. [7] carried out high speed machining on AISI 4340 is carried out by using coated tools with TiN/TiCN/TiAlN multi-coating, TiAlN + TiN coating, TiCN + NbC coating, and AlTiN coating, respectively. The cutting performance evaluation of the coated tools is revealed by the chip morphology, cutting force, cutting temperature, and tool wear. The burrs and the smoothness's degree of chip surfaces flowing from the rake face can reflect tool wear. S Lubis et.al [8] determined wear on ceramic cutting tools during cutting cast iron. They concluded that cutting speed has an effect on wear on the edge of the cutting tool. They identified that the roughness of the workpiece ( $R_a$ ) is directly proportional to the value of the cutting tool ( $VB$ ) wear. Mehmet Boy et.al [9] aimed to improve the machining performance of coated ceramic cutting tool under the turning of powder metallurgical hardened (from 30 to 60 HRC) Bohler K490 steel and after experimentation concluded that the most sustainable method, in terms of power consumption, is the nano-MQL3 condition, with 149.8 W in turning of Bohler K490 tool steel at a cutting speed of 150 m/min, a feed rate of 0.1 mm/rev, and a cutting depth of 0.2 mm. Bipin Kumar Singh et.al [10] fabricated the Zirconia toughened alumina (ZTA) ceramic inserts infused with CuO solid lubricant by Hot Press technique and after characterization concluded that the prepared composites ZTA/CuO having homogeneous microstructure. SIA Qadri et.al [11] performed series of experiments on plain turning of Inconel 718 with Al-Oxide (620), mixed oxide (6050) and silicon nitride (6190) ceramic cutting tools. They studied the effect of cutting speed and hardness of material (being cut) on flank wear of tools and surface finish of work piece and concluded that the cutting forces presented higher values for harder work piece, lower cutting speed and for mixed oxide cutting tool. However, they identified that, in case of harder work piece reduction in cutting forces occurred; especially at higher cutting speed due to thermal softening of the work piece. Sushil Kumar et.al [12] studied the effects of machining parameters on tool life. For this purpose, high Chromium & High Carbon steel is machined at dry condition with ceramic insert at three different cutting speeds (95, 130, 170 m/min), feed rates (.005, 0.008, 0.1 mm/ rev) and depth of cut 0.2 mm. Two factor three level full factorial design was adopted for the experiment and concluded on the effect of edge preparation on tool life by comparing with other type of edges in order to have a better understanding of different edge formations such as chamfer for ceramic insert. Dmitriy Morozow et.al [13] did experimental investigations on ion implanted cutting tools made out of  $Si_3N_4$  with additives Ti-6Al-4V alloy. Distribution of ions on the tool surface was measured and concluded that the wear of cutting edges after ion implantation was smaller than unimplanted ones, thus providing longer lifetime and better performance of tools with ion implanted surfaces. Yahya ISIK et.al. [14] compared TiN (PVD) coated  $Al_2O_3+Ti[C,N]$  mixed alumina-based (KY4400) ceramic and CVD coated carbide  $TiC+Al_2O_3+TiN$  (ISO P25) cutting tools in turning austempered ductile irons and concluded the flank wear increase over tool life influence surface roughness, which remained nearly constant throughout tool lives, especially for the experiments with alumina-based ceramic tool.

Since dry machining doesn't require cutting fluid, it's getting more and more common now a days. It's also thought to be the safest, most cost-effective and cleanest manufacturing method. In particular, dry machining reduces the negative impacts of coolant fluids as well as the expenses associated with coolant disposal, cleaning, and filtering, which lowers overall machining costs. When it comes to dry machining, the key aspects of the machining process, such as the work piece and cutting tool materials,

must be properly taken into account in order to ensure optimal machining results. The most suitable tool materials for dry machining include ceramics, cemented carbides and cubic boron nitride. Hence, in the current work, EN 36 hardened steel samples are dry-machined using microwave sintered alumina ceramic tool inserts, and the machining performance of the alumina ceramic insert is compared with that of commercial carbide tool insert's machining performance in terms of weight loss of the tool inserts during machining and surface roughness of machined EN 36 samples.

## EXPERIMENTAL STUDIES

Pure alumina tool inserts (shown in Fig. 2(a)) according to standard SNGN 120404 are prepared initially from pure alumina powder using a hydraulic press under a compression load of 6 T using a tungsten die. These samples were then sintered using microwave sintering technique at 1500°C [15].



**Fig. 2: Tool Inserts**

### (a) Microwave sintered pure alumina tool insert (b) Carbide Tool Inserts

Carbide tool insert (shown in Fig. 2(b)) was the commercial tool used in this investigation. On EN 24 hardened steel samples, turning operations are performed at different machining parameters (as indicated in Table 1), such as cutting speed, feed and depth of cut, using both commercial tool inserts and alumina ceramic tool inserts for five minutes without the use of coolant (dry machining).

**Table 1: Machining Parameters**

Machining Parameter	Levels of Variation
Speed	100, 300 and 500 rpm
Feed	0.3, 0.5 and 0.8 mm/rev
Depth of Cut	0.1, 0.3 and 0.5 mm

Surface roughness of the machined EN 36 sample surfaces and cutting tool insert wear were used to evaluate the machining performance of the tool inserts. Tool insert wear is calculated using Eq. 1 by weighing the cutting tool inserts before and after each machining process using an electronic weighing equipment.

$$\text{Wear of the tool inserts /min} = (W_f - W_i) / \text{Total machining time in min} \quad \dots \text{Eq. 1}$$

$W_i$  = Initial weight of tool inserts

$W_f$  = Final weight of tool inserts (after machining)

Surface roughness tester (SURF TEST SJ-210) is used to measure the surface roughness of EN 36 sample surfaces that are machined using both alumina and commercial tool inserts. Table 2 presents the wear and surface roughness values acquired during machining with both tool inserts under various machining conditions. Graphs illustrating the results are shown in Fig. 6.

**Table 2: The obtained values during machining with both tool inserts at different conditions**

		Machining of EN36 at 100RPM (Ceramic tool insert)		Machining of EN36 at 100RPM (Commercial tool insert)	
Feed (mm/rev)	Depth of cut(mm)	Weight Loss (gram/min)	Surface Roughness (microns)	Weight Loss (gram/min)	Surface Roughness (microns)
0.3	0.1	0.078	8.23	0.083	7.30
	0.3	0.087	8.30	0.091	7.35

Two-day International Conference on Recent Advances in Mechanical and Industrial Engineering – 2024  
(ICRAMIE-2024)

	0.5	0.093	8.50	0.098	7.30
0.5	0.1	0.089	8.40	0.096	7.60
	0.3	0.096	8.58	0.098	7.72
	0.5	0.099	8.70	0.102	7.78
0.8	0.1	0.099	8.53	0.103	7.56
	0.3	0.105	8.65	0.108	7.77
	0.5	0.109	8.99	0.121	7.90

(a) 100 RPM of Cutting Speed

		Machining of EN36 at 100RPM		Machining of EN36 at 100RPM (Commercial tool insert)	
Feed (mm/rev)	Depth of cut(mm)	Weight Loss (gram/min)	Surface Roughness (microns)	Weight Loss (gram/min)	Surface Roughness (microns)
0.3	0.1	0.199	8.16	0.122	7.38
	0.3	0.105	8.22	0.126	7.11
	0.5	0.121	8.40	0.138	7.40
0.5	0.1	0.102	8.20	0.118	7.52
	0.3	0.132	8.48	0.139	7.59
	0.5	0.142	8.61	0.161	7.70
0.8	0.1	0.192	8.30	0.199	7.63
	0.3	0.214	8.57	0.228	7.82
	0.5	0.218	8.70	0.239	7.96

(b) 300 RPM of Cutting Speed

		Machining of EN36 at 100RPM		Machining of EN36 at 100RPM (Commercial tool insert)	
Feed (mm/rev)	Depth of cut(mm)	Weight Loss (gram/min)	Surface Roughness (microns)	Weight Loss (gram/min)	Surface Roughness (microns)
0.3	0.1	0.315	8.03	0.391	7.51
	0.3	0.343	8.21	0.400	7.60
	0.5	0.353	8.2	0.421	7.82
0.5	0.1	0.342	8.05	0.401	7.56
	0.3	0.355	8.25	0.413	7.71
	0.5	0.369	8.35	0.418	7.82
0.8	0.1	0.350	8.21	0.423	7.56
	0.3	0.359	8.35	0.433	7.62
	0.5	0.370	8.51	0.453	7.73

(c) 500RPM of Cutting Speed

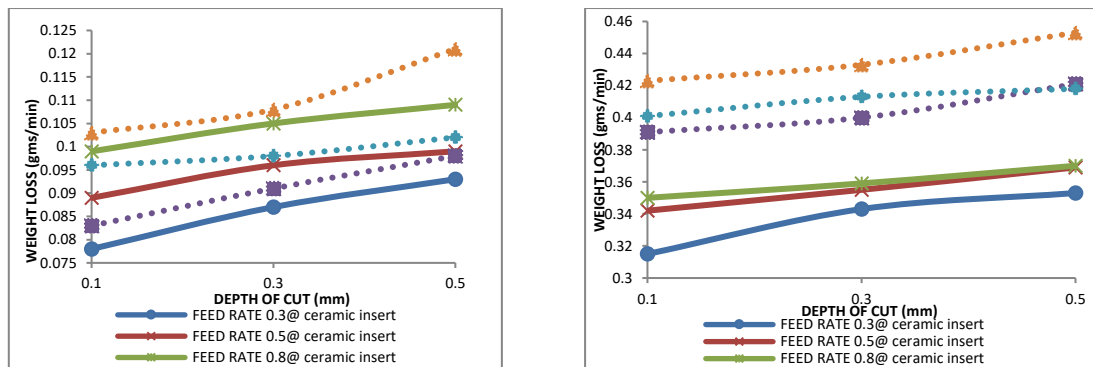


**Fig. 3:** Wear in both the tool inserts during machining on EN 36 hardened steel samples  
(a) 100 rpm speed (b) 500 rpm speed

From the Fig. 3 it was identified that, that wear in both the inserts was increasing with the increasing speed, feed and depth of cut during machining EN 36 hardened samples. It is observed that, the increase in wear rate was more for both inserts with the increase in the speed, when compared with the rate of increase of wear during increase of feed and depth of cut. This may be due to the increased rubbing action between the tool insert and material with increased speed, which augmented the friction. This might resulted generation of more heat between the tool insert and work piece and amplified the material loss particularly at high speeds. Moreover, the feed rate during machining was also seemed to be having greater influence on the weight loss of the tool inserts when compared with the depth of cut at considered speed levels. This wear was observed to be less in alumina tool inserts when compared to commercial tool inserts during machining of EN 36 steel samples at all machining conditions. After completion of turning operations at different machining conditions with both the inserts, surface roughness of machined surfaces of EN 36 samples was measured using surface roughness tester and was displayed in comparison with both the tool inserts in the Fig. 4

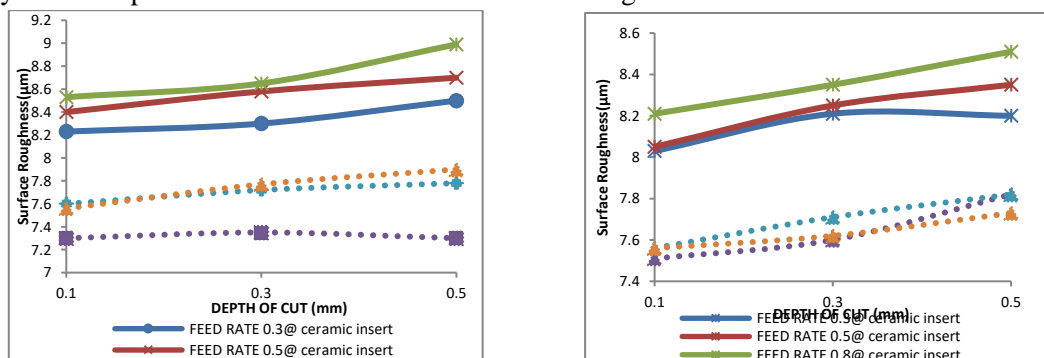


**Fig. 4:** Surface roughness of EN 36 hardened steel samples surface after machining with both the inserts  
(a) 100 rpm speed (b) 500 rpm speed

From the Fig. 4, it was observed that, surface roughness values of EN 36 hardened steel samples machined with alumina tool insert was a bit high when compared with surface roughness values of steel samples machined with commercial tool inserts at same machining conditions. This high surface roughness values can be attributed to high hardness of ceramic tool inserts, which needs grater cutting force during machining of samples, which may contribute more surface roughness to machined samples. It was also identified that with the increased speed of machining, surface roughness values of EN 36 hardened steel samples were observed to be decreased irrespective of type of tool insert used for machining. An increasing trend in surface roughness was observed for EN 36 machined surfaces in case of machining with both the inserts with the increasing feed rate at the constant speed and depth of cut. The effect of depth of cut on surface roughness is seems to be minimum when compared with the speed and feed rate.

## RESULTS AND DISCUSSION

The percentage change in the wear (weight loss) of both the inserts and generated surface roughness on EN 36 machined samples during machining with both the inserts are computed and analysed for the lower (100 rpm speed, 0.3 mm/rev feed, 0.1 mm depth of cut) and higher (500 rpm, 0.8 mm/rev, 0.5 mm depth of cut) machining conditions and are presented in the following Table 3.

**Table 3:** Percentage variation in monitored parameters at different machining conditions of Alumina tool inserts to Commercial tool inserts

Machining conditions			Wear of tool insert (grams/min)			Surface roughness (microns)		
Speed (rpm)	Feed (mm/rev)	Depth of cut (mm)	Alumina ceramic insert	Commercial tool inserts	% Change	Alumina ceramic insert	Commercial carbide tool Inserts	% Change
100	0.3	0.1	0.078	0.083	6.41	8.23	7.30	-11.30
500	0.8	0.5	0.370	0.453	22.43	8.51	7.73	-9.16

From the Table 3, it is observed that the wear of alumina tool insets was less than the wear of commercial tool inserts by 6.41% and 22.43% at lower and higher machining conditions respectively. The surface roughness values yielded by alumina inserts on EN 36 samples was 11.30% and 9.16% higher than the surface roughness values yielded by commercial tool inserts at the at lower and higher conditions of machining respectively.

## CONCLUSIONS

The following conclusions have been drawn after analyzing the results obtained through experimentation.

The alumina ceramic tool inserts have shown less wear (weight loss) when compared to commercial tool inserts during machining of EN 36 samples at all machining conditions.

Surface roughness of machined EN 36 hardened steel samples yielded by alumina tool insert was observed to be little higher than that of the surface roughness yielded by commercial tool inserts during machining at all machining conditions.

Hence, it can be concluded that alumina ceramic tool inserts can be employed for dry machining of EN 36 hardened steels as are observed to be competing with the commercial tool inserts in performance.

In the future, alumina ceramic tool inserts may have a greater influence on mass production machining processes since the alumina ceramic material is more ecologically friendly and because it exhibits less wear during dry machining than commercial tool inserts.

## References

- [1] Ch Sateesh Kumar , Saroj Kumar Patel , Filipe Fernandes , “Performance of Al<sub>2</sub>O<sub>3</sub>/TiC mixed ceramic inserts coated with TiAlSiN, WC/C and DLC thin solid films during hard turning of AISI 52100 steel”, Material Research and technology, Vol. 19, 2022, pp.3380-3393. <https://doi.org/10.1016/j.jmrt.2022.06.092>.
- [2] M. Junaid Mir, M.F. Wani, “Performance evaluation of PCBN, coated carbide and mixed ceramic inserts in finish-turning of AISI D2 steel”, Tribologi, Vol. 14, 2017, pp.10-31.
- [3] Yahya IŞIK,” The performance evaluation of ceramic and carbide cutting tools in machining of austempered ductile irons”, The faculty of Engineering, Vol. 19, 2014, pp. 67-76.
- [4] Biswanath Mondal,Amit Jyoti Banerjee,” Performance Evaluation of Indigenously Developed Zirconia Toughened Alumina Ceramic Cutting Tool Insert”, Vol. 209, 1994, pp. 443-448.
- [5] Syed Sohail Akhtar , Rashid Ali Laghari , Amer D. Alotaibi , Abba A. Abubakar , Samir Mekid ,”A critical review on functionally graded ceramic material for cutting tools”, Review on Advanced Materials and Science,Vol.62, 2023, pp.1-43.

- [6] Naresh Kumar Wagri , Neelesh Kumar Jain , Anand Petare , Sudhansu Ranjan Das , Mohammed Y. Tharwan , Abdulkarim Alansari , Bader Alqahtani , Majed Fattouh , Ammar Elsheikh ,” Investigation on the Performance of Coated Carbide Tool during Dry Turning of AISI 4340 Alloy Steel”, Materials, Vol.16, 2023, pp.668, <https://doi.org/10.3390/ma16020668>.
- [7] Yuan Li, Guangming Zheng,\* Xiang Cheng, Xianhai Yang, Rufeng Xu, and Huaqiang Zhang,” Cutting Performance Evaluation of the Coated Tools in High-Speed Milling of AISI 4340 Steel”, Materials(Basel), Vol.19, 2019, pp. 3266, doi: [10.3390/ma12193266](https://doi.org/10.3390/ma12193266).
- [8] S Lubis, S Darmawan , Rosehan , W Winata , M Zulkarnain,” Tool wear analysis of ceramic cutting tools in the turning of gray cast iron materials”, Materials Science and Engineering, , Vol. 857, 2019, pp.1-7.
- [9] Mahmet boy , “Performance evaluation of coated ceramic tools in nano-MQL assisted turning of powder metallurgical manufactured Bohler K490 steel”, vol.47, 2022, pp. 180. <https://doi.org/10.1007/s12046-022-01959-3.S>
- [10] Bipin kumar singh, Sourav Goswami, Kunal Ghosh, Himadri Roy, Nilrudra Mandal, “Performance evaluation of self lubricating CuO added ZTA ceramic inserts in dry turning application”, Refractory Metals and Hard Materials, vol. 98, 2021, <https://doi.org/10.1016/j.ijrmhm.2021.105551>.
- [11]SIA Qadri, G.A Hermain,M.F Wani.” The effect of cutting speed and work piece hardness on turning performance of nickel based super alloy-718 using ceramic cutting inserts”, Engineering Research Express ,Vol. 2, 2020, <https://doi.org/10.1088/2631-8695/ab40f0>.
- [12] Sushil Kumar,D.p.Singh,Abhishek Chaudhary,”Comparative performance evaluation of ceramic tools for hard turning of high chromium high carbon steel”, Engineering Research and Technology, vol.5, 2016, pp. 186-190.
- [13] DmitriMorozow, Zbigniew Siemiałkowski , Edwin Gevorkyan 2, Mirosław Ruck, Jonas Matijošius , Arturas Kilikevičius, Jacek Caban ,Zbigniew Krzysiak .”Effect of Yttrium and rhenium ion implantation on the performance of nitride ceramic cutting tools”, Materials, Vol. 13, 2020, doi:10.3390/ma13204687.
- [14] Yahya ISIK “The performance evaluation of ceramic and carbide cutting tools in machining of austempered ductile irons”, Vol. 2, 2014, pp. 67-75.
- [15] K. I. Vishnu Vandana, K. N. S. Suman, “Finite element modelling and experimental investigation on mechanical properties and micro structural studies of alumina-graphene composites”, New Materials, Compounds and Applications, vol. 5, no. 3 pp. 156-170, 2021, doi: 10.1016/j.tca.2016.06.016.

## The Automated Rope Line: A Revolution in Industrial Automation

Dr. K Srinivas <sup>1</sup>, Divya Singhi <sup>2</sup>, D. Kasim Moula<sup>3</sup>, P. Jai Tarun Sai<sup>4</sup>, A. Shyam Sundar<sup>5</sup>,  
K. Subrahmanyam<sup>6</sup>

<sup>1</sup>\*Department of mechanical engineering, VRSEC, Vijayawada, Andhra Pradesh.

\*corresponding author: E-mail: [srrinwaas@gmail.com](mailto:srrinwaas@gmail.com)

### ABSTRACT

The emergence of the automated rope line system marks a groundbreaking advancement in industrial automation, revolutionizing manual labor practices across multiple sectors. Engineered for seamless material transport in all directions, its versatility extends from optimizing meat drying processes to handling hazardous materials and even creating automated clotheslines for diverse settings. With notable advantages such as reduced manual labor, heightened operational efficiency, and enhanced safety measures, the system integrates seamlessly with sensors and offers tailored solutions to meet specific industry needs. Its inherent programming flexibility ensures efficiency and customization across tasks and industries, positioning it as a cost-effective and indispensable solution in the evolving landscape of industrial automation.

**Keywords:** automation, rope line, material, industry, material handling

### INTRODUCTION

The ever-evolving landscape of industrial automation has ushered in a new era of efficiency, safety, and adaptability with the introduction of the Automated Ropeline system. This innovative solution stands at the forefront of transformative technologies, challenging conventional manual labor practices and redefining material transport across diverse sectors. Engineered to seamlessly carry materials in all three directions, the Automated Ropeline represents a paradigm shift in the way industries handle a myriad of tasks, from optimizing meat drying processes in butcher factories to ensuring the safe and efficient transport of hazardous materials in chemical industries.

In essence, the Automated Ropeline is a testament to the relentless pursuit of automation, driven by the need to simplify complex tasks and enhance operational processes. Its versatility extends beyond traditional applications, encompassing various industries and scenarios. Picture a butcher factory streamlining its meat drying operations, or a chemical industry optimizing the handling of hazardous materials with minimal human intervention. The adaptability of the system doesn't end there; it extends to the creation of automated clotheslines designed for use in diverse settings, including hotels, hospitals, and domestic environments.

The significance of the Automated Ropeline lies not only in its capacity to revolutionize material transport but also in the tangible benefits it brings to the forefront. A substantial reduction in manual labor, a heightened level of operational efficiency, and improved safety measures are among the noteworthy advantages offered by this automated system. The integration of various sensors further enhances its functionality, paving the way for tailored applications that cater to the specific requirements of different industries.

Moreover, the Automated Ropeline boasts an inherent programming flexibility that allows seamless adjustments, ensuring the system remains efficient and customizable across diverse tasks and industries. This adaptability is a key feature, offering industries the ability to fine-tune the system according to their evolving needs and technological advancements. The result is a versatile and cost-effective solution that not only addresses current challenges but also anticipates future demands. As we explore the current capabilities of the Automated Ropeline system in this paper, we delve into its applications, advantages, and the role it plays in shaping the future of industrial automation. Beyond its immediate impact, this technology has the potential to spark further advancements in the field, setting the stage for a new era of efficiency, safety, and innovation. Join us on a journey into the heart of the Automated

Ropeline system—a technological marvel that transcends traditional boundaries and signifies a transformative leap in industrial automation.

### LITERATURE SURVEY

[1] AthayaAtsiq. Electrical Engineering, Universitas Negeri Padang, Indonesia, Automatic Clothing Drying Using Rain Sensors and Ldr Sensors Based on Arduino UNO

In this automatic clothesline when light and rain sensors are used as input to detect the presence of light and water. When the light sensor detects light, the clothesline will move out. When water is detected by the rain sensor, the clothesline will move inside. To control the rotation of the motor using the H-Bridge circuit. So to rotate the motor, you must use the c language in the Arduino program. That way, this circuit can be controlled by Arduino.

[2] Lim Jia Chun, Noor Anida Abu Talib<sup>1</sup>, Haryati Jaafar<sup>1</sup>, Nordiana Shariffudin<sup>1</sup>, Nur Hidayah Ramli<sup>1</sup>. Development of Intelligent Clothesline Sytem, [Proceedings of The 2nd International Conference On Advance And Scientific Innovation, ICASI 2019, 18 July, Banda Aceh, Indonesia](#)

The project successfully developed an intelligent clothesline system using an Arduino UNO R3 microcontroller. It utilized an LDR sensor to detect light intensity, with voltage values exceeding 4V before 6:00 a.m. and after 8:00 p.m. indicating darkness. A rain sensor detected raindrops by monitoring voltage changes, which decreased linearly with increased water volume. Threshold values of 20 for LDR and 657 for the rain sensor were set after digital conversion, distinguishing between brightness and darkness for the LDR and rain or no rain for the rain sensor.

[3] T .Rammohan , Karpagam college of engineering, Coimbatore-32. International Journal of Pure and Applied Mathematics Volume 118 No. 20 2018, 1851-1856.

Automatic retractable roof for clothesline with notification system is contrived cinch to a facile problem. If this project needs further implementation, it must be in design section. As due to user's needs and environmental surroundings controller part can vary. Raspberry pi, a system on chip conceit and a purpose computer. This computer can be used for better controlling and improved performance than Arduino. Combination of Arduino and Esp8266 module for notification combined with a single Raspberry pi. As Rpi acts a computer with both built-in processor and plugins of internet connection. Finally ARRC with notification system built with an economic and simpler design.

[4] Sathish Kumar B. S Mechanical Engineering, Bannari Amman Institute of Technology, ; International Journal of Advance Research, Ideas and Innovations in Technology. (Volume3, Issue2)

When the battery is charged by the solar panel through the solar controller, it provides power to the motor which will operate the pulley and reel the clothes in. In another condition where the photocell is exposed to sunlight, the resistance is approximately and currently is able to flow to the relay to move the electromagnet. This is why under hot sunlight; the clothes will remain under the sun to dry until the sun is gone. This project is advantageous towards the environment and also for us. It is good for the environment because of its solar energy source. We, on the other hand, are able to go out and leave our clothes out in the open without the constant worrying that our clothes might get drenched or so on. For example, even if it starts to rain, we no longer need to rush home for our clothes will be in safe hands.

[5] Lumitha Seema Cutinha<sup>1</sup>, Manasa k<sup>2</sup>, Venkatesh Pai<sup>3</sup>, Sadhana B<sup>4</sup> AUTOMATIC CLOTH RETRIEVER SYSTEM International Research Journal of Engineering and Technology (IRJET) e-ISSN: 2395 -0056 Volume: 03 Issue: 03 | Mar-2016

This project employs a Microcontroller PIC16F877A to automate laundry based on weather conditions. It addresses the challenge of finding a suitable laundry day for a busy working couple. The system uses a DC motor for retrieving clothes, with temperature sensors for accurate weather detection. LDR sensors measure light intensity, contributing to weather condition assessments. A rain detector with a moisture impedance sensor is incorporated to sense the onset of rain. A rotary knob switch sets the dry-time for clothes, and a DC motor retrieves them automatically. The project utilizes LCD or LED indicators to display day condition, temperature, and dry-time. The focus is on efficient cloth retrieval during sunny days and automatic retrieval during rainy days. The integration of various sensors enhances the accuracy

of weather and light detection. Overall, the system aims to streamline laundry by responding to changing weather conditions automatically.

[6] Mohd Nasrudin Abd Latif<sup>1,a</sup>, Nurul Ashykin Abd Aziz<sup>2,b</sup>, Mohamad Rohieszan Ramdan<sup>3,c</sup>, Nor Hafiza Othman<sup>2,d</sup> <sup>1</sup>Unit Academic and Continuing Education, Kolej Komuniti Kemaman, Lot K-148E, Bangunan Majlis Perbandaran Kemaman, Kijal 24100 Kemaman, Terengganu. <sup>2</sup>Faculty of Entrepreneurship and Business, Universiti Malaysia Kelantan, Locked Bag 36, Pengkalan Chepa, 16100, Kota Bahru, Kelantan <sup>3</sup>Faculty of Management and Economics, Universiti Pendidikan Sultan Idris, 35900 Tanjong Malim, Perak.

The S.M.A.R.T Automated Clothesline features a rain sensor module retracting clotheslines during rain, preventing dampness. The project achieves climate-friendly automation through an Arduino-controlled suspension system. The prototype, using components like Arduino UNO and 12V actuator, successfully meets its objectives. With commercial potential in apartment housing areas, it offers flexibility, time-saving, and affordability. Addressing a common household concern, the innovation not only presents a practical solution but also holds promise as a commercially viable and convenient approach to managing laundry in unpredictable weather conditions.

[7] Multidisciplinary Applied Research and Innovation Vol. 2 No. 1 (2021) 401–410. Siti Nur Aisyah Abdul Hei, Effa Nadzirah Nazri, Nurin Faqihah Mohamed Rafik, Mazniha Berahim\* Department of Information Technology, Centre for Diploma Studies, Universiti Tun Hussein Onn Malaysia KM 1, Jalan Panchor, Muar, 84000 Johor, MALAYSIA.

The Automatic Clothesline Retrieval System with Humidity Sensor is an IoT innovation designed to retrieve and deploy clotheslines based on surrounding weather conditions. Developed to aid busy individuals, the project aims to enhance a prototype ACR system with a Humidity sensor and application. Using a DHT22 Humidity Sensor and Micro Servo, the prototype achieved 100% success in aligning with surrounding humidity and light readings. Commercially viable, it targets students, with 100% interest shown in surveys, offering convenience and peace of mind.

[8] Engineering Technology International Conference (ETIC 2022). M. Y. Hew; A. M. Andrew; Y. Z. Q. Faith; Y. Y. Low; M. K. Y. Natasha

An Automated Cloth Hanging System for laundry in Malaysia utilizes Light Dependent Resistor (LDR) and raindrop sensors to detect weather conditions. The system, integrated with the Blynk application through Wi-Fi, notifies users to either retrieve or hang clothes based on sunlight and rain detection. This Internet of Things (IoT) concept addresses the challenges of manual clothesline operation, ensuring efficiency and convenience in unpredictable weather conditions.

[9] Vol. 14 No. 2 July - December 20 Journal of Engineering and Technology. S. F. Sulaiman\*<sup>1</sup>, M. D. A. Sabri<sup>1</sup>, K. Osman<sup>1</sup>, S. I. Samsudin<sup>1</sup>, N. A. Sulaiman<sup>1</sup> and K. N. Khamil

This project revolutionizes conventional clothesline systems by introducing an automated retrieval system with smart features. Utilizing DC geared motors and a rain sensor connected to NodeMCU, the system responds to external weather conditions. Integrated with a home Wi-Fi network and Blynk server, it provides real-time rainfall monitoring and push notifications. The impressive results showcase the system's ability to autonomously shelter clothes during rain and resume exposure when conditions improve, enhancing household laundry routines with convenience and efficiency.

[10] Jurnal Integrasi Sains dan Qur'an (JISQu) Vol. 2 No. 02 (2023): Agustus: 2023-09-05

In response to the challenges posed by manual clothesline systems in uncertain weather conditions, we developed an automatic clothesline prototype using Arduino Uno. Acting as a data processing center, the Arduino Uno integrates a steam sensor for rain detection, an ambient light sensor for sunlight detection, and a servo for roof folding/unfolding. Testing results demonstrate the prototype's effectiveness, with the system automatically folding the roof during sunny weather and unfolding it, along with activating infrared light, when detecting darkness or rain. This innovation streamlines the clothes drying process, providing a solution to unpredictable weather-related inconveniences.

[11] OIPEEC conference- La Rochelle-April 2017. Slesarev D., Sukhorukov D., Shpakov I.

Continuous rope monitoring represents a novel application of non-destructive testing (NDT) for enhanced safety in industrial settings like drilling rigs and steel mills. The system addresses challenges unique to these environments, requiring rugged design to withstand harsh conditions (extreme temperatures, humidity, dust, vibration, and explosive surroundings) while minimizing maintenance needs. Automation ensures user-friendly operation, offering clear and unambiguous indications suitable for machine operators. The optimized monitoring system, exemplified by Intros-Auto in drilling rigs, demonstrates effective solutions for improving safety and reliability in critical industrial rope installations.

[12] 2021 IEEE International Conference on Artificial Intelligence and Computer Applications (ICAICA) Mehreen Naeem; Shoaib Aslam; Muhammad Suhaib; Seemab Gul; Zeeshan Murtaza; Muhammad Jawad Khan

This research introduces an autonomous pick and pack system designed for industrial use, comprising a 4-DOF robotic manipulator and vision perception capabilities. The system can identify and pick up products from a production line, placing them in a packaging box with specified orientations. The manipulator, configured as RRPR and equipped with an electromagnetic end-effector, utilizes inverse kinematics to determine motion sequences for precise positioning within its workspace. Feetech SC servo motors with built-in PID controllers ensure accurate joint angle movements. An RGB camera captures the region of interest, and image processing techniques extract object orientation. Arduino Mega 2560 serves as the control board, interfacing with PC, while a MATLAB GUI enables monitoring and control in both manual and automatic modes for the end-to-end pick and pack system.

[13] Modeling and advanced sliding mode controls of crawler cranes considering wire rope elasticity and complicated operations, Mechanical Systems and Signal Processing Volume 103, 15 March 2018, Pages 250-263

The paper presents a new mathematical model and robust control strategies for crawler cranes, which are widely used for material handling in confined spaces. Unlike previous studies that focused on specific crane motions, this research considers simultaneous cargo-lifting and boom-luffing actions while accounting for internal and external disturbances like wire rope elasticity and wind.

Three robust control methods—sliding mode control (SMC), terminal SMC, and fast terminal SMC—are proposed to precisely track cargo and boom movements while minimizing swings. The effectiveness of these controllers is evaluated through numerical simulations.

Key contributions include:

1. Development of a comprehensive dynamic model for crawler cranes.
2. Introduction of robust control strategies to handle various disturbances.
3. Simulation-based validation of the proposed control systems.

The paper is structured as follows:

1. Development of the dynamic model.
2. Introduction of robust control methods.
3. Simulation and analysis of control system performance.
4. Conclusion and discussion on future research avenues.

[14] Design of Components and Layout of Machines for Material Handling, Published: February 2001 Volume 17, pages 371–382, (2001)

The paper explores how efficient material handling can streamline manufacturing operations without sacrificing component functionality. It introduces two models:

1. Model I focuses on selecting optimal component routes within a manufacturing system, especially when limited information about machine layout is available.
2. Model II integrates component route selection with machine location determination and layout design, considering both single-row and multi-row machine configurations. Mathematical formulations and algorithms are provided for each model, offering practical solutions to minimize material flow and handling costs in manufacturing. Additionally, potential areas for further exploration include equipment

flexibility, automation, lean principles, and simulation techniques to enhance material handling efficiency.

**[15]** A Time Window Approach to Simultaneous Scheduling of Machines and Material Handling System in an FMS [Ümit Bilge, Gündüz Ulusoy](#) Published Online: 1 Dec 1995

The paper tackles the intertwined challenges of machine scheduling and material handling system scheduling in Flexible Manufacturing Systems (FMS). It focuses on systems where Automated Guided Vehicles (AGVs) transfer materials between machines without returning to the load/unload station after each delivery, causing sequence-dependent travel times for AGVs. The objective is to minimize makespan, formulated as a nonlinear mixed integer programming model. The approach involves iterative procedures: generating a new machine schedule using heuristics, constructing time windows for trips based on operation completion times, and searching for a feasible solution for the vehicle scheduling subproblem, treated as a sliding time window problem. The proposed method is tested on 90 example problems to demonstrate its effectiveness. Overall, the paper offers a practical solution for optimizing system performance and reducing makespan in FMS by simultaneously addressing machine and material handling system scheduling complexities.

**[16]** The influence of superstructure vibrations on operational loads in the undercarriage of bulk material handling machine Damian Pietrusiak, Tadeusz Smolnicki, Mariusz Staníco

The article explores the relationship between vibrations in the ŁZKS 1600 stacker-re-claimer superstructure and harmonic variations in loads on the undercarriage supports. It investigates how vibrations in the superstructure affect the center of gravity's movement, subsequently influencing loads on the undercarriage elements. The research and analysis demonstrate a clear correlation between the dynamic behavior of the superstructure and changes in loads on the undercarriage. It indicates that the harmonic changes in these loads stem from the global vibrations of the superstructure, leading to dynamic shifts in the center of mass position. Overall, the findings highlight the interconnectedness of superstructure vibrations and undercarriage load variations, providing valuable insights into the dynamic behavior of stacker-re-claimer systems.

**[17]** Material handling machines and systems – umi-twinn project contribution péter telek béla illés christian landschützerfabian schenkflavien massi

The paper discusses the pervasive influence of the Industry 4.0 concept on various sectors, including industrial, economic, social, and personal domains. Key transformations highlighted include automation and digitalization, particularly in material handling processes. These processes increasingly rely on automated machinery, and logistics planning, operation, and optimization are driven by data collected from material flow processes. The paper emphasizes the emergence of new methods and devices necessitating innovative solutions and defining new research directions. It outlines the state of the art in material handling research and underscores the role of partner institutes within the UMi-TWINN project in advancing these fields. Through the H2020 EU project, the University of Miskolc aims to enhance its scientific excellence and initiate new research activities in material handling. Overall, the project aims to leverage the opportunities presented by Industry 4.0 to drive innovation and progress in material handling research.

**[18]** Performance evaluation of an automated material handling system for a machining line using simulation

The paper discusses the pervasive influence of the Industry 4.0 concept on various sectors, including industrial, economic, social, and personal domains. Key transformations highlighted include automation and digitalization, particularly in material handling processes. These processes increasingly rely on automated machinery, and logistics planning, operation, and optimization are driven by data collected from material flow processes. The paper emphasizes the emergence of new methods and devices necessitating innovative solutions and defining new research directions. It outlines the state of the art in material handling research and underscores the role of partner institutes within the UMi-TWINN project in advancing these fields. Through the H2020 EU project, the University of Miskolc aims to enhance its scientific excellence and initiate new research activities in material handling. Overall, the project aims

to leverage the opportunities presented by Industry 4.0 to drive innovation and progress in material handling research.

**[19] Material Handling Automation in Production and Warehouse Systems**

This chapter explores advancements in material handling automation for production and warehouse management systems. With innovations in information interface, system design, and intelligent control technologies, sophisticated systems are enhancing productivity. Utilizing wireless devices like RFID tags and mobile computers streamlines tracking and provides more accurate data. Flexible and efficient automated systems are designed for various industries, with recent integration into large-scale integrated systems. High-level automation in material handling benefits modern supply chain management by synchronizing sales, procurement, and production, leading to enhanced enterprise efficiency.

**[20] Development of Unmanned Guided Vehicle for Material Handling Automation for Industry 4.0**  
C. Maheswari, E.B.Priyanka, S.Thangavel, P. Parameswari

The proposed project aims to enhance material handling efficiency in industries by implementing automation. A Unmanned Ground Vehicle (UGV) equipped with a robotic arm and controlled by an ARDUINO UNO R3 ATMEGA 328P controller is used for picking raw materials from the storehouse and transporting them to the workshop for machining. The robotic arm, powered by five servo motors, facilitates material handling tasks. The vehicle, with three wheels, is guided by three IR sensors to detect and follow a black line path. When the vehicle reaches the storehouse, indicated by the third sensor, it stops, and the arm is activated to pick up the goods. The vehicle then autonomously transports the materials to the workshop without human intervention, reducing labor costs and processing time. The project components include the robotic arm with a gripper, the UGV, ARDUINO UNO R3 controller, motor driver, three IR sensors, and a Single-Mode Power Supply (SMPS). Overall, the project aims to streamline material handling processes in industries through automation.

**[21] Stochastic Modeling for Automated Material Handling System Design and Control**

The paper discusses the challenges and benefits of automated Material Handling Systems (MHSs), which have seen significant progress in recent years due to advancements in automation technology. While automated MHSs offer lower material handling costs and increased production efficiency, they also present new challenges in design, operation, and control. One key challenge is the stochastic nature of the operational environment, which includes random demands for material handling, flexible vehicle routing, and variable processing times. To address these challenges, analytical models that incorporate stochastic elements are crucial for effective design and control of automated MHSs. The paper focuses on reviewing research related to the design and control of two types of automated MHSs: Automated Storage and Retrieval Systems (AS/RS) and Automated Guided Vehicle Systems (AGVS). It evaluates existing literature and identifies areas requiring further research to improve the efficiency and reliability of automated MHSs. Overall, the paper provides insights into the complexities of designing and controlling automated MHSs in stochastic environments, highlighting the importance of advanced analytical models and the need for ongoing research in this field.

**[22] The design of an automated material handling system for a job shop**

The paper applies Flexible Manufacturing Systems (FMS) techniques to a traditional job shop manufacturing sheet metal parts. It focuses on designing an automated Material Handling Subsystem (MHS) to optimize shop operations. Detailed simulation models compare the existing setup with the MHS and various loading algorithms. Key highlights include the use of CAPS for rapid model generation and the downstream pull scheduling method. Results show a significant increase in shop output, with orders per day rising from 26 to 45 and turnaround time decreasing from ten days to two days. Overall, the study showcases the effectiveness of automated material handling and advanced scheduling techniques in improving job shop manufacturing efficiency.

**[23] automation of packaging and material handling using plc**

The paper demonstrates the application of Flexible Manufacturing Systems (FMS) techniques in traditional job shop manufacturing of sheet metal parts. It focuses on designing an automated Material Handling Subsystem (MHS) to enhance shop operations. Through detailed simulation models, it

compares the performance of the existing setup with the MHS and various loading algorithms. Key highlights of the study include the utilization of CAPS for quick model generation and the implementation of the downstream pull scheduling method. Results indicate a substantial improvement in shop output, with orders per day increasing from 26 to 45 and turnaround time decreasing from ten days to two days. Overall, the research underscores the effectiveness of automated material handling and advanced scheduling techniques in optimizing job shop manufacturing efficiency.

**[25] Effect of cognitive automation in a material handling system on manufacturing flexibility**

The study investigates the impact of cognitive and mechanical automation in the material handling system on manufacturing flexibility. Cognitive automation reduces operators' cognitive workload by providing relevant information, while mechanical automation decreases physical workload. Using a truck-body production line case study, the researchers applied modified DYNAMO++ for the material handling system and utilized AnyLogic 6.9.0 for simulation. Results showed that increasing levels of cognitive and mechanical automation improved manufacturing flexibility by 14.2% in cycle time, 53.3% in downtime, and 26.3% in the number of tasks. Notably, cognitive automation significantly contributed to total improvements in cycle time and downtime by 64.2% and 74.1%, respectively. This highlights the critical role of cognitive automation in enhancing manufacturing flexibility in material handling systems.

**[26] Development of an automated mechanical lift for material handling purposes, Peter Kayode Farayibiac\*\*, Taiwo Ebenezer Abioyea and & Olagoke Zephaniah Ayodejib**

This paper outlines the development of an automated mechanical lift designed for material handling in a manufacturing environment. With a rated load capacity of 10 kg, the lift utilized a 1-hp electric motor for operation. Power transmission was achieved through belt-pulley, worm gear, and chain-sprocket mechanisms, while system automation was facilitated using contactors and limit switches. Performance evaluation revealed a third-order polynomial relationship between the time required to raise and return loads within a range of 5–15 kg over a distance of 1070 mm. High correlation coefficients of 0.996 and 0.998 were observed, indicating strong correlations. The lifting behavior was characterized by a three-region trend polynomial curve: a gradual decrease in slope to near zero, a region with a near-zero slope over a load range of 7–10.60 kg, and consistent travel time of about  $5.67 \pm 0.03$  sec, and finally, an increase in slope to 0.64 sec/kg. Overall, the automated mechanical lift successfully performed vertical displacement of materials, fulfilling its intended design purpose.

**[27] Advanced Material Handling: Automated Guided Vehicles in Agile Ports**

This report details the collaborative efforts between the Center of Advanced Transportation Technologies (CATT) at the University of Southern California (USC) and the Center for Commercial Deployment of Transportation Technologies (CCDoTT) at the California State University at Long Beach (CSULB). Task 1.2.6.1, titled "Advanced Material Handling: Automated Guided Vehicles," within the project "USTRANSCOM/MARAD/CCDoTT: Agile Port," is the focus of this report. In collaboration with August Design, Inc., the objective of Task 1.2.6.1 is to explore the use of Automated Guided Vehicles (AGVs) and automation to enhance terminal capacity and efficiency within the agile port concept. The report outlines the development and evaluation of various automated container terminal concepts employing AGVs, utilizing a computer-based performance and cost model. The report also presents the comparison of the most promising AGV concepts with other competitive terminal concepts such as the Grid RAIL (GRAIL) and Automated Storage/Retrieval System (AS/RS). Future projections provided by ports regarding container volume and the accommodation of larger ships inform the design characteristics of an Automated Container Terminal (ACT) to meet projected demands. A general layout of the ACT is proposed, specifying interfaces with ship, inland trucks, and trains, as well as desired storage capacity, to accommodate projected demands efficiently. The flexible layout allows for consideration of different storage yard concepts and container movement methods without major configuration changes to the ACT.

**[28] Modularized control algorithm for automated material handling systems**

The paper introduces a modular control algorithm for automated material handling systems, aiming to streamline the engineering process of control software development. Unlike traditional approaches that involve extensive manual programming, this algorithm adopts a two-layer architecture separating hardware control from material flow control. The modular control algorithm facilitates the creation of predefined modules for both conveyor hardware and material flow elements. These modules can then be assembled as needed, allowing for the customization of control software without manual programming. This approach offers flexibility and efficiency in developing control software for custom-built material handling systems. The functionality of the control algorithm is validated through a simulation example using emulated hardware, demonstrating its effectiveness in controlling material handling processes. This modular approach presents a promising solution to optimize the engineering process and maximize the potential of automated material handling systems in industry.

**[29]** Estimating arrival times of transportation jobs for automated material handling in LCD fabrication facilities.

This paper addresses the crucial need for accurate estimation of transportation times in modern LCD fabrication facilities, where automated material handling systems play a pivotal role in optimizing manufacturing competitiveness. The efficient movement of jobs between process toolsets is essential for achieving shorter cycle times, faster deliveries, and higher product quality. The paper introduces a novel heuristic method, leveraging stochastic approaches, to estimate the arrival times of transportation jobs to their final destinations within the facility. By providing expected arrival times compared to arrival due times, this approach enables dynamic prioritization of transportation tasks, thus enhancing the performance of material handling systems. To validate the effectiveness of the proposed method, the author collected actual transportation data from the industry. The analysis demonstrates that the new heuristic method outperforms existing approaches that rely on simple statistics based on historical data. This highlights the significance of adopting advanced stochastic techniques for transportation time estimation in LCD fabrication facilities, contributing to improved operational efficiency and manufacturing competitiveness.

**[30]** Robotic materials handling for automated building construction technology☆, Author links open overlay panel Mirosław J. Skibniewski, Stephen C. Wooldridge

The construction industry is witnessing a transformative shift with the development of fully automated, self-rising platforms by leading Japanese firms for high-rise building construction. These innovative systems integrate robotized cranes, finishing robots, computer workstations, and other automated equipment to create a comprehensive construction environment. Anticipated benefits of these automated building construction systems include enhanced productivity, reduced reliance on labor, and improved safety and quality standards. The coordinated deployment of resources and processes, coupled with streamlined information transfer, is expected to yield significant efficiency gains. To further advance this integrated automation approach, several research issues require attention, particularly the design of materials handling systems to support the efficiency of automated building construction. This paper outlines a concept for an automated materials handling system, leveraging proven automation technologies and a distributed computer network. A prototype robotic materials handling workcell, incorporating micro-robot and barcode technology, is also introduced for integration within the automated materials handling system. This system represents a promising avenue for enhancing the efficiency and effectiveness of automated building construction processes.

**[31]** Introduction to Automated Material Handling Systems in LCD Panel Production Lines

This paper provides an overview of the automated material handling systems (AMHS) employed in thin-film-transistor liquid-crystal-display (TFT-LCD) panel manufacturing. These AMHS are hardware systems designed to transport discrete parts between processing machines within the manufacturing facility. The TFT-LCD panel industry has experienced rapid growth over the past decade, driven by advancements in process equipment facilitating technological innovation. However, while process equipment has evolved significantly, AMHS equipment has seen limited improvement. Many TFT-LCD factories continue to utilize the same AMHS concepts from a decade ago. As production efficiency

becomes a critical factor in competitiveness, the role of AMHS in TFT-LCD production lines has become increasingly vital. Manufacturers are now focusing on enhancing productivity by adopting efficient material handling methods and technologies. This paper underscores the importance of modernizing AMHS in TFT-LCD manufacturing to meet the demands of a rapidly evolving industry landscape.

**[32]** Framework for the control of automated material-handling systems using the holonic manufacturing approach

In the current global economy, manufacturing companies face the challenge of adapting to changes in product variety and production quantity without disrupting the production process. An efficient manufacturing system must possess a flexible control system capable of transitioning between different states seamlessly, without causing significant delays. To address the limitations of traditional hierarchical and heterarchical control systems, this paper proposes a control architecture based on the holonic concept. The holonic control architecture offers a novel approach by integrating both hierarchical and heterarchical control elements. The paper introduces the general holonic control architecture and then delves into its application in designing an automated material-handling control system. In a manufacturing context, where transport activities are crucial, the holonic system's architecture allows it to function both as a hierarchical system, adhering to a predefined schedule during normal operations, and as a heterarchical system in response to disturbances. By leveraging the holonic control concept, manufacturing systems can achieve greater flexibility and resilience, enabling them to adapt to changing production requirements while minimizing disruptions to the production process. This innovative approach represents a promising solution for enhancing the efficiency and agility of modern manufacturing systems.

**[33]** An integrated methodology for automating the determination of layout and materials handling system P. S. WELGAMA & P. R. GIBSON

This paper addresses the complex problem of determining layout and materials handling systems when neither are fixed, an issue for which existing models and solution techniques are limited. To tackle this challenge, the paper proposes a novel integrated methodology that combines knowledge-based reasoning with optimization techniques. The methodology comprises two key components: a knowledge base and an optimization model. The knowledge base incorporates facts and rules to evaluate the feasibility of using specific materials handling equipment for a given move. On the other hand, the optimization model focuses on determining the layout of machines to minimize materials handling costs, aisle space usage, and dead space, employing a multi-criteria optimization approach. The primary objective of the methodology is to optimize materials handling costs, aisle space utilization, and dead space within the resulting layout, with a particular emphasis on heavy manufacturing environments. The output of the system includes the optimal location, configuration, and orientation of machines, as well as the types and design capacities of materials handling equipment, their utilization, and the assignment of moves to each equipment item. The paper concludes by presenting the results of a successful application of the methodology to an example problem, highlighting its effectiveness in addressing complex layout and materials handling challenges in manufacturing environments.

**[34]** A New Generation of Collaborative Robots for Material Handling Conference Paper · June 2012

This paper presents a breakthrough in material handling technology for manufacturing industries, particularly in construction. It introduces modular intelligent power assist systems, also known as collaborative robots or COBOTS, which enhance productivity while ensuring worker safety. Developed by leading companies like Stanley Cobotics and IPK, these systems bridge the gap between manual and fully automatic handling methods. The prototype showcased in the paper features a modular design, sophisticated control system, and advanced human-machine interface, highlighting the potential of this innovative approach to material handling.

**[35]** Material Handling Equipment Michael G. Kay Fitts Dept. of Industrial and Systems Engineering North Carolina State University January 12, 2012

Material handling (MH) is crucial for the efficient movement of goods within facilities like plants or warehouses and between these locations and transportation hubs. While it doesn't alter the form of products like manufacturing does, MH plays a vital role in creating time and place utility. This utility enhances the overall value of products by ensuring they are available when and where they are needed, ultimately contributing to improved efficiency and customer satisfaction. Thus, while MH may not directly shape products, its role in streamlining operations and facilitating timely delivery can significantly enhance the value of goods.

**[36]** A bi-objective stochastic programming model for optimising automated material handling systems with reliability consideration, Madjid Tavana, Hamed Fazlollahtabar & Reza Hassanzadeh

Material handling (MH) is essential for the smooth flow of goods within facilities, such as plants or warehouses, and between these locations and transportation hubs. Unlike manufacturing, which changes the form of products, MH focuses on creating time and place utility. This utility ensures that products are accessible when and where they are required, thereby enhancing their overall value. While MH itself may not physically alter products, its ability to streamline operations and enable timely delivery plays a crucial role in improving efficiency and satisfying customers. As a result, MH significantly contributes to enhancing the value of goods in the supply chain.

**[37]** Scheduling automated transport vehicles for material distribution systems, Author links open overlay panel Humyun Fuad Rahman a, Izabela Nielsen b

The advancement of manufacturing technology has led to more efficient material handling equipment, particularly in manufacturing and container terminal environments. To fully leverage this technology, novel scheduling approaches are needed to coordinate multiple automated transport vehicles effectively. This research presents a methodology for scheduling these vehicles to ensure smooth material flow in such environments. The approach combines a mixed-integer programming model with two meta-heuristic-based algorithms to generate high-quality schedules efficiently. The results demonstrate significant improvements in material delivery timeliness and overall operational performance, highlighting the effectiveness of the proposed scheduling approaches in optimizing material distribution.

**[38]** Design of an automated guided vehicle-based material handling system for a flexible manufacturing system

This paper focuses on the design and operation of Automated Guided Vehicle (AGV)-based Material Handling Systems (MHSs) within Flexible Manufacturing Systems (FMS). It addresses various critical aspects such as determining the required number of vehicles, designing track layouts, managing traffic patterns along AGV tracks, and solving traffic control issues. The paper analyzes challenges arising from multi-vehicle systems and explores strategies to address them through analytical and simulation models.

**[39]** An investigation of a human material handler on part flow in automated manufacturing systems

This paper introduces a formal approach to address the integration of human operators into computerized manufacturing systems. It emphasizes the need to model human functional specifications for task execution and integrate them into the control scheme. The complexity of control is analyzed to develop an effective control mechanism. Specifically focusing on human material handlers, the paper proposes a formal model for human task execution processes, considering part and location aspects. It classifies human material handling tasks based on this model and explores human errors and their impact on part flow. The complexity of part flow in manufacturing systems is then analyzed from a control perspective, considering human tasks and errors. The paper includes a shop floor control example to demonstrate the proposed model.

**[40]** Automation in material handling, Author links open overlay panel Volker Lutz, Hans-Christian Früh, Thomas Gries, Josef Klingele

Automated handling plays a crucial role in meeting the increasing demands of the textile industry. Textiles, being flexible materials, possess unique properties that differ significantly from traditional mechanical engineering materials. This presents challenges in handling due to variations and inhomogeneities both within and between different materials. Over the past few decades, there has been

significant progress in automating processes for non-garment materials such as composite preforms. Various grippers have been developed for tasks like separation, handling, and forming, aiming at damage-free manipulation of textile materials. Looking ahead, emerging transport technologies for light and non-rigid materials hold promise for addressing the challenges in textile transport within garment manufacturing.

## CONCLUSION

The extensive exploration of automated material handling systems (MHSs) presented in the collection of papers underscores the critical role of automation in enhancing efficiency, productivity, and flexibility across various industries. From the development of unmanned guided vehicles (UGVs) equipped with robotic arms to stochastic modeling for optimized MHS design and control, each paper contributes valuable insights into different aspects of automated material handling.

One prominent theme that emerges from the papers is the growing significance of automation in addressing the evolving challenges of modern manufacturing environments. With the advent of Industry 4.0, there is a pressing need for advanced technologies that can streamline material handling processes, reduce labor costs, and improve overall operational efficiency. The integration of robotics, artificial intelligence, and advanced control systems, as demonstrated in several papers, holds immense promise for achieving these objectives.

Furthermore, the papers highlight the multidisciplinary nature of automated material handling, with contributions spanning engineering, computer science, operations research, and management. This interdisciplinary approach is essential for developing comprehensive solutions that address the complex requirements of industrial automation while optimizing performance and cost-effectiveness.

Moreover, the focus on practical applications and case studies underscores the real-world relevance of the research presented. Whether it is optimizing material flow in job shop manufacturing, enhancing container terminal operations with automated guided vehicles (AGVs), or improving manufacturing flexibility through cognitive automation, the papers offer valuable insights into the challenges and opportunities associated with implementing automated material handling solutions.

In conclusion, the papers collectively demonstrate the transformative potential of automated material handling systems in revolutionizing industrial processes across various sectors. By leveraging cutting-edge technologies and innovative methodologies, these systems pave the way for enhanced efficiency, productivity, and competitiveness in the era of advanced manufacturing and Industry.

## APPLICATIONS

- 1. Manufacturing Assembly Lines:** Automated material handling systems can efficiently transport raw materials, components, and finished products between different stations on assembly lines, reducing cycle times and improving productivity.
- 2. Warehousing and Distribution Centers:** In warehouses and distribution centers, automated systems can streamline the movement of goods from receiving docks to storage locations and then to outbound shipping areas, optimizing inventory management and order fulfillment processes.
- 3. Automotive Manufacturing:** In the automotive industry, automated material handling systems play a crucial role in transporting vehicle components and parts along production lines, ensuring timely assembly and minimizing downtime.
- 4. Food and Beverage Processing:** Automated systems are utilized in food and beverage processing plants to handle ingredients, packaging materials, and finished products, maintaining hygiene standards and enhancing throughput.
- 5. Pharmaceutical Production:** In pharmaceutical manufacturing facilities, automated material handling systems help transport delicate and sensitive materials such as active pharmaceutical ingredients (APIs), ensuring precise handling and minimizing contamination risks.

6. **Aerospace and Defense:** Automated systems are employed in aerospace and defense industries for handling large and heavy components, tooling, and equipment, facilitating efficient manufacturing processes for aircraft, spacecraft, and military hardware.

7. **E-commerce Fulfillment Centers:** With the rise of e-commerce, automated material handling systems are used in fulfillment centers to manage the storage, picking, packing, and shipping of orders, enabling rapid order processing and delivery to customers.

8. **Hospital and Healthcare Facilities:** In hospitals and healthcare facilities, automated material handling systems assist in the transportation of medical supplies, equipment, and patient samples, enhancing operational efficiency and patient care.

9. **Textile and Apparel Manufacturing:** Automated systems are employed in textile and apparel manufacturing for handling fabrics, garments, and accessories, improving production efficiency and quality control.

10. **Automated Ports and Container Terminals:** In port and terminal operations, automated material handling systems, such as automated guided vehicles (AGVs) and robotic cranes, streamline container handling processes, optimizing throughput and reducing turnaround times for vessels.

These are just a few examples of the diverse applications of automated material handling systems across different industries. As technology continues to advance, we can expect to see further innovations and implementations in various industrial sectors.

## REFERENCE

- [1] AthayaAtsiq. Electrical Engineering, Universitas Negeri Padang, Indonesia, Automatic Clothing Drying Using Rain Sensors and Ldr Sensors Based on Arduino UNO <https://journals.insparagonsociety.org/index.php/spectrum/article/view/174>
- [2] Lim Jia Chun, Noor Anida Abu Talib<sup>1</sup>, Haryati Jaafar<sup>1</sup>, Nordiana Shariffudin<sup>1</sup>, Nur Hidayah Ramli<sup>1</sup>, Development of Intelligent Clothesline Sytem, Proceedings of The 2nd International Conference On Advance And Scientific Innovation, ICASI 2019, 18 July, Banda Aceh, Indonesia <https://eudl.eu/doi/10.4108/eai.18-7-2019.2288530>
- [3] T. Rammohan, Karpagam college of engineering, Coimbatore-32. International Journal of Pure and Applied Mathematics Volume 118 No. 20 2018, 1851-1856 <https://acadpubl.eu/jsi/2018-118-20/articles/20c/73.pdf>
- [4] Sathish Kumar B. S Mechanical Engineering, Bannari Amman Institute of Technology, ; International Journal of Advance Research, Ideas and Innovations in Technology. (Volume3, Issue2) <https://www.ijariit.com/manuscripts/v3i2/V3I2-1152.pdf>
- [5] Lumitha Seema Cutinha, Manasa K, Venkatesh Pai, Sadhana B; Automatic Cloth Retriever System, International Research Journal Of Engineering And Technology (IRJET) Volume: 03 Issue: 03 Mar-2016 <https://www.irjet.net/archives/V3/i3/IRJET-V3I347.pdf>
- [6] Mohd Nasrulddin Abd Latif<sup>1,a</sup>, Nurul Ashykin Abd Aziz<sup>2,b</sup>, Mohamad Rohieszan Ramdan<sup>3,c</sup>, Nor Hafiza Othman<sup>2,d</sup> <sup>1</sup>Unit Academic and Continuing Education, Kolej Perak. <http://hdl.handle.net/123456789/2148>
- [7] Multidisciplinary Applied Research and Innovation Vol. 2 No. 1 (2021) 401–410. Siti Nur Aisyah Abdul Hei, Effa Nadzirah Nazri, Nurin Faqihah Mohamed Rafik, Mazniha Berahim\* Department of Information Technology, Centre for Diploma Studies, Universiti Tun Hussein Onn Malaysia KM 1, Jalan Panchor, Muar, 84000 Johor, MALAYSIA. <https://publisher.uthm.edu.my/periodicals/index.php/mari/article/view/404/173>
- [8] Engineering Technology International Conference (ETIC 2022). M. Y. Hew; A. M. Andrew; Y. Z. Q. Faith; Y. Y. Low; M. K. Y. Natasha <https://ieeexplore.ieee.org/abstract/document/10106726>
- [9] Vol. 14 No. 2 July - December 20 Journal of Engineering and Technology. S. F. Sulaiman\*<sup>1</sup>, M. D. A. Sabri<sup>1</sup>, K. Osman<sup>1</sup>, S. I. Samsudin<sup>1</sup>, N. A. Sulaiman<sup>1</sup> and K. N. Khamil <https://jet.utem.edu.my/jet/article/view/6402>

- [10] **Jurnal Integrasi Sains dan Qur'an (JISQu)** Vol. 2 No. 02 (2023): Agustus: 2023-09-05  
<https://www.jisqu.trensains.sch.id/index.php/journal/article/view/29>
- [11] OIPEEC conference- La Rochelle-April 2017. Slesarev D., Sukhorukov D., Shpakov I . [chrome-extension://efaidnbnmnibpcajpcglclefindmkaj/https://www.intron.ru/en/img/PRESS/NEWS/En/15.05.17\\_Intron\\_Plus\\_Rope\\_Monitoring\\_OIPEEC.pdf](chrome-extension://efaidnbnmnibpcajpcglclefindmkaj/https://www.intron.ru/en/img/PRESS/NEWS/En/15.05.17_Intron_Plus_Rope_Monitoring_OIPEEC.pdf)
- [12] 2021 IEEE International Conference on Artificial Intelligence and Computer Applications (ICAICA) Mehreen Naeem; Shoaib Aslam; Muhammad Suhaib; Seemab Gul; Zeeshan Murtaza; Muhammad Jawad Khan <https://ieeexplore.ieee.org/abstract/document/9466074>
- [13] Modeling and advanced sliding mode controls of crawler cranes considering wire rope elasticity and complicated operations, *Mechanical Systems and Signal Processing* Volume 103, 15 March 2018, Pages 250-263 <https://www.sciencedirect.com/science/article/abs/pii/S0888327017305241>
- [14] Design of Components and Layout of Machines for Material Handling Published: February 2001 Volume 17, pages 371–382, (2001) <https://link.springer.com/article/10.1007/PL00003946>
- [15] A Time Window Approach to Simultaneous Scheduling of Machines and Material Handling System in an FMS [Ümit Bilge, Gündüz Ulusoy](https://doi.org/10.1287/opre.43.6.1058) Published Online: 1 Dec 1995  
<https://doi.org/10.1287/opre.43.6.1058>
- [16] The influence of superstructure vibrations on operational loads in the undercarriage of bulk material handling machine Damian Pietrusiak, Tadeusz Smolnicki, Marusz Stańco  
<https://www.sciencedirect.com/science/article/abs/pii/S1644966517300316>
- [17] MATERIAL HANDLING MACHINES AND SYSTEMS – UMI-TWINN PROJECT CONTRIBUTION Péter Telek Béla Illés Christian Landschützer Fabian Schenk Flavien Massi  
<https://als.uni-miskolc.hu/index.php/als/article/view/81>
- [18] Performance evaluation of an automated material handling system for a machining line using simulation <https://dl.acm.org/doi/abs/10.1145/224401.224746>
- [19] Material Handling Automation in Production and Warehouse Systems  
[https://link.springer.com/chapter/10.1007/978-3-540-78831-7\\_55](https://link.springer.com/chapter/10.1007/978-3-540-78831-7_55)
- [20] Development of Unmanned Guided Vehicle for Material Handling Automation for Industry 4.0 C. Maheswari, E.B.Priyanka, S.Thangavel, P. Parameswari  
[https://www.researchgate.net/profile/Maheswari-Chenniappan/publication/330846976\\_Development\\_of\\_unmanned\\_guided\\_vehicle\\_for\\_material\\_handling\\_automation\\_for\\_industry\\_40/links/5d0b0895458515ea1a7336f5/Development-of-unmanned-guided-vehicle-for-material-handling-automation-for-industry-40.pdf](https://www.researchgate.net/profile/Maheswari-Chenniappan/publication/330846976_Development_of_unmanned_guided_vehicle_for_material_handling_automation_for_industry_40/links/5d0b0895458515ea1a7336f5/Development-of-unmanned-guided-vehicle-for-material-handling-automation-for-industry-40.pdf)
- [21] Stochastic Modeling for Automated Material Handling System Design and Control  
<https://pubsonline.informs.org/doi/abs/10.1287/trsc.30.4.330>
- [22] The design of an automated material handling system for a job shop  
<https://www.sciencedirect.com/science/article/abs/pii/S0166361583900192>
- [23] AUTOMATION OF PACKAGING AND MATERIAL HANDLING USING PLC  
<https://www.indianjournals.com/ijor.aspx?target=ijor:ijset1&volume=3&issue=6&article=016>
- [25] Effect of cognitive automation in a material handling system on manufacturing flexibility  
<https://www.sciencedirect.com/science/article/abs/pii/S0925527315000304>
- [26] Development of an automated mechanical lift for material handling purposes Peter Kayode Farayibi \*\*, Taiwo Ebenezer Abioyea and Olagoke Zephaniah Ayodejib  
<https://journals.co.za/doi/abs/10.1080/20421338.2020.1765478>
- [27] Advanced Material Handling: Automated Guided Vehicles in Agile Ports  
<https://catt.usc.edu/catt/files/2018/02/68519-27tn8xx.pdf>
- [28] Modularized control algorithm for automated material handling systems  
<https://ieeexplore.ieee.org/abstract/document/795981>
- [29] Estimating arrival times of transportation jobs for automated material handling in LCD fabrication facilities  
<https://www.sciencedirect.com/science/article/abs/pii/S0278612514001460>

- [30] Robotic materials handling for automated building construction technology☆  
Author links open overlay panelMirosław J. SkibnieStephen C. Wooldridge  
<https://www.sciencedirect.com/science/article/abs/pii/092658059290017E>
- [31] Introduction to Automated Material Handling Systems in LCD Panel Production Lines  
<https://ieeexplore.ieee.org/abstract/document/4120350>
- [32] Framework for the control of automated material-handling systems using the holonic manufacturing approach  
<https://www.tandfonline.com/doi/abs/10.1080/00207540410001705284>
- [33] An integrated methodology for automating the determination of layout and materials handling system P. S. WELGAMA &P. R. GIBSON  
<https://www.tandfonline.com/doi/abs/10.1080/00207549608905023>
- [34] A New Generation of Collaborative Robots for Material Handling Conference Paper · June 2012  
[https://www.researchgate.net/profile/Ernesto-Gambao/publication/320392042\\_A\\_New\\_Generation\\_of\\_Collaborative\\_Robots\\_for\\_Material\\_Handling/links/5dc05970a6fdcc2128046dd6/A-New-Generation-of-Collaborative-Robots-for-Material-Handling.pdf](https://www.researchgate.net/profile/Ernesto-Gambao/publication/320392042_A_New_Generation_of_Collaborative_Robots_for_Material_Handling/links/5dc05970a6fdcc2128046dd6/A-New-Generation-of-Collaborative-Robots-for-Material-Handling.pdf)
- [35] Material Handling Equipment Michael G. Kay Fitts Dept. of Industrial and Systems Engineering North Carolina State University January 12, 2012  
[https://www.academia.edu/download/56980917/Material\\_Handling\\_Equipment.pdf](https://www.academia.edu/download/56980917/Material_Handling_Equipment.pdf)
- [36] A bi-objective stochastic programming model for optimising automated material handling systems with reliability consideration, Madjid Tavana,Hamed Fazlollahtabar &Reza Hassanzadeh  
<https://www.tandfonline.com/doi/abs/10.1080/00207543.2014.887232>
- [37] Scheduling automated transport vehicles for material distribution systems  
Author links open overlay panelHumyun Fuad Rahman a, Izabela Nielsen b  
<https://www.sciencedirect.com/science/article/abs/pii/S156849461933321>
- [38] Design of an automated guided vehicle-based material handling system for a flexible manufacturing system <https://www.tandfonline.com/doi/abs/10.1080/00207549008942819>
- [39] An investigation of a human material handler on part flow in automated manufacturing systems  
<https://ieeexplore.ieee.org/abstract/document/1561478>
- [40] Automation in material handling Author links open overlay panelVolker Lutz, Hans-Christian Früh, Thomas Gries, Josef Klingele  
<https://www.sciencedirect.com/science/article/abs/pii/B9780081012116000070>

## **EDM input parameter optimization for SS-316 steel using the fuzzy logic technique and an analysis of the micro structural features of the EDM machining surface**

**G.Sridevi<sup>1</sup>, Sneha.H.Dhoria<sup>2</sup>, Dr.Putta Nageswara rao<sup>3</sup>, Dr. Siva Sankara Babu Chinka<sup>4</sup>,  
Nelakuditi Naresh babu<sup>5</sup>**

sridevi@cutm.ac.in , snehadhoria@gmail.com , vvitpnr@gmail.com, sivachinka@gmail.com,  
[nareshbabu338@micttech.ac.in](mailto:nareshbabu338@micttech.ac.in)

1. Centurion university of technology and management, Odisha.
2. R.V.R&J.C College of engineering, , chowdavaram, Guntur
3. Vasireddy venkatadri Institute of Technology, Guntur
4. Lakireddy Bali Reddy College of Engineering, Mylavaram
5. DVR & Dr.HS MIC College Of Technology

### **ABSTRACT**

The current study aims to improve output performance parameters in the SS-316 steel EDM machining material with a copper electrode. The experiments are designed to analyze the process response such as material removal rate (MRR), tool wear rate (TWR), and tool over cut (TOC) using a Taguchi L9 orthogonal array with three process parameters such as current, TON, and TOFF .The input-output relationship was modeled using fuzzy logic. The experimental and predicted fuzzy logic results are compared. Fuzzy logic modeling results achieve approximately 95% accuracy when compared to experimental results, allowing for better optimization of EDM machining parameters. Micro structural characterizations were carried out on EDM machining surface through Scanning electron microscope. It was observed that there were micro cracks, craters and Globules on the EDM machining surface .Certainly, the density of the cracks can reduce with lower pulse current and pulse on-time.

**Keywords:** EDM, Fuzzy logic, MRR, Taguchi Method, SS-316 Steel, Micro structural characterization, recast layer

### **1. INTRODUCTION**

Electrical Discharge Machining (EDM) is a precision machining process that uses electrical discharges to remove material from a work piece. This method is particularly effective for creating complex shapes and intricate details in materials that are challenging to machine using traditional methods. EDM is widely used in industries such as aerospace, automotive, electronics, and tool and die making. The technique of optimization plays a critical role in improving product quality .The Principal operation of EDM involves the uses of electrical sparks or discharges to erode material from work piece. The work piece and a tool known as the electrode are submerged in a dielectric fluid (usually oil or deionized water) to facilitate the machining process. EDM is primarily used for machining hard-to-machine materials and temperature resistant high strength alloys. This is the comprehensive and successfully applied method in the advance industries for different work piece materials[1]. Electrically conductive material for the work piece to be machined by EDM should be . There have been several research project to model the EDM process and review process efficiency to enhance MRR, TWR and OC. Improvement of these parameters is still challenging and limits the extended application of the technology. Studies have been performed from various investigators in this field. Jitendra et al. performed WEDM tests using EN31 as a work piece and molybdenum wire as an electrode to analyze the effect of input parameters such as Ton, Toff, discharge current, wire speed on performance parameters such as the rate of material removal, wear rate of the instrument, and roughness on the surface. The experiments were performed based on the orthogonal array Taguchi L9 and the outputs were further used for fuzzy modeling using MATLAB. It was found that Fuzzy model's values and

experimental values were to be interconnected with an accuracy of 88%. [2]. Further, Singh et al. modeled the EDM machining input parameters using Fuzzy logic for Die steel skd 61 as work-piece, and reported optimize process parameters for WEDM process. Fuzzy model found 75% correlation with experimental result [4]. To minimize the number of experiments, a taguchi method configuration with fuzzy logic optimization method in WEDM parameters has been used to reduce the number of experiments by Rajyalakshmi et. al. [2]. Mukherjee and Ray [3] worked on a generic framework for controlled optimization. Their modelling results for input-output process parameters found to be in optimal cutting conditions. Mohanty and Nayak work for machining parameters and 3- factor level Taguchi specification on EN 31 work pieces. For input parameters such as Ton  $8\mu\text{s}$ , Toff  $2\mu\text{s}$ , Wire feed 6 m/min, Table Feed 8m/min, Servo Voltage 7V the minimum surface roughness obtained as  $1.467\ \mu\text{m}$ , whereas with the input parameters as Ton  $10\mu\text{s}$ , Toff  $2\mu\text{s}$ , Wire feed 4 m/min, Table Feed 10 m/min, Servo Voltage 7V, the maximum MRR obtained to be 3.522 mm/min. Moreover, Rahman et al. [6] presented machining process in electric discharge machining for austenitic stainless steel 304. The analysis shows that the MRR and surface roughness are generated with increasing current. J.T. Huyang, N.Kumar et al. [7, 8] conducted experiments to reduce the number of experiments using Taguchi Methods of Experimental Runs (L9, L18, and L27 designs). Orthogonal Taguchi L27 array has been used for optimizing the parameters and responses of WEDM using EN31 working material. Fuzzy model provides a more accurate and easier range to an accuracy of 97% Arindam Majumder [9]. The results test showed that the proposed fuzzy model can be used positively for the optimum EDM machining method parameters. Santosh patro, I. Harish and P.S.Rao [10] has modeled a fuzzy model which was correlation with experimental results. They found that there is rise in Pulse ON time and Peak Current in Increases in the material removal rate. Increased peak current and reduced wire feed capability decreases in the Wire Wear Rate. The reduction of the Spark Voltage and Peak Current decreases Surface roughness. Subrat Kumar Barik, G. Sridevi, P.S.Rao [11,12] worked on EDM machining optimize the process parameters. G.Sridevi et al [13,14] worked on machining to optimize the process parameters using Fuzzy logic approach and they found that the Fuzzy logic modeling results achieve approximately 95% accuracy when compared to experimental results, allowing for better optimization of EDM machining parameters. Three factors pulse on time, current and feed rate are considered as input parameters. Taguchi design of experiments method is used to reduce the number of experiments and Taguchi method has been used for process parameter optimization. Extremely pulse on time among the three input parameters MRR factors, accompanied by current and feed rate utilization electrodes of copper and brass. The impact of the instrument over cut and tool wear rate. The parameter is the copper electrode pulse on time and the Servo feed rate using brass is an affected parameter with an electrode.

This paper exposed to forecast the optimal parametric data set with extreme Material removal rate and nominal tool wear, over cut during machining SS-316 stainless steel. An experimental design maintained L9 orthogonal array based experimental design is engaged during this experiment. The second step involved the development of an effective correlation using the fuzzy modelling approach between the experimental values and the modelled values. To estimate the optimum machining conditions, a fuzzy-based model is used. The third step involves micro structural characterization of machined surface.

The micro structural research shows that SS-316 steel's crystalline structure is altered by the EDM technique. The mechanical characteristics of the machined surface are impacted by the development of a recast layer and the discovery of micro cracks. The goal of research is to comprehend how the micro structural characteristics that are produced by EDM process parameters—like pulse duration and discharge energy—relate to one another. This information is crucial for process optimization to produce the appropriate material qualities and surface quality.

The literature review highlights the significance of optimizing EDM process parameters using Fuzzy Logic techniques for SS-316 steel. The integration of Fuzzy Logic provides a systematic approach to handle the complexities of the EDM process. Concurrently, the investigation of micro structural

characteristics is crucial for understanding the impact of EDM on the integrity of SS-316 steel. Future research should aim at developing a comprehensive model that integrates both process parameter optimization and micro structural analysis to enhance the overall efficiency and quality of EDM machining for SS-316 steel.

## 2. INVESTIGATIONAL SETUP.

The experiment was administrated using Electronica ECO plus 500 model EDM diesinker machine as shown in fig-1. SS-316 steel is taken as work material copper is taken as tool material. The key points of all the process parameters with its levels are mentioned in table -1. The calculated output response are the rate of material removal-MRR, Tool wear-TWR and Over cut-OC..A 16mmx25mm round diameter copper electrode is used as tool .The experiments specific gravity= 0.773, freezing point= 94°C. It's recycled for every cycle and works as a coolant



**Fig -1** Die Sinker EDM machining with tool and work piece (Model: Electronica Eco plus 500 model) A set of nine experiments were done as per the Taguchi design of experiments by orthogonal array. the work piece SS-316 stainless steel is machined using changed amalgamation of process parameters as per the orthogonal array and the values of MRR, TWR and OC of copper electrode are calculated are shown in Table 2. The formulas of the calculations are discussed below:

i) Material removal rate calculation:

The rate of material removal is determined as the percentage of the weight change of the work piece before and after machining to the product of the machining time and material density..  $MRR = (W_{bm} - W_{am}) / t \times \rho$  in  $mm^3/s$

Whereas:  $W_{bm}$  = Weight of work piece before machining.  $W_{am}$  = Weight of work piece after machining.  $t$  = Machining period  $\rho$  = Density of SS 316 stainless-steel work piece =  $7800 \text{ kg/m}^3$

ii) TOOL WEAR RATIO=(Volume of electrode wear)/ (Volume of fabric exclusion arte from the work piece.

iii) Overcut =  $(R_h - R_e) / R_e$

where,  $R_h$  – radius of the opening on the work piece,  $R_e$  – radius of the electrode

**Table 1** Machining parameters and their level

Sl.No	Parameters	Unit	Level-1	Level-2	Level-3
1	Pulse on time	$\mu s$	50	200	750
2	Discharge current	Amps	10	25	40
3	Feed rate	$\mu m/s$	3	5	7

The response table expressions the calculated values of MRR, TOC and TWR are laterally with the input factors.

**Table 2:** Calculated performance characteristics using Copper electrode.

Exp.No	T-on time	Discharge current	Servo feed	MRR	TOC	TWR
1	50	10	3	0.039	0.035	0.09208
2	50	25	5	0.039	0.13	0.09208
3	50	40	7	0.078	0.0275	1.3813
4	200	10	5	0.273	0.0175	0.7893
5	200	25	7	0.078	0.0375	0.9209

6	200	40	3	0.429	0.0825	0.1675
7	750	10	7	0.234	0.035	0.04605
8	750	25	3	0.312	0.1625	1.036
9	750	40	5	0.351	0.04606	0.2046

### 3. FUZZY MODELING:

Using Mat lab software Fuzzy method (Mamdani) the experimental values are demonstrated using Fuzzy method (Mamdani approach) to get the most elevated and accurate machining parameters, Fig.2. The 3 levels of input parameters are articulated in triangular membership function shown in figures 3 to 8. The input parameters levels were uttered in linguistic forms such as small (S), Medium (M), Large (L).

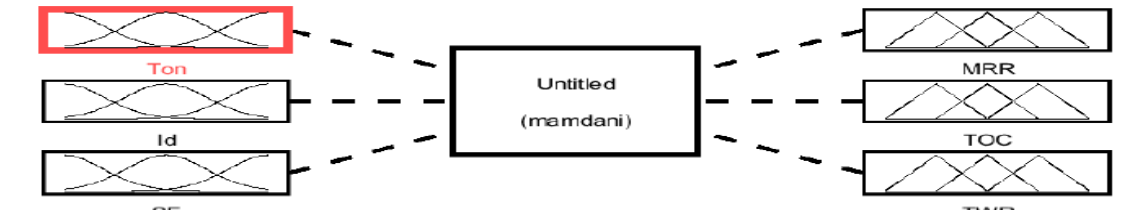


**Fig-2** Fuzzy logic for copper electrode

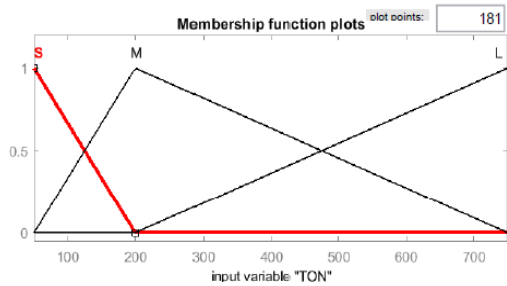


**Fig. 3** Membership Function for TON

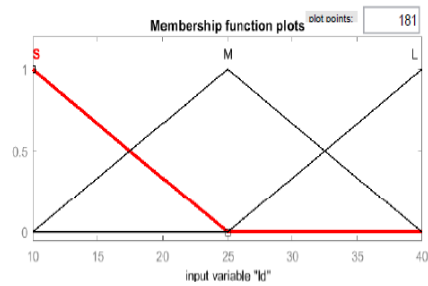


**Fig. 4** Membership Function for T OFF

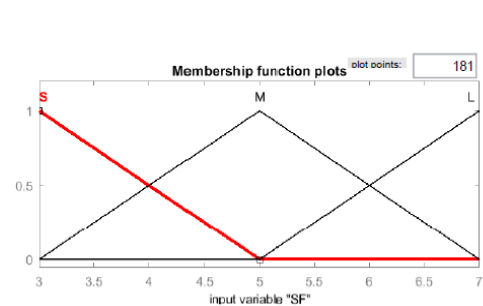


**Fig. 5** Membership Function for SF

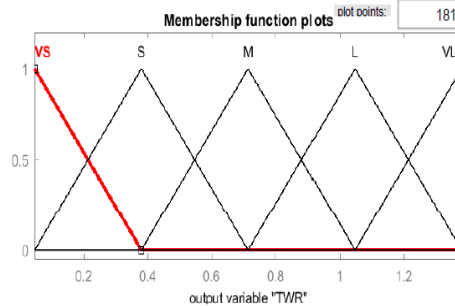


**Fig.6** Membership Function for TWR

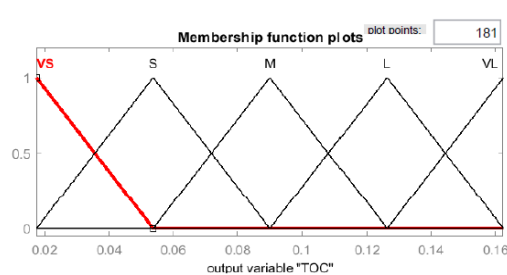


**Fig. 7** Membership Function for TOC

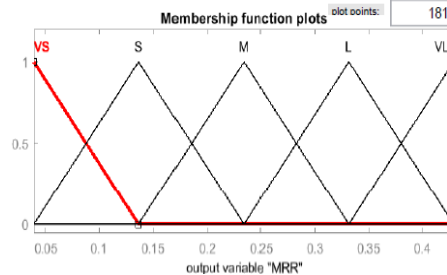


**Fig.8** Membership Function for MRR

### 4. RESULTS AND DISCUSSIONS:

The input variable and output variable associations were developed by setting the rules in the form of if-then statements. A over-all set of 9 rules are fired as copper electrodes separately. The expression of a rule is as follows

Rule 1: If Ton is Small , discharge current is small and servo feed is small then MRR is very small tool wear and over cut is small.

Rule -2: If Ton is Small, discharge current is medium and servo feed is medium then MRR is very small tool wear small and over cut is large.

Rule 3: If Ton is Small , discharge current is large and servo feed is large then MRR is very small tool wear small and over cut is small.

The 9 rules are fired taking altered arrangements. The fuzzified output as originate using fuzzy modeling is defuzzified using centroid method to need a output as obtained using fuzzy modeling is defuzzified using centroid method to get a accurate value. The graphical illustration of modelled values gained using fuzzy approach is shown in fig. 4. These demonstrated values are then compared with the experimental values and consequently the accuracy of demonstrated values was checked. The modelled values obtained using fuzzy logic methodology is compared with the experimental values for copper as shown in Table 3. It has been found that the modeled values were analogous with the experimental values with more than 93 percent accuracy in more number of the cases. The graphical illustrations of variation of MRR, TWR and TOC for dissimilar values of input parameters for copper are shown in fig. 10.

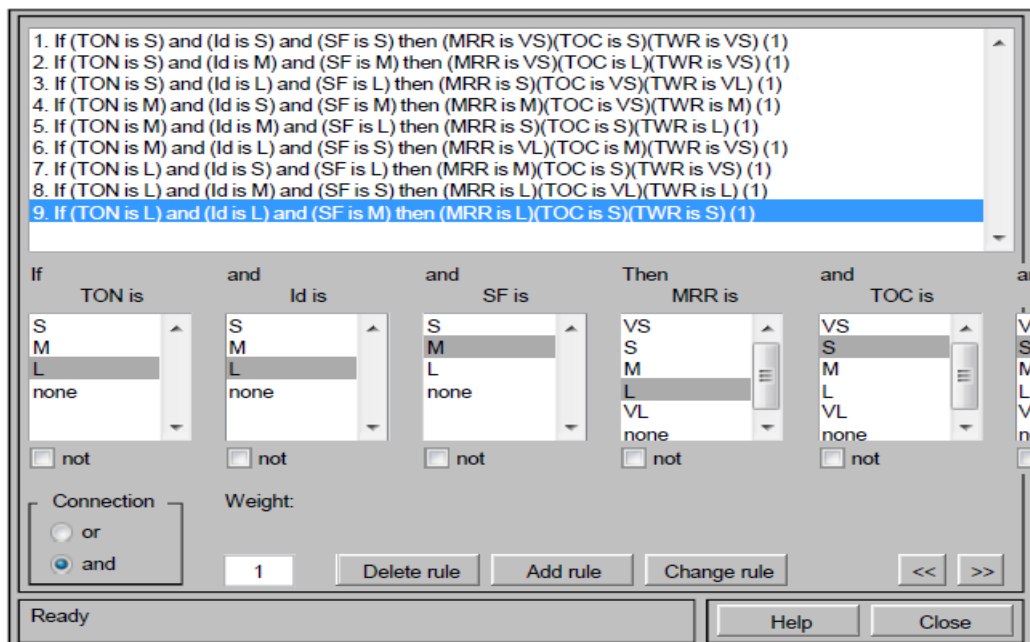


Fig-9 Fuzzy rules fired for copper electrodes

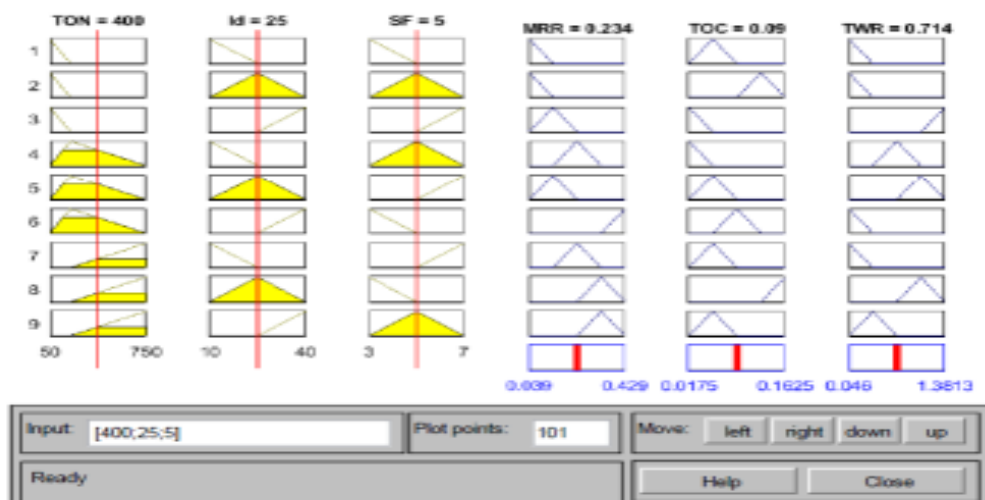


Fig-10 Graphical illustrations of fuzzy values for copper electrodes

**Table 3** Comparison between Experimental Values and Modelled Values for Copper electrode

Exp. No.	Experimental Values			Modelled Values			Percentage Accuracy		
	MRR	TWR	TOC	MRR	TWR	TOC	MRR	TWR	TOC
	mm <sup>3</sup> /s	μm	μm	mm <sup>3</sup> /s	μm	μm	%	%	%
1	0.039	0.035	0.09208	0.0702	0.0537	0.153	96.88	98.13	93.908
2	0.039	0.13	0.09208	0.0702	0.126	0.153	96.88	99.6	93.908
3	0.078	0.0275	1.3813	0.137	0.0291	1.27	94.1	99.84	88.87
4	0.273	0.0175	0.7893	0.234	0.0291	0.714	96.1	98.84	92.47
5	0.078	0.0375	0.9209	0.137	0.0537	1.05	94.1	98.38	87.09
6	0.429	0.0825	0.1675	0.398	0.09	0.153	96.9	99.25	98.55
7	0.234	0.035	0.04605	0.234	0.0537	0.153	100	98.13	89.305
8	0.312	0.1625	1.036	0.331	0.151	1.05	98.1	98.85	98.6
9	0.351	0.04606	0.2046	0.331	0.0537	0.38	98	99.236	82.46

The modelled values obtained using fuzzy logic approach (Mamdani approach) is compared with the experimental values as shown in table 3. It was found that the modelled values were comparable with the experimental values with more than 93 percent accuracy in most of the cases.

The graphical representation of variation of MRR, TWR and TOC for different values of input parameters is shown in fig. 11 to 13.

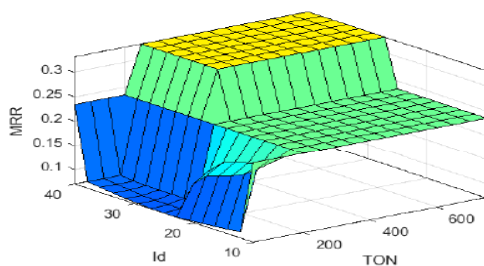


**Fig-11** Variation of MRR

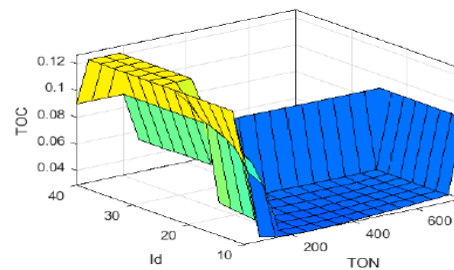


**Fig-12** Variation of TWR

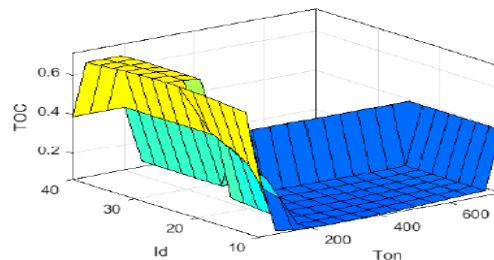


**Fig-13** Variation of TOC

### MICRO STRUCTURAL CHARACTERISATION OF MACHINING SURFACE.

One of the most important factors influencing the integrity of machined is surface micro-crack, and directly affecting the fatigue resistance and performance of the parts. The micro-cracks on the machined surfaces are formed as a result of residual stresses generated in the subsurface. Residual stresses during electrical discharge machining are generated because of reasons such as non-uniformity in thermal stresses, metallurgical phase transformation and local crystal plastic deformation. However, in EDM the scale of plastic deformation and its effects on the residual stresses is very small as there is no contact between the electrode and part and local crystal plastic deformation in EDM is resulted because of very high thermal stress generated during the process.

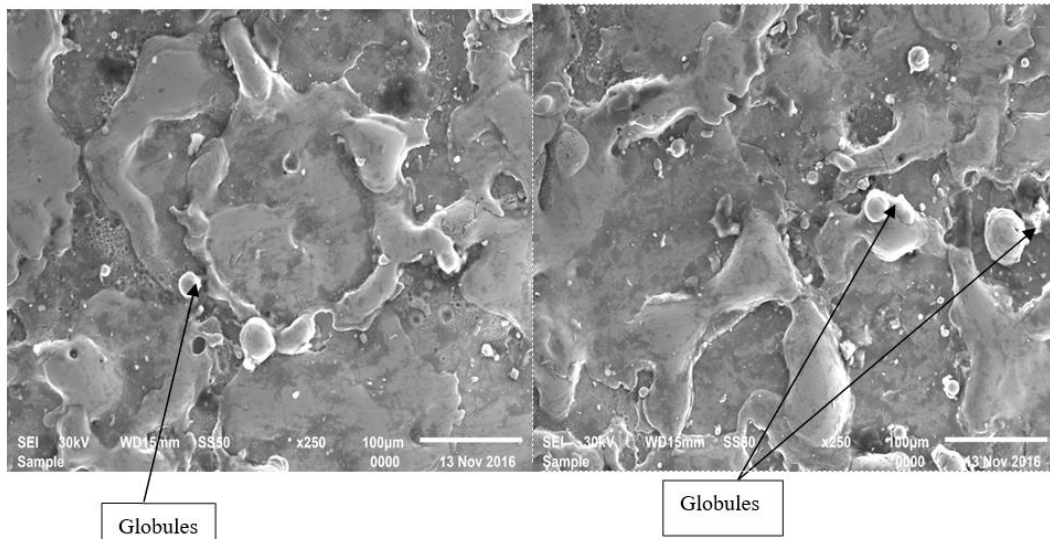


**Figure 14 & 15:** Microstructure of experiments 1 & 2 with Pulse on time  $50 \mu\text{s}$  and current 10amp & 25 amp at magnification X250

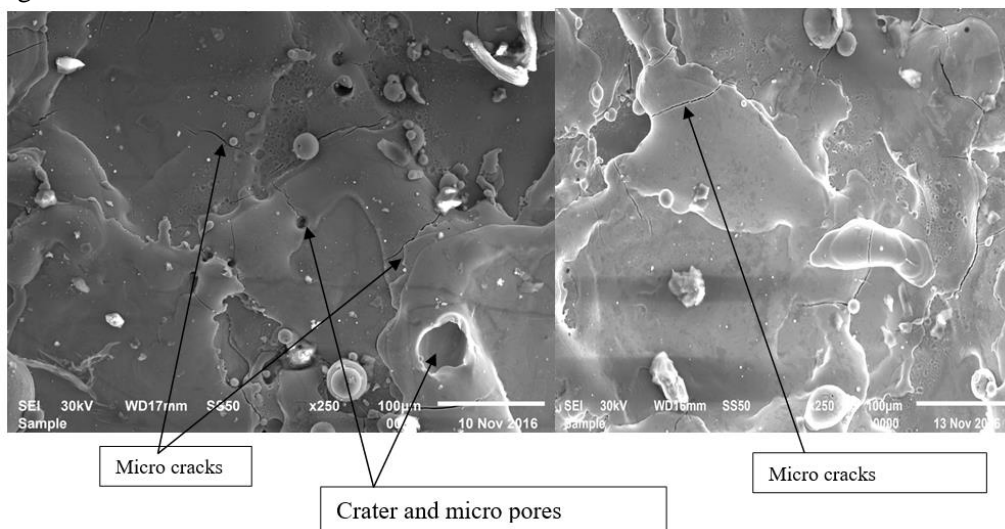


**Figure 16 & 17:** Microstructure of experiments 4 & 6 with Pulse on time  $200\mu\text{s}$  and current 10 amp & 40 amp at magnification X250

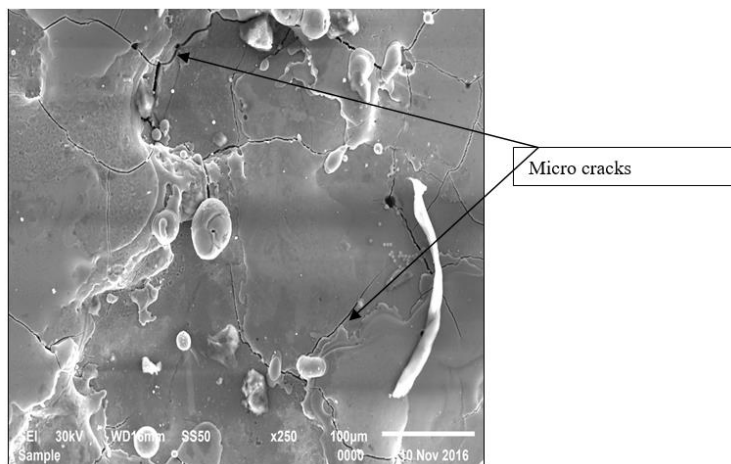


**Figure 18 & 19:** Microstructure of experiments 7 & 8 with Pulse on time  $750 \mu\text{s}$  and current 10 amp & 25 amp at magnification X250

It was observed from the above scanning microscope images that, there is no trace of surface micro-cracks for the pulse on time  $50 \mu\text{s}$ , while relatively wide and large micro-cracks are present on the surface when a higher pulse on time  $200\mu\text{s}$  or  $750 \mu\text{s}$  is used.

With increasing current in EDM, the size and number of micro-cracks increase rapidly.

In machined parts with higher Ton time, the length of micro-cracks is increased, and the span width of the surface cracks is larger.

This is mainly due to a higher thermal gradient, which results in the generation of tensile stresses exceeding the maximum tensile strength of the material.

In higher pulse-on time, energy input in the discharge zone will be increased, which increases the supplied heat energy and thermal gradient on the machined surface; and this consequently increases the micro-cracks density

## 5. CONCLUSIONS:

The conclusion found from the present paper are mentioned below:

1. The experimental values and the proposed fuzzy models are nearly equal i.e the accuracy level for all the parameters for copper the value is more than 93%.
2. The material removal rate is very high with increase of Ton and discharge current using copper electrode.
3. The tool wear decreases with an increase in discharge current and a decrease in the servo feed.
4. An increase Ton time leads to the expansion of surface micro-cracks, which endangers the integrity of the surface being machined. Therefore, it is recommended that low currents are used for machining of sensitive parts that will be subjected to cyclic loads and fatigue to prevent or lower the possibility of formation of micro-cracks on the surface.

## References:

- [1] Subrat Kumar Barik, P Srinivasa Rao, G Sridevi “Optimization of Performing Parameters of SS-316 in Diesinker EDM”INTERNATIONAL JOURNAL OF ENGINEERING, SCIENCE AND - Volume 6, Issue 8,, December 2017 (Special Issue)
- [2] Jitendra Kumara, Tarun Sootaa, S.K. Rajput, “Modelling and optimization of EN 31 work material on wire electric discharge machining” Materials Today: Proceedings 18 (2019) 2984–2992, ICMPC-2019
- [3] I. Mukherjee and P.K. Ray, A review of optimization techniques in metal cutting processes. Computers & Industrial Engineering, Vol. 50, pp. 2006, pp.15-34.
- [4] R.K. Singh, D.K. Singh and V. Kumar, Parametric Optimization of Wire – EDM by Using Fuzzy Logic. IJBSTR RESEARCH PAPER VOL 1 ISSN (2013) pp.2320 – 6020.
- [5] D. Mohanty and N.C. Nayak, Effect of process parameters on performance of EN 31 steel using WEDM: Experimentation and optimization, International Journal of Engineering Research & Technology, Vol. 5 Issue 7, 2016 pp 536-547.
- [6] M.M. Rahman, M.S. Chua, Y.S. Wong and H.T. Loh, Determination of the Optimal Conditions using DOE and Optimization Techniques, International Journal of Mach. Tools Manufacture. Vol. 33. (2), 1993, pp. 297-305.
- [7] J.T. Huang, Y.S. Liao, Optimization of machining parameters of Wire-EDM based on Grey relational and statistical analyses, Int. J. Prod. Res. 41 (8) (2003) 1707–1720.
- [8] Jaganathan Pa, N. Kumar, R. Siva Subramanian, Optimization of WEDM parameters using Taguchi method, Int. J. Sci. Res. Publication. 2 (2012) 1–4.
- [9] Arindam Majumder Process parameter optimization during EDM of AISI 316 LN stainless steel by using fuzzy based multi-objective PSO,, Journal of Mechanical Science and Technology 27 (7) (2013) 2143~2151
- [10] Santosh patro, I. Harish and P.S. Rao “A Fuzzy Modelling for Selection of Machining Parameters in Wire Electrical Discharge Machining of D2 Steel” International Journal of Recent Technology and Engineering (IJRTE) ISSN: 2277-3878, Volume- January 2020.8 Issue-5,
- [11] Subrat Kumar Barik, G. Sridevi “ Optimization of Performing Parameters of SS-316 in Diesinker EDM” International Journal of Science and Research (IJSR), search (IJSR) ISSN (Online): 2319-7064. Dept. of Mech. Engg. PVPSIT

[12].Subrat Kumar Barik, P Srinivasa Rao, G Sridevi “Optimization of Performing Parameters of SS-316 in Diesinker EDM”INTERNATIONAL JOURNAL OF ENGINEERING, SCIENCE AND - Volume 6, Issue 8,, December 2017 (Special Issue)

[13] G.Sridevi, Santosh patro, Sujit Mishra, N.Jeevaratnam ” A Fuzzy Logic approach for the selection of machining parameters in Electric Discharge Di-Sinker Machine using Copper electrode” Shodh Sanchar Bulletin, Volume 10, Issue-40,ISSN 2229-3620,2020

[14] G.Sridevi, Santosh patro, Sujit Mishra, ” A Fuzzy Logic approach for the selection of machining parameters in Electric Discharge Di-Sinker Machine using Brass electrode” Shodh Sanchar Bulletin, Volume 10, Issue-40,ISSN 2229-3620,2020

## **Enhancing the Thermal Properties of Ultra-High Molecular Weight Polyethylene through the Addition of Carbon Nanotubes: A Promising Approach for Total Joint Replacement Applications**

**V.Chittaranjan Das<sup>a\*</sup>, K.Praveen Kumar<sup>a</sup>, U.Sai Pranay<sup>b</sup>, P.S.Rama Sreekanth<sup>c</sup>**

<sup>a</sup>Department of Mechanical Engineering, R.V.R. & J.C. College of Engineering, Guntur 522 019, A.P., India <sup>b</sup>Student, Department of Mechanical Engineering, R.V.R. & J.C. College of Engineering, Guntur 522 019, A.P., India <sup>c</sup>Department of Mechanical Engineering, VIT-AP University, Amaravati 522 237, A.P., India

\*Corresponding author email: vemulapalli.chittaranjandas@gmail.com

### **ABSTRACT**

Ultra-high molecular weight polyethylene (UHMWPE) is commonly utilized in orthopaedic applications, particularly joint arthroplasty, due to its exceptional qualities. However, the limitations of pure UHMWPE, such as inadequate wear resistance and potential joint issues, necessitate further advancements to enhance its longevity and reduce the need for revision procedures. This study investigates the integration of multi-walled carbon nanotubes (MWCNTs) as reinforcements in the UHMWPE matrix. The mechanical properties of MWCNTs at varying concentrations were assessed following ASTM standards, while thermal characteristics were evaluated to gauge the impact of MWCNT incorporation. The results demonstrate that the addition of MWCNTs significantly enhances the thermal properties of UHMWPE. Differential scanning calorimetry (DSC) and thermo gravimetric analysis (TGA) reveal a reduction in weight loss from 4.3% to 1.3% and an increase in crystallinity from 52% to 64%. These findings underscore the potential of MWCNT-reinforced UHMWPE as a viable option for total joint replacement, as it improves thermal characteristics and material durability. This research contributes to the advancement of superior orthopaedic materials with enhanced thermal properties, consequently extending the lifespan of joint arthroplasty devices by addressing the challenges associated with pure UHMWPE.

**Keywords:** UHMWPE, MWCNTs, compression moulding and Thermal Properties

### **1. INTRODUCTION**

Ultra-high molecular weight polyethylene (UHMWPE) has revolutionized the field of total joint replacement since its introduction by Sir John Charnley in the 1960s [1]. Its exceptional physical and mechanical properties, including low moisture absorption, remarkable durability, and excellent resistance to material oxidation with the addition of antioxidant compounds such as Vitamin E, have made UHMWPE a preferred choice for hip arthroplasty treatments [2]. However, the longevity of UHMWPE implants can be compromised by challenges such as osteolysis and wear debris formation, necessitating further advancements [3].

To address these limitations, researchers have explored the incorporation of nanomaterials to enhance the properties of UHMWPE, among which multi-walled carbon nanotubes (MWCNTs) have shown promise. These nanotubes have demonstrated significant improvements in biomechanical strength and antibacterial activity, making them attractive for constructing biomimetic extracellular matrices for bone cell applications, thus driving extensive research in the materials science community [4-5]. This study focuses on the mechanical and thermal characterization of UHMWPE reinforced with varying weight percentages (0.5% to 2.0%) of MWCNTs [6]. The addition of MWCNTs resulted in notable enhancements, including a 28.44% increase in tensile strength, a significant 48% rise in hardness, and a substantial 14.2% increase in density, highlighting their potential as reinforcing agents [6]. Additionally, a composite material was developed by blending UHMWPE (80%) with high-density polyethylene (20%) and reinforcing it with MWCNTs in the range of 0.2% to 2.0% weight to improve

thermal properties and prevent oxidation [6]. While MWCNTs exhibited minimal effects on creep behavior, they significantly influenced the material's wear resistance. Specifically, incorporating 2% MWCNTs led to a considerable reduction in both tensile strength and hardness, resulting in gains of 6% and 2.4%, respectively [7]. Furthermore, an electrostatic spraying approach was employed to manufacture UHMWPE/MWCNTs nanocomposite films, resulting in an sample of introducing 5 sample of MWCNTs to UHMWPE improved tensile strength by 38%, albeit with a 5% reduction in toughness [8-9]. Similarly, the addition of 2 weight percent MWCNTs led to an 80% a rise in Young's modulus but a 35% decrease in toughness [10]. Although some studies, such as that by *K. Esumi et al.* [11], reported that a concentration of 1.5% wt MWCNTs enhanced mechanical properties, none of the reviewed papers identified an optimal MWCNT concentration in UHMWPE. The composite exhibited improved thermal properties and increased resistance to material oxidation. Gradually increasing the concentration of MWCNTs from 0.5% wt to a total of 2% resulted in enhanced crystallization and a significant 24°C improvement in thermal stability [12]. Additional references by *Gu J et al.* [13] and *Suhaib Umer Ilyas et al.* [14] indicated that adding MWCNTs up to 1.5 wt% to UHMWPE improved thermal properties and reduced weight loss, but further addition led to increased weight loss due to the presence of amorphous carbon in the carbon nanotubes. Similarly, *Melk L et al.* [15] found that increasing the carbon concentration in MWCNTs from 1.5 wt% to 3.5 wt% caused composite heat degradation.

This research aims to determine the optimal concentration of MWCNTs in medical-grade UHMWPE, as well as investigate the underlying processes responsible for the reported improvements and eventual degradation. The choice of consolidation technique, MWCNT aspect ratio, and chemical processing all play crucial roles in determining the suitable MWCNT concentration in UHMWPE. Regardless of variations in these factors, the fundamental principles driving property enhancement and degradation remain constant. By elucidating these factors, this study seeks to contribute to the advancement of UHMWPE composites for joint replacement applications.

## 2. MATERIALS AND METHODS

### 2.1 Materials

The MWCNTs used in this study were provided by Ad-Nano Technologies Private Limited (ANT). The MWCNTs had a diameter of 5 to 15 nm and a length of approximately 10  $\mu$ m. They exhibited a high purity of 99 wt.%, a density of 0.14 g/cm<sup>3</sup>, and a surface area of 260 m<sup>2</sup>/g. The UHMWPE employed in the study was supplied by M/s Ticona, a German corporation. Specifically, GUR 1020 was the grade of UHMWPE utilized. The molecular mass of UHMWPE was 4 x 10<sup>6</sup> g/mol, the average particle size was about 140  $\pm$  20  $\mu$ m, and the density was 930 kg/m<sup>3</sup>. These specifications provide essential information about the materials employed in the study, including the properties of the MWCNTs and UHMWPE.

### 2.2 Preparation of composites

The fabrication of UHMWPE/MWCNTs composite samples followed established procedures as described in the literature [16-18]. Raw Multi-Walled Carbon Nanotubes (MWCNTs) were chemically processed and then combined with UHMWPE powder at different loadings ranging from 0.5 to 2.0 wt% (refer to **Table 1** for specific details). The MWCNTs and UHMWPE powder mixture was subjected to milling using a horizontal axis ball milling machine (PULVERISETTE 6 Ball Mono mill) to ensure uniform dispersion of MWCNTs within the UHMWPE matrix. The milling process lasted for 60 minutes at a rotation speed of 300 RPM. To prevent polymer overheating, the milling operation was intermittently paused for 15 minutes, followed by a five-minute interval before resuming. After milling, the resulting UHMWPE/MWCNTs composite powder was physically combined and crushed making use of a compression moulding machine under a pressure of 10 MPa. The compression cycle included phases of consolidation, sintering, and cooling. For one hour, both the top and bottom heating plates were kept at 230°C and 210°C, respectively. Subsequently, water circulation was employed to cool the mould to room temperature. This process yielded sheet-shaped

samples with cross-sectional dimensions of 16 cm x 16 cm<sup>2</sup> and thicknesses up to three millimetres, meeting the required standards for mandatory testing. The objective of the manufacturing process was to achieve homogeneous dispersion of chemically treated MWCNTs within the UHMWPE matrix. The milling and compression moulding procedures played a vital role in producing a well-consolidated composite material suitable for subsequent evaluation and characterization. The resulting samples were then subjected to comprehensive testing to assess the mechanical and thermal properties of the UHMWPE/MWCNTs composites and to investigate the impact of different MWCNT concentrations on the material's performance.

Table 1

Composites	Composites compositions
Pure	UHMWPE 100%
0.5	(99.5% UHMWPE) + (0.5 wt. % MWCNTs)
1.0	(99.0% UHMWPE) + (1.0 wt. % MWCNTs)
1.5	(98.5% UHMWPE) + (1.5 wt. % MWCNTs)
2.0	(98.0% UHMWPE) + (2.0 wt. % MWCNTs)

### 2.3 Tensile Testing

A microtensile test was carried out to assess the mechanical characteristics of the specimens using the Tinius Olsen 10 KL universal testing equipment. The test adhered to the guidelines outlined in ASTM D638-14, with a temperature range of 22 to 24°C and a crosshead speed of 2 mm/min. To ensure consistency, the samples were subjected to a maximum strain rate of 50%. Stress-strain curves were constructed based on the original dimensions of the samples during the testing procedure, while load-displacement curves were continually observed and recorded.

### 2.4 Micro Hardness

The hardness tests on UHMWPE composite samples were conducted using a Mitutoyo- HB210 micro-Vickers hardness tester equipped with a 136° 3-side pyramid angle. All tests were performed at room temperature. To ensure consistency and accuracy in the measurements, a specific subset of samples was selected for analysis. During the testing procedure, a standardized weight of 0.3 kg was consistently applied to each sample for a duration of five seconds. This established protocol was crucial in maintaining uniform testing conditions across all samples and obtaining precise hardness values.

### 2.5 Density

The density of the micro samples from five distinct compositions was determined by applying Formula (1) and measuring the mass of the samples through a weight balancing method. Furthermore, a chemical technique involving the addition of 500 cc of water was utilized. The density measurements were conducted at room temperature using a standardized method.

$$\text{Density} = \text{mass} / \text{volume} \quad (1)$$

### 2.6 Fabrication procedure

The procedure for enhancing the thermal properties through the immersion of MWCNT into UHMWPE was carried out according to the flow chart presented in Figure 1. The steps involved in the procedure are as follows: The weight of MWCNT and UHMWPE was measured as per the calculated amounts, with the assistance of steel balls. The raw material and steel balls were placed in the ball milling machine, following the specifications for the sample and machine. The sample was loaded tightly into horizontal jars, ensuring they were leak-proof. The ball jars were securely fixed in the ball milling machine using screws with program settings. After completion of the milling process, the jars were unloaded from and the blended powder was carefully collected. The powder obtained from the ball milling process was poured into a mould cavity and then placed in a compression moulding machine.

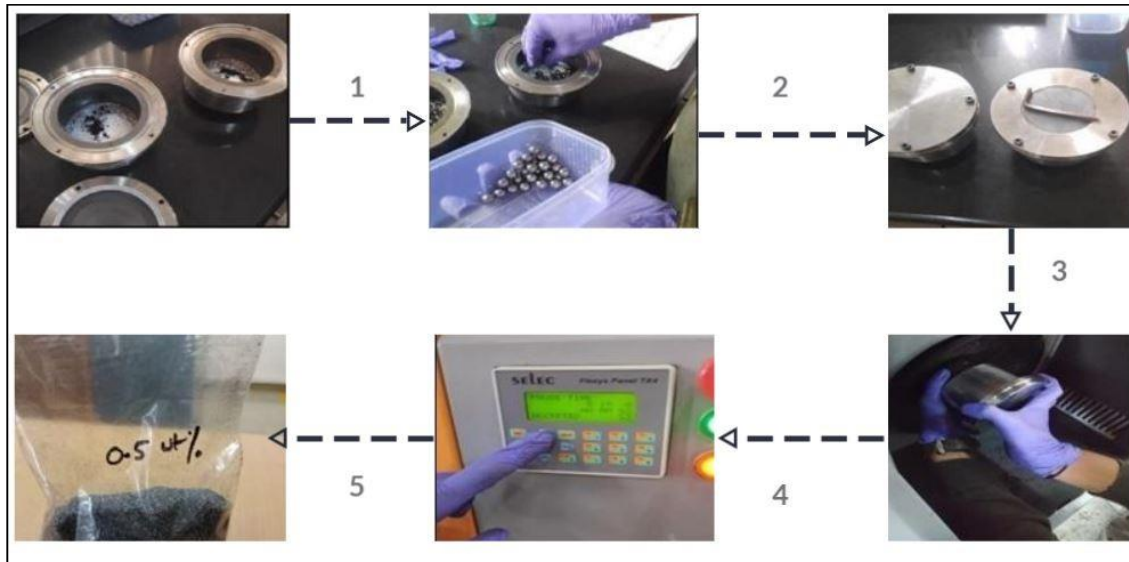


**Fig 1** Fabrication Procedure of the UHMWPEs with MWCNTs

By applying both heat and pressure within the moulding machine, the powder contained in the cavity undergoes a shaping process, resulting in the formation of sheets. Multiple sheets are produced, each containing various weight ratios of MWCNTs, namely 0%, 0.5%, 1%, 1.5%, and 2%. To facilitate further thermal testing, the sheets are then trimmed to the required dimensions (Fig.2).

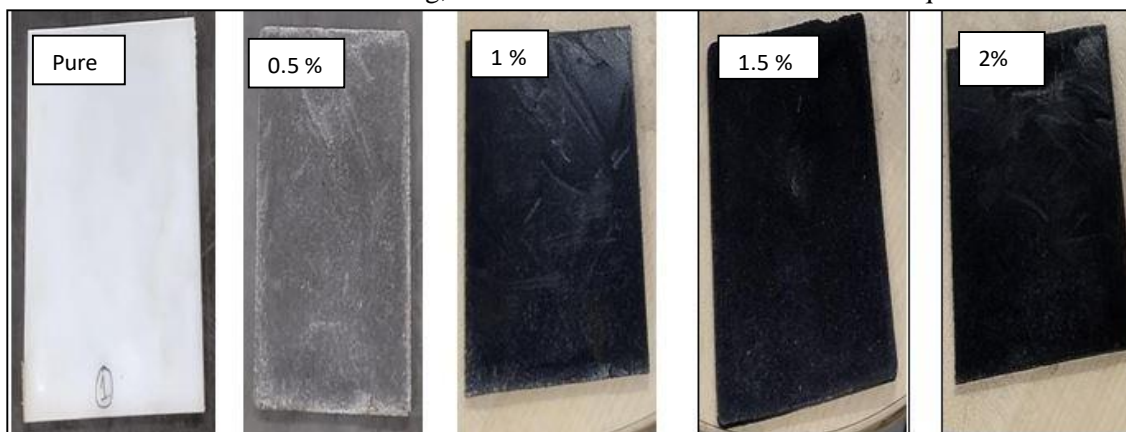


**Fig 2.** UHMWPE/MWCNT composite samples

### **2.7 Thermal Gravimetry Analysis (TGA)**

The Thermal Gravimetric Analysis (TGA) experiments were conducted using a Thermo Gravimetry Analyzer SDT Q600 manufactured by TA Instruments, United States. The TGA instrument employed had a temperature range spanning from ambient temperature to 1200°C, and a balance sensitivity of 0.1 µg. It was equipped with a regulated and variable heat-up rate capability, allowing adjustments between 0.1 and 200°C/min as required. For the testing phase, a total of five samples underwent heating cycles from 30 to 700°C and vice versa, employing a uniform heating rate of 10°C/min. Throughout the experiment, precise temperature measurements and corresponding weight loss data were recorded for all five samples, strictly adhering to the specified temperature ranges and initial sample sizes.

### **2.8 Differential Scanning Calorimetry (DSC)**

The DSC analysis was performed using Setaram Inc.'s TG-DSC Themys One+ instrument, which features a temperature range of 1600°C. The instrument allows for a customizable heating rate ranging from 0.01 to 100°C/min, and it has a sensitivity of 0.1g. To determine the test sample's heat flow rate and known reference materials, measurements were conducted. The experiment involved heating the five samples from 30 to 200°C at a continuous rate of 10°C/min. Throughout the experiment, temperature versus heat flow rate data for each sample was meticulously recorded within the specified temperature ranges for measuring crystallization.

### 3. RESULTS AND DISCUSSION

#### 3.1 Tensile test on UHMWPE/MWCNTs compositions

For conducting tensile testing on nanocomposites, microtensile test specimens were employed in this study. These specimens consisted of varying weight concentrations of MWCNTs, ranging from pure UHMWPE to 2.0 wt.%. Through a combination of experimental testing and theoretical formulation (2), it was determined that an optimal concentration of 1.5 wt.% MWCNTs led to improved mechanical properties of UHMWPE. It ought to be noted that the literature has previously discussed both the underlying mechanism responsible for this enhancement in properties, as well as the decline in performance beyond the optimum concentration [19].

$$\text{Tensile Stress} = \text{Load Applied} / \text{Cross sectional area of the sample} \quad (2)$$

Table 2

UHMWPEs/MWCN TEs Composites	(Tensile Strength) (MPa)	
	Theoretical Approach	Practical Approach
Pure	9.66	12.5
0.5% wt	8.87	12
1.0% wt	7.92	11.8
<b>1.5% wt</b>	<b>14.3</b>	<b>16.6</b>
2.0% wt	13.5	16.2

The selection of 1.5 wt.% as the optimal concentration is supported by the observed rise in crystallinity of the core fibers, which can be attributed to the rearranging of molecular chains that occurs during the hot stretching process. Moreover, the increasing values of Tensile Strength, as presented in **Table 2**, demonstrate that the stress steadily rises until the point of breakage with the continuous exposure to higher temperatures. This trend persists up to the 1.5 wt.% concentration, emphasizing the significance of this particular concentration in facilitating improved mechanical properties, as illustrated in Figure 3 [20-21].

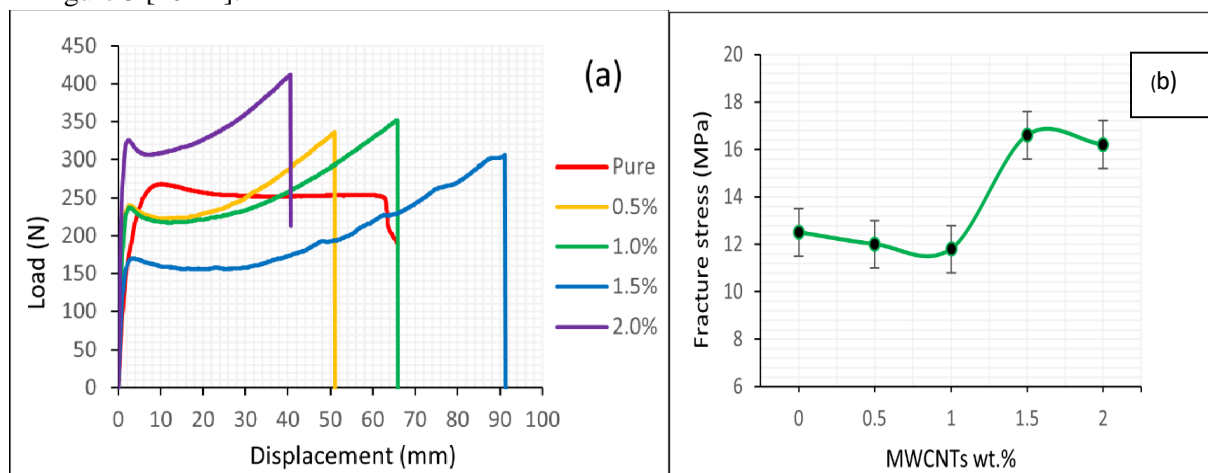


**Fig 3** Tensile response of samples

#### 3.2 Hardness on UHMWPE/MWCNTs compositions

In this study, a comprehensive analysis was conducted to determine the optimal concentration among the five samples. The assessment involved a series of experimental tests along with the utilization of a theoretical methodology. The results obtained from these investigations revealed a noteworthy enhancement in hardness.

Table 3

UHMWPEs/MWCNTs Composites	(Hardness)	
	Theoretical Approach	Practical Approach
Pure	51	54
0.5% weight sample	60	69
1.0% weight sample	72	74
<b>1.5% weight sample</b>	<b>85</b>	<b>88</b>
2.0% weight sample	78	84

This section possesses the results and discussions related to the incorporation of MWCNTs into UHMWPE composites. The UHMWPE/MWCNTs composites' hardness was assessed using the Vickers scale, and the findings are illustrated in Figure 4. As the weight percentages of MWCNTs increased, a notable variation in the hardness parameters of the composites was observed. This indicates a strong correlation between the inclusion of MWCNTs and increased hardness within the UHMWPE matrix. The initial hardness of pure UHMWPE, measured on the Vickers scale, was found to be 54. With the addition of MWCNTs at weight percentages of 0.5%, 1.0%, and 1.5%, the hardness values increased to 69, 74, and 88, respectively. Notably, the composite achieved maximum hardness at a weight percentage of 1.5%, exhibiting a significant improvement of approximately 48% compared to pure UHMWPE. This increase in hardness suggests enhanced resistance to indentation and deformation, which is crucial for extending the lifespan of joint components. However, it is important to consider the potential challenges associated with higher weight percentages of MWCNTs. The increased concentration may lead to the agglomeration or clustering of the nanofillers, which can compromise their uniform distribution within the composite matrix and reduce their reinforcing effectiveness. This phenomenon was observed in the 2% weight percentage composite, resulting in a hardness rating of 84 (refer to **Table 3**). The higher hardness observed in the UHMWPE/MWCNTs composites is expected to improve their wear resistance, indicating better durability against friction and mechanical stress. This increased wear resistance can lessen the development of wear debris and, as a result, the chance of discomfort produced by such debris.

It is worth noting that a study conducted by *Avinash Patil et al.* [23] reported a decline in hardness when the concentration of MWCNTs exceeded 2% weight. This decline in hardness was attributed to the presence of excessive carbon and alumina particles in the composite sample. In summary, the results indicate a positive correlation between the weight percentage of MWCNTs and the hardness of UHMWPE composites with optimal weight percentage of 1.5% demonstrated the highest hardness, offering improved wear resistance and potential benefits in joint component longevity. However, careful consideration should be given to avoid excessive MWCNT concentrations that could lead to agglomeration and negatively impact the composite's properties.

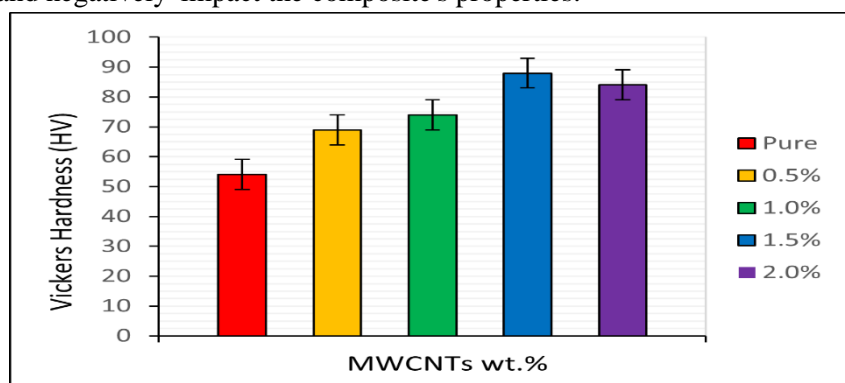


Fig 4 Hardness of the UHMWPE & MWCTs composites

### 3.3 Density on UHMWPE/MWCNTs compositions

Through an extensive investigation utilizing both theoretical and practical techniques, as cited in reference (1), a significant conclusion has been derived. The study focused on the gradual incorporation of MWCNTs into UHMWPEs and its impact on the porosity of the samples. The results obtained indicate a notable improvement in the porosity of the samples when MWCNTs are incorporated. This enhanced porosity plays a crucial role in promoting superior biocompatibility, allowing for normal cellular activity without eliciting any toxic effects on the host tissue.

Table 4

UHMWPEs/MWCNTs	(Density)(g/cm <sup>3</sup> )		
	Composites	Theoretical Approach	Practical Approach
Pure		0.97	0.82
0.5% weight sample		0.973	0.84
1.0% weight sample		0.977	0.87
<b>1.5% weight sample</b>		<b>0.980</b>	<b>0.90</b>
2.0% weight sample		0.984	0.92

In accordance with the research conducted by *Ashrith H.S. et al.* [22], the incorporation of MWCNTs into UHMWPE samples has been found to yield significant improvements in interfacial strength and fracture toughness within the composite material. This enhancement is attributable to the crosslinking within the filler (MWCNTs) and matrix (UHMWPEs), which synergistically contributes to the overall performance increase of composite. The higher density of the hybrid composite specimens in comparison to the UHMWPE matrix alone is a result of the lower density of the UHMWPE matrix in comparison to carbon fiber. Notably, the addition of 2.0 wt% carbon nanotubes to polyethylene results in a 1.5% increase in density [23]. Moreover, these particles are specifically designed to reduce or fill gaps and imperfections within the UHMWPE matrix, thus enhancing the density and structural integrity of the composite. It is critical to emphasise the existence of imperfections on the surface of MWCNTs and the non-homogeneous distribution of MWCNTs within UHMWPE contribute to a practical density that is lower than the theoretical density, as illustrated in **Table 4**. This disparity between practical and theoretical densities directly influences the porosity of the composite material. A larger difference in density leads to the presence of synthesized nano-hydroxyapatite (nHA) with increased permeability, resulting in a higher number of pores with more consistent stiffness. These characteristics are advantageous for cell attachment and promote a favorable environment for cellular activity [24].

### 3.4 Impact of crystallization on polyethylene with added carbon nano-tubes

To investigate the impact of the samples on parameters such as crystallinity and melting temperature, differential scanning calorimetry (DSC) studies were conducted. Figures 5(a) to 5(f) depict the DSC plots of different weight fractions of MWCNT in UHMWPE. The temperature range covered by the DSC analysis ranged from 0 to 200°C. Figure 5(a) illustrates that the pure nanocomposites exhibited a melting temperature of approximately 142.87°C, with a temperature spectrum between 140°C to 142°C. This observation aligns with the reported melting temperature of the irradiated sample, stated as 131.5°C by *Sreekanth et al.* (2014). Crosslink generation during the irradiation process, as indicated by *Premnath et al.* (1999) and *Sreekanth et al.* (2014), could account for the delayed increase in the evaporation temperature of the nanocomposites with increasing level of irradiation. It is worth noting that higher irradiation doses resulted in a greater degree of crosslinking within the tested material, suggesting that the melting process would occur at a higher temperature, as suggested by *Ries et al.* (2005).

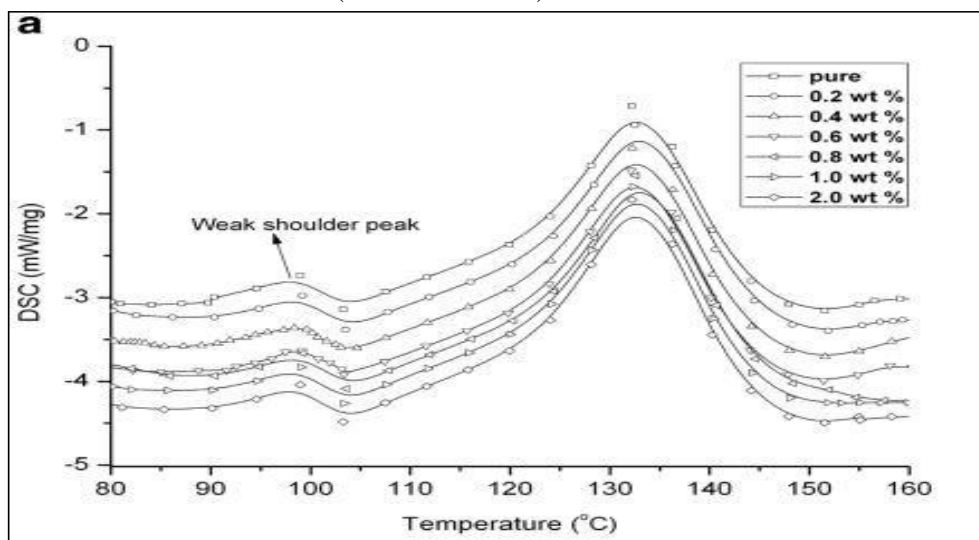


**Fig 5(a)** DSC plots of nanocomposites at unirradiate [Sreekanth P.S. et al 2014]

Figures 5(b) to 5(f) exhibit the variations in crystallization peak temperatures for all samples as the cooling rate is increased. These graphs present temperature versus heat flow charts obtained at a cooling rate of 5°C/min, utilizing different concentrations of MWCNTs.

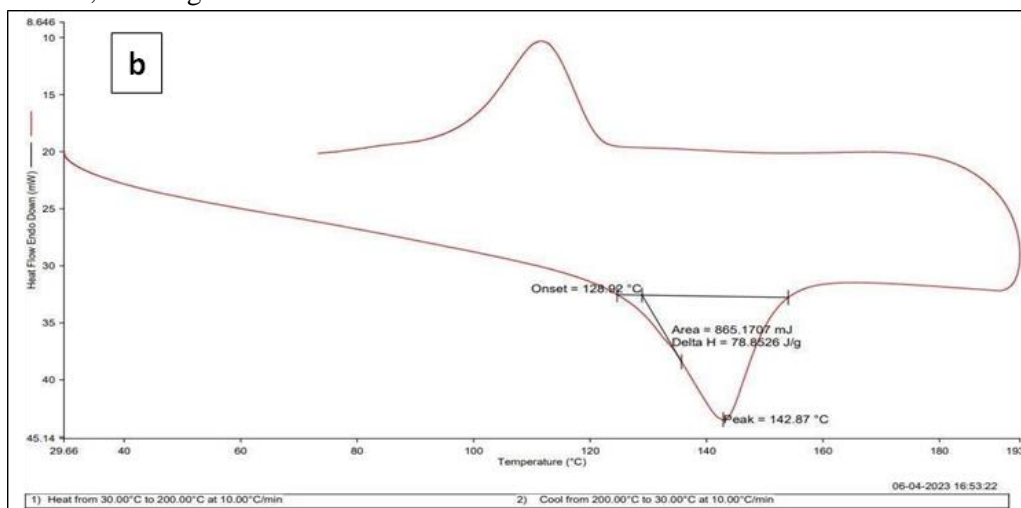


**Fig 5(b)** DSC plots for pure UHMWPE

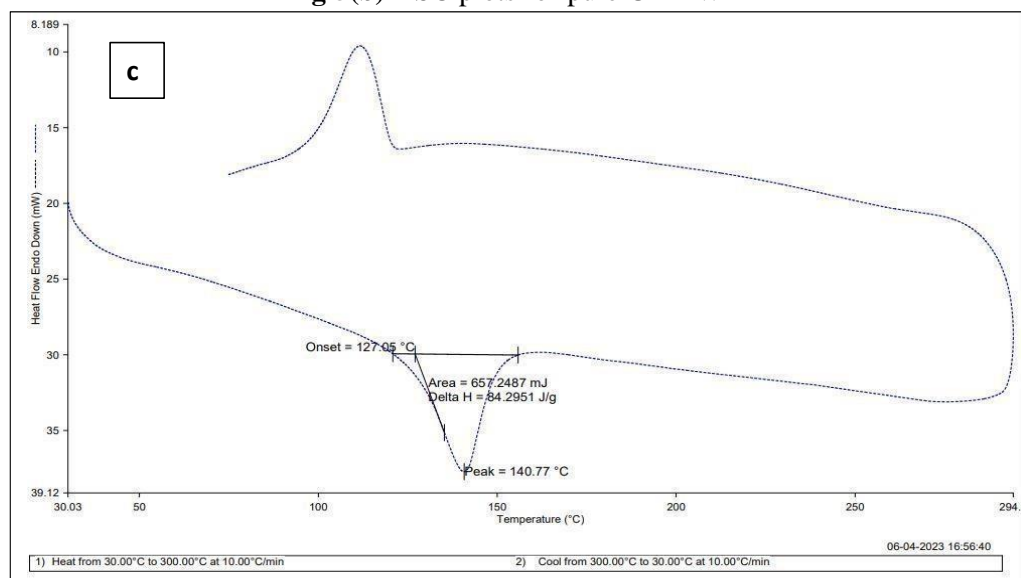


**Fig 5(c)** DSC plots for 0.5% MWCNTs in UHMWPE

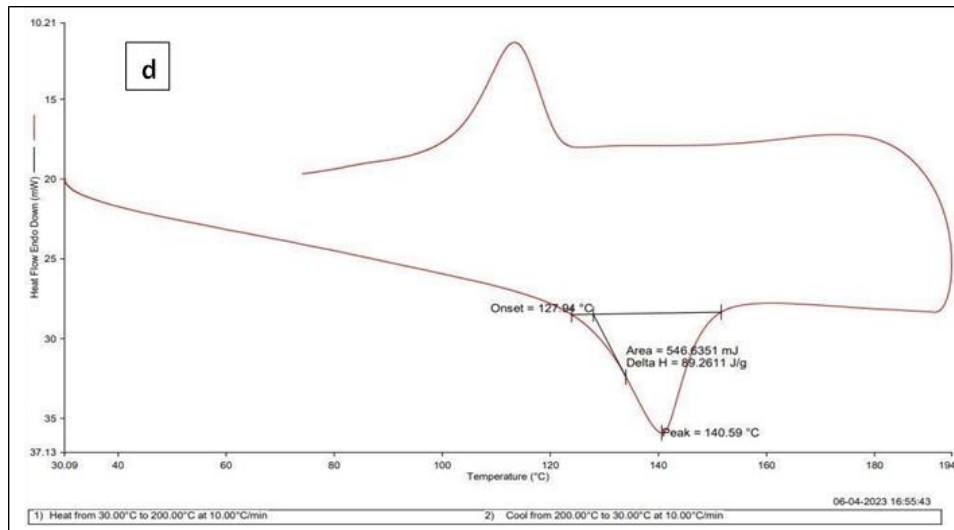


**Fig 5(d)** DSC plots for 1% MWCNTs in UHMWPE

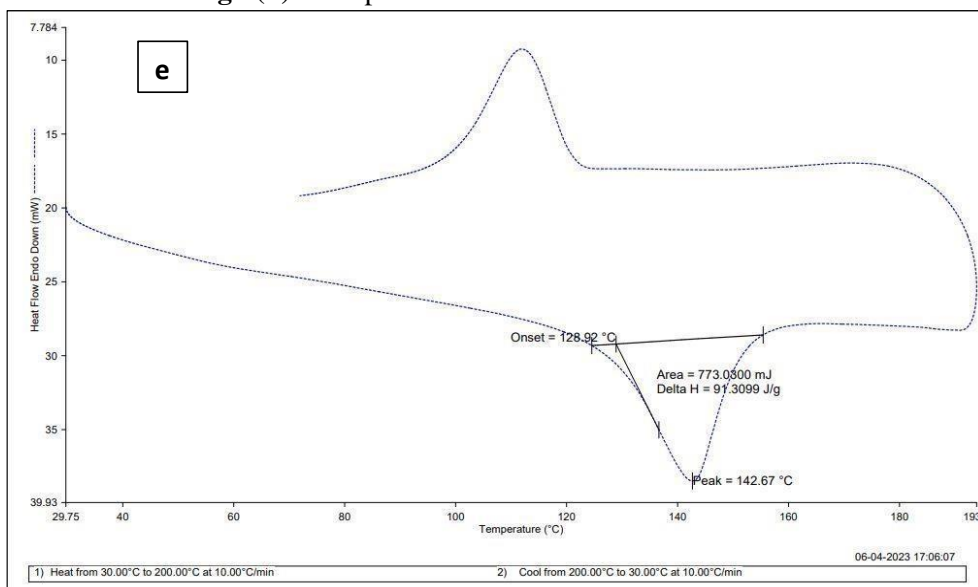


**Fig 5(e)** DSC plots for 1.5 % MWCNTs in UHMWPE

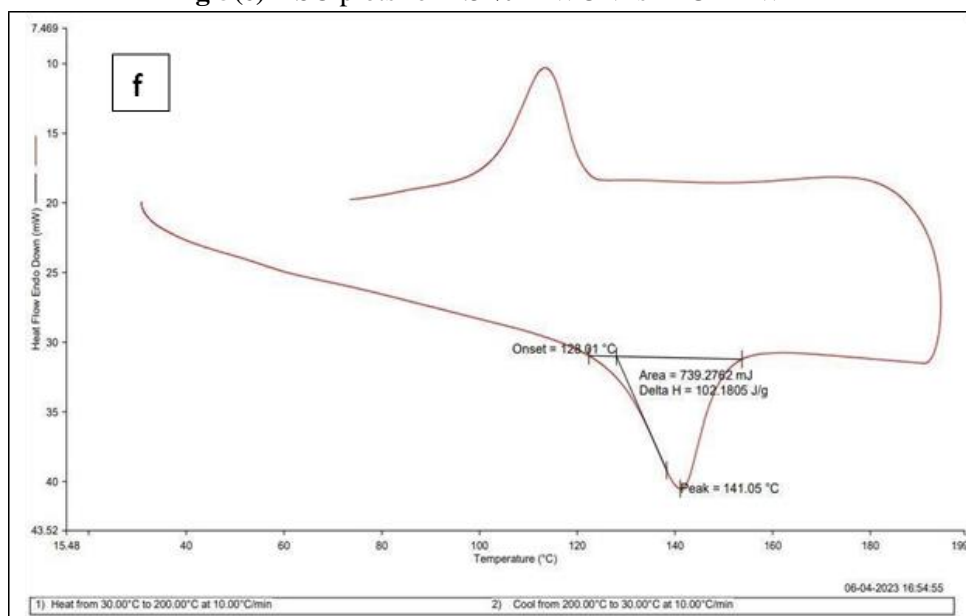


**Fig 5(f)** DSC plots for 2 % MWCNTs in UHMWPE

The measured crystallization temperatures UHMWPE with varying concentrations of MWCNTs reveal an interesting pattern. Initially, as the concentration of MWCNTs increases, the crystallization

temperatures of UHMWPE also increase. However, beyond a certain point, the crystallization temperatures start to decrease. For instance, at cooling rate of 5 °C/min, the addition of 0.5% mass of MWCNTs raises the crystallization temperature of UHMWPE from 142.87 °C (pure sample) to 140.77 °C (sample with 0.5% MWCNTs). This finding indicates that MWCNTs presence modifies the crystallization behavior of UHMWPE, initially leading to a higher crystallization temperature followed by a subsequent decrease. A distinct pattern emerges when the MWCNTs concentration approaches 0.5% mass, contrary to the initial increase observed at lower concentrations. Moreover, the investigation conducted by *Wu et al. (2020)* and *Qun Yang et al. (2023)* supports the observation that when the concentration of MWCNTs exceeds 10% mass, the crystallization temperatures of UHMWPE decline. These findings shed light on the crystallinity behavior of UHMWPE when MWCNTs are introduced. The crystallinity of pure UHMWPE was determined to be 54.2%, whereas the addition of 1.5% wt of MWCNTs resulted in improved crystallinity of 64.9%, indicating a 10.4% enhancement. However, when 2 wt% MWCNTs were utilised, the crystallinity dropped to 59.1%. This decline is due to the restricted impact of MWCNTs on the macromolecular chain motion of UHMWPE, which hinders crystallization more significantly than the heterogeneous nucleation provided by MWCNTs. These findings align with the observations made by *Anqi Li et al. (2019)* and *P.S. Rama Sreekanth et al. (2012)* regarding the impact of MWCNTs on the condensation behavior of UHMWPE. Based on the presented observations and analyses, it is hypothesized that the interplay between the heterogeneous crystallization provided by MWCNTs and the limitation of macromolecular chain motion of UHMWPE induced by MWCNTs influences the crystallization temperatures of UHMWPE composites. It is proposed that a composite sample containing 1.5 wt% MWCNTs exhibits desirable properties, such as high crystallinity, striking a balance between crystallization promotion through heterogeneous crystallization and limitation of macromolecular chain mobility, ultimately leading to enhanced crystallinity in the UHMWPE composite.

### **3.5 Impact of weight loss on polyethylene with added carbon nano-tubes**

Thermogravimetric Analysis (TGA) was used to evaluate the effect of MWCNTs on the thermal stability and oxidative degradation of nanocomposites. The breakdown curves for both the nanocomposites and pure UHMWPE are depicted in Figures 6(a) through 6(e). The thermal stability of UHMWPE was significantly enhanced through two key factors: irradiation dosage and the integration of MWCNTs as reinforcements.

The thermal stability of unirradiated pure UHMWPE was found to have starting temperature of 484.67°C. However, the inclusion of MWCNTs in nanocomposites led to an improvement in thermal stability. For instance, the initiation temperature of a nanocomposite containing 1.5 wt% MWCNTs was measured to be 491.64°C, indicating an enhancement in thermal stability. This trend was noticed for additional MWCNT doses up to 1.5 wt%, with a slight reduction observed at a composition of 2 wt% nanocomposite. The experiments conducted demonstrated the presence of MWCNTs raised the temperature at which the highest breakdown rate occurred. This phenomenon can be attributed to the favorable thermal characteristics and high thermal stability exhibited by MWCNTs. Additionally, it was observed that the heat required to achieve a certain temperature increase in the polymer was three times greater compared to that needed for MWCNTs. This observation is in conformity with the results of *Rezgar Hasanzadeh et al. (2023)*, supporting the notion of MWCNTs' superior thermal properties. By enhancing the nanocomposites' thermal endurance, the inclusion of MWCNTs contributes to their improved resistance to thermal degradation, making them suitable for applications where high-temperature environments are encountered.

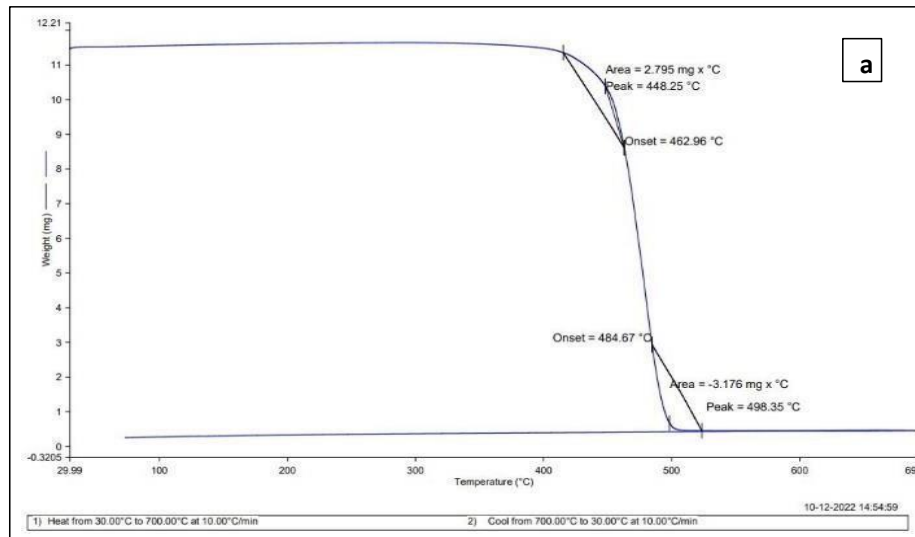


Fig 6(a) TGA plot for pure UHMWPE

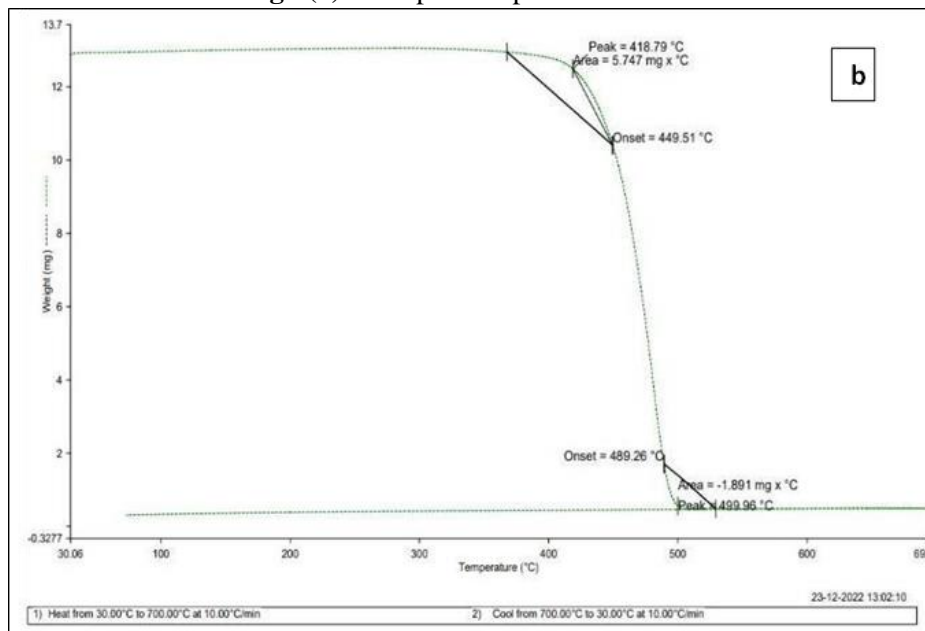


Fig 6(b) TGA curve for 0.5% MWCNTs in UHMWPE

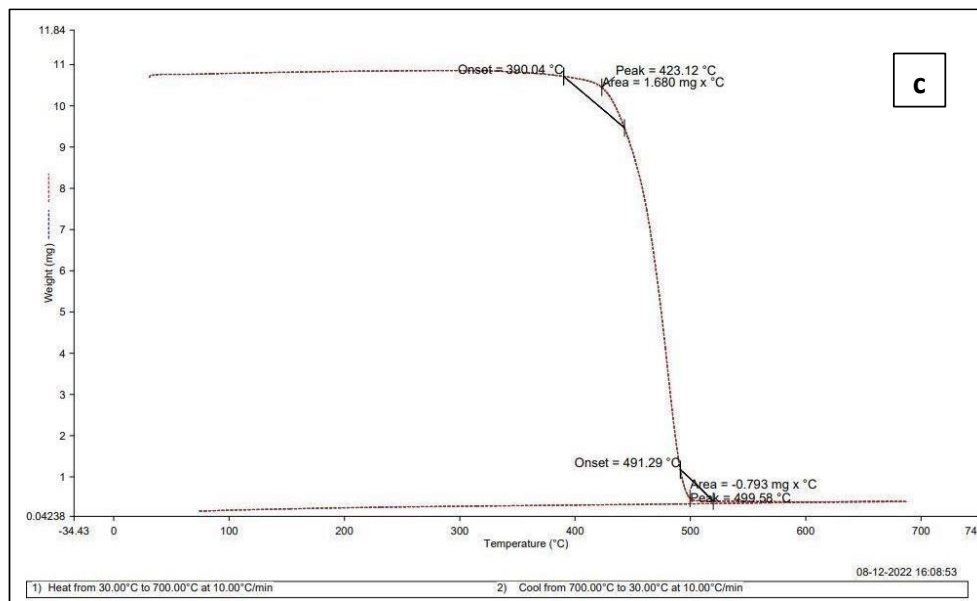
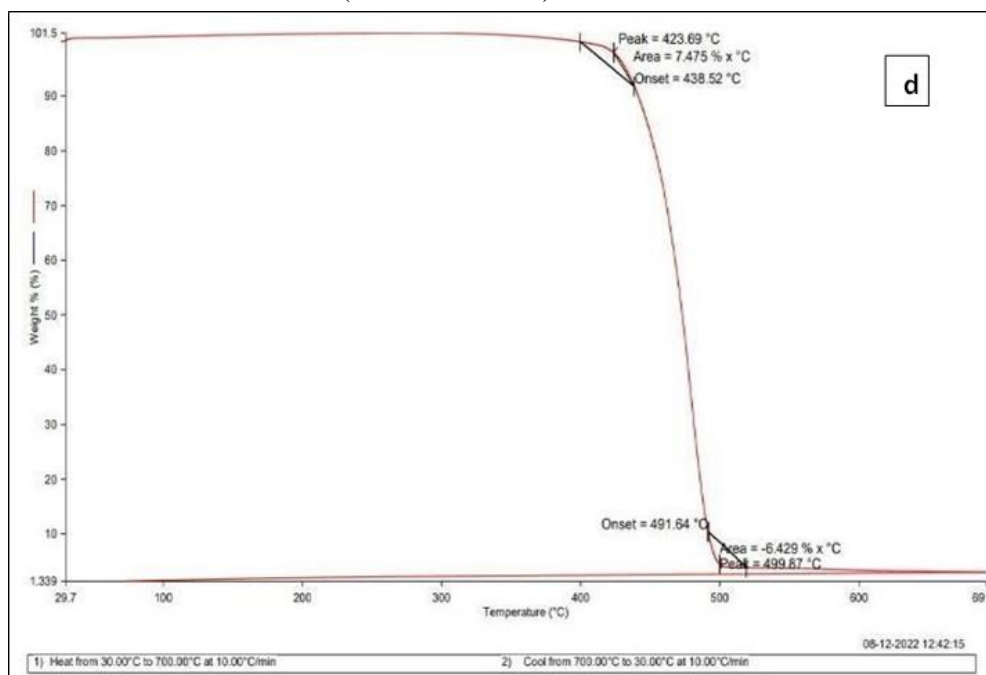
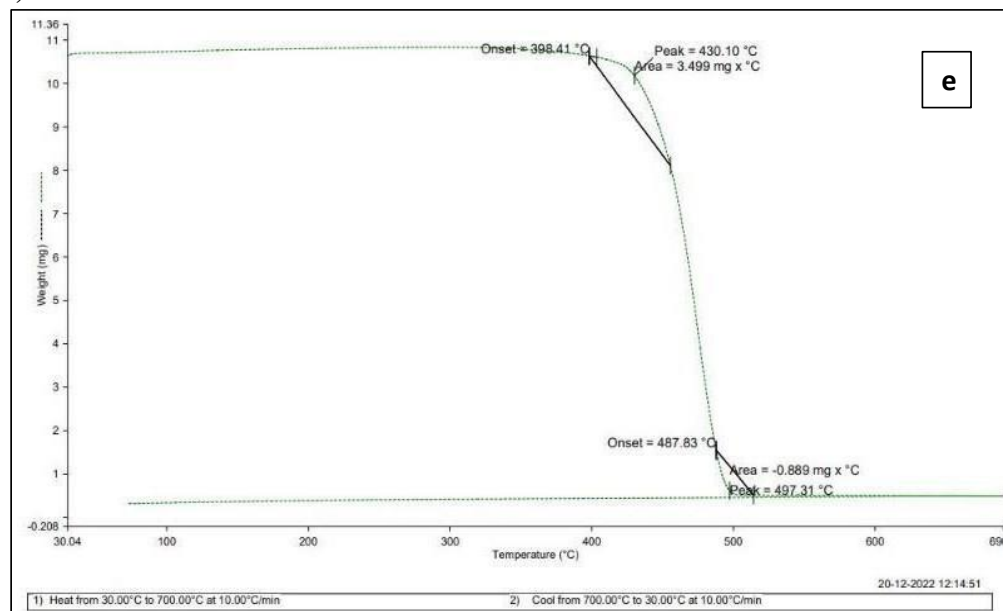


Fig 6(c) TGA curve for 1% MWCNTs in UHMWPE



**Fig 6(d)** TGA curve for 1.5% MWCNTs in UHMWPE



**Fig 6(e)** TGA curve for 1.5% MWCNTs in UHMWPE

When the same amount of heat is supplied to MWCNTs, the temperature rise is larger than that of UHMWPE. This is attributed to the superior MWCNT thermal coercivity compared to the polymer matrix. Heat tends to follow the path of least resistance, resulting in a greater heat flow via the MWCNTs rather than the polymer. Consequently, as concentration of MWCNTs increases, the temperature at which UHMWPE begins to break down also rises. This is due to the enhanced thermal stability provided by the presence of MWCNTs, which promotes better heat dissipation within the nanocomposite system. Moreover, the irradiation process induces the formation of crosslinks within the polyethylene structure, enhancing the thermal resilience of the polymer, particularly at higher temperatures. As the MWCNT concentration approaches 1.5 wt%, the weight loss of the sample increases. This is because the carbon tubes include crystalline carbon and other carbonaceous particles, which oxidize at lower temperatures than the MWCNTs. Consequently, the onset temperature decreases, resulting in higher weight loss in the nanocomposite system. These findings are supported by the research conducted by *Deepak J et al. (2023)* and *Michael N. Durso et al. (2022)*, highlighting the impact of MWCNTs across thermal enhancements and oxidative degradation behavior of UHMWPE

nanocomposites. The combination of MWCNTs' enhanced thermal conductivity and the irradiation-induced crosslinking in UHMWPE contributes to the overall improvement in thermal stability and resilience exhibited by the nanocomposite system.

#### 4. CONCLUSION

According to the results of this study, the inclusion of multi-walled carbon nanotubes significantly affects the inherent thermal properties of ultra-high molecular weight polyethylene. Previous research has demonstrated that the amalgamating MWCNTs enhances various inherent attributes of UHMWPE, including tensile strength, hardness, and density. Moreover, improvements in other mechanical characteristics such as crystallization behavior and weight reduction have also been observed. The optimal concentration of MWCNTs for achieving the most notable enhancements in the aforementioned properties has been determined to be 1.5 wt.%. Beyond this threshold, the viscosity of the composite melt increases, limiting the amount of polymer available to fully cover the expanded surface area of MWCNTs. However, despite this limitation, MWCNTs have shown promising results in improving the mechanical strength and hardness of UHMWPE. These enhanced properties are anticipated to positively impact the abrasion resistant, particularly in context of total joint replacements. By incorporating MWCNTs into UHMWPE, it is possible to create novel materials with superior performance characteristics, specifically tailored for total joint replacement applications. In conclusion, this research's findings suggests the inclusion of MWCNTs in UHMWPE holds great potential for the development of innovative materials with improved thermal properties. Further research and development in this area could lead to advancements in the field of total joint replacements, offering enhanced durability and performance in such applications.

#### Acknowledgment

The author's motivation for interaction with their sincere gratitude for the financial support extended by the All India Council for Technical Education (AICTE) through the Research Promotion Scheme (RPS). This support made it possible to bring to fruition the project identified with reference number 8-45/FDC/RPS/POLICY-1/2021-22. The authors are grateful for the instrumental role played by AICTE in enabling the successful execution of this research endeavor. The authors thank the Research Centre, Department of Mechanical Engineering, R.V.R. & J.C. College of Engineering (A), Guntur, for providing necessary support in conducting the experiments and their support in characterization of materials/composites.

#### References

1. Fahad Alam, M.Choosri, Tejendra K. Gupta, K.M. Varadarajan, D.Choi and S.Kumar(2018) Electrical,mechanical and thermal properties of graphene nanoplatelets reinforced UHMWPE nanocomposites. *Material Science & Engineering B* 241, 82-91
2. Samy Yousef, Annamaria Visco, Giovanna Galtieri, Davide Nocita(2017) Wear behavior of UHMWPE reinforced by carbon nanofiller and paraffin oil for joint replacements *Materials Science & Engineering C* 73,234-244
3. J.Park, R.S. Lakes(2007) *Biomaterials- an introduction* Springer New York,
4. M.M.J. Treacy, T.W. Ebbesen and J.M. Gibson(1996) Exceptionally high Young's modulus observed for individual carbon nanotubes *Nature* 381,678-680
5. Sita Shrestha, Bishnu Kumar Shrestha, Sung Wong Ko, Rupesh Kandel, Chan Hee Park, Cheol Sang Kim(2021) Engineered cellular microenvironments from functionalized multiwalled carbon nanotubes integrating Zein/Chitosan @ Polyurethane for bone cell regeneration *Carbohydrate Polymers* 251
6. Jong Hyun Eun, Do Hyun Kim, In Uk Jang, Sun Min Sung, Ming Seong Kim, Bo Kyoung Choi, Sun Woo Kang, Min Soo Kim, Joon Seok Lee(2022) A Study on mechanical properties and

thermal properties of UHMWPE/MWCNT composite fiber with MWCNT content and draw ratio  
*Journal of Engineered Fibers and Fabrics* 17, 1-10

7. Xue, Y., Wu, W., Jacobs, O., Schadel, B., (2006). The tribological behavior of UHMWPE/HDPE blends reinforced with multi-wall carbon nanotubes. *Polymer Testing* 25, 221–229.
8. Bakshi, S.R., Tercero, J.E., Agarwal, A., (2007) Synthesis and characterization of multi-walled carbon nanotube reinforced ultra-high molecular weight polyethylene composite by electrostatic spraying technique. *Composites: Part A* 38, 2493–2499.
9. Morlanes, M.J.M., Castell, P., Nogue´s, V.M., Martinez, M.T., Alonso, P.J., Pue´rtolas, J.A., (2011) Effects of gamma-irradiation on UHMWPE/MWNT nanocomposites. *Composites Science and Technology* 71, 282–288.
10. Fonseca, A., Kanagaraj, S., Oliveira, M.S.A., Simões, J.A.O. (2011) Enhanced UHMWPE reinforced with MWCNT through mechanical ball-milling. *Defect and Diffusion Forum* 312–315, 1238–1243.
11. K. Esumi, M. Ishigami, A. Nakajima, K. Sawada, H. Honda (1996) Chemical treatment of carbon nanotubes, *Carbon* 34 279–281.
12. Ayat Bozeya, Yahia F. Makableh, Laith A. Al-Mezead, Rund Abu-Zurayk (2023) Wet Ball milling and hot press for the preparation of UHMWPE/modified MWCNTs nanocomposite with enhanced mechanical and thermal properties *Polymer Bulletin* 70
13. Gu, J., Guo, Y., Lv, Z., Geng, W., Zhang, Q., (2015) Highly thermally conductive POSS-g-SiCp/UHMWPE composites with excellent dielectric properties and thermal stabilities *Composites: Part A* 78, 95-101
14. Suhaib Umer Ilyas, Rajashekhar Pendyala, Marneni Narahari (2017) Stability and thermal analysis of MWCNT-thermal oil-based nanofluids *Colloids and Surfaces A: Physicochemical and Engineering aspects* 527, 11-22
15. Melk L, Emami N (2018) Mechanical and thermal performances of UHMWPE blended vitamin E reinforced carbon nano particles *Composites Part B: Engineering* 146, 20-27
16. Sreekanth, P.S.R., Kanagaraj, S., (2013) Assessment of bulk and surface properties of medical grade UHMWPE based nano composites using Nano indentation and micro tensile testing. *Journal of Mechanical Behavior of medical Materials* 18, 140–151.
17. Nilesh Dalai, P.S. Rama Sreekanth (2021) UHMWPE/nanodiamond nanocomposites for orthopaedic applications: A novel sandwich configuration based approach, *Journal of Mechanical behavior of Biomedical applications* 116
18. J.A. Puertolas, S.M. Kurtz (2014) Evaluation of carbon nanotubes and graphene as reinforcements for UHMWPE-based composites in arthroplastic applications: A review, *Journal of Mechanical behavior of Biomedical applications* 39, 129-145
19. Samaneh Salkhi Khasraghi and Mostafa Rezaei (2013) Preparation and characterization of UHMWPE/HDPE/MWCNT melt-blended composite *Journal of Thermoplastic Composite Materials* 28, 305-326
20. Seung Yoon On, Steve Park, Seong Su Kim (2019) Preparation and Characterization of Hybrid Structured MWCNT/UHMWPE Fiber Sensors for Strain Sensing and Load Bearing of Composite Structure *Advanced Material Technologies* 4
21. I.A. Markevich, G. Ye. Selyutin, V.A. Poluboyarov, N.A. Drokin, A.G. Selyutin and M.A. Matzko (2020) Influence of ultrasonic treatment on mechanical and electro-physical characteristics of UHMWPE/MWCNT composites *Materials Today: Proceedings* 25, 532-535
22. Ashrith, H.S.; Jeevan, T.P.; Xu, J., (2023) A Review on the Fabrication and Mechanical Characterization of Fibrous Composites for Engineering Applications *J. Compos. Sci.*, 7, 252
23. Tamara R. Kadhim, Jawad K. Oleiwi, Qahtan A. Hamad (2022) Investigation of Compression and Hardness for UHMWPE Bio-composites as Internal Bone Plate Fixation *Engineering and Technology Journal* 40, 1771-1782

24. Ali Sadeghinia, Somaieh Soltani, Marziyeh Aghazadeh, Javad Khalilifard, Soodabeh Davaran(2020) Design and fabrication of clinoptilolite-nanohydroxyapatite/chitosan-gelatin composite scaffold and evaluation of its effects on bone tissue engineering Journal of Biomedical Materials Research 108,221-233
25. PS Rama Sreekanth, S Kanagaraj(2014) Influence of MWCNTs and gamma irradiation on thermal characteristics of medical grade UHMWPE Bull.Mater.Sci, Vol 37 2, 347-356
26. Premnath V, Bellare A, Merrill E W, Jasty M and Harris W H(1999) Molecular rearrangements in ultra high molecular weight polyethylene after irradiation and long-term storage in air Polymer 40, 2215-2229
27. Ries Michael D MD, Pruitt,Lisa PHD(2005) Effect of Cross-linking on the microstructure and Mechanical Properties of Ultra-High Molecular Weight Polyethylene Clinical Orthopaedics and Related Research 440, 149-156
28. Wu Zexiong, Li Anqi, Zhang Zishou, Mai Kancheng(2022) Crystallization of UHMWPE nanocomposites filled by multi-wall carbon nanotubes Journal of Thermal Analysis and Calorimetry 146, 2223-2232
29. Qun Yang, Run Zhang, Jing Tian, Hailong He, Ping Xue, Xiaonong Chen, Mingyin Jia,”Isothermal and non-isothermal crystallization kinetics of UHMWPE composites incorporating with GNP/MWCNT”,Journal of Polymer Research 30 2023,152
30. Anqi Li, Zexiong Wu, Zishou Zhang, Kancheng Mai(2020) Preparation and characterization of ultrahigh molecular weight polyethylene composites with high content of multiwall carbon nanotubes Polymer Composites 41,1972-1978
31. P.S. Rama Sreekanth, S. Kanagaraj(2013) Assessment of bulk and surface properties of medical grade UHMWPE based nanocomposites using Nanoindentation and microtensile testing”,Journal of the mechanical Behavior of Biomedical Materials 18, 140-151
32. Rezar Hasanzadeh, Taher Azdast, Patrick C. Lee, Chul B. Park(2023) A review of the state-of-the-art on thermal insulation performance of polymeric foams Thermal Science and Engineering Progress 41
33. J. Deepak, H.Adarsha, R. Keshavamurthy , N.P. Ramkumar(2023) Analysis of Thermal Behaviour of Carbon Nanotubes-Reinforced HDPE Composites Developed using FDM Process Journal of the institution of Engineers(India): Series D 25
34. Michael N. Durso, A.John Hart(2022) Purification of dense carbon nanotube networks by subcritical hydrothermal processing Carbon Trends 9

## Investigating the Performance and Emission Characteristics of Diesel Engine Fuelled with Rice Bran Biodiesel

K.Sai Babu<sup>1</sup>, V.Dhana Raju<sup>2</sup>, Devarakonda Vamsi<sup>3</sup>, Emmanuel Buradagunta<sup>4</sup>

<sup>1,2,3</sup>Lakireddy Bali Reddy College of Engineering, Mylavaram, A. P. -521230

<sup>4</sup>DVR & Dr. HSMIC College of Technology, Andhra Pradesh, India

Corresponding author mail id: [saibabu@lbrce.ac.in](mailto:saibabu@lbrce.ac.in)

### ABSTRACT

Biodiesel is an oil which is extracted from the seeds and nuts of vegetables then blended with diesel. This biodiesel is used for the transportation fuel. But these organic fuels easily react with the oxygen. Due to this reaction, it is transformed into crystal like formation. This kind of fuel does not suitable for the engine. So, this paper is concentrated on the improving oxidation stability of rice bran biofuel along with analyzing the diesel engine characteristics. Performance outcomes exposed that rice bran biodiesel gave favorable brake thermal efficiency and minor brake specific fuel consumption. Moreover, the HCs, CO<sub>x</sub> and NO<sub>x</sub> emissions decreased as load increased as compared with diesel. From the outcomes B20+1500ppm showed optimum oxidation stability as 7.35hr. At peak load, B20+1500ppm showed BTE and BSFC were 32.04% and 0.27kg/kW-hr respectively.

**Key words:** Biodiesel, Rice-bran oil, Oxidation stability, Performance parameters and emission characteristic

### 1. INTRODUCTION

Energy is defined as the ability to do work. Usually in thermodynamics, heat energy often called as energy, whereas heat energy is the energy on the account of temperature difference. As per first law of thermodynamics energy can neither be created and nor be destroyed. Naturally heat is transmission from grater thermal section to the lower thermal section but with the aid of external device it may transfer from low to high. Biodiesel is a nonconventional, recyclable oil made-up locally from vegetal oils, animal fats, or biodegradable restaurant oil. Bio-diesel is not same petroleum-based oil. Biodiesel has been low emissions than petroleum fuel. It is an alternative fuel like conventional. The most effective issue regarding biodiesel is that it is made of animal fat, plants and used cookery oil. The way to alter these oils to biofuels is titled transesterification. Biofuel is a less harmful to the atmosphere if spilled. Antioxidants are natural constituents that may avoid or adjournment the oxidation issues. Oxidation nothing but the damage due to reactions of oxygen with products. This reaction can toxic or spoil the properties of items. To overcome this kind of problems, we should add some additives with the products called anti-oxidants, these facilitate the counter attack to oxidation reaction.

#### 1.1 Literature Survey

Literature survey helped a lot to move the wok forward. This literature not only focussed on the diesel engine characteristics but also focused on the fuel additive, ignition improvers and advancements in the biodiesels etc. Mourad (2021) et al. directed experimentation on engine for improving the performance and discharge characteristics. By exhaust gas recirculation (EGR) and pre heated biodiesel on a CI engine with a percentage is reduced to 25% of EGR and preheated biodiesel. There is a clear reduction of emitted gases by using these biofuels [1]. Janakiraman (2021) et al. inspected the effects of triple (diesel + biodiesel + bio-ethanol) oil mixed with nano additives on an engine. Following an analysis of the engine outcomes, it was determined that the blend with 65 ppm TiO<sub>2</sub> nano additions is the favourable substitute oil, balancing global energy needs in a timely manner [2]. Kaya (2020) et al. looked at the emissions and performance metrics of B20 and B100 in comparison to waste frying oil biodiesel under full circumstances. Transesterification is used to convert waste frying oil to biodiesel in this experiment. The outcomes were showed that decrement in emissions, BSFC and increment in BTE [3]. Asokan (2020) et al. examined the performance and emission features engine by diesel and

watermelon kernel oil mixes. The goal of this framework is to explore the emissions, combustion, and performance of engine that runs on a diesel and watermelon kernel oil (WMB) blend. This test result demonstrated that the WMB B20 mixture is the best substitute oil for engines [4]. Sivasubramanian (2019) et al. studied the impact of ammonia on biodiesel-fuelled single cylinder diesel engine emissions. Ammonia was introduced to mustard methyl ester mixes and tested under various load settings in this experiment. This experiment resulted in lower CO, HC, and NO<sub>x</sub> emissions as well as more air in the combustion chamber [5]. Gowtham (2021) et al. inspected the emissions and performance features of engine running on fumigated calophylluminophyllum vapours. Calophylluminophyllum oil derived through the transesterification process and biodiesel in various amounts were employed in this experiment. The outcomes exhibited that BTE, BSFC, heat release, and peak pressure increase, whereas HC, CO, and NO<sub>x</sub> emissions decrease [6]. Saibabu (2019) et al. compared the different types of antioxidants as an additive in tamarind biodiesel with different proportions. This work not only focussed on the stabilization factor but also focussed on engine characteristics. Among all the blends TSME 20 BHA 2000ppm showed better results as per standards [7]. T. Srinivasa Rao (2023) et al. analysed the oxidation stability and CI engine parameters by mixing the BHT and TBHQ with TSME. From the fair outcomes B20 with BHT 2000ppm showed the augmented oxidation stability i.e., 7.9 hrs and favourable diesel engine characteristics [8].

By the literature survey, biodiesels gave great impact by reducing the emissions and better results in performance point of view but ignition improvers helped to augment the performance parameters.

## 2 MATERIALS AND METHODS

The crude rice bran oil has highest viscosity and density compared to the diesel. transesterification is one of the approaches that can used to decrease the fluid thickness of the crude oil. Higher viscosity and density of crude rice bran oil is reduced by using transesterification process also transesterification method helped to prepare the engine suitable fuel from raw material.

### 2.1 Butylated Hydroxytoluene Additive (BHT)

BHT also recognized as dibutylated hydroxytoluene as presented in Fig. 1, is a lipophilic organic complex, chemically a derivative of phenol, that is beneficial for its antioxidant properties. By literature survey BHT 1500ppm showed the optimum results.



Fig. 1. Butylated hydroxytoluene.

### 2.2 Properties of Fuel

The following fuel samples were arranged and tried in a CI engine. These fuel samples were prepared after the transesterification process and BHT mixed with the samples as presented in Fig. 2. as per literature survey.



Fig. 2. RBO with 1500ppm BHT.

Fuel properties were calculated by using standard apparatus. The properties of rice bran oil and diesel were listed in table 1.

**Table 1.** Fuel properties

S.No	Properties	Diesel	Rice bran oil	B20+ BHT 1500ppm	B30+ BHT 1500ppm	B40+ BHT 1500ppm
1	Calorific Value(kJ/kg)	42500	37900.8	41380	40820	40260
2	Specific gravity	0.83	0.92	0.830	0.842	0.846
3	Kinematic Viscosity(cts)	4.3	6.29	4.60	4.89	5.19
4	Flash Point( <sup>0</sup> C)	54	166	64.5	75	85.5
5	Fire Point( <sup>0</sup> C)	65	198	75.5	86	96.5
6	Cetane number	43	54	44	45	46

### 2.3 Investigational Arrangement

The arrangement comprises of single cylinder, four stroke, diesel engine associated to eddy electricity kind of dynamometer for loading as mentioned in Fig.3. The CI engine works on the principle of diesel cycle. This cycle consists of four strokes named as intake, compression, expansion and exhaust strokes. In CI engine through intake stroke air alone arrives the engine and fuel enter in compression stroke with the help of fuel injector. Then required power developed in working stroke and finally exhaust gases were sent out in exhaust stroke.



**Fig. 3.** Diesel engine set up.

### 2.4 Fatty Acid Content

A gas chromatograph shown in Fig. 4, is used for extricating the chemicals in a complex sample and it is a chemical analysis instrument. Gas chromatograph is a method of separating the volatile compounds from a mixture.



**Fig. 4.** Photographic view for gas chromatograph.

From the above test rig, the quantity of palmitic acid, stearic acid, ricinoleic acid and arachidic acid were 5.4%, 2.6%, 11.6% and 0.5% respectively.

### 2.5 Oxidation Stability Test

To overcome the auto-oxidation damage in the bio-diesels it is important to blend with the counter oxidants called as antioxidants or anti-oxidants. The storage constancy of the biofuel is relying upon its oxidation constancy. So, the evolution of oxidation stability is must. In this project the oxidation constancy is estimated with rotating bomb oxidation tester (RBOT), as presented in Fig. 5 and the related outcomes tabulated in table 2



**Fig. 5.** Rotating bomb oxidation tester.

**Table 2.** Oxidation stability values among B20 and other BHT blends with different proportions.

Test	Sample name			
Oxidation stability test 110°C (hr)	B20	B20+1500ppm	B30+1500ppm	B40+1500ppm
	5.23	7.35	7.21	7.11

### 3. RESULTS AND DISCUSSIONS

By the experimentation like oxidation stability test and diesel engine test the outcomes are obtained. Those were analyzed with graphical representation as below.

#### 3.1 Analysis on Oxidation Stability

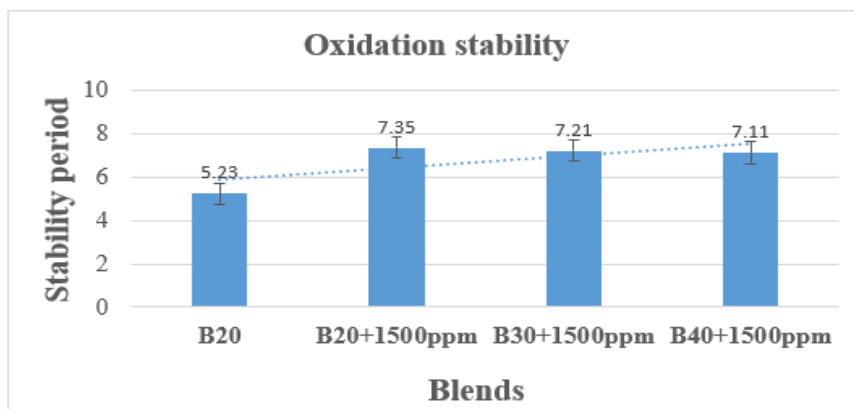


**Fig. 6.** Graphical representation on oxidation stability among B20 and other BHT blends.

As per standard the oxidation stability must be 6hr. As compared with biodiesel, diesel showed better stability because of low carbon content. The blend B20 showed poor oxidation stability as 5.23hr. After mixing of BHT remaining blend showed optimum results. However, at B20+1500ppm showed best results as compared with other blends as 7.35hrs as represented Fig. 6, because of effect of BHT anti-oxidant and more diesel quantity.

#### 3.2 Analysis on Diesel Engine Characteristics

The tests were directed on the CI engine at constant speed with fluctuating 0 to 100% loads with diesel and dissimilar mixtures of rice bran oil and optimum blend with BHT. All these values are compared with diesel.

**3.2.1 Performance Parameters.** The performance constraints, such as BTE, BSFC were calculated from the experiential constraints and were represented in the form of graphs from the measured values.

**3.2.1.1 Brake Thermal Efficiency.** The discrepancy of BTE with load for various fuels is presented in below Fig 7. BTE is the proportion of BP to the energy provided by the oil.

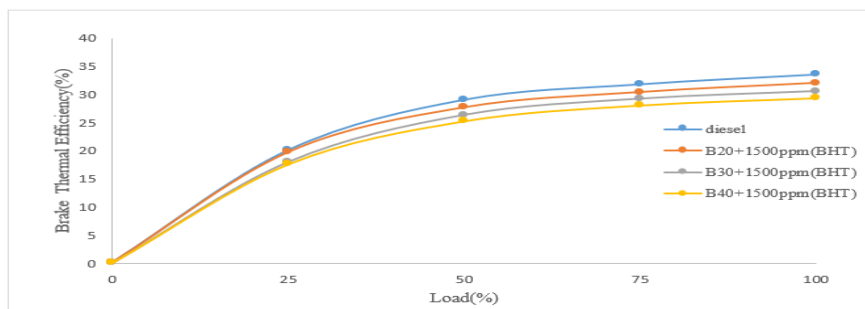


**Fig. 7.** Variation in brake thermal efficiency.

By the above graph, in all situations, BTE rises with increment in load. BTE is greater for diesel because of greater heating value. At full load conditions diesel has 33.58% and whereas for B20+ BHT 1500ppm, B30+ BHT 1500ppm and B40+ BHT 1500ppm has 32.04%, 30.54% and 29.34%. For B20+ BHT 1500ppm has 4.81% difference with diesel, B30+ BHT 1500ppm has 10% difference with diesel and B40+ BHT 1500ppm has 14.5% difference with the diesel. So B20+ BHT 1500ppm is best because it near to diesel.

**3.2.1.2 Brake Specific Fuel Consumption.** The Fig. 8, was drawn between BSFC and Load. The discrepancy in BSFC with load for diverse blends is mentioned in graph and BSFC is the proportion of quantity of oil feeding and brake effective power.

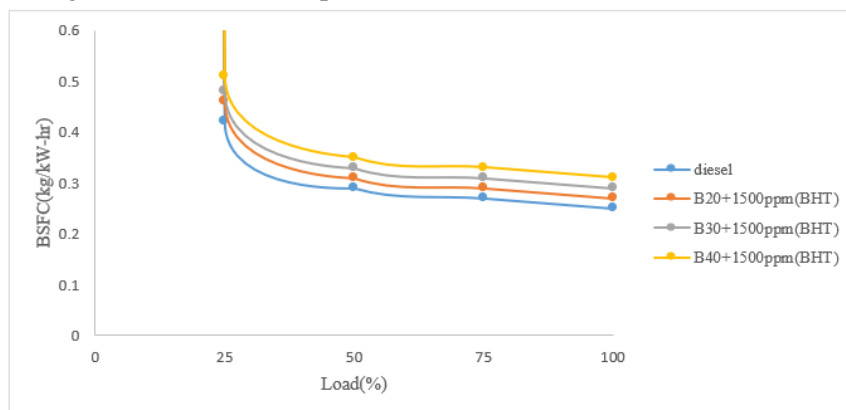


**Fig. 8.** Variation in Brake Specific Fuel Consumption.

From the above graph, BSFC reduced gradually with growth in BP. The chief cause for this could be relatively less portion of the heat is lost at higher loads. The BSFC for B20+BHT 1500rpm is 0.27 kg/kW-hr, it is best because it is near that of diesel.

**3.2.2 Emission Analysis.** The emission parameters such as carbon monoxide, smoke opacity, HC, NO<sub>x</sub> were carried for rice bran oil with BHT at 1500ppm and results were plotted in the form of graphs in the below.

**3.2.2.1 Smoke Opacity.** The below Fig. 9, show the trend of smoke with respect to load. The smoke increases with increase in load. This may be due improper mixing of air and oil due to less time available for mixing at full load.

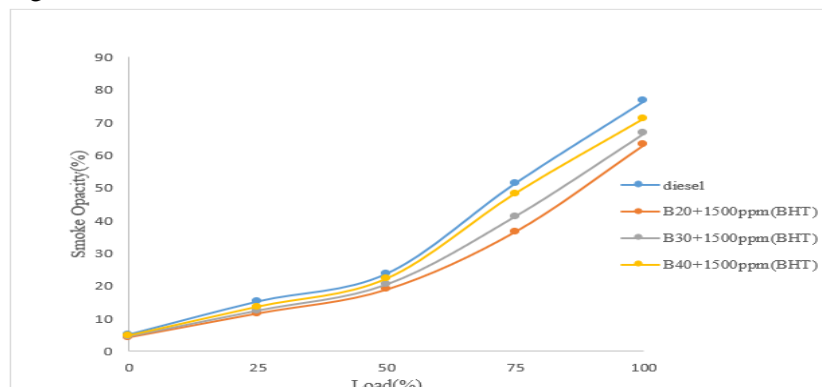


**Fig. 9.** Variation in Smoke.

Through the above graph, at full load smoke is very much less for B20+BHT 1500ppm to that of diesel because of better mixing of air and fuel in case of B20+BHT 1500ppm. At full load minimum Smoke is obtained for B20+BHT 1500ppm, is 63.2% whereas for diesel it is 76.6%.

3.2.2.2 *Carbon Monoxide (CO)*. CO discharge depends on constraints such as A/F proportion and the engine temperature etc. It is one the poisonous products of burning caused because of incomplete combustion of the fuel.

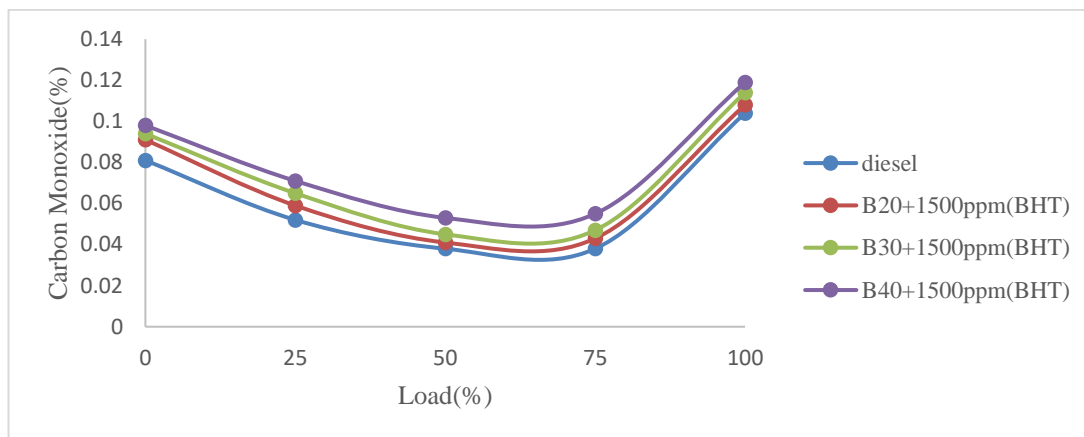


**Fig. 10.** Variation in Carbon Monoxide.

The above Fig. 10, shown the trend of CO emissions regarding the percentage of load. At full load diesel has CO emission of 0.104% whereas for B20+BHT 1500ppm it is 0.108%. There is a reduction about 18% decrease in CO releases at peak load with respect to diesel. This could be due to the better burning because of inferior atomization and shortening ignition delay. Due to this the degree of mingling of fuel and air could have improved leading to proper ignition resulting decrease in CO discharges.

3.2.2.3 *Oxides of Nitrogen (NO<sub>x</sub>)*. The NO<sub>x</sub> emission from the diesel engine depends on the highest temperature and oxygen accessibility during the burning.

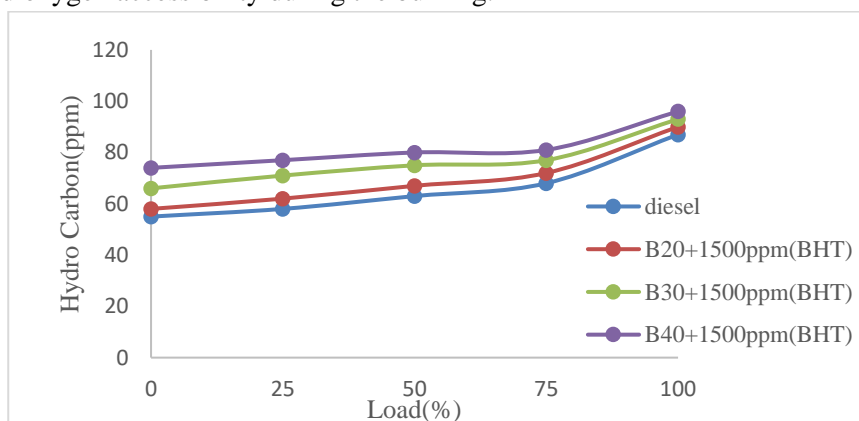


**Fig. 11.** Variation in NO<sub>x</sub>.

The above Fig. 11, demonstrations the trend of NO<sub>x</sub> emissions regarding the load for blends of B20+BHT 1500ppm, B30+BHT 1500ppm and B40+BHT 1500ppm. At Peak load diesel showed 2056ppm and for B20+BHT 1500ppm was 1854 ppm. At full load NO<sub>x</sub> is reduced for B20+BHT 1500ppm.

3.2.2.4 *Hydro Carbon (HC)*. The discrepancy of HC with load is exposed in the Fig. 12. The below figures of shows that HC releases rises with growth in load and maximum HC emission is observed at full load.

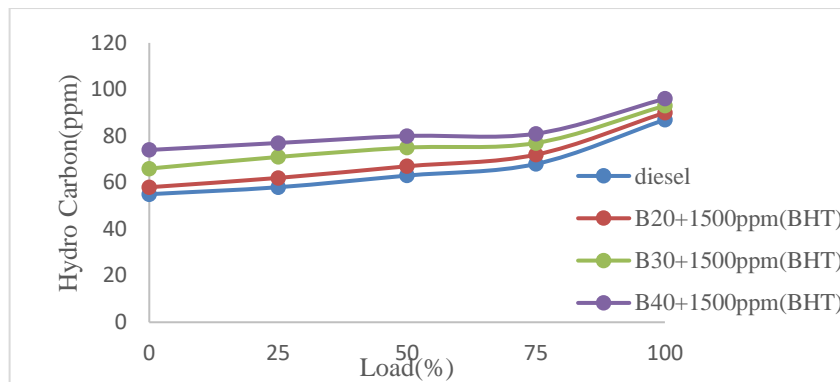


**Fig. 12.** Variation in hydro carbon.

With the help of above graph, the minimum HC emission at full load was observed for B20+BHT 1500ppm. The HC emission of B20+BHT 1500ppm is 90ppm whereas diesel has 87ppm. This may be due to well mixing of air and fuel which led to well burning. Due to this complete combustion in the engine cylinder, there is decrease in HC discharges.

#### 4 CONCLUSIONS

This investigation of experimentations is directed on CI engine using blends of rice bran oil. Among the blends with B20+ BHT 1500ppm showed better results.

- It is observed that among the tested biodiesel blends of rice bran oil with BHT, B20+ BHT 1500ppm produced well performance and emission features associated to B30+ BHT 1500ppm and B40+ BHT 1500ppm, so B20+ BHT 1500ppm is taken as optimum blend.
- The BTE rises with growth in ignition improver by volume fraction in mixtures. By the outcomes of biodiesel blends with added ignition improver, B20+ BHT 1500ppm showed better result with improvement of brake thermal efficiency about 5% than that of diesel.
- Results obtained in this work shows that B20+ BHT 1500ppm has 8% lower BSFC compared to diesel.
- As far as emissions are concerned obtained B20+ BHT 1500ppm produced lesser smoke, CO, NO<sub>x</sub> and HC, then that diesel among the blends. For B20+ BHT 1500ppm the reduction in smoke is about 21% and reduction in CO emissions is about 11%. Among the blends of B20+ BHT 1500ppm produced better emission characteristics than that of diesel.

From the above results it can conclude that rice bran oil has considered as a good substitute fuel for diesel. The performance and emission parameters of B20+ BHT 1500ppm showed better results, so it is taken as optimum blend.

#### References:

1. M.Mourad, El-sadek H.NourEldeen.2021. "Improving diesel engine performance and emissions characteristics fuelled with biodiesel", vol.302. <https://doi.org/10.1016/j.fuel.2021.121097>
2. S.Janakiraman, T.Lakshmanan, P.Raghu.2021. "Experimental investigation analysis of ternary(diesel+biodiesel+bio-ethanol) fuel blended with metal\_doped titanium oxide nanoadditives tested on a diesel engine", vol.235. <https://doi.org/10.1016/j.energy.2021.121148>
3. Cenk kaya and Gorkem Kokkulunk.2020. "Biodiesel as alternative additive fuel for diesel engine and an experimental and theoretical investigation on emissions and performance characteristics", vol. 45(2):1-23. <https://doi.org/10.1080/15567036.2020.1774685>
4. Asokan M-A, S.S.Prabu, V.s.Akhil,P.S.Bhuvan,Y.B.Reddy.2020. "Performance and emission behaviour of diesel and blends of watermelon seed oil biodiesel in direct injection diesel engine", vol.45. <https://doi.org/10.1016/j.matpr.2020.12.469>
5. R.Sivasubramanian, J.B.Sajin and Gokul Omanakuttan Pillai.2019. "Effect of ammonia to reduce emission from biodiesel fuelled diesel engine", vol.43. <https://doi.org/10.1080/01430750.2019.1663367>

6. M Gowtham, R Prakash.2021. “Influence of fumigated calophyllum inophyllum vapours on the combustion, performance and emission characteristics of a diesel engine”,vol.43. <https://doi.org/10.1080/15567036.2019.1636159>
7. K. Saibabu, V. Dhana Raju, K. Appa Rao, S. Rami Reddy & P. Tharun Sai.2019. “Experimental studies on the influence of antioxidant additive with waste tamarind biodiesel on the diverse characteristics of diesel engine”, vol.43. <https://doi.org/10.1080/01430750.2019.1636871>
8. T. Srinivasa Rao, K. Sai Babu, V. Dhana Raju, Ch. Raghavendra, N. Kishan.2023. “Augmentation of oxidation stability of biodiesel and investigation on diesel engine characteristics fuelled with tamarind biodiesel”, vol.2810 issue 1. <https://doi.org/10.1063/5.0146837>

## Experimental Investigation of Performance R134a Vapour Compression Refrigeration System Permanent Magnetic Field After Condenser and Diffuser at Compressor Outlet

P.Tejomurthi<sup>a</sup>, K.Dilip Kumar<sup>b</sup> and B.BalaKrishna<sup>c</sup>

<sup>a</sup>Department of Mechanical Engineering Seshadri Rao Gudlavalleru Engineering College Guldavalleru <sup>b</sup>Department of Mechanical Engineering, Lakireddy Bali Reddy College of Engineering, Mylavaram <sup>c</sup>Department of Mechanical Engineering JNTUK Kakinada <sup>a</sup>Department of Mechanical Engineering Seshadri Rao Gudlavalleru Engineering College Guldavalleru <sup>b</sup>Department of Mechanical Engineering, Lakireddy Bali Reddy College of Engineering, Mylavaram <sup>c</sup>Department of Mechanical Engineering JNTUK Kakinada

### ABSTRACT

The performance improvement of vapour compressor system is very identical in current days. The refrigeration and air conditioning systems are operated by compressor (Operated by electrical power) and phase change gas (Ex: R134a). The load these systems increases due to increase in population and needs (comfort of their life). The power consumption and global warming is important one. This consideration the new techniques are introduced to control the electrical power consumption and global warming, one is arrange a diffuser at compressor, and apply magnetic field at liquid line. The experiments are conducted by with and without magnetic pairs (each magnet having 100gauss) by with and without diffuser, results are observed the COP of the system, cooling load increased and compressor work is decreased.

**Keywords-** Magnetic field, Diffuser, HFC refrigerant and COP

### 1. INTRODUCTION

Vapour compression refrigeration (VCR) system, the refrigerant undergoes phase change from liquid to vapour and vice versa by absorbing the heat from evaporator and rejecting it at the condenser. The system performance mainly depends on the ratio of heat transfer rate at the evaporator and input improved by various methods.

The Industrial revolution increased after the second half of the twentieth century, the new technological products in our daily life. This effect more energy consumption as a part of human life. The developed countries become success ceaselessly, safely and sufficient in rate of energy consumption per capita. It is necessary to have implementing activities in this area, Identify 3 policies related to energy currently [1]. VCR system commonly used refrigeration cycle, first reported in 1748 by Professor Williams Cullen of Glasgow University who produced refrigeration by partial vacuum over ethyl ether. This system next level modified to a hand-operated compressor machine working on ether, by Jacob Perkins. The same system was further improved by motor driven compressor and in present days commonly used in most of the household refrigerators as well as in large commercial refrigeration systems.

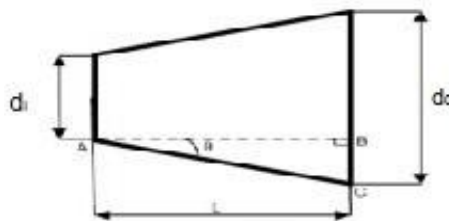
The implication of Chlorofluorocarbon (CFC) and Hydro chlorofluorocarbon (HCFC) refrigerants damage the on stratosphere layers of the earth such as ODP (Ozone Depletion potential) and GWP (Global Warming Potential). These refrigerants replacement is necessary as per the Montreal protocol and Kyoto these refrigerants need to replaced with less harmful ones, having zero ODP and GWP. The Hydro fluorocarbon (HFC) refrigerants having zero ozone depletion potential were recommended as alternatives to the CFC and HCFC, refrigerant R134a is the long term replacement refrigerant for R12 because of its favourable characteristics such as 0 ODP and 0.29 GWP [2,3]. The system performance improved by better operating techniques and less power used, In the VCR system generally operated by phase change refrigerant fluids. These Refrigerants were react with sun

light and released harmful gases to the environment, chlorofluorocarbons (CFC) gases, hydrochlorofluorocarbon (HCFC) ozone-depleting potential (ODP) and global warming potential (GWP). These kinds of refrigerant fluids replaced by (environment save) eco-friendly refrigerant by chlorine-free refrigerant, i.e., Hydrofluorocarbon (HFC) Zero Ozone depletion [4]. CFC's and HFC134a refrigerant fluids replaced by the R290/R600a refrigerant fluids mixture, designed by CFC<sub>12</sub> suitable vapour compression refrigeration system. The test results the refrigerant R290/R600a had 19.9-50.1% higher refrigerating capacity than R12 and 28.6 to 87.2% than R134a. The mixture R290/R600a consumed 6.8 to 17.4% more energy compared to R12. The COP of R290/R600a refrigerant mixture increased from 3.9 to 25.1% than R12 at lower evaporating temperature 11.8-17.6% at higher evaporating temperatures. The magnetic field effect reduced the compressor energy consumption by 1.5-2.5% than with no magnets. The COP of system was higher in the range 1.5-2.4% with the effect of magnetic field force. The mixture R290/600a (68/32 by wt.%) excellent than refrigerant for CFC<sub>12</sub> and HFC134a systems [5]. MCE for a magnetic field defined as the heating or cooling of magnetic materials upon variation of magnetic field [6,7]. Physical properties of materials such as entropy, heat capacity, and thermal conductivity strongly influenced by magnetic [8-14]. The thermal effect of metal iron varying magnetic field first discovered by Warburg in 1881; known as MCE (Magneto-Caloric Effect) [15].

The main work focused on the improving coefficient of performance (COP) of the Vapour compression Refrigeration system (VCR) system by experimentally, arranged permanent magnetic field after condenser and before evaporator (liquid line). The main function of magnetic field in liquid line is decrease the coefficient friction factor in the cylinder wall, increased the kinetic energy of the fluid flow. The compressor effect is decreased by decreasing the coefficient of friction in the pipe and increasing the fluid flow. The COP of the system tested by varying magnetic pairs in the tested pipe (Liquid Line) vs with and without diffuser at compressor outlet.

## 2. DESIGN AND FABRICATION OF DIFFUSER

The diffuser cross-section area should reduce in the flow direction for supersonic flows and should increase for subsonic flows. The available kinetic energy is converted into the pressure energy. The diameter gradually increases



The diffuser design details

Inlet diameter =  $d_i$

Outlet diameter =  $d_o$

Length of the diffuser =  $l$

Divergence angle =  $\phi$

$$\tan \phi = \frac{\text{Outlet diameter} - \text{Inlet diameter}}{2l}$$

$$\text{Length of diffuser } l = \frac{(d_o - d_i)}{2 \tan \phi}$$

Assume  $d_i = 6.35 \text{ mm}$ ,  $d_o = 7.937 \text{ mm}$  and  $\phi = 1.5$  Length  $l = 30.16 \text{ mm}$

## 3. EQUIPMENT CONSTRUCTION PROCEDURE

Vapour compression refrigeration system was constructed and investigated by R134a refrigerant. The system consists of compressor, condenser, capillary tube, evaporator and rotameter. A single loop

connects all VCR system. Hermetically Sealed reciprocating compressor is used in this system. A rotameter is used to measure the flow or control the flow in the circuit it is connected before evaporator and the capacity of meter is 0 to 20 LPH. A 650 gauss capacity 5 magnetic pairs arranged between Condenser out let and evaporator.

The magnetic pairs placed by varying distance over the length of the pipe shown in Fig.1, a 6 channel K-type digital thermocouple used to measure the system temperature at various points. Four pressure gauges were used to measure the pressure inlet and outlet of the compressor and Condenser. The Temperature at various points in the system was noted with the help of 4-channel k-type sensor.

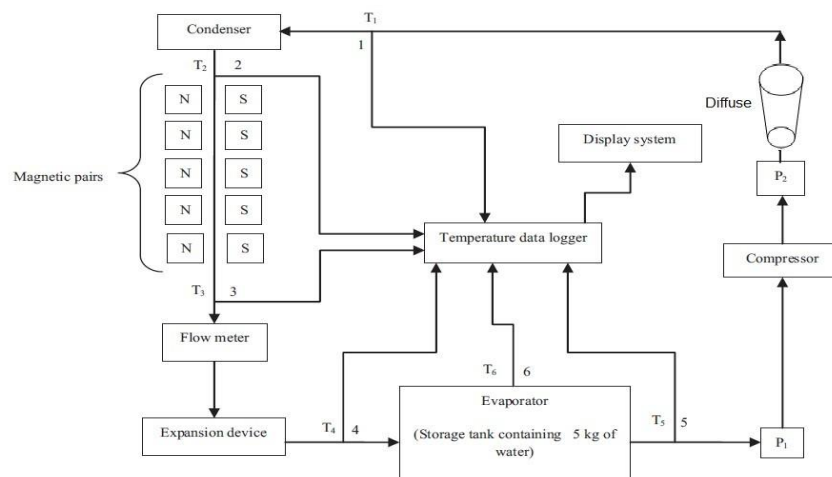


**Fig. 2.2** Experimental setup

- T1-Condenser inlet temperature
- T2-Condenser Outlet temperature
- T3-Temperature at inlet of rotameter or flow meter
- T4-Evaporater Inlet Temperature
- T5- Evaporator outlet Temperature
- T6- Water temperature
- P1-Compressor inlet pressure (Suction line Pressure)
- P2- Compressor outlet pressure (Discharge line Pressure)

#### 4. PERFORMANCE TEST

The performance test was conducted by variable magnetic pairs in the liquid line, these experimental values compared to without magnetic pairs in the liquid line. The system performance tested by variable incremental pairs 0 to 5. The refrigeration effect and compressor work calculated.

The compressor work

$$W_{\text{compressor}} = V \times I \quad \text{Watts or J/s} \quad (4.1)$$

Where V= voltage in Volts (digital measuring instrument/ by multimeter)

I= current in Amperes (By digital clamp meter)

$$\text{Refrigeration effect } Q_{\text{Refr}} = m \times c_{pw} \times (T_2 - T_1) \quad \text{Watts or J/s} \quad (4.2)$$

where  $m$  = mass of the water w.r.t to time in m/s

$c_{pw}$  = Specific heat of water in kJ/m

$T_1$  = Initial temperature of the water  $^{\circ}\text{C}$

$T_2$  = Final temperature of the water  $^{\circ}\text{C}$

Coefficient of performance of refrigeration system COP calculated

$$\text{COP} = \frac{\text{Refrigerating Effect}}{\text{Compressor Power}} \quad (4.3)$$

## 5. RESULTS AND DISCUSSIONS

### a) Effect of Magnetic field in refrigeration effect

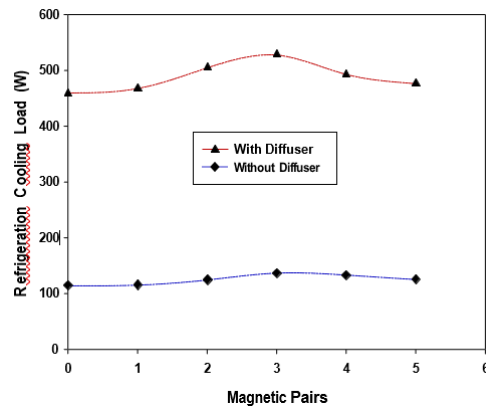


**Fig.5.1** Effect of Diffuser, Magnetic field Vs Refrigeration Effect (Load)

Magnetic Pairs	Without Diffuser	With diffuser
	Cooling Load (W)	
0	349.0	459.9
1	398.9	468.3
2	444.5	506.1
3	469.5	529.2
4	478.6	493.5
5	284.6	476.7

**Table.5.1.** Refrigeration cooling effect With and Without diffuser

The vapour compressor refrigeration system working on compressor, it compresses the vapour refrigerant at low pressure and temperature to high pressure and temperature. Fig.3. represents effect of magnetic field on the instantaneous power consumption of compressor, experimentally found that effect of magnetic field reduce the compressor work, and viscosity of refrigerants decreases with proportional to magnetic field. Viscosity of refrigerant decreases due to increases in magnetic field and decrease the delivery pressure of the fluid, result decreases the compressor work, same amount of refrigerant send by less compression work. Magnetic field effect increases by number of pair's proportional to refrigeration effect also increases. The molecular strength depends on molecular attractive forces between them. The change of phase of a refrigerant depends on the intermolecular forces. Kinetic energy of liquid change is response to increase in change of phase of a liquid Increase, improvement affect the Molecular covalent bond [16].The magnetic field the liquid in the pipe line increase the frequency of vibration of molecules effect in the molecules and enhance heat transfer at magnetic field location [17]. The entropy generated due to internal irreversibility of molecular motion, at a certain magnetic field it is suitable beyond that drop in refrigeration effect. this observed experimentally with and without diffuser by number of magnetic pairs.

b) Effect of Compressor energy

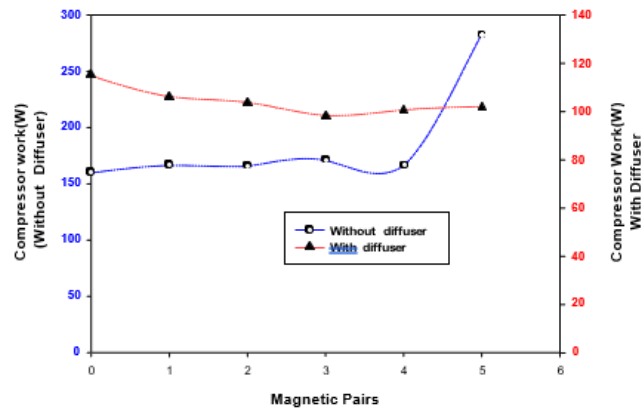


Fig .5.2 Compressor Work Vs Diffuser and magnetic field

Magnetic Pairs	Without Diffuser	With diffuser
	Energy Consumption (W)	
0	161.13	115.19
1	159.27	106.33
2	153.04	103.81
3	147.36	98.22
4	161.56	100.60
5	168.77	102.03

Table5.2. Energy consumption Magnetic Pairs Vs Diffuser

Compressor work decreases proportional to magnetic field, minimum energy consumed to run the compressor up to 3<sup>rd</sup> magnetic pair for system operated with and without diffuser. The delivery power on the line decrease due to increase in the magnetic pairs, because decreases the viscosity of the refrigerant till 3<sup>rd</sup> pair after increase hence 3<sup>rd</sup> magnetic pair is the optimum limit further there is no any decrease in the power experimentally observed.

Coefficient of Performance (COP)

Permanent magnetic field application has a positive result in COP of a system, when it is compared to arrangement of diffuser at compressor out let .The result observed fig with and without diffuser COP improved with application of 3<sup>rd</sup> magnetic pair. The COP of the system has magnetic field improved 25.97% with diffuser and 7.11% without diffuser, beyond the 3<sup>rd</sup> pair the evaporator capacity decreases and drops in the COP of the system.

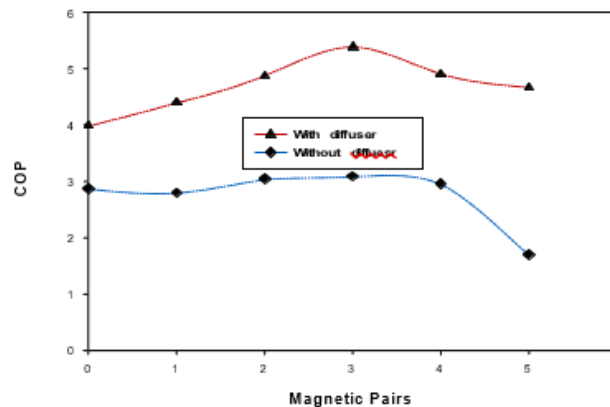


Fig.5.3.Magnetic Field Effect on COP

Magnetic Pairs	Without Diffuser	With diffuser
	Coefficient of performance(COP)	
0	2.17	3.99
1	2.50	4.40
2	2.90	4.88
3	3.19	5.39
4	2.96	4.91
4	1.69	4.67

**Table 5.3:** COP of VCR system

## 6. CONCLUSION

An experimental investigation carried out in our Laboratory on performance of Vapour compressor Refrigeration system with R-134a as a refrigerant under influence of magnetic field and diffuser the test results are compared with and without magnetic field and diffuser, for this experimental study clearly observed that effect of magnetic field, diffuser and field strength on COP.

The result shows that, with the application of magnetic field, diffuser and compressor energy. The compressor consumed energy reduced and improvement in refrigeration effect and COP of the Vapour compressor system. The molecules viscosity of refrigerant decrease and increase the fluid velocity (mass flow rate of refrigerant) due to de-clusterization principle, which leads to drop in compressor work and enhance evaporator capacity. COP of the system enhanced by number of magnetic pairs up to certain magnetic strength up to third pair, and same system operated by diffuser the COP of system increased. The compressor work without diffuser and without magnetic field is 160.49 W, compressor work decreased by diffuser and magnetic field 39.8 % and 9.5% , overall compressed work reduced by both magnetic field and diffuser the percentage of reduction at optimum at 3<sup>rd</sup> pair is 64.3%. The refrigeration effect and COP are 34.0% and 59.85% respectively.

## References

1. Brown S. Single-site and industrial-scale schemes. *Applied Energy* 1996;53:149–55.
2. Mani Kolandavel, Selladurai Velappan. Energy savings with the effect of magnetic field using R290/600a mixture as substitute for CEC12 and HFC 134a. *Therm Sci* 2008;12:111–20.
3. Devotta S, and Gopichand S. Comparative assessment of HFC 134a and some refrigerants as alternatives to CFC 12. *Int J Refrig* 1992;15(2):112–8.
4. Devotta, S., Gopichand, S., Comparative Assessment of HFC 134a and Some Refrigerants as Alternatives to CFC 12, *International Journal of Refrigeration*, 15 (1992), 2, pp.112- 18
5. Kolandavel MANI and Velappan Selladurai “Energy savings with the effect of magnetic field using R290/600a mixture as substitute for CFC12 and HFC134a” *Thermal Science: Vol. 12 (2008), No. 3*, pp. 111-120
6. Khovaylo VV, Rodionova VV, Shevyrtalov, Novosad SN. Magnetocaloric effect in reduced” dimensions: thin films, ribbons, and microwires of Heusler alloys and related compounds. *Physica Status Solidi* 2014;251:2104–13.
7. Brück E. Developments in magnetocaloric refrigeration. *J Phy D: Appl Phy* 2005;38(23):381.
8. Trevizoli PV, Barbosa JR, Oliveira PA, Ferreira RT. The reversibility of the magnetocaloric effect and its consequences for the active magnetic regenerator refrigeration cycle. In: *Proceedings of ENCIT. Uberlandia, MG, Brazil.*
9. Christensen DV, Bjørk R, Nielsen KK, Bahl CRH, Smith A, Clausen S. Spatially resolved measurement of the magnetocaloric effect and the local magnetic field using thermography. *J Appl Phy* 2010;108:063913.
10. Pecharsky KV, Karl Gschneidner Jr A. Magnetocaloric effect and magnetic refrigeration. *J Magn Magn Mater* 1999;200:44–56.

11. Pecharsky KV, Karl Gschneidner Jr A. Magnetocaloric effect from indirect measurements: magnetization and heat capacity. *J Appl Phy* 1999;86:565–75.
12. Pecharsky VK, Gschneidner Jr KA, Pecharsky AO, Tishin AM. Thermodynamics of the magnetocaloric effect. *Physical Rev B* 2001;64:1444061–14440613.
13. Tagliafico LA, Scarpa F, Canepa F, Cirafici S. Performance analysis of a room temperature rotary magnetic refrigerator for two different gadolinium compounds. *Int J Refrig* 2006;29:1307–17.
14. Bansal Pradeep, Vineyard Edward, Abdelaziz Omar. Status of not-in-kind refrigeration technologies for household space conditioning, water heating, and food refrigeration. *Int J Sustain Built Environ* 2012;1:85–101.
15. Warburg E. Magnetische Untersuchungen über einige Wirkungen der Koerzitivkraft. *Ann Phys* 1881;13:141–64.
16. Suba R, Megha M, vairam S, Kumar R, Pande PP, Jeevannanda T, et al. *Engineering chemistry*. 1st ed. India: Wiley; 2012. p. 4–6.
17. Ghasemian M, Najafian Ashrafi Z, Goharkhah M, Ashjaee M. Heat transfer characteristics of Fe<sub>3</sub>O<sub>4</sub> ferrofluid flowing in a mini channel under constant and alternating magnetic fields. *J Magn Mater* 2015;381:158–67.

## **Analytical Optimization of Crystalline Nano Cellulose-Dispersed H<sub>2</sub>O/C<sub>2</sub>H<sub>6</sub>O<sub>2</sub> Nano Fluids Using Response Surface Methodology**

**Vidya Chaparala<sup>1,2\*</sup>, G. Ravi Kiran Sastry<sup>1</sup>, P. Phani Prasanthi<sup>2</sup>**

<sup>1</sup> Mechanical Engineering Department, National Institute of Technology, Andhra Pradesh, India

<sup>2</sup> Mechanical Engineering Department, P.V.P. Siddhartha Institute of Technology, Vijayawada, Andhra Pradesh, India

### **ABSTRACT**

This work investigates the use of Response Surface Methodology (RSM) to optimize heat exchanger characteristics, namely the pressure drop across the flow conduit and the heat transfer coefficient. The principal aim is to enhance our understanding of the complex interrelationships between crucial variables and determine ideal parameters for pressure loss and heat transfer coefficient. A forced convective heat transfer system was used in the experiment, with the concentration of nanoparticles, coolant flow rate, air velocity, and coolant temperature at the system's entrance being the main points of interest. The outcomes demonstrated how input parameters affect heat exchange performance and how well RSM captures intricate relationships. The output characteristics are mostly influenced by discharge and dispersion concentration, according to an analysis of the optimal settings. In addition to offering insights into how flow conditions affect the system's ability to dissipate heat, RSM made it easier to identify stable conditions that promote increased heat exchange with less pressure loss across the flow channels. The conclusions drawn from this research make significant contributions to the broader field of thermal management systems, highlighting RSM's potential as a potent tool for analysing and predicting the heat transfer performance of heat exchangers. This approach offers the advantage of obviating the need for extensive experimental tests, thereby saving valuable time and resources.

**Keywords:** Response surface methodology, heat transfer coefficient, Pressure drop, nanofluids

### **INTRODUCTION**

In recent years, researchers have been focused on comprehending how various design parameters influence response variables. They have acknowledged the interdependence of design variables and interactions among responses. Response Surface Methodology (RSM) is a promising mathematical tool designed to optimize process parameters. A process involves a sequence of steps to convert input energy into a specific output form. RSM facilitates the assessment of connections between response variables and a set of independent variables through iterative tests for regression analysis [1-3]. Factorial design analysis is another suitable technique for identifying the most favorable conditions in a process [4].

Single-objective and multi-objective optimization problems can be classified into two types. A single objective issue pertains to optimizing a major variable that predominantly governs the process. Conversely, in scenarios with multiple objectives, several parameters naturally govern the process, and it is unclear how each parameter influences the outcome. Previous studies were limited to optimizing the viscosity ratio and thermal conductivity properties by using one factor at a time.

In the present study, we examined the effects of four independent factors on the pressure drop and heat transfer coefficient in a forced convection heat rejection mode. This work presents a novel method for investigating the best circumstances for input variables, such as the ideal concentration of nanoparticles in volume, the best coolant temperature and discharge, and the air velocity within a certain range. Design of experiments software is used in this study. In order to evaluate their impact on the heat transfer coefficient and pumping power as reactions, the research takes into account four design parameters: air velocity, sample temperature, pump discharge, and nanoparticle concentration. In addition, response factor analysis was done using contour plots and interaction plots.

### OPTIMIZATION ANALYSIS USING RESPONSE SURFACE METHODOLOGY

Utilizing the statistical technique called Response Surface Methodology (RSM), a mathematical model is developed to establish a connection between the desired response variable and the input governing variables [5]. RSM aims to streamline the number of experiments required by identifying the set of input variables that produces the optimal response value [6]. To collect data on both the contribution variables and the response variable, RSM employs various experimental designs. Following a statistical analysis of the data, a mathematical model is generated to elucidate the relationship between the input factors and the response variable [7].

In the present study, the impact of four operational parameters—coolant discharge rate, air velocity, coolant temperature, and nano fluid volume concentration—on the convective heat transfer coefficient and pressure drop in a cross-flow heat exchanger was investigated. The RSM approach, capable of analysing interactions between specified parameters, was employed to determine the optimal conditions for the variables within the studied domain.

The parameters of the model's range are as follows.

Volume concentration of nano particles between 0.1 to 0.9% with a step size of 0.4%,

air velocity between 15 to 25m/sec with a step size of 5m/sec,

temperature of coolant suspension ranging between 50° to 90° with a step size of 20°

and the coolant flow rate within the limit of 5 to 15 LPM with a step size of 5LPM.

All the influencing variables are selected with three levels. Further the statistical model table of L27 was prepared with the chosen parameters and concerned three levels. Defined test codes of -1,0 and +1 are assigned respectively for lower, equal and higher values with respect to central point. Parameter variations along with their concerned levels are summarized here in Table 1. Details of operating variables with designated codes and the experimental outcome of the response variables are presented in Table 2.

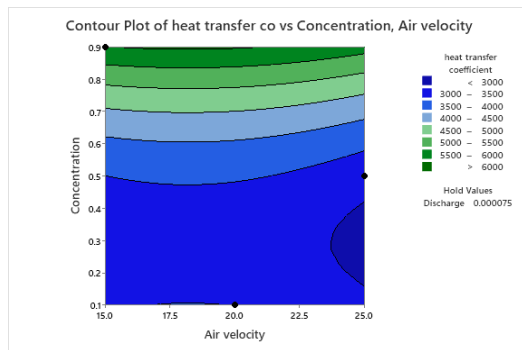
Table 1: List of input variables with the details of levels

Input variable name	Notation	Level -1	Level 0	Level +1
Volume fraction of nanoparticles	Ø %	0.1	0.5	0.9
Velocity of air	V m/sec	15	20	25
Coolant temperature	T °C	50	70	90
Discharge of coolant	Q LPM	5	10	15

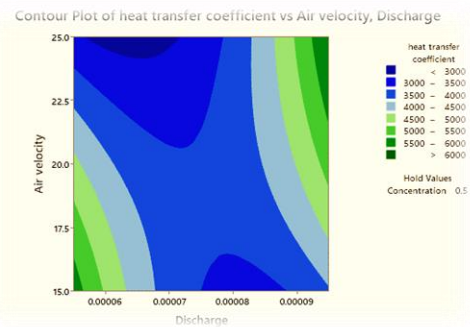
Table 2: Operating variables data with designated codes and the experiment results of response variables

Exp No	Test codes of variables				Input variable ranges				Pressure drop W	heat transfer coefficient W/m <sup>2</sup> K
					Discharge of Coolant Q LPM	Air velocity V m/sec	Temperature T ° C	Nano particle Concentration ø %		
1	-1	-1	-1	-1	5	15	80	0.1	864	163.9218
2	-1	-1	0	0	5	15	90	0.5	528	184.0269
3	-1	-1	+1	+1	5	15	100	0.9	240	221.4244
4	-1	0	-1	0	5	20	80	0.5	2240	170.9924
5	-1	0	0	+1	5	20	90	0.9	1280	194.7572
6	-1	0	+1	-1	5	20	100	0.1	960	215.8137
7	-1	+1	-1	+1	5	25	80	0.9	4400	182.4742
8	-1	+1	0	-1	5	25	90	0.1	3200	200.7094
9	-1	+1	+1	-1	5	25	100	0.5	2400	225.4776
10	0	-1	-1	+1	10	15	80	0.9	1104	150.2527
11	0	-1	-1	+1	10	15	80	0.9	816	168.331
12	0	-1	-1	+1	10	15	80	0.9	432	202.2141

13	0	0	0	-1	10	20	90	0.1	4160	172.1882
14	0	0	0	-1	10	20	90	0.1	2560	192.4691
15	0	0	0	-1	10	20	90	0.1	1600	219.9952
16	0	+1	+1	0	10	25	100	0.5	6400	203.6492
17	0	+1	+1	0	10	25	100	0.5	5200	219.3913
18	0	+1	+1	0	10	25	100	0.5	2800	255.0911
19	+1	-1	-1	0	15	15	80	0.5	1392	142.5588
20	+1	-1	-1	0	15	15	80	0.5	1224	154.6129
21	+1	-1	-1	0	15	15	80	0.5	1032	171.5485
22	+1	0	0	+1	15	20	90	0.9	1024	213.5218
23	+1	0	0	+1	15	20	90	0.9	736	236.9445
24	+1	0	0	+1	15	20	90	0.9	576	264.3227
25	+1	+1	+1	-1	15	25	100	0.1	5200	218.4649
26	+1	+1	+1	-1	15	25	100	0.1	4400	230.4601
27	+1	+1	+1	-1	15	25	100	0.1	3400	247.7794



(a)



(b)

**Fig 1:** Contour plots of heat transfer coefficient as a function of effective parameters (a)  $\phi$ -V and (b) V-Q

Contour plots, a graphical representation in a design of experiments (DOE) study, illustrate the response surface and are commonly employed alongside analysis of variance to identify crucial variables influencing a specific response variable [8]. In ANOVA analysis, a contour map is utilized to demonstrate how two or more factors impact the response variable. These plots depict the changes in the response variable when two factors simultaneously change, while other variables remain constant [9]. The point of intersection among the contour lines on the plot signifies the optimal value for the response variable, with the contour lines themselves representing the response value at a specific level of the response variable. To explore the interaction between independent variables (such as volume concentration, coolant discharge, and air velocity) and the response variable, such as heat transfer coefficient, the contour plot was generated using RSM software (Figure 1).

Figure 8 illustrates the impact of variations in volume concentration and air velocity on the heat transfer coefficient of the coolant. According to Response Surface Methodology (RSM), the highest convective heat transfer coefficient is achieved within concentration ranges of 0.2% to 0.5% and airflow speeds between 24 and 25 m/sec. In Figure 2a, the circular arcs evident in the contour plot indicate that the parameters of velocity and discharge exhibit a quadratic relationship with the response variable. Conversely, Figure 2b displays nearly linear parallel curves, indicating that the operating variables, specifically concentration and air flow velocity, have a linear relationship with the response.

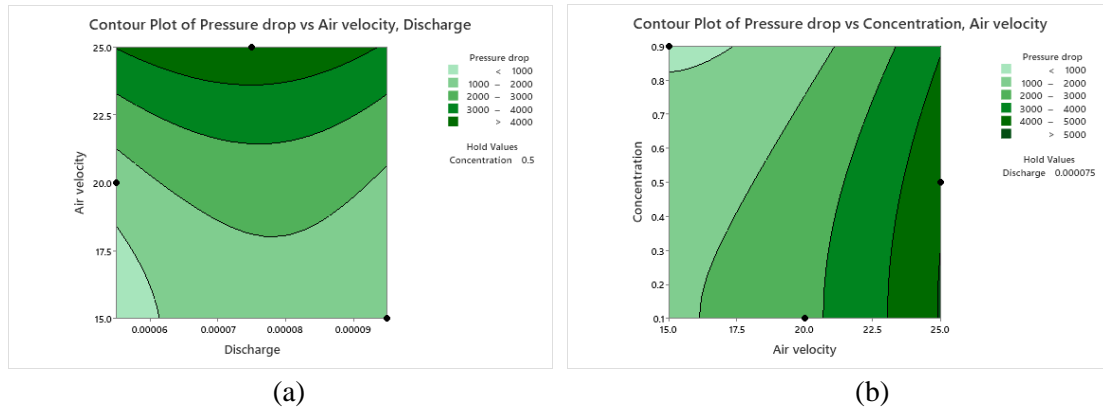


**Fig 2:** Contour plots of pressure drop as a function of effective parameters (a)  $Q-\phi$  and (b)  $\phi -V$

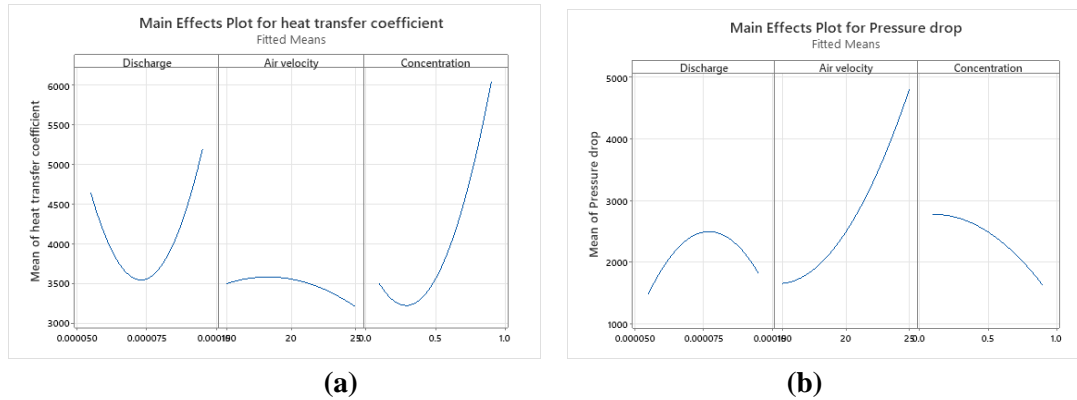


**Fig 3:** Diagram presenting main effects plot of (a) heat transfer coefficient (b) Pressure drop  
The main effect plot illustrates that an increase in volume concentration of nano particles and discharge rate of coolant beyond certain value intensifies the heat transfer coefficient as presented in Fig. 3. Conversely the pressure drop is being effected by the air velocity predominantly.

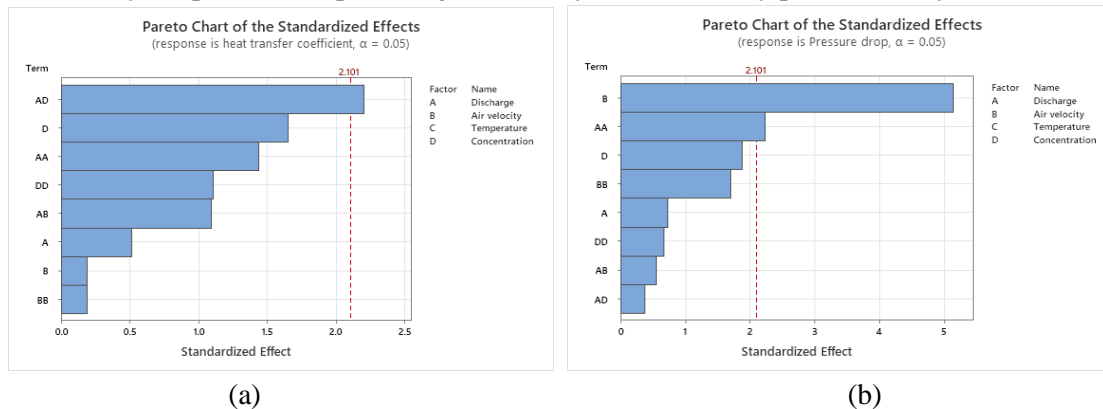


**Fig.4** Pareto chart of standardized effects for various operating parameters (a) heat transfer coefficient (b) Pressure drop

The outcomes of the Pareto chart for the operating parameters are depicted in Figure 4. The Pareto chart visually highlights the operating parameter that exerts the most substantial influence on the responses based on the experimental data. It is evident from the chart that the volumetric flow rate and nanofluid concentration play pivotal roles in determining the heat transfer coefficient. As discussed in the preceding section, the Pareto chart indicates that the sluggish air speed and the second-order fluctuation of discharge significantly impact the pressure drop within the flow conduit. The normal probability plots of the residuals, as indicated in Figure 4, demonstrate a satisfactory fit.

The residual plots may be found in Figs. 5 (a) and (b). The residual plots are used to assess the model's suitability. These charts are based on the following four underlying assumptions: Normal plot: A line is drawn through the data since the residual values and data must be normal. Residual and Predicted: Variations must hold steady. If the residual changes don't adhere to the predetermined process and have

a random distribution, the necessity for the constant variance is established. Residual versus Run: Data need to be time-independent. If the data dispersion falls between two lines and deviates from a predetermined pattern, the requirement is met. Comparison of findings between predictions and observations: The reference line is formed by the meeting of two axes. The data are more trustworthy if the line is surrounded by a large amount of variation. Additionally, these two Figures' residual histogram distributions are less skewed and more asymmetrical. The residual graphs show a strong connection amongst the observed and fitted values when compared to the fitted values.

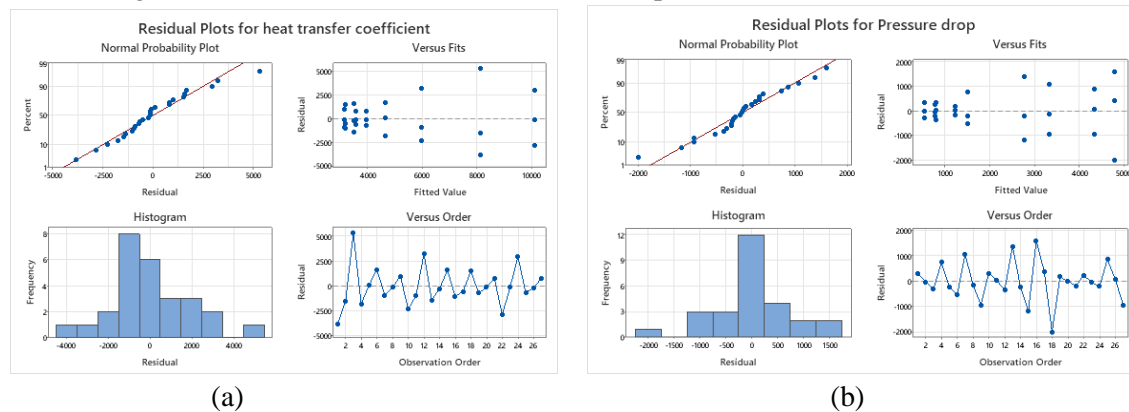


**Fig.5** Residual plots of a) heat transfer coefficient b) pressure drop

## CONCLUSIONS

In summary, the present study has yielded significant insights into the optimization of heat exchanger parameters, particularly the pressure drop across the flow conduit and the heat transfer coefficient, by employing Response Surface Methodology (RSM) for analysis. The main conclusions and findings of this investigation can be summed up as follows:

- By applying RSM, we were able to ascertain the ideal values for the heat transfer coefficient and pressure loss in the studied heat exchanger system, which furthered the development of effective heat exchange procedures.
- The analysis has demonstrated the significant influence of input parameters, with particular attention to variables like the concentration of nanoparticles, the flow rate of coolant, air velocity, and the temperature of coolant at the system entrance. A thorough comprehension of these factors is necessary to attain the intended heat transfer efficiency.
- Analysis of the optimal settings has revealed that the main factors affecting the output parameters are discharge and dispersion concentration. This discovery is critical to the advancement of heat exchangers designed for optimal performance.
- RSM has made it easier to identify strong conditions that limit pressure loss throughout the flow channels and improve heat exchange efficiency. These results have applications in the efficient design and management of heat exchanger systems.
- The incorporation of RSM into this research highlights how it can improve the efficiency of time and resources while studying heat exchanger systems. One notable benefit is that significant insights can be obtained without the need for extensive experimentation.

## References

- [1] L. Sun, C.-L. Zhang, Evaluation of elliptical finned-tube heat exchanger performance using CFD and response surface methodology, *Int. J. Therm. Sci.* 75 (2014) 45–53, <http://dx.doi.org/10.1016/j.ijthermalsci.2013.07.021>.
- [2] J.S. Nam, D.H. Kim, H. Chung, S.W. Lee, Optimization of environmentally benign micro-drilling process with nanofluid minimum quantity lubrication using response surface methodology and genetic algorithm, *J. Clean. Prod.* 102 (2015) 428–436, <http://dx.doi.org/10.1016/j.jclepro.2015.04.057>.

- [3] M. Rahimi-Gorji, O. Pourmehran, M. Hatami, D.D. Ganji, Statistical optimization of microchannel heat sink (MCHS) geometry cooled by different nanofluids using RSM analysis, *Eur. Phys. J. Plus.* 130 (2015) 1–21, <http://dx.doi.org/10.1140/epjp/i2015-15022-8>.
- [4] Gheshlaghi, R. E. Z. A., Scharer, J. M., Moo-Young, M., & Douglas, P. L. (2008). Application of statistical design for the optimization of amino acid separation by reverse-phase HPLC. *Analytical biochemistry*, 383(1), 93-102.
- [5] Najafi, G., Ghobadian, B., Yusaf, T., Ardebili, S. M. S., & Mamat, R. (2015). Optimization of performance and exhaust emission parameters of a SI (spark ignition) engine with gasoline–ethanol blended fuels using response surface methodology. *Energy*, 90, 1815-1829.
- [6] Gelis, K., & Akyurek, E. F. (2021). Entropy generation of different panel radiator types: Design of experiments using response surface methodology (RSM). *Journal of Building Engineering*, 41, 102369.
- [7] Anderson, M. J., & Whitcomb, P. J. (2017). DOE simplified: practical tools for effective experimentation. CRC press.
- [8] Ranganath, M. S., & Vipin, H. (2014). Optimization of process parameters in turning operation using response surface methodology: a review. *International Journal of Emerging Technology and Advanced Engineering*, 4(10), 351-360.
- [9] Abubakar, A., Manogaran, M., Yakasai, H. M., Yasid, N. A., & Shukor, M. Y. (2022). Response Surface Method for the Optimization of *E. cloacae* Strain UPM2021a Growth on Acrylamide as a Nitrogen Source. *Bioremediation Science and Technology Research*, 10(2), 29-39.
- In conclusion, the results of this RSM-based analysis provide a useful framework for raising thermal management efficiency and open up new directions for study and application in the optimization of heat exchangers.

## Heat Transfer Analysis of Cylindrical Horizontal Jet Impinging on Vertical Plate

Kunapuli Siva Satya Mohan<sup>1</sup>, K. Ravi Kumar<sup>2</sup>, Panthangi Ravi Kumar<sup>3</sup>, K.P.V. Krishna Varma<sup>4</sup>, M. Rambabu<sup>5</sup>, P V S Muralikrishna<sup>6</sup>

<sup>1</sup>Associate Professor, <sup>2</sup>Assistant Professor, <sup>3</sup>Professor, <sup>4</sup>Associate Professor, <sup>5</sup>Assistant Professor, <sup>6</sup>Sr. Assistant Professor

<sup>1,5,6</sup>Aditya College of Engineering & Technology, Surampalem, 533437 <sup>2</sup>V R Siddhartha Engineering college, Vijayawada <sup>3</sup>CMR College of Engineering & Technology, Telangana <sup>4</sup>Raghu Engineering College, Visakhapatnam, India.

<sup>1</sup>kunapulisiva46@gmail.com, <sup>2</sup>ravi\_24k@yahoo.com <sup>3</sup>pravikamar@cmrcet.ac.in, <sup>4</sup>varmamtech2005@gmail.com.

### ABSTRACT

In this paper determination of heat flux for horizontal jet impingement on vertical plate is found out. Experiment work is compared with CFD analysis. diameter of jet is fixed to be 12mm and the gap between jet to plate was set to be 6, 12, 18 and 24mm. Jet to plate distance (e) Ratio ranging from 0 to 2 and Re for turbulent flow is considered in this analysis. Air and CO<sub>2</sub> are compared by experimental and CFD simulation. It was found that CFD simulation can give close to experimental results.

**KEY WORDS:** *Computational fluid dynamics, vertical plate, Heat flux, H/D, Re*

### 1. INTRODUCTION

Impinging jets have more demand in industrial applications viz. heating of metals etc. Keyon *et al.* [1] explained the impact of fluid flow on flat plate. The results shows that as the blowing ratio is greater, greater is the cooling effectiveness. Gokulnath. [2] explained about Jet impingement cooling mechanism. The results shows that heat transfer is to be obtained from the heat transfer coefficients with limited area. Khudheyer. [3] studied computationally for the impingement heat transfer for the inside channel. It is concluded that the heat flux is enhancing. It is also found out that as the jet size increases heat transfer also increases.

Akshay. [4] explained about theoretical and experimental developments in heat transfer. The results shows that jet impingement method provides best way of getting more heat transfer rate. Muhsincan. [5] described the effects of different phase heat transfer improvements through impact of jet cooling. The results shows that use of nano rods enhances surface area of the plate. Pallavi and Ashish. [6] experimented and simulated to achieve an elementary perceptive. Results shows that heat transfer is increased by varying the parameters. Vipin *et al.* [7] studied enhancement of heat transfer in pulsed jet impingement cooling at different frequencies. Results shows that there is a considerable increase in average Nusselt number. Mahesh. [8] studied different CFD techniques used. The results are,  $r_{ib}$  with more perforation gives enhancement of Nusselt number. Chaina. [9] numerically studied the single impinging jet on concave surface. The results shows that more in Re gives increase in Nusselt number. Reji Kumar. [10] determined the cooling of impinging jet to increase the temperature. Results shows that cooling is used for more density applications. In this paper comparing heat transfer rate for CFD and experiment for air and CO<sub>2</sub> has been found out.

### 2. MATERIALS AND METHODOLOGY

The components used, their materials and working fluids used for the present analysis were as shown in Table 2.1. Three different jets were fabricated with different diameters. Parameters considered and their ranges are pivoted in Table.2.

Specifications of the jet and plate used for the analysis were pivoted in Table 2.2. Thermal properties of fluids at 30°C temperature are shown in the Table 2.3. It shows that thermal conductivity of air is more than that of CO<sub>2</sub>.

Table 1 Materials and working substance

Component	Material	Working substance
Cylinder and jet	Steel	Air
Plate	Copper	CO <sub>2</sub>

Table 2.1 Parameters and their ranges

Parameter	Value
Surface temperature range, T <sub>s, ∞</sub> °C	30- 80°C
Nozzle diameter, mm	10 - 14
Nozzle to plate distance to jet diameter (H/D)	0.5 – 2

Table 2.2 Specifications of jet and plate

D <sub>1</sub> mm	L <sub>1</sub> mm	D mm	H mm	H/D	L <sub>2</sub> mm
76	140	10, 12 and 14	5, 6 and 7	0.5	180
76	140	10, 12 and 14	10, 12 and 14	1	180
76	140	10, 12 and 14	15, 18 and 21	1.5	180
76	140	10, 12 and 14	20, 24 and 28	2	180

## 2.1 Experimental Set Up and Procedure



Fig 1 Pictorial view of horizontal jet on flat plate

Fig.1 shows the proposed experimental set up for Horizontal jet impingement on vertical flat plate

## 2.2 Data Reduction

Heat flux can be calculated from the mathematical equation from Heat Transfer. Table 4, 5 and 6 shows the calculated values of heat transfer coefficient from e=0.5 to 2.

Table 4 Reynolds number of air and CO<sub>2</sub> for  $\theta = 90^\circ$ ,  $\alpha = 0^\circ$  and  $\theta = 0^\circ$ ,  $\alpha = 90^\circ$  at D=10mm

	Fluid	Re		h, W/m <sup>2</sup> K	
		Air	CO <sub>2</sub>	Air	CO <sub>2</sub>
e	0.5	6.25 x 10 <sup>5</sup>	8.54 x 10 <sup>5</sup>	2527	1903
	1	9.38 x 10 <sup>5</sup>	12.81 x 10 <sup>5</sup>	3497	2633
	1.5	12.51 x 10 <sup>5</sup>	17.08 x 10 <sup>5</sup>	4399	3313
	2	15.64 x 10 <sup>5</sup>	21.35 x 10 <sup>5</sup>	5261	3962

Table 5 Reynolds number of air and CO<sub>2</sub> for  $\theta = 90^\circ$ ,  $\alpha = 0^\circ$  and  $\theta = 0^\circ$ ,  $\alpha = 90^\circ$  at D=12mm

	Fluid	Re		h, W/m <sup>2</sup> K	
		Air	CO <sub>2</sub>	Air	CO <sub>2</sub>

<b>e</b>	0.5	$5.21 \times 10^5$	$3.07 \times 10^5$	1820	1370
	1	$7.82 \times 10^5$	$4.60 \times 10^5$	2517	1896
	1.5	$10.42 \times 10^5$	$6.14 \times 10^5$	3168	2386
	2	$13.03 \times 10^5$	$7.68 \times 10^5$	3788	2853

Table 6 Reynolds number of air and CO<sub>2</sub> for  $\theta = 90^\circ$ ,  $\alpha = 0^\circ$  and  $\theta = 0^\circ$ ,  $\alpha = 90^\circ$  at D=14mm

		Re		h, W/m <sup>2</sup> K	
		Air	CO <sub>2</sub>	Air	CO <sub>2</sub>
<b>e</b>	0.5	$4.47 \times 10^5$	$6.10 \times 10^5$	1380	1039
	1	$6.70 \times 10^5$	$9.16 \times 10^5$	1907	1437
	1.5	$8.94 \times 10^5$	$12.21 \times 10^5$	2401	1809
	2	$11.17 \times 10^5$	$15.25 \times 10^5$	2870	2162

### 2.3 Flow Diagram in CFD

Figure 3 and 4 shows model and meshing of horizontal jet impinging on vertical plate.



Figure 2 Horizontal jet & plate

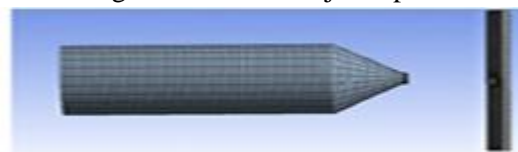


Figure 3 Meshing

### 2.4 BOUNDARY CONDITIONS IN CFD

Boundary conditions are the input and output conditions for which analysis is to be done.

## 3. RESULTS AND DISCUSSION

### 3.1 Experimental results and discussion

#### 3.1.1 Experimental results and discussion for air at D=10mm

Fig. 4 shows the heat transfer rate enhancement at various **e** ratios and at various **Re**

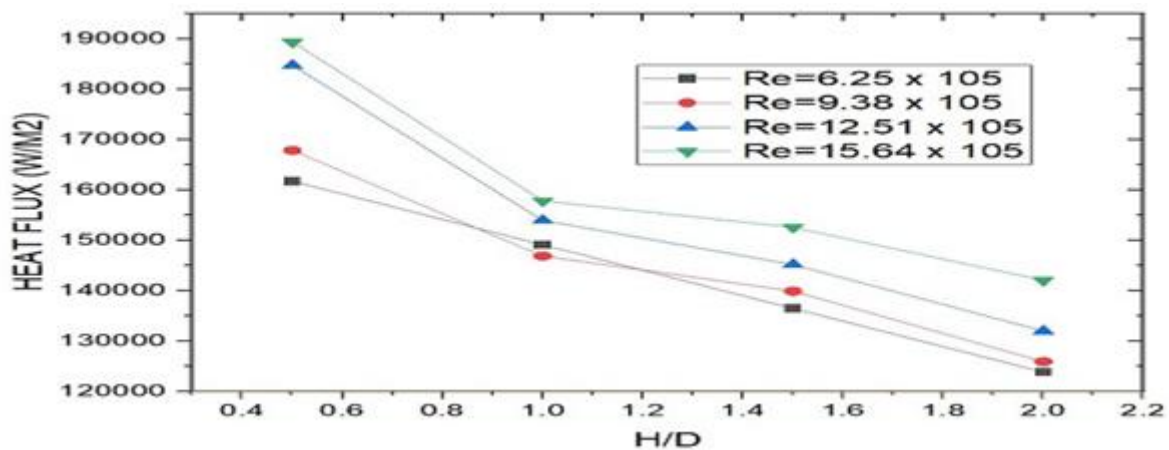


Fig. 4 heat transfer rate vs H/D at different Reynolds numbers at D=10mm

### 3.1.2 Experimental results and discussion for CO<sub>2</sub> at D=10mm

Fig.5 shows the heat transfer rate enhancement at various H/D and Re

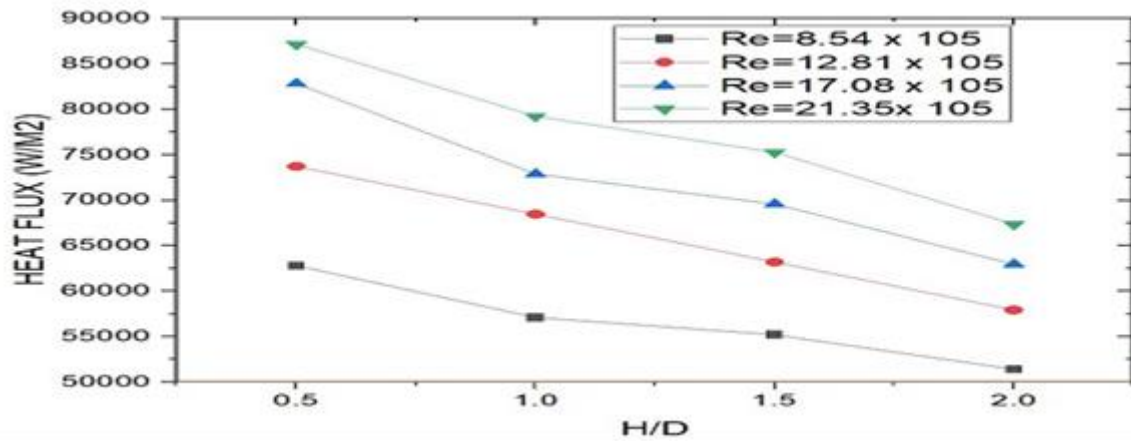


Fig. 5 heat transfer rate vs H/D at different Reynolds numbers at D=10mm

### 3.1.3 Experimental results and discussion for air at D=12mm

Fig.6 shows the heat transfer rate enhancement at e ratios and at various Re

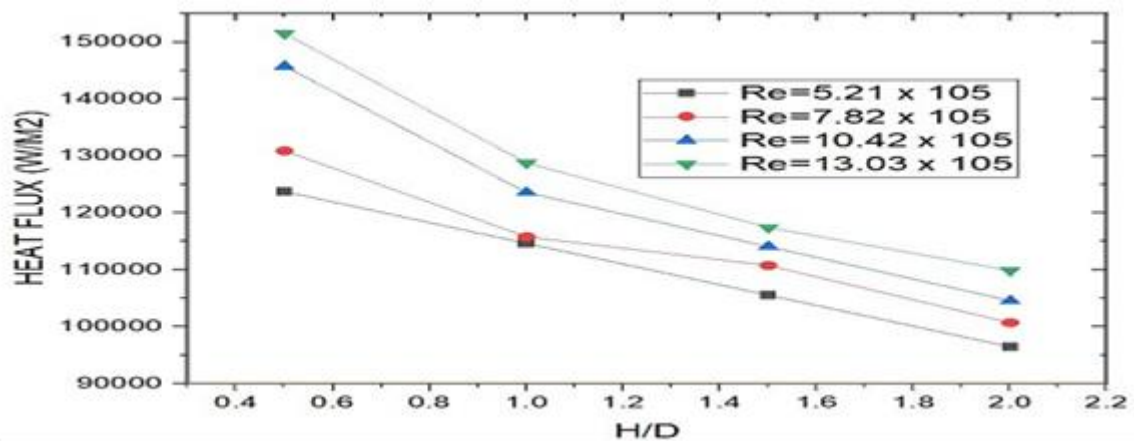


Fig. 6 heat transfer rate vs e at different Reynolds numbers at D=12mm

### 3.1.4 Experimental results and discussion for CO<sub>2</sub> at D=12mm

Fig. 7 shows the heat transfer rate enhancement at e ratios and at various Re

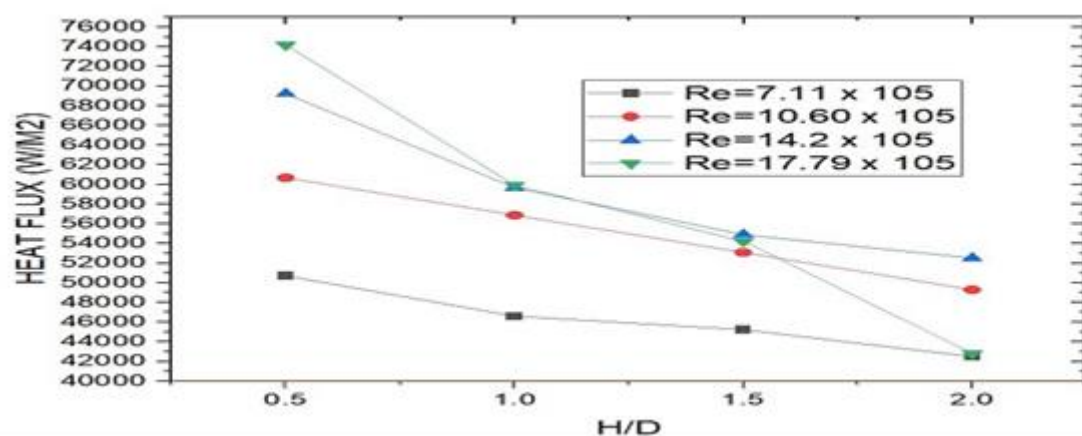


Fig. 7 heat transfer rate vs e at different Reynolds numbers at D=12mm

### 3.1.5 Experimental results and discussion for air at D=14mm

Fig. 8 shows the heat transfer rate enhancement at various  $e$  ratios and at various  $Re$

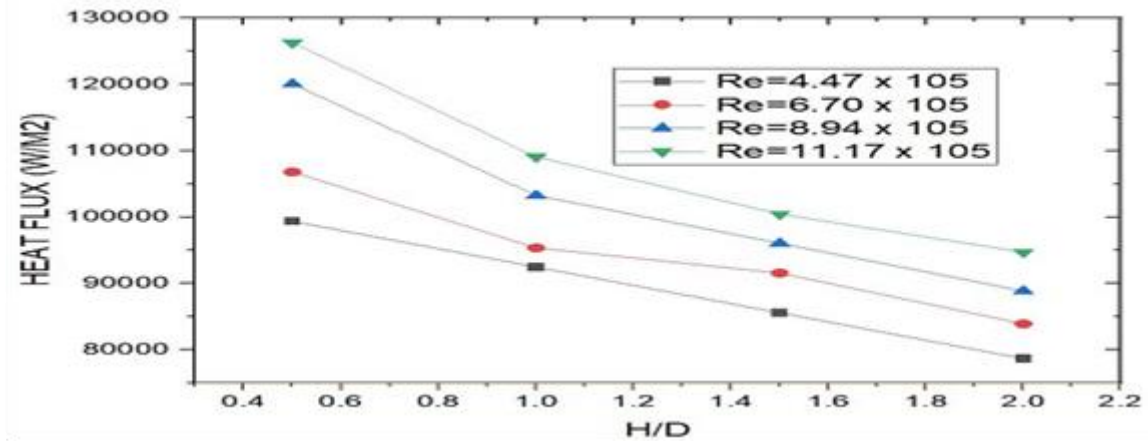


Fig. 8 heat transfer rate vs  $e$  at different Reynolds numbers at D=14mm

### 3.1.6 Experimental results and discussion for CO<sub>2</sub> at D=14mm

Fig. 9 shows the heat transfer rate enhancement at various  $e$  ratios and at various  $Re$

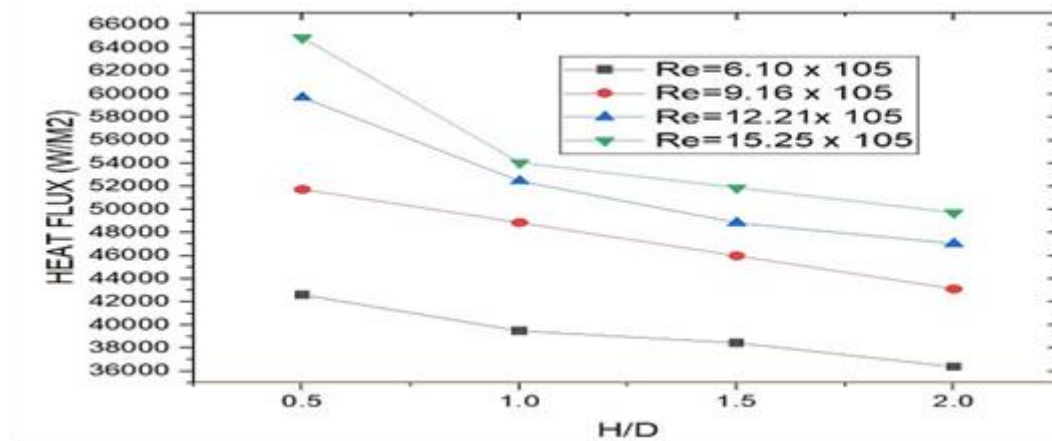


Fig. 9 heat transfer rate vs  $e$  at different Reynolds numbers for CO<sub>2</sub> at D=14mm

## 3.2 CFD Analysis Results and Discussion

### 3.2.1 for air at D=10mm

Fig.10 shows the heat transfer rate enhancement at various  $e$  ratios and at various  $Re$  in CFD.

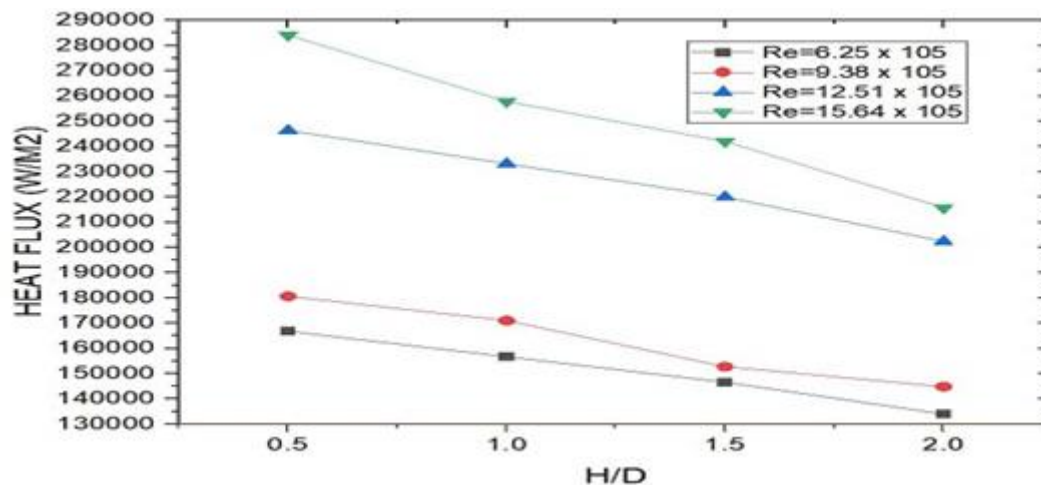


Fig. 10 heat transfer rate vs  $e$  at different  $Re$

Fig.11 and 12 shows the temperature and heat flux of the jet and plate.

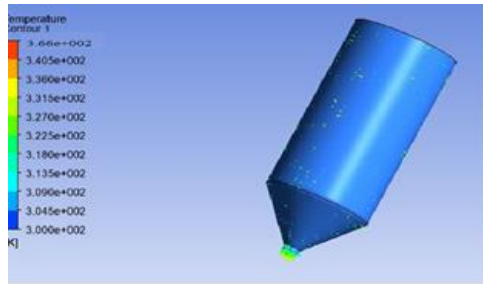


Figure 11 Outlet temperature of Jet

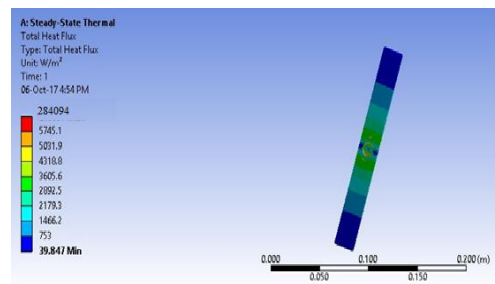


Figure 12 Total heat flux of flat plate

### 3.2.2 For CO<sub>2</sub> at D=10mm

Fig 13 shows the variation of heat transfer rate enhancement at various  $e$  ratios and at various  $Re$  in CFD.

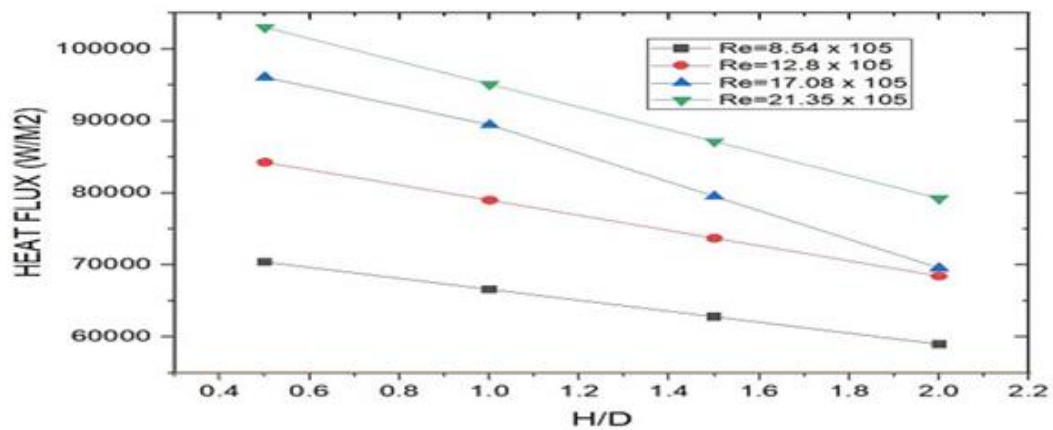


Fig. 13 heat transfer rate vs  $e$  at different  $Re$

Fig.14 and 15 shows the temperature and heat flux of the jet and plate.

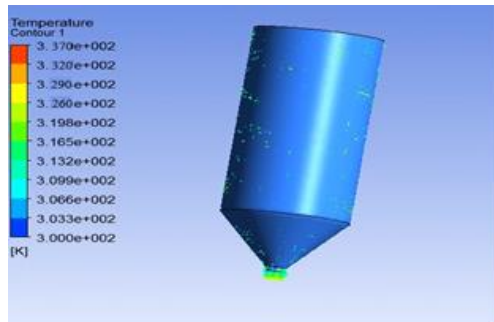


Fig. 14 Outlet temperature of jet

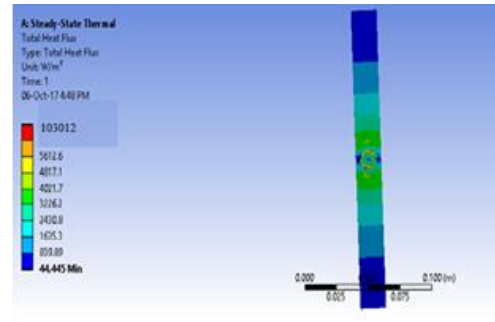


Fig.15 Total heat flux of flat plate

### 3.2.3 For air at D=12mm

Fig.16 shows the variation of heat transfer rate enhancement at various  $e$  ratios and at various  $Re$  in CFD.

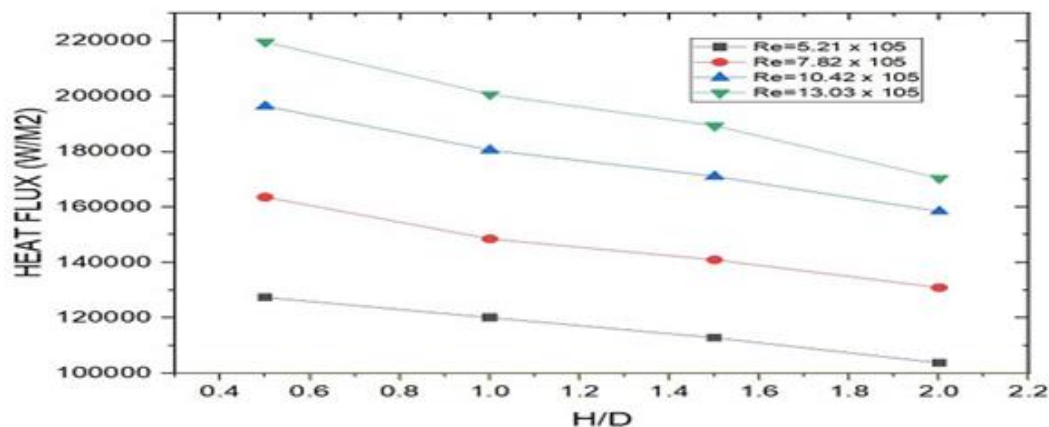


Fig. 16 heat transfer rate vs  $e$  at different  $Re$

Fig.17 and 18 shows the temperature and heat flux of the jet and plate.

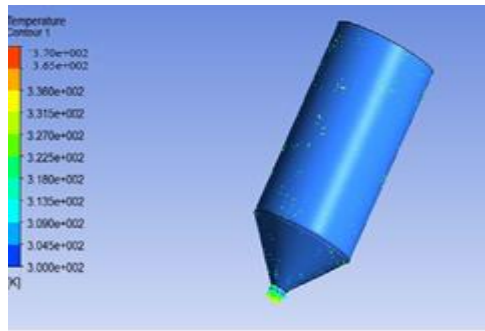


Fig. 17 Outlet temperature of Jet

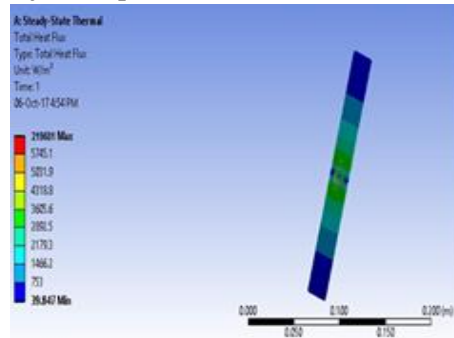


Fig. 18 Total heat flux of flat plate

### 3.2.4 For CO<sub>2</sub> at D=12mm

Fig. 19 shows the variation of heat transfer rate at various  $e$  ratios and at various  $Re$  in CFD.

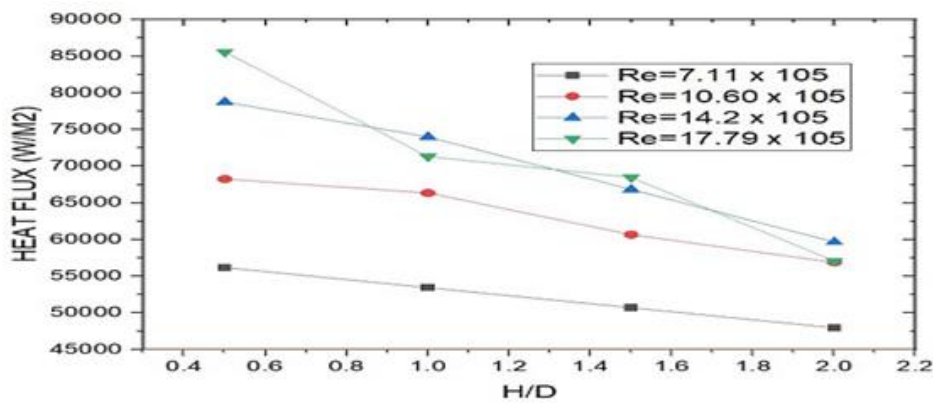


Fig. 19 heat transfer rate vs e at different  $Re$

Fig. 20 and 21 shows the temperature and heat flux of the jet and plate.

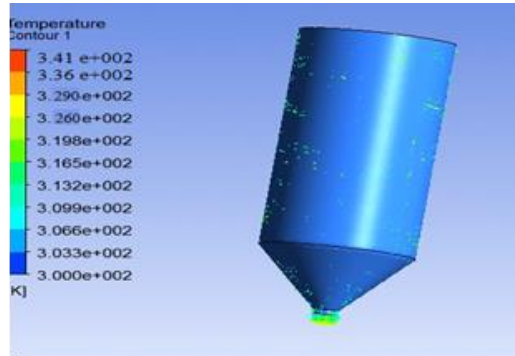


Figure 20 Outlet temp.of cylindrical jet

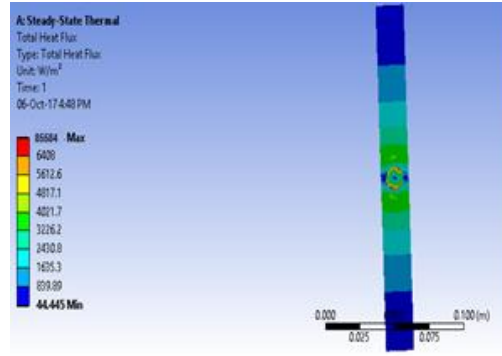


Figure 21 Total heat flux of flat plate

### 3.2.5 For Air at D=14mm

Fig.22 shows the heat transfer rate enhancement at various  $e$  ratios and at various  $Re$  in CFD.

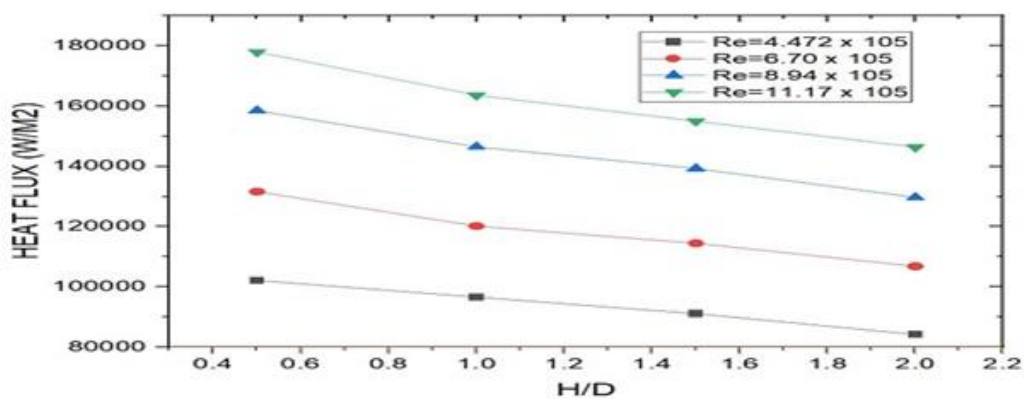


Figure 22 heat transfer rate vs e at different  $Re$

Fig.23 and 24 shows the temperature and heat flux of the jet and plate.

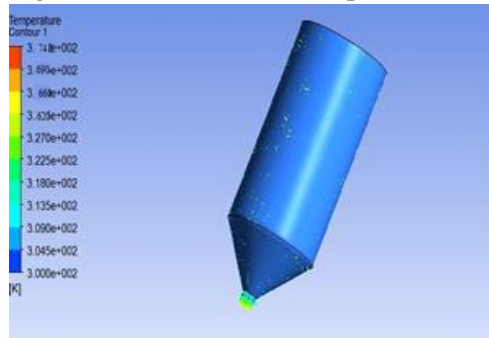


Figure 23 Outlet Temp. of cylindrical Jet

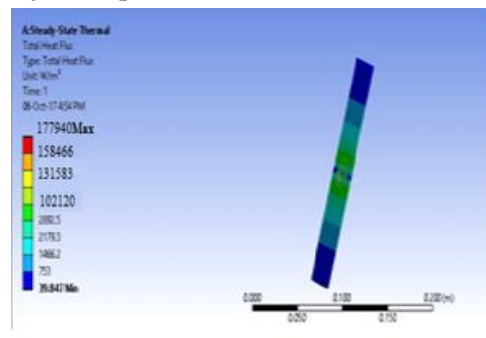


Figure 24 Total heat flux of flat plate

### 3.2.6 For CO<sub>2</sub> at D=14mm

Fig 25 shows the heat transfer rate enhancement at various e ratios and at various Re in CFD.

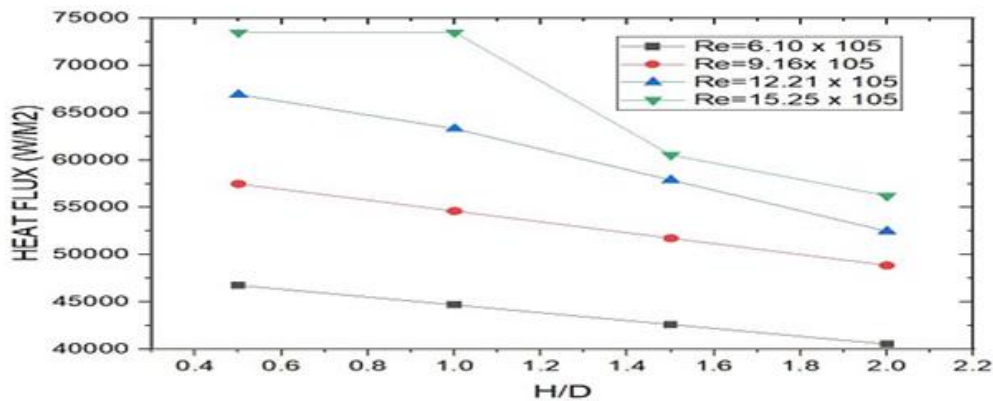


Fig. 25 heat transfer rate vs e at different Re

Fig.26 and 27 shows the temperature and heat flux of the jet and plate.

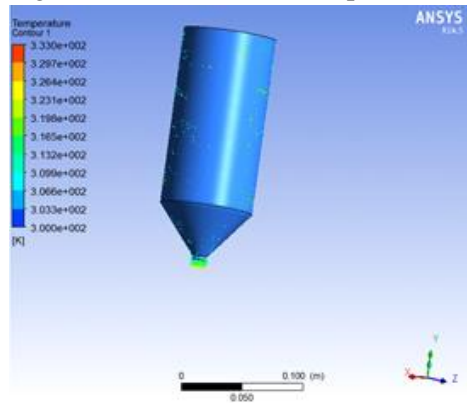


Fig. 26 Outlet temperature of cylindrical jet

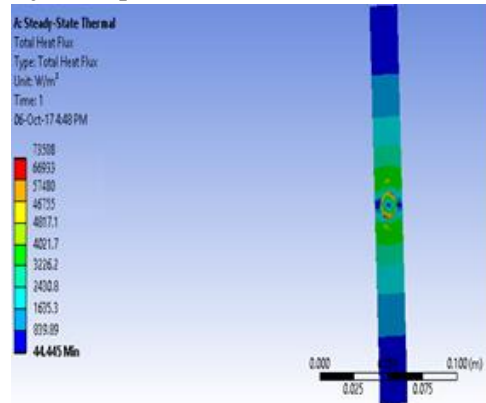


Fig. 27 Total heat flux of flat plate

## 4. CONCLUSIONS AND RECOMMENDATIONS

From results it is shown that  $e=0.5$  gives more heat flux than  $e=1, 1.5$  and  $2$ .

From results it is shown that at massflow rate of  $0.25$  kg/s gives more heat flux.

It is concluded that CFD validation is correlated to experimental value and is more for air.

## REFERENCES

1. Keyon Cheng, Xiulan Huai, Jun Cai, Zixionguo “Numerical simulation of Impinging Cooling on the leading edge of a Turbine blade” International Mechanical Engineering Congress and Exposition, 10, 2011.
2. GokulnathR “ Review on Jet Impingement Cooling of Heated Plate” International Journal of Innovative and Emerging Research in Engineering, 4(5), 2017.

3. Khudheyer S. Mushatet. "Thermal and Hydrodynamic Analysis of the Impingement Cooling inside a Backward Facing Step Flow" Research Journal of Recent Sciences , 1, 2012.
4. Akshay R. Nangare. "Multiple Jet Impingement: A Promising method of cooling" International journal of latest trends in engineering and technology, 6(4), 2016.
5. Muhsincan S. "Submerged jet impingement cooling using nano structured plates" International Journal of Heat and Mass Transfer, 59, 2013.
6. Pallavi C. Chaudhari, Ashish N. Sarode. "Performance analysis of jet impingement cooling on copper square plate" International Conference Proceeding ICGTETM, 2017.
7. Vipin .R , Sabu .Kurian , Tide P. S. "STUDY ON PULSED JET IMPINGEMENT COOLING" International Journal of Science, Engineering and Technology Research (IJSETR), 4(10), 2015.
8. Mahesh T. "A numerical investigation on jet impingement cooling aided with cross flow and ribs on target plate", International Journal of Science, Engineering and Technology Research (IJSETR), 4(10), 2015.
9. Chaina Ram. "computational study of leading edge jet impingement cooling with a conical converging hole for blade cooling" ARPN Journal of Engineering and Applied Sciences, 12(22), 2017.
10. RejiKumar "Inline Array Jet Impingement Cooling Using Al<sub>2</sub>O<sub>3</sub> / Water Nanofluid In A Plate Finned Electronic Heat Sink" American Journal of Engineering Research (AJER), 03(03),2014.

## Heat Transfer Enhancement of An Automobile Engine Radiator Using Al<sub>2</sub>O<sub>3</sub>/CuO Water Base Nanofluids

K. Venkatarao<sup>1</sup>, Ch. Lakshmi Kanth<sup>2</sup>, V. Sravani<sup>3</sup>, N. Manoj Kumar<sup>4</sup>, V. Eswar Balaji<sup>5</sup>,  
V. Veera Manikanta<sup>6</sup>, Sk. Suhail<sup>7</sup>

<sup>1,2,3</sup>Assistant Professor, Department of Mechanical Engineering, Prasad V Potluri Siddhartha Institute of  
Technology, Vijayawada, A.P, India.

<sup>4,5,6,7</sup>UG Student, Department of Mechanical Engineering, Prasad V Potluri Siddhartha Institute of  
Technology, Vijayawada, A.P, India

### ABSTRACT

This study investigates convective heat transfer and the performance characteristics of a uniformly heated car radiator using Al<sub>2</sub>O<sub>3</sub>-CuO/water nanofluids. The experimental approach involves preparing nano-composite powders of Al<sub>2</sub>O<sub>3</sub> and CuO suspended in water through a sonication process. Various combinations of these nanoparticles, with concentrations ranging from 0.01% to 0.16%, are examined alongside different flow rates from 3.5 to 4.5. The fluid enters the system uniformly at 50°C, and experimental results reveal varying Nusselt and Reynolds numbers at different concentrations and flow rates. Specifically, 0.16% CuO/water nanofluids exhibit slightly higher heat transfer coefficients compared to other volume concentrations and flow rates of Al<sub>2</sub>O<sub>3</sub>/water nanofluids. Empirical correlations for Nusselt number and friction factor align well with the experimental data. Additionally, Computational Fluid Dynamics (CFD) simulations are performed using ANSYS 18.0 Fluent to model the car radiator design, employing a coarse mesh and applying boundary conditions. The analysis shows laminar flow, and the CFD results are in close agreement with the experimental findings, depicting temperature, velocity, and pressure contours.

**Keywords:** Heat Transfer in Internal flows, Radiator, Volume concentrations, flow rates

### 1. INTRODUCTION

Theoretically, it is widely accepted that the utilization of nanoparticles can improve heat transfer efficiency. This research project investigates the real-world implementation of nano-fluids in a heat exchanger experiment.

Nano-fluids consist of engineered colloids merging a base fluid with nanoparticles, typically sized between 1 to 100nm. These fluids exhibit superior thermal conductivity and enhanced heat transfer coefficients compared to their base counterparts. The concept involves suspending metallic or non-metallic nanoparticles in the base fluid, forming a novel heat transfer fluid. Factor such as nanoparticle properties, size, and concentration within the fluid influence the heat transport capabilities of nano-fluids.

This study explored the convective heat transfer properties of silver-water nanofluids across laminar, transition, and turbulent flow regimes. [1]. Nano fluid is a suspension of nanoparticles with superior thermal, rheological, and wettability properties, improving various applications like heat transfer, lubrication, drug delivery, and oil recovery. This article discusses Nano fluid stability from preparation to implementation in practical applications, focusing on factors like temperature, pressure, confinement, composition, salinity, external magnetic field, and shear rate. [2]. This study focuses on synthesizing pristine Cu-Al layered double hydroxide (LDH) Nano fluid using a one-step method and studying its thermal properties. Characterization techniques were employed to determine crystallite size, composition, morphology, and interlayer anion vibration. [3]. This study used mono-type nanoparticle suspensions, with CuNPs showing the greatest enhancement. Hybrid suspensions did not show the same improvement. Experimentally measured thermal conductivities were consistently greater than theoretical predictions. Mechanisms for this enhancement are discussed [4]. The framework analyzes

Alumina and Copper-water Nano fluid over a sheet with thermal radiation effects. It incorporates effective thermal conductivity and viscosity for nanoparticles, analyzing temperature influence in the restricted domain. Partial differential equations are obtained from momentum and energy equations [5]. This study evaluates the performance of an automobile radiator using nanofluid compared to distilled water as a coolant in a heat exchanger-based radiator. The radiator consists of upright tubes with an elliptical cross-section. The results show that increasing air flow rate and flow rate improves heat transfer performance. The maximum enhancement in heat transfer rate was found to be 44.29% at 0.2% volume fraction of alumina-distilled water-based Nano fluid compared to distilled water [6]. This paper presents a best practice for analyzing Nano fluids in heat transfer applications, specifically for car radiators. The study investigates aluminum oxide and titanium dioxide nanoparticles, focusing on their anti-corrosive properties and comprehensive characterization. Results show a maximum enhancement of thermal performance by 24.21% using  $\text{Al}_2\text{O}_3$  at a 0.3% volume fraction. [7].

This paper presents findings on the thermal conductivity, viscosity, density, and specific heat of  $\text{Al}_2\text{O}_3$  nanoparticles in water and ethylene glycol-based coolants used in car radiators. Thermal conductivity, viscosity, and density increased with volume concentrations, while specific heat decreased with nanoparticle volume concentrations [8].

This investigation analyzes the effect of adding  $\text{Al}_2\text{O}_3$  nanoparticles to MQL cooling fluid on cutting tool temperature distribution using finite element analysis and a discrete phase model [9]. Experimental investigation of temperature and particle volume concentration on water- $\text{Al}_2\text{O}_3$  Nano fluid dynamic viscosity using a commercial viscometer. Results show increased viscosity with particle volume fraction but decrease with temperature increase [10].

The study investigates the thermal conductivity of  $\text{Al}_2\text{O}_3$ -Cu/EG nanoparticles in ethylene glycol at different concentrations and temperatures. Results show Nano fluid has higher thermal conductivity than base fluid, depending on volume concentration and temperature [11]. A laminar convective heat transfer and pressure drop technique is presented using  $\text{Al}_2\text{O}_3$ -Cu/water hybrid Nano fluid in a uniformly heated circular tube [12]. This study investigated the effect of  $\text{TiO}_2$ -water Nano fluid on radiator performance, comparing results with pure water and  $\text{TiO}_2$ -water Nano fluid. The main objective was to check heat transfer aspects [13].

The study investigated the effects of silica Nanospheres, MWCNTs, and hybrids H1 and H2 on distilled water viscosity and density. Results showed that Nano fluids increased with concentration, while temperature reduced them. H2 showed the least increase in viscosity at high concentrations, while H1 showed the least increase in base fluid density [14]. The study prepared hybrid carbon Nano fluids (HCNFs) using an acetylene flame synthesis system for heat exchange applications. [15].

This study investigates thermoelectric power generation from cavities with ventilation ports using a rotating conic object and carbon nanotube particles. It examines the effects of parameters like Reynolds numbers, object size, and nanoparticle volume fractions on fluid flow, interface temperature, and output power [16]. This study aims to attract young scholars and experts in heat transfer by discussing hybrid Nano fluids applications and challenges. The authors identify important work orientations and existing problems that hinder their performance and implementation [17]. This paper reviews 160 papers from 1995-2017 on hybrid or composite Nano fluids, focusing on their preparation and thermo physical properties. It also discusses the applications and challenges of these fluids, aiming to stimulate further research in this field [18]. Conventional heat transfer fluids like water and engine oil are widely used in automobile radiators. To improve thermal performance, nano-sized solid particles can enhance thermal conductivity in working fluid [19].

Nano fluids have gained significant attention in recent years, with numerous papers discussing their applications. This paper reviews their use in different PHE geometries [20]. Hybrid Nano fluids offer promising thermo physical properties, heat transfer rate, and stability, offering potential in various heat transfer applications. This paper summarizes factors affecting their performance and presents conclusions based on data [21]. Rapid research on Nano fluids shows their potential as heat transfer fluids in engineering applications, influenced by nanoparticle thermal conductivity, particle volume

concentrations, and flow rates [22]. The experiment examined the impact of particle size, weight fraction, and working temperature on the thermal conductivity ratio of alumina/water Nano fluids [23]. The thermodynamic analysis evaluates Nano fluid's effect on improving PV/T hybrid solar collector efficiency in Qatar climate using experimental and computational data [24]. Researchers have shown the potential of Nano fluids in various systems, particularly automotive thermal management. Their idiosyncratic thermal and hydrodynamic behaviors make them ideal candidates for evaluation [25].

The study evaluates the enhancement of convective heat transfer performance of hybrid Nano fluids (Ag, Cu, SiC, CuO, TiO<sub>2</sub>) in Al<sub>2</sub>O<sub>3</sub> Nano fluid as coolants for louvered FN automobile radiators [26]. Conventional heat transfer fluids like water and engine oil are widely used in automobile radiators. To improve thermal performance, nano-sized solid particles can enhance thermal conductivity in working fluid [27]. Radiator heats and cools fluids, such as automotive engine cooling and HVAC dry cooling towers, to improve efficiency and effectiveness in IC engines. Enhancing radiator performance is crucial for overall performance improvement [28]. The automobile industry aims to maximize engine efficiency while maintaining compactness. This can be achieved by decreasing the frontal area of a car, enhancing aerodynamics. Higher thermal conductivity coolants transfer heat faster, reducing engine volume, pumping power, and radiator size. This leads to smaller frontal areas, improved fuel economy, and reduced emissions. Nano-fluids, with their enhanced thermal conductivity, offer better heat dissipation than conventional coolants, making them a potential practical application [29].

## 2. THERMOPHYSICAL PROPERTIES OF NANOFLUIDS

At a temperature of 50°C, the thermophysical attributes of Al<sub>2</sub>O<sub>3</sub>-CuO nanofluids are calculated, encompassing density, dynamic viscosity, specific heat capacity, and thermal conductivity, based on the given equations.

Base fluid properties are calculated by

$$\rho_w = 1000 \times \left[ 1.0 - \frac{(T_w - 4.0)^2}{119000 + 1365 \times T_w - 4 \times (T_w)^2} \right]$$

$$\mu_w = 0.00169 - 4.2526e-5 \times T_w + 74.9255e-7 \times (T_w)^2 - 2.09935e-9 \times (T_w)^3$$

$$k_w = 0.56112 + 0.00193 \times T_w - 2.60152e-6 \times (T_w)^2 - 6.08803e-8 \times (T_w)^3$$

Density of Nano fluid is calculated by

$$\rho_{nf} = \left( \frac{\phi}{100} \right) \rho_p + \left( 1 - \frac{\phi}{100} \right) \rho_w$$

Specific heat of Nano fluid is calculated by

$$C_{nf} = \frac{\frac{\phi}{100} (\rho C_p)_p + \left( 1 - \frac{\phi}{100} \right) (\rho C_p)_w}{\rho_{nf}}$$

Thermal conductivity of the Nano fluid is calculated by using

$$k_r = \frac{k_{nf}}{k_w} = \left[ 0.8938 \left( 1 + \frac{\phi}{100} \right)^{1.37} \left( 1 + \frac{T_{nf}}{70} \right)^{0.27} \left( 1 + \frac{d_p}{150} \right)^{-0.0336} \left( \frac{\alpha_p}{\alpha_w} \right)^{0.01737} \right]$$

$$k_{nf} = k_w \times k_r$$

Dynamic Viscosity of Nano fluid is calculated by using

$$\mu_r = \frac{\mu_{nf}}{\mu_w} = \left( 1 + \frac{\phi}{100} \right)^{11.3} \left( 1 + \frac{T_{nf}}{70} \right)^{-0.038} \left( 1 + \frac{d_p}{170} \right)^{-0.061}$$

$$\mu_{nf} = \mu_r \times \mu_w$$

### 3. METHODOLOGY

The figure illustrates the project architecture, depicting the functionality of the system and the interaction among different devices. The process of system design began with the choice of a suitable heat exchanger, and in our scenario, we decided on a car radiator paired with a fan.

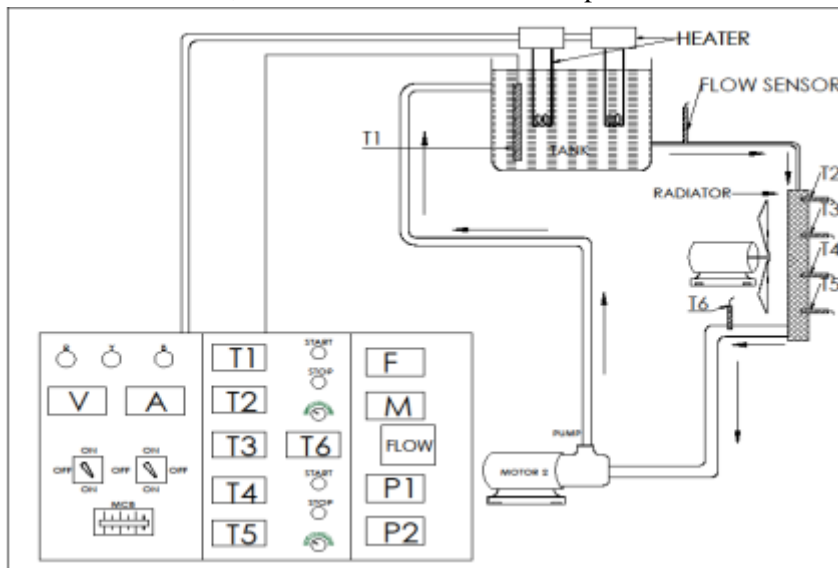


**Figure: 1** Project architecture diagram

The figure encompasses a water tank, heaters, thermocouples, fan, radiator, flow meter, motor, pressure gauge, and water pump. However, it's important to note that the conventional water pump used in cars, mechanically linked to the engine, doesn't meet the requirements of our experiment. By selecting a water pump tailored to our experimental needs, we ensure the smooth operation of the entire system. The project architecture illustrated in the figure offers a comprehensive overview of the interaction and collaboration among the devices, facilitating a clear understanding of the system's design and functionality. It acts as a visual aid in conveying the technical aspects of the project.

#### 3.1 Geometry Specifications of car radiator

**Table-1**

Parameters	Dimensions
Height of radiator	0.75m
Width of radiator	0.55 m
No. of radiator tubes	53
Each tube diameter	0.016 m
Length of the radiator tube	16.25m

#### 3.2 Fluid Preparation:

In our experiment, we begin with water as the initial fluid, utilizing a total volume of 60 liters. Water is frequently chosen as a base fluid in heat transfer applications due to its exceptional thermal properties and widespread availability. With 60 liters of water, we ensure ample fluid volume to facilitate smooth flow and circulation throughout the system. Water's high heat capacity and thermal conductivity make it an efficient heat transfer medium, and its abundance and affordability make it practical for experimentation. Using water as the base fluid establishes a reference point for comparing the performance of the nanofluid. Incorporating 60 liters of water in our experiment enables us to investigate how nanofluids enhance heat transfer capabilities compared to traditional base fluids. The nanofluids were prepared through sonication at 90°C over a period of 2 hours.

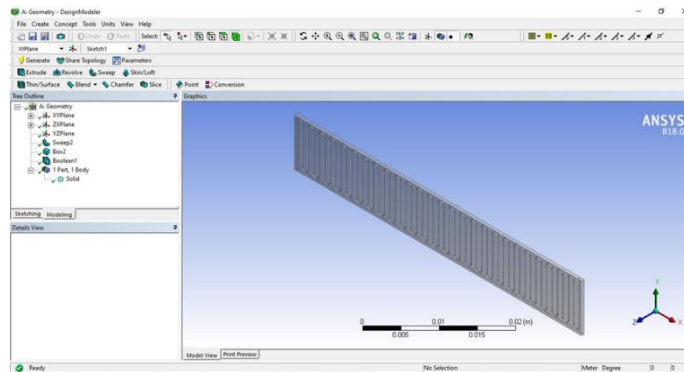
#### 3.4 Input parameters.

**Table-2**

Parameter	Range
Inlet Temperature	50°C

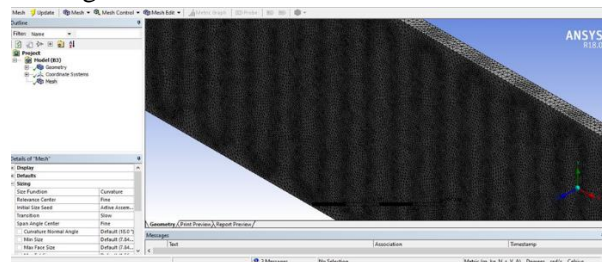
Volume Concentrations	0.01% - 0.16%
Flow rates	3.5m <sup>3</sup> /hr -4.5m <sup>3</sup> /hr
Reynolds Number	

The dimensions mentioned in Table-1 are used for creating a 3D model of the test section and the input parameters mentioned in Table-2 are used for the analysis. The solid models of the test section are shown in Fig. 1 and Fig. 2 respectively. In Fig. 1, Hexahedral meshing is used, number of nodes are 924798 and number of elements are 798995.



**Figure.2** Geometry model of Car Radiator.

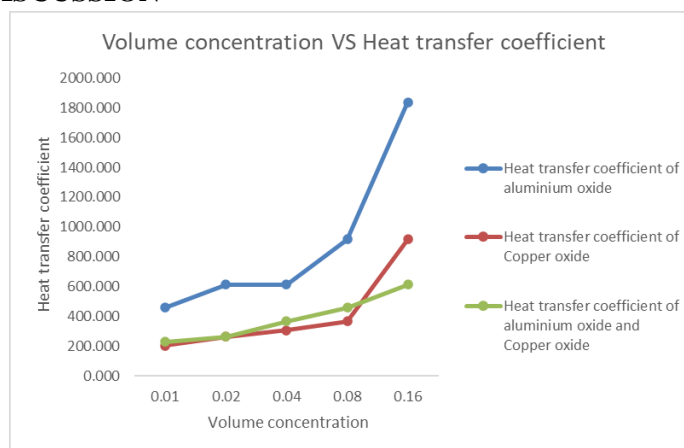
After selecting the window geometry, we transition to the design modeler page. Initially, a sketch is drawn on the XY plane to outline a circle with a 1 mm diameter, which is then extruded to a length of 16.25 meters. Through a Boolean operation, the two solid bodies are merged into a single part. Subsequently, employing a Pattern operation, a pitch distance of 10 mm is entered, and 53 copies are generated, resulting in a total length of 16.25 meters.



**Figure.3** Meshed model detail view

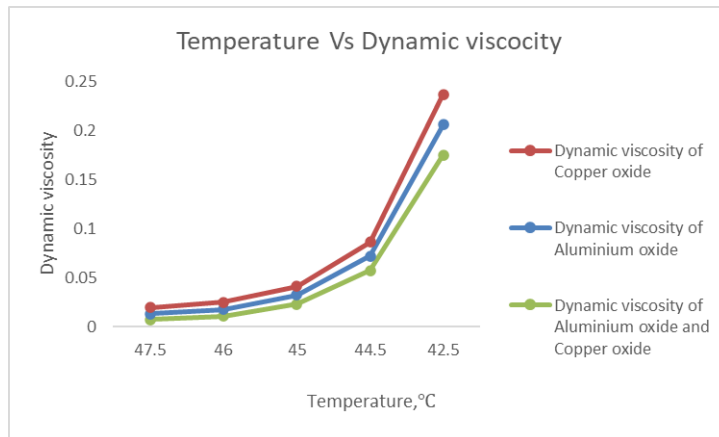
**Figure.3** once the model is finalized, the next step involves meshing. The material for the entire domain is designated as FLUENT, with each edge of the domain slated for division to achieve either hexahedral or tetrahedral meshing.

#### 4. RESULTS AND DISCUSSION



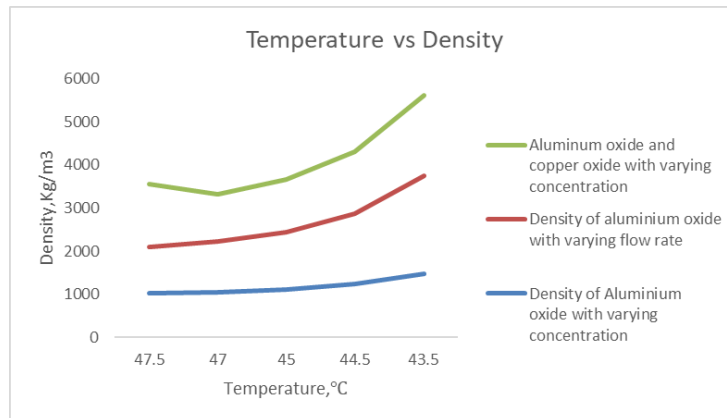
**Figure: 4** Graph between Volume Fraction and Heat Transfer Coefficient

**Figure: 4** shows that the graphical representation effectively illustrates the correlation between the Volume Concentration and heat transfer coefficient. In this context, Heat transfer coefficient of the aluminium oxide increases with increase in volume concentration.



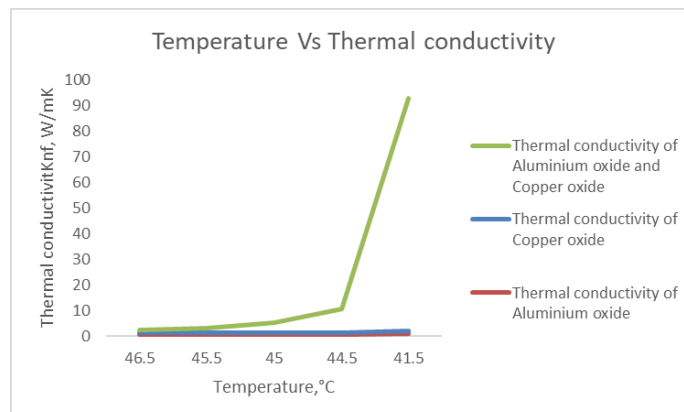
**Figure: 5** Graph between Temperature and Dynamic Viscosity

The graphical representation effectively illustrates the correlation between the Temperature and Dynamic viscosity of different fluids. The Dynamic viscosity of copper oxide increases accordingly to temperature.



**Figure: 6** Graph between Temperature and Density

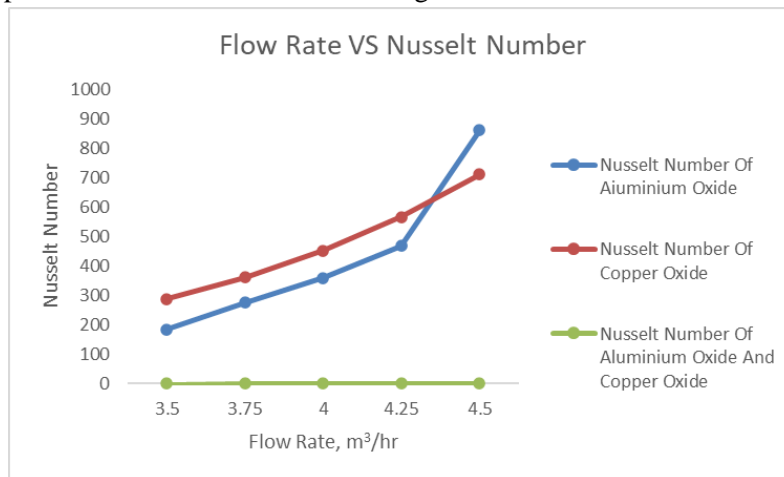
The visual representation efficiently demonstrates the connection between the Temperature and Density. The Density of oxide increases constantly with raises of Temperature. The hybrid nano-fluid which is mixed with both Aluminium Oxide and Copper Oxide had a high density with the temperature ranges when compared to the nanofluids. The Density of nano fluid Aluminium Oxide is lowest compared to other nanofluids.



**Figure: 7** Graph between Temperature and Thermal Conductivity

The visual representation efficiently demonstrates the connection between the Nusselt number and the Heat transfer coefficient. It's important to highlight that, in every scenario investigated; Copper oxide consistently surpasses other fluids. These results emphasize the superior performance of copper oxide in

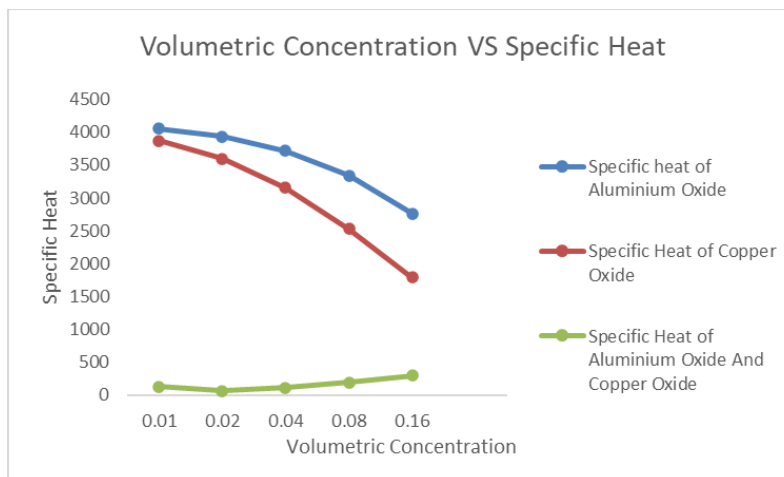
enhancing the friction factor across different flow rates. This lower value positions the Nano fluid as an ideal option for applications related to radiator cooling.



**Figure: 8** Graph between Flow Rate and Nusselt Number

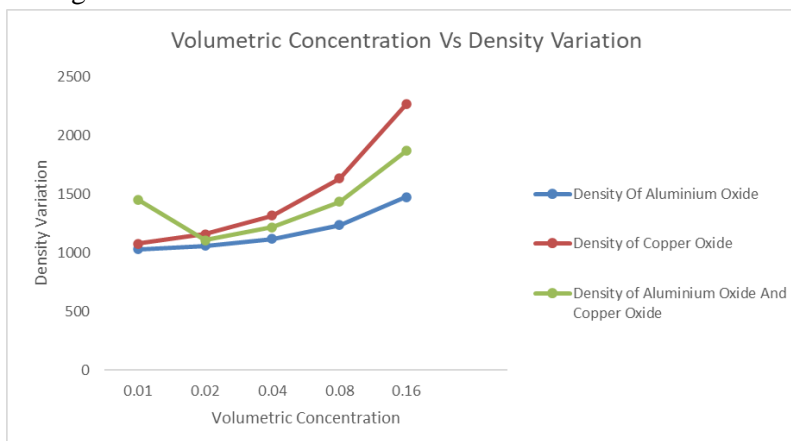
The graphical representation effectively illustrates the correlation between the flow rate and Nusselt number. In this context, it is noteworthy that Aluminium oxide consistently outperforms other fluids in each scenario examined. These findings underscore Aluminium Oxide superior performance when it comes to enhancing the Nusselt number across various flow rates.

**Validation:**



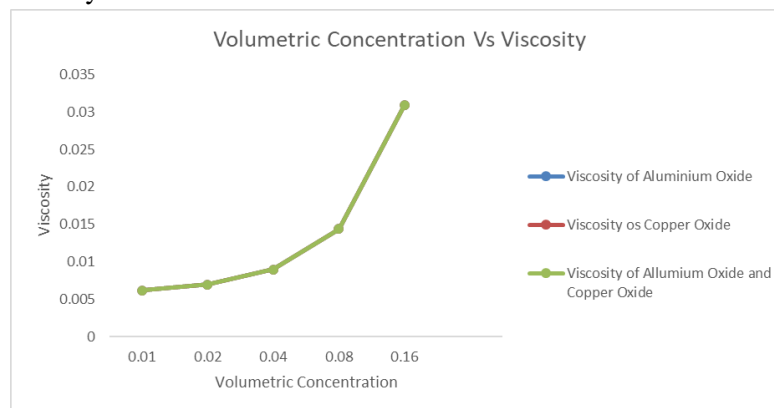
**Figure: 9** Graph between Volumetric Concentration Vs Specific Heat

Figure 9 represents the Graph is plotted between Volumetric Concentration and Specific Heat of analytical and experimental values. The specific heat of Aluminium Oxide and Copper Oxide nanofluids are decreasing with the increasing of volumetric concentration. The Specific heat of hybrid nano fluid increases with increasing volumetric concentration.



**Figure: 10** Graph between Volumetric Concentration Vs Density Variation

Figure 10 represents the Graph is plotted between Volumetric Concentration and Density Variation of analytical and experimental values. The Density of hybrid nanofluid decreases first and after certain Volumetric Concentration, Density increases constantly. The both Aluminium oxide and Copper Oxide nanofluid are continuously increases the with Volumetric Concentration.



**Figure: 11 Graph between Volumetric Concentration Vs Viscosity**

Figure 11 represents the Graph is plotted between Volumetric Concentration and Viscosity of analytical and experimental values. All the nanofluid and hybrid nanofluids are having the similar values of viscosity with respective to Volumetric Concentration. The graph shows that the Viscosity increases with the increases of Volumetric Concentration.

## 5. CONCLUSION

The experimental findings indicate that Nano fluids with 0.16%  $\text{Al}_2\text{O}_3$  and CuO in water exhibit slightly elevated heat transfer coefficient values in comparison to different volume concentrations. Additionally, the performance metrics outperform those associated with other volume concentrations and flow rates. Empirical correlations developed to analyze the Nusselt number and friction factor closely match the experimental data, offering valuable insights into the heat transfer characteristics of these Nano fluids. Through Computational Fluid Dynamics (CFD) analysis, the study comprehensively dissects temperature fluctuations, pressure distributions, and velocity profiles. These factors are intricately interrelated, and their coordinated optimization plays a vital role in enhancing a car's radiator performance. In essence, CFD analysis serves as an essential tool, acting as a linchpin in the pursuit of improving the cooling capabilities of automotive radiators. It is through a meticulous examination of temperature, pressure, and velocity distributions that the overall effectiveness of the car's radiator system is carefully examined and enhanced.

## References:-

1. Chakraborty, S., &Panigrahi, P. K. (2020). Stability of nanofluid: A review. *Applied Thermal Engineering*, 174, 115259. <https://doi.org/10.1016/j.applthermaleng.2020.115259>
2. Asirvatham, L. G., Raja, B., Lal, D. M., &Wongwises, S. (2011). Convective heat transfer of nanofluids with correlations. *Particuology*, 9(6), 626–631. <https://doi.org/10.1016/j.partic.2011.03.014>
3. Chakraborty, S., Sarkar, I., Haldar, K., Pal, S. K., &Chakraborty, S. (2015). Synthesis of Cu–Al layered double hydroxide nanofluid and characterization of its thermal properties. *Applied Clay Science*, 107, 98–108. <https://doi.org/10.1016/j.clay.2015.01.009>
4. Jana, S., Salehi-Khojin, A., &Zhong, W. (2007). Enhancement of fluid thermal conductivity by the addition of single and hybrid nano-additives. *ThermochimicaActa*, 462(1–2), 45–55. <https://doi.org/10.1016/j.tca.2007.06.009>
5. Rezania, A., Rosendahl, L., &Brouwer, J. (2012). Experimental investigation of thermoelectric power generation versus coolant pumping power in a microchannel heat sink. *International*

*Communications in Heat and Mass Transfer*, 39(8), 1054–1058.  
<https://doi.org/10.1016/j.icheatmasstransfer.2012.07.010>

6. Chaurasia, P., Kumar, A., Yadav, A. K., Kumar, P., Kumar, V. & Prasad, L. (2019). Heat transfer augmentation in automobile radiator using Al<sub>2</sub>O<sub>3</sub>–water based nanofluid. *SN applied sciences*, 1(3). <https://doi.org/10.1007/s42452-019-0260-7>
7. Said, Z., Assad, M. E. H., Hachicha, A. A., Ghobadian, B., Abdelkareem, M. A., Alazaizeh, D. Z., & Yousef, B. A. (2019). Enhancing the performance of automotive radiators using nanofluids. *Renewable & Sustainable Energy Reviews*, 112, 183–194. <https://doi.org/10.1016/j.rser.2019.05.052>
8. Choi, J., & Zhang, Y. (2012). Numerical simulation of laminar forced convection heat transfer of Al<sub>2</sub>O<sub>3</sub>–water nanofluid in a pipe with return bend. *International Journal of Thermal Sciences*, 55, 90–102. <https://doi.org/10.1016/j.ijthermalsci.2011.12.017>
9. Khanafer, K., & Vafai, K. (2021). Analysis of turbulent two-phase flow and heat transfer using nanofluid. *International Communications in Heat and Mass Transfer*, 124, 105219. <https://doi.org/10.1016/j.icheatmasstransfer.2021.105219>
10. Rashid, I., Haq, R. U., Khan, Z. A., & Al-Mdallal, Q. M. (2017). Flow of water based alumina and copper nanoparticles along a moving surface with variable temperature. *Journal of Molecular Liquids*, 246, 354–362. <https://doi.org/10.1016/j.molliq.2017.09.089>
11. Sundar, L. S., Sharma, K. S., Singh, M. K., & Sousa, A. (2017). Hybrid nanofluids preparation, thermal properties, heat transfer and friction factor – A review. *Renewable & Sustainable Energy Reviews*, 68, 185–198. <https://doi.org/10.1016/j.rser.2016.09.108>
12. Ahmed, S., Özkaymak, M., Sözen, A., Menlik, T., & Fahed, A. (2018). Improving car radiator performance by using TiO<sub>2</sub>-water nanofluid. *Engineering Science and Technology, an International Journal*. <https://doi.org/10.1016/j.jestch.2018.07.008>
13. Baghbanzadeh, M., Rashidi, A., Soleimansalim, A. H., & Rashtchian, D. (2014). Investigating the rheological properties of nanofluids of water/hybrid spherical silica/MWCNT nanostructure. *Thermochimica Acta*, 578, 53–58. <https://doi.org/10.1016/j.tca.2014.01.004>
14. Hung, Y. H., Wang, W., Hsu, Y., & Teng, T. P. (2017). Performance evaluation of an air-cooled heat exchange system for hybrid nanofluids. *Experimental Thermal and Fluid Science*, 81, 43–55. <https://doi.org/10.1016/j.expthermflusci.2016.10.006>
15. Shafahi, M., Bianco, V., Vafai, K., & Manca, O. (2010). An investigation of the thermal performance of cylindrical heat pipes using nanofluids. *International Journal of Heat and Mass Transfer*, 53(1–3), 376–383. <https://doi.org/10.1016/j.ijheatmasstransfer.2009.09.019>
16. Akash, A., Abraham, S., Pattamatta, A., & Das, S. K. (2019). Experimental Assessment of the Thermo-Hydraulic Performance of Automobile Radiator with Metallic and Nonmetallic Nanofluids. *Heat Transfer Engineering*, 41(3), 235–251. <https://doi.org/10.1080/01457632.2018.1528055>
17. Karlapalem, V., & Dash, S. K. (2021). Design of perforated branching fins in laminar natural convection. *International Communications in Heat and Mass Transfer*, 120,
18. Nguyen, C. N., Desgranges, F., Galanis, N., Roy, G., Maré, T., Boucher, S., & Mintsa, H. A. (2008). Viscosity data for Al<sub>2</sub>O<sub>3</sub>–water nanofluid—hysteresis: is heat transfer enhancement using nanofluids reliable? *International Journal of Thermal Sciences*, 47(2), 103–111. <https://doi.org/10.1016/j.ijthermalsci.2007.01.033>
19. Sahoo, R. R., & Sarkar, J. (2016). Heat transfer performance characteristics of hybrid nanofluids as coolant in louvered fin automotive radiator. *Heat and Mass Transfer*. <https://doi.org/10.1007/s00231-016-1951-x>
20. Qasim, M., Kamran, M., Ammar, M., Jamal, M., & Javaid, M. (2020). Heat Transfer Enhancement of an Automobile Engine Radiator using ZnO Water Base Nanofluids. *Journal of Thermal Science*, 29(4), 1010–1024. <https://doi.org/10.1007/s11630-020-1263-9>
21. Said, Z., Assad, M. E. H., Hachicha, A. A., Ghobadian, B., Abdelkareem, M. A., Alazaizeh, D. Z., & Yousef, B. A. (2019b). Enhancing the performance of automotive radiators using nanofluids. *Renewable & Sustainable Energy Reviews*, 112, 183–194. <https://doi.org/10.1016/j.rser.2019.05.052>

22. Carvalho, C. J. (2022). A Review on Nanofluids the next Super Coolant for Radiator. *IJERT*. <https://doi.org/10.17577/IJERTV11IS020096>
23. Aditi, N. V., Farooque, Z., & Chauhan, N. R. (2022). Comparative study of Nano-fluids as Coolants in a Car Radiator. *IOP Conference Series: Materials Science and Engineering*, 1228(1), 012011. <https://doi.org/10.1088/1757-899x/1228/1/012011>
24. Selimefendigil, F., & Oztop, H. F. (2021). Thermoelectric generation from vented cavities with a rotating conic object and highly conductive CNT nanofluids for renewable energy systems. *International Communications in Heat and Mass Transfer*, 122, 105139. <https://doi.org/10.1016/j.icheatmasstransfer.2021.105139>
25. Kumar, D. D., & Arasu, A. V. (2018). A comprehensive review of hybrid nanofluids' preparation, characterization, properties, and stability. *Renewable & Sustainable Energy Reviews*, 81, 1669–1689. <https://doi.org/10.1016/j.rser.2017.05.257>
26. Sidik, N. a. C., Cheong, N. K., & Fazeli, A. (2014). Computational analysis of nanofluids in vehicle radiator. *Applied Mechanics and Materials*, 695, 539–543. <https://doi.org/10.4028/www.scientific.net/amm.695.539>
27. Geetha, Y. (2019). Numerical Study of Heat Transfer Enhancement using Water and Ethylene Glycol Mixture based Nanofluids as Coolants in Car Radiators 1296. <https://www.semanticscholar.org/paper/Numerical-Study-of-Heat-Transfer-Enhancement-using-Geetha-Babu/adb88ae831e7026221d13d0737b88d08335d2ce0>
28. Huminic, G., & Huminic, A. (2018). Hybrid nanofluids for heat transfer applications – A state-of-the-art review. *International Journal of Heat and Mass Transfer*, 125, 82–103. <https://doi.org/10.1016/j.ijheatmasstransfer.2018.04.059>
29. Kumar, V., & Sarkar, J. (2019). Numerical and experimental investigations on heat transfer and pressure drop characteristics of Al<sub>2</sub>O<sub>3</sub>-TiO<sub>2</sub> hybrid nanofluid in minichannel heat sink with different mixture ratio. *Powder Technology*, 345, 717–727. <https://doi.org/10.1016/j.powtec.2019.01.061>

## A Brief Overview of Magnetic Refrigeration

**K.Nithin<sup>1</sup>, J.Jathin<sup>1</sup>, G.Hemanth kumar<sup>2</sup>, M.Virinchi<sup>3</sup>, G.V.S.Ravi Teja<sup>4</sup>, G.Bhargav<sup>5</sup>,  
B.Prem sai<sup>6</sup>, K.Raju<sup>7</sup>, B. Sai Kausik<sup>1</sup>, Dr.P.Anusha<sup>1\*</sup>, Dr.M.Naga Swapna Sri<sup>1\*</sup>**

<sup>1,2,3,4,5,6</sup>B.Tech Student, Department of Mechanical Engineering, P V P Siddhartha Institute of  
Technology, Vijayawada.

<sup>1\*</sup>Assistant Professor, Department of Mechanical Engineering, P V P Siddhartha Institute of  
Technology, Vijayawada. [anusha.peyyala@pvsiddhartha.ac.in](mailto:anusha.peyyala@pvsiddhartha.ac.in)

### ABSTRACT

Magnetic refrigeration is a relatively new technology compared to traditional refrigeration methods like compression-based systems. The concept of magnetic refrigeration dates back to the early 20th century, but significant advancements have been made in recent decades. The idea of using magnetic materials to achieve cooling was first proposed by a German physicist named Emil Warburg in 1881. He suggested that applying a magnetic field to certain materials could cause them to heat up or cool down, depending on their magnetic properties. However, it wasn't until the late 20th century that practical applications of magnetic refrigeration began to emerge. In the 1970s and 1980s, researchers began experimenting with various magnetic materials and developing prototypes of magnetic refrigeration systems. One of the key breakthroughs came in the 1990s when researchers discovered the magnetocaloric effect (MCE) in certain materials. The magnetocaloric effect is the phenomenon in which a material heats up when exposed to a magnetic field and cools down when the magnetic field is removed. This effect forms the basis of magnetic refrigeration technology. Today, magnetic refrigeration is seen as a promising alternative to traditional refrigeration methods due to its potential for higher energy efficiency, reduced environmental impact, and compatibility with environmentally friendly refrigerants. Researchers continue to work on refining magnetic refrigeration technology and bringing it to commercial applications in areas such as refrigeration, air conditioning, and cryogenics. While it has yet to become widely adopted, ongoing advancements suggest that magnetic refrigeration could play a significant role in the future of cooling technology. Present Review focused on Studies done by various researchers in the field of Magnetic Refrigeration and its applications in various fields of Engineering.

**KEY WORDS:** Magnetic Refrigeration, Magnetocaloric Effect [MCE], Magnetic Field, Future Of Cooling Technology.

### 1. INTRODUCTION

Investigating four samples of Gd with varying purities using multiple methods including ac susceptibility, magnetization, heat capacity, and direct measurements of the magnetocaloric effect in both quasistatic and pulse magnetic fields, it was found that they consistently indicate a zero-field Curie temperature of approximately 294 K. The Curie temperature determined from inflection points in magnetic susceptibility and heat capacity aligns well with those from magnetocaloric effect and Arrot plots. Beyond 2 T, the transition temperature increases nearly linearly with magnetic field at a rate of around 6 K/T up to 7.5 T. Spin reorientation transition, occurring at approximately 227 K without magnetic field, was confirmed through susceptibility, magnetization, and heat-capacity measurements. Magnetic fields above 2–2.5 T seem to suppress the spin reorientation transition, maintaining Gd's simple ferromagnetic structure from TC(H) down to about 4 K. The anomaly observed above 132 K in ac susceptibility measurements along the c axis is discussed. High levels of interstitial impurities lower the second-order paramagnetic↔ferromagnetic transition temperature, potentially leading to inaccuracies in magnetocaloric effect measurements in pulsed magnetic fields. The magnetocaloric effect was assessed using three experimental techniques across the same samples, showing consistent results among them, barring one exception, within experimental error bounds.[1]

The study examined the exergetic and thermal efficiency of hybrid systems utilizing various solid oxide fuel cell (SOFC) intermediate-temperature electrolytes at different temperatures and electrolyte thicknesses. Electrolytes investigated included lanthanum strontium gallate magnesite, yttria-stabilized zirconium, and gadolinium-doped ceria oxide (GDC). By integrating the Wagner mass transfer model (MTM), encompassing solid-state oxygen-ion, hole, and electron conduction, into a thermodynamic model for a basic hybrid system, the simulated performance trends of different electrolytes aligned closely with experimental observations. This paper attends to demonstrate the usefulness of Design of Experiments (DOE) method in magnetic refrigeration (MR) understanding and optimization. A numerical DOE is applied to a simple 1D finite difference model describing an Active Magnetic Regenerative Refrigeration (AMRR) system. The heat transfer fluid is water, the regenerator consists of stacked gadolinium plates and the model is based on the assumption of an equivalent single plate. A two-level 27-3 fractional DOE based on Box methodology is used to evaluate the effect of seven parameters on the temperature span, namely material and fluid thicknesses, length, equivalent width, mass flow rate, cycle frequency and magnetocaloric effect (MCE).[2]

Magnetic refrigeration utilizes the magnetocaloric effect (MCE) to achieve cooling by altering magnetic fields. However, MCE typically yields only a small temperature change at room temperature. To enhance cooling efficiency, an Active Magnetic Regenerator (AMR) has been developed. This paper conducts analytical evaluation and performance projection for a magnetic refrigerator incorporating AMR. An analytical model is devised, featuring small channels, jet flow, and retention regions within a test sectional tube to simulate fluid flow through a packed bed of spherical gadolinium particles, serving as magnetocaloric materials. The analysis and projection of the AMR magnetic refrigeration system via the analytical model reveal temperature performance and highlight the existence of optimal operating conditions, dependent on suitable flow volume and volumetric flow rate.[3]

Magnetic cooling, an age-old concept, is now being explored for everyday applications to address the limitations of traditional vapor compression refrigeration systems, such as reduced power consumption and environmental concerns like Ozone Depletion and Global Warming. Historically, it has found success in cryogenic temperature ranges. Magnetic refrigeration relies on the magneto-caloric effect, a property inherent in magnetic materials and their alloys, wherein their temperature changes upon magnetization or demagnetization. Magnetization corresponds to gas compression (heating), while demagnetization mimics gas expansion (cooling). Key requirements include achieving these variations rapidly, repeatedly, reversibly, and with minimal energy losses. This paper investigates the feasibility of employing this method for room temperature refrigeration and air conditioning. Firstly, it compares magnetic refrigeration with vapor compression systems. Secondly, it outlines the magneto-caloric materials and their prerequisites. Thirdly, it examines the impact of various parameters such as magnetic field strength, regenerator configuration, temperature span, and refrigerant fluid on magnetic refrigeration performance. Lastly, it discusses the advantages and disadvantages. Magnetic refrigeration shows promising potential for future applications.[4]

The refrigeration system holds significant importance in various industries, with ongoing efforts directed towards mitigating environmental impact. Magnetic refrigeration, an emerging eco-friendly technology, relies on a magnetic solid functioning as a refrigerant through the magneto-caloric effect (MCE). In ferromagnetic materials, MCE induces warming as atomic magnetic moments align under a magnetic field. Magnetic phase changes, occurring at the Curie point, may involve first-order (FOMT) or second-order (SOMT) transitions. The active magnetic regenerative cycle (AMR) serves as the reference cycle for magnetic refrigeration. Here, the magnetic material matrix serves dual purposes as a refrigerant and heat regenerator, with a fluid flowing through the porous matrix facilitating heat transfer. Regeneration involves reciprocating blowing of a heat transfer fluid through a regenerator comprised of magnetocaloric material, alternately magnetized and demagnetized. Numerous magnetic refrigeration prototypes with diverse designs and software models have been developed globally. This paper aims to elucidate magnetic refrigeration's efficacy compared to conventional methods.[5]

Research into room-temperature magnetic refrigeration is driven by the aim to surpass the energy efficiency of vapor-compression technology. Despite this, the development of commercially viable magnetic refrigeration systems with competitive performance and pricing remains elusive. One significant barrier is the insufficient properties of current magnetocaloric materials. This article explores the necessary enhancements in these materials' properties. Using two established vapor-compression refrigerators as benchmarks, the study employs numerical simulations to assess magnetic refrigerators. Beyond factors like uniformity of transition temperature and mechanical durability, the research underscores the need for magnetocaloric materials with an adiabatic entropy change 2.35 times greater than existing options to surpass vapor-compression systems.[6]

Magnetic refrigeration, utilizing the magnetocaloric effect (MCE), presents a promising avenue for energy-efficient and environmentally friendly cooling technology, potentially rivaling traditional vapor compression systems in the future. MCE refers to the temperature changes observed in certain ferromagnetic materials upon exposure to a magnetic field, forming the basis for this innovative cooling approach. Active magnetic regenerative (AMR) refrigeration cycles harness the MCE of materials like Gd through a four-stage regenerative process. Over the past two decades, research in this field has flourished, exploring various aspects such as materials selection, magnetic field generation, and system design. This study provides a chronological overview and comparison of recent advancements in AMR refrigeration. It examines findings from the literature, focusing on magnetocaloric materials, geometric parameters (including regenerator geometry), and operational variables such as cycle frequency, utilization, heat transfer fluid, heat rejection temperature, and cooling load. Performance metrics like no-load temperature span, cooling capacity, and system coefficient of performance are evaluated and compared. Parametric sensitivity and performance trends are identified and analysed. Additionally, key barriers to achieving optimal system performance and the commercial viability of this technology are discussed.[7]

This paper provides a comprehensive overview of magnetic refrigeration research, encompassing various studies in the field. It discusses the principle of magnetic refrigeration at ambient temperature and its significance. The discussion includes explanations of phase transitions, distinguishing between first-order and second-order transitions, highlighting their respective advantages and drawbacks. First-order materials are noted for their high magnetic entropy and adiabatic temperature change, although they are burdened by significant magnetic hysteresis. Conversely, second-order phase transition materials exhibit contrasting characteristics. Additionally, the review includes an examination of existing materials and an analysis of the magnetocaloric effect.[8]

This paper discusses a new type of refrigeration system that operates based on the magnetic field's cooling effect, known as the Magneto-Caloric effect (MCE). The aim of the study is to elucidate the working principle and operational cycle of this cooling method. The MCE occurs when a magnetic material, such as gadolinium, is exposed to a magnetic field generated by a magnet, causing its temperature to rise. Upon removal of the magnetic field source, the material returns to its original temperature. The cooling effect is harnessed by employing gadolinium, which heats up as it passes through the magnetic field and undergoes the magneto-caloric effect. To dissipate the heat from the metal when it is subjected to the magnetic field, cooled water is circulated. Upon exiting the magnetic field, the material cools back to its initial temperature due to the magnetic effect. This cooled gadolinium is then utilized to extract heat from the refrigerator coils.[9]

Magnetic refrigeration stands out as a compelling alternative to traditional refrigeration methods, leveraging the unique property of certain materials known as the magnetocaloric effect (MCE). This study offers a comprehensive exploration of various magnetic refrigeration technologies, employing diverse models to assess key performance indicators like the coefficient of performance (COP) and specific cooling capacity. The research categorizes magnetic refrigeration models into four types: rotating, reciprocating, C-shaped magnetic refrigeration, and active magnetic regenerator, detailing their operational principles and comparative performance. Furthermore, the investigation delves into factors such as the magnetocaloric effect's impact, magnetization area, and thermodynamic processes and

cycles, aiming to optimize efficiency and achieve maximal cooling capacity. Previous research on magnetocaloric materials is synthesized, emphasizing their magnetic properties and potential. The study also underscores essential features of magnetic refrigeration systems, elucidating their advantages, challenges, limitations, and feasibility considerations. Additionally, a cost analysis is presented to assess the commercial viability of these systems.[10]

Magnetic refrigeration represents an emerging, eco-friendly technology that harnesses the magnetocaloric effect (MCE) of a magnetic solid to function as a refrigerant. In ferromagnetic materials, the MCE involves a heating process as the alignment of magnetic moments occurs upon the application of a magnetic field, followed by cooling when the field is removed. Two types of magnetic phase changes, first order magnetic transition (FOMT) and second order magnetic transition (SOMT), can occur at the Curie point. The active magnetic regenerative (AMR) cycle serves as the reference cycle for magnetic refrigeration, where the magnetic material matrix serves both as a refrigerating and heat regenerating medium, with a fluid flowing through the porous matrix facilitating heat transfer. Regeneration is achieved by cyclically blowing a heat transfer fluid through the regenerator made of magnetocaloric material, which is alternately magnetized and demagnetized. This study focuses on the near room-temperature range, comparing the energy performance of a commercial R134a refrigeration plant to that of a magnetic refrigerator operating with an AMR cycle. Special attention is given to evaluating the environmental impact in terms of greenhouse gas emissions. Through mathematical modeling, the comparison reveals that Gd<sub>5</sub>Si<sub>2</sub>Ge<sub>2</sub> and LaFe<sub>11.384</sub>Mn<sub>0.356</sub>Si<sub>1.26</sub>H<sub>1.52</sub> consistently exhibit lower TEWI indices than those of vapor compression plants. Moreover, the TEWI of the AMR cycle using FOMT materials consistently outperforms that of SOMT materials, with Gd<sub>5</sub>Si<sub>2</sub>Ge<sub>2</sub> identified as the most effective FOMT material.[11]

S.No	Author	Summary
1.	S. Yu. Dan'kov et al.	Gd samples of varying purity showed a Curie temperature of 294 K independent of measurement technique, with a linear rise under high magnetic fields, a spin reorientation at 227 K suppressed by stronger fields, and magnetocaloric effects influenced by interstitial impurities and measurable with consistent techniques
2.	M. Williams <i>et al.</i>	This study explores optimal conditions for solid oxide fuel cells (SOFCs) by analyzing material properties, thermodynamics, and experimental data, identifying gadolinium-doped ceria as promising for high efficiency.
3.	J. ROUDAUT et al.	A numerical DOE approach in this paper reveals the influence of seven parameters on temperature span in an AMRR system, highlighting its effectiveness for optimizing magnetic refrigeration.
4.	Hirano et al.	An analytical model in this paper simulates jet flow and retention regions to evaluate a magnetic refrigerator with gadolinium particles, identifying flow parameters for optimal temperature performance.
5.	Dr. L.C.Singal et al.	This paper presents magnetic cooling, utilizing the magnetocaloric effect, as a potential alternative to traditional refrigeration, analyzing materials, performance factors, and its environmental benefits.
6.	N A Mezaal et al.	This paper explores magnetic refrigeration, an eco-friendly alternative to traditional methods, explaining its principles, comparing it to existing technology, and emphasizing its potential applications.

7.	Behzad Monfareda et al.	Room-temperature magnetic refrigeration offers potential energy efficiency as a vapor-compression replacement, but requires significant improvements in magnetocaloric materials, particularly a 2.35-fold increase in entropy change.
8.	Muhammad Sajid Kamran et al.	Magnetic refrigeration, using MCE and materials like Gd, shows promise for energy-efficient cooling through AMR cycles, but faces challenges in material performance and commercialization.
9.	Souheila Mellari et al.	This review explores room-temperature magnetic refrigeration, comparing first-order (high entropy change but large hysteresis) and second-order (low hysteresis but lower entropy change) materials, and analyzes existing materials and characterization methods.
10.	Pranav Pachpande et al.	This study thoroughly explores magnetic refrigeration technologies, evaluating their performance and categorizing them into four types. It analyzes key factors impacting efficiency, including magnetocaloric effects, operational principles, and cost considerations, to optimize cooling capacity and commercial viability.
11.	C Aprea et al.	This study compares the energy performance and environmental impact of a commercial R134a refrigeration plant to a magnetic refrigerator using an AMR cycle at near room temperature. Results show that magnetic refrigerants Gd <sub>5</sub> Si <sub>2</sub> Ge <sub>2</sub> and LaFe <sub>11.384</sub> Mn <sub>0.356</sub> Si <sub>1.26</sub> H <sub>1.52</sub> exhibit lower Total Equivalent Warming Impact (TEWI) indices compared to vapor compression plants, with Gd <sub>5</sub> Si <sub>2</sub> Ge <sub>2</sub> identified as the most effective FOMT material.

## CONCLUSIONS

In conclusion, the investigation into magnetic refrigeration, utilizing the magnetocaloric effect (MCE), offers promising insights for energy-efficient and environmentally friendly cooling technology, with potential to rival traditional vapor compression systems. The study encompasses diverse methodologies and analyses, ranging from experimental studies on gadolinium samples to numerical simulations of active magnetic regenerative (AMR) refrigeration cycles. Key findings include the consistent determination of a zero-field Curie temperature around 294 K in gadolinium samples, along with observations of spin reorientation transitions and their suppression by magnetic fields. The examination of hybrid systems incorporating solid oxide fuel cell (SOFC) electrolytes highlights the importance of material selection and electronic conductivity in achieving optimal performance. Additionally, Design of Experiments (DOE) methods are demonstrated as valuable tools for understanding and optimizing magnetic refrigeration systems.

The analysis of AMR refrigeration cycles underscores the significance of magnetocaloric materials and regenerator geometry in achieving efficient cooling. Comparisons with traditional vapor compression systems, considering factors such as coefficient of performance (COP) and environmental impact, reveal the potential of magnetic refrigeration to outperform conventional methods, particularly when utilizing certain magnetocaloric materials like Gd<sub>5</sub>Si<sub>2</sub>Ge<sub>2</sub>. Overall, this comprehensive overview consolidates recent advancements in magnetic refrigeration research, emphasizing the importance of material

properties, system design, and operational variables in realizing the commercial viability and environmental benefits of this innovative cooling technology.

### ACKNOWLEDGMENT

We would like to thank SAGTE and PVP Siddhartha Institute of Technology for Providing us Technical and Financial Assistance to carry out this work.

### REFERENCES

1. S. Yu. Dan'kov, A. M. V. K. Pecharsky, K. A. Gschneidner, Jr., "Magnetic phase transitions and the magnetothermal properties of gadolinium", PHYSICAL REVIEW B, VOLUME 57, NUMBER 6, 1 FEBRUARY 1998-II., 1998 The American Physical Society.
2. M. Williams, K. Yamaji, T. Horita, N. Sakai and H. Yokokawa " Exergetic Studies of Intermediate-Temperature, Solid Oxide Fuel Cell Electrolytes" , Journal of The Electrochemical Society, Volume 156, Number 4, 24 February 2009, © 2009 ECS - The Electrochemical Society.
3. J. Roudaut, H. Bouchekara , A. Kedous-Lebouc , J.L. Coulomb, " Optimization Of Active Magnetic Regenerative Refrigeration Systems Using Design Of Experiments" Theory And Modeling, May 2009.
4. Hirano , Shigeki ; Kawanami, Tsuyoshi ; Ikegawa, Masahiro ; Fumoto , Koji ; Hirasawa , Shigeki "Analytical Investigation on Regenerative Magnetic Refrigeration with Particle Packed Bed", Transactions of the Japan Society of Refrigerating and Air Conditioning Engineers, Volume 27, Issue 1, pp. 39-47 (2011).
5. Dr. L.C.Singal, Aishna Mahajan, Rajwinder Singh, "Magnetic Refrigeration- A Review- A boon for the coming generations", SSRG International Journal of Mechanical Engineering (SSRG – IJME ) – Volume 3 Issue 5 – May 2016.
6. N A Mezaal, K V Osintsev, T B Zhirgalova , "Review of magnetic refrigeration system as alternative to conventional refrigeration system" IOP Publishing, N A Mezaal et al 2017 IOP Conf. Ser.: Earth Environ. Sci. 87 032024. IOP Conf. Series: Earth and Environmental Science 87 (2017).
7. Behzad Monfareda, Björn Palm, "Material requirements for magnetic refrigeration applications" International Journal of Refrigeration, 19 August 2018.
8. Muhammad Sajid Kamran, Hafiz Ozair Ahmad, Hua Sheng Wang, "Review on the developments of active magnetic regenerator refrigerators – Evaluated by performance" Volume 133, November 2020.
9. Souheila Mellari, " Introduction to magnetic refrigeration: magnetocaloric materials "International Journal of Air-Conditioning and Refrigeration, Mellari Int. J. Air-Cond. Ref. (2023).
10. Pranav Pachpande, " Magnetic Refrigeration: The Modern Refrigeration Technique- A Review", International journal of Analytical Experimental and Finite Element Analysis, Vol. 7, Issue. 1, April 2020, pp 1-8 .
11. C Aprea , A Greco, A Maiorino , C Masselli, " Magnetic refrigeration: an eco-friendly technology for the refrigeration at room temperature" . Journal of Physics: Conference Series. : C Aprea et al 2015 J. Phys.: Conf.

## Structural and Thermal Analysis of Brake Drum

Shaik.Chand Mabhu Subhani<sup>1\*</sup>, A.Pavan Kumar<sup>2</sup>, Dr.D.venkata rao<sup>3</sup> and K.Anna Purnaiah<sup>4</sup>

<sup>1</sup>Asst.professor, Department of Mechanical Engineering, Narasaraopeta Institute of Technology, Narasaraopet, Guntur(Dt), A.P., India. [skcmsubhani@gmail.com](mailto:skcmsubhani@gmail.com)

<sup>2</sup>Asst.professor, Department of Mechanical Engineering, Narasaraopeta Institute of Technology, Narasaraopet, Guntur(Dt), A.P., India. [pavan.litam2006@gmail.com](mailto:pavan.litam2006@gmail.com)

<sup>3</sup>Professor and head, Department of Mechanical Engineering, Narasaraopeta Institute of Technology, Narasaraopet, Guntur(Dt), A.P., India. [dvrcrec@gmail.com](mailto:dvrcrec@gmail.com)

<sup>4</sup>M.Tech student, Thermal engineering, Narasaraopeta engineering college, Narasaraopet, Guntur(Dt), A.P., India. [academicsnitn@gmail.com](mailto:academicsnitn@gmail.com)

**ABSTRACT.** The brake drum is a specialized brake that uses the concept of friction to decelerate or to stop the vehicle. The deceleration is achieved by the assistance of the friction generated by a set of brake shoes or pads. During the brake operation heat is ejected out this causes damage to the brake. Disc (Rotor) brakes are exposed to large thermal stresses during routine braking and extraordinary thermal stresses during hard braking. To satisfy this condition the drum material should possess a high thermal conductivity, thermal capacity and high strength. The common material used for construction of brake drum is cast iron.

The aim of the project is to design, model a disc. Modeling is done using catia. Structural and Thermal analysis is to be done on the drum brakes using four materials Stainless Steel, grayCast iron, carbon carbon composite & aluminium metal matrix. The shoes of this kind of brake are contained within the drum and expand outwards when the brake is applied. Such kind of brakes is used in medium heavy-duty vehicles. Structural analysis is done on the drum brake to validate the strength of the drum brake and thermal analysis is done to analyze the thermal properties. Comparison can be done for deformation; stresses, temperature etc. from the three materials to check which material is best. Catia is a 3D modeling software widely used in the design process. ANSYS is general-purpose finite element analysis (FEA) software package. Finite Element Analysis is a numerical method of deconstructing a complex system into very small pieces (of user-designated size) called elements.

**Keywords:** Rotor brake, CATIA, FEA, Thermal analysis, Static analysis.

### 1. INTRODUCTION

A brake is a device which is used to bring to rest or slow down a moving body. Safe operation of vehicle demands dependable brakes is required to absorb the kinetic energy of the moving parts or the potential energy of the object being lowered by host when the rate of descent is controlled. The energy absorbed by brakes is dissipated in the form of heat. This heat is dissipated in the surrounding atmosphere to stop the vehicle, The working principle of the drum brakes involves a set of shoes or pads that create friction against a drum connected to the rotating wheel. Brake drum components include the back plate, brake drum, shoe, wheel cylinder, and various springs and pins. Brake drum was invented by Louis Renault in 1902.

He used woven asbestos lining for the brake drum lining as no alternative dissipated heat like the asbestos lining, though Maybach has used a less sophisticated brake drum. In the first brake drums, levers and rods or cables operated the shoes mechanically. From the mid-1930's, oil pressure in a small wheel cylinder and pistons operated the brakes, though small vehicles continued with purely mechanical systems for decades. Some designs have two wheel cylinders. The shoes in brake drums wear thinner, and brakes required regular adjustment until the introduction of self-adjusting brake drums in 1950's. The brake drum is used widely on road vehicles and consists of a drum attached to the rotating wheel.

The drum has an internal machined cylindrical surface. Inside the drum and protected from the environment are two shoes lined with friction material which can be pivoted to make a forced contact with the internal cylindrical surface. A drum brake unit consists of two brake shoes mounted on a stationary backing plate. When the brake pedal is pressed, a hydraulically activated wheel cylinder pushes the shoes out to contact a rotating drum which creates friction and slows the vehicle. As the pedal is released, return springs retract the shoes to their original position.

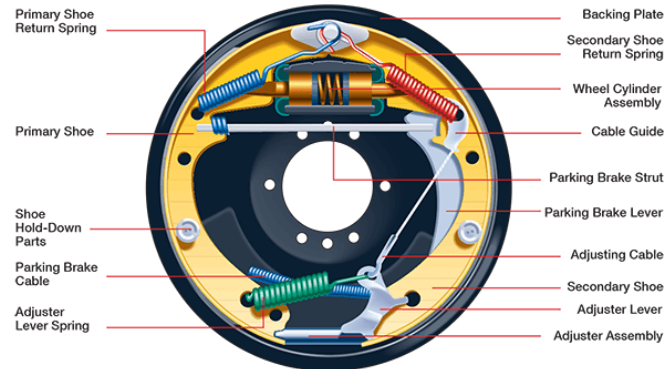


**Fig1: Brake Drum Assembly**

The important requirements of the brake drum are following

- It should provide a surface having well anti wear qualities.
- It should allow the optimum rate of heat transfer.
- Heat is generated during each brake application and
- It must be dissipated to the atmosphere immediately, because the next brake application would again produce more heat. Any excess heating of brakes would cause the drum to expand resulting in loss of effective pedal travel and fading of brake lining.
- It should have sufficient strength but minimum weight.
- It should be able to be accommodated within the wheel space available.

### 1.1 Introduction to Catia

Catia is the standard in 3D product design, featuring industry-leading productivity tools that promote best practices in design while ensuring compliance with your industry and company standards.

### 1.2 Introduction to FEA

FEA consists of a computer model of a material or design that is stressed and analyzed for specific results. It is used in new product design, and existing product refinement. A company is able to verify a proposed design will be able to perform to the client's specifications prior to manufacturing or construction. Modifying an existing product or structure is utilized to qualify the product or structure for a new service condition. In case of structural failure, FEA may be used to help determine the design modifications to meet the new condition. FEA uses a complex system of points called nodes which make a grid called a mesh. This mesh is programmed to contain the material and structural properties which define how the structure will react to certain loading conditions. Nodes are assigned at a certain density throughout the material depending on the anticipated stress levels of a particular area. In practice, a finite element analysis usually consists of three principal steps.

### 1.3 Introduction to ANSYS

ANSYS is general-purpose finite element analysis (FEA) software package. Finite Element Analysis is a numerical method of deconstructing a complex system into very small pieces (of user-designated size) called elements. The software implements equations that govern the behaviour of these elements and solves them all; creating a comprehensive explanation of how the system acts as a whole. These results then can be presented in tabulated, or graphical forms. This type of analysis is typically used for the design and optimization of a system far too complex to analyze by hand. Systems that may fit into this category are too complex due to their geometry, scale, or governing equations.

## 2. LITERATURE REVIEW

**Ramesha.D.K et al [1]** in his thesis concluded that the maximum temperature obtained for aluminum alloy brake drum is less as compared to the cast iron brake drum for a truck. Also, concluded that thermal deformation is less for aluminum alloy brake drum than the cast iron brake drum. As his study states that the weight of Aluminum is lesser than the Cast iron, it is better to use the Aluminum material in the construction of brake drum.

**Nurulhuda Binti Khalid [2]** in his project concluded that the temperature changes on the brake drum during the deceleration providing the heat distribution and the distribution of temperature depends on the various factors such as friction, surface roughness, speed, and others.

**Ray W.Murphy et al [3]** in their report concluded that the braking efficiency of trucks and can be improved by careful distribution of braking effort among the axles of the vehicle.

**W.S.Chung[4]** In thier paper The heat flux generated in the disc brake module is calculated by assuming that the braking energy changes into thermal energy. Temperature rise and deformation of a disc are estimated by performing the thermo-mechanical analysis.

**Faramarz Talati[5]** In their report theyconcluded that the heat generated due to friction between the disk and the pad should be ideally dissipated to the environment to avoid decreasing the friction coefficient between the disk and the pad and to avoid the temperature rise of various brake components and brake fluid vaporization due to excessive heating.

## 3. SCOPE OF PRESENT WORK

Braking systems and brake drums have been reviewed. Static and Thermal analyses on the brake drum on different materials such as aluminium alloy and cast iron have been done. A thermal analysis of different materials such as materials Stainless Steel, grayCast iron, carbon carbon composite& aluminium metal matrix brake drum will be done as this type of analysis has not been done before.

The objectives of this study are:

- To model & meshing the brake drum
- To apply the boundary conditions
- To calculate the maximum temperature, stress, heat flux and strain that is developed on brake drum materials Stainless Steel, grayCast iron, carbon carbon composite& aluminium metal matrix brake drums.
- To calculate the thermal deformation that is produced due to the application of brake as it exerts an amount of force for the above stated materials.
- To compare all the three results and conclude a best material for the selection of a brake drum.

## 4. METHODOLOGY

1. Model design
2. Meshing
3. Material Properties
4. Boundary condition
5. Results & Discussion

### 4.1 The model design and braking conditions

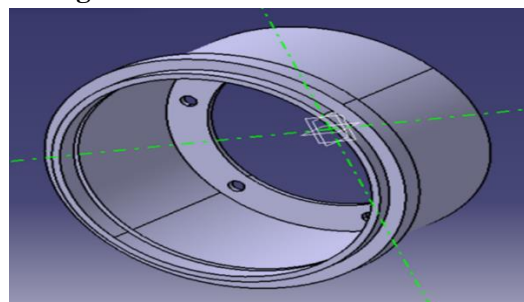


**Fig 2:** Brake drum model in CATIA

A three-dimensional solid with shape and dimensions is modeled in catia. It is imported to ANSYS in igs formate.

#### 4.2 Meshed Model

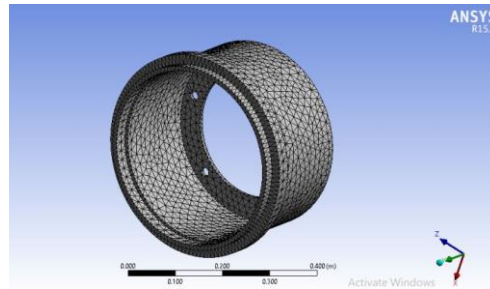


**Fig.3** :Meshed Model of Rotor Disc

The elements used for the meshing of the full and ventilated disc are tetrahedral three-dimensional elements with nodes (iso-parametric). In this simulation, the meshing was refined in the contact zone (disc-pad). This is important because in this zone, the temperature varies significantly. Indeed, in this strongly deformed zone, the Thermo mechanical gradients are very high. This is why an accurate account of the contact conditions involve the use of a refined mesh. Three meshes have been tested automatically using an option called convergence in ANSYS Workbench Multi physics.

#### 4.3 Material Properties

**Table 1: Material properties**

MATERIAL / PROPERTY	Stainless Steel	Gray Cast iron	Carbon carbon composite	Aluminum metal matrix
Density (kg/m <sup>3</sup> )	8000	7200	1800	2800
Young's modulus (GPa)	19	110	95	98
Poison's ratio	0.30	0.28	0.31	0.33
Thermal conductivity (w/m-k)	21.5	54.4	40	15
Specific heat (j/kg-k)	500	570	755	850
Coefficient of friction	0.22	0.2	0.3	0.3

#### 4.4 . Results and discussion

##### 4.4.1 Static Structural Analysis by using ANSYS R15

Static structural analysis is a technique used to obtain the deformation, equivalent stresses and the equivalent strains in the brake drum.

The boundary conditions for this analysis are the pressure applied on inner surface of drum is 1.5MPa and fixed at back face

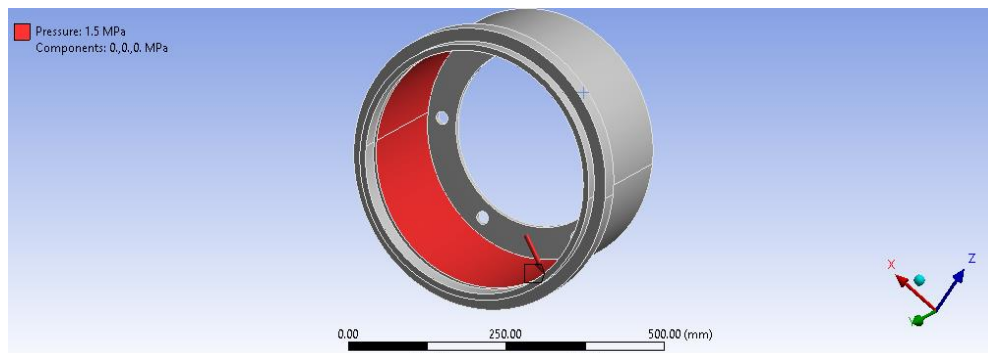


**Fig 4:** pressure on inner walls of drum

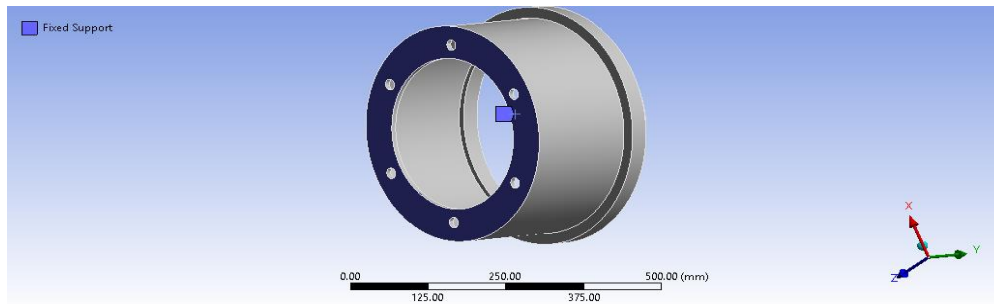


Fig 5: fixed support of drum

#### 4.4.2 Static Structural Analysis on stainless steel material

Following fig. shows results of total deformation, equivalent stress and strain of stainless steel after analysis.

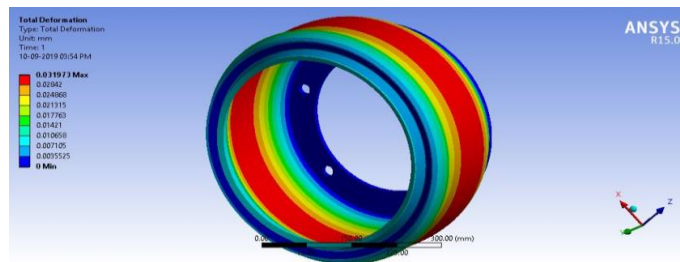


Fig 6: Deformation for stainless steel material brake drum

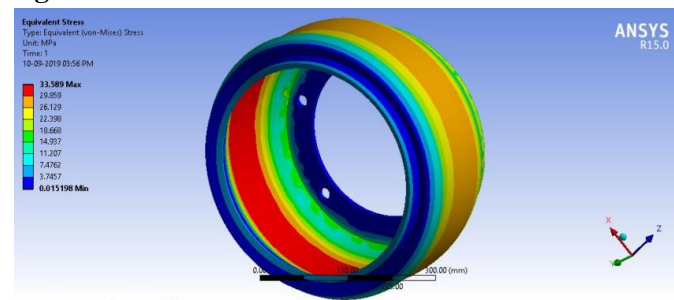


Fig 7: Equivalent stress for stainless steel material brake drum

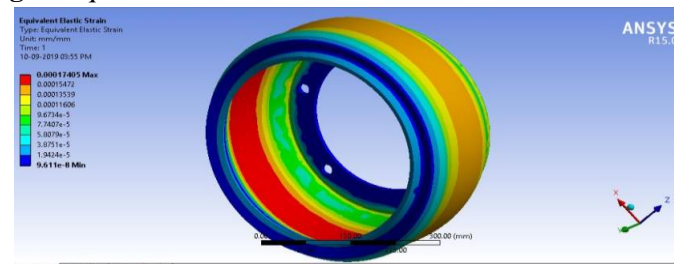


Fig 8: Equivalent elastic strain for stainless steel material brake drum

#### 4.4.3 Static Structural Analysis on gray cast iron material

Following fig. shows results of total deformation, equivalent stress and strain of gray cast iron after analysis.

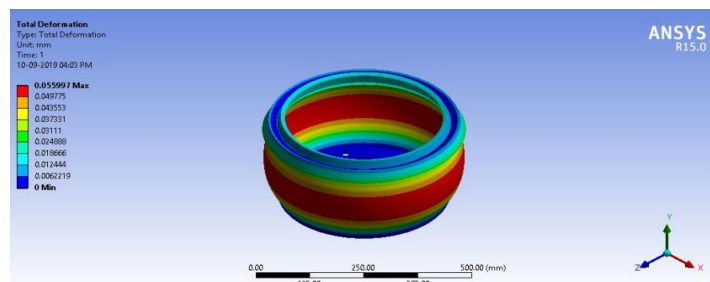


Fig 9: Deformation for gray cast iron material brake drum

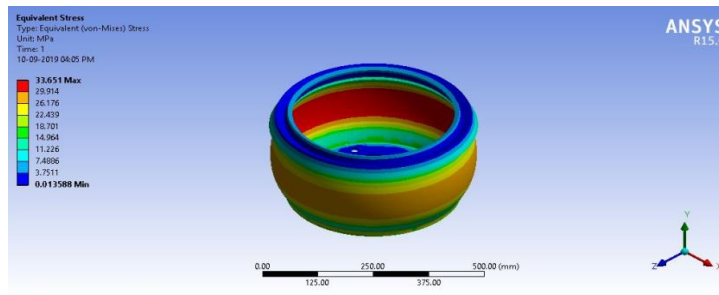


Fig 10: Equivalent stress for gray cast iron material brake drum

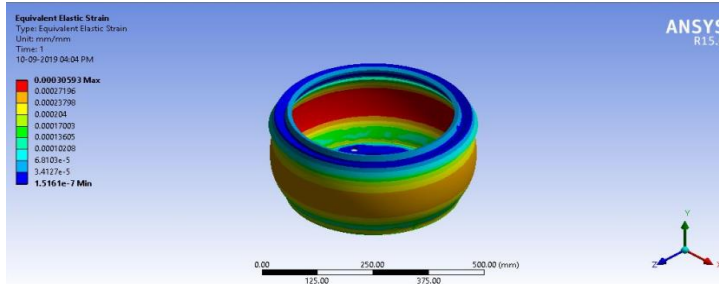


Fig 11: Equivalent elastic strain for gray cast iron material brake drum

#### 4.4.4 Static Structural Analysis on carbon carbon composite material

Following fig. shows results of total deformation, equivalent stress and strain of carbon carbon composite after analysis.

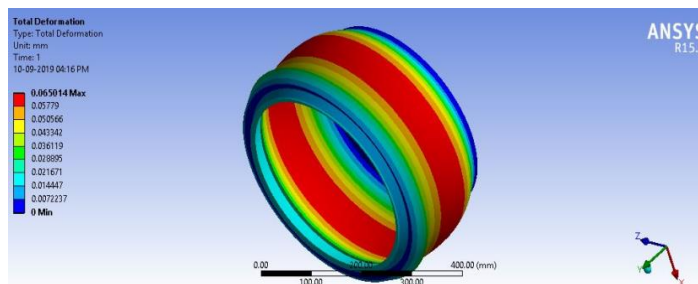


Fig 12: Deformation for carbon carbon composite material brake drum

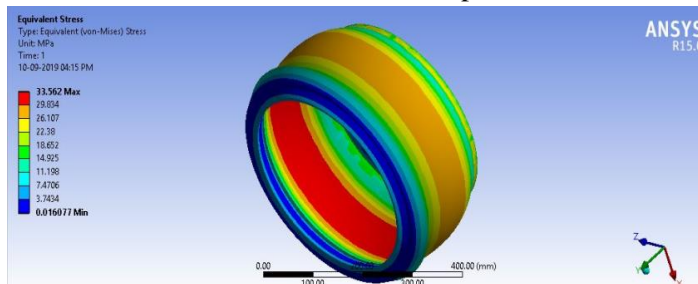


Fig 13: Equivalent stress for carbon carbon composite material brake drum

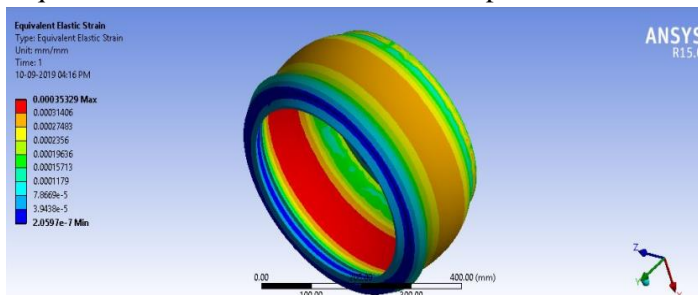
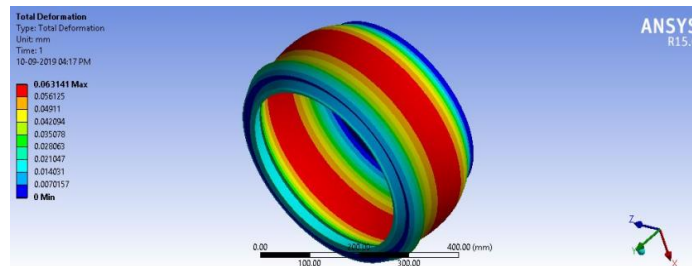


Fig 14: Equivalent elastic strain for carbon carbon composite material brake drum

#### 4.4.4 Static Structural Analysis on Aluminium metal matrix material

Following fig. shows results of total deformation, equivalent stress and strain of aluminium metal matrix after analysis.



**Fig 15:** Deformation for aluminium metal matrix material brake drum

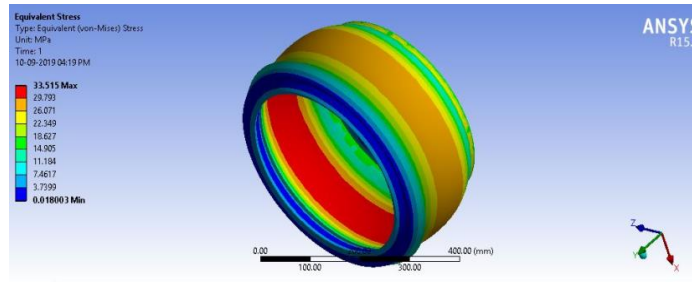


**Fig 16:** Equivalent stress for aluminium metal matrix material brake drum

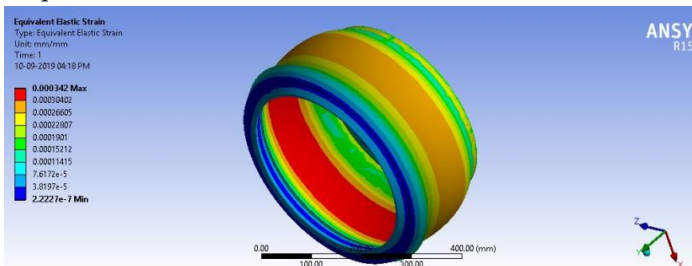


**Fig 17:** Equivalent elastic strain for aluminium metal matrix material brake drum

#### 4.5 Thermal analysis by using ANSYS R15

In acceleration, heat energy of the fuel is converted by the engine into kinetic energy to move the vehicle. In braking, the kinetic energy is converted into heat by means of friction produced between the two mating surface of the brake drum. The amount of friction developed between the two surfaces in contact is independent of the area of the surface in contact. However the magnitude of the force of friction or retarding force created between the brake lining and the brake drum depends upon the pressure or force exerted on the shoes by the retarding mechanism and the coefficient for the materials.

#### Boundary conditions:

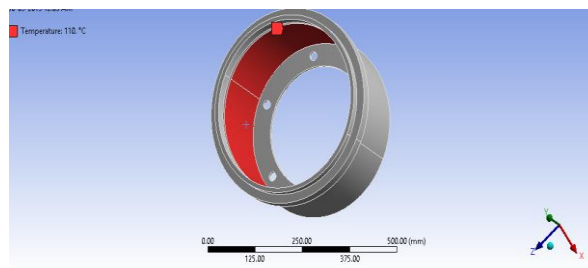


**Fig 18:** Temperature application in inner side of brake drum

The temperature of 110°C applied at inner walls of drum

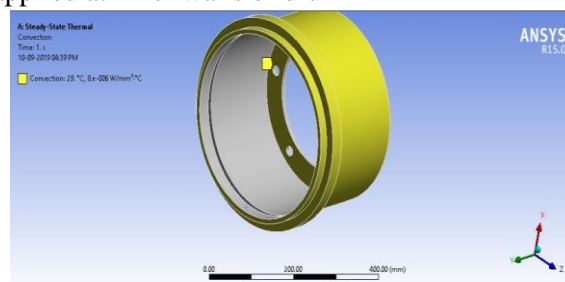


**Fig19:** The convection application on outer surface

The convection of  $8 \text{ e-}6 \text{ W/mm}^2\text{C}$  and temperature of  $29^{\circ}\text{C}$  applied on outer surface of drum  
Thermal analysis is a technique used to obtain temperature distribution and heat flux in the brake drum.

#### 4.5.1 Thermal analysis on stainless steel

Following fig. shows results of obtain temperature distribution and heat flux of stainless steel after analysis.

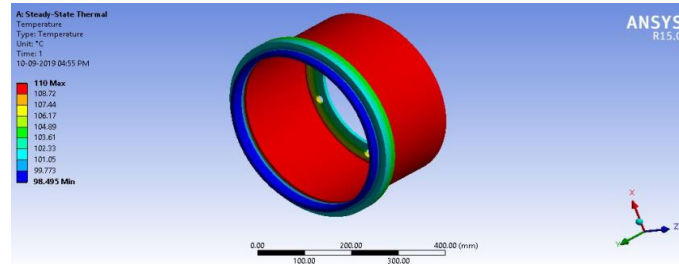


Fig 20: Temperature distribution for stainless steel material

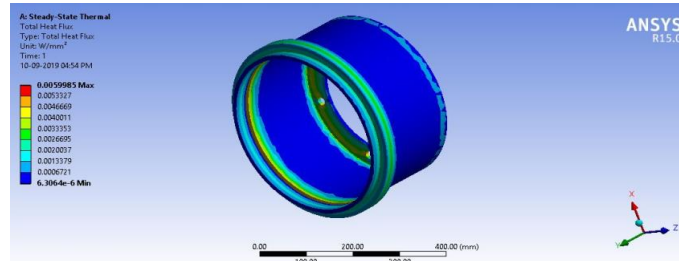


Fig 21: Heat flux for stainless steel material

#### 4.5.2. Thermal analysis on gray cast iron

Following fig. shows results of obtain temperature distribution and heat flux of gray cast iron after analysis.

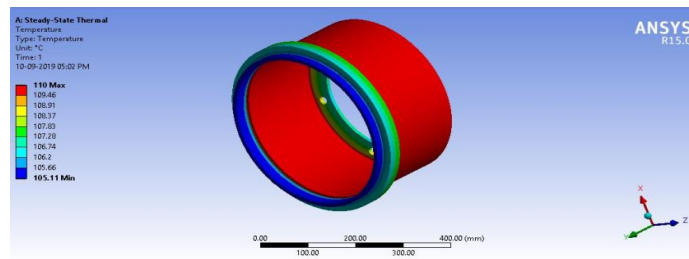


Fig 22: Temperature distribution for gray cast iron material

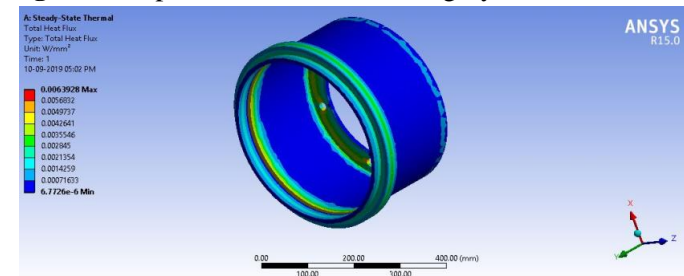


Fig 23: Heat flux for gray cast iron material

#### 4.5.3. Thermal analysis on carbon carbon composite

Following fig. shows results of obtain temperature distribution and heat flux of carbon carbon composite material after analysis

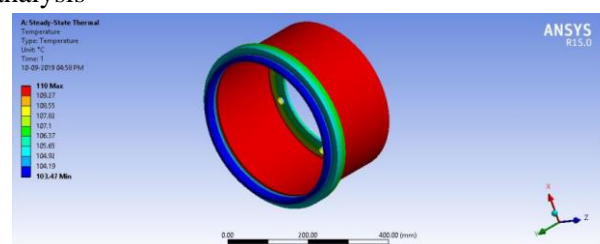


Fig 24: Temperature distribution for carbon carbon composite

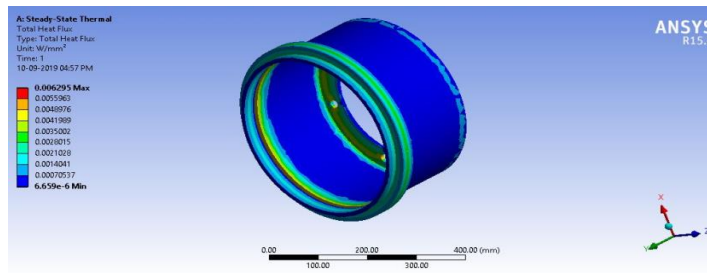


Fig 25: Heat flux for carbon carbon composite material

#### 4.5.4. Thermal analysis on Aluminium metal matrix

Following fig. shows results of obtain temperature distribution and heat flux of aluminium metal matrix material after analysis

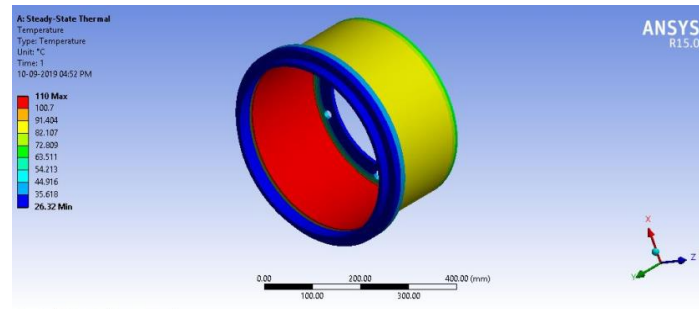


Fig 26: Temperature distribution for aluminium metal matrix

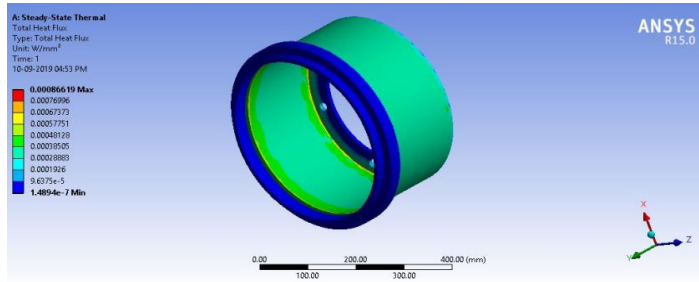


Fig27: Heat flux for aluminium metal matrix material

### 4.6 DISCUSSIONS

Table 2: static analysis results

RESULTS	Total deformation(mm)	Equivalent elastic strain mm/mm	Equivalent elastic stress(MPa)
Stainless steel	0.031973	0.00017405	33.589
Gray cast iron	0.055997	0.00030593	33.651
Aluminium metal matrix	0.063141	0.000342	33.515
Carbon carbon composite	0.065014	0.00035329	33.562

Table 3: Thermal analysis results

RESULTS	Temperature °C		Heat flux w/mm <sup>-2</sup>
	min	max	
Stainless steel	98.495	110	0.0059985
Gray cast iron	105.11	110	0.0063928
Aluminium metal matrix	26.32	110	0.0008619
Carbon carbon composite	103.4	110	0.006295

### 5. CONCLUSION

The static and thermo analysis of brake drum in brake applications has been per-formed. The present study can provide a useful de-sign tool and improve the brake performance of Drum brake system. The

values obtained from the analysis are less than their allowable values. Hence the brake design is safe based on the strength and rigidity criteria.

The use of these kinds of materials in brake drum manufacturing provides a range of heat flow values. This range of values is useful in the selection of material comparing with these two materials in different applications. The aluminium metal matrix have low heat flux when compared with the others and minimum temperature also. Although the deformation is high when compared with the stainless steel It is observed that the stainless steel has low deformation and low strain which can provide better brake performance than others from deformation point of view whereas gray cast iron has higher from stress point of view.

## 6. SCOPE FOR FUTURE WORK

Similar type of investigation can be replicated on some other materials.

Similar analysis can be carried out on a disc and drum brake.

Static, Steady and transient thermal analysis can be carried out at various heat flux and different braking cycles.

## 7. REFERENCES

- [1] Ramesha.D.K et al - “Temperature distribution analysis of aluminum alloy and cast iron brake drum using Ansys” - an International Journal of Emerging trends in Engineering and Development, ISSN 2249-6149, Issue 2, Vol.3 in April 2012.
- [2] Nurulhuda Binti Khalid - Thermal stress analysis on brake drum (simulation) - Mechanical Engineering (Thermal-Fluid) of the Kolej University Teknikal Kebangsaan, Malaysia, in November 2005.
- [3] Ray W. Murphy et al - Summary final report on “Bus, truck, tractor/trailer braking system performance” - Contract FH-11-7290 Highway Safety Research Institute-The University of Michigan-Ann Arbor, January 1970.
- [4] W. S. Chung, S. P. Jung and T. W. Park, Numerical analysis method to estimate thermal deformation of a ventilated disc for automotives, Journal of Mechanical Science and Technology, 24 (11) (2010) 2189-2195.
- [5] F. Talati and S. Jalalifar, Analysis of heat conduction in a disc brake system, Heat Mass Transfer, 45 (2009) 1047-1059.
- [6] J. T. Kim and B. J. Baek, A numerical study of thermal performace in ventilated disk brake, Journal of the Korean Society of Tribologists & Lubrication Engineers, 17 (5) (2001) 358-364.
- [7] Y. Choi, J. W. Choi, H. M. Kim and Y. W. Seo, Thermal dissipation performance of the ventilated brake disc having helical grooved vent, Journal of the Korean Society of Precision Engineering, 21 (3) (2004) 117-123.
- [8] Esmail M.A. Mokheimer, “Performance of annular fins with different profiles subject to variable heat transfer coefficient”, International Journal of Heat and Mass Transfer, Vol. 45, pp 3631–364, 2002.

## Comparative Analysis of Semi Monocoque Structured Aircraft Nose Cone Made of Different Titanium Graded Alloys at different operating conditions

T J Prasanna Kumar<sup>1a\*</sup>, V Sravani<sup>1b</sup>, B Kamala Priya<sup>2</sup>, Y Ayyappa<sup>3a</sup>, M Kiran Kumar<sup>3b</sup>, Sk Roshan<sup>3c</sup>, P Tarun kumar<sup>3d</sup>

<sup>1\*a,b</sup> Assistant Professor, Department of Mechanical Engineering, PVP Siddhartha Institute of Technology, Kanuru, Vijayawada, AP, India-520007

<sup>2</sup> Assistant professor, Department of Mechanical engineering, Lakireddy Bali Reddy College of Engineering, Mylavaram, - 521230, AP, India

<sup>2abcd</sup> UG Students, Department of Mechanical Engineering, PVP Siddhartha Institute of Technology, Kanuru, Vijayawada, AP, India-520007

\*Corresponding Author Email: [tjpk.mech@gmail.com](mailto:tjpk.mech@gmail.com)

### ABSTRACT

The aim of this article is to carry static structural analysis on a semi-monocoque structured aircraft nose cone made of titanium with different graded alloys, in order to predict the optimum values for structural deformation and von mises stresses under various operational load conditions. In general the passenger aircrafts will fly at maximum altitude of about 50000 Feet and minimum at sea level and hence the environmental impact or atmospheric pressure will influence on strength of the nose cone structure when the aircraft is flying at different altitudes are considered. In present research it is proposed to design a scaled model of nose cone section with semi monocoque structure having 4 segments and each segment is a shell parabolic configuration. Among several nose cone configurations such as conical, O-give, sears hack, Parabolic, and elliptical, our investigation is carried on parabolic configuration because of lowest tip temperature and less mean shear stress distribution at various operational conditions. For the present work Titanium with graded alloys are chosen because of its excellent physical properties, which is currently most widely used in various fields, has been adopted for aircraft nose cones and has achieved good results. A major challenge facing the aerospace industry is designing the nose shape of a fast-moving aircraft with optimal values of air resistance. This study involves a computer analysis of the parabolic nose cone profile of a commercial aircraft. The effect of material transition to pure grade titanium alloys and the change in material properties on the structure of the nose fairing under various pressure loads are studied. The paper objective is to identify the better Titanium graded alloy with minimum structural deformation at all operating altitudes. The scope of this work is to develop a nose cone configuration with variable shell thickness the structure should yield optimum material strength to withstand loads at all operating conditions.

**Keywords:** *Nose cone, Titanium alloys, operating pressure, total deformation, von mises stress*

### 1. INTRODUCTION

#### 1.1 Nose cone material consideration

A nose cone is the conical shape foremost section of aircraft, rockets, and missiles, designed to regulate the behaviour of oncoming airflow and reduce air resistance. The cone configurations generally used for aerospace applications are conic, spherically blunted conic, bi-conic, tangent ogive, spherically blunted tangent ogive, secant ogive, elliptic, parabolic, power series and Haack series etc. The most widely used materials for aircraft nose cone structure includes: magnesium alloys, aluminium, magnesium alloys, molybdenum, titanium, carbon-carbon composites, and hafnium Diboride. While composite materials perform well in terms of strength-to-weight ratio they have some disadvantages in terms of raw material costs storage and limited lifetime of the model in addition to having use adverse measures in many cases.

In this study, to determine the observed behaviour of these titanium materials used to build the nose of a parabolic model for aircraft, the parabolic shape was selected because the average shear stress

distribution was small and the tip temperature was the lowest. First, we will focus on nose cone structural deformation at different atmospheric pressures, and then, the investigation continues to predict the optimum values of induced stresses for the subjected loads on nose cone made of different Titanium graded alloys. And comparing the above materials with their ability to withstand the Pressure loads at various operating conditions based on altitudes range from 10000 feet to 50000 feet.

## 2. LITERATURE SURVEY

[1] P. Venkata Suresh et al, carried their investigation on aircraft nose cone at specified altitude (40,000ft) for different materials such as stainless steel, structural steel, titanium alloy (pure grade), and aluminium alloy. In present research it is proposed to design a scaled model of nose cone section with semi monocoque structure having 4 segments and each segment is a shell parabolic configuration. Among several nose cone configurations such as conical, elliptical, Parabolic, O-give, and sear shack, our investigation is carried on parabolic configuration because of lowest tip temperature and less mean shear stress distribution at mach number having 0.8 to 1.0. [2] C.M.V Priya et al, investigated aircraft nose of conical and elliptical configuration with titanium alloys at a standard pressure of  $10 \times 10^5$  MPa. [4] P. V. D Aditya et. al, carried their analysis on missile nose cone of conical and elliptical configuration made of Titanium grade-I and Titanium  $\alpha$ -alloy and concluded that total structural deformation is less for titanium grade-1 alloy when compared with titanium  $\alpha$ -alloy. [3] M. Srinivasula et al. In his article discussing a new nose concept that promises to enhance the performance of the existing nose, the word nose is used to refer to a part of a rocket, missile or aircraft. The conical shape provides very little air. Titanium Ti-6Al-6V-2 SN namely Grade-1 and other titanium It is stronger than pure titanium. Although they have the same energy and thermal properties, analysis results for model loads, instantaneous pressure loads and bubble nose cones are used for model analysis with ANSYS. [8] Sanjay Varma et al.: Different nose contours should be compared to understand performance against existing traditional nose contours discussed in this article. The purpose of this article is to determine the type of nose profile and its specific aerodynamic characteristics by means of the minimum pressure coefficient and the critical Mach number. The purpose of this article is to develop prototype wings with excellent aerodynamic properties and low cost for use in missile construction projects to increase their range and impact on targets. For the present work Titanium with graded alloys are chosen because of its excellent physical properties, which is currently most widely used in various fields, has been adopted for aircraft nose cones and has achieved good results. [7] The main challenge facing in the aerospace industry is to design the shape of the nose of a flying object moving at high speed with an optimal air resistance value. This study involves a computer analysis of the parabolic nose cone profile of a commercial aircraft. The effect of change in material properties on nose cone structure is studied different pressure loads.

## 3. TITANIUM ALLOYS AND THEIR MATERIAL PROPERTIES

Titanium is an important metal that is generally considered one of the strongest. Titanium is used in many industries and is in high demand today. Titanium materials are better and suitable for products that require high strength and lightness. Titanium is also resistant to corrosion and high temperatures. These properties make titanium ideal for many industries, including medical, aerospace, military and defense.

### 3.1 Properties of Titanium

Proper forging of titanium requires an understanding of the metal's properties and how the material behaves when heated, to prepare for forging at the microstructural level. During heating, two phases associated with titanium and titanium alloys appear in the product.

These phases are called alpha and beta phases, and a good understanding of them is crucial to making good titanium.

### 3.1.1 Alpha ( $\alpha$ ) Phase

The low temperature alpha phase is a heterogeneous body with a hexagonal tight packed structure. The alpha phase exists between room temperature and 1625°F. "Alpha" grade titanium offers highest corrosion resistance among other titanium grades.

### 3.1.2 Beta ( $\beta$ ) Phase

Titanium transforms into its hot allotrope, a body centered cubic beta phase, at 1625°F and retains its beta phase up to its melting point at 3038°F. This alloy is ideal for forging, heat treating, and welding when machining titanium. This level of material has excellent strength and high corrosion resistance to form strong alloys, titanium can be easily combined with other metals, resulting in three types of titanium alloys such as  $\alpha$  alloys,  $\beta$  alloys, and  $\alpha$ - $\beta$  alloys.

Alpha alloys generally retain their original alpha phase which makes them creep resistant up to 5537.778°C. The alpha stabilizers that make up alpha titanium alloys are aluminium, nitrogen-carbon and oxygen.

Alpha and beta alloys constitute microstructures of both alpha and beta that are customized at room temperature. This alloy is capable of high-strength heat treatment and contains neutral elements such as tin and zirconium. A well-known alpha-beta alloy is Ti-6AL4V.

Beta alloys are highly heat treatable titanium alloys that contain enough other alloys to maintain the beta phase at room temperature. This titanium alloy class includes beta stabilizers such as molybdenum, vanadium, niobium, and tantalum.

## 3.2 Material Properties considered for the Analysis

Table-1 Mechanical properties and real constants used for present analysis

Properties	Titanium-Gr1	Titanium-Gr2	Ti- $\alpha$ alloy	Ti- $\beta$ alloy
Modulus of Elasticity (Pa)	1.02E+11	1.02E+11	1.10E+11	1.01E+11
Density (kg/m <sup>3</sup> )	4540	4540	4540	4420
Poisson's Ratio	0.34	0.37	0.31	0.31
Thickness (m)	0.001	0.001	0.001	0.001

[6] (Titanium and their alloys material properties are taken from the reference: *Metals Hand Book ASM International, 1990*)

## 4. METHOD OF APPROACH (Modelling and Analysis using ANSYS)

### 4.1 Introduction to Finite Element Analysis (FEA)

In general Ansys [5] is a finite element modelling tool used for the numerical solution of various mechanical problems. These problems involve static/dynamic, structural, heat transfer, fluid flow, acoustics and electromagnetic problems. Finite element solutions can be divided into three steps and typical general engineering problems.

**Pre-Processing:** Problem Definition:

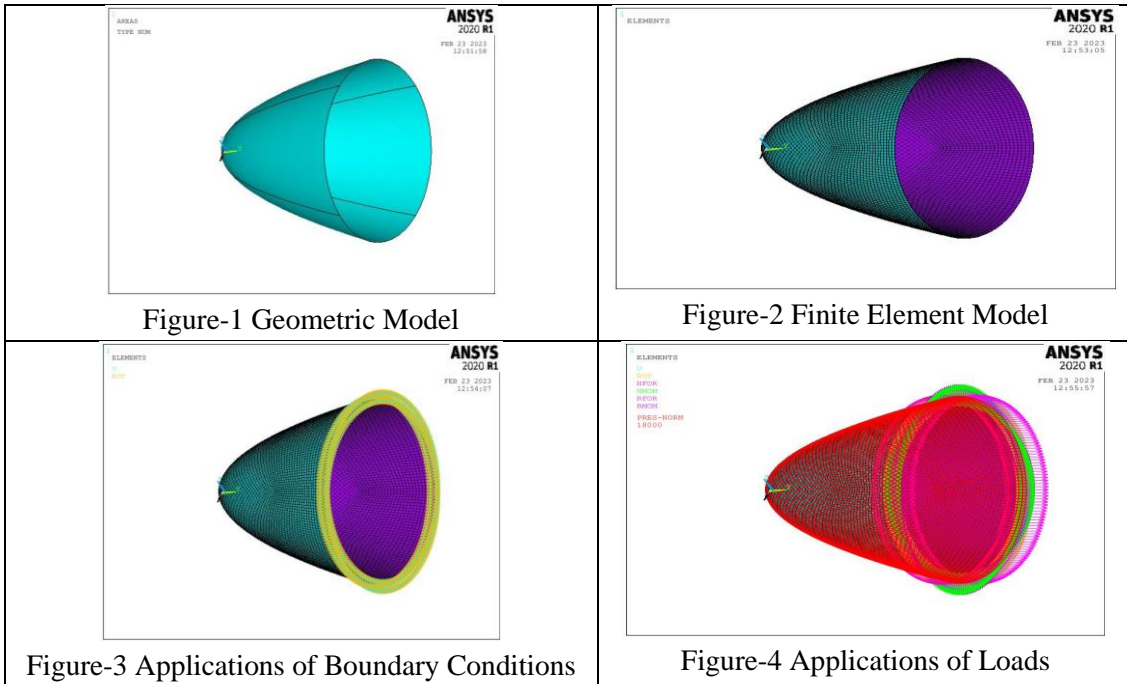
The first important step is to define the elements/line/area/volume, object types and material/geometric properties, and the desired mesh line/area/volume. The amount of detail required depends on the measurement length, 1D, 2D and 3D.

**Solutions:** Load assignments, constraints and solutions. Here you need to show the loads (point or pressure), constraints (translational and rotational) and finally solve the resulting system of equations.

**Post-Processing:** further processing and viewing results. At this stage, you can get a list of node displacements, forces and moments, deflection plots, and stress profiles or temperatures for the element.

In the present investigation, the aircraft nose cone structure is proposed to model in parabolic configuration [3] in ANSYS 2020 R1 APDL to study the static structural behaviour at different loading conditions.

Considering four different materials such as Titanium ASTM Grade-1(pure), Titanium ASTM Grade-2 (pure), Titanium  $\alpha$ -Grade alloy Ti-5Al-2.5Sn, Titanium  $\beta$ -Grade alloy: Ti-13V-11 Cr- 3 Al with slight changes in material properties like [6] modulus of elasticity, density, poisson's ratio etc., keeping the SHELL thickness as constant ie. 0.0016 m, (presented in the above Table-1) the model is tested each time with different Pressure load conditions. Upon solving the solution at given load step, the individual structures are examined for Total Deformation and maximum- minimum von mises stresses and respective contour plots were captured and results are compared.



### 5. RESULTS AND DISCUSSIONS

The nose cone when it is tested under a wide range of operating conditions about 10000 ft to 50000 ft of altitudes, however the respective pressure values in Pascal's are taken from standard atmospheric table as shown below:

Table-2: Pressure values from Standard Atmospheric table

Altitude in Feet	Pressure (Pa)
10000	70326.52
20000	44126.4
30000	29647.5
40000	18615.8
50000	11031.6

ANSYS 2020 R1 tool is used to analyse this nose cone structure made of different materials with different material properties as mentioned in above Table-2. The proposed model is tested for total deformation and von mises stresses when it is operating under different loading conditions as shown in above table.

The tested model is subjected to the various ranges of Total deformation. The minimum value and maximum value of von mises stresses induced in the nose structure made of 4 different materials subjected to pressure at various altitudes are presented in the below Table-3 to 7.

Table-3 Total Deformation and von mises results obtained from static structural analysis at an altitude of 10000 Ft

<b>PRESSURE (Pa)</b>		<b>70326.52</b>	
Material	Total Deformation	Von mises Stress	
		(max)	(min)
Ti-Gr1	0.001782	8.34E+07	9.88E+06
Ti-Gr2	0.002842	1.33E+08	1.60E+07
Ti- $\alpha$ alloy	0.002734	1.32E+08	1.61E+07
Ti- $\beta$ alloy	0.002974	1.32E+08	1.61E+07

Table-4 Total Deformation and von mises results obtained from static structural analysis at an altitude of 20000 Ft

<b>PRESSURE (Pa)</b>		<b>44126.4</b>	
Material	Total Deformation	Von mises Stress	
		(max)	(min)
Ti-Gr1	0.001819	8.33E+07	1.01E+07
Ti-Gr2	0.001096	5.26E+07	6.19E+06
Ti- $\alpha$ alloy	0.001716	8.31E+07	1.01E+07
Ti- $\beta$ alloy	0.001866	8.31E+07	1.01E+07

Table-5 Total Deformation and von mises results obtained from static structural analysis at an altitude of 30000 Ft

<b>PRESSURE (Pa)</b>		<b>29647.5</b>	
Material	Total Deformation	Von mises Stress	
		(max)	(min)
Ti-Gr1	8.35E-04	3.38E+07	4.21E+06
Ti-Gr2	6.81E-04	3.53E+07	4.16E+06
Ti- $\alpha$ alloy	7.08E-04	3.50E+07	4.17E+06
Ti- $\beta$ alloy	0.001254	5.58E+07	6.77E+06

Table-6 Total Deformation and von mises results obtained from static structural analysis at an altitude of 40000 Ft

<b>PRESSURE (Pa)</b>		<b>11031.6</b>	
Material	Total Deformation	Von mises Stress	
		(max)	(min)
Ti-Gr1	4.55E-04	2.08E+07	2.52E+06
Ti-Gr2	4.46E-04	2.09E+07	2.52E+06
Ti- $\alpha$ alloy	4.29E-04	2.08E+07	2.52E+06
Ti- $\beta$ alloy	4.67E-04	2.08E+07	2.52E+06

Table-7 Total Deformation and von mises results obtained from static structural analysis at an altitude of 50000 Ft

<b>PRESSURE (Pa)</b>		<b>11031.6</b>	
Material	Total Deformation	Von mises Stress	
		(max)	(min)
Ti-Gr1	4.55E-04	2.08E+07	2.52E+06
Ti-Gr2	4.46E-04	2.09E+07	2.52E+06
Ti- $\alpha$ alloy	4.29E-04	2.08E+07	2.52E+06
Ti- $\beta$ alloy	4.67E-04	2.08E+07	2.52E+06

Contour Plots are captured for the above analysis carried out using Ansys 2020 R. Total Deformation and von mises stresses maximum and minimum values are plotted in comparison with structural deformation of nose cone made of different titanium graded alloys at various operating conditions.

**5.1 Contour Plots At 50000 ft, Total Deformation and von mises stresses of Nose cone structure with different Titanium graded alloys are shown below Figure-5 & Figure-6**

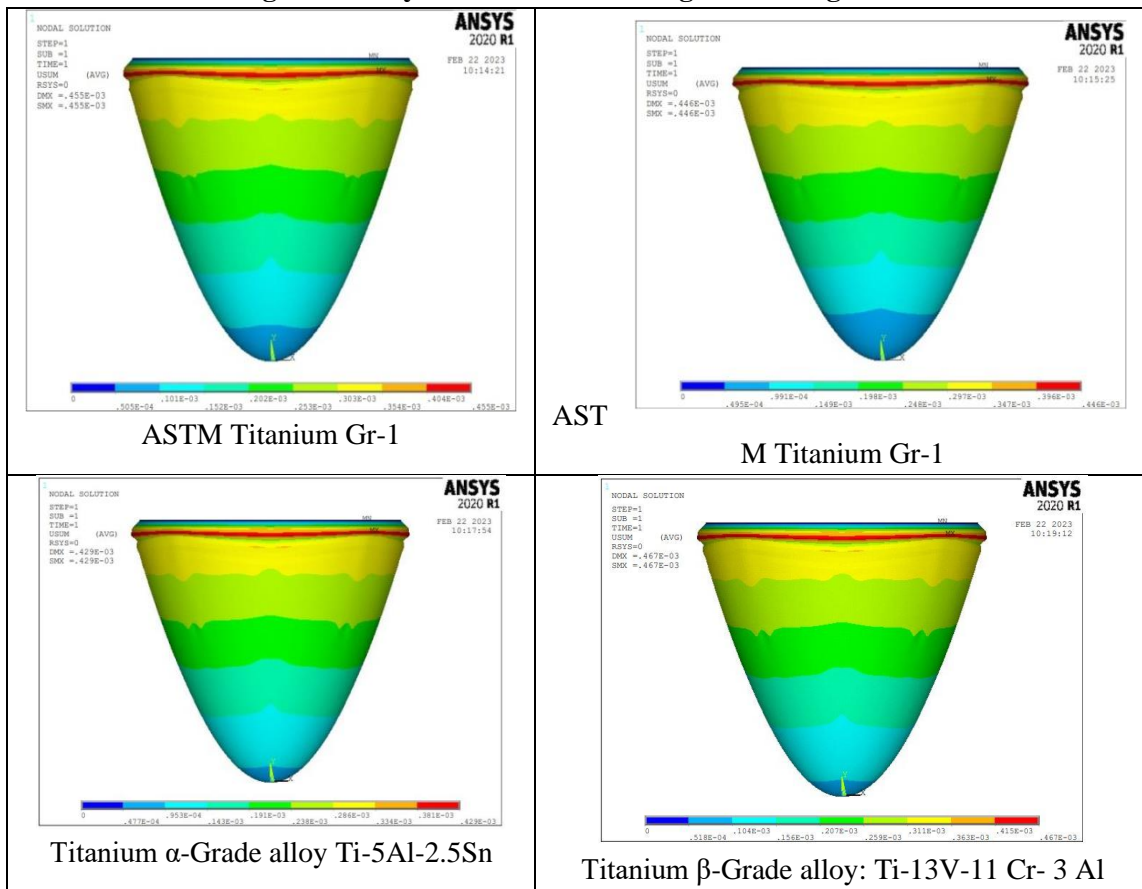


Figure-5 Contour plots for Nose cone structure subjected to Total Deformation under operating pressure of **11031.6 (Pa)**

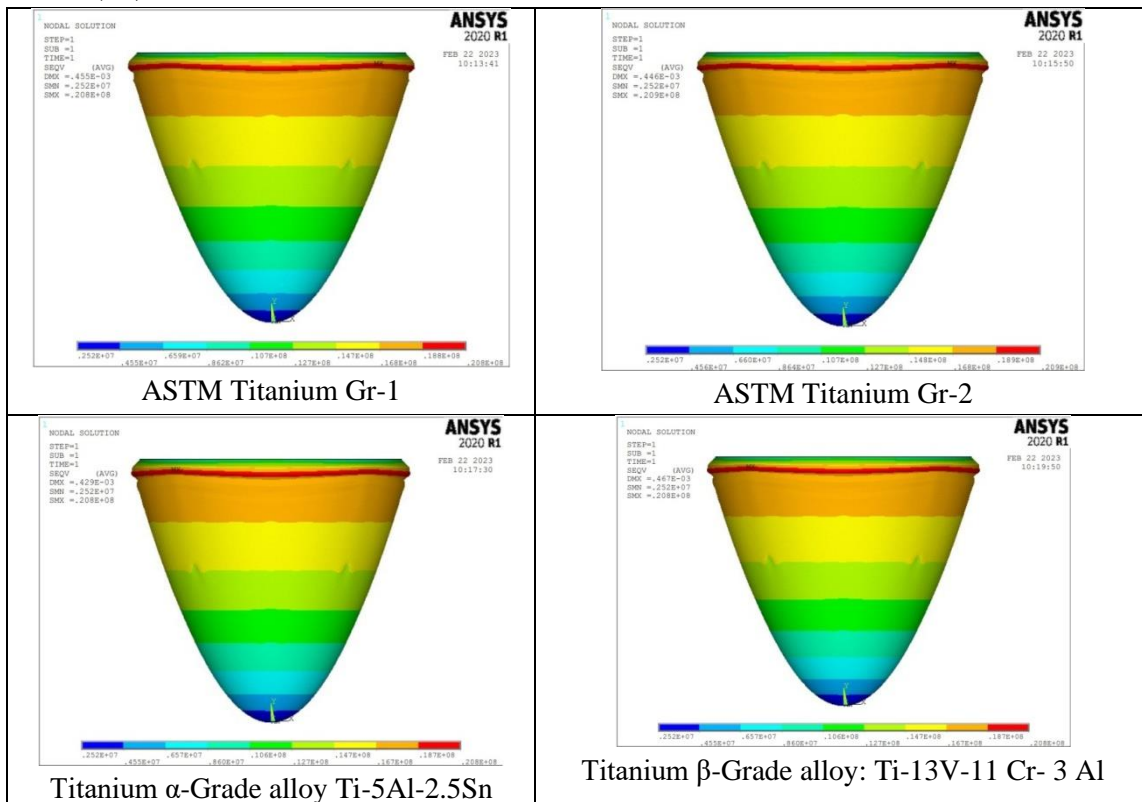


Figure-6 Contour plots for Nose cone structure subjected to von mises stresses under operating pressure of **11031.6 (Pa)**

At an altitude of 50000 Ft and pressure of **11031.6 Pa**, the proposed nose cone model with different Titanium Graded alloys yielded promisable values. However the model made of Ti-  $\alpha$  alloy has less total deformation of 4.29E-04 m when compared with Ti-Gr1, Ti-Gr2 and Ti- $\beta$  alloy. It is also noticed that the nose cone structure with Gr-1, Ti-  $\alpha$  alloy and Ti- $\beta$  alloy are induced with less von mises stress about 2.08E+07 Pa.

**5.2 Contour Plots At 40000 ft, Total Deformation and von mises stresses of Nose cone structure with different Titanium graded alloys are shown below Figure-7 & Figure-8**

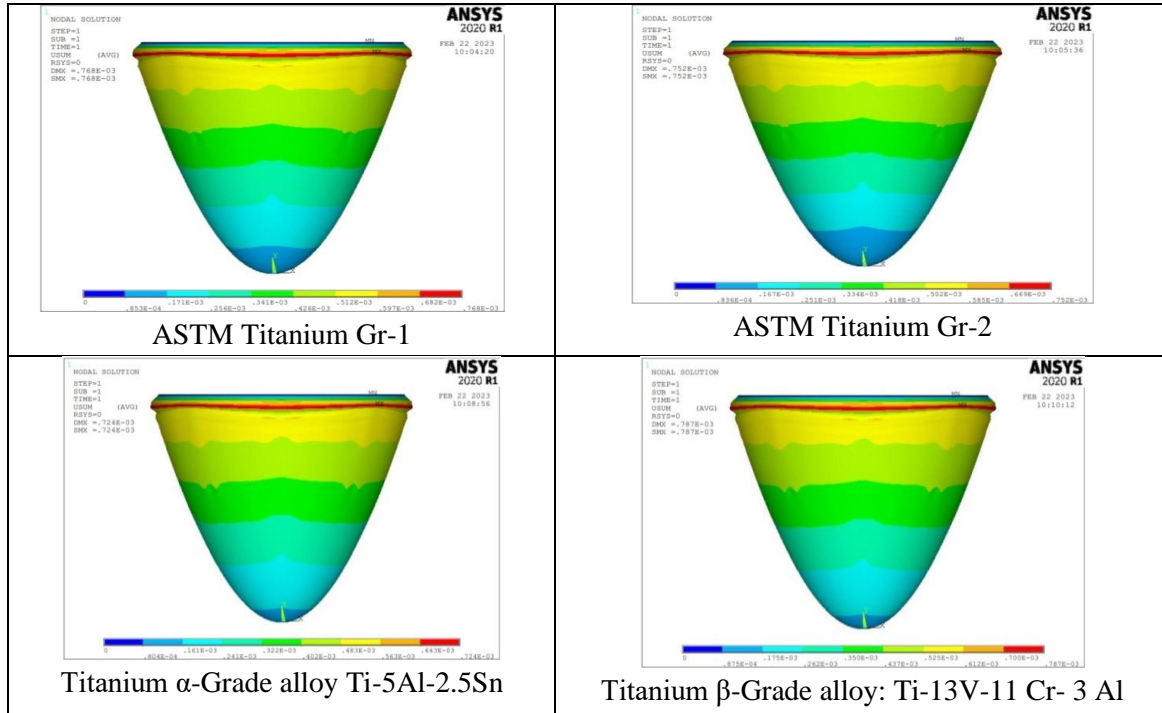


Figure-7 Contour plots for Nose cone structure subjected to Total Deformation under operating pressure of **18658.2 (Pa)**

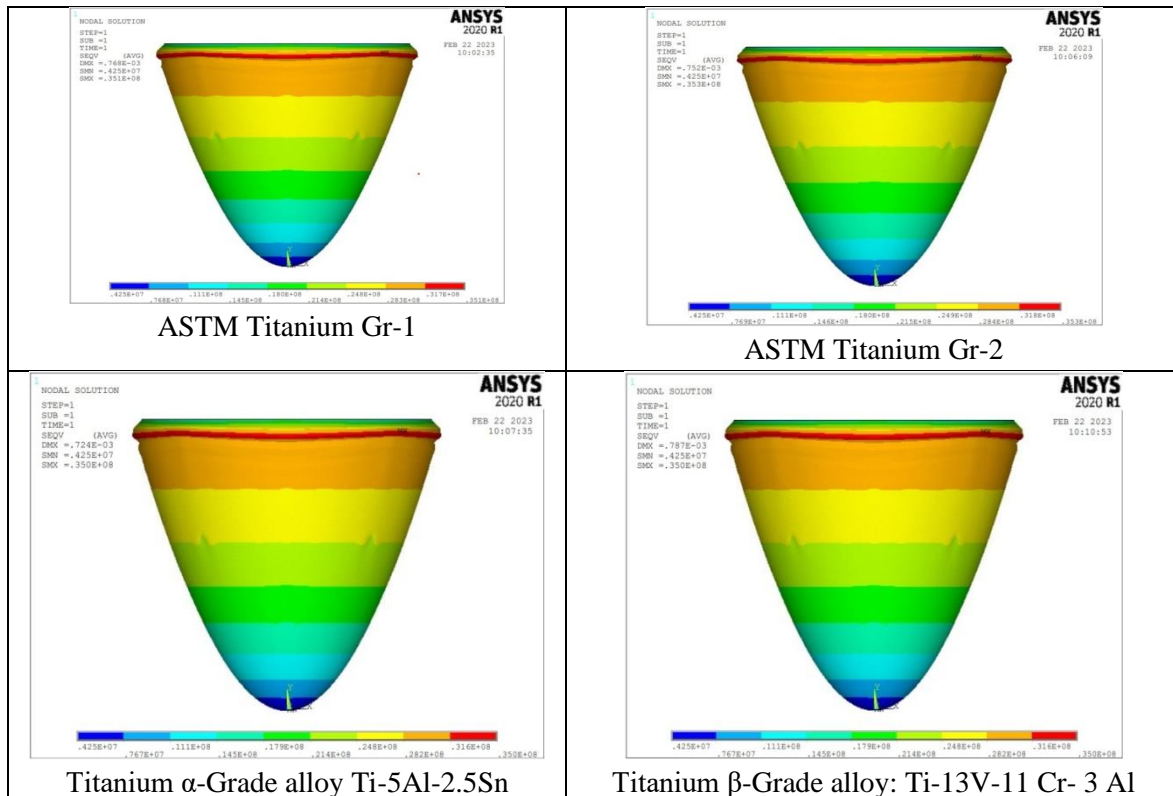


Figure-8 Contour plots for Nose cone structure subjected to von mises stresses under operating pressure of **18658.2 (Pa)**

From the above contour plot results, at an altitude of 40000 Ft and pressure of **18615.8 Pa**, the proposed nose cone model with different Titanium Graded alloys yielded promisable values. However the model made of Ti-  $\alpha$  alloy has less total deformation of  $7.24E-04$  m when compared with Ti-Gr1, Ti-Gr2 and Ti- $\beta$  alloy. It is also noticed that the nose cone structure with Ti-  $\alpha$  alloy and Ti- $\beta$  alloy are induced with less von mises stress about  $3.50E+07$  Pa.

**5.3 Contour Plots At 30000 ft, Total Deformation and von mises stresses of Nose cone structure with different Titanium graded alloys are shown below Figure-9 & Figure-10**

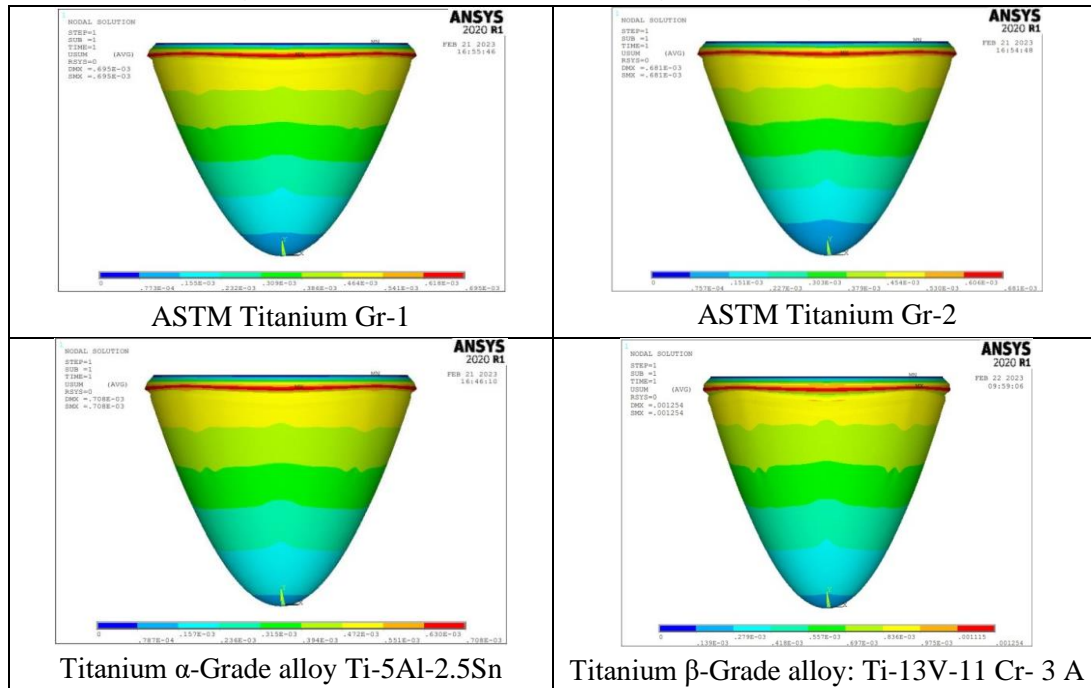


Figure-9 Contour plots for Nose cone structure subjected to Total Deformation under operating pressure of **29647.5 (Pa)**

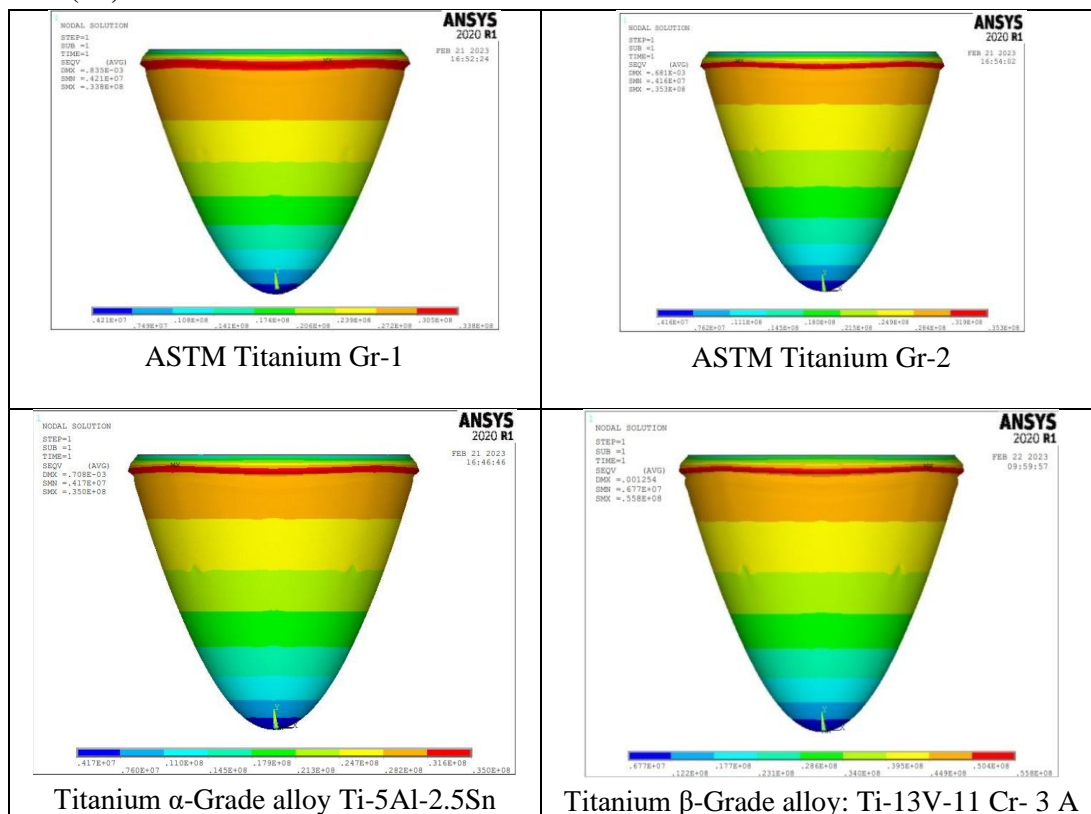


Figure-10 Contour plots for Nose cone structure subjected to von mises stresses under operating pressure of **29647.5 (Pa)**

When compared at an altitude of 30000 Ft and pressure of **29647.5 Pa**, the proposed nose cone model with different Titanium Graded alloys yielded promisable values. However the model made of Ti-β alloy has less total deformation of 0.001254 m when compared with Ti-Gr1, Ti-Gr2 and Ti-α alloy. It is also noticed that the same structure is induced with less von mises stress about 5.58E+07 Pa.

**5.4 Contour Plots At 20000 ft, Total Deformation and von mises stresses of Nose cone structure with different Titanium graded alloys are shown below Figure-11 & Figure-12**

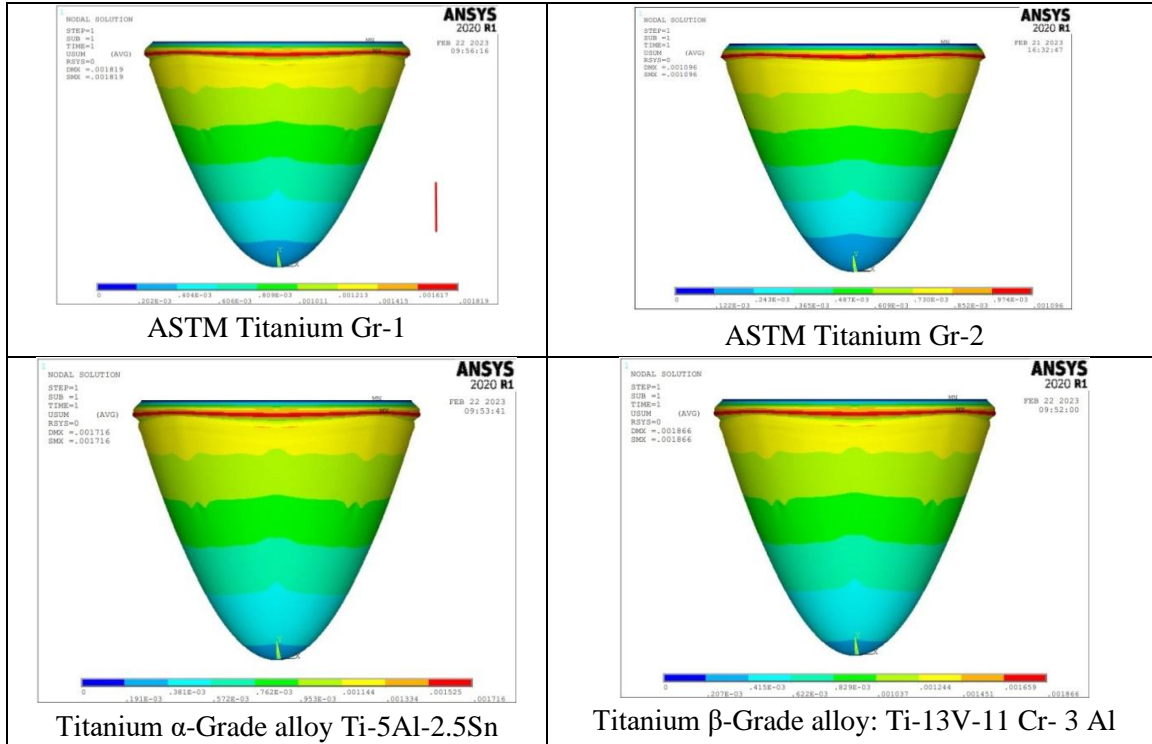


Figure-11 Contour plots for Nose cone structure subjected to Total Deformation under operating pressure of **44126.4 (Pa)**

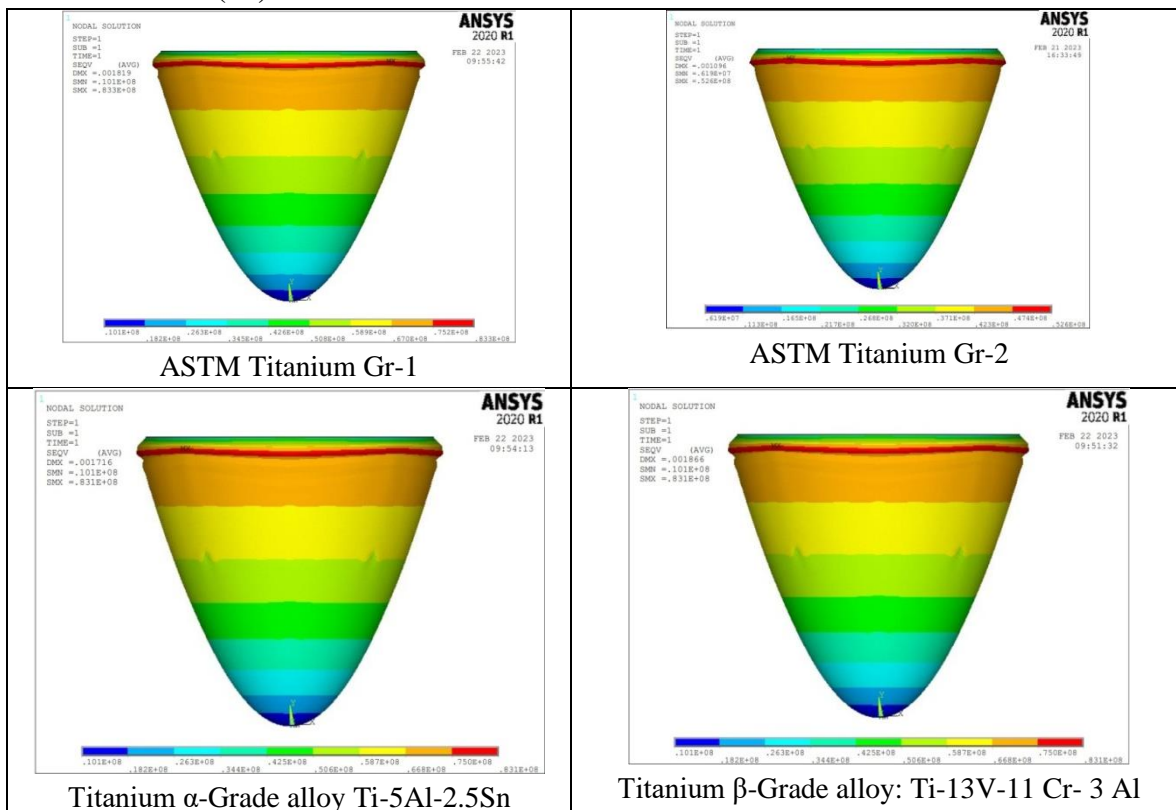


Figure-12 Contour plots for Nose cone structure subjected to von mises stresses under operating pressure of **44126.4 (Pa)**

Similarly, at an altitude of 20000 Ft and pressure of **44126.4 Pa**, the proposed nose cone model with different Titanium Graded alloys yielded promisable values. However the model made of Ti-Gr2 has less total deformation of 0.001096 m when compared with Ti-Gr1, Ti- $\alpha$  alloy and Ti- $\beta$  alloys. It is also noticed that the same structure is induced with less von mises stress about  $5.26E+07$  Pa.

**5.5 Contour Plots At 10000 ft, Total Deformation and von mises stresses of Nose cone structure with different Titanium graded alloys are shown below Figure-13 & Figure-14**

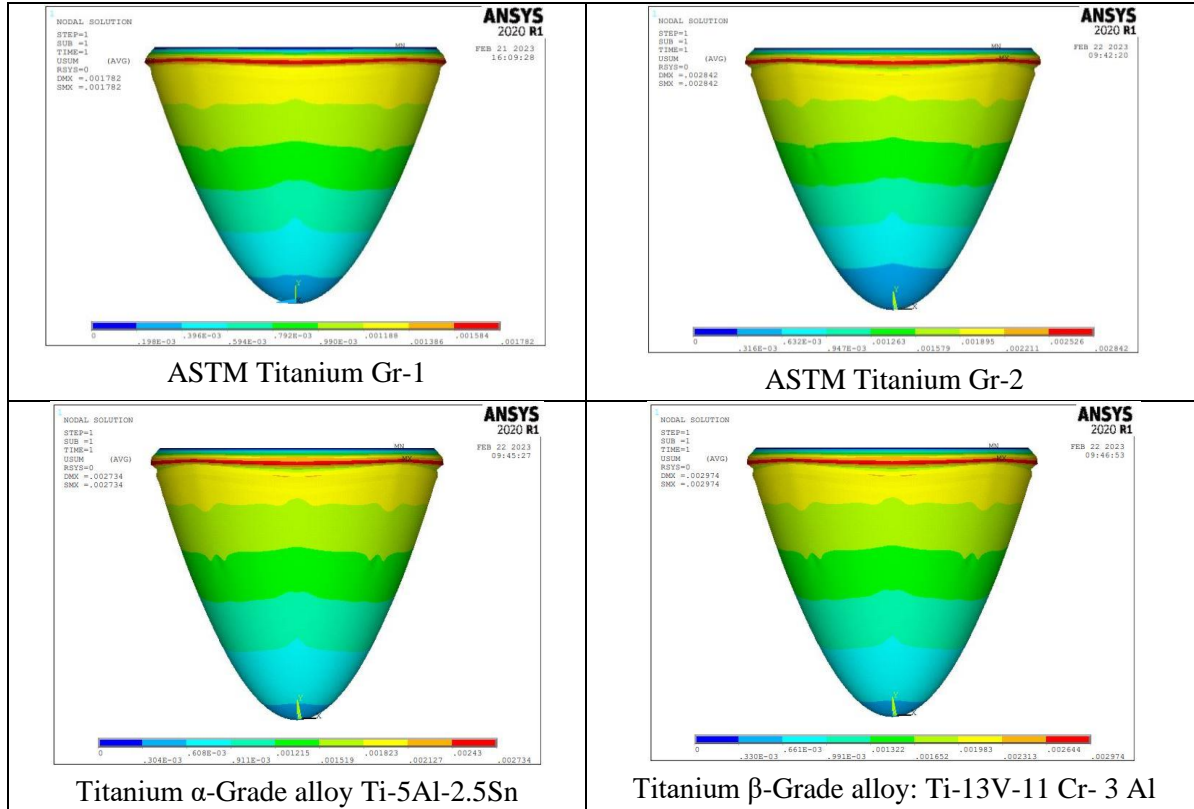


Figure-13 Contour plots for Nose cone structure subjected to Total Deformation under operating pressure of **70326.2 (Pa)**

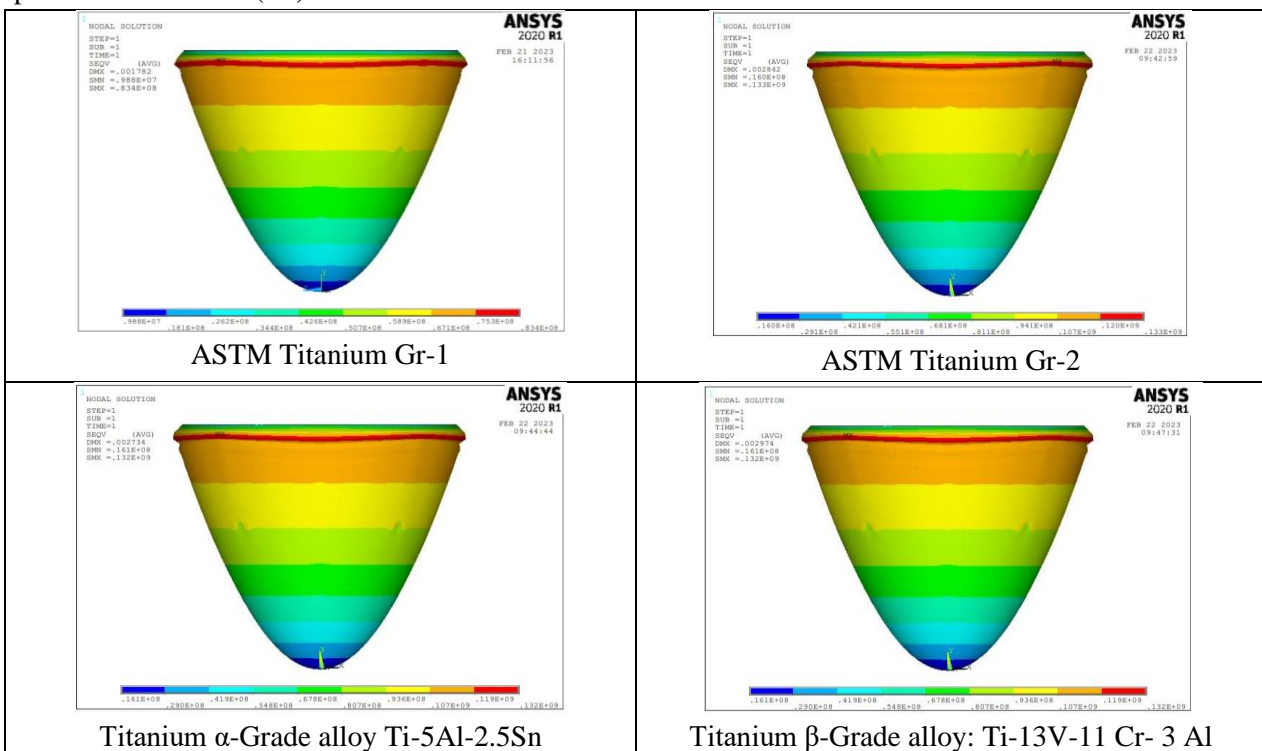


Figure-14 Contour plots for Nose cone structure subjected to von mises stresses under operating pressure of **70326.2 (Pa)**

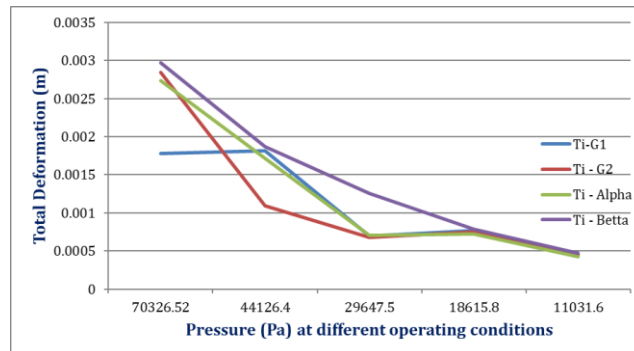
From the above observations, it is noticed that at an altitude of 10000 Ft and pressure of 70326.2 Pa, the proposed nose cone model with different Titanium Graded alloys yielded promisable values. However the model made of Ti-Gr1 has less total deformation of 0.001782 m when compared with Ti-Gr2, Ti- $\alpha$  alloy and Ti- $\beta$  alloys. It is also noticed that the same structure is induced with less von mises stress about 8.34E+07 Pa.

### 6. Comparison Plots for nose cone structure made of Titanium graded alloys subjected to Total Deformation and Von mises stresses at different operating conditions

Table-8: Total Deformation values for nose cone structure noticed for 4 different Ti grade and alloy materials

Total Deformation of nose cone with different materials at various operational conditions				
Pressure (Pa)	Ti - Gr1	Ti-Gr2	Ti- $\alpha$ alloy	Ti- $\beta$ alloy
70326.52	0.001782	0.002842	0.002734	0.002974
44126.4	0.001819	0.001096	0.001716	0.001866
29647.5	6.95E-04	6.81E-04	7.08E-04	0.001254
18615.8	7.68E-04	7.52E-04	7.24E-04	7.87E-04
11031.6	4.55E-04	4.46E-04	4.29E-04	4.67E-04

The nose cone with Titanium-Grade1, Titanium- Grade2, Titanium-  $\alpha$  alloy and Titanium- $\beta$  alloy materials are modelled and analyzed in Ansys tool to investigate the Total deformation and von mises stress values. In contrast from the obtained results, a comparison graph was plotted and presented for different operating conditions such as 10000 Ft to 50000 Ft.



Graph-1 Total Deformation Vs Pressure (Pa) of nose cone with 4 different Ti Gr & alloys

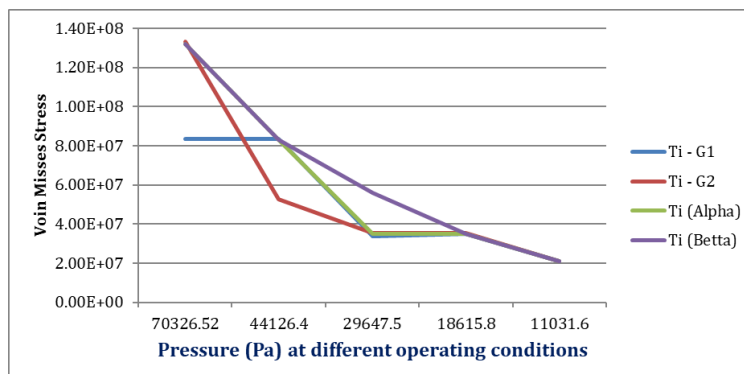
From the Graph Total Deformation Vs Pressure, it is noticed that almost all titanium graded alloy structures have gradual increment in Total deformation as the (Pressure) increases and altitude decreases. However Among these Titanium family nose cone structure made of Titanium Grade-2 has yielded optimum values of less total deformation for the operating conditions range from 10000 Ft to 30000 Ft.

Whereas cone structure made of Titanium Grade-1 and Titanium- $\alpha$  alloy both has decrement in total deformation range from 20000 Ft to 30000 Ft linearly. However at a range from 30000 Ft to 40000 ft nose cone structure made of Ti- Gr1, Ti- Gr2 and Ti- $\alpha$  alloy materials have increment in total deformation. Also observed that at a range from 40000 Ft to 50000 Ft structure made of all Titanium graded alloys have decrement in total deformation.

Table-9: Maximum von mises stress values for nose cone structure captured for 4 different Ti grade and alloy materials

Von mises stress values of nose cone structure with different materials at various operational conditions				
Pressure (Pa)	Ti - G1	Ti-G2	Ti- $\alpha$ alloy	Ti- $\beta$ alloy
70326.52	8.34E+07	1.33E+08	1.32E+08	1.32E+08
44126.4	8.33E+07	5.26E+07	8.31E+07	8.31E+07

<b>29647.5</b>	3.38E+07	3.53E+07	3.50E+07	5.58E+07
<b>18615.8</b>	3.51E+07	3.53E+07	3.50E+07	3.50E+07
<b>11031.6</b>	2.08E+07	2.09E+07	2.08E+07	2.08E+07



**Graph-2 von mises stress Vs Pressure (Pa) for a nose cone model tested with 4 different Ti Gr & alloys**

From the Graph von mises stresses Vs Pressure, it is noticed that almost all titanium graded alloy structures have gradual increment in von mises stresses as the (Pressure) increases and altitude decreases. However Among these Titanium family nose cone structure made of Titanium Grade-2 has yielded optimum values of minimum von mises stress for the operating conditions range from 10000 Ft to 30000 Ft.

Whereas cone structure made of Titanium Grade-1 and Titanium- $\alpha$  alloy both have decrement in stresses at range from 20000 Ft to 30000 Ft linearly. However at a range from 30000 Ft to 40000 ft nose cone structure made of Ti- Gr1, Ti- Gr2 and Ti- $\alpha$  alloy material have increment in stresses. Also observed that at a range about 40000 Ft to 50000 Ft, the structure made of all Titanium graded alloys have decrement in von mises stresses.

## 7. Conclusion & Future Scope

In the present study, the nose cone is modelled and analyzed using Finite Element tool ANSYS. From the above results, Titanium- grade 1 and Titanium grade 2 materials yielded less total deformation at specified operational conditions i.e., At higher altitudes range about 40000 Ft to 50000 Ft and at lower altitudes about 10000 Ft to 30000 Ft, these materials failed to withstand high pressures and yields maximum von mises stresses and subjected to maximum total deformation.

On the other side, the nose cone structure made of Titanium  $\alpha$  – alloy : Ti-5Al-2.5Sn and Titanium  $\beta$  – alloy: Ti-13V-11 Cr- 3 Al have better strength than pure grade titanium materials since these materials yielded less von mises stress and a gradual increment in Total deformation as the pressure load increases and vice-versa. After overall observation of obtained results, the Titanium  $\beta$  – alloy: Ti-13V-11 Cr- 3 Al material is preferable and also it has high quality, low weight proportion and great erosion resistance over wide range of operating conditions.

**Future scope:** The scope of this work is to develop a nose cone configuration with variable shell thickness the structure should yield optimum material strength to withstand loads at all operating conditions. Similarly, the longerons and bulkheads of the nose cone structure made with different material and can be analyzed to predict the strength of such materials under all operating conditions.

## 8. References

- [1] P. Venkata Suresh, K. Ayyappa, V. Anjalee Kumari, M. Koteswararao, J. Venumurali  
Design of an Air Craft Nose Cone and Analysis of Deformation under the Specified Conditions with Different Materials using ANSYS  
International Journal of Engineering Research & Technology (IJERT)

ISSN: 2278-0181, Vol. 4 Issue 02, February-2015

[2] C.M.Vamsi Priya

New Aerodynamic Design and Structural Analysis of Missile Nose Cone using different materials

JETIR May 2019, Volume 6, Issue 5, ISSN-2349-5162

[3] M. Sreenivasula reddy, Keerthi, “Design and Structural Analysis Of Missile Nose Cone”

Australian Journal of Basic and Applied Sciences, 11(11) August 2017, Pages: 30-40

ISSN: 1991-8178

[4] P. V. Devendra Aditya, Y. Rajesh Kumar, “Design and Structural Analysis of Missile Nose Cone Using Different Materials”

International Journal of Advanced Technology and Innovative Research

Volume- 10, IssueNo.12, December-2018, Pages: 1147-115, ISSN 2348–2370

[5] Adrian Bogdan Şimon-Marinică1 , Nicolae-Ioan Vlasin1 , Florin Manea1 , Gheorghe-Daniel Florea

Finite element method to solve engineering problems using ansys

MATEC Web of Conferences 342, 01015 (2021)

UNIVERSITARIA SIMPRO 2021

[6] Metals Hand Book, Properties & Selection Iron, Steel, and High Performance Alloys

ASM International 1990.

[7] A.Yeshwanth, P V.Senthiil, “Nose Cone Design And Analysis Of An Avion”

International Journal of Pure and Applied Mathematics

Volume 119 No. 12 2018, 15581-15589 ISSN: 1314-3395

[8] A Sanjay Varma, ,G Sai Satyanarayana, Sandeep “CFD Analysis Of Various Nose Profiles”,

International Journal of Aerospace and Mechanical Engineering , ISSN (O): 2393-8609, Volume 3 – No.3, June 2016

## Performance And Emission Characteristics of VCR Engine Fueled with Tyreoil and Cotton Seed Oil Blends

Dr.G.NagaMalleswara Rao<sup>1\*</sup>, Shaik Chand Mabhu Subhani<sup>2</sup>

<sup>1</sup>Principal & Professor, Dept. of Mechanical Engg, Eswar College of Engineering, Kesanupalli(Po),  
Narasaraopet(Md), Palanadu(Dt), AP

<sup>2</sup>Assistant Professor, Dept. of Mechanical Engg, Eswar College of Engineering, Kesanupalli(Po),  
Narasaraopet(Md), Palanadu(Dt), AP.

### ABSTRACT

In this paper, the biodiesel from non-edible tyre oil and edible cotton seed oil is prepared by the method of two-step 'acid-base' process. An experimental investigation has been carried out to analyze the performance and combustion characteristics of a VCR diesel engine fueled with tyre oil & cotton seed oil and its blends for different compression ratios. The blends will be prepared by the varying of 5% of biofuel with diesel with effect of using cotton seed and tyre and its diesel blends at different loads.

The results will show that maximum cylinder pressure and maximum rate of heat release increased with the increase in bio diesel blends. The carbon monoxide (CO) and smoke emissions may find significantly lower when operating on biodiesel & diesel blends, Nitrogen Oxide (NOx) emissions will found at full load. This study will reveal that the performance of the engine with these biodiesel blends differ marginally from diesel and its blends. The performance of individual and mixture of both biofuels will be compared.

**KEYWORDS:** VCR Engine, bio fuel, cotton seed oil, Tyre oil, blends, performance, emissions

### 1. INTRODUCTION

Energy is very important for society as it is used to sustain and improve well-being. It exists in various forms, from many different sources. Historically, with economic development, energy needs grew, utilizing natural resources such as wood, hydro, fossil fuels, and nuclear energy in the preceding century.

The difference between bio-diesel and petroleum diesel lies in the name itself. Petroleum diesel is created and is 100% petroleum based, considered as a fossil fuel. On the other hand bio-diesel is composed of biological mass. Bio-diesel is created from live feed stock such as vegetable oil, peanut oil, coconut oil, even algae oil. Bio-Diesel can be used as a direct fuel considered B100, or in its unrefined form of Straight Vegetable Oil (S.V.O.). Since many of these S.V.O. (Straight Vegetable Oil) are similar in properties to those of petroleum diesel.

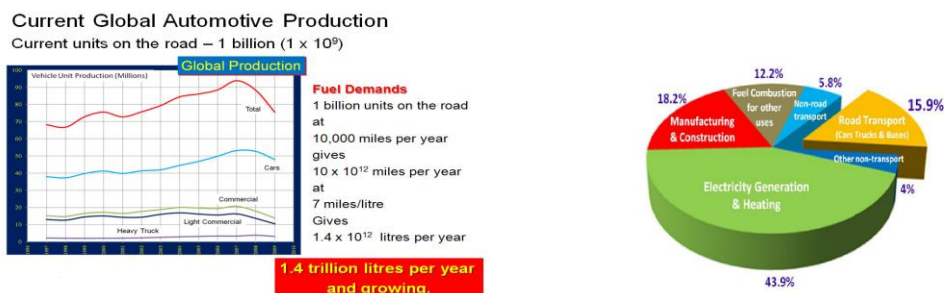


**Figure 1: Current global automotive productions and fuel usage**

First-generation bio-fuels are produced in two ways. One way is through the fermentation of either a starch-based food product, such as corn kernels, or a sugar-based food product, such as sugar cane, into ethanol, also known as ethyl alcohol, or "gasohol." Another way is by processing vegetable oils, such as soy, rapeseed and palm, into bio-diesel, a nonpetroleum-based diesel fuel.

**Second Generation bio-fuel** Second-generation bio-fuels (hydrogenated vegetable oil (HVO), synthetic diesel, bio ethanol (more advanced than 1st generation) can be produced from 'plant biomass'

which tends to refer to lignocelluloses materials (whole parts of plants). These second-generation, or "advanced," bio-fuels, are made from non-food sources, and hold significant promise as a low-carbon, renewable transportation fuel that can complement traditional petroleum-based fuels in meeting the world's future some of energy needs. The process of making alcohol from lignocelluloses biomass, in principle, is relatively simple: after hydrolysis and a subsequent fermentation, the ethanol can be refined by distillation

Recent improvement of the injection systems (common rail system) and application of supercharged or turbocharged engines satisfy the requirements regarding the output power. Moreover, the exhaust gaseous emissions are improved against older engine and injection systems. Unfortunately, the exhaust gaseous emissions of NO<sub>x</sub> and soot from the compression ignition (CI) engine are still high and limited by the legislation norms.

## 2. LITERATURE REVIEW

**S. Sinha et al** [1] investigated that that emissions of carbon monoxide and un burnt hydrocarbon reduce as load increases for all the blends of bio-diesel tested on the engine up to 80% of maximum engine load beyond that these emissions further increase. It has been found that nitrogen oxide emission increases slightly as the engine load increases on the engine up to 80% of maximum engine load beyond that it further decreases. The fuel samples containing 0%, 10%, 20%, 30%, 40%, 50%, 75% & 100% blends of jatropha biodiesel and conventional diesel, have been tested on single cylinder, four stroke, water cooled, direct injection diesel engine of Kirloskar Make (Rated Power 10 hp at 1500 rpm). It is observed that blend of 10-20% Jatropha bio-diesel with conventional diesel is found to be the best proportion as far as brake thermal efficiency and brake specific fuel consumption is concerned. Emission characteristics of engine show that the use of Jatropha bio-diesel is reducing harmful emissions from the exhaust such as un-burnt hydrocarbon, carbon monoxide and smoke. Nitrogen oxide emission is found to be little bit higher with some blends of bio-diesel for some range of brake power

**Bhojraj N. Kale et al** [2] investigated that performance of a diesel engine using diesel fuel and cottonseed oil (CSO) biodiesel in terms of brake thermal efficiency and indicated thermal efficiency for conventional diesel, cottonseed oil, as well as for jatropha oil on a Single Cylinder, 4-stroke vertical, water-cooled, self-governed diesel engine developing 5 HP at 1500 rpm (Rope brake dynamometer with spring balances and loading screw). In his evaluation of theoretical data showed that the brake thermal efficiency and indicated thermal efficiency of CSO biodiesel was slightly higher than that of diesel fuel and jatropha oil. He finally concluded that the use of cottonseed oil biodiesel improves the performance parameters of CI engine compared to conventional diesel fuel.

**Jinang M. Patel et al** [3] in his study the oil is obtained from pyrolysis of waste tire. He evaluated the use of various tire pyrolysis oil (TPO) blends with diesel fuel investigated and compared the results of performance and emissions characteristics TPO blends with diesel on a 4 cylinder direct injection engine. He was maintained A constant speed off 1500rpm throughout the experiment. He was blended TPO with diesel fuel at the volumetric ratios of 5 % (D5), 10% (D10) and 15 % (D15) in his study the results showed that brake thermal efficiency of the engine was maximum, BSFC was also found to be less and no significant increase in exhaust gas temperature for D10 blend than diesel at same loading conditions

**Jawalkar et al.** [4] investigated and compared the results of performance and emissions characteristics of single cylinder vertical direct injection Kirloskar diesel engine by using different blend of mahua and linseed oil. They founded that with an increase of injection pressure, the Bth Eff was increased and BSFC was reduced more for mahua biodiesel in comparison to Linseed biodiesel. They observed that as proportion of blend is increased the brake thermal efficiency was decreased. They observed that, the BthEff of M50 was 13.49% lower than that of L50 at 160 bar pressure at full load. They also observed that as the proportion of blend increased the BSFC was decreased. They investigated that CO emissions were lower for mahua oil than from linseed oil. They also observed that at 20% load, the HC emission of engine

**Sk.Mohammad Younus et al [5]** investigated oil taken is the tyre pyrolysis oil which was obtained by the pyrolysis of the waste automobile tyres. He conducted the test on four stroke single cylinder diesel engine by using diesel. In his investigation the tyre pyrolysis oil blended with diesel in different proportions such as T10, T20 and T30 with Ethanol and Ethyl Hexyl Nitrate (EHN) as additives to the diesel-biodiesel blends .he did that Ethanol was added as 5% and 10% by volume to the diesel-biodiesel blends and Ethyl Hexyl Nitrate (EHN) was added as 0.5% and 1% to the diesel-biodiesel blends. He concluded that the Brake thermal efficiency increased and The Brake specific fuel consumption is decreased and CO, CO<sub>2</sub> and HC emissions are decreased significantly with all blends when compared to the conventional diesel fuel.

**Alp Tekin ERGENC et al [6]** analyzed that Conventional diesel and soybean-based biodiesel blends and tests were conducted on an air-cooled single cylinder DI diesel engine. He found that by using soybean ester–diesel blends, the engine operated smoothly without any notable problems. He finally concluded that the maximum torque generated by the soybean ester blends (B20, B50) and CO, NO<sub>x</sub>, and CO<sub>2</sub> emissions were very similar or lower than those of diesel fuel. He found that rate and maximum value of heat release decreased with the higher percentage of soybean ester in the blends

**K.Naveen et al[7]** he examined that Ziziphus jujuba(Indian jujube), which is the edible in nature, first time introduced as fuel to run single cylinder, four stroke ,variable compression ratio diesel engine. His Experimental investigation of diesel engine was made with 20% (B20),40% (B40) and 60% (B60) blending of Ziziphus jujuba oil with diesel for compression ratio from 15:1 to 18:1 .in his investigation he finally concluded that SFC decreases with increasing load for the compression ratio from 15:1 to 18:1 and increases with increasing percentage blending of bio fuel ,BTE and EGT increases with increasing the load for all the compression ratio (18:1 to 15:1) and all the blending (B20, B40 & B60).B20 register higher BTE when compared to B40 & B60 except the compression ratio of 17:1. And EGT decreases with increasing the compression ratio and blending percentage. B60 register lower EGT at all compression ratio comparing with B20 & B40 as well as Diesel.

**Miqdam Tariq Chaichan et al [8]** investigated that the effect of the biodiesel produced from restaurant waste feed stocks on engine. Bio diesel blends were prepared from restaurants waste yellow grease of different vegetable oils. The neat fuels and their 20% blends with diesel fuel were studied at steady-state engine operating conditions in a four-cylinder direct injection. In his investigation he found that Brake specific fuel consumption was found to have minimum, The brake thermal efficiency was found to increase with increase in load when compared with neat diesel and he examine that biodiesel fuels provided significant reductions in carbon monoxide, unburned hydrocarbons and particulate matters, oxides of nitrogen increased by 7 and 11% for the yellow grease B20 and B100 respectively.

**Dr. Hiregoudar Yerrennagoudaru et al [9]** in his investigation he highlight the usage of Methanol (30%) blended with Cottonseed oil (70%) for a twin cylinder compression ignition engine and the performance characteristics of this blended fuel. He found that Methanol Blends with vegetable oils emits less pollutants compared to diesel, he examined that The HC, CO emissions are measured in exhaust gases using gas analyzer and it is observed that HC, CO emissions in Methanol Blend with vegetable oil are less compare to diesel.

**M.Harinatha reddy et al [10]** his paper gives the brief out line about the worldwide production cottonseed & its oil, Cotton Seed Oil (CSO) properties, its comparison with diesel and Jatropa biodiesel he investigated that the performance of a diesel engine using diesel fuel and cottonseed oil (CSO) biodiesel in terms of brake thermal efficiency and indicated thermal efficiency for conventional diesel, cottonseed oil, as well as for Jatropa oil. The test is conducted on A Single Cylinder, 4-stroke vertical, water-cooled, self-governed diesel engine developing 5 HP at 1500 rpm (Rope brake dynamometer with spring balances and loading screw. Brake drum diameter = 0.400 m.). His evaluation of theoretical data showed that the brake thermal efficiency and indicated thermal efficiency of CSO biodiesel was slightly higher than that of diesel fuel and Jatropa oil. This study reveals that the use of cottonseed oil biodiesel improves the performance parameters of CI engine compared to conventional diesel fuel.

**Aydin et al. [11]** described the effects of different blends like 5% (B5), 20% (B20), and 50% (B50) of cottonseed oil methyl ester in a single cylinder, direct injection, air-cooled diesel engine at partial and full load condition. They investigated the effects of blend on the engine fuel consumption and exhaust emissions at 2000 rpm of engine speed. They observed that for both, half load engine condition and easy loaded engine operation, at 2000 rpm engine speed the BSFCs of B5 were lower than those of others fuels. According to them at partial loads, for diesel and B5 fuels the exhaust gas temperatures were found to be higher than those of B20 and B50 as a result of higher thermal efficiencies of B5 and diesel fuels. They observed that the lowest CO emissions were obtained for biodiesel blends, at 50% load due to their rich oxygen content and optimal air–fuel ratio. They stated that the NO<sub>x</sub> emissions were decreased with the use of B20 and B50 blends. They observed that SO<sub>2</sub> emissions were decreased with increase on biodiesel content in the blend. The lowest SO<sub>2</sub> values were found for B50 usage for all loads

**Adaileh et al. [12]** measured the performance of diesel engine fuelled by a biodiesel extracted from waste cooking oil for a four stroke single cylinder diesel engine loaded at variable engine speed between 1200-2600 rpm. According to them B20 produced significant reductions in the CO, HC, and smoke emissions compared with standard diesel and B5. They observed that biodiesel had more volumetric consumption than diesel due to its more oxygen content. They investigated that exhaust emissions were reduced and performance was improved with biodiesel as fuel. They also observed that biodiesel can be safely used in engines up to lower amount of blending up to 20%. According to them after treatment of engine was required for the reduction of particulate emissions. They observed that NO<sub>x</sub> emissions were increased with the amount of blending and with the use EGR, these emissions could be reduced. They evaluated that with the increase in engine speed fuel consumption rate, brake thermal efficiency, equivalence ratio, and exhaust gas temperature were increased while at the same time the BSFCs, emission of CO<sub>2</sub>, CO and the NO<sub>x</sub> were reduced with the engine speed.

**Sharma et al. [13]** discussed the latest aspects of development of biodiesel. Effect of molar ratio, moisture content, reaction temperature, specific gravity, stirring had been discussed in this research paper. Apart from this biodegradability and satiability of biodiesel had also been discussed. According to their observation methanol being cheaper was the commonly used alcohol during transesterification reaction. They observed that among the catalysts, homogeneous catalysts such as sulphuric acid, sodium hydroxide, potassium hydroxide are commonly used at industrial level production of biodiesel. They also investigated the use of heterogeneous catalysts such as calcium oxide, magnesium oxide and others are to decrease the catalyst amount and production cost of biodiesel. According to them transesterification reaction can be completed even without catalyst by using supercritical methanol but it would increase the production cost of biodiesel as it was energy intensive. They observed that the molar ratio of alcohol to oil required for acid transesterification was from 6:1 and 18:1 for alkaline transesterification it ranged from 5:1 and 12:1. They observed that the temperature ranged between 45OC and 65OC as the boiling point of methanol is 64.7OC and heating beyond this temperature would burn methanol. However, they observed that higher temperature was employed while using supercritical methanol (200OC–300OC). They described that a balance had to be maintained between the composition of saturated and unsaturated fatty acid in the biodiesel fuel. According to them high saturated fatty acid content would increase the oxidative stability but the pour point and cloud point were increases which is not desirable and on the other hand higher un saturation content increased the pour point and cloud point but decreased the oxidative stability.

**Jawalkar et al. [14]** investigated and compared the results of performance and emissions characteristics of single cylinder vertical direct injection Kirloskar diesel engine by using different blend of mahua and linseed oil. They founded that with an increase of injection pressure, the BthEff was increased and BSFC was reduced more for mahua biodiesel in comparison to Linseed biodiesel. They observed that as proportion of blend is increased the brake thermal efficiency was decreased. They observed that, the BthEff of M50 was 13.49% lower than that of L50 at 160 bar pressure at full load. They also observed that as the proportion of blend increased the BSFC was decreased. They investigated that CO emissions

were lower for mahua oil than from linseed oil. They also observed that at 20% load, the HC emission of engine were higher for mahua oil in comparison with linseed oil.

### 3. EXPERIMENTAL SETUP AND METHODOLOGY

#### 3.1 Production of Tyre Pyrolysis Oil

##### 3.1.1 Availability and Composition of Tyres

Since the number of automobiles used in India is less than the developed countries, the problems related to disposal of waste tyres is not seriously realized as on today. But it is supposed to become a serious problem in the near future. Hence, proper treatment methods for waste tyres have to be put in place in advance.

**Table 1: Input Tyres to Finished Products Output Ratio**

Input Material	Input Quantity	Output quantity
Waste mixed plastic scrap	10,000kgs	- 6,500 to 9,000 lit of Pyrolysis Oil - 500 to 1,000 Kg of Hydrocarbon Gas - 500 to 700 Kg of carbon Black
Nylon Scrap Tyres	10,000kgs	- 4,500 to 5,000 lit of Pyrolysis Oil - 1,000 to 1,200 Kg of Hydrocarbon Gas - 3,000 to 3,500 Kg of carbon Black
Radial Scrap Tyres	10,000kgs	- 4,000 to 4,500 lit of Pyrolysis Oil - 800 to 1,000 Kg of Hydrocarbon Gas - 2,750 to 3,250 Kg of carbon Black - 800 to 1,000 kgs of Mild steel wire scrap

A tyre is artificially engineered by the human mind. It contains chemicals, rubber, steel and fabric. Approximately 80% of the original constituents remain at the end of its service. The theory to reduce, reuse and recycle is difficult to implement with tyres owing to their complex nature, durability, varying size, numbers involved and different dimensions.

##### 3.1.2 Pyrolysis of tyres

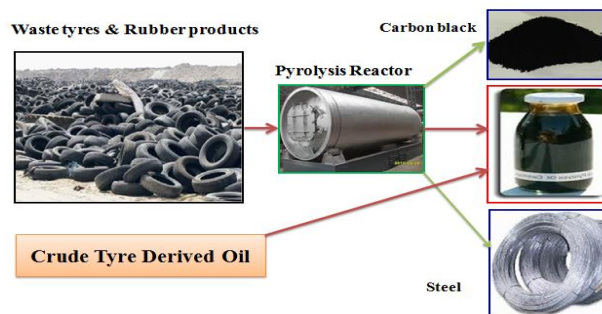


**Figure 2 Products from Waste Tyres after Pyrolysis**

A car tyre has a mass of about 8.5 kg, whereas the mass of a tyre of a passenger or light duty vehicle is around 11 kg. The constituents of truck tyre are given in Table .The various parts of an automobile tyre include bead, bundle, body, belt, cap sidewall and tread.

The raw materials used in tyres include synthetic and natural rubber, nylon, polyester cord, carbon black, sulphur, oil resin and other chemicals. These constituents provide the tyre with a good strength and flexibility to ensure adequate road holding properties under all conditions. About 80% of mass of car tyres and 75% of mass of truck tyres are rubber compounds. The components of tyre manufactured by different manufacturers are very similar. The tread portion of a tyre is primarily used for energy recovery to obtain TPO, pyro gas and carbon black.

**Table 2: Components of truck Tyre**

Component	Proportion (%)
Carbon Black	40
Oil	43.5
Steel Wire	16.5

### 3.3 PREPARATION OF BLENDS

The different types of blended bio fuels used in these projects are

DIESEL	:	100% PURE DIESEL
C0T10N90	:	0%CSO 10% TYREOIL 90% DIESEL
C0T20N80	:	0%CSO 20% TYREOIL 80% DIESEL
C10T0N80	:	10%CSO 0% TYREOIL 80% DIESEL
C20T0N80	:	20%CSO 0% TYREOIL 80% DIESEL
C10T10N80	:	10%CSO 10% TYREOIL 80% DIESEL
C10T20N70	:	10%CSO 20% TYREOIL 70% DIESEL
C20T10N70	:	20%CSO 10% TYREOIL 70% DIESEL



**Figure 3: Blended Fuels**

**Table 3 : properties of the biodiesel**

S.No	Blend	Viscosity (Stokes)	CALORIFIC VALUE (Kj/)	Flash Point(°C)	Fire Point(°C)	Density 45° C (Kg/m <sup>3</sup> )
1	DIESEL	2.65	46000	55	61	640
2	C0T10N90	2.43	45750	54	59	650
3	C0T20N80	2.32	45670	52	57	660
4	C10T0N90	3.59	45730	54	60	660
5	C10T10N80	3.42	45520	53	57	670
6	C10T20N70	3.31	45360	51	55	680
7	C20T0N80	4.53	45600	57	63	660
8	C20T10N70	4.23	45330	56	62	680
9	TYRE OIL	1.64	41320	46	49	780
10	COTTON SEED OIL	6.92	40200	134	146	780

### 3.7.5 Test rig specification

<b>Engine</b>	:	4 - stroke 1- cylinder water cooled Diesel engine
Make	:	Kirloskar
Rated power	:	3.7KW (5 HP)
Bore dia	:	80mm
Stroke length	:	110mm
Connecting rod length	:	234mm

Swept volume : 562cc  
 Compression ratio : 16.5: 1  
 Rated Speed : 1500 rpm

### 3.7.6 Dynamometer

**Dynamometer:** Eddy current dynamometer

Make: POWER MAG

Rated torque: 24N-m

Arm length: 150mm

**3.7.7 INDUS 5 GAS ANALYSER:** it is used to measure the concentration of exhaust gases



Figure 3: INDUS 5 GAS ANALYSER

## 4. RESULTS AND DISCUSSIONS

### 4.1 PERFORMANCE PARAMETERS

#### 4.1.1 Brake power (kW) Vs COMPRESSION RATIO

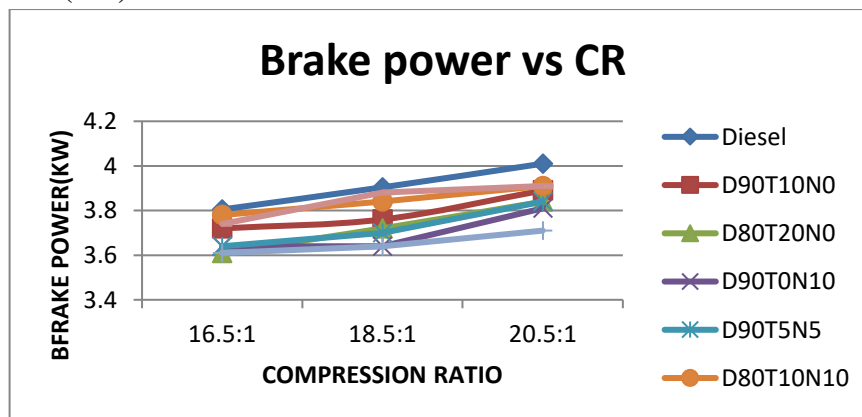


Figure 4: Brake power (kW) Vs COMPRESSION RATIO at maximum torque of 24 Nm

#### 4.1.2 Brake Thermal Efficiency (%) Vs COMPRESSION RATIO

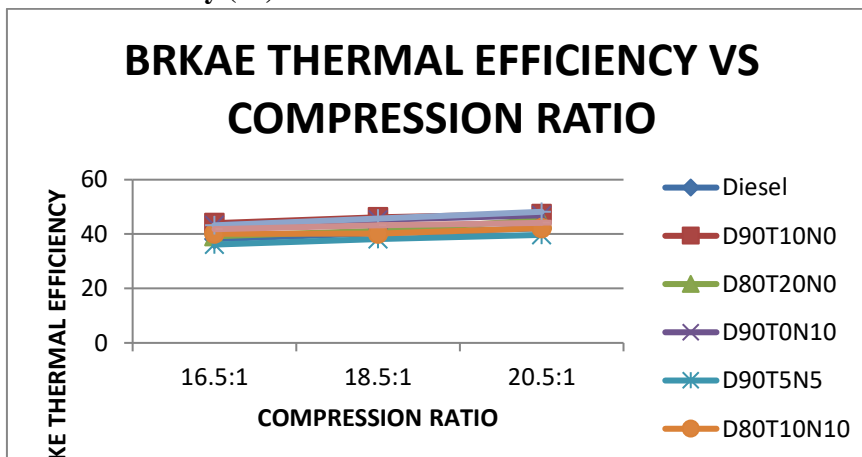


Figure 5 : Brake Thermal Efficiency (%) Vs COMPRESSION RATIO at maximum torque of 24 Nm

4.1.6 Volumetric efficiency (%) Vs COMPRESSION RATIO

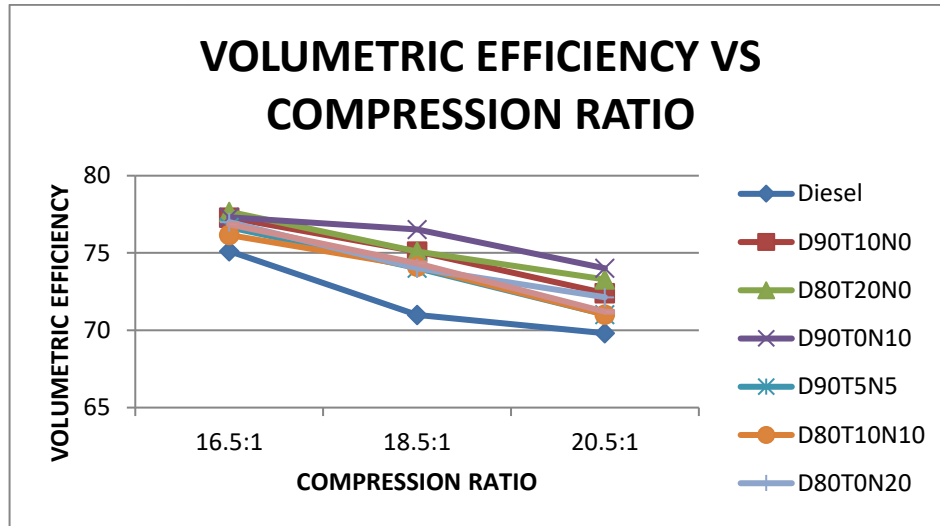


Figure 6: Volumetric efficiency (%) Vs COMPRESSION RATIO at maximum torque of 24 Nm  
4.1.4 Exhaust Gas Temperature (0C) Vs COMPRESSION RATIO

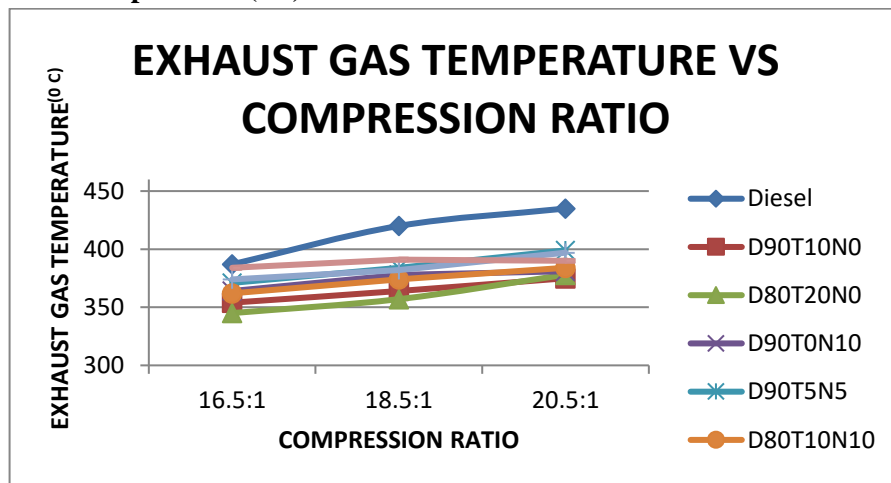


Figure 7: Exhaust Gas Temperature (°C) Vs COMPRESSION RATIO at maximum torque of 24 Nm  
4.1.5 Brake Specific fuel consumption (Kg/Kw Hr) Vs COMPRESSION RATIO

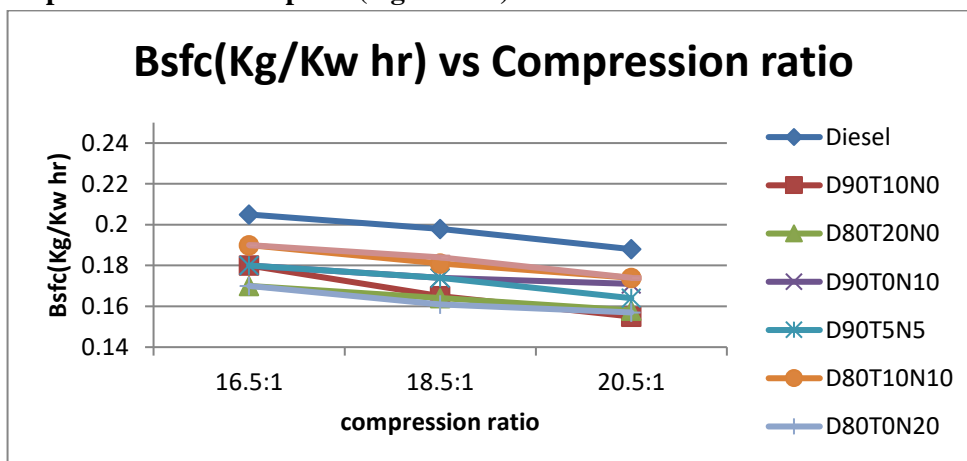
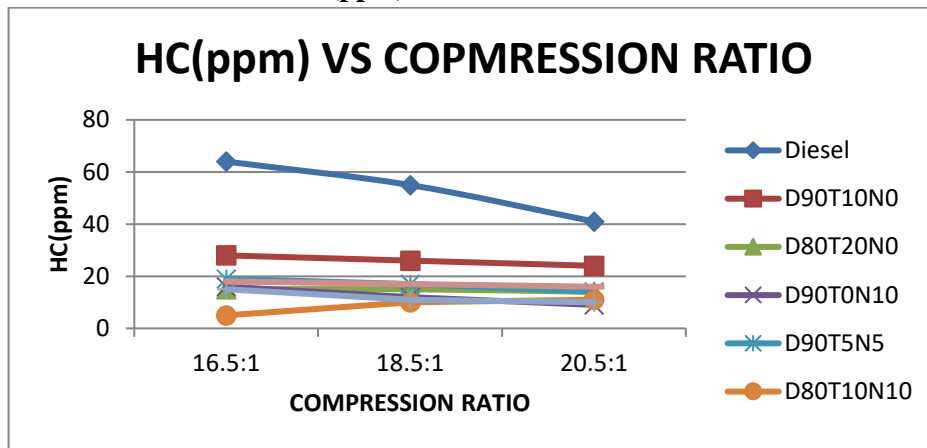


Figure 8: Brake Specific fuel consumption (Kg/Kw Hr) Vs COMPRESSION RATIO at maximum torque of 24 Nm

## 4.2 EMISSION ANALYSIS

### 4.2.1 HYDRO CARBON EMISSION (ppm) Vs COMPRESSION RATIO



**Figure 9:** HYDRO CARBON EMISSION (ppm) Vs COMPRESSION RATIO at maximum torque of 24 Nm

### 4.2.2 NITROGEN OXIDE EMISSION (ppm) Vs COMPRESSION RATIO

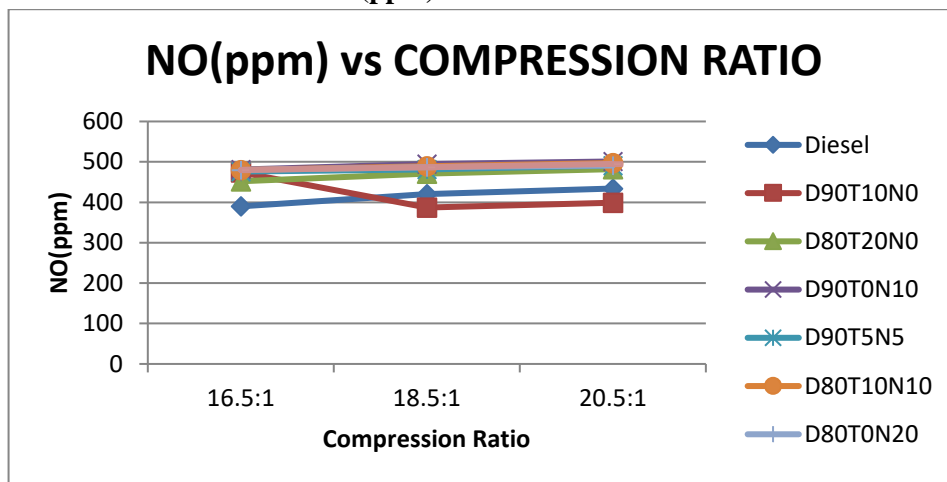


**Figure 10:** NITROGEN OXIDE EMISSION (ppm) Vs COMPRESSION RATIO at maximum torque of 24 Nm

### 4.2.3 CARBON MONOXIDE (%) Vs COMPRESSION RATIO

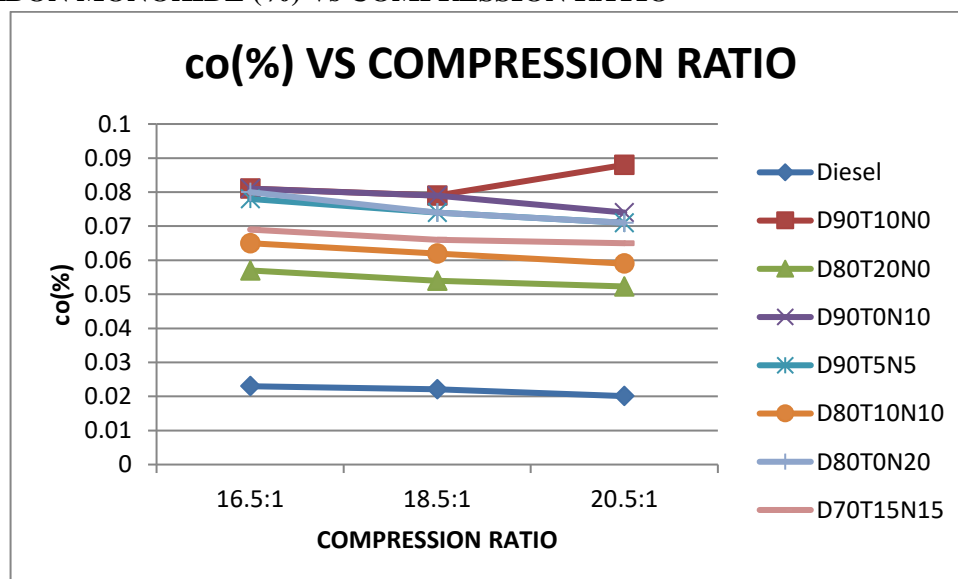


**Figure 11:** CARBON MONOXIDE (%) Vs COMPRESSION RATIO at maximum torque of 24 Nm

#### 4.2.4. CARBON DI OXIDE (%) Vs COMPRESSION RATIO

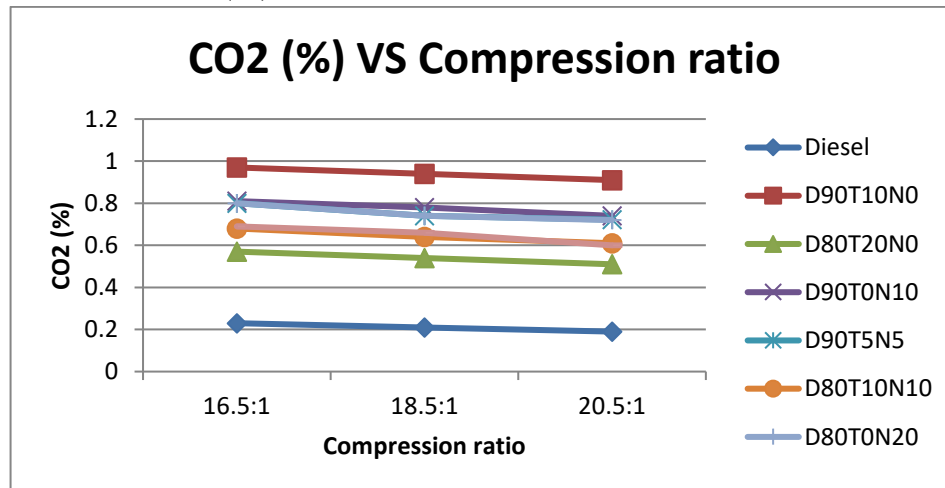


Figure 12: CARBON DIOXIDE (%) Vs COMPRESSION RATIO at maximum torque of 24 Nm

## 5. CONCLUSION

The experimental results shown in this paper that engine performance and emissions of all blends were run on the diesel engine and compared with standard diesel fuel

- Properties of all blends are nearly equal to the diesel fuel. The brake power for C20T10N70 is 1.183% more than the diesel and for C0T20N80 is 5.125% less than diesel. The highest is recorded with and C20T10N70 lowest with C0T20N80 at higher compression ratio
- As the applied torque is maximum at 24 KN m, the brake thermal efficiency of the fuel blends also increases at all compression ratios. The maximum brake thermal efficiency at full torque of 24Nm is 45.36% for C10T0N90
- The brake specific fuel consumption for C0T20N80, C10T0N90 and C20T0N80 is 0.17Kg/Kw Hr and diesel has 0.205 Kg/Kw Hr the specific fuel consumption only increases for higher percentages of blends at higher compression ratios.
- The volumetric efficiency was decreases for blend. The decrease in volumetric efficiency is due to increase in compression ratio
- The increasing compression ratio at maximum Torque the exhaust gas temperature is also increases. The exhaust temperature is highest for C10T20N70 and lowest for C10T10N80 at 20.5:1 compression ratio
- It can be observed from the figure that there was a gradual increase in NOx emission with increase in the blend concentration but lesser than that of diesel fuel. Due to higher heat release rates there is an increase in cylinder temperature resulting in increase in NOx emissions
- Due to incomplete combustion and inadequate supply of oxygen carbon dioxide emission of the fuel blends C0T10N90 low at full load decreases.
- The carbon monoxide emission of the blend C10T10N80 is found to be higher for low and medium torque and closer to that of standard diesel at high Torque. For the blends of C10T20N70 and C20T0N80 are having the carbon monoxide lower than that of the diesel Cotton seed oil and tyre oil promising as a best alternative fuel source of diesel engine because of its high heat content. It can be directly used as diesel fuel but having a major problem was cottonseed oil having high viscosity. From this investigation, test results showed that 20% cottonseed oil 10% tyre oil and 70% diesel (C20T10N70) and for suitable it to be used as diesel fuel without any modification of engine.

## 6. REFERENCES

- [1] Palash M. Mendhe, Mirzamunawwar Baig And Chetan D. Madane “ Cottonseed oil used as an alternative fuel for the performance characteristics of CI engine by blending with diesel” international journal for research in emerging science and technology, volume-2, special issue-1, march-2015

- [2] Bhojraj N. Kale<sup>1</sup>, Dr.S.V.Prayagi “ Performance analysis of cottonseed oil methyl ester for compression ignition engines” international journal of emerging technology and advanced engineering website: www.ijetae.com (issn 2250-2459, volume 2, issue 8, august 2012)
- [3] Jinang M.Patel, Krunal J.Patel,Vatsal V.Patel and Kalpesh V.Vaghela “ performance studies of tire pyrolysis oil blends with diesel fuel” international journal of engineering and advanced technology (ijeat) issn: 2249 – 8958, volume-3, issue-2, December 2013
- [4] Ashish Jawalkar, Kalyan Mahantesh, M Jagadish “performance and emission characteristics of mahua and linseed biodiesel operated at varying injection pressures on CI engine” international journal of modern engineering research (ijmer), 2, page 1142-1149, 2012.
- [5] Sk.Mohammad Younus, V.Ranjith Kumar, DR.Y.V.Hanumantha Rao” Performance and emissions characteristics of diesel engine fueled with tyre pyrolysis oil & diesel blends with additives” international journal of engineering science invention issn (online): 2319 – 6734, issn (print): 2319 – 6726 www.ijesi.org volume 2 issue 5 || may. 2013 || pp.32-37
- [6] Alp Tekin Ergenc., Levent Y”Uksek, Orkun ”Ozener “ Performance, emission, and heat release analyses of a direct injection diesel engine running on diesel and soybean ester blends” turkish j eng env sci (2013) 37: 23 – 32
- [7] K.Naveen,T.Parameshwaran Pillai, Azhagiri Pon” Experimental investigation of variable Compression ratio diesel engine using ziziphus jujuba oil” international journal of innovative research in science, engineering and technology volume 3, special issue 3, march 2014, issn (online) : 2319 – 8753 issn (print) : 2347 – 6710
- [8] Miqdam Tariq Chaichan, Prof. Dr. Sabah Tarik Ahmed “ Evaluation of performance and emissions characteristics for compression ignition engine operated with disposal yellow grease” the international journal of engineering and science (ijes) ||volume|| 2 ||issue|| 2 ||pages|| 111-122 ||2013|| issn: 2319 – 1813 isbn: 2319 – 1805
- [9] Dr. Hiregoudar Yerrennagoudaru, Manjunatha K. Chandragowda ” Performance and emission characteristics of twin cylinder CI engine using cottonseed oil blended with methanol” iosr journal of mechanical and civil engineering (iosr-jmce) e-issn: 2278-1684,p-issn: 2320-334X, volume 12, issue 1 ver. I (jan- feb. 2015), pp 47-53
- [10] M.Harinathareddy, DR P.Nageswara Reddy, DR.K.Vijayakumar Reddy ” Experimental investigation of compressed ignition engine using cotton seed oil methyl ester as alternative fuel” research invent: international journal of engineering and science isbn: 2319-6483, issn: 2278-4721, vol. 2, issue 1 (january 2013), pp 06-10
- [11]M. Ozcanli, H. Serin, O. Y. Saribiyik, K. Aydin, And S. Serin “ Performance and emission studies of castor bean (*ricinus communis*) oil biodiesel and its blends with diesel fuel” energy sources, 34, page 1808–1814, 2012
- [12] W.M Adaileh, K.S. Alqdah “performance of diesel engine fuelled by a biodiesel extracted from waste cooking oil” energy *procedia* ,18, page 1317-1334, 2012.
- [13] jinang m.patel, krunal j.patel,vatsal v.patel, kalpesh v.vaghela” Performance studies of tire pyrolysis oil blends with diesel fuel” international journal of engineering and advanced technology (ijeat) issn: 2249 – 8958, volume-3, issue-2, December 2013
- [14] Ashish Jawalkar<sup>1</sup>, Kalyan Mahantesh<sup>1</sup>, M Jagadish “Performance and emission characteristics of mahua and linseed biodiesel operated at varying injection pressures on ci engine” *international journal of modern engineering research (ijmer)*, 2, page 1142-1149, 2012.
- [15] R. K. Yadav And S. L. Sinha” performance of diesel engine using blends of Conventional diesel and jatropa bio-diesel as alternative fuel for clean environment” international journal for research in emerging science and technology, volume-2, issue-2, february-2015, volume-2, issue-2, february-2015

## **Experimental and CFD Analysis of Thermal Performance Improvement of Automobile Radiator Using Al<sub>2</sub>O<sub>3</sub>-TiO<sub>2</sub> Water Base Nanofluids**

**1.K. Venkatarao, 2.Ch. Lakshmi Kanth, 3.V, Sravani, 4.T. Hari Krishna, 5.T. Kiran Kumar, 6.V. Chandra Sekhar, 7.V. Chinna Murali Krishna**

1,2,3 Assistant Professor, Department of Mechanical Engineering, Prasad V Potluri Siddhartha Institute of Technology

4,5,6,7 B. Tech Students, Department of Mechanical Engineering, Prasad V Potluri Siddhartha Institute of Technology

### **ABSTRACT:**

This investigation explores the convective heat transfer dynamics and operational characteristics of a uniformly heated car radiator utilizing Al<sub>2</sub>O<sub>3</sub>-TiO<sub>2</sub> water nanofluids. The experimental methodology involves preparation of nano fluids of Al<sub>2</sub>O<sub>3</sub> and TiO<sub>2</sub> suspended in water through sonication. Various combinations of nano fluids at different concentrations and at different flow rates. The fluid is uniformly introduced into the system at 50°C, with experimental outcomes revealing varying Nusselt and Reynolds numbers at different concentrations and flow rates. Notably, at 0.16% volume concentration of TiO<sub>2</sub>/water nanofluids displays maintain pressure drop as constant compared to other nanofluids. Empirical correlations for the Nusselt number and friction factor exhibit good alignment with the experimental data. Additionally, Computational Fluid Dynamics (CFD) simulations are conducted using ANSYS 18.0 Fluent to model the car radiator design, employing a Fine mesh and applying boundary conditions. The analysis indicates turbulent flow, and the CFD results closely correspond with the experimental findings, depicting temperature, velocity, and pressure contours.

**Keywords:** Pressure drop, Radiator, Volume concentrations, Flow rates.

### **1. INTRODUCTION:**

In theory, it is widely recognized that the incorporation of nanoparticles can significantly enhance heat transfer efficiency. This research Mainly focuses on the practical implementation of nanofluids in a heat exchanger experiment. Nanofluids, which are engineered colloids, blend a base fluid with nanoparticles typically ranging in size from 1 to 100 n-m. These nanofluids exhibit heightened thermal conductivity and improved heat transfer coefficients compared to their original base fluids. The concept of nanofluids revolves around integrating metallic or non-metallic nanoparticles into base fluids to create a novel heat transfer medium. The heat transfer capabilities of nanofluids are influenced by various factors, including the properties and dimensions of the nanoparticles, as well as the concentration of solid particles within the fluid.

The utilization of nanoparticle-dispersed coolants in automobile radiators enhances heat transfer rates and facilitates a reduction in the overall size of the radiators. This study investigates the heat transfer characteristics of a water/propylene glycol-based TiO<sub>2</sub> nanofluid through experimental analysis, comparing it with pure water and a water/propylene glycol mixture. Two different concentrations of nanofluids were prepared by adding 0.1 vol.% and 0.3 vol.% of TiO<sub>2</sub> nanoparticles into the water/propylene glycol mixture (70:30). The experiments varied the coolant flow rate from 3 to 6 liters per minute for different coolant temperatures (50°C, 60°C, 70°C, and 80°C) to assess the effect of flow rate on heat transfer. Results indicate that the Nusselt number of the nanofluid coolant increases with an increase in flow rate. While the water/propylene glycol mixture demonstrates higher heat transfer rates at low inlet coolant temperatures, at higher operating temperatures and flow rates, the 0.3 vol.% TiO<sub>2</sub> nanofluid enhances heat transfer rates by 8.5% compared to the base fluids. [1].

Nanofluids represent a novel category of heat transfer fluids achieved through dispersing metallic or non-metallic nanoparticles, typically smaller than 100 nm in size, into traditional heat transfer fluids.

Their application significantly enhances the heat transfer capabilities of the base liquids. This study investigates the heat transfer coefficient and friction factor of  $\text{TiO}_2$  water nanofluids flowing in a horizontal double-tube counter-flow heat exchanger under turbulent flow conditions through experimental means.  $\text{TiO}_2$  nanoparticles, with diameters of 21 nm, are dispersed in water at volume concentrations ranging from 0.2% to 2%. Results demonstrate that the heat transfer coefficient of the nanofluid surpasses that of the base liquid, increasing with rising Reynolds numbers and particle concentrations. Specifically, the heat transfer coefficient of the nanofluids is approximately 26% higher than that of pure water at 2 vol.%, while at the same concentration, it is approximately 14% lower compared to the base fluids under given conditions. Regarding pressure drop, nanofluids exhibit a slightly higher pressure drop than the base fluid, escalating with increasing volume concentrations. Additionally, new correlations are proposed for predicting the Nusselt number and friction factor of nanofluids, focusing on their enhanced heat transfer properties. [2]. The stability of nanoparticle dispersion in liquid media holds significant importance for practical applications. This study aims to explore the impact of mechanical dispersion methods on the dispersal of functionalized  $\text{TiO}_2$  nanoparticles in transformer oil. Various dispersion techniques, including stirring, ultrasonic bath, and probe processes, were systematically evaluated to assess their effectiveness in producing stable nanofluids. Test outcomes indicate that the combination of ultrasonic bath processing and stirring yields the highest dispersion efficiency, resulting in nanofluids with superior AC breakdown strength. Specifically, even after aging for 168 hours, the nanoparticle size in the nanofluids prepared using the combined method exhibits no significant change, whereas those produced via the other three methods exhibit noticeable increases. [3].

Hybrid nanofluids, a novel class of nanofluids, are created by suspending various types of nanoparticles in a base fluid. This paper presents an experimental investigation into the influence of temperature and nanoparticle concentration on the thermal conductivity of  $\text{ZnO-TiO}_2/\text{EG}$  hybrid nanofluids. The experiments were conducted over a temperature range of 25 to 50°C and a solid volume fraction range of 0% to 3.5%. Results indicate that thermal conductivity increases with both higher solid volume fractions and temperatures. Interestingly, the thermal conductivity enhancement of nanofluids exhibits a greater variation with solid volume fraction at higher temperatures compared to lower temperatures. Similarly, the variation of thermal conductivity enhancement with temperature is more pronounced at higher solid volume fractions than at lower ones. Additionally, a correlation is proposed based on experimental data to predict the thermal conductivity ratio of  $\text{ZnO-TiO}_2/\text{EG}$  hybrid nanofluids. Deviation analysis of the thermal conductivity ratio is also conducted, showing good accuracy between experimental data and the proposed correlation outputs.[4].

Nitrogen-doped graphene (NDG) nanofluids are synthesized using a two-step method in an aqueous solution containing 0.025wt.% Triton X-100 as a surfactant, with various nanosheet concentrations (0.01, 0.02, 0.04, 0.06wt.%). This study presents experimental results on the thermal conductivity, specific heat capacity, and viscosity of NDG nanofluids, as well as their convective heat transfer behaviour within a double-pipe heat exchanger. Various water-based nanofluids were employed as coolants to analyze parameters such as the total heat transfer coefficient, convective heat transfer coefficient, percentage of wall temperature reduction, pressure drop, and pumping power in a counter-flow double-pipe heat exchanger. A novel MATLAB code was utilized for calculations across Reynolds numbers ranging from 5000 to 15,000 (indicating turbulent flow) and nanosheet weight percentages between 0.00% and 0.06%. Increasing the Reynolds number or the percentage of nanomaterial could potentially enhance the heat transfer characteristics of the working fluid. For instance, utilizing 0.06wt.% nanomaterial in the base fluid resulted in a 15.86% enhancement of the convective heat transfer coefficient compared to water. However, the increase in pumping power was relatively minimal. Nevertheless, for a specific material, increasing the Reynolds number or nanomaterial weight percentage would lead to an increase in pumping power. Across all examined cases, power consumption, heat removal, and heat transfer rate were higher for nanofluids than for water under the

same pumping power. On average, the heat transfer coefficient increased by nearly 16.2%. Consequently, opting for NDG/water as the working fluid can enhance the performance of double-pipe heat exchangers. [5].

Thermal conductivity models for nanofluids containing nanotubes are less prevalent compared to those for nanofluids incorporating spherical nanoparticles. This study introduces an updated Hamilton–Crosser model to estimate the effective thermal conductivity of nanofluids based on carbon nanotubes (CNTs), achieved by simulating an equivalent anisotropic nanoparticle. The thermal conductivity of this anisotropic nanoparticle is derived by analyzing the heat conduction process of a single CNT with an interfacial layer in any given direction. The proposed model incorporates the effects of CNT diameter, aspect ratio, and interfacial layer, and it is examined and validated against other models and available experimental data. Results indicate that the proposed model demonstrates a more moderate rate of variation influenced by CNT diameter and aspect ratio. This characteristic yields better adaptability compared to other models when compared with certain available experimental results [6].

This paper presents an experimental investigation into the impact of hybrid nano-additives, consisting of magnesium oxide (MgO) and functionalized multi-walled carbon nanotubes (FMWCNTs), on the thermal conductivity of ethylene glycol (EG). The experiments were conducted over a temperature range of 25°C to 50°C and a solid volume fraction range of 0% to 0.6%. Results indicate a significant enhancement in the thermal conductivity of nanofluids with an increase in the percentage of the solid volume fraction. Furthermore, while the thermal conductivity of EG notably increased with rising temperature, the enhancement in thermal conductivity of the hybrid nanofluid was slighter. Thermal conductivity measurements revealed a maximum enhancement of 21.3% in the nanofluid's thermal conductivity, occurring at a solid volume fraction of 0.6% and a temperature of 25°C. Additionally, efforts were made to establish an accurate correlation for predicting thermal conductivity at various temperatures and concentrations. Deviation analysis of the thermal conductivity ratio was conducted, and the comparison between experimental results and correlation outputs demonstrated good agreement [7].

Exploring further the potential of nanofluids, a novel type of solid/liquid suspension, is essential, particularly when their measured thermal conductivity significantly surpasses classical predictions, especially when they contain specially shaped particles such as nanorods. While various thermal conductivity models exist for nanofluids containing spherical or tubular nanoparticles, none are specifically tailored for nanorod-based nanofluids. This paper addresses this gap by developing a physical model of a nanorod with an interfacial layer in a fluid medium, which is dissected into axial and radial directions to formulate different sets of differential equations. Subsequently, a new thermal conductivity model for nanorod-based nanofluids is proposed by combining the analytical solutions of these differential equations. The distribution of heat conduction in the axial and radial directions in this model depends on the ratio of the nanorod's flanking and end (top and bottom) surface areas. Finally, the present model is compared with some classical models using available experimental data on the thermal conductivity of nanorod-based nanofluids. The comparative analysis demonstrates that the present model achieves greater precision. [8].

The escalating heat load poses a significant obstacle to industrial development. Addressing this challenge involves enhancing heat transfer rates, achievable through methods such as increasing temperature gradients, enlarging heat transfer surface areas, or enhancing the thermophysical properties of heat transfer fluids. The advent of modern technology has enabled the production of particles within the nano-meter scale (1-100 nm), known as nanoparticles, which boast high specific surface areas. When these nanoparticles are suspended in conventional fluids, forming colloidal suspensions termed nanofluids, the resulting mixtures exhibit heightened thermal conductivity compared to traditional fluids. However, ensuring the long-term stability of nanofluids is crucial for their effective utilization in heat transfer applications, presenting a significant technical challenge. This study aims to review the research conducted by various scholars over the past two decades, summarizing the techniques

employed for the preparation of stable nanofluids. Furthermore, the paper delves into emerging challenges that require resolution to enhance the industrial applicability of nanofluids. [9].

The increasing heat load presents a significant obstacle to industrial progress. However, this challenge can be addressed by enhancing the rate of heat transfer, which can be achieved through various means such as increasing temperature differentials, expanding heat transfer surfaces, or enhancing the thermophysical properties of heat transfer fluids. Modern technological advancements offer opportunities to manufacture particles within the size range of 1-100 nm, known as nanoparticles, which possess high specific surface areas. When these nanoparticles are dispersed in conventional fluids, forming colloidal suspensions known as nanofluids, the resulting mixtures exhibit superior thermal conductivity compared to conventional fluids. Ensuring the long-term stability of nanofluids is essential for their effective utilization in heat transfer applications, representing a significant technical challenge. Consequently, the primary focus of this study is to review research conducted by various scholars over the past two decades and summarize the preparation and analytical techniques employed for producing stable nanofluids. Additionally, the paper addresses emerging challenging issues that require resolution to enhance the industrial application of nanofluids. [10].

In recent years, there has been a notable surge in research focused on nanofluids, revealing their potential as advantageous heat transfer fluids for engineering applications. The efficacy of nanofluids in enhancing heat transfer primarily hinges on factors such as the thermal conductivity of nanoparticles, particle volume concentrations, and mass flow rates. When particle volume concentrations and flow rates remain constant, the degree of heat transfer enhancement is solely determined by the thermal conductivity of the nanoparticles. This property can be manipulated by producing hybrid (composite) nanoparticles, which consist of two or more different materials at the nano-meter scale. The resulting fluids containing these hybrid nanoparticles are termed hybrid nanofluids. The rationale behind developing hybrid nanofluids is to further enhance heat transfer by augmenting the thermal conductivity of these nanofluids. This review encompasses the synthesis of hybrid nanoparticles, the preparation of hybrid nanofluids, thermal properties, heat transfer characteristics, friction factor analysis, and available correlations for Nusselt number and friction factor. It also underscores that hybrid nanofluids outperform single-nanoparticle-based nanofluids and conventional fluids in terms of heat transfer effectiveness. However, a comprehensive understanding of the mechanisms underlying the heat transfer enhancement of hybrid nanofluids is still lacking, necessitating significant research efforts in this domain. [11].

Nanofluid refers to a colloidal suspension of nanoscale solid particles, such as metals or metal oxides, within conventional fluids like water and ethylene glycol. Owing to its distinct property of enhancing heat transfer in comparison to conventional fluids, nanofluid has garnered considerable attention from the research community. Numerous researchers have investigated the forced convection heat transfer of nanofluids. This paper provides a critical review of studies published on experimental investigations of forced convection heat transfer and pressure drop using  $\text{Al}_2\text{O}_3$ ,  $\text{TiO}_2$  and  $\text{CuO}$ -based nanofluids dispersed in water, ethylene glycol, and water-ethylene glycol mixtures. Most studies have indicated a marginal increase in pressure drop when nanofluids are used in plain tubes. The literature suggests that significant increases in pumping power are only observed at very high particle concentrations, exceeding 5%. Consequently, as nanofluids demonstrate the ability to enhance heat transfer at low particle concentrations, the majority of researchers have employed volume concentrations of less than 3% in their studies. While there is generally a consensus on pressure drop results among different researchers, there is no unanimous agreement on the magnitude and mechanism of heat transfer enhancement. Some studies have reported anomalous increases in heat transfer even at low particle concentrations, whereas others have observed minimal heat transfer enhancement at similar particle concentrations. A considerable variation (2-3 times) in Nusselt number has been observed in certain studies conducted under similar conditions. [12].

Nanofluids have emerged as promising thermodynamic fluids due to their remarkable properties regarding stability, thermal conductivity, thermal convection, and boiling heat transfer. The exploration

of their thermal physical properties, potential benefits, and applications has seen explosive growth. While numerous reviews have attempted to offer comprehensive summaries encompassing the preparation, properties, heat transfer, and application performance of various nanofluids, this task has become challenging given the vast volume of related literature, numbering in the tens of thousands. Consequently, a selective and comprehensive summary focusing on specific aspects of particular nanofluids holds significant value. This review centers on the heat transfer characteristics of TiO<sub>2</sub> nanofluid, as it is considered one of the most promising candidates for practical applications due to its excellent dispersibility, chemical stability, and non-toxicity. Additionally, this review highlights the challenges and opportunities for future studies in this field. It is anticipated that this review will offer a comprehensive overview of research progress in the heat transfer applications of TiO<sub>2</sub> nanofluids.[13].

This paper provides a comprehensive review of the current state of research and development concerning the conduction (thermal conductivity) and convection heat transfer properties of nanofluids based on ethylene glycol. Methods for preparing and stabilizing nanofluids are summarized and discussed. The impact of nanoparticle type, size, concentration, and temperature on the thermal conductivity of ethylene glycol-based nanofluids, as well as ethylene glycol/water mixtures, is critically analyzed and discussed individually. Furthermore, studies on the convective heat transfer of these nanofluids are reviewed, and the results from different studies are compared. The review unequivocally demonstrates that these nanofluids exhibit significantly higher thermal conductivity and convective heat transfer characteristics compared to their base fluids, namely ethylene glycol and its aqueous mixture. These enhanced thermal properties of nanofluids are crucial factors for their performance in thermal management and energy applications. With their improved thermal conductivity and convective heat transfer coefficients, nanofluids offer substantial potential in energy harvesting and storage, as well as advanced cooling applications. [14].

This paper provides a historical overview of the development of water-based, ethylene glycol (EG)-based, and EG: mixture nanofluids over the past two decades. The main objective is to review significant research pertaining to EG: water mixture nanofluids and their applications. In recent years, there has been a rapid increase in fundamental studies of nanofluids for engineering applications. The review includes an examination of forced convection heat transfer and pressure drop in nanofluid flow within tubes, presenting both experimental and numerical findings. Additionally, other relevant research studies are discussed. While a considerable amount of literature exists on water-based nanofluids in fundamental engineering studies, the use of EG: water mixture nanofluids for evaluating forced convection heat transfer has been limited. Nonetheless, several research studies have investigated the transport properties of EG: water mixture nanofluids through experimental or numerical approaches. Researchers have conducted experimental works using various types of potential nanofluids to verify the performance of EG: water mixture nanofluids. Consequently, nanofluids have found application in specific engineering domains such as automotive, transportation, cooling of electronic components, solar energy, and nuclear reactor coolant. [15].

Nanofluids, which consist of nano-sized particles dispersed in fluids, show great promise for enhancing heat transfer. Several studies have investigated heat transfer through such mediums, highlighting the substantial influence of temperature on the thermal conductivity of nanofluids. However, discrepancies in reported values underscore the need for a critical examination of this issue and a thorough discussion of the controversies surrounding it. This paper provides a concise literature review on the impact of temperature on the thermal conductivity of nanofluids, discussing key theoretical studies and significant experimental investigations. Additionally, it addresses the discrepancies observed among these studies. [16].

Over the past decade, the rapid advancement of nanotechnology has captured the attention of scientists, scholars, and engineers alike. One of the remarkable outcomes of this technology is nanofluids, which have the potential to significantly enhance the efficiency of thermal systems. Nanofluids containing solid nanoparticles typically exhibit higher viscosity compared to conventional working fluids, making it essential to measure viscosity for the design of thermal systems and estimation of required pumping

power. In this review study, the latest experimental investigations on the viscosity of nanofluids are covered. Experimental inquiry is crucial for analysis as theoretical models often underestimate nanofluid viscosity. Through experiments, the actual effects of volume fraction, temperature, particle size, and shape on nanofluid viscosity will be determined. [17]

The evaluation of thermo-physical properties, particularly thermal conductivity and viscosity, plays a crucial role in assessing heat transfer coefficients, whether for single-phase or two-phase flow. Measurements of thermo-physical properties and observations of heat transfer are typically conducted with nanoparticles sized above 10nm. Numerous researchers have undertaken measurements and modeling efforts to determine the thermal conductivity and viscosity of nanofluids. Many investigators have formulated equations to estimate thermal conductivity and viscosity as functions of volume concentration percentage, temperature, and occasionally particle size, within the range of their experimental conditions. Nanofluids are recognized for their significant potential in enhancing heat transfer and are thus employed in various heat transfer processes. Numerous studies have been conducted to explore this phenomenon. The primary objective of this study is to provide a comprehensive review of research advancements concerning the enhancement of effective thermal conductivity and effective dynamic viscosity of nanofluids.[18]

Over the past few decades, there has been a rapid increase in research focusing on nanofluids. Nanofluids, characterized by traditional heat transfer fluids containing nanoparticles ranging in size from 1 to 100 nano-meters, have emerged as superior heat transfer mediums despite variations in results reported by different research teams. This article aims to provide a comprehensive review and summary of recent experimental and theoretical investigations into convective heat transfer in heat exchangers operating under constant heat flux boundary conditions. It presents and compares the use of various types of nanoparticles with different base fluids as employed by different research groups. Additionally, it offers an overview of experimental findings regarding the heat transfer capabilities of hybrid nanofluids sourced from the available literature. Finally, the article discusses the challenges and future directions for advancing research in this field. [19].

This review aims to compile and analyze recent research articles concerning heat transfer and fluid flow behaviours in curved tubes, employing both conventional fluids and nanofluids as working fluids. Over recent years, several researchers have explored the utilization of nanofluids in curved tubes, seeking novel opportunities to enhance thermo-hydrodynamical performances. Curved tubes are categorized into three groups based on their curvature configurations: helically coiled tubes, spirally coiled tubes, and other types of curved tubes. The review encompasses experimental, numerical, and analytical studies published in the literature on this subject. [20].

The recent advancements in nanotechnology have introduced the concept of incorporating suspended nanoparticles into heat transfer fluids to enhance the heat transfer coefficient of the base fluids. This study primarily focuses on reviewing numerical investigations to gain a comprehensive understanding and detailed summary of how various parameters, including nanoparticle type, host liquid, particle volume concentration, particle size, particle shape, Brownian diffusion, and thermophoresis, influence the hydrodynamic and thermal characteristics of convective heat transfer using nanofluids. Furthermore, the paper offers comprehensive insights into the commonly used correlations employed to predict the effective thermophysical properties of nanofluids. Ultimately, the main objective of this work is to provide a thorough review of different computational fluid dynamics (CFD) approaches utilized in the numerical simulation of nanofluid flow, evaluating the advantages and disadvantages of each approach, and identifying the most suitable technique that yields results consistent with experimental findings. [21]

New methods for cooling, particularly for dissipating heat fluxes, are under exploration. Recent research has emphasized heat transfer in micro/mini-channels (M/MCs) utilizing nanofluids to harness the combined benefits and achieve enhanced single-phase heat transfer. The demand for high-efficiency applications such as cooling electronic devices, solar cells, and automotive technology is increasingly pressing, necessitating solutions to reduce operating costs. This review article aims to consolidate recent

studies in this domain, focusing on two main aspects. The first part elucidates key concepts including scaling effects of M/MCs, physical properties, and convective heat transfer. The second part delves into recent applications of M/MCs with nanofluids, addressing the challenges impeding their widespread adoption. The objective of this article is to furnish a comprehensive review of the latest developments in this emerging field, offering overarching conclusions. [22]

Recent advancements in nanotechnology have spurred innovations in the conventional applications of nanofluids, particularly in car engine cooling systems. This study investigates the potential enhancement of a car engine radiator through the utilization of TiO<sub>2</sub>-water nanofluid as a coolant. Experimental analyses were conducted to evaluate the impact of TiO<sub>2</sub>-water nanofluid on radiator performance, with comparisons made against pure water and existing studies on the vehicle engine system FIAT DOBLO 1.3 MJTD ENG. The primary objective was to assess the heat transfer aspects of TiO<sub>2</sub>-water nanofluid as a substitute for conventional coolant systems. To this end, experiments were conducted using TiO<sub>2</sub> nanofluid at volume concentrations of 0.1%, 0.2%, and 0.3%, with flow rates ranging from 0.097 to 0.68 m<sup>3</sup>/h in the laminar flow regime, covering Reynolds numbers from 560 to 1650. Our findings indicate a reduction in friction factor with increasing Reynolds number and volume concentration. Additionally, TiO<sub>2</sub>-water nanofluid at a concentration of 0.2% demonstrates a 47% enhancement in radiator effectiveness compared to concentrations of 0.1% and 0.3%, as well as pure water coolant. Furthermore, the average heat transfer coefficient is directly influenced by the rise in Reynolds number and volume concentration fraction of the nanofluid.[23]

An experimental investigation was conducted to examine the impact of temperature and particle volume concentration on the dynamic viscosity of water– Al<sub>2</sub>O<sub>3</sub> nanofluid. Viscosity data were collected using a commercial viscometer of the 'piston-type' for temperatures ranging from ambient conditions up to 75 °C. Two different particle sizes, namely 36 and 47 nm, were considered in the study. The findings indicate that, in general, the dynamic viscosity of nanofluid substantially increases with the particle volume fraction but decreases with temperature elevation. The viscosity values for particle sizes of 36 and 47 nm exhibit relatively close proximity, except at high particle fractions. The comprehensive viscosity dataset is presented. Results reveal the presence of a critical temperature beyond which the properties of particle suspension appear to undergo significant alteration, leading to a hysteresis phenomenon. This critical temperature is notably influenced by both particle concentration and size. The occurrence of the hysteresis phenomenon raises concerns about the reliability of nanofluids for heat transfer enhancement applications. Moreover, the data suggest that Einstein's formula and similar models derived from classical linear fluid theory may have limitations when applied to nanofluids with high particle fractions. [24]

The current investigation focuses on enhancing the convective heat transfer performance of ethylene glycol (EG) brine-based hybrid nanofluids, including Ag, Cu, SiC, CuO, and TiO<sub>2</sub>, with volume fractions ranging from 0% to 1% of Al<sub>2</sub>O<sub>3</sub> nanofluid, serving as coolants for louvered fin automobile radiators. The study evaluates the impact of nanoparticle combinations and operating parameters on the thermophysical properties, heat transfer efficiency, effectiveness, pumping power, and overall performance index of these hybrid nanofluids. Furthermore, a comparative analysis of the studied hybrid nanofluids is conducted based on radiator size and pumping power. Among the various hybrid nanofluids examined, the 1% Ag hybrid nanofluid (comprising 0.5% Ag and 0.5% Al<sub>2</sub>O<sub>3</sub>) demonstrates the highest effectiveness, heat transfer rate, and pumping power. However, the SiC + Al<sub>2</sub>O<sub>3</sub> dispersed hybrid nanofluid exhibits the maximum performance index, making it a recommended coolant choice. Using Ag hybrid nanofluids increases pumping power, which subsequently enhances engine thermal efficiency and reduces engine fuel consumption for a given radiator size and heat transfer rate. Additionally, employing Ag hybrid nanofluids decreases radiator size, weight, and cost while maintaining the same coolant flow rate and heat transfer rate. [25]

Sophisticated heat dissipation technologies are imperative for optimizing the performance of automotive engines. Current conventional fluids, typically composed of a blend of distilled water (DW) and ethylene glycol (EG), expand the operational temperature range but may limit heat removal efficiency.

Consequently, the adoption of nanofluids to enhance heat transfer performance has gained significant traction in recent years. However, many existing reports predominantly focus on short-term heat transfer outcomes, which may not accurately represent long-term performance. In this study, a proposed best practice for analyzing the utilization of nanofluids in heat transfer applications, specifically within an actual car radiator context, is presented. The investigation involves the use of aluminium oxide ( $\text{Al}_2\text{O}_3$ ) and titanium dioxide ( $\text{TiO}_2$ ) nanoparticles dispersed in DW and EG at a volumetric ratio of 50:50. The selection of these oxide-based nanofluids is motivated by their inherent anti-corrosive properties, and aspect often overlooked in existing literature. Moreover, the study emphasizes providing a comprehensive characterization of the nanofluids, including thermophysical properties (particle size, density, viscosity, thermal conductivity, corrosive behaviour), and long-term stability (zeta potential), essential for end-user assessment. Results indicate a maximum thermal performance enhancement of 24.21% using  $\text{Al}_2\text{O}_3$  at a volume fraction of 0.3%. Friction and performance evaluation criterion (PEC) for the radiator experiments are computed to assess the pressure drop penalty accurately. The calculated PEC values fall within the range of 1.03–1.31, indicating a significant flow enhancement. [26].

The automotive industry has been actively exploring strategies to optimize engine efficiency while maintaining compact vehicle designs. One such approach involves reducing the frontal area of vehicles, which not only enhances compactness but also improves aerodynamic performance. The effectiveness of a car radiator hinges significantly on its heat transfer rate, which, in turn, relies on the properties of the coolant utilized. Coolants with higher thermal conductivity can expedite heat transfer, resulting in quicker engine cooling, enhanced engine efficiency, reduced coolant volume requirements, pumping power, and ultimately, radiator size. This reduction in radiator size subsequently contributes to improved engine efficiency, compact vehicle designs, enhanced fuel economy, and reduced emissions. Through our research, we have demonstrated that nanofluids, with their superior thermal conductivity, offer superior heat dissipation capabilities compared to conventional coolants, thus holding promising practical applications in this regard. [27]

Nanofluids have emerged as promising heat transfer fluids, comprising a mixture of solid nanoparticles suspended in a liquid base. The presence of these nanoparticles significantly enhances the effective thermal conductivity of the fluid, thereby improving its heat transfer characteristics. Incorporating a single nanoparticle into the base fluid has proven effective in enhancing flow and heat transfer properties. However, recent research has shifted focus towards utilizing hybrid or composite nanofluids, which involve impregnating two or more nanoparticles into the base fluid. Studies have demonstrated that hybrid nanofluids offer superior thermal and rheological enhancements compared to mono nanoparticle-based nanofluids. This paper provides a comprehensive review of research studies on the preparation, characterization, properties, and stability of hybrid nanofluids. Models for predicting properties such as thermal conductivity, viscosity, density, specific heat, friction factor, and heat transfer coefficient of hybrid nanofluids are presented. Additionally, the paper discusses the potential applications of hybrid nanofluids, along with the challenges associated with their stability and measures to address them. [28]

In recent years, a new category of working fluids, known as hybrid nanofluids, has garnered significant attention and research focus. These fluids consist of two solid materials dispersed within a conventional fluid. This paper provides a comprehensive review of recent research findings about thermo-physical properties (such as thermal conductivity, viscosity, density, and specific heat) as well as the heat transfer and flow characteristics of hybrid nanofluids used in various heat exchangers. The incorporation of hybrid nanoparticles in nanofluids results in increased thermal conductivity, thereby enhancing heat transfer in heat exchangers. Both experimental and numerical findings discussed in this review suggest that hybrid nanofluids have the potential to significantly improve heat transfer efficiency in heat exchangers. However, further research is needed to explore different combinations of hybrid nanoparticles, their mixing ratios, and the stability of hybrid nanofluids, and to better understand the underlying mechanisms contributing to heat transfer enhancement. [29]

Experimental and numerical analyses were conducted to examine the heat transfer and pressure drop characteristics of a mini-channel heat sink utilizing hybrid nanofluids. The heat sink comprised nine parallel mini channels with rectangular shapes, each having a depth of 3 mm and a width of 1 mm. An  $\text{Al}_2\text{O}_3\text{-TiO}_2$  hybrid nanofluid, with a nanoparticle volume concentration of 0.1%, was utilized as a coolant, with different nanoparticle mixture ratios ranging from 10:0 to 0:10. The study aimed to assess the impact of volume flow rate (ranging from 0.1 to 0.5 LPM), Reynolds number (in the range of  $90 < \text{Re} < 500$ ), and inlet temperature (ranging from 20 to 40 °C). The two-phase mixture model provided better agreement with the experimental data compared to the single-phase approach. Moreover, the use of hybrid nanofluids resulted in a slight increase in the developing length. Notably, a maximum enhancement of 8.5% (numerical) and 12.8% (experimental) was observed in the convective heat transfer coefficient with  $\text{Al}_2\text{O}_3$  (10:0) hybrid nanofluid. Both numerical and experimental findings indicated that pressure drop and friction factor increased with decreasing temperature and increasing nanoparticle volume fraction. However, it was concluded that the hybrid nanofluids did not exhibit any synergistic effect in heat transfer when dissimilar nanoparticles with similar shapes and sizes were mixed. [30]

### Thermophysical properties of Nanofluids:

The thermophysical properties of  $\text{Al}_2\text{O}_3$  and  $\text{TiO}_2$  nano-fluids are subsequently estimated at a temperature of 50°C. Additionally, thermal characteristics such as density, dynamic viscosity, specific heat capacity, and thermal conductivity are also estimated at the same temperature by using the relations given below.

Base fluid properties are calculated by

$$\rho_w = 1000 \times \left[ 1.0 - \frac{(T_w - 4.0)^2}{119000 + 1365 \times T_w - 4 \times (T_w)^2} \right]$$

$$\mu_w = 0.00169 - 4.2526 e - 5 \times T_w + 74.9255 e - 7 \times (T_w)^2 - 2.09935 e - 9 \times (T_w)^3$$

$$k_w = 0.56112 + 0.00193 \times T_w - 2.60152 e - 6 \times (T_w)^2 - 6.08803 e - 8 \times (T_w)^3$$

The density of Nanofluid is calculated by

$$\rho_{nf} = \left( \frac{\phi}{100} \right) \rho_p + \left( 1 - \frac{\phi}{100} \right) \rho_w$$

The specific heat of Nanofluid is calculated by

$$C_{nf} = \frac{\frac{\phi}{100} (\rho C_p)_p + \left( 1 - \frac{\phi}{100} \right) (\rho C_p)_w}{\rho_{nf}}$$

The thermal conductivity of the Nanofluid is calculated by using

$$k_r = \frac{k_{nf}}{k_w} = \left[ 0.8938 \left( 1 + \frac{\phi}{100} \right)^{1.37} \left( 1 + \frac{T_{nf}}{70} \right)^{0.27} \left( 1 + \frac{d_p}{150} \right)^{-0.0336} \left( \frac{\alpha_p}{\alpha_w} \right)^{0.01737} \right]$$

$$k_{nf} = k_w \times k_r$$

Dynamic Viscosity of Nanofluid is calculated by using

$$\mu_r = \frac{\mu_{nf}}{\mu_w} = \left( 1 + \frac{\phi}{100} \right)^{11.3} \left( 1 + \frac{T_{nf}}{70} \right)^{-0.038} \left( 1 + \frac{d_p}{170} \right)^{-0.061}$$

$$\mu_{nf} = \mu_r \times \mu_w$$

## 2. METHODOLOGY

The figure represents the project architecture, showcasing the system's functionality and the interaction between various devices. The system design process commenced by selecting a suitable heat exchanger, and in our case, we opted for a car radiator equipped with a fan.



**Figure: 1** Project architecture diagram

The figure consists of the water tank, heaters, thermocouples, fan, radiator, flow meter, motor, pressure gauge, and water pump. However, it should be noted that the water pump commonly used in cars is mechanically connected to the engine and does not align with the requirements of our experiment. By selecting a water pump specifically suited for our experimental needs, we ensure the smooth operation and functionality of the entire system. The project architecture depicted in the figure provides a clear overview of how the devices within the system interact and work together to achieve the desired goals. It serves as a visual representation of the system's design and operation, aiding in the understanding and communication of the project's technical aspects.

### 3.1 Geometry Specifications of Car Radiator

**Table-1**

Parameter	Dimensions
Height of radiator	0.75m
Width of radiator	0.55 m
No. of radiator tubes	53
Each tube diameter	0.016 m
Length of the radiator tube	16.25m

### 3.2 Fluid Preparation:

In our study, we initially utilize water as the fluid. A total volume of 60 liters of water is utilized for the setup. Water serves as a widely used base fluid in numerous heat transfer applications due to its exceptional thermal characteristics and widespread availability. With the use of 60 liters of water, we ensure ample fluid quantity to facilitate flow and circulation throughout the system. Water possesses high heat capacity and thermal conductivity, making it an effective medium for heat transfer. Its abundant supply and economical cost further establish it as a pragmatic choice for experimental endeavors. Employing water as the base fluid establishes a reference point for comparing the performance of the Nanofluid. In essence, the incorporation of 60 liters of water in our experiment enables us to scrutinize and assess the Nanofluid's impact on enhancing heat transfer capabilities in contrast to the conventional base fluid. The nanofluids are prepared through a sonication process at a temperature of 90°C for a duration of 2 hours.

### 3.4 Input parameters

**Table-2**

Parameter	Range
Inlet Temperature	50°C
Volume Concentrations	0.01% - 0.16%
Flow rates	3.5m <sup>3</sup> /hr -4.5m <sup>3</sup> /hr
Reynolds Number	

The dimensions mentioned in Table 1 are used for creating a 3D model of the test section and the input parameters mentioned in Table 2 are used for the analysis. The solid models of the test section are shown in Fig. 1 and Fig. 2 respectively. In Fig. 1, Hexahedral meshing is used, the number of nodes is 924798, and the number of elements is 798995.

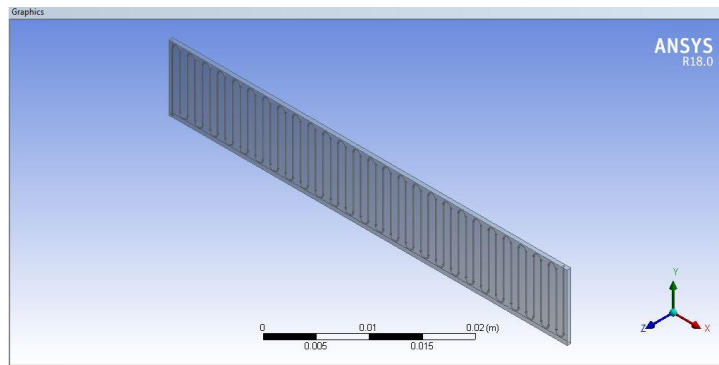


**Figure 2** Geometry model of Car Radiator

In this window geometry is selected, once the geometry is selected, we will be on the design modeler page. Initially, the sketch was created on the XY plane to create a circle with a 1 mm diameter and was extruded to 16.25m which means the total length is 16.25m. In this window geometry is selected, once the geometry is selected, I shall be on the design modeler page. Initially, the sketch is created on XY plane to create a circle with 1mm diameter and draw the pipe of diameter 1 mm and length 16.25m. By using Boolean operation, the two solid bodies form a single part. Then using the Pattern operation, enter 10mm pitch distance and enter 53 copies which means the total length is 16.25m.

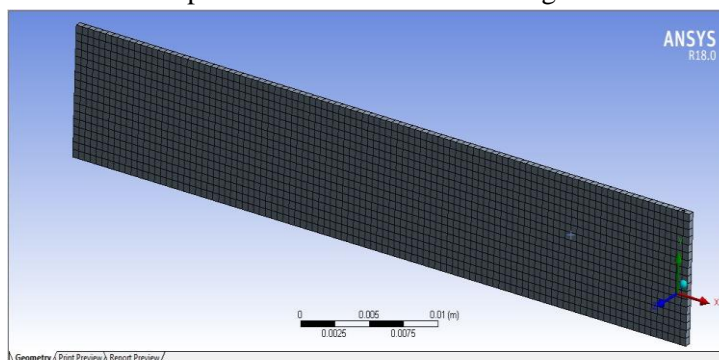


**Figure 3** Meshed model detail view

**Figure 3** represents the meshing as the next step once the model is completed. The entire domain material is assigned as FLUENT, and every edge of the domain is planned to divide to gain hexahedral or tetrahedral meshing.

### 3. RESULTS AND DISCUSSION

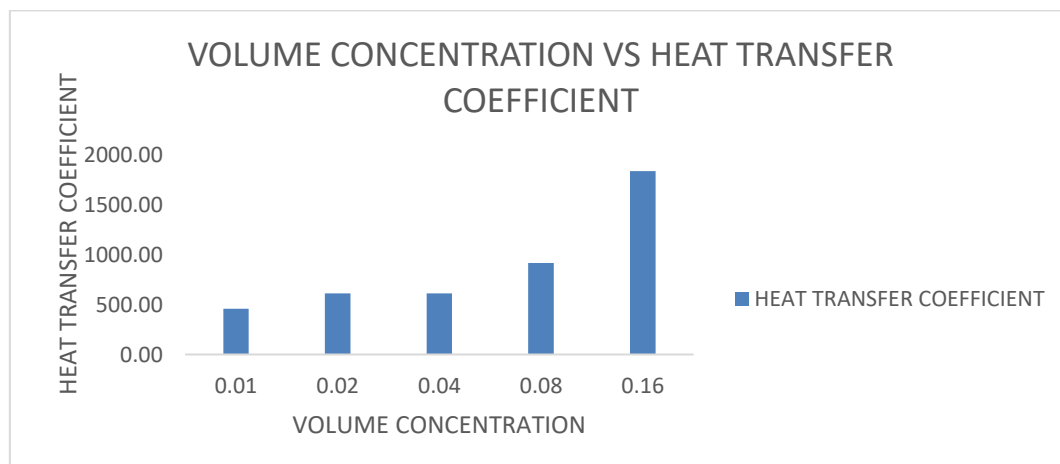


**Figure: 4** Graph between Volume Concentration and Heat transfer coefficient

**Figure: 4** shows that the graphical representation effectively illustrates the correlation between the Volume Concentration and Heat transfer coefficient. In this context, it is noteworthy that Aluminium oxide consistently outperforms other fluids in each scenario examined. These findings underscore as the volume concentration increases the heat transfer coefficient of aluminium oxide increases.

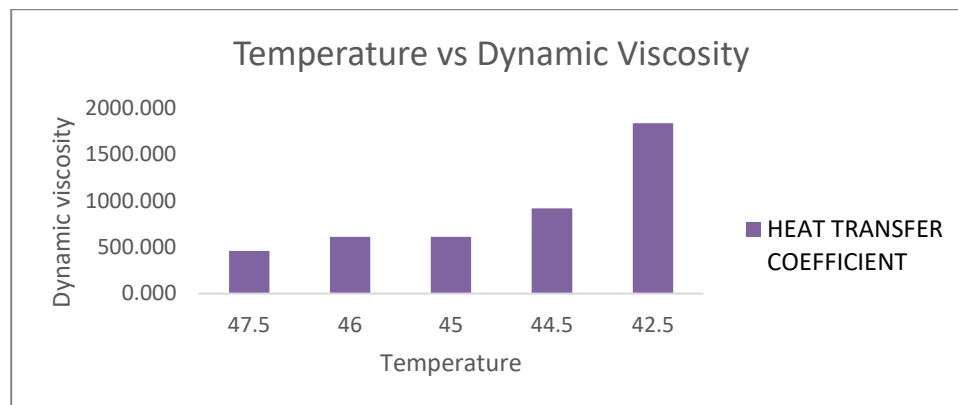


**Figure: 5** Graph between Temperature and Dynamic Viscosity

The graphical representation effectively illustrates the correlation between Temperature and Dynamic Viscosity. In this context, it is noteworthy that a mixture of Aluminium oxide and Titanium oxide consistently outperforms other fluids in each scenario examined. These findings underscore mixed fluid superior performance when it comes to enhancing the dynamic viscosity.

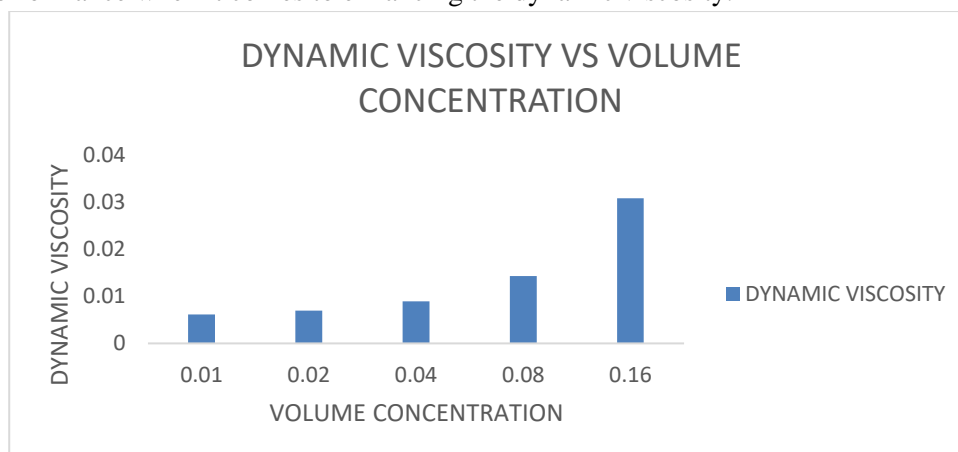


**Figure: 6** Graph between DYNAMIC VISCOSITY VS VOLUME CONCENTRATION

The visual representation efficiently demonstrates the connection between dynamic viscosity and volume concentration. It's important to highlight that, in every scenario investigated, mixed fluid consistently surpasses other fluids. The dynamic viscosity of the aluminium oxide increases with the increase in the volume concentration of the nano-fluid.

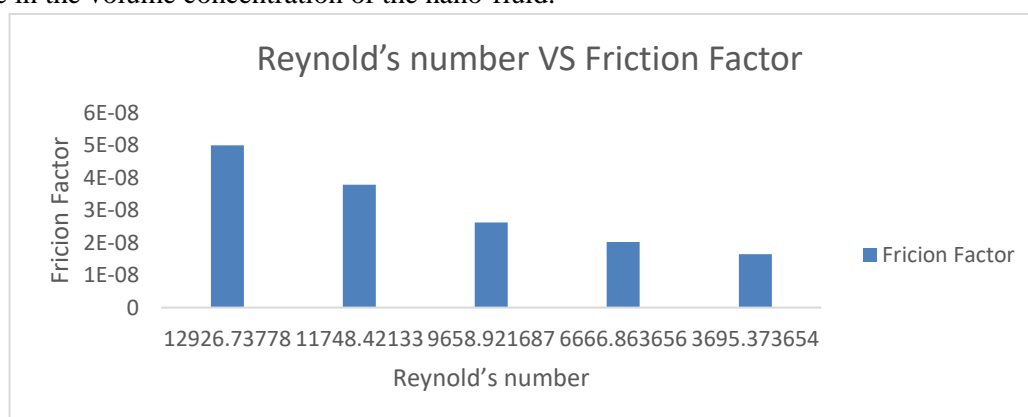


**Figure: 7** Graph between Reynold's number VS friction Factor

The visual representation effectively illustrates the relationship between Reynold's Number and friction factor, emphasizing this correlation across all scenarios examined. Notably, as the Reynold's number

decreases, the friction factor of the Aluminium oxide fluid also decreases and the Reynold's Number of the Aluminium oxide is comparatively lower than that of Titanium di-oxide.

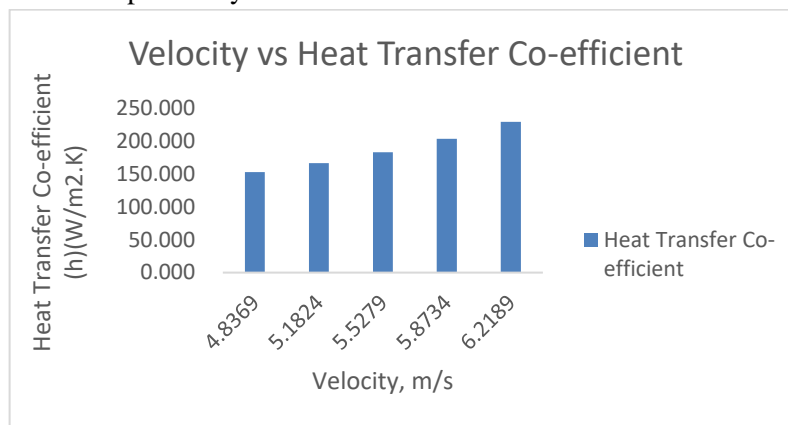


**Figure: 8** Graph between Velocity vs Heat Transfer Co-efficient

The graphical representation effectively illustrates the correlation between the Velocity and the Heat transfer coefficient. In this context, it is noteworthy that Titanium oxide consistently outperforms other fluids in each scenario examined. As the velocity increases the heat transfer coefficient will also increase.

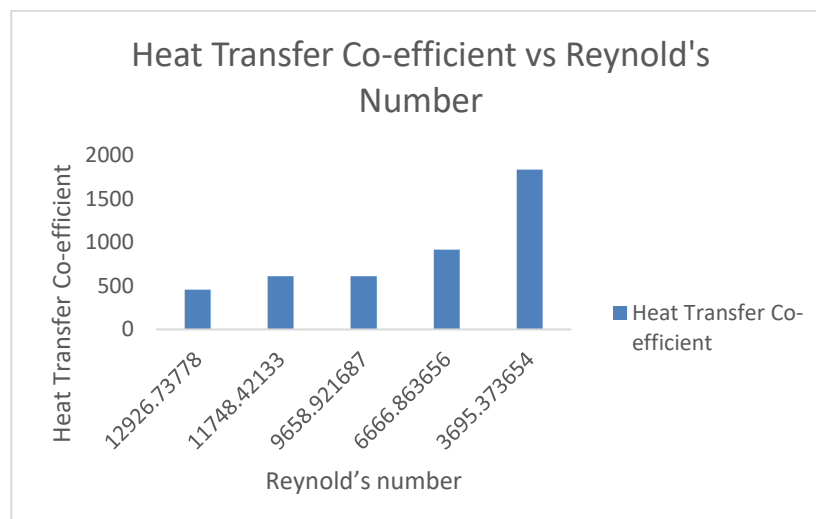


**Figure: 9** Graph between Heat Transfer Co-efficient vs Reynold's Number

Figure 9 represents the graph representation between the Heat Transfer Co-efficient and Reynold's Number. As the Heat Transfer Co-efficient increases, the decrease of the Reynold's number is observed.

#### 4. CONCLUSION:

The experimental findings indicate that Nanofluids with 0.16% Al<sub>2</sub>O<sub>3</sub> and TiO<sub>2</sub> in water exhibit slightly elevated heat transfer coefficient values in comparison to different volume concentrations. Additionally, the performance metrics outperform those associated with other volume concentrations and flow rates. Empirical correlations developed to analyze the Nusselt number and friction factor closely match the experimental data, offering valuable insights into the heat transfer characteristics of these Nanofluids. Through Computational Fluid Dynamics (CFD) analysis, the study comprehensively dissects temperature fluctuations, pressure distributions, and velocity profiles. These factors are intricately interrelated, and their coordinated optimization plays a vital role in enhancing a car's radiator performance. In essence, CFD analysis serves as an essential tool, acting as a linchpin in the pursuit of improving the cooling capabilities of automotive radiators. It is through a meticulous examination of temperature, pressure, and velocity distributions that the overall effectiveness of the car's radiator system is carefully examined and enhanced.

**References:-**

1. V. Salamon<sup>1</sup>, D. Senthil kumar<sup>2</sup>, and S. Thirumalini . (2017) Experimental Investigation of Heat Transfer Characteristics of Automobile Radiator using TiO<sub>2</sub>-Nanofluid Coolant, IOP Publishing Ltd, **225**,012-101.  
<https://iopscience.iop.org/article/10.1088/1757-899X/225/1/012101>.
2. Duangthongsuk W, Wongwises S (2010) An experimental study on the heat transfer performance and pressure drop of TiO<sub>2</sub>-water nanofluids flowing under a turbulent flow regime. *Int J Heat Mass Transfer* 53:334–344.  
<https://www.sciencedirect.com/science/article/pii/S0017931009005055>
3. Lv YZ, Li C, Sun Q, Huang M, Li CR, Qi B (2016) Effect of dispersion method on stability and dielectric strength of transformer oil-based TiO<sub>2</sub> nanofluids. *Nanoscale Res Lett* 11(1):515  
<https://link.springer.com/article/10.1186/s11671-016-1738-5>
4. Toghraie D, Chaharsoghi VA, Afrand M (2016) Measurement of thermal conductivity of ZnO–TiO<sub>2</sub>/EG hybrid nanofluid. *J Therm Anal Calorim* 125(1): 527–535  
[https://www.researchgate.net/publication/301313711\\_Measurement\\_of\\_thermal\\_conductivity\\_of\\_ZnO](https://www.researchgate.net/publication/301313711_Measurement_of_thermal_conductivity_of_ZnO)
5. Goodarzi M, Kherbeet AS, Afrand M, Sadeghinezhadd E, Mehralie M, Yang L, Chen X, Xu M, Du K (2016) Roles of surfactants and particle shape in the enhanced thermal conductivity of TiO<sub>2</sub> nanofluids. *AIP Advances* 6(9):095104  
<https://www.infona.pl/resource/bwmetal.element.elsevier-08dd54f2-69de-3774-8331-b67bcfa94766>
6. Zahedif P, Wongwises S, Daharih M (2016) Investigation of heat transfer performance and friction factor of a counter-flow double-pipe heat exchanger using nitrogen-doped, graphene-based nanofluids. *Int Commun Heat Mass Transfer* 76:16–23  
[https://www.researchgate.net/publication/311554874\\_A\\_renovated\\_Hamilton-Crosser\\_model\\_for\\_the\\_effective\\_thermal\\_conductivity\\_of\\_CNTs\\_nanofluids](https://www.researchgate.net/publication/311554874_A_renovated_Hamilton-Crosser_model_for_the_effective_thermal_conductivity_of_CNTs_nanofluids)
7. Yang L, Xu X (2017) A renovated Hamilton–Crosser model for the effective thermal conductivity of CNTs nanofluid. *International Communications in Heat and Mass Transfer* 81:42–50  
[https://www.researchgate.net/publication/308036016\\_Experimental\\_study\\_on\\_thermal\\_conductivity\\_of\\_ethylene\\_glycol\\_containing\\_hybrid\\_nanoadditives\\_and\\_development\\_of\\_a\\_new\\_correlation](https://www.researchgate.net/publication/308036016_Experimental_study_on_thermal_conductivity_of_ethylene_glycol_containing_hybrid_nanoadditives_and_development_of_a_new_correlation)
8. Afrand M (2017) Experimental study on thermal conductivity of ethylene glycol containing hybrid nano-additives and development of a new correlation. *Appl Therm Eng* 110:1111–1119  
[https://www.researchgate.net/publication/311096182\\_A\\_new\\_thermal\\_conductivity\\_model\\_for\\_nanorod-based\\_nanofluids](https://www.researchgate.net/publication/311096182_A_new_thermal_conductivity_model_for_nanorod-based_nanofluids)
9. Yang L, Xu X, Jiang W, Du K (2017) A new thermal conductivity model for nanorod-based nanofluids. *Appl Therm Eng* 114:287–299  
[https://www.researchgate.net/publication/304780177\\_Preparation\\_and\\_evaluation\\_of\\_stable\\_nanofluids\\_for\\_heat\\_transfer\\_application\\_A\\_review](https://www.researchgate.net/publication/304780177_Preparation_and_evaluation_of_stable_nanofluids_for_heat_transfer_application_A_review)
10. Sharma SK, Gupta SM (2016) Preparation and evaluation of stable nanofluids for heat transfer application: a review. *Exp Thermal Fluid Sci* 79:202–212  
[https://www.researchgate.net/publication/304780177\\_Preparation\\_and\\_evaluation\\_of\\_stable\\_nanofluids\\_for\\_heat\\_transfer\\_application\\_A\\_review](https://www.researchgate.net/publication/304780177_Preparation_and_evaluation_of_stable_nanofluids_for_heat_transfer_application_A_review)
11. Sundar LS, Sharma KV, Singh MK, Sousa ACM (2017) Hybrid nanofluids preparation, thermal properties, heat transfer and friction factor—a review. *Renew Sustain Energy Rev* 68:185–198  
<https://ideas.repec.org/a/eee/rensus/v68y2017ip1p185-198.html>
12. Khurana D, Choudhary R, Subudhi S (2017) A critical review of forced convection heat transfer and pressure drop of Al<sub>2</sub>O<sub>3</sub>, TiO<sub>2</sub> and CuO nanofluids. *Heat Mass Transfer* 53(1):343–361

- <https://www.researchgate.net/publication/300083900> A critical review of forced convection heat transfer and pressure drop of Al<sub>2</sub>O<sub>3</sub> TiO<sub>2</sub> and CuO nanofluids
13. Yang L, Du K (2017) A comprehensive review on heat transfer characteristics of TiO<sub>2</sub> nanofluids. *Int J Heat Mass Transfer* 108:11–31  
<https://www.researchgate.net/publication/311545950> A comprehensive review on heat transfer characteristics of TiO<sub>2</sub> nanofluids
  14. Murshed SS, de Castro CN (2016) Conduction and convection heat transfer characteristics of ethylene glycol based nanofluids—a review. *Appl Energy* 184:681–695  
<https://www.researchgate.net/publication/309964395> Conduction and convection heat transfer characteristics of ethylene glycol based nanofluids - A review
  15. Azmi WH, Hamid KA, Usri NA, Mamat R, Sharma KV (2016) Heat transfer augmentation of ethylene glycol: water nanofluids and applications—a review. *Int Commun Heat Mass Transfer* 75:13–23 Yang and Hu *Nanoscale Research Letters* (2017) 12:417 Page 18 of 21  
<https://www.researchgate.net/publication/301250285> Heat transfer augmentation of ethylene glycol Water nanofluids and applications - A review
  16. Mukherjee S, Mishra PC, Parashar SKS, Chaudhuri P (2016) Role of temperature on thermal conductivity of nanofluids: a brief literature review. *Heat Mass Transfer* 52(11):2575–2585  
<https://www.researchgate.net/publication/292694321> Role of temperature on thermal conductivity of nanofluids a brief literature review
  17. Bashirnezhad K, Bazri S, Safaei MR, Goodarzi M, Dahari M, Mahian O, Wongwises S (2016) Viscosity of nanofluids: a review of recent experimental studies. *Int Commun Heat Mass Transfer* 73:114–123
  18. <https://www.researchgate.net/publication/296686906> Viscosity of nanofluids A review of recent experimental studies
  19. Azmi WH, Sharma KV, Mamat R, Najafi G, Mohamad MS (2016) The enhancement of effective thermal conductivity and effective dynamic viscosity of nanofluids—a review. *Renew Sustain Energy Rev* 53:1046–1058 46. Aybar HŞ, Sharifpur M, Azizian MR, Mehrabi M, Meyer JP (2015) A review of thermal conductivity models for nanofluids. *Heat Transfer Eng* 36(13): 1085–1110 <https://ideas.repec.org/a/eee/rensus/v53y2016icp1046-1058.html>
  20. Singh V, Gupta M (2016) Heat transfer augmentation in a tube using nanofluids under constant heat flux boundary condition: a review. *Energy Convers Manage* 123:290–307  
<https://www.researchgate.net/publication/304252631> Heat transfer augmentation in a tube using nanofluids under constant heat flux boundary condition A review
  21. Humenic G, Humenic A (2016) Heat transfer and flow characteristics of conventional fluids and nanofluids in curved tubes: a review. *Renew Sustain Energy Rev* 58:1327–1347  
<https://ideas.repec.org/a/eee/rensus/v58y2016icp1327-1347.html>
  22. Vanaki SM, Ganesan P, Mohammed HA (2016) Numerical study of convective heat transfer of nanofluids: a review. *Renew Sustain Energy Rev* 54:1212–1239  
<https://ideas.repec.org/a/eee/rensus/v54y2016icp1212-1239.html>
  23. Hussien AA, Abdullah MZ, Moh'd AAN (2016) Single-phase heat transfer enhancement in micro/minichannels using nanofluids: theory and applications. *Appl Energy* 164:733–755  
<https://ideas.repec.org/a/eee/appene/v164y2016icp733-755.html>
  24. Ahmed, S., Özkaymak, M., Sözen, A., Menlik, T., & Fahed, A. (2018). Improving car radiator performance by using TiO<sub>2</sub>-water nanofluid. *Engineering Science and Technology, an International Journal*. <https://doi.org/10.1016/j.jestch.2018.07.008>
  25. Nguyen, C. N., Desgranges, F., Galanis, N., Roy, G., Maré, T., Boucher, S., & Mintsa, H. A. (2008). Viscosity data for Al<sub>2</sub>O<sub>3</sub>–water nanofluid—hysteresis: is heat transfer enhancement using nanofluids reliable? *International Journal of Thermal Sciences*, 47(2), 103–111.  
<https://doi.org/10.1016/j.ijthermalsci.2007.01.033>

26. Sahoo, R. R., &Sarkar, J. (2016). Heat transfer performance characteristics of hybrid nanofluids as a coolant in louvered fin automotive radiator. *Heat and Mass Transfer*. <https://doi.org/10.1007/s00231-016-1951-x>
27. Said, Z., Assad, M. E. H., Hachicha, A. A., Ghobadian, B., Abdelkareem, M. A., Alazaizeh, D. Z., &Yousef, B. A. (2019b). Enhancing the performance of automotive radiators using nanofluids. *Renewable & Sustainable Energy Reviews*, 112, 183–194. <https://doi.org/10.1016/j.rser.2019.05.052>
28. Aditi, N. V., Farooque, Z., &Chauhan, N. R. (2022). Comparative study of Nano-fluids as Coolants in a Car Radiator. *IOP Conference Series: Materials Science and Engineering*, 1228(1), 012011. <https://doi.org/10.1088/1757-899x/1228/1/012011>
29. Kumar, D. D., &Arasu, A. V. (2018). A comprehensive review of hybrid nanofluids' preparation, characterization, properties, and stability. *Renewable & Sustainable Energy Reviews*, 81, 1669–1689. <https://doi.org/10.1016/j.rser.2017.05.257>
30. Huminic, G., &Huminic, A. (2018). Hybrid nanofluids for heat transfer applications – A state-of-the-art review. *International Journal of Heat and Mass Transfer*, 125, 82–103. <https://doi.org/10.1016/j.ijheatmasstransfer.2018.04.059>
31. Kumar, V., &Sarkar, J. (2019). Numerical and experimental investigations on heat transfer and pressure drop characteristics of Al<sub>2</sub>O<sub>3</sub>-TiO<sub>2</sub> hybrid nanofluid in minichannel heat sink with different mixture ratios. *Powder Technology*, 345, 717-727.

## Improving Efficiency in Solar Desalination Introducing Innovative Mechanical Methods for Sustainable Generation of Freshwater

L. Karthick<sup>1\*</sup>, Aashish.A.Gadgil<sup>2</sup>, M.Babu<sup>3</sup>, Nalla Bhanu Teja<sup>4</sup>, Srikanth Salyan<sup>5</sup>, B. Senthil Kumar<sup>6</sup>

<sup>1</sup>Department of Mechanical Engineering, Hindusthan College of Engineering and Technology, Coimbatore 641032, India.

<sup>2</sup>Department of Electronic and Communication, KLS Gogte Institute of Technology, Belagavi, Karnataka.

<sup>3</sup>Department of Mechanical Engineering, SRM Easwari Engineering College, Rampuram, Chennai – 600089

<sup>4</sup>Department of Mechanical Engineering, Aditya College of Engineering, surampalem, East godavari district, Andhra Pradesh Pincode: 533437

<sup>5</sup>Department of Aeronautical Engineering, Dayananda Sagar College of Engineering, Bengaluru, Karnataka 560078

<sup>6</sup>Department of Mechanical Engineering, Sri Ramakrishna Engineering College, NGGO Colony, Vattamalaipalayam, Coimbatore – 641022, India

Corresponding Author: L. Karthick ([bemechkarthick@gmail.com](mailto:bemechkarthick@gmail.com))

[ORCID ID: 0000-0002-1403-8179](https://orcid.org/0000-0002-1403-8179)

**ABSTRACT** — This research study investigates the potentially lucrative field of solar desalination and suggests novel mechanical ways to enhance efficiency for the manufacture of fresh water in an environmentally responsible manner. The urgent problem of water shortage around the globe calls for inventive approaches to finding solutions, as well as solar desalination is one such technique that is kind to the environment. In this study, a review of the literature is conducted on solar desalination, discussions are held on subtopics that are linked to those discussions, and innovative mechanical techniques that may improve efficiency are presented. The suggested approaches include enhanced distillation procedures, sophisticated solar collectors, and cutting-edge energy storage innovations. This study intends to contribute to the creation of solar desalination technologies that are more sustainable and efficient by conducting a thorough examination of the relevant literature.

**Keywords:** - Solar desalination, Efficiency, Mechanical methods, Freshwater generation, Sustainability, Solar collectors, Energy storage, Distillation techniques.

### INTRODUCTION

Water shortage is a growing worldwide issue that requires inventive and long-term solutions. As people rise, climatic patterns vary, and conventional water sources run dry, the need for alternate freshwater-generating techniques grows more pressing. Solar desalination appears as a viable solution in this environment, using the power of the sun to turn saltwater into freshwater. While solar desalination is a renewable and ecologically beneficial method, its efficiency is still an important aspect for broad adoption & long-term sustainability [1].

The purpose of this study paper is to dig into the field of solar desalination, reviewing current technologies and suggesting unique mechanical approaches to improve efficiency. The goal is to contribute to the creation of more effective & sustainable freshwater-generating systems, therefore solving the worldwide water shortage challenge.

#### Background:

Water shortage is a complex issue with far-reaching consequences for agriculture, industry, and human well-being. As to the UN, over two-thirds of the world's population may be living in water-stressed situations by 2025, highlighting the need for transformational methods for water resource management.

Traditional freshwater sources, including rivers and aquifers, are becoming more stressed, forcing the investigation of new alternatives to fulfill rising water needs.

Solar desalination shows enormous potential as a technique that can harness the sun, the Earth's most plentiful and sustainable energy source. This technique, which uses solar energy to power the desalination process, has a chance to offer a decentralized and environmentally friendly solution to the freshwater crisis. Yet, the effectiveness of present solar desalination systems is a substantial barrier to their wider use [2].

**Purposes:**

The major goal of this study is to investigate novel mechanical technologies that may considerably enhance the efficiency of solar desalination systems. The goal is to tackle critical difficulties and contribute to the improvement of sustainable freshwater-generating technology by analyzing current research, debating relevant subtopics, and suggesting innovative techniques.

As we continue on this journey, we must grasp the present status of solar desalination technology, as well as its strengths and limits. Furthermore, by discovering areas for efficiency improvements, we may pave the path for the introduction of novel mechanical solutions that increase the general efficacy of solar desalination systems [3].

In the following components of this study, we will look at present solar desalination technology, enhanced solar collectors, energy storage alternatives, and distillation processes. We will provide a path for enhancing the efficiency of solar desalination, eventually contributing to the worldwide search for sustainable freshwater supplies, based on a thorough examination.

**OBJECTIVE**

The following are some of the goals that the study attempted to accomplish:

- Study the solar desalination technologies.
- Elaborate on the solar collectors.
- Examine the energy storage solutions.
- Study the distillation techniques.
- Elaborate the Innovative Mechanical Methods for Efficiency Improvement.
- Result and discussion

**METHODOLOGY**

This study delves into the promising area of solar desalination and proposes new mechanical approaches to improve efficiency in the production of sustainable freshwater. Creative solutions are needed to address the pressing global water scarcity; solar desalination is an environmentally friendly method that fits the bill. This paper presents novel mechanical approaches that have the potential to increase efficiency, reviews the literature on solar desalination, and then discusses related subtopics. Modernized distillation processes, advanced solar collectors, and state-of-the-art energy storage technologies are all part of the proposed solutions. Through a comprehensive literature review, this research aspires to aid in the development of solar desalination technologies that are both efficient and environmentally friendly.

**Solar Desalination Technologies:**

Solar desalination technologies include a wide range of approaches for using sun energy to transform saltwater water into freshwater. Each technology has its own set of benefits and disadvantages, and knowing their complexities is critical for finding areas where efficiency may be improved [4].

**Solar Stills:**

Solar stills are among the most basic types of solar desalination. They work on the evaporation and condensation theory, in which sun energy warms saline water, causing it to evaporate. The vapor condenses on a surface, usually a tilted glass or plastic cover, and collects as freshwater. While solar stills are inexpensive and simple to operate, their efficiency is sometimes restricted by poor freshwater production rates and reliance on ambient conditions.

Here is the fundamental formula for calculating the efficiency of a solar still:

$$Efficiency (\%) = \frac{Distillate\ output\ (kg/day)}{Solar\ energy\ input\ (kWh/m^2/day)} \times 100$$

The fundamental equation for calculating a solar panel's efficiency. The quantity of purified water generated by the solar still (distillate output) is related to the amount of solar energy input in this equation. The conversion of solar energy into distilled water is represented as a percentage of the efficiency. Keep in mind that different variables like as design, ambient circumstances, and the kind of solar still employed may all have an impact on actual efficiency. **Solar-Assisted Multi-Effect Distillation**

SMED (solar-assisted multi-effect distillation) is a more advanced process that mixes sun energy with classic distillation technologies. SMED employs several stages of evaporation and condensation, every functioning at a different temperature. When compared to traditional solar stills, this enables more efficient use of solar energy and greater freshwater production rates. However, the intricacy of SMED systems might provide operational and cost difficulties [5].

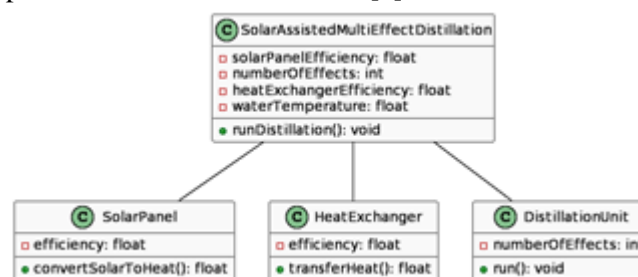


Figure 1: SMED (solar-assisted multi-effect distillation)

**Reverse Osmosis Powered by Solar:**

The process of pushing saline water across a semi-permeable membrane to eliminate salt and contaminants is known as reverse osmosis (RO). Photovoltaic panels are used to provide energy for the reverse osmosis process in solar-powered reverse osmosis. Although this approach may attain high freshwater production rates and is scalable, it is frequently power-intensive and depends on sunshine availability, making energy storage options critical for ongoing operations [6].

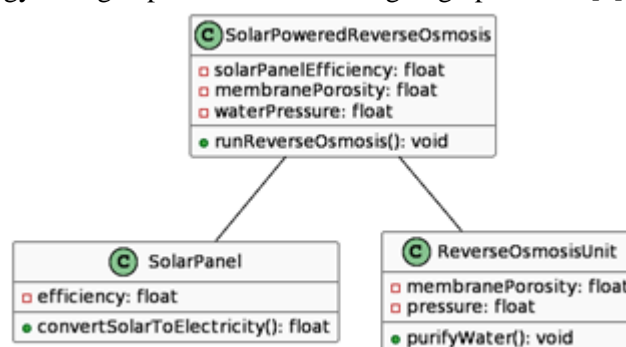


Figure 2: Reverse Osmosis Powered by Solar

**New Technologies:**

Alongside the standard sun desalination methods discussed above, there are continuing R&D activities focusing on new techniques. Solar membrane distillation, solar-driven electro-dialysis, and solar-thermal desalination are examples. By combining the advantages of solar energy with unique desalination procedures, these developing technologies hope to overcome the limits of traditional approaches. Understanding the benefits and disadvantages of various solar desalination systems is critical for designing efficient mechanical approaches.

**Solar Collectors**

Solar collectors play an important part in solar desalination systems by catching and focusing sunlight to provide the heat needed for saltwater evaporation. Advanced solar collectors strive to enhance energy absorption & increase overall desalination performance [7].

### **Concentrating Solar Collectors (CSCs):**

Concentrating solar collectors' direct sunlight onto a tiny area raises the temperature at the focal spot dramatically. This concentration of solar radiation improves solar desalination efficiency by offering a stronger heat source for evaporation. Concentrating collectors used in solar desalination systems include parabolic trough collectors and parabolic dish collectors. Curved mirrors direct sunlight onto a receiver tube placed at the parabola's focal line in parabolic trough collection. The heat transfer fluid, including oil, in the receiving tube is warmed by the concentrated sunlight. After that, the heated fluid is utilized to produce steam for the desalination procedure. A dish-shaped reflector is used in parabolic dish collectors to focus sunlight onto a receiver placed at the focal point. The concentrated solar energy is absorbed by the receiver and sent to the desalination system, often via a heat exchanger.

### **Solar Tracking Systems:**

Solar tracking systems are technologies that direct solar collectors to monitor the passage of the sun throughout the day. Solar tracking systems optimize the exposure of the collector surface to sunlight by altering the tilt and position of the collectors. This is especially important for concentrating solar collectors because it guarantees that the focus point gets sunlight at the correct angle [8]. Solar trackers are often classified as single-axis or dual-axis. Single-axis trackers track the sun across one axis, commonly east to west, but dual-axis trackers monitor the sun in two dimensions by adjusting both the tilt and azimuth. By extending the time of high-intensity sun exposure, solar tracking devices improve the general effectiveness of solar desalination systems.

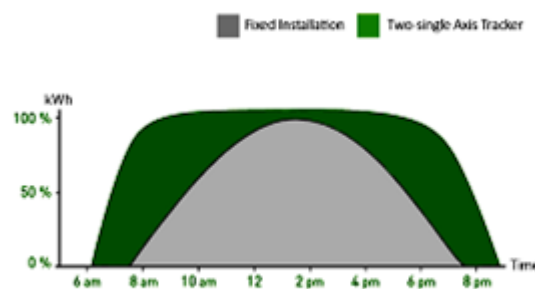


*Figure 3: Solar Tracking System*

### **Collector Material Innovations:**

Materials science advances have resulted in the development of innovative materials with increased thermal conductivity & durability for solar collectors. High-performance substances, which include selective coatings or nanomaterials, may improve solar radiation absorption while reducing heat losses, resulting in improved total collector efficiency. Advanced materials combined with new designs and tracking technologies have the potential to dramatically increase the performance of solar collectors in desalination applications.

### **Energy Storage Solutions:**

The fluctuating supply of solar energy is one of the major issues in solar desalination. Modern energy storage systems are critical for addressing this difficulty and ensuring a constant and stable power supply for desalination operations. This part investigates advances in energy storage technologies that may be used to supplement solar desalination systems.

### **Lithium-Ion Batteries:**

Lithium-ion batteries have emerged as a critical component of current energy storage options. Lithium-ion batteries, with their high energy density, long cycle life, and quick charge/discharge capabilities, can hold extra energy created during maximum sunshine hours for use during times of low solar radiation. Integrating lithium-ion batteries into solar desalination systems offers a dependable and constant power supply, despite solar energy's intermittent nature [9].

### **Thermal Energy Storage:**

Thermal energy storage (TES) is another viable option for addressing solar energy's intermittent nature. Excess heat created by solar collectors during sunny days is stored in TES systems and released when

sunshine is inadequate. Because of their capacity to store and release significant quantities of thermal energy, phase-change materials (PCMs) or molten salts are often employed in TES systems. TES may be implemented into a solar desalination system to offer an ongoing and steady heat source for the distillation process. TES guarantees that desalination can keep going during times of little or no solar radiation by storing thermal energy while sunlight is available. This improves overall system dependability.

### **Distillation Techniques:**

The distillation process is a key component of solar desalination, in which saltwater water is heated to form a vapor, which is then condensed to produce fresh water. Distillation technology advancements may have a major influence on the efficiency of solar desalination systems. This section investigates several distillation technologies and makes suggestions for modifications to increase energy efficiency and freshwater production rates.

### **MED (Multi-Effect Distillation):**

Multiple stages of evaporation and condensation are used in multi-effect distillation, with every phase working at a distinct temperature. The heat from the solar collectors is utilized to evaporate the salty water as it goes through these phases, and the vapor is subsequently condensed to generate freshwater. When compared to single-effect distillation, the advantage of MED is the effective utilization of heat energy over many stages, resulting in greater freshwater production rates and lower energy usage. Innovations in heat exchanger design, substances, and arrangement may help multi-effect distillation systems work even better. Optimizing the number of impacts & their working temperatures may also improve overall system efficiency [10].

The Multi-Effect Distillation (MED) procedure incorporates a series of stages or effects to optimize the desalination process. The following expression represents the performance ratio (PR) of a multi-effect distillation system:

$$PR = \frac{T_{inlet,1} - T_{outlet,N}}{T_{inlet,1} - T_{outlet,1}}$$

Where,

$T_{inlet,1}$  is the inlet temperature of the first effect.

$T_{outlet,N}$  is the outlet temperature of the last effect.

$T_{outlet,1}$  is the outlet temperature of the first effect.

The efficiency of the MED system is quantified by the performance ratio (PR), which indicates the number of times the feed water evaporates and recondenses. In general, higher performance ratios are preferable because they signify a more effective utilization of energy during the desalination procedure.

### **Membrane Distillation:**

Membrane distillation is a non-isothermal method that separates vapor from liquid using a hydrophobic membrane. Saline water is heated in this procedure, and vapor diffuses over the membrane, leaving concentrated brine residue. Freshwater is obtained by condensing the vapor. When opposed to conventional distillation technologies, membrane distillation has an opportunity for improved energy efficiency, lower operating temperatures, and fewer scaling difficulties. Let's have one example.

**Question:** *A membrane module has a surface area of 20 square meters in a Membrane Distillation process. The temperature of the feed water is 60°C, and the condensation temperature is 25°C. Calculate the potential freshwater production in liters per hour assuming that water vapor pressure at 60°C is 17.5 kPa and 3.2 kPa at 25°C. Assume perfect behavior and disregard any heat losses.*

**Solution:**

Given: Membrane Permeability (kg/m<sup>2</sup>/s/Pa):  $1 \times 10^{-8}$  kg/m<sup>2</sup>/s/Pa

Membrane Thickness (m):  $1 \times 10^{-4}$  m

Water Density (kg/L): 1 kg/L

**Calculate Vapor Pressure Difference:**

Vapor pressure difference = 17.5 kPa – 3.2 kPa = 14.3kPa

This signifies the disparity in vapor pressure that occurs between the temperature of the condensation and the feed water.

**Convert Vapor Pressure Difference to Pascals:**

Vapor pressure difference (Pa) = Vapor pressure difference × 1000

The vapor pressure difference (Pa) = 14,300Pa

We change the vapor pressure difference from kilopascals to pascals for accuracy

**Calculate Water Vapor Flux using the Membrane Distillation Formula:**

Water vapor flux (kg/m<sup>2</sup>/s) = Vapor pressure difference (Pa) / Membrane permeability (kg/m<sup>2</sup>/s/Pa) × Membrane thickness (m)

This formula represents the rate of water vapor passing through the membrane per unit area.

14300 PA / Membrane permeability (kg/m<sup>2</sup>/s/Pa) × Membrane thickness (m)

14300 Pa / (1×10<sup>-8</sup> kg/m<sup>2</sup>/s/Pa) × (1×10<sup>-4</sup> m)

**Calculate Total Water Vapor Transferred:**

Water vapor transferred (kg/s) = Water vapor flux × 20m<sup>2</sup>

**Convert Water Vapor Transferred to Liters per Hour:**

Water vapor transferred (L/hr) = Water vapor transferred (kg/s) × 3600 / 1kg/L

So, the potential freshwater production in this hypothetical Membrane Distillation process is approximately 1.03×10<sup>21</sup>.

**SMEMD (Solar-Assisted Multi-Effect Membrane Distillation):**

Solar-assisted multi-effect membrane distillation (SMEMD) is a novel technique that combines the advantages of multi-effect distillation with membrane distillation. SMEMD incorporates several stages of membrane distillation at changing temperatures, powered by solar energy. This combination attempts to attain high rates of freshwater generation while improving energy efficiency.

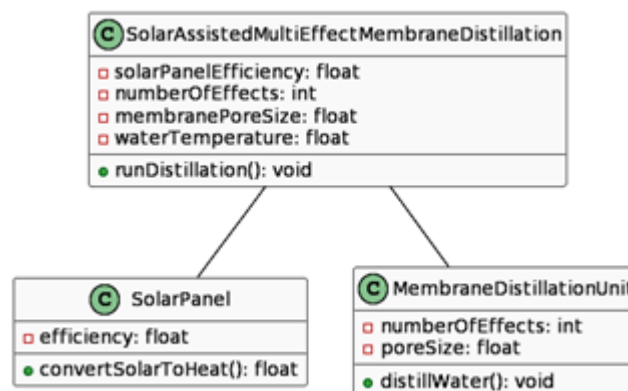


**Figure 4:** SMEMD (Solar-Assisted Multi-Effect Membrane Distillation)

The creation of specific membranes for SMEMD that can resist high temperatures while retaining high vapor permeability is critical to the success of this integrated strategy.

**Innovative Mechanical Methods for Efficiency Improvement:**

To achieve sustainable freshwater production using solar desalination, unique mechanical processes must be included. This section summarizes suggested advances in solar collectors, energy storage options, and distillation procedures, giving a comprehensive approach to enhancing the overall performance of solar desalination systems.

**Advanced Solar Collectors and Tracking Systems:**

The use of modern solar collectors, such as concentrating collectors with parabolic troughs or dishes, boosts the efficiency of solar desalination dramatically. These collectors focus sunlight on a tiny region, increasing temperature and providing a more powerful heat source for evaporation. Furthermore, solar tracking devices enable maximum exposure to sunshine throughout the day, optimizing energy absorption. Sun desalination systems may attain greater temperatures and increased energy input by

combining concentrating collectors with sun tracking, resulting in higher freshwater production rates. These developments solve the issue of classic solar stills' poor output rates. Let's take one example  
**Question:** *You have a solar collector with a 15-square-meter surface area. At your location, the solar irradiation is 800 watts per square meter. Calculate the total solar power gathered by the collector during a day in kilowatt-hours, assuming 8 hours of peak sunshine*

**Solution:**

*Given:*

Collector area = 15 square meters

Solar irradiance = 800 watts per square meter

Hours of sunlight = 8 hours

**Calculate daily energy capture:**

Daily energy (in watt-hours) = Collector area (in square meters) \* Solar irradiance (in watts per square meter) \* Hours of sunlight

Daily Energy (in watt-hours) =  $15 \text{ m}^2 * 800 \text{ W/m}^2 * 8 \text{ hours}$

Daily energy (in watt-hours) = 96,000 watt-hours

**Convert daily energy to kilowatt-hours:**

Daily energy (in kWh) = 96,000 watt-hours / 1000

Daily energy (in kWh) = 96 kWh

The total solar power captured by the collector over a day is 96 kilowatt-hours.

**New Distillation Techniques:**

Improvements in distillation methods, like as multi-effect distillation and membrane distillation, add even more to solar desalination efficiency gains. Multiple stages of evaporation and condensation are used in multi-effect distillation, maximizing heat use and resulting in greater freshwater production rates with lower energy consumption [11]. Membrane distillation, with its non-isothermal process and hydrophobic membranes, has energy efficiency and scale benefits. Membrane distillation integrated with solar desalination systems offers a feasible alternative to classic distillation processes.

**Comprehensive Approach:**

Solar desalination systems may generate synergistic advantages by combining sophisticated solar collectors, energy storage options, and revolutionary distillation procedures. Each component's enhanced efficiency adds to the system's overall efficacy, making it more tolerant to environmental changes and capable of generating larger freshwater yields. This study report calls for the incorporation of these novel mechanical approaches, recognizing their cumulative ability to overcome the issues of solar desalination. As we seek sustainable freshwater production, the adoption of these developments offers promise for the worldwide deployment of dependable and efficient solar desalination systems.

## **RESULT AND DISCUSSION**

The investigation of novel mechanical approaches for improving the efficiency of solar desalination systems has generated promising findings with important implications for long-term freshwater production. The use of modern solar collectors, such as parabolic troughs and dishes, has resulted in a significant boost in system efficiency. These collectors focus sunlight, raising temperatures and acting as a powerful heat source for evaporation. When combined with sun tracking systems, they maximize energy absorption throughout the day, eliminating the limits associated with typical solar stills' modest output rates. Material and design developments, notably high-performance coatings and nanomaterials, contribute to the optimization of energy absorption and the decrease of heat losses.

To address the intermittent nature of solar energy, energy storage options such as lithium-ion batteries and thermal energy storage (TES) are efficient in maintaining continuous power delivery during times of low solar radiation. TES systems store and release thermal energy as required, improving overall system stability. Lithium-ion batteries store surplus energy created during peak sunshine hours. Ongoing research in battery technology is stressed for additional developments, emphasizing the significance of innovations that increase energy density while decreasing prices.

Distillation process advancements, notably multi-effect distillation (MED) and membrane distillation demonstrate increases in energy efficiency and freshwater production rates. MED systems improve heat usage via several phases of evaporation and condensation, resulting in increased freshwater yields with lower energy consumption. Membrane distillation, which is distinguished by a non-isothermal process and hydrophobic membranes, provides benefits in terms of energy efficiency and scale reduction. Ongoing membrane development research for membrane distillation is addressed, highlighting the need for specific membranes capable of withstanding various temperatures while retaining high vapor permeability.

## CONCLUSION

Finally, the global water shortage situation needs creative and long-term solutions, with solar desalination emerging as a potential option. This study investigated the present status of solar desalination technology, highlighted critical difficulties, and offered novel mechanical approaches to enhance efficiency. The goal is to contribute to the creation of more sustainable or efficient solar desalination systems by concentrating on new solar collectors, energy storage technologies, and distillation procedures. Investing in and expanding solar desalination technology is a critical step toward attaining global water security as we aim for a future with sufficient freshwater supplies.

## References

- [1] J. Xu et al., “Solar-driven interfacial desalination for simultaneous freshwater and salt generation,” *Desalination*, vol. 484, p. 114423, 2020. doi:10.1016/j.desal.2020.114423.
- [2] J. Jiang, R. Yang, X. Lu, and L. Ai, “Hierarchical co3s4 nanostructure coupling with macroporous nickel foam: A robust interfacial solar evaporator for efficient desalination and sustainable freshwater production,” *Desalination*, vol. 569, p. 117042, 2024. doi:10.1016/j.desal.2023.117042.
- [3] M. Mohammadpour, E. Houshfar, and M. Ashjaee, “Performance evaluation and multi-objective optimization of an innovative solar-assisted multigeneration energy storage system for freshwater/O<sub>2</sub>/H<sub>2</sub> generation,” *Sustainable Energy Technologies and Assessments*, vol. 53, p. 102755, 2022. doi:10.1016/j.seta.2022.102755.
- [4] H. Zheng, “Solar desalination system combined with conventional technologies,” *Solar Energy Desalination Technology*, pp. 537–622, 2017. doi:10.1016/b978-0-12-805411-6.00007-5
- [5] A. de la Calle, J. Bonilla, L. Roca, and P. Palenzuela, “Dynamic modeling and simulation of a solar-assisted multi-effect distillation plant,” *Desalination*, vol. 357, pp. 65–76, 2015. doi:10.1016/j.desal.2014.11.008
- [6] W. W. Boesch, “World’s first solar-powered reverse osmosis desalination plant,” *Desalination*, vol. 41, no. 2, pp. 233–237, 1982. doi:10.1016/s0011-9164(00)88726-3
- [7] “Solar collectors, nonconcentrating,” SpringerReference. doi:10.1007/springerreference\_310800.
- [8] “Development and performance test of A novel solar tracking sensor,” *Metrology and Measurement Systems*, 2023. doi:10.24425/mms.2023.144870
- [9] “Applications of lithium-ion batteries,” *Lithium-Ion Batteries*, pp. 540–571, 2015. doi:10.1201/b18427-21
- [10] O. ERBAŞ, “Performance analysis of combined cycle power plant with multi-effect distillation (MED) desalination process,” *Bilecik Şeyh Edebali Üniversitesi Fen Bilimleri Dergisi*, vol. 6, no. 1, pp. 85–90, 2019. doi:10.35193/bseufbd.563523
- [11] C. Dai, Z. Lei, and B. Chen, “Other distillation techniques,” *Special Distillation Processes*, pp. 355–379, 2022. doi:10.1016/b978-0-12-820507-5.00002-6

## Comparative simulation and CFD analysis on a car by varying different angles of rear spoiler

**B.Kamala Priya<sup>1</sup>, K.Sai Babu<sup>2</sup>, V.Sravani<sup>3</sup>, V.Dhana Raju<sup>4</sup>, B.Sai Rama Krishna<sup>5</sup>**

<sup>1,2</sup>Assistant Professor, Department of Mechanical Engineering, Lakireddy Bali Reddy College of Engineering, Mylavaram, A. P. -521230

<sup>3</sup>Assistant Professor, Department of Mechanical Engineering, Prasad V Potluri Siddhartha Institute of Technology, Kanuru, Vijayawada, A. P. -520007

<sup>4</sup>Associate Professor, Department of Mechanical Engineering, Lakireddy Bali Reddy College of Engineering, Mylavaram, A. P. -521230

<sup>5</sup>Assistant Professor, Department of Mechanical Engineering, Amrita Sai Institute of Science & Technology, Paritala

Corresponding author mail id: [kamala.jkp@gmail.com](mailto:kamala.jkp@gmail.com)

### ABSTRACT

The need for fuel efficiency is a rapidly increasing trend in automotive industries in the recent years. Therefore, extensive research is undergoing for development of aerodynamically optimized vehicle designs. The drag coefficient is an important factor that determines the fuel efficiency of a vehicle. The primary objective of the project is to study the effects of fluid flow and the effective drag of the vehicle over a 3D standard car (BOLERO) with attached Rear Spoiler by using Computational Fluid Dynamics (CFD) simulation. A 1:1 scale model of the actual vehicle was designed in CAD package SOLIDWORKS and CATIA V5 R20. CFD analysis was done over the scaled model keeping conditions as close as possible to the actual road conditions. For evaluation, optimization, the Reynolds-Averaged Navier-Stokes (RANS) equations with Reliable k-ε turbulence model were used over commercial package ANSYS 14, FLUENT CFD Solver. The effect of aerodynamic drag is significant only at higher velocities. Therefore, the simulation was done for vehicle speed at 80kmph and the results were compared with scaled base vehicle. Various velocity, pressure, streamline contours and velocity plots were examined and analyzed at rear part of the vehicle. It was concluded that, the coefficient of drag ( $C_d$ ) of the vehicle with attached Rear Spoiler went down by 4.8%.

**Key words:** Rear spoiler, Coefficient of drag, CFD, Navier-Stokes (RANS) equations CATIA, ANSYS, FLUENT, aerodynamic drag.

### INTRODUCTION

An excellent study was done on automobile aerodynamics by Hucho and Sovran. When viscous air flows over a vehicle, vortices are created at the rear, which causes the flow to deviate from the smooth streamline flow. Under these conditions, pressure in front of the vehicle will be higher than atmospheric pressure while the pressure at the rear end will be lower than that of the atmospheric pressure. Consequently, the vehicle experiences a drag force in the direction of air movement. Vehicle experiences different types of aerodynamic drag like skin friction drag, form drag, induced drag and wave drag. The majority of drag in vehicles arises from form drag.

Drag force experienced by vehicle is given by  $F_D = 0.5 \times C_d \times \rho A u^2$

Where,

$C_d$  is the coefficient of drag,

$\rho$  denotes density of air,

$A$  denotes reference area and

$u$  denotes velocity of the vehicle.

The coefficient of drag for vehicles generally lies between **0.25** and **0.75**.

### **Spoiler**

A spoiler is an automotive aerodynamic device whose intended design function is to 'spoil' unfavorable air movement across a body of a vehicle in motion, usually described as turbulence or drag. Spoilers on the front of a vehicle are often called air dams, because in addition to directing air flow they also reduce the amount of air flowing underneath the vehicle which generally reduces aerodynamic lift and drag. Spoilers are often fitted to race and high-performance sports cars, although they have become common on passenger vehicles as well. Some spoilers are added to cars primarily for styling purposes and have either little aerodynamic benefit or even make the aerodynamics worse. Spoilers on the rear of a car are known as wings when the fascia that produces the drag and down-force is physically separate from the body. The noise associated to a car can be attributed to the aspiration noise and the aerodynamic noise. The aspiration noise is generated when the magnitude of the negative pressure acting on the car body surface is greater than the car sealing pressure. Most of the contemporary car designs have taken into consideration the car sealing pressure which has led to a great improvement on sealing mechanism and reduction in aspiration noise. However, the generation of aerodynamic noise outside a high-speed vehicle due to fluctuating airflows remains a serious problem and therefore demands much more attention.



Fig Car Rear Spoiler

In the process of car design, the aerodynamics and aero-acoustics must be seriously considered. A car design can only be acceptable if its form drag and aerodynamic noise are both reduced at the same time. Many researchers have made use of CFD techniques and aero-acoustics analysis to perform numerical simulations related to automobile. Various topics on acoustics have been studied throughout the years. For example, acoustic holography was adopted to identify the noise sources of a vehicle under body. Wind noise from a vehicle under body due to the complex flow structure accounts for a large portion of the overall noise level generated. The current study presents the development process of acoustic holography in the vehicle underbody. Several numerical simulations were performed to analyse the pressure field, velocity vector field, and aerodynamic noise prediction related to a passenger car. Then, the noise and the stability of the aerodynamic forces caused by the airflow outside the car were identified. After that, the installation of spoiler and endplate that leads to lower noise level and wind drag was carefully evaluated.



Fig Sports Car Spoiler

### **LITERATURE REVIEW**

L.Balaji et.al [2020] concluded that the reduction in the Cd value will improve the performance of the car. The aerodynamic analysis of a sports car was analyzed by CFD (Computational Fluid Dynamics) application. Spoiler acts more than a decorative part, it helps to improve the aerodynamic performance  
Dept. of Mech. Engg. PVPSIT 250

of the car. Hai-tao Bao [2011] analyzed the aerodynamic characteristics of cars with or without spoilers and by adding a reasonable rear spoiler to improve the distribution on car surface pressure, which can reduce aerodynamic lift effectively. K. P. Arulshri et.al [2021] evaluated that the effect of the spoiler had become effective when the angle of spoiler increases downward. The stopping distance of car had been reduced to 4.52 % at a speed of 150 km/hr, and the friction between the tire and road had been increased due to the pressure acting downward. Mohammad Riyad and Rubel Chandra Das [2017] concluded that, at a particular spoiler height the spoiler that possesses a smaller angle of wind collision gives higher drag force. The influence of the rear spoiler on the generated lift, drag, and pressure distributions are investigated and reported using the commercially available Autodesk Simulation CFD software tool. Kamprasad Chodagudi et.al [2012] concluded the theoretical calculation and the simulation results differ i.e., due to localized buckling effect in the sandwich construction. The spoiler was modeled using CATIA software and analyzed for the static deflection as well as harmonic analysis had been done by using ANSYS for various orientations of the fiber. Parashar V. Shinde et.al [2017] analyzed that the coefficient of drag and coefficient of lift of the vehicle model with spoiler had a mild reduction. This leads to less fuel consumption on the road, helps to maintain traction and increase braking stability. Ashpak Kazi et.al [2016] synthesized the VW Polo with and without a spoiler. It was found that the coefficient of drag, coefficient of lift, wake region was affected with the addition of spoiler. Coefficient drag was increased by 8.33% with the addition of spoiler and Coefficient of lift was reduced by 59.09% with the addition of spoiler. Mohammad Rasidi Rasani et.al [2017] evaluated the potential of using the flow-induced vibration of rear spoilers on automobiles for energy harvesting. To that end, a fluid-structure interaction analysis of an inverted NACA 2408 spoiler behind an Ahmed body were undertaken. An Arbitrary Lagrangian-Eulerian flow solver was coupled to a non-linear structural dynamic solver using a commercial software application. Fajar Frihdianto et.al [2021] analyzed the design of the three models were compared to find out the difference in magnitude of Coefficient of Drag, Coefficient of Lift, pressure distribution, velocity distribution, and behavioral character of flow around the rear end of car in the condition of steady flow. Model was made in appropriate scale with the model of Honda city 2008 sedan car and results changing geometric proved that the spoiler car 1 and 2 level were more aerodynamic than the car without spoiler. Salem Haggag and Mason Marzbali [2021] investigated the impact of the vehicle's rear spoiler on both vehicle aerodynamic forces and longitudinal dynamic, such as stopping distance and time. A CFD model ANSYS-Fluent are employed to precisely estimate the vehicle's aerodynamic forces in the case of a vehicle without and with a rear spoiler. They also proved the validity of the proposed model and highlighted the potential benefits of equipping the vehicle with a rear spoiler in braking control system design.

From the above reviews, it is concluded that rear spoiler will help to reduce the drag force on the vehicle and subsequently it will improve the fuel economy and gives better traction of the vehicles. From the above reviews, it is concluded that rear spoiler with below  $20^\circ$  will help to reduce the drag force on the vehicle based on its vehicle architecture.

## DESIGN AND METHODOLOGY

Spoiler designed with 3 proposals at different lift angle conditions like  $28^\circ$ ,  $15^\circ$  and  $3^\circ$  which we carried out in the CFD analysis to know the drag force reduction. We picked best condition to reduce the drag force and further it fine-tuned to have better curvature continuity with the vehicle which gives aesthetic look and smooth surface finish. Solid model of spoiler designed with mountings on vehicle from frozen spoiler surface in CFD analysis. We conducted Structural and Mould flow analysis for same solid model to make feasible in manufacturing. Finally Fabricated Spoiler is made with 1.2mm thick Mild steel sheets (which is readily available in market) by bending and welding. Fabricated spoiler fitted in the vehicle and mileage test carried out.

**Model description:** The base model vehicle over which design modifications were done is shown in figures

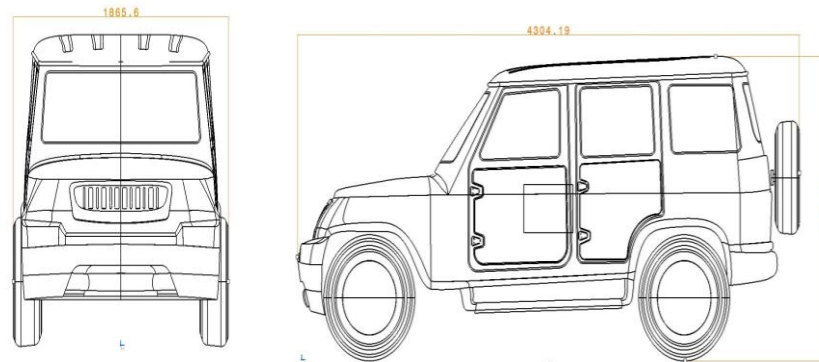


Fig.3.2. Bolero outer dimensions

### Design of bolero car model

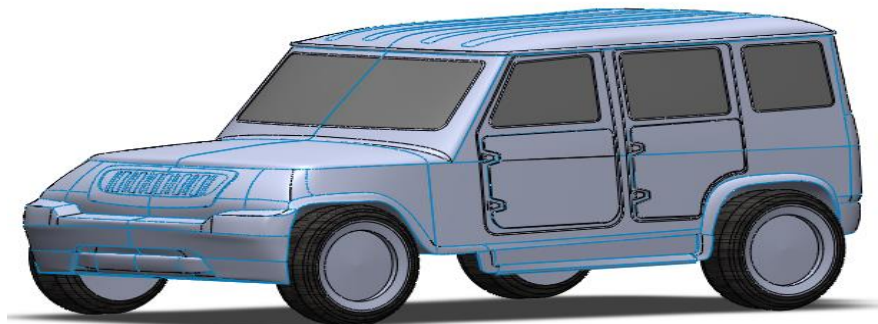


Fig 3.11 Overall View of Bolero Car Model

### Design of spoiler

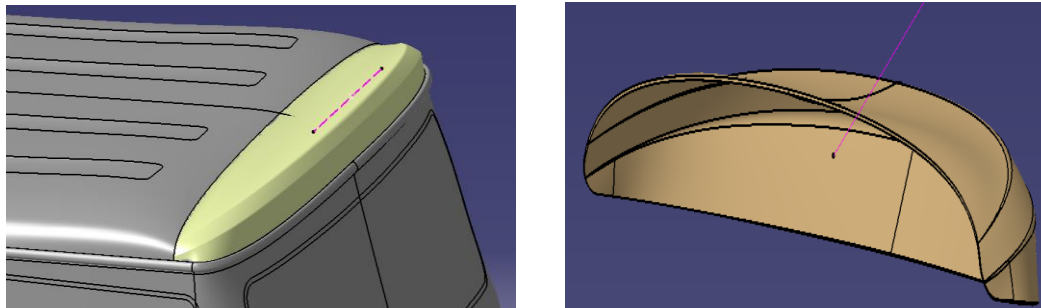


Fig. Surface modeling and solid modelling of Spoiler

### CFD analysis of spoiler

The ANSYS Workbench platform is the framework upon which the industry’s broadest and deepest suite of advanced engineering simulation technology is built. An innovative project schematic view ties together the entire simulation process, guiding the user through even complex multi physics analyses with drag-and-drop simplicity.

#### Table: Boundary conditions

Boundary Conditions		
Velocity Inlet	Magnitude (Measured normal to Boundary)	22 m/s (constant)
	Turbulence Specification Method	Intensity and Viscosity Ratio
	Turbulence Intensity	1.00%
	Turbulence Viscosity Ratio	20
Pressure Outlet	Gauge Pressure magnitude	0 pascal
	Gauge Pressure direction	normal to boundary
	Turbulence Specification Method	Intensity and Viscosity Ratio
	Backflow Intensity	10%
	Backflow Viscosity Ratio	10
Wall Zones	- vehicle surface-noslip wall B/c - Ground face- inviscid wall B/C -Side faces -inviscid wall B/C	
Fluid Properties	Fluid Type	Air
	Density	$\rho = 1.175 \text{ (kg/m}^3 \text{)}$
	Kinematic viscosity	$\nu = 1.7894 \times 10^{-5} \text{ (kg(m}\cdot\text{s))}$

**Turbulent viscosity ratio**

The turbulent viscosity ratio is simply the ratio of turbulent to laminar (molecular) viscosity:

$$\beta = \frac{\nu_t}{\nu}$$

For internal flows  $\beta$  may be scaled with the Reynolds numbers. Some guidelines (determined with numerical experiments) for fully developed pipe flows are as follows:

Table: Reynolds number and turbulent viscosity ratio

Re	3000	5000	10,000	15,000	20,000
$\beta$	11.6	16.5	22	32.0	45.1

For a Reynolds numbers of 100,000 or greater a constant value of  $\beta = 100$  is a reasonable estimate. For external flows the freestream turbulent viscosity will be on the order of laminar viscosity so small values of bare appropriate, say  $\beta = 0.1 - 0.2$ .

**Results and Discussions:**

The velocity stream line without spoiler is represented in the figure 1. As it seen, the velocity increases and Fig 2 represents the completed pressures of bolero car with 3° spoiler. The simulator will run with an increased pressure.

**CFD analysis of bolero car without spoiler:**

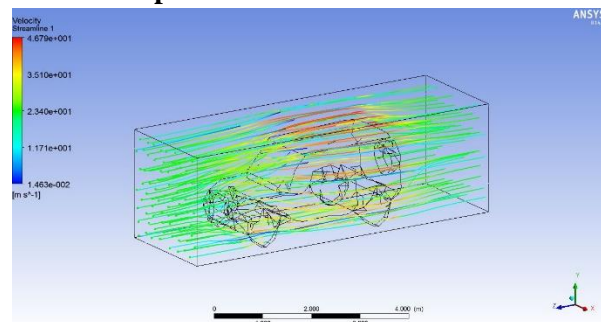


Fig1. Velocity stream line without spoiler

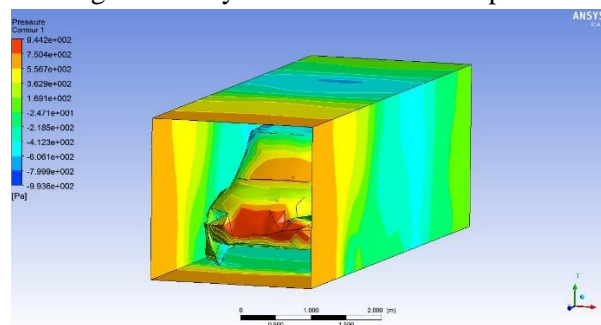


Fig 2. Pressure contour without spoiler

Simulation of bolero car has been performed and Fig 3,4 5,6 shows the behavior of velocity stream line and pressure flow field with 3° spoiler and 28° respectively.

**CFD analysis of bolero car with 3° spoiler:**

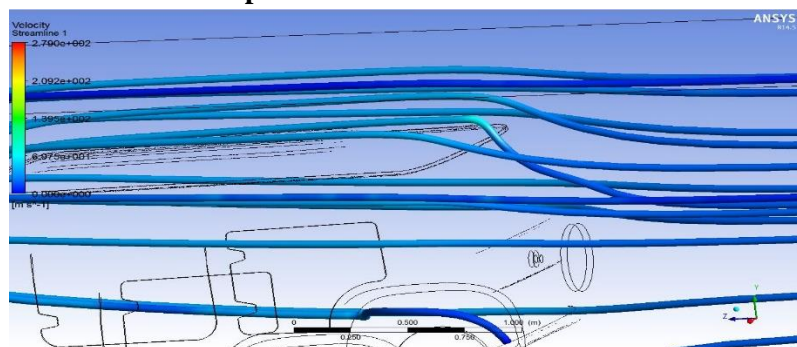


Fig 3. Velocity streamline with 3° spoiler

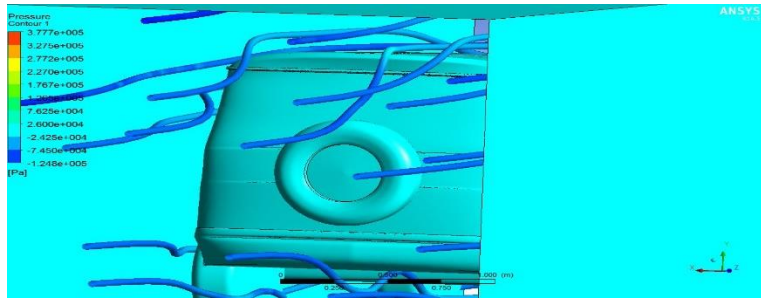


Fig 4. Pressure contour with 3° spoiler

**CFD analysis of bolero car with 28° spoiler:**

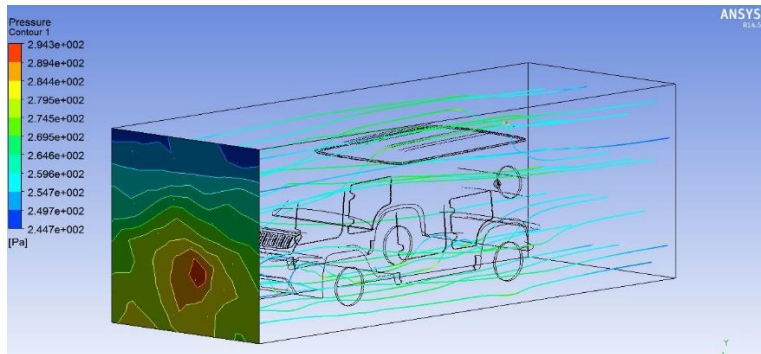


Fig 5. Pressure contour with 28° spoiler

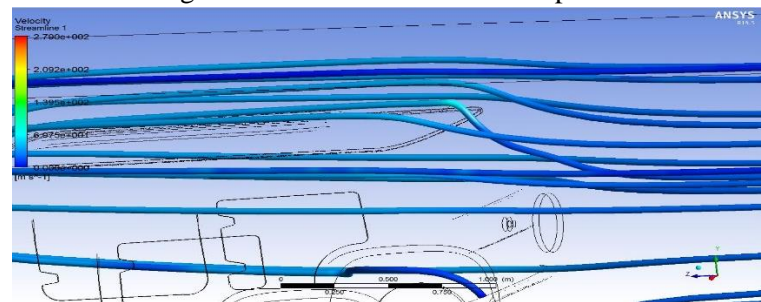


Fig 6. Velocity streamline step with 28° spoiler

From the Fig 7, it was observed that the coefficient of drag value,  $C_d$  is 0.62 for bolero car without spoiler.

**Co-efficient of drag ( $C_d$ ) Values Comparison:**

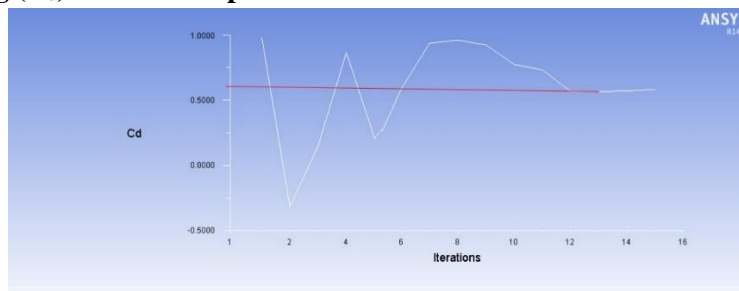


Fig 7. Bolero car without spoiler  $C_d = 0.62$

And from the Fig 8,9 shows that the coefficient of drag,  $C_d$  is 0.59 and 0.69 for bolero car with 3° and 28° spoiler.

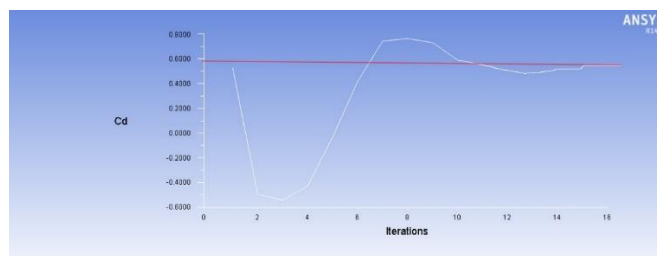


Fig 8. Bolero car with 3° spoiler  $C_d = 0.59$

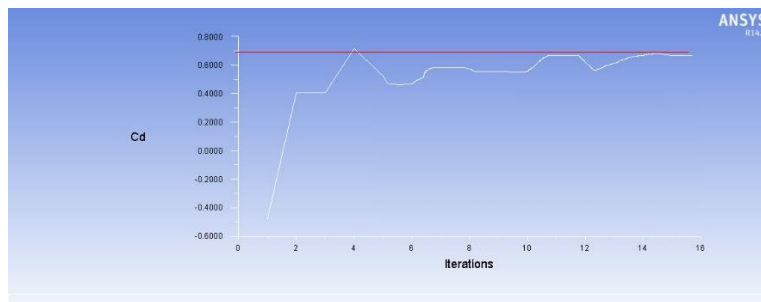


Fig 9. Bolero car with 28° spoiler  $C_d = 0.69$

**Table: Co-efficient of drag ( $C_d$ ) Values Comparison**

	Without Spoiler	With 3° Spoiler	With 28° Spoiler
Co-efficient of Drag	0.62	0.59	0.69

## CONCLUSIONS

Computational fluid dynamics (CFD) simulations of the steady flow field around Bolero car model with and without Spoiler were presented and compared the simulated data to each other. The ANSYS-14.5 Fluent with the steady model is used for the simulations of aerodynamics. In this analysis, the coefficient of drag has been reduced by 4.8%. The Spoiler objective is to reduce aerodynamic drag acting on the vehicle and thus improve the fuel efficiency of passenger car which we resulted 3.2% increase of fuel economy in On Road mileage test at 80km/h speed. Hence, the drag force can be reduced by using add on devices on vehicle and fuel economy, stability of a passenger car can be improved.

### Future enhancement:

- Verifying the computational results by building and testing both models in a wind tunnel.
- Building a practical model (More accurate proto by silicon moulding or injection moulding) of the designed rear spoiler and carrying out experimental tests on it to verify the obtained computational results.
- Gathering data on the actual environmental conditions that the car is exposed to and using that data in the CFD analysis.

## REFERENCES:

1. L.Balaji, P.Deepak prasad, V.Ashok, Surendra Kumar Yadav and Sovan Samanta.“ Design And Analysis Of Rear Spoiler To Reduce Drag Coefficient Of A Sports Car ” 2020 ISSUE VOLUME 1 ISBN 978-93-5406-579-8.
2. B. Hai-tao, "Study the effect of rear spoiler on car aerodynamics characteristics," 2011 6th International Conference on Computer Science & Education (ICCSE), Singapore, 2011, pp. 460-463, <https://ieeexplore.ieee.org/stamp/stamp.jsp?tp=&arnumber=6028679&isnumber=6028569>
3. K. P. Arulshri, S.Selva Kumar and R.Nesalingam “CFD ANALYSIS OF AUTOMOBILE REAR DYNAMIC SPOILER” International Journal of Aquatic Science, Vol 12, Issue 03, 2021 [https://www.journal-aquaticscience.com/article\\_149873\\_5428615476281eeee0f3702a1e8797b1.pdf](https://www.journal-aquaticscience.com/article_149873_5428615476281eeee0f3702a1e8797b1.pdf)
4. Mohammad Riyad and Rubel Chandra Das “CFD Analysis of Passenger Vehicle at Various Angle of Rear End Spoiler” Volume 194, 2017, Pages 160-165, ISSN 1877-7058, <https://doi.org/10.1016/j.proeng.2017.08.130>
5. Kamprasad Chodagudi, T.B.S Rao, 2012, “Analysis Of Naca 2412 For Automobile Rear Spoiler Using Composite Material” , INTERNATIONAL JOURNAL OF ENGINEERING RESEARCH & TECHNOLOGY (IJERT) Volume 01, Issue 07 (September 2012) .
6. [Analysis Of Naca 2412 For Automobile Rear Spoiler Using Composite Material – IJERT](#)

7. Parashar V. Shinde ,Arshad Shaikh ,Saad Mirza, Haidar Khan ,Prof. Irshad Shaikh, “Analysis Of the Spoiler” Volume 03, Issue 03; Month - 2017 [ISSN: 2455-1457]  
<https://scholar.archive.org/work/pqlqeclwsje7dbbfn2kgdd4kga/access/wayback/http://www.ijrter.com/papers/volume-3/issue-3/analysis-of-the-spoiler.pdf>
8. Ashpak Kazi, Pradyumna Acharya, Akhil Patil and Aniket Noraje, “EFFECT OF SPOILER DESIGN ON HATCHBACK CAR” (IJMTER) Volume 03, Issue 09, [September– 2016] ISSN (Online):2349–9745; ISSN (Print):2393-8161 [EFFECT OF SPOILER ON HATCHBACK CAR.PDF](#)
9. M. R. Rasani, M. S. Aldlemy, and Z. Harun, “Fluid-structure interaction analysis of rear spoiler vibration for energy harvesting potential”, JMES, vol. 11, no. 1, pp. 2415–2427, Mar. 2017.  
<https://doi.org/10.15282/jmes.11.1.2017.2.022>
10. Fajar Frihdianto, Nyeyep Sri Wardani, Indah Widiastuti ,2021“ANALYSIS OF THE USE OF SPOILER ONE LEVEL AND TWO LEVELS IN CONDITIONS OF STEADY AGAINST THE DRAG AND LIFT COEFFICIENTS ON A SEDAN TYPE CAR BY USING CFD” ISSN: 2615-5699 (Online) <https://doi.org/10.20961/jomeve.v1i2.25066>
11. Salem Haggag and Mason Marzbali, 2021 “Impact of Rear Spoiler on Vehicle Braking Longitudinal Dynamics” ISSN: 1946-3995, e-ISSN: 1946-4002 <https://doi.org/10.4271/06-14-01-0003>

## Single Cylinder Engine Fueled with Petrol and Enriched Hydrogen and Hydroxy for Better Performance

Sukumar Kalapati, Dr. Venkatasubbaiah K, Dr. Narayana Rao K

Lecturer in Automobile Engg., (Dept. of Technical Education) Govt. Polytechnic for Minorities, Guntur,  
A.P., India.

Vice-Chancellor JNTU Gurajada, Vizianagaram, (Council Member, IEI & ISTE.,) Andhra Pradesh,  
India.

Joint Secretary, A.P.S.B.T & T., (Dept. of Technical Education) Vijayawada, A.P., India.

**ABSTRACT:** Hydroxy and hydrogen blended gases offer a promising catalyst fuel for enhancing efficiency and reducing NO<sub>x</sub> emissions in petrol engines. However, challenges related to the production, storage, and distribution of these gases exist. The narrow flammability limits of petrol, compared to hydrogen, may lead to partial burning or misfires in engines relying solely on petrol when operating with lean mixtures. This paper addresses these concerns and presents experimental findings on the impact of introducing enriched hydroxy and hydrogen mixed gases (referred to as HHO++) on a petrol engine's performance. Parameters such as effective power, brake specific fuel consumption (BSFC), and emissions (NO<sub>x</sub>, HC) are investigated. The experiments, conducted on a dynamometer, precede implementation in commercially modified two-wheeler vehicles, specifically the Honda Activa and Suzuki Access 125. A specialized valve, positioned between the intake and air filter, is added to the engines. Tests encompass various operating conditions and air-fuel ratios, with the injection of hydrocarbons and hydrogen-rich gases into the engine cylinder. Prior to injection, experiments are carried out to separate positive and negative ions of the gas phase, and gas compounds are analysed for hydrocarbon specificity using Gas Chromatography-Mass Spectrometry (GC-MS) at the Sophisticate Analytical Instruments Facility (SAIF) at IIT Bombay. This paper provides a brief overview of some key results obtained from these experiments.

**Keywords:** IC engines, Enriched HHO++, Engine thermal efficiency, Brake power, Emission control.

### INTRODUCTION:

In the current societal landscape, the escalating concerns among individuals from all walks of life centre around the continuously rising fuel prices and the detrimental effects caused by heightened pollutant levels in the atmosphere. However, the harmful emissions associated with the use of fossil fuels over the years have minimized their applications in IC engines [1,2]. To reduce the dependency on conventional fossil fuels, numerous studies have focused on the use of renewable and non-conventional energy sources, such as hydrogen [3, 4], natural gas [5,6], liquefied petroleum gas [7] and alcohols [8,9]. In the above perspective, hydrogen is a promising fuel for IC engines because of its superior properties, such as a wide flammability range, high laminar flame velocity, high adiabatic flame temperature, high heating value, low ignition energy, and a smaller quenching gap [10, 11]. Kassaby et al. [12] investigated the effect of hydroxy (HHO) gas on SI engine performance and emissions. They reported that the addition of HHO improved thermal efficiency and reduced fuel consumption and exhaust emissions, even for nitrogen oxides (NO<sub>x</sub>). Kamil et al. [13] analyzed the effect of hydrogen gas on the performance of gasoline and methane. Duan et al. [14] investigated the effect of hydrogen addition on cyclic variation on a large-bore SI engine operating on lean burn natural gas. They found that the in-cylinder pressure increased with an increasing hydrogen energy share. However, the combustion duration and cyclic variation decreased with increasing hydrogen energy share.

Addressing these pressing issues, the evolution of hybrid vehicles emerges as one of the closest solutions. Defined as any vehicle that integrates one or more on-board power sources capable of directly or indirectly providing propulsion power, hybrid vehicles aim to significantly enhance mileage and reduce emission levels in both gasoline-powered and diesel engines. The water hybrid vehicle,

specifically, employs an HHO (Oxy Hydrogen) generator to supply hydrogen on demand through electrolysis.

This process takes place in an HHO Fuel Cell, where the flow of current through the stainless steel plate initiates electrolysis between the two terminals. As a result, electrolyte molecules separate into hydrogen-rich hydrocarbon gases. The integration of these modules yields highly favourable outcomes. During operation, the internal combustion (IC) engine of the hybrid vehicle simultaneously charges the battery using an alternator, which, in turn, functions as a generator. The hybrid system represents an endeavour to provide an affordable, low-emission, and fuel-efficient vehicle with performance standards surpassing those of most conventional engines.

During the design and development stage, our primary objectives encompassed variables such as indicated power, brake power, brake-specific fuel consumption, exhaust emissions, engine cooling, and maintenance-free operation. Another crucial aspect of the development project involved reducing costs while enhancing torque output and engine reliability. To achieve these goals, various design concepts incorporating other stored renewable energy sources were employed. Following the design and development of the prototype, the working model, as depicted in Fig. 1, was created. To validate the developed engine, testing and performance evaluations were conducted using the traditional dynamometer test setup method.

### 1. EXPERIMENTATION AND OBSERVATIONS:

This experimentation involves the study of hydrocarbon presence using a specifically designed reactor, which was tested at the GC MS machine in the IIT Bombay SAIF test facility to separate positive and negative ions.

The reactor jar is constructed from borosilicate to withstand temperatures exceeding 200 degrees Celsius. It features two outlets; one serves as the exit path for positive ions, and the other for negative ions. The electrodes, designed cylindrically from graphite, aim to minimize corrosion effects. The electrolyte solution consists of a 0.1 N concentration of sodium salt dissolved in HPLC grade distilled water. Positive and negative electrodes are connected to a pulsating power source, with pulse characteristics controlled by an electronic control circuit to vary pulse amplitude and frequency. The experimental setup of the reactor is depicted in Figure 1 below.

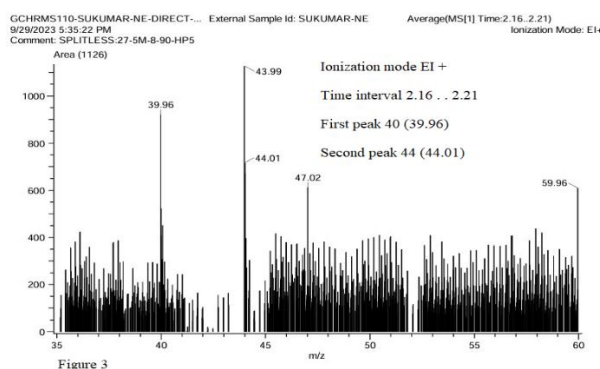
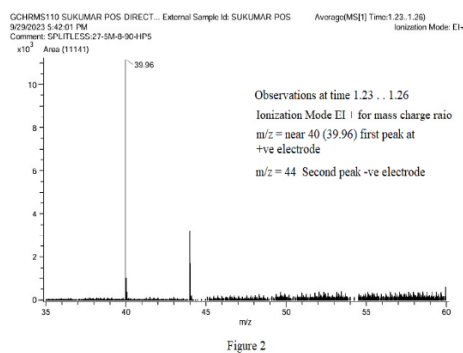


Figure 1

The distinct separation of gas molecule compounds is clearly illustrated in Figure 2 and Figure 3. This capability to separate gas ions enhances the specificity of molecules, thereby contributing to improved reactor design for more efficient combustion processes. The clear visualization of separated gas molecules is a valuable insight that can be leveraged for optimizing combustion dynamics and enhancing the overall performance of reactors in various applications.

## **2. WORKING OF CONVENTIONAL HHO CELL:**

The electrolysis process initiates when an electric current passes through the stainless steel plate, occurring between the two terminals and resulting in the separation of water molecules into HHO gas. This gas is then directed through a bubbler tank equipped with a non-return valve to prevent gas backpressure. From the bubbler, the HHO gas travels through a P.V.C pipe connected to the outlet valve, and using a silicon pipe, it is directed to the air intake of the carburettor.

Water, as the most abundant resource on our planet, can serve as a fuel. Hydrogen Generators, extracting Hydrogen and Oxygen (HHO) from water, have become integral for internal combustion engine applications. By introducing this hydrogen/oxygen gas alongside regular fuel, our experimentation with a modified Hydrocarbon-rich generator aims to enhance the fuel economy of internal combustion engines by 20-35% and significantly reduce emissions to meet clean standards.

## **3. IC ENGINE WITH HHO++ GAS:**

Within the combustion chamber, the fuel undergoes mixing with air, along with the introduction of enriched hydrogen gas (HHO++), sourced from the engine manifold. The HHO++ gas mixer enhances the fuel mixture, leveraging the combustible nature of hydrogen. This facilitates an efficient combustion process, leading to the removal of carbon deposits within the cylinder. The result is a cleaner engine operation, contributing to an overall improvement in engine performance.

### **Combustion process w.r.t. Temperature:**

The process commences with water and various electrolytes, and the application of pulsed DC current induces the breakdown of  $H_2O$  into H (ortho), H (para), and O (atomic), collectively known as HHO. This HHO++ is introduced into the engine cylinder using the engine's vacuum. Upon mixing with air, HHO++ undergoes combustion within the chamber. After combustion, it reverts to hot  $H_2O$  vapor molecules, absorbing engine heat within the temperature range of 350 to 450°F CHT. The vapor then transforms into superheated dry steam, expelled through the tailpipe during the exhaust stroke. Upon release, it condenses back into water vapor, eventually returning to its liquid state. Significantly, this process results in a substantial reduction of emissions to cleaner, lower levels.

## **4. REVIEW OF ENERGY CONSUPTION AND PERFORMANCE:**

This review encompasses hydrogen-diesel experiments, sharing commonalities such as the use of naturally aspirated diesel engines and maintaining constant engine speeds, typically around 1500 rev/min to emulate generator conditions. A small quantity of either hydrogen-rich or HHO++ compounds is introduced to gasoline engines for the analysis of fuel consumption and NOx emissions, employing an eddy current dynamometer.

Throughout the paper, all gas mass flow rates are standardized to volumetric flow rates at standard temperature and pressure (273.15°K and 101.325 kPa). In our experiment, the production of 1L of HHO++ required nearly 8 kJ. Additionally, the net efficiency of converting equivalent gasoline energy to HHO++ energy ranged between 11.4% and 16%. Notably, it took almost 4.4 Wh of electrical energy to produce 1L of HHO++ in our experiment, accounting for losses from the switch mode power supply. Considering the HHO++ conversion efficiency of 15-20%, the production of 1L of HHO++ would necessitate approximately 52 kJ or 14.43 Wh of gasoline energy.

## OBSERVED RESULTS:

### COMBUSTION CHARACTERISTICS:

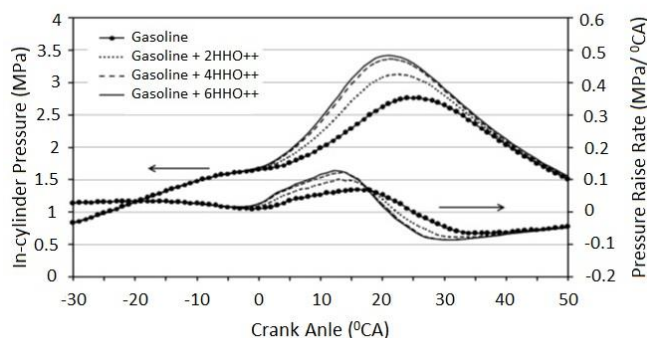


Fig. 1.1. Effect of HHO++ gas flow rate on In-cylinder pressure and pressure raise Rate at 3000 rpm, WOT and  $\lambda=1.4$

Figure 1.1 illustrates the profiles of in-cylinder pressure and pressure rise rate against crank angle (CA) at 3000 rpm, WOT (Wide Open Throttle) and  $\lambda$  (air-fuel ratio) set at 1.4. The introduction of hydrogen-rich HHO++ gas, depicted in Gasoline + 2 HHO++, Gasoline + 4 HHO++ and Gasoline + 6 HHO++ cases, results in earlier pressure rise curves compared to the original engine pressure curve, attributable to hydrogen's fast burn characteristic. Additionally, the peak in-cylinder pressure increases due to the high flame temperature and speed of hydrogen combustion. Consequently, a smaller amount of fuel is burnt during the expansion stroke, leading to a quicker drop in in-cylinder pressure after reaching its peak value, as observed with HHO++ gas enrichment.

The variations in pressure rise rate when adding HHO++ gas are more pronounced than those observed in an engine using pure gasoline, as depicted in Fig. 1.1. The findings indicate that combustion durations decrease with the addition of HHO++ gas. Specifically, the combustion duration reduces by approximately 18.34%, 29.23% and 29.31% when adding 2, 4, and 6 litres/min of HHO++ respectively.

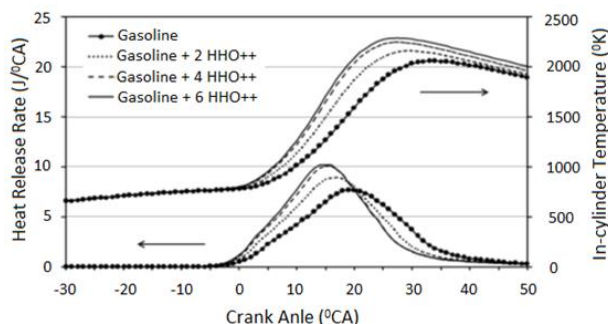


Fig. 1.2 Effect of addition HHO++ gas flow rate on HRR and In-cylinder temperature at 3000 rpm, WOT and  $\lambda = 1.4$ .

Figure 1.2 presents profiles of heat release rate (HRR) and in-cylinder temperature with crank angle at 3000 rpm, WOT and  $\lambda = 1.4$ . The figure highlights that both the peaks of temperature and HRR increase and move closer to top dead centre with the incremental addition of HHO++ gas, whether under rich or lean conditions. This behaviour is attributed to the high adiabatic flame temperature and the rapid flame speed of hydrogen combustion.

### ENGINE THERMAL EFFICIENCY:

The figure 2.1 illustrates the relationship between engine thermal efficiency and lambda (the air-fuel ratio). This improvement can be attributed to the unique properties of hydrogen. With a flame speed five times that of gasoline and a much wider flammability range, the HHO++ gas/gasoline mixture exhibits a faster burning velocity and an extended flame limit compared to gasoline alone. This results in a shorter burning duration and more complete combustion. The heightened flame speed of the gasoline-HHO++ gas mixture enhances constant volume combustion, bringing the engine closer to the ideal cycle and yielding higher thermal efficiency compared to pure gasoline at the same lambda.

Moreover, hydrogen's broader flammable range allows for high efficiency across a wide range of lambda values beyond stoichiometry. Therefore, as lambda increases, a HHO++ gas-enriched gasoline engine moves toward relatively more complete combustion, even though engine power decreases due to the gradual reduction in fuel flow. This highlights the potential for achieving efficient combustion with HHO++ gas enrichment across a spectrum of air-fuel ratios.

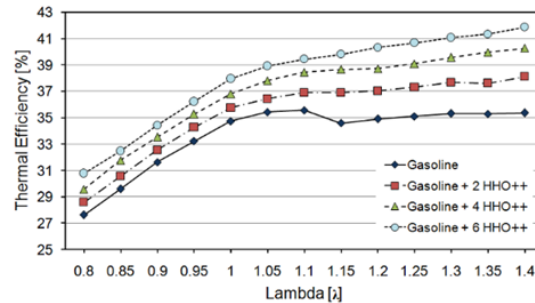


Fig. 2.1 Effect of addition HHO++ gas flow rate on Thermal Efficiency against lambda (λ) at 3000 rpm, WOT

**SPECIFIC FUEL CONSUMPTION:**

Observation of Specific Fuel Consumption for Test Engine with HHO++ and without HHO++

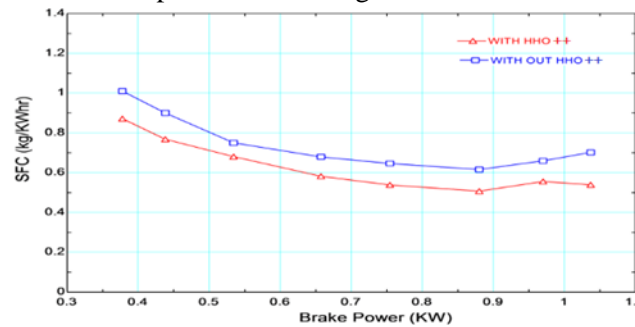


Fig.3.1. Specific fuel consumption v/s Brake Power

The figure 3.1 depicting Specific Fuel Consumption (SFC) versus Brake Power reveals a notable improvement in the SFC of the test engine when utilizing HHO++. In comparison to running without HHO++, the maximum reduction in SFC occurs at 1.03 kW brake power, reaching 25%, while the minimum reduction is observed at 0.55 kW brake power, amounting to 10.2%. On average, the use of HHO++ results in a Brake SFC decrease ranging from 10% to 25%.

This reduction in fuel consumption can be attributed to enhanced combustion facilitated by the uniform mixture of air, particularly oxygen, and the enriched gas maintaining the original ratio during the combustion process. The distinctive properties of hydrogen in oxyhydrogen gas, such as a short quenching distance, high flame speed, and a wide flammability range, contribute to the comprehensive combustion of petrol fuel. This synergy allows for a more efficient combustion process, leading to a significant reduction in Specific Fuel Consumption across varying brake power levels.

**REDUCTION OF ENVIRONMENTAL POLLUTION: (CO, CO<sub>2</sub> & HC):**

Observation of CO for test engine with HHO++ and without HHO++:

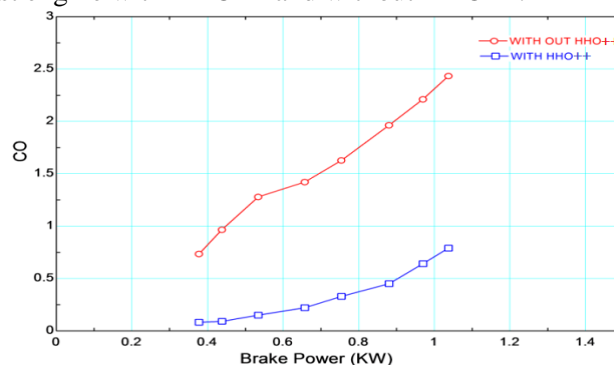


Fig. 4.1 Brake Power v/s CO

Figure 4.1 depicting CO versus Brake Power illustrates a significant improvement in the CO levels of the test engine when utilizing HHO++ compared to running without it. The maximum decrease is observed at 1.03 kW brake power, reaching 75%, while the minimum decrease occurs at 0.3 kW brake power, amounting to 25%. On average, CO levels decrease by 25-80% with the use of HHO++.

This improvement can be attributed to the combustion characteristics of the air-hydrogen mixture. The presence of engine lubrication oil film sticking onto the cylinder wall and burning with the air-hydrogen mixture may contribute to carbon emissions. The absence of carbon in the hydroxyl gas, generated through the use of HHO++, is a significant factor in the reduction of CO emissions. The combustion process facilitated by HHO++ appears to mitigate the production of carbon monoxide, leading to a substantial decrease in CO levels across various brake power levels.

b) Observation of CO<sub>2</sub> for Test Engine:

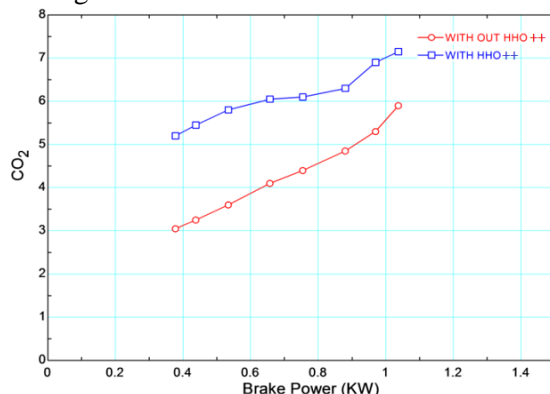


Fig. 4.2. CO<sub>2</sub> v/s Brake Power

It has been observed from figure 4.2 depicting CO<sub>2</sub> versus Brake Power that CO<sub>2</sub> levels in the test engine show improvement when using HHO++ compared to running without it. The maximum increase is noted at 0.3-0.6 kW brake power, approximately 40%, while the minimum decrease occurs at 1.03 kW brake power, around 15%. On average, CO<sub>2</sub> levels decrease by approximately 15-50% with the use of enriched gas.

This improvement can be associated with the combustion characteristics of the air-hydrogen mixture introduced by HHO++. The specific conditions at different brake power levels contribute to variations in CO<sub>2</sub> levels. Overall, the use of HHO++ appears to positively impact the CO<sub>2</sub> emissions, resulting in a notable reduction across various brake power levels.

b) Observation of HC for Test Engine:

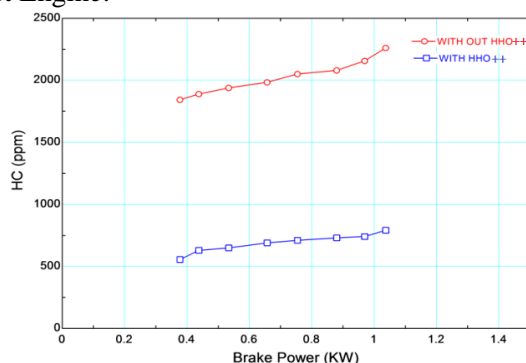


Fig. 4.3 HC v/s Brake Power

Observations from Figure 4.3, illustrating Hydrocarbon (HC) levels versus Brake Power, indicate an improvement in HC emissions in the test engine when using HHO++ compared to operating without it. The maximum decrease is noted at 1.03 kW brake power, approximately 80%, while the minimum decrease occurs at 0.5 kW brake power, around 55%. On average, HC emissions decrease by approximately 50-80% with the use of HHO++.

This improvement in HC emissions can be attributed to the combustion characteristics facilitated by the air-hydrogen mixture introduced by HHO++. The short quenching distance and wide flammability range

of hydrogen contribute to the engine expelling lower HC emissions. The combustion process enhanced by HHO++ appears to mitigate the production of hydrocarbons, resulting in a substantial reduction in HC levels across various brake power levels.

## 5. CONCLUSION:

This study primarily focuses on mitigating pollution levels and enhancing fuel efficiency through experimentation, specifically investigating the feasibility of HHO++ utilization in a four-stroke petrol engine without modifications. The engine underwent testing to assess the impact of HHO++ usage on fuel consumption and carbon emissions. Further experimentation is necessary to align with on-road BS standards.

### Key findings include:

**Specific Fuel Consumption Reduction:** The study observed a reduction in specific fuel consumption by approximately 10-25%. This improvement is attributed to the high lower heating value of HHO++ compared to gasoline.

**HC Emissions:** Traces of hydrocarbon (HC) emissions were detected during HHO++ operation, likely arising from the vaporization of lubricating oil. Further investigation is needed to address this emission concern.

**Conversion Efficiency Increase:** The conversion efficiency showed an increase of 15-20% when the engine operated with HHO++. This suggests that the presence of HHO++ positively influences the efficiency of the combustion process.

Overall, while the study demonstrates promising results in terms of fuel efficiency and reduced specific fuel consumption, addressing trace HC emissions is an important consideration for further refinement and alignment with on-road emission standards.

## REFERENCES:

- [1] A. Elfasakhany, Investigations on the effects of ethanol–methanol–gasoline blends in a spark-ignition engine: performance and emissions analysis, *Eng. Sci. Technol. Int. J.* 18 (4) (2015) 713–719.
- [2] J. Pan, N. Li, H. Wei, J. Hua, G. Shu, Experimental investigations on combustion acceleration behavior of methane/gasoline under partial load conditions of SI engines, *Appl. Therm. Eng.* 139 (2018) 432–444.
- [3] X. Yu, Z. Guo, L. He, W. Dong, P. Sun, Y. Du, et al., Experimental study on lean-burn characteristics of an SI engine with hydrogen/gasoline combined injection and EGR, *Int. J. Hydrogen Energy* 44 (26) (2019) 13988–13998.
- [4] S. Pan, J. Wang, Z. Huang, Effects of hydrogen injection strategy on the hydrogen mixture distribution and combustion of a gasoline/hydrogen SI engine under lean burn condition, *Int. J. Hydrogen Energy* 47 (57) (2022) 24069–24079.
- [5] Z. Chen, T. Zhang, X. Wang, H. Chen, L. Geng, T. Zhang, A comparative study of combustion performance and emissions of dual-fuel engines fueled with natural gas/methanol and natural gas/gasoline, *Energy* 237 (2021), 121586.
- [6] R. Madihi, M. Pourfallah, M. Gholinia, M. Armin, A.Z. Ghadi, Thermofluids analysis of combustion, emissions, and energy in a biodiesel (C<sub>11</sub>H<sub>22</sub>O<sub>2</sub>)/natural gas heavy-duty engine with RCCI mode (Part II: fuel injection time/Fuel injection rate), *Int. J. Thermofluids* 16 (2022), 100200.
- [7] G.T. Hashem, M.F. Al-Dawody, I.E. Sarris, The characteristics of gasoline engines with the use of LPG: an experimental and numerical study, *Int. J. Thermofluids* 18 (2023), 100316.
- [8] S. Sarıkoç, Effect of H<sub>2</sub> addition to methanol-gasoline blend on an SI engine at various lambda values and engine loads: a case of performance, combustion, and emission characteristics, *Fuel* 297 (2021), 120732.
- [9] M.K. Mohammed, H.H. Balla, Z.M.H. Al-Dulaimi, Z.S. Kareem, M.S Al-Zuhairy, Effect of ethanol-gasoline blends on SI engine performance and emissions, *Case Stud. Therm. Eng.* 25 (2021), 100891.

- [10] S.T.P. Purayil, M.O. Hamdan, Al-Omari SAB, M.Y.E. Selim, E. Elnajjar, Review of hydrogen–gasoline SI dual fuel engines: engine performance and emission, *Energy Reports* 9 (2023) 4547–4573.
- [11] E. Elnajjar, S.A.B. Al-Omari, M.Y.E. Selim, Purayil STP. CI engine performance and emissions with waste cooking oil biodiesel boosted with hydrogen supplement under different load and engine parameters, *Alexandria Eng. J.* 61 (6) (2022) 4793–4805.
- [12] M.M. El-Kassaby, Y.A. Eldrainy, M.E. Khidr, K.I. Khidr, Effect of hydroxy (HHO) gas addition on gasoline engine performance and emissions, *Alexandria Eng. J.* 55 (1) (2016) 243–251.
- [13] M. Kamil, M.M. Rahman, Performance prediction of spark-ignition engine running on gasoline-hydrogen and methane-hydrogen blends, *Appl. Energy* 158 (2015) 556–567.
- [14] X. Duan, B. Deng, Y. Liu, S. Zou, J. Liu, R. Feng, An experimental study the impact of the hydrogen enrichment on cycle-to-cycle variations of the large bore and lean burn natural gas spark-ignition engine, *Fuel* 282 (2020), 118868.
- [15] Boden, T.A., G.Marland, and R.J. Andres, 2011, Global, Regional, and National Fossil fuel CO<sub>2</sub> Emissions. Carbon dioxide Information Analysis Center, Oak Ridge National Laboratory, U.S. Department of Energy, Oak Ridge, Tenn., U.S.A. doi10.3334/CDIAC/00001\_V2011.
- [16] Effect of Hydroxy (HHO) gas addition on performance and exhaust emissions in compression ignition engines (2010) by Ali Can Yilmaz, Erinclu, U dumar, Kadir Aydin.
- [17] D.R. Gabhane., S.S. Deshmukh. A Review on effect of Oxy-Hydrogen (HHO) gas addition on the performance of Internal Combustion Engines. *IJSRO-International for Scientific Research & development/Vol.3, Issue 04, 2015/ISSN (online): 2321-0613.*
- [18] Sanjib Das, Diptanu Dey, Bharath kumar Boyanapalli, Priyanath Das. Design of a petrol – HHO hybrid fuel system for 110 CC, 4-stroke I.C. Engine/*IJEREEEE/Vol.2, Issue 12, December, 2016/ISSN (online) 2395-2717.*
- [19] Yasin Karagoz, Emre Orak, Levent Yuksek, Tarkan Sandalci. Effect of Hydrogen addition on exhaust emissions and performance of a Spark Ignition engine, *Environmental Engineering and Management journal/March, 2015, Vol.14, No.3, 665-672.*
- [20] S. Manigandan, P. Gunasekar, S. Poorchilamban, S. Nithya, J. Devipriya, G. Vasanthkumar, Effect of addition of hydrogen and TiO<sub>2</sub> in gasoline engine in various exhaust gas recirculation ratio, *Int. J. Hydrogen Energy* 44 (21) (2019) 11205–11218.
- [21] E. Zervas, Correlations between cycle-to-cycle variations and combustion parameters of a spark ignition engine, *Appl. Therm. Eng.* 24 (14–15) (2004) 2073–2081.
- [22] E. Galloni, Analyses about parameters that affect cyclic variation in a spark ignition engine, *Appl. Therm. Eng.* 29 (5–6) (2009) 1131–1137.
- [23] J.B. Heywood, *Internal Combustion Engine Fundamentals*, McGraw-Hill Education, 2018.
- [24] R.A. Bakar, K. Kadirgama, D. Ramasamy, T. Yusaf, M.K. Kamarulzaman, N. Aslfattahi, et al., Experimental analysis on the performance, combustion/ emission characteristics of a DI diesel engine using hydrogen in dual fuel mode, *Int. J. Hydrogen Energy* (2022).
- [25] J. Etheridge, S. Mosbach, M. Kraft, H. Wu, N. Collings, A detailed chemistry multi-cycle simulation of a gasoline fueled HCCI engine operated with NVO, *SAE Int. J. Fuels Lubr.* 2 (1) (2009) 13–27.
- [26] A.K. Sen, S.K. Ash, B. Huang, Z. Huang, Effect of exhaust gas recirculation on the cycle-to-cycle variations in a natural gas spark ignition engine, *Appl. Therm. Eng.* 31 (14–15) (2011) 2247–2253.
- [27] X. Yu, Y. Du, P. Sun, L. Liu, H. Wu, X. Zuo, Effects of hydrogen direct injection strategy on characteristics of lean-burn hydrogen–gasoline engines, *Fuel* 208 (2017) 602–611.
- [28] M.A. Ceviz, A.K. Sen, A.K. Küleri, I.V. Öner, Engine performance, exhaust emissions, and cyclic variations in a lean-burn SI engine fueled by gasoline–hydrogen blends, *Appl. Therm. Eng.* 36 (2012) 314–32.